PLASTICITY
THEORY AND ENGINEERING APPLICATIONS

SÁNDOR KALISZKY

AKADÉMIAI KIADÓ, BUDAPEST

Plasticity

Theory and Engineering Applications

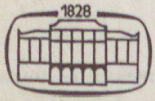
Plasticity

Theory and Engineering Applications

by

Sándor Kaliszky

Professor, Department of Civil Engineering Mechanics
Technical University of Budapest



Akadémiai Kiadó
Budapest 1989

507680

This monograph is published by Elsevier Science Publishers
as Vol. 21 in the series "Studies in Applied Mechanics".

This book is the revised English version of
Képlékenységtan. Elmélet és mérnöki alkalmazások
published by Akadémiai Kiadó, Budapest.

MAGYAR
TUDOMÁNYOS AKADÉMIA
KÖNYVTÁRA

ISBN 963 05 4708 2

© S. Kaliszky, 1989

Joint edition published by Akadémiai Kiadó, Budapest, Hungary
and Elsevier Science Publishers, Amsterdam, The Netherlands

All rights reserved. No part of this book may be reproduced by any means, or transmitted, or translated into machine language without the prior written permission of the publishers.

Printed in Hungary
by Akadémiai Kiadó és Nyomda Vállalat, Budapest

M. TUD. AKADÉMIA KÖNYVTÁRA
Könyvtár 7959 /19 89 sz.

To my wife, Klara
for her patience and encouragement

PREFACE

This book is a revised English edition of the author's book published in Hungarian in 1975 and in German in 1984. The text of the Hungarian edition was based on the author's lectures over several years to civil engineers on a graduate course in plasticity at the Technical University of Budapest.

A number of excellent books on plasticity are available, but their purpose, subject, level and method of presentation vary. The present book has been written primarily for the research engineer and the graduate student of engineering. The author has tried to keep a balance between theory and application, to present the text in a precise mathematical framework and, at the same time, to explain the physical phenomena.

In order to keep the book to a reasonable size, attention is focussed mainly on the formulation and structural applications of the fundamental physical properties, methods and solution of linearly elastic-perfectly plastic bodies. The treatment is purely phenomenological, and does not enter into micro structure or the thermodynamics of irreversible deformation processes. Plastic hardening and strain rate effects are only briefly discussed, and the assumption of infinitesimal deformations is adopted. The detailed presentation of experimental results and numerical methods and solutions is beyond the scope of the book.

The main emphasis is placed on the fundamental relations and theorems of the incremental theory of plastic bodies and on the principles and methods of incremental and limit analysis, optimal design, and shakedown analysis of bar structures, plates and shells. In addition, however, the elasto-plastic analysis of prismatic bars under torsion and of thick-walled cylinders and spheres subjected to internal pressure is also discussed, and a chapter is devoted to the theory and application of plane strain and to plane stress problems of plasticity. In the last chapter a detailed survey of the dynamic response of plastic structures is given.

Fundamental relations are described in terms of Cartesian tensors; for the solution of specific problems, however, scalar notations are used. In order to facilitate study and understanding of the text, the applications of the methods are illustrated by the solution of a large number of simple problems. The bibliography contains nearly 400 references but, is not intended to be exhaustive.

Compared with the Hungarian and German editions, this English version has a more detailed discussion of several topics, such as the application of mathematical

programming and the finite element method, and the problems of dynamically loaded structures. On the other hand, some classical problems and methods of solution which are no longer of practical importance have been omitted.

The author is greatly indebted to all those who have contributed to the publication of this book. He is particularly grateful to *Dr. L. Berke*, who corrected the English translation of the Hungarian text, contributed to the improvement of the manuscript and commented on it. Thanks are due to Ms. *D. Hadházy* and Mrs. *L. Czeglényi* for their neat and precise typing and drawing work.

In conclusion, the author wishes to express his gratitude to the Publishers, Elsevier, and Akadémiai Kiadó, for the excellent preparation of this book.

S. Kaliszky

CONTENTS

PREFACE 7

1. BASIC CONCEPTS AND NOTATIONS 19

1.1. The mechanical properties of materials 19
1.2. Material models 24
1.3. Historical remarks 28
1.4. Notations 31

2. FUNDAMENTAL RELATIONS AND GOVERNING EQUATIONS 36

2.1. State of stress 36
2.1.1. Stress vector and stress tensor 36
2.1.2. Principal stresses. Stress invariants 38
2.1.3. Principal shear stresses 41
2.1.4. Stress deviator tensor 42
2.1.5. Graphical representation of the stress state. Mohr's circle 43
2.1.6. Equilibrium equations 45
2.2. State of strain 47
2.2.1. Relative displacement tensor 47
2.2.2. Strain vector and strain tensor 50
2.2.3. Principal strains. Strain invariants 52
2.2.4. Principal shear strains. Octahedral strains 53
2.2.5. Strain deviator tensor 53
2.2.6. Strain increments and strain rates 54
2.2.7. Kinematic equations. Compatibility equations 55
2.3. Stress–strain relations 57
2.3.1. Constitutive equations for linearly elastic, isotropic bodies 58
2.3.2. Yield conditions for perfectly plastic materials 60
2.3.2.1. General remarks 60

2.3.2.2. The Huber–v. Mises–Hencky yield condition 63
2.3.2.3. The Tresca yield condition 65
2.3.2.4. Comparison of yield conditions 66
2.3.3. Constitutive equations for linearly elastic—perfectly plastic bodies 67
2.3.3.1. General relationships 67
2.3.3.2. Prandtl–Reuss and Lévy–v. Mises constitutiv equations 73
2.3.3.3. The plastic multiplier $d\lambda$ 75
2.3.3.4. The Hencky constitutive equations 77
2.4. The governing equations for linearly elastic—perfectly plastic bodies 81
2.4.1. The linearly elastic body 82
2.4.2. The Prandtl–Reuss elasto-plastic body 83
2.4.3. The Hencky elasto-plastic body 85
2.4.4. The Lévy–v. Mises rigid-plastic body 85
2.4.5. Notes on the solution of elasto-plastic problems 86

3. VARIATIONAL PRINCIPLES 88

3.1. Introductory remarks 88
3.2. Principle of virtual work and complementary virtual work 90
3.2.1. Virtual work and complementary virtual work 91
3.2.2. Principle of virtual work 91
3.2.3. Principle of complementary virtual work 93
3.3. Variational principles of elasticity 94
3.3.1. Principle of stationary potential energy 94
3.3.2. Principle of minimum complementary energy 97
3.4. Variational principles of plasticity 99
3.4.1. General remarks 99
3.4.2. Incremental load history analysis 100
3.4.2.1. Introduction 100
3.4.2.2. Principle of minimum complementary energy rate 101
3.4.2.3. Principle of minimum potential energy rate 103
3.4.3. Limit analysis 104
3.4.3.1. General remarks 104
3.4.3.2. Theorem of constant stress 105
3.4.3.3. Static principle 106
3.4.3.4. Kinematic principle 107
3.4.3.5. Remarks 109
3.4.4. Shakedown analysis 112
3.4.4.1. Introduction 112
3.4.4.2. Static principle 114

3.4.4.3. Kinematic principle 118
3.4.4.4. Remarks 119
3.5. Discontinuity of stress and velocity fields 119
3.5.1. Discontinuity in stress field 120
3.5.2. Discontinuity in velocity field 121

4. ELASTO-PLASTIC ANALYSIS OF SOME SIMPLE PROBLEMS 123

4.1. Analysis of a simple bar structure 123
4.1.1. Elastic analysis 123
4.1.1.1. Solution by the use of field equations 124
4.1.1.2. Solution by the use of variational principles 125
4.1.2. Elasto-plastic analysis 127
4.1.2.1. Loading 127
4.1.2.2. Unloading and reloading 128
4.1.2.3. Remarks 131
4.1.3. Limit analysis 133
4.1.4. Two-parameter loading 136
4.1.4.1. Limit analysis 136
4.1.4.2. Shakedown analysis 138
4.1.5. Optimal design 140
4.2. Torsion of prismatic bars 142
4.2.1. Notations and assumptions 142
4.2.2. Basic relationships 143
4.2.2.1. Compatibility conditions 143
4.2.2.2. Equilibrium conditions 144
4.2.3. Elastic torsion 147
4.2.3.1. Analytical solution 147
4.2.3.2. Membrane analogy 148
4.2.3.3. Bar with elliptical cross-section 149
4.2.4. Elasto-plastic torsion 151
4.2.4.1. Analytical solution 151
4.2.4.2. Membrane analogy 154
4.2.4.3. Bar with circular cross-section 155
4.2.5. Fully plastic torsion 157
4.2.5.1. Analytical solution 157
4.2.5.2. Sand hill analogy 157
4.2.6. Torsion of hollow bars 158
4.2.7. Unloading 160
4.3. Thick-walled spheres and cylinders under internal pressure 162
4.3.1. Thick-walled spheres 162
4.3.1.1. Basic relationships 162

4.3.1.2. Elasto-plastic state 163
4.3.1.3. Elastic state 166
4.3.1.4. Fully plastic state 166
4.3.1.5. Displacements 166
4.3.1.6. Unloading and reloading 167
4.3.2. Thick-walled cylinders 168
4.3.2.1. Basic relationships 168
4.3.2.2. Elasto-plastic state 170
4.3.2.3. Elastic state 173
4.3.2.4. Fully plastic state 173
4.3.2.5. Displacements 174
4.3.2.6. Unloading and reloading 175

5. PLASTIC ANALYSIS OF PLANE STRAIN AND PLANE STRESS PROBLEMS 176

5.1. Basic relationships 176
5.1.1. Introduction 176
5.1.2. Governing equations of the elastic state 178
5.2. Plane plastic flow 180
5.2.1. General remarks 180
5.2.2. Stress relationships 182
5.2.3. Strain rate and velocity relationships 186
5.2.4. Shear line theory 188
5.2.4.1. Properties of shear line fields 189
5.2.4.2. Numerical and geometrical solutions 194
5.2.4.3. Approximate solutions 196
5.2.5. Applications 198
5.3. Plane stress problems 212
5.3.1. Basic relationships 212
5.3.2. Solution based on the Huber–v.Mises–Hencky yield condition 213
5.3.2.1. Basic relationships 213
5.3.2.2. Hyperbolic domain 216
5.3.2.3. Parabolic and elliptical domains 218
5.3.2.4. Determination of the velocity field 218
5.3.2.5. Lines of discontinuity 219
5.3.2.6. Extension of notched plates 219
5.3.3. Solution based on the Tresca yield condition 221
5.4. Application of the finite element method 224
5.4.1. Introductory remarks 224
5.4.2. Fundamental equations 225
5.4.3. Incremental elasto-plastic analysis 230

5.4.4. Limit analysis 233
5.4.4.1. Lower bound solution 234
5.4.4.2. Upper bound solution 234

6. PLASTIC ANALYSIS AND DESIGN OF BAR STRUCTURES 236

6.1. Introductory remarks 236
6.2. Yield conditions for bar members 238
6.2.1. General relationships 238
6.2.2. Members under combined loading 242
6.2.2.1. Bending and tension or compression 242
6.2.2.2. Bending and shear 249
6.2.2.3. Bending and torsion 251
6.2.2.4. Asymmetrical bending 252
6.2.2.5. Approximate yield conditions 255
6.2.3. Members under pure bending 256
6.2.3.1. Loading 257
6.2.3.2. Unloading, reloading, reverse loading, cyclic loading 263
6.3. Elasto-plastic analysis 264
6.3.1. Beams 264
6.3.1.1. Simply supported beams 265
6.3.1.1.1. Stress distribution 265
6.3.1.1.2. Plastic hinge 267
6.3.1.1.3. Deflections 268
6.3.1.2. Continuous beams 271
6.3.2. Frames 275
6.4. Limit analysis 277
6.4.1. Theorems of limit analysis 277
6.4.2. Applications 278
6.4.3. Distributed loading 287
6.4.4. General loading 291
6.4.4.1. Basic relationships 291
6.4.4.2. Illustrative example 294
6.4.4.3. Approximate solutions 296
6.4.5. Effect of combined internal forces 297
6.4.5.1. General remarks 297
6.4.5.2. Illustrative examples 297
6.5. Deflections 302
6.5.1. Introductory remarks 302
6.5.2. Deflections in the case of proportional loading 302

6.5.2.1. Estimate of deflections at collapse 302
6.5.2.1.1. Assumptions and basic relationships 302
6.5.2.1.2. Illustrative example 305
6.5.2.2. Permanent deflections 307
6.5.3. Deflections in the case of general loading 309
6.5.3.1. Accumulating and alternating plastic deformations 309
6.5.3.2. Shakedown analysis 311
6.5.4. Effect of deflections on the collapse load 316
6.5.4.1. Introduction 316
6.5.4.2. Non-linear elasto-plastic analysis of frames 318
6.6. Plastic design 321
6.6.1. Basic principles 321
6.6.2. Optimal plastic design 323
6.6.2.1. Introduction 323
6.6.2.2. Minimum weight design 323
6.6.2.3. Structures with piece-wise variable plastic moments 325
6.6.2.4. Structures with continuously variable plastic moments 333
6.6.2.4.1. Constrained minimum weight design 333
6.6.2.4.2. Unconstrained minimum weight design 335
6.6.3. Plastic design of structures under general loading 341
6.7. Application of mathematical programming 342
6.7.1. Introduction 342
6.7.2. Formulation of linear and quadratic programming 342
6.7.3. Governing equations of elasto-plastic discretized bar structures 344
6.7.4. Incremental elasto-plastic analysis 346
6.7.5. Limit analysis 347
6.7.6. Shakedown analysis 348
6.7.7. Minimum weight design 349

7. PLASTIC ANALYSIS AND DESIGN OF PLATES AND SHELLS 350

7.1. Assumptions 350
7.2. Limit analysis of plates 351
7.2.1. Governing equations 351
7.2.1.1. Kinematic equations 351
7.2.1.2. Equilibrium equations 352
7.2.1.3. Yield conditions 354

7.2.1.4. Constitutive equations 356
7.2.1.5. Dissipation function 357
7.2.1.6. Basic concepts of analysis 357
7.2.2. Axially symmetrically loaded circular plates 358
7.2.2.1. Governing equations 358
7.2.2.2. Simply supported circular plate under uniform load 359
7.2.2.3. Clamped circular plate under uniform load 360
7.2.2.4. Circular plates on plastic subgrade 363
7.2.3. Rectangular plates 366
7.2.3.1. Lower bound solution 367
7.2.3.2. Upper bound solution 368
7.2.4. Yield-line theory of reinforced concrete plates 370
7.3. Limit analysis of shells 371
7.3.1. Circular cylindrical shells 371
7.3.1.1. Governing equations 371
7.3.1.2. Clamped cylindrical shell under uniform radial pressure 378
7.3.2. Circular conical shells 382
7.3.2.1. Governing equations 382
7.3.2.2. Clamped conical shell under uniform pressure 386
7.3.3. Shallow reinforced concrete shell 390
7.4. Optimal design of plates and shells 393
7.4.1. Fundamentals 393
7.4.2. Applications 399
7.4.2.1. Circular sandwich plate 399
7.4.2.2. Reinforced concrete plates 402
7.4.2.3. Axisymmetric reinforced concrete shells 403

8. VARIOUS INELASTIC MATERIAL PROPERTIES 407

8.1. Introductory remarks 407
8.2. Plastic hardening materials 408
8.2.1. Fundamental relationships 408
8.2.2. Plastic hardening theories 410
8.2.2.1. Uniaxial state of stress 410
8.2.2.2. Isotropic hardening 411
8.2.2.3. Kinematic hardening 412
8.2.2.4. Generalized hardening rules 414
8.3. Granular materials 415
8.3.1. Yield conditions 415
8.3.1.1. Coulomb yield condition 415

8.3.1.2. The generalized Huber–v.Mises–Hencky and Tresca yield conditions 417
8.3.1.3. Stassi D'Alia yield condition 418
8.3.2. Flow rule 420
8.3.3. Plane strain problem 421
8.4. Viscous materials 423
8.4.1. Viscous properties of materials 423
8.4.2. Visco-elastic materials 427
8.4.3. Visco-plastic materials 435

9. DYNAMIC RESPONSE OF PLASTIC STRUCTURES 440

9.1. Introduction 440
9.2. Fundamental relationships 442
9.3. Simple rigid-plastic theory 444
9.3.1. General relationships 444
9.3.2. Solutions to simple problems 444
9.3.2.1. One-degree-of-freedom model 444
9.3.2.2. Two-degree-of-freedom model 448
9.3.3. Time history analysis 455
9.3.3.1. General remarks 455
9.3.3.2. Kinematic principle 456
9.3.3.3. Dynamic principle 456
9.3.4. Mode approximation 457
9.3.4.1. Basic concepts 457
9.3.4.2. Solution technique 457
9.3.4.3. Example 458
9.3.5. Kinematic approximation 460
9.3.5.1. Basic concepts 460
9.3.5.2. Response time and final displacements 460
9.3.5.3. Example 461
9.3.6. Bounding theorems 464
9.3.7. Optimal design 464
9.3.7.1. Basic concepts 464
9.3.7.2. Example 465
9.4. Effect of strain rate sensitivity 468
9.4.1. Constitutive law 467
9.4.2. Linearization of the constitutive law 469
9.4.3. Mode approximation 470
9.4.4. Kinematic approximation 470
9.5. Effect of large displacements 471
9.5.1. Mode approximation 471

9.5.2. Kinematic approximation 472
9.5.3. Bounding theorem 473
9.5.4. Example 473
9.6. Effect of elastic deformations 476
9.6.1. General remarks 476
9.6.2. Mode approximation 476
9.6.3. Kinematic approximation 476
9.7. Applications 479
9.7.1. Circular plate 479
9.7.2. Shallow spherical shell 482
9.7.3. Thick-walled tube 483
9.7.3.1. Dynamic analysis 483
9.7.3.2. Optimal design 486
9.8. Concluding remarks 488

REFERENCES 489

SUBJECT INDEX 503

1. BASIC CONCEPTS AND NOTATIONS

In this introductory chapter, the mechanical properties of materials will be briefly discussed. We will then describe the time- and temperature-independent elastic and plastic material models and discuss in more detail the behaviour of linearly elastic–perfectly plastic materials in simple tension and compression.

Next, a brief survey of the historical development of the theory of plasticity and limit analysis will be presented.

Finally, we will review the Cartesian tensor notation and present the notations to be used most frequently in this book.

1.1. THE MECHANICAL PROPERTIES OF MATERIALS

(1) The response of solids and structures to external agencies largely depends upon the mechanical properties of their materials. The actual mechanical behaviour of materials is, however, very complex, therefore, in order to facilitate the study of problems, several idealizations and simplifications have to be introduced.

In engineering mechanics it is a generally used idealization that the atomic and molecular structure of matter can be disregarded and that matter can be considered a *continuum* without gaps or empty spaces. The state variables of a continuum are described by continuous functions of the coordinates.

Another simplification connected with the continuum approach is the *phenomenological description* of material's properties. Hence, in the description of a material's behaviour, changes (deformations, dislocations etc.) in the crystal structure of the material under the action of mechanical agencies are also disregarded (Hult 1966; Polukhin, Gorelik, Vorontsov 1983) and the mechanical properties of the material are characterized by *material models* based on the observation of simple experiments (tension, compression, torsion etc.).

Because of the complexity of material behaviour a great number of material models can be developed. Each model, however, describes only one or a few properties. The selection of the most suitable model to be used depends on the material under consideration, the nature of the problem to be solved, the accuracy required and the computational facilities available.

In this book the *continuum approach* and the *phenomenological models* of materials will be used. In addition, we will assume that the continuum (body or structure) is *homogeneous and isotropic*, i.e. that the material's parameters are independent of the coordinates and the directions of the stresses and strains. It will also be assumed that the *displacements and deformations are small*, and therefore the relationships will be referred to coordinates prior to deformation (Lagrangian formulation).

Only problems where the change of temperature is negligibly small, and therefore its effect on the material's properties can be disregarded, will be treated; that is to say, we will assume that the material is *temperature-independent*.

The dynamic response of a material depends, among other things, upon the magnitude of the strain rate. In addition, strain may increase under constant stress *(creep)* and stress may decrease under constant strain *(relaxation)*. These *time-dependent* phenomena are those of *viscosity*. In certain materials (e.g. plastics, concrete) and at high strain rates and elevated temperatures, viscous effects may play an important role.

The discussion of the theory of viscosity is beyond the scope of this book; in the constitutive equations and in the solution of problems, viscous properties will therefore be disregarded and it will be assumed that the material is *time-independent*. In the last part of the book, however, the most important models and constitutive equations of viscous materials will be briefly discussed and their application to some dynamic problems will also be presented.

(2) The basic experiment in which the simplest but most characteristic mechanical properties of a material are studied is a standard *tension test*. By measuring the applied force and the elongation of the tensile specimen during the loading process, and assuming homogeneous states of stress and strain in the observed part of the specimen, a stress–strain relationship is obtained and may be plotted in a *stress–strain diagram*. By considering the characteristics of the diagrams of structural materials and disregarding the temperature and strain rate effects, three different types of material can be distinguished.

(a) *Elastic materials* follow the same stress–strain relationship during both the loading and the unloading processes (Fig. 1—1(a)). Hence, after unloading, no permanent strain remains and the strain energy stored in the specimen during the loading procedure is fully recovered. An elastic material is *reversible*, *non-dissipative* and *time-independent* under isothermal conditions. Depending on the shape of the stress–strain diagram *linear and nonlinear elastic materials* can be distinguished.

(b) In the case of *plastic materials*, the loading and unloading processes are described by different relationships and therefore we no longer have a one-to-one correspondence between stress and strain (Fig. 1—1(b)). Hence, after unloading, permanent strain remains and the strain energy stored during the loading procedure is partly or fully dissipated and transformed into heat. The plastic material is *irreversible*, *dissipative* and *time-independent* under isothermal conditions.*

* In the terminology of the theory of plasticity time independence of material properties is understood despite the frequent use of terms such as "strain rate" and "velocity". Time always enters homogeneously in all equations of statics. A given loading path produces the same deformation regardless of the variation in time of the loading.

(c) Most materials under lower stresses behave elastically but under higher stresses undergo plastic deformation. These are called *elasto-plastic materials.* For most elasto-plastic materials, the definition of the elastic and plastic ranges is a matter of convention since the transition from elastic to plastic behaviour is gradual. There are, however, some materials (e.g. mild steel, bronze) which at a well defined stress σ_0, called the *yield stress*, exhibit a sudden transition from elastic to plastic behaviour (Fig. 1—1(c)).

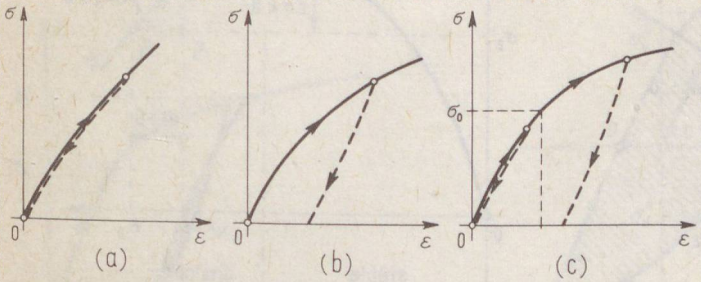


Fig. 1–1

(3) On the basis of energetical considerations D. C. Drucker elaborated *phenomenological postulates* according to which two types of material can be distinguished: *stable and unstable materials* (Drucker 1949, 1952a, 1959).

Let us consider the state of stress and strain of a point within a body under prescribed external loads, and assume that under isothermal conditions some external agency statically applies and removes additional stress and strain increments. *Then the network* $\mathrm{d}W_0$ *performed by these increments during the entire cycle of loading and unloading is non-negative:* $\mathrm{d}W_0 \geq 0$. This postulate follows from the 2nd Law of Thermodynamics, expressing the fact, that during a loading and unloading process no mechanical energy can be extracted from a body.

Now consider the work $\mathrm{d}W_1$ done by the stress and strain increments during the *loading process.* A material is described as *stable* if $\mathrm{d}W_0 \geq 0$ and $\mathrm{d}W_1 \geq 0$; otherwise it is *unstable.*

In the case of a *uniaxial state of stress* this *stability postulate* can be illustrated in the stress–strain diagram shown in Fig. 1—2(a). The point P_1 in the diagram and the corresponding stress σ_1 and strain ε_1 represent the initial state. Now the external agency moves the point P_1 to P_2 and the stress and strain will change from σ_1 to σ_2 and from ε_1 to ε_2, respectively. The corresponding increments are $\mathrm{d}\sigma = \sigma_2 - \sigma_1$ and $\mathrm{d}\varepsilon = \varepsilon_2 - \varepsilon_1$ and the work done during the loading process is $\mathrm{d}W_1 \approx 0.5\,\mathrm{d}\sigma\,\mathrm{d}\varepsilon$. The latter is identical with the area of the triangle $P_1 P_2 P_3$. In the stress–strain diagram of Fig. 1—2(a) $\mathrm{d}\sigma > 0$ and $\mathrm{d}\varepsilon > 0$, and consequently the energy increment $\mathrm{d}W_1 > 0$. It means, that in this range the behaviour of the corresponding material is *stable.*

During unloading the stress regains its initial magnitude σ_1. The strain, however, does not generally regain its initial value but changes from ε_2 to ε_3. Hence, after unloading the state of the material is represented by the point P_4 in Fig. 1—2(a). The work done during unloading is $\mathrm{d}W_2 \approx 0.5\,\mathrm{d}\sigma\,\mathrm{d}\varepsilon'$, where $\mathrm{d}\varepsilon' = \varepsilon_2 - \varepsilon_3$, and the work

performed during the entire cycle of loading and unloading is $dW_0 = dW_1 - dW_2 \approx$ $\approx 0.5\, d\sigma\, d\varepsilon''$, where $d\varepsilon'' = \varepsilon_3 - \varepsilon_1$. This work, represented by the area of the lined triangle $P_1 P_2 P_4$, is dissipated and transformed into heat. Since dW_0 cannot be negative, ε_3 must be greater than or at least equal to ε_1.

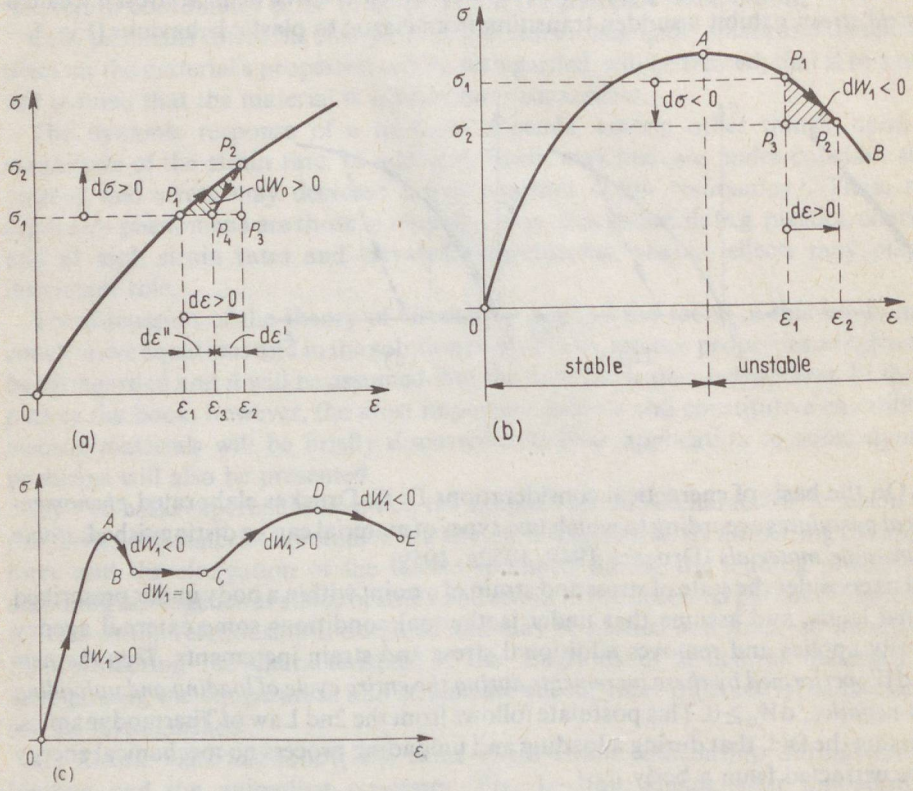


Fig. 1–2

The stress–strain diagram of Fig. 1—2(b) has a decreasing part where $d\sigma = \sigma_2 - \sigma_1 < 0$ and $d\varepsilon = \varepsilon_2 - \varepsilon_1 > 0$ consequently, $dW_1 \approx 0.5\, d\sigma\, d\varepsilon < 0$. It means that in the range represented by the line *A–B* of the diagram the behaviour of the corresponding material is *unstable*.

We can conclude that a material with a monotonically increasing stress–strain curve is stable, but that if the curve has a decreasing part then the behaviour of the material is unstable in that range.

Figure 1—2(c) illustrates the idealized stress–strain diagram of mild steel. The behaviour of mild steel in the ranges *O–A* and *C–D* is *stable* ($dW_1 \geq 0$) and in the ranges *A–B* and *D–E* is *unstable* ($dW_1 < 0$).

As will be seen in Chapters 2 and 3 in the theory of plasticity the constitutive equations and variational theorems are based on the assumption of stable materials. Thus, materials with decreasing stress–strain curves are ruled out from the classical theory of plasticity.

Finally, we note that in the case of nonisothermal processes the stability postulate has to be modified.

(4) In the case of plastic materials, the problem of *repeated loading and unloading* plays an important role and therefore we will now discuss it in more detail.

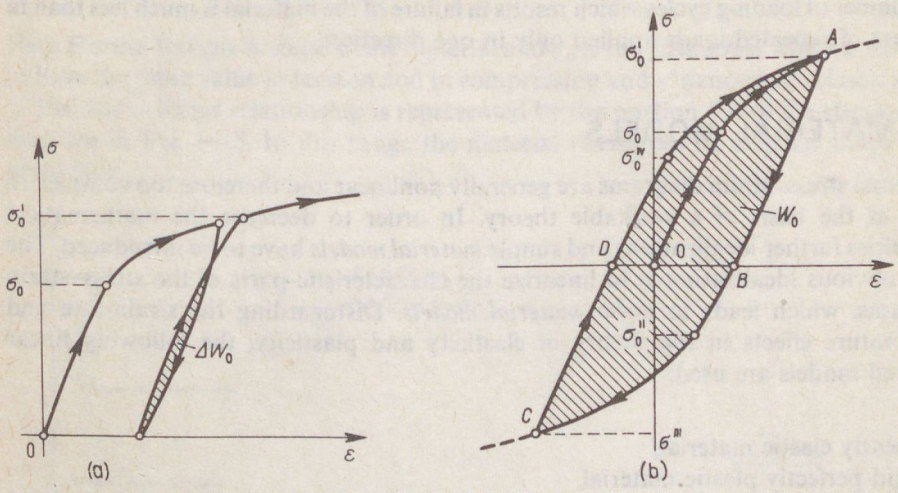


Fig. 1–3

When a tension specimen is subjected to a stress exceeding the limit σ_0 and then unloaded, the slope of the stress–strain diagram for unloading is approximately the same as at the beginning of the first loading (Fig. 1—3(a)). When the specimen is reloaded, the stress–strain diagram does not exactly follow the stress–strain diagram for unloading. The lines corresponding to unloading and reloading form a narrow *elastic hysteresis loop* whose area ΔW_0 is the mechanical energy dissipated during the unloading and reloading process. The stress–strain curve for reloading will nearly pass through the point where the last but one reversal of the sense of deformation occurred. During reloading, before reaching the stress σ_0^{I} corresponding to this point the specimen undergoes only elastic deformations. Thereafter, the stress–strain diagram corresponding to the further loading continues as if the loop had never been formed and in this range plastic deformations occur. Hence, during this loading process the yield stress of the material has been increased from σ_0 to σ_0^{I}.

Next, let us assume that after the removal of the tensile force the specimen is reloaded in the opposite direction (Fig. 1—3(b)). The specimen starts to yield in compression at the stress σ_0^{II} which is less than the initial yield stress σ_0 by approximately the same amount as σ_0^{I} is greater than σ_0. Hence, the yield stress in compression decreases at the same rate as it grows in tension. Thus, we can write $|\sigma_0|-|\sigma_0^{\mathrm{II}}|\approx|\sigma_0^{\mathrm{I}}|-|\sigma_0|$, from which it follows that $|\sigma_0^{\mathrm{I}}|+|\sigma_0^{\mathrm{II}}|\approx 2\sigma_0$.

Now, let us assume that reaching the compressive stress σ_0^{III} the specimen is unloaded and reloaded again in tension. The specimen starts to yield at the stress σ^{IV} which approximately fulfills the relationship $|\sigma_0^{\mathrm{III}}|+|\sigma_0^{\mathrm{IV}}|\approx 2\sigma_0$.

The phenomenon described above is called the *Baushinger effect*. The line corresponding to the complete loading, unloading and reloading cycle forms a *plastic*

hysteresis loop the area W_0 of which gives the mechanical energy dissipated by the specimen during the alternating loading cycle. This dissipated energy is much larger than the energy dissipated during a simple loading and unloading process in tension or in compression (see Fig. 1—3(a)). This is the reason why if alternating loads are applied, the number of loading cycles which results in failure of the material is much less than in the case of repeated loads applied only in one direction.

1.2. MATERIAL MODELS

(1) Actual stress–strain diagrams are generally nonlinear and therefore too complex to serve as the basis of a workable theory. In order to decrease the mathematical difficulties further idealizations and simple *material models* have to be introduced. The most obvious idealization is to linearize the characteristic parts of the stress–strain diagrams, which leads to *linear material models.* Disregarding the strain-rate and temperature effects in the theory of elasticity and plasticity, the following linear material models are used:

(a) linearly elastic material,
(b) rigid-perfectly plastic material,
(c) rigid-plastic hardening material,
(d) linearly elastic–perfectly plastic material,
(e) linearly elastic–plastic hardening material.

The corresponding stress–strain diagrams are shown in Fig. 1—4. Here σ_0 designates the *yield stress* of the material. In tension and in compression the behaviour of the material is assumed to be identical. The unloading and reloading process is also described by straight lines the slopes of which have the same value as that of the initial line.

The behaviour of linearly elastic and rigid-perfectly plastic materials can be illustrated by a spring and a block resting on a rough surface, respectively (see Figs 1—4(a) and 1—4(b)). In these *mechanical models* the force acting on the spring and on the block represents the stress; the elongation of the spring and the displacement of the block, respectively, correspond to the strain. The elongation of the spring is proportional to the acting force corresponding to the linear stress–strain relationship. The block remains in standstill until the force becomes large enough to overcome the frictional force between the block and the rough surface. Then, with a constant force, the block will keep moving. If the force decreases, the block stops in its new position. It is obvious that this mechanical model exactly describes the behaviour of rigid-perfectly plastic materials.

Figure 1—4 shows that by series and parallel connections of the above simple models the mechanical models of elasto-plastic and plastic hardening materials can be constructed.

(2) The classical theory of plasticity with which this book is concerned assumes a *linearly elastic–perfectly plastic material.* We will now discuss the properties of this material in more detail.

(a) Assuming that no initial stresses are present, for sufficiently small values of stress the material behaves elastically. Hence, to this state Hooke's Law applies

$$\text{if } |\sigma| < \sigma_0, \quad \text{then} \quad \varepsilon^e = \frac{\sigma}{E}. \tag{1—1}$$

Here E is the *Young's modulus* of the material and σ_0 is the *yield stress* which is assumed to have the same value in tension and in compression and ε^e denotes the elastic strain.

The above linear relationship is represented by the portion OA of the stress–strain diagram in Fig. 1—5. In this range the material reassumes its original shape upon unloading.

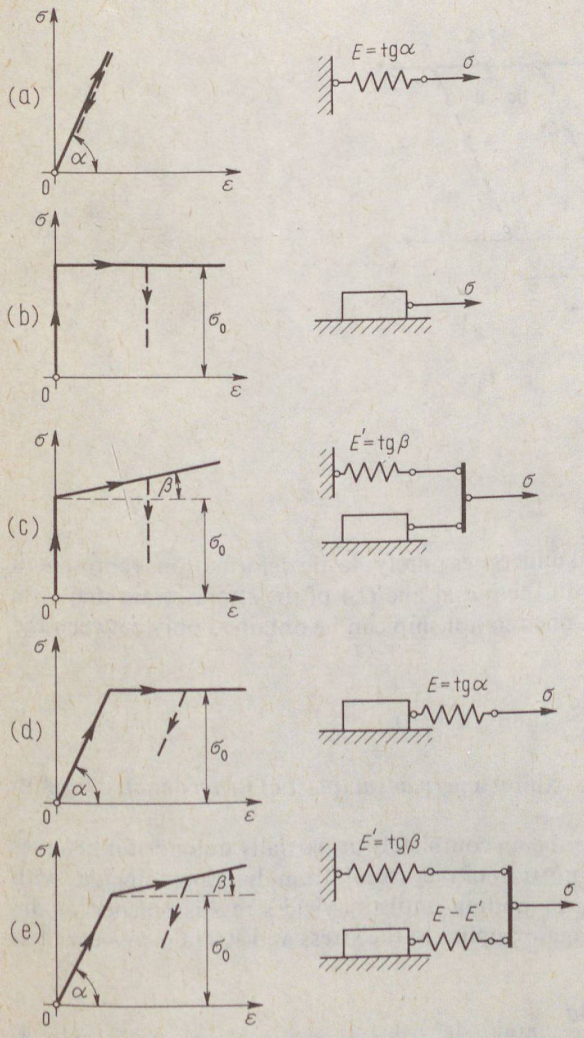


Fig. 1–4

(b) Once the stress reaches the yield stress, i.e. $|\sigma| = \sigma_0$, and is maintained there, the material might *flow plastically without limits* (exhibits unrestricted plastic flow) under the constant stress σ_0. During this flow the stress increment $d\sigma$ must be zero and we no longer have a one-to-one relationship between stress and strain. The only statement which can be made is that the sign of the *plastic strain increment* $d\varepsilon^p$ must be equal to the sign of the stress. Thus,

$$\text{if } \left\{ \begin{matrix} |\sigma| = \sigma_0 \\ \text{and } d\sigma = 0, \end{matrix} \right\} \quad \text{then} \quad \sigma d\varepsilon^p \geq 0. \tag{1—2}$$

The plastic flow under constant stress is represented by the line AB of the diagram in Fig. 1—5.

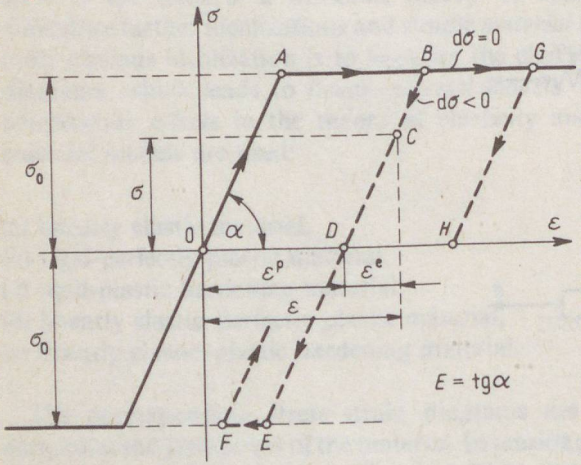


Fig. 1–5

(c) During *unloading* the material undergoes purely elastic deformations represented by the straight line BD parallel with the initial line OA of the stress–strain diagram. Hence, during unloading a one-to-one relationship can be obtained only between the *increments* in stress and strain

$$\text{if } \left\{ \begin{matrix} |\sigma| \leq \sigma_0 \\ \text{and } \sigma d\sigma < 0, \end{matrix} \right\} \quad \text{then} \quad d\varepsilon^e = \frac{d\sigma}{E} \quad \text{and} \quad d\varepsilon^p = 0. \tag{1—3}$$

After unloading the material will exhibit a *permanent* (plastic) *strain* denoted by ε^p in Fig. 1—5.

(d) If the material is *reloaded* after being completely or partially unloaded it behaves elastically, and the corresponding portion of the stress–strain diagram coincides with the straight line for the preceding unloading until the yield stress is reached again. Hence, in this state Hooke's Law again applies to the stress and strain *increments* and we can write

$$\text{if } \left\{ \begin{matrix} |\sigma| < \sigma_0 \\ \text{and } \sigma d\sigma > 0, \end{matrix} \right\} \quad \text{then} \quad d\varepsilon^e = \frac{d\sigma}{E} \quad \text{and} \quad d\varepsilon^p = 0. \tag{1—4}$$

On reaching the yield stress during reloading, the material starts to flow plastically again as if the unloading and reloading had never taken place. Hence, eq. (1—2) applies to this state, too.

The above statements are also valid for the case where the material is completely unloaded and then *reloaded in the reverse sense*. This is indicated by the portion *DEF* of the diagram in Fig. 1—5.

(e) During an *arbitrary loading process* only points in the infinite strip bounded by the parallels *AG* and *EF* can be reached. At a typical point *C* in this strip, corresponding to the stress σ the total strain may be considered as the sum of the *elastic strain* ε^e and the *plastic strain* ε^p

$$\varepsilon = \varepsilon^e + \varepsilon^p = \frac{\sigma}{E} + \varepsilon^p. \tag{1—5}$$

Here ε^e is the strain which vanishes and ε^p is the permanent strain which remains after complete unloading. The first can be uniquely determined by Hooke's Law while the second is obtained by the integration of the plastic strain increments $d\varepsilon^p$ occurring during the preceding loading process: $\varepsilon^p = \int d\varepsilon^p$. Hence, *the permanent strains depend on the load path.** For example, if the load paths are defined by the lines *O–A–B–D* and *O–A–G–H* in the diagram in Fig. 1—5 then the permanent strains are equal to the lengths *OD* and *OH*, respectively. This is the reason why in the theory of plasticity no one-to-one relationships can be constructed between the stress and the *total* strain. Only *incremental stress–strain relationships* are used, and in order to determine the total stresses and strains one has to take the complete loading process into consideration.

The model of the linearly elastic–perfectly plastic material constitutes a far-reaching idealization of the actual mechanical behaviour of typical structural materials. Nevertheless, this model appears adequate for the treatment of a great number of engineering problems and provides important and reliable information about the behaviour of structures beyond the elastic limit. There are, however, some problems where plastic hardening of the material cannot be neglected (e.g. the analysis of metal-forming processes) while there are others (e.g. plastic limit analysis of structures) where elastic deformations can be disregarded. Again, in some problems (e.g. analysis of structures subjected to short-time dynamic loading or to elevated temperatures) the strain rate and temperature effects have to be taken into consideration. These special problems will be discussed in Chapters 8 and 9.

(3) The actual behaviour of materials can be more accurately approximated by the use of *nonlinear stress–strain diagrams*. If it is assumed that for loading and unloading the same relationship exists, the corresponding material is called *nonlinearly elastic*. On the other hand, if the stress–strain curves for loading and unloading are different the material is called *nonlinearly elasto-plastic*. In the case of a uniaxial state of stress, the use of nonlinear stress–strain relationships is relatively simple; but in problems where the state of stress is bi- or triaxial there are serious computational difficulties, and therefore only numerical solutions can be achieved.

* Note, that the linearly elastic–perfectly plastic material itself is *path-independent* since its material constants (E and σ_0) do not depend on the loading process.

To illustrate this two nonlinear stress–strain relationships will now be briefly discussed.

The stress–strain diagram in Fig. 1—6(a) is defined by the function

$$\varepsilon = C\sigma^n, \tag{1—6}$$

where C and $n \geq 1$ are constants. By appropriate choices for their values, the stress–strain curve can be fitted to the actual stress–strain diagram.

Ramberg and Osgood (1943) proposed the following stress–strain relationship

$$\frac{\varepsilon}{\varepsilon_1} = \frac{\sigma}{\sigma_1} + \frac{3}{7}\left(\frac{\sigma}{\sigma_1}\right)^n, \tag{1—7}$$

where ε_1, σ_1 and $n \geqq 1$ also denote appropriately chosen constants. Figure 1—6(b) shows the corresponding stress–strain curves for different values of n. The cases $n = 1$ and $n \to \infty$ correspond to the stress–strain diagrams for linearly elastic and linearly elastic–perfectly plastic materials, respectively.

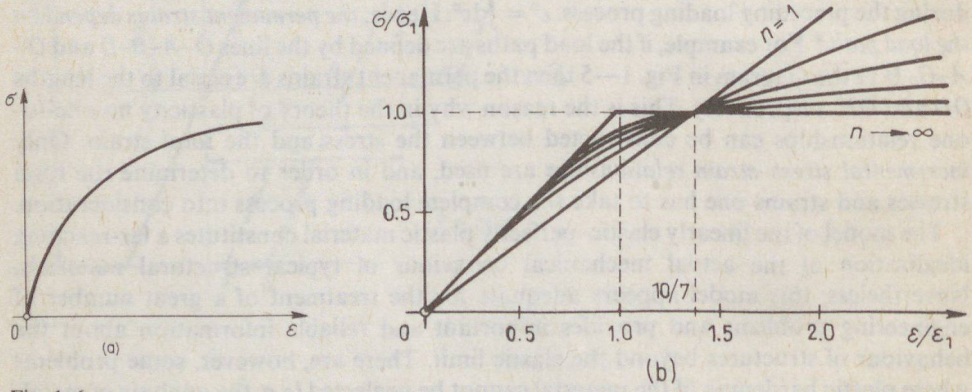


Fig. 1–6

1.3. HISTORICAL REMARKS

We will now make a brief survey of the historical development of the *theory of plasticity* and *limit analysis*.

(1) Plastic behaviour and the failure of soil and other materials were first investigated by Galilei (1638) and Coulomb (1773). The results were applied to the analysis of retaining walls by Coulomb (1773), Poncelet and Rankine (1859) and Tresca (1864) investigated the conditions for plastic flow of metals, and developed a theory according to which plastic flow occurs when the maximum shear stress reaches a critical value. On the basis of this yield condition, Saint-Venant (1870) proposed the first constitutive equation for plastic materials in plane strain, in which the stress was related to the strain increment. These relationships were generalized by Lévy (1870) for triaxial problems.

At the end of the last century Guest studied metal tubes subjected to internal pressure and tension and verified the Tresca yield condition experimentally. Later, Huber (1904), v. Mises (1913) and Hencky (1924) independently proposed another yield condition. In 1925 Prandtl, using this Huber–v. Mises–Hencky yield condition, developed a constitutive equation for plane problems of perfectly plastic materials; this was generalized by Reuss (1930) for triaxial states of stress. These Prandtl–Reuss constitutive equations form the basis of the *incremental or flow theory of plasticity*. Hencky (1924) had previously proposed an other theory in which stresses were related to strains rather than to strain increments. He had thus established the basis of the *deformation theory of plasticity* which was later developed and applied to numerous problems by Ilyushin and Lenski (1948, 1959, 1967). In 1923 Hencky had also carried out other pioneering work in the *theory of shear lines* of plane plastic problems. His theorems and results were further developed and used by Geiringer (1930). In 1925 Kármán applied the theory of plasticity to the analysis of metal-forming processes. Further progress was made in this field by Sachs (1927) and Siebel (1931).

The first comprehensive book on plasticity was written by Nádai in 1927. After World War II several monographs were published which, even today, form a very important source of the theory of plasticity (Ilyushin 1948; Freudenthal 1950; Nádai 1950; Sokolovski 1950; Prager, Hodge 1951; Hoffman, Sachs 1953).

(2) The earliest example of the application of the concepts of *limit analysis* can be found in Galileo's *Discorsi* (1638). Galieo considered the failure of a cantilever beam, and essentially used the kinematic method of limit analysis to determine the collapse load (Fig. 1—7). The design of masonry vaults and domes provides further examples of early forms of limit analysis. De La Hire (1695; 1712) investigated circular voussoir arches of constant thickness. His analysis may be as an attempt to construct statically admissible stress fields in order to determine the collapse load. Coulomb (1773) and later Lamé and Clapeyron (1823) also investigated the failure of stone and masonry arches and domes and derived rules and simple methods for the design of this type of structures.

Other early examples of limit analysis are found in soil mechanics. Here again Coulomb (1773) developed a simple method for the calculation of the pressure acting on a retaining wall. Following his work Poncelet (1840), Moseley (1843), Rankine (1859), Rebhann (1871), Kötter (1899) and Massan (1899) elaborated several graphical and mathematical methods for the determination of soil pressure which were also based on the application of the concepts of limit analysis.

The application of limit analysis to structures other than arches and domes started with the attempt to predict the collapse loads of steel structures. In 1914 Kazinczy concluded from his experiments on clamped steel beams that the theory of elasticity could not provide a realistic estimate the load-carrying capacity (Kazinczy 1914). He introduced the concept of *plastic hinges* and developed several principles and methods which even today are valid and used in engineering practice (Kazinczy 1933, 1942). Kazinczy's early work failed to receive the attention it merited, partly because it was written in Hungarian and partly because of the war. Hence, a few years later Kist (1917) independently presented similar ideas. Taking plastic behaviour of the material into account, Maier–Leibnitz (1928) carried out experiments with continuous steel beams and Ingerslev (1921) and Johansen (1932) investigated the plastic behaviour of

reinforced concrete slabs. The *yield-line theory*, developed on the basis of these results, is widely used in engineering practice even today (see e.g. Wood 1961; Johansen 1962; Sawczuk, Jaeger 1963; Kaliszky 1967).

The problem of accumulating plastic deformations was first investigated by Grüning (1926). Girkmann (1931) and Bleich (1932) dealt with the load-carrying capacity of steel frames. This work was continued by Baker (1936) who carried out intensive experimental and theoretical investigations, and published the first book on plastic analysis of steel frames (Baker, Horne and Heyman 1956).

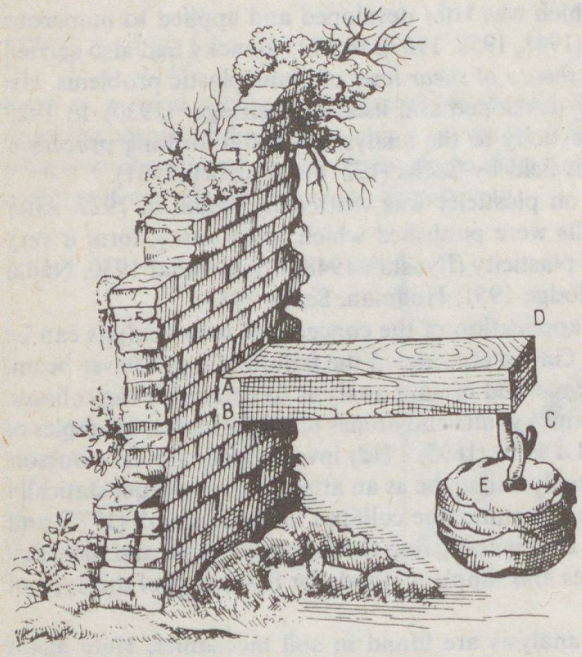


Fig. 1–7

The upper and lower bound theorems of limit analysis were first established—for frames and plates—by Gvozdev (1936) and later Feinberg (1948). Like Kazinczy's work Gvozdev's results did not attract attention because of the war. Thus, these theorems were independently derived for continua by Greenberg, Prager and Durcker (1951, 1952b). Once the fundamental principles were clearly understood, the field of application of limit analysis expanded rapidly and was extended to such problems as optimal design and shakedown analysis.*

Today, the theory of plasticity and limit analysis is an important and developing part of solid mechanics which, at the same time, provides an efficient and reliable method of solving many engineering problems.

* More detailed surveys of the historical development of the theory of plasticity and limit analysis are found elsewhere (Ziegler 1972; Prager 1974.)

1.4. NOTATIONS

(1) Since continuum mechanics involves a number of second-order tensors, such as stress and strain tensors, the use of *Cartesian tensor notation* is convenient and efficient. In this book we will use both scalar notation and tensor notation; the fundamental equations and theorems will be presented by making use of both notations while particular problems will be solved using only the scalar notation. For convenience, in the discussion of discrete systems vector and matrix notations will also be used.

The essential simplifications in Cartesian tensor notation are achieved by the systematic use of *letter subscripts* and the adoption of the *summation convention.*

(a) In tensor notation whenever a small *letter subscript* occurs in a term it is understood to take on the values 1, 2, 3. The rectangular Cartesian coordinates are denoted by x_1, x_2, x_3 or briefly by x_i instead of x, y, z.* Hence, a_i for example stands for a *vector* with the components a_1, a_2, a_3.

(b) Whenever the same small letter subscript appears *twice* in a single term, it is understood to represent a summation over the range of 1, 2, 3. This is the *summation convention.* Hence, a *scalar product* of the vectors a_i and b_i is written as

$$a_i b_i = a_1 b_1 + a_2 b_2 + a_3 b_3.$$

(c) The *linear transformation* of the vector a_i is expressed as

$$c_{11}a_1 + c_{12}a_2 + c_{13}a_3 = b_1,$$

$$c_{21}a_1 + c_{22}a_2 + c_{23}a_3 = b_2,$$

$$c_{31}a_1 + c_{32}a_2 + c_{33}a_3 = b_3,$$

which leads to the concept of the *second-order tensor* c_{ij}. The *matrix* of this tensor is

$$c_{ij} = \begin{pmatrix} c_{11} & c_{12} & c_{13} \\ c_{21} & c_{22} & c_{23} \\ c_{31} & c_{32} & c_{33} \end{pmatrix}.$$

The above linear transformation can now be written in the form

$$c_{ij}a_j = b_i.$$

Here $j = 1, 2, 3$ is the *summation subscript* and $i = 1, 2, 3$ is the *free subscript.*

In the following the *stress tensor* and the *strain tensor* will be denoted by σ_{ij} and ε_{ij}, respectively. The matrices of these tensors are as follows

$$\sigma_{ij} = \begin{pmatrix} \sigma_{11} & \sigma_{12} & \sigma_{13} \\ \sigma_{21} & \sigma_{22} & \sigma_{23} \\ \sigma_{31} & \sigma_{32} & \sigma_{33} \end{pmatrix} = \begin{pmatrix} \sigma_{xx} & \sigma_{xy} & \sigma_{xz} \\ \sigma_{yx} & \sigma_{yy} & \sigma_{yz} \\ \sigma_{zx} & \sigma_{zy} & \sigma_{zz} \end{pmatrix},$$

* In two-dimensional problems, of course, the subscript takes on only the values 1 and 2.

$$\varepsilon_{ij}=\begin{pmatrix}\varepsilon_{11} & \varepsilon_{12} & \varepsilon_{13}\\ \varepsilon_{21} & \varepsilon_{22} & \varepsilon_{23}\\ \varepsilon_{31} & \varepsilon_{32} & \varepsilon_{33}\end{pmatrix}=\begin{pmatrix}\varepsilon_{xx} & \varepsilon_{xy} & \varepsilon_{xz}\\ \varepsilon_{yx} & \varepsilon_{yy} & \varepsilon_{yz}\\ \varepsilon_{zx} & \varepsilon_{zy} & \varepsilon_{zz}\end{pmatrix}.$$

In this notation the shear stresses and shear strains are denoted by σ and ε instead of τ and $\frac{1}{2}\gamma$, respectively.

In the following we shall need the *unit tensor* also called *Kronecker delta*

$$\delta_{ij}=\begin{pmatrix}1 & 0 & 0\\ 0 & 1 & 0\\ 0 & 0 & 1\end{pmatrix} \text{ or } \delta_{ij}=\begin{cases}1, & \text{if } i=j,\\ 0, & \text{if } i\neq j.\end{cases}$$

(d) The summation convention is generalized for *double summation*. Then, the *inner product* of the tensors a_{ij} and b_{ij} which results in a *scalar* c is expressed in the form

$$a_{ij}b_{ij}=\sum_{i=1}^{3}\sum_{j=1}^{3}a_{ij}b_{ij}=c,$$

and the *outer product* of the tensors a_{ij} and b_{ij} which results in a *fourth-order tensor*,* is written as

$$a_{ij}b_{kl}=d_{ijkl}.$$

A fourth-order tensor d_{ijkl} defines the linear transformation of a second-order tensor a_{ij}

$$d_{ijkl}a_{kl}=b_{ij}.$$

A summation such as

$$\sigma_{ii}=\sigma_{11}+\sigma_{22}+\sigma_{33}$$

results in a scalar.

(e) Considering a *scalar function* $\lambda(x_i)$ and a *vector function* $\phi_i(x_j)$ and introducing the *vector operator*

$$\nabla_i=\frac{\partial}{\partial x_1}\mathbf{e}_1+\frac{\partial}{\partial x_2}\mathbf{e}_2+\frac{\partial}{\partial x_3}\mathbf{e}_3$$

the *gradient* of the scalar function and the *divergence* of the vector function can be written as

$$\nabla_i\lambda=\frac{\partial\lambda}{\partial x_1}\mathbf{e}_1+\frac{\partial\lambda}{\partial x_2}\mathbf{e}_2+\frac{\partial\lambda}{\partial x_3}\mathbf{e}_3$$

* In three-dimensional space a tensor of N-th order has 3^N components.

and

$$\nabla_i \phi_i = \frac{\partial \phi_1}{\partial x_1} + \frac{\partial \phi_2}{\partial x_2} + \frac{\partial \phi_3}{\partial x_3},$$

respectively. Here $\mathbf{e}_1$, $\mathbf{e}_2$ and $\mathbf{e}_3$ denote the unit vectors in the directions of the coordinate axes.

To simplify our notations, in addition to the summation convention we introduce the *differential convention*. Accordingly, whenever a letter subscript occurs in a single term following a *comma*, it is understood to differentiate with respect to the corresponding coordinates i.e.

$$,_i = \frac{\partial}{\partial x_i}.$$

Hence, for example

$$\lambda_{,i} = \nabla_i \lambda = \frac{\partial \lambda}{\partial x_1}\mathbf{e}_1 + \frac{\partial \lambda}{\partial x_2}\mathbf{e}_2 + \frac{\partial \lambda}{\partial x_3}\mathbf{e}_3,$$

$$\phi_{i,i} = \frac{\partial \phi_1}{\partial x_1} + \frac{\partial \phi_2}{\partial x_2} + \frac{\partial \phi_3}{\partial x_3},$$

$$a_{i,j} = \begin{pmatrix} a_{1,1} & a_{1,2} & a_{1,3} \\ a_{2,1} & a_{2,2} & a_{2,3} \\ a_{3,1} & a_{3,2} & a_{3,3} \end{pmatrix} = \begin{pmatrix} \frac{\partial a_1}{\partial x_1} & \frac{\partial a_1}{\partial x_2} & \frac{\partial a_1}{\partial x_3} \\ \frac{\partial a_2}{\partial x_1} & \frac{\partial a_2}{\partial x_2} & \frac{\partial a_2}{\partial x_3} \\ \frac{\partial a_3}{\partial x_1} & \frac{\partial a_3}{\partial x_2} & \frac{\partial a_3}{\partial x_3} \end{pmatrix}$$

$$\sigma_{1j,j} = \sigma_{11,1} + \sigma_{12,2} + \sigma_{13,3} = \frac{\partial \sigma_{11}}{\partial x_1} + \frac{\partial \sigma_{12}}{\partial x_2} + \frac{\partial \sigma_{13}}{\partial x_3},$$

$$a_{1,23} = \frac{\partial^2 a_1}{\partial x_2 \partial x_3},$$

$$\sigma_{ij,j} = \begin{cases} \frac{\partial \sigma_{11}}{\partial x_1} + \frac{\partial \sigma_{12}}{\partial x_2} + \frac{\partial \sigma_{13}}{\partial x_3} \\ \frac{\partial \sigma_{21}}{\partial x_1} + \frac{\partial \sigma_{22}}{\partial x_2} + \frac{\partial \sigma_{23}}{\partial x_3} \\ \frac{\partial \sigma_{31}}{\partial x_1} + \frac{\partial \sigma_{32}}{\partial x_2} + \frac{\partial \sigma_{33}}{\partial x_3} \end{cases}$$

(2) The most *frequent notations* to be used in this book are as follows:

σ_{ij}; σ_{xx}, σ_{yy}, σ_{zz}, σ_{xy}, σ_{yz}, σ_{xz}: stress tensor and stress components,

s_{ij}; s_{xx}, s_{yy}, s_{zz}, s_{xy}, s_{yz}, s_{xz}: stress deviator and stress deviator components,

σ_{I}, σ_{II}, σ_{III}: principal normal stresses,

τ_{I}, τ_{II}, τ_{III}: principal shear stresses,

$\sigma_m = \frac{1}{3}(\sigma_{xx}+\sigma_{yy}+\sigma_{zz}) = \frac{1}{3}(\sigma_I+\sigma_{II}+\sigma_{III}) = \frac{1}{3}\sigma_{kk}$: mean normal stress,

$s = 3\sigma_m = (\sigma_{xx}+\sigma_{yy}+\sigma_{zz})$,

$\dot{\sigma}_{ij}$; $\dot{\sigma}_{xx}$, $\dot{\sigma}_{yy}$, $\dot{\sigma}_{zz}$, $\dot{\sigma}_{xy}$, $\dot{\sigma}_{yz}$, $\dot{\sigma}_{xz}$: stress-rate tensor and stress-rate components,

τ_{oct}: octahedral shear stress,

I_1, I_2, I_3: invariants of the stress tensor,

K_1, K_2, K_3: invariants of the stress deviator,

ε_{ij}; ε_{xx},ε_{yy}, ε_{zz}, ε_{xy}, ε_{yz}, ε_{xz}: strain tensor and strain components,

ε^{e}_{ij}, ε^{p}_{ij}: strain tensors of the elastic and plastic deformations,

e_{ij}; e_{xx}, e_{yy}, e_{zz}, e_{xy}, e_{yz}, e_{xz}: strain deviator and strain deviator components,

ε_{I}, ε_{II}, ε_{III}: principal normal strains,

γ_{I}, γ_{II}, γ_{III}: principal shear strains,

$\varepsilon_m = \frac{1}{3}(\varepsilon_{xx}+\varepsilon_{yy}+\varepsilon_{zz}) = \frac{1}{3}(\varepsilon_I+\varepsilon_{II}+\varepsilon_{III}) = \frac{1}{3}\varepsilon_{kk}$: mean normal strain,

$e = 3e_m = (\varepsilon_{xx}+\varepsilon_{yy}+\varepsilon_{zz})$: dilatation,

γ_{oct}: octahedral shear strain,

$\dot{\varepsilon}_{ij}$; $\dot{\varepsilon}_{xx}$, $\dot{\varepsilon}_{yy}$, $\dot{\varepsilon}_{zz}$, $\dot{\varepsilon}_{xy}$, $\dot{\varepsilon}_{yz}$, $\dot{\varepsilon}_{xz}$: strain-rate tensor and strain-rate components,

I'_1, I'_2, I'_3: invariants of the strain tensor,

u_i; u_x, u_y, u_z: displacement vector and displacement components,

v_i; v_x, v_y, v_z: velocity vector and velocity components,

E and ν: Young's modulus and Poisson's ratio,

$G = \frac{E}{2(1+\nu)}$: shear modulus,

$K = \frac{E}{3(1-2\nu)}$: bulk modulus,

ρ: density of material

σ_0 and τ_0: yield stress in tension or compression and in shear,

k: plasticity constant,

μ: viscosity coefficient,

t: time,

S: surface,

V: volume,

x_i: Cartesian coordinate,

n_i: unit normal vector,

f_i: body force per unit volume,

q_i: surface force per unit area,

f: yield function,

$d\lambda$, $\dot{\lambda}$: plastic multipliers,

m_s, m_k, m_c: statically admissible, kinematically admissible and collapse load multipliers.

2. FUNDAMENTAL RELATIONS AND GOVERNING EQUATIONS

In the first part of this chapter the state of stress and strain at a point in a body will be studied and the equilibrium and the kinematic equations will be derived. We will then discuss the general properties of yield conditions and will present the Huber–v. Mises–Hencky and Tresca yield conditions in detail. From the yield conditions the plastic flow rule can be derived which allows the derivation of the constitutive equations of plastic bodies. The Prandtl–Reuss incremental theory and the Hencky deformation theory will be discussed. Finally, we will present the governing equations for linearly elastic-perfectly plastic bodies based both on the incremental and on the deformation theory and will briefly describe the problems that arise in the solution of these equations.

2.1. STATE OF STRESS

2.1.1. STRESS VECTOR AND STRESS TENSOR

Let us consider a section that passes through a point $P(x_i)$ of a body and is defined by a unit outward normal vector n_i $(n_1\ n_2\ n_3)$. The *stress vector* $p_i^{(n)}$ at the point $P(x_i)$ acting on this section is defined

$$p_i^{(n)} = \lim_{\Delta A \to 0} \frac{\Delta Q}{\Delta A},$$

where ΔQ is the force acting on the infinitesimal area ΔA of this section. This vector specifies the stress state of the point P associated with the section under consideration. It can be decomposed into *normal stress* and *shear stress components* σ_n and τ_n, respectively (Fig. 2—1(a)) or into the components $p_1{}^{(n)}$, $p_2{}^{(n)}$ and $p_3{}^{(n)}$ corresponding to the Cartesian coordinate axes x_1, x_2 and x_3.

The stress vector $p_i^{(n)}$ is a function of the normal vector n_i. To specify completely the state of stress at a point it is necessary to specify the stress vectors associated with any section at the point A. That is, one has to specify the vector–vector function

$$p_i^{(n)} = F(n_i). \tag{2—1}$$

To derive this function, we assume that the stress vectors acting on the sections perpendicular to the coordinate axes x_1, x_2 and x_3 are given (Fig. 2—1(b)) and are denoted by*

$$\left.\begin{aligned} p_i^{(1)}(\sigma_{11}\,\sigma_{12}\,\sigma_{13}) &= p_i^{(x)}(\sigma_{xx}\,\sigma_{xy}\,\sigma_{xz}) \\ p_i^{(2)}(\sigma_{21}\,\sigma_{22}\,\sigma_{23}) &= p_i^{(y)}(\sigma_{yx}\,\sigma_{yy}\,\sigma_{yz}) \\ p_i^{(3)}(\sigma_{31}\,\sigma_{32}\,\sigma_{33}) &= p_i^{(z)}(\sigma_{zx}\,\sigma_{zy}\,\sigma_{zz}) \end{aligned}\right\}. \qquad (2—2)$$

Now considering an arbitrary section with the normal vector n_i the components of the corresponding stress vector $p_i^{(n)}$ can be obtained by writing the force equilibrium

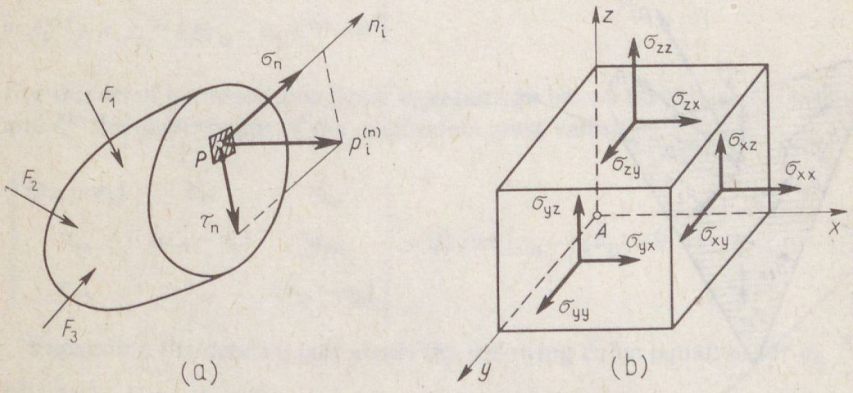


Fig. 2–1

equations of an infinitesimal tetrahedron formed by the four plane sections under consideration** (Fig. 2—2):

$$\left.\begin{aligned} p_x^{(n)} &= \sigma_{xx}n_x + \sigma_{yx}n_y + \sigma_{zx}n_z \\ p_y^{(n)} &= \sigma_{xy}n_x + \sigma_{yy}n_y + \sigma_{zy}n_z \\ p_z^{(n)} &= \sigma_{xz}n_x + \sigma_{yz}n_y + \sigma_{zz}n_z \end{aligned}\right\} \; p_i^{(n)} = \sigma_{ij}n_j. \qquad (2—3)$$

It can be stated that (2—1) is a linear relationship and that the stress state of a point is entirely determined by the 9 components of the three stress vectors of eq. (2—2), that is, by the second order *stress tensor* σ_{ij}. In the Cartesian system of coordinates the matrix of the scalar components of this second-order tensor has the form

$$\sigma_{ij} = \begin{pmatrix} \sigma_{11} & \sigma_{12} & \sigma_{13} \\ \sigma_{21} & \sigma_{22} & \sigma_{23} \\ \sigma_{31} & \sigma_{32} & \sigma_{33} \end{pmatrix} = \begin{pmatrix} \sigma_{xx} & \sigma_{xy} & \sigma_{xz} \\ \sigma_{yx} & \sigma_{yy} & \sigma_{yz} \\ \sigma_{zx} & \sigma_{zy} & \sigma_{zz} \end{pmatrix}. \qquad (2—4)$$

* In the following the subscripts 1, 2, 3 and x, y, z will be used interchangeably.

** The body forces are of a smaller order of magnitude and therefore can be neglected in these equations.

Furthermore, writing the moment equilibrium equations for an infinitesimal rectangular parallelepiped shown in Fig. 2—1(b) one obtains the relations

$$\left.\begin{aligned}\sigma_{xy}&=\sigma_{yx}\\ \sigma_{yz}&=\sigma_{zy}\\ \sigma_{xz}&=\sigma_{zx}\end{aligned}\right\}\ \sigma_{ij}=\sigma_{ji}. \tag{2—5}$$

Thus, the *stress tensor* is *symmetric* and therefore the stress state of a point can be defined by six independent scalar components.*

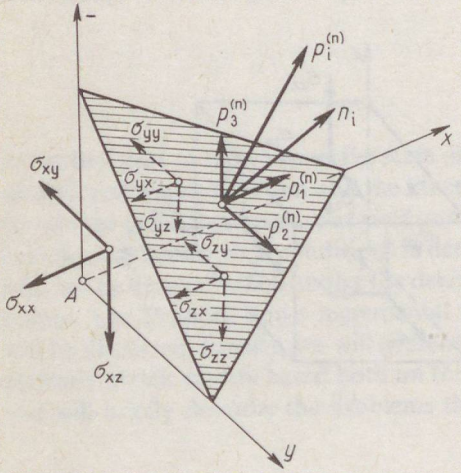


Fig. 2–2

2.1.2. PRINCIPAL STRESSES. STRESS INVARIANTS

A well-known property of symmetric second-order tensors is the existence of principal directions (see e.g. Flügge 1972). In the case of stress tensors, this implies that at a point in a body at least three orthogonal normal vectors $l_i^{(k)}$, $(k=\mathrm{I, II, III})$ can be found such that the corresponding stress vectors are parallel to the normal vectors, i.e.

$$p_i^{(k)}=\sigma_k l_i^{(k)}. \tag{2—6}$$

The directions of the normal vectors $l_i^{(k)}$ and the corresponding coordinate axes are called *principal directions* and *principal axes* (I, II, III), respectively, while the normal stresses σ_k are the *principal (normal) stresses* $(\sigma_{\mathrm{I}}, \sigma_{\mathrm{II}}, \sigma_{\mathrm{III}})$. On the planes corresponding to the principal directions the shear stresses are by definition equal to zero.

* In the case of the *Cosserat-continuum* not only *force stresses* σ_{ij} but also *couple stresses* are assumed to be acting on the infinitesimal parallelepiped. Consequently, the *force stress tensor* σ_{ij} is not symmetric and in order to define the stress state at a point a *moment stress tensor* has to be given as well (E. Cosserat and F. Cosserat 1909).

To determine the principal stresses and directions the transformation (2—3) should be applied to the normal vectors $l_i^{(k)}$. Then, considering eq. (2—6) one obtains

$$\left.\begin{aligned} p_x^{(k)} &= \sigma_k l_x^{(k)} = \sigma_{xx} l_x^{(k)} + \sigma_{xy} l_y^{(k)} + \sigma_{xz} l_z^{(k)} \\ p_y^{(k)} &= \sigma_k l_y^{(k)} = \sigma_{yx} l_x^{(k)} + \sigma_{yy} l_y^{(k)} + \sigma_{yz} l_z^{(k)} \\ p_z^{(k)} &= \sigma_k l_z^{(k)} = \sigma_{zx} l_x^{(k)} + \sigma_{zy} l_y^{(k)} + \sigma_{zz} l_z^{(k)} \end{aligned}\right\} \; p_i^{(k)} = \sigma_k l_i^{(k)} = \sigma_{ij} l_j^{(k)} \qquad (2—7)$$

or, by rearranging these equations

$$\left.\begin{aligned} (\sigma_{xx} - \sigma_k) l_x^{(k)} + \sigma_{xy} l_y^{(k)} + \sigma_{xz} l_z^{(k)} &= 0 \\ \sigma_{yx} l_x^{(k)} + (\sigma_{yy} - \sigma_k) l_y^{(k)} + \sigma_{yz} l_z^{(k)} &= 0 \\ \sigma_{zx} l_x^{(k)} + \sigma_{zy} l_y^{(k)} + (\sigma_{zz} - \sigma_k) l_z^{(k)} &= 0 \end{aligned}\right\} (\sigma_{ij} - \sigma_k \delta_{ij}) l_j^{(k)} = 0. \qquad (2—8)$$

For this set of homogeneous linear equations to have a nontrivial solution for $l_x^{(k)}$, $l_y^{(k)}$ and $l_z^{(k)}$ the determinant of the coefficients must vanish

$$\left.\begin{vmatrix} (\sigma_{xx} - \sigma_k) & \sigma_{xy} & \sigma_{xz} \\ \sigma_{yx} & (\sigma_{yy} - \sigma_k) & \sigma_{yz} \\ \sigma_{zx} & \sigma_{zy} & (\sigma_{zz} - \sigma_k) \end{vmatrix} = 0 \right\} \det |\sigma_{ij} - \sigma_k \delta_{ij}| = 0.$$

Expanding the determinant yields the following cubic equation for σ_k

$$\sigma_k^3 - I_1 \sigma_k^2 - I_2 \sigma_k - I_3 = 0, \qquad (2—9)$$

where

$$\left.\begin{aligned} I_1 &= \sigma_{xx} + \sigma_{yy} + \sigma_{zz} = \sigma_{ii} \\ I_2 &= -\begin{vmatrix} \sigma_{xx} & \sigma_{xy} \\ \sigma_{yx} & \sigma_{yy} \end{vmatrix} - \begin{vmatrix} \sigma_{yy} & \sigma_{yz} \\ \sigma_{zy} & \sigma_{zz} \end{vmatrix} - \begin{vmatrix} \sigma_{xx} & \sigma_{xz} \\ \sigma_{zx} & \sigma_{zz} \end{vmatrix} = \\ &= -(\sigma_{xx}\sigma_{yy} + \sigma_{yy}\sigma_{zz} + \sigma_{zz}\sigma_{xx}) + (\sigma_{xy}^2 + \sigma_{yz}^2 + \sigma_{xz}^2) = \frac{1}{2}[\sigma_{ij}\sigma_{ij} - (\sigma_{ii})^2] \\ I_3 &= \begin{vmatrix} \sigma_{xx} & \sigma_{xy} & \sigma_{zx} \\ \sigma_{yx} & \sigma_{yy} & \sigma_{yz} \\ \sigma_{zx} & \sigma_{zy} & \sigma_{zz} \end{vmatrix} = \\ &= \sigma_{xx}\sigma_{yy}\sigma_{zz} + 2\sigma_{xy}\sigma_{yz}\sigma_{xz} - (\sigma_{xx}\sigma_{yz}^2 + \sigma_{yy}\sigma_{xz}^2 + \sigma_{zz}\sigma_{xy}^2) = \\ &= \frac{1}{6}[3\sigma_{ii}\sigma_{jk}\sigma_{jk} - 2\sigma_{ij}\sigma_{jk}\sigma_{ki} - (\sigma_{ii})^3]. \end{aligned}\right\} \qquad (2—10)$$

It can be proved that eq. (2—9) has three real roots and consequently there are at least three principal stresses designated by σ_I, σ_{II} and σ_{III}. The subscripts of the principal stresses will be chosen in such a manner that the relationships $\sigma_I \geq \sigma_{II} \geq \sigma_{III}$ are satisfied.

Then, σ_I and σ_{III} denote the largest and the smallest normal stresses, respectively, among all those which act on any possible section passing through the point under consideration.

Substituting any of the principal stresses into eqs (2—8) and considering the identity $(l_x^{(k)})^2+(l_y^{(k)})^2+(l_z^{(k)})^2=1$ one can solve eq. (2—8) for the corresponding direction cosines $l_x^{(k)}$, $l_y^{(k)}$ and $l_z^{(k)}$. If σ_I, σ_{II} and σ_{III} are distinct, the three corresponding principal directions will be unique and orthogonal. If two of the principal stresses are equal, one principal direction will be unique and the two others can be in any direction orthogonal to the first one. If all three principal stresses are equal, there are no unique principal directions, which is the case of the state of hydrostatic stress.

Because the principal stresses are physical quantities they cannot depend on the coordinate axes chosen, and the quantities I_1, I_2, I_3 in eq. (2—9) must also have this property. Thus, I_1, I_2 and I_3 are called the first, second and third principal *invariants* of the stress tensor, respectively.

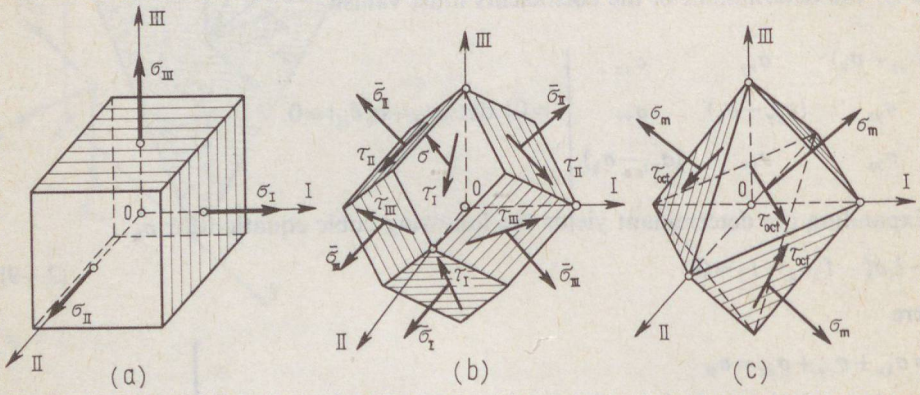


Fig. 2–3

Choosing the principal directions as the directions of the coordinate axes, the stress tensor and the invariants have the simple forms (Fig. 2—3(a)):

$$\sigma_{ij}=\begin{pmatrix}\sigma_I & 0 & 0\\ 0 & \sigma_{II} & 0\\ 0 & 0 & \sigma_{III}\end{pmatrix} \tag{2—11}$$

$$\left.\begin{aligned} I_1&=\sigma_I+\sigma_{II}+\sigma_{III},\\ I_2&=-(\sigma_I\sigma_{II}+\sigma_{II}\sigma_{III}+\sigma_{III}\sigma_I),\\ I_3&=\sigma_I\sigma_{II}\sigma_{III}. \end{aligned}\right\} \tag{2—12}$$

2.1.3. PRINCIPAL SHEAR STRESSES

Using the transformation (2—3) the shear and normal stresses acting on the section containing one of the principal axes and bisecting the angle between the two others can be obtained as follows:*

$$\tau_{\mathrm{I}}=\frac{1}{2}(\sigma_{\mathrm{II}}-\sigma_{\mathrm{III}}),\quad \tau_{\mathrm{II}}=\frac{1}{2}(\sigma_{\mathrm{I}}-\sigma_{\mathrm{III}}),\quad \tau_{\mathrm{III}}=\frac{1}{2}(\sigma_{\mathrm{I}}-\sigma_{\mathrm{II}}), \tag{2—13}$$

$$\bar{\sigma}_{\mathrm{I}}=\frac{1}{2}(\sigma_{\mathrm{II}}+\sigma_{\mathrm{III}}),\quad \bar{\sigma}_{\mathrm{II}}=\frac{1}{2}(\sigma_{\mathrm{I}}+\sigma_{\mathrm{III}}),\quad \bar{\sigma}_{\mathrm{III}}=\frac{1}{2}(\sigma_{\mathrm{I}}+\sigma_{\mathrm{II}}). \tag{2—14}$$

τ_{I}, τ_{II} and τ_{III} are called the *principal shear stresses*. One of these stresses among all of those which act on any possible plane passing through the point under consideration is the *maximum shear stress*. If the relationship $\sigma_{\mathrm{I}}\geq\sigma_{\mathrm{II}}\geq\sigma_{\mathrm{III}}$ holds, the maximum shear stress is

$$\tau_{\max}=\tau_{\mathrm{II}}=\frac{1}{2}(\sigma_{\mathrm{I}}-\sigma_{\mathrm{III}}). \tag{2—15}$$

The sections of the principal shear stresses form a dodecahedron and the stresses acting on these sections are given by eqs (2—13) and (2—14) as illustrated in Fig. 2—3(b).

Using the transformation (2—3) again, one can derive the shear and normal stresses acting on the sections which make equal angles with all the three principal axes. These *octahedral shear* and *normal stresses* are

$$\begin{aligned}\tau_{\mathrm{oct}}&=\frac{1}{3}[(\sigma_{xx}-\sigma_{yy})^2+(\sigma_{yy}-\sigma_{zz})^2+(\sigma_{zz}-\sigma_{xx})^2+\\&\quad+6(\sigma_{xy}^2+\sigma_{yz}^2+\sigma_{xz}^2)]^{1/2}=\\&=\frac{1}{3}[(\sigma_{\mathrm{I}}-\sigma_{\mathrm{II}})^2+(\sigma_{\mathrm{II}}-\sigma_{\mathrm{III}})^2+(\sigma_{\mathrm{I}}-\sigma_{\mathrm{III}})^2]^{1/2},\end{aligned} \tag{2—16}$$

$$\sigma_{\mathrm{oct}}=\sigma_{\mathrm{m}}=\frac{1}{3}(\sigma_{xx}+\sigma_{yy}+\sigma_{zz})=\frac{1}{3}(\sigma_{\mathrm{I}}+\sigma_{\mathrm{II}}+\sigma_{\mathrm{III}}) \tag{2—17}$$

where σ_{m} is called the *mean normal stress*.

The sections of the octahedral stresses form an octahedron which can be used to illustrate the octahedral stresses (Fig. 2—3(c)).

Finally, the notation

$$s=3\sigma_{\mathrm{m}}=\sigma_{xx}+\sigma_{yy}+\sigma_{zz}=\sigma_{kk} \tag{2—18}$$

will also be used in the presentations that follow.

* For example τ_{I} and $\bar{\sigma}_{\mathrm{I}}$ designate the shear and normal stresses, respectively, which act on the plane containing the principal axis I and bisecting the angle between the principal axes II and III.

2.1.4. STRESS DEVIATOR TENSOR

It is convenient in plasticity to separate the stress tensor into two parts

$$\sigma_{ij}=\sigma_{ij}^{0}+s_{ij}. \tag{2—19}$$

Here the *spherical stress tensor* σ_{ij}^{0} corresponds to the hydrostatic part of the state of stress and is of the form

$$\sigma_{ij}^{0}=\begin{pmatrix}\sigma_m & 0 & 0\\ 0 & \sigma_m & 0\\ 0 & 0 & \sigma_m\end{pmatrix}=\delta_{ij}\sigma_m. \tag{2—20}$$

Then from (2—19) it is apparent that the *stress deviator tensor* s_{ij} can be expressed as

$$s_{ij}=\sigma_{ij}-\sigma_m\delta_{ij}=\begin{pmatrix}(\sigma_{xx}-\sigma_m) & \sigma_{xy} & \sigma_{xz}\\ \sigma_{yx} & (\sigma_{yy}-\sigma_m) & \sigma_{yz}\\ \sigma_{zx} & \sigma_{zy} & (\sigma_{zz}-\sigma_m)\end{pmatrix} \tag{2—21}$$

or introducing the notations

$$\left.\begin{aligned} &s_{xx}=(\sigma_{xx}-\sigma_m), \quad s_{yy}=(\sigma_{yy}-\sigma_m), \quad s_{zz}=(\sigma_{zz}-\sigma_m),\\ &s_{xy}=\sigma_{xy}, \qquad\quad s_{yz}=\sigma_{yz}, \qquad\quad s_{xz}=\sigma_{xz},\end{aligned}\right\} \tag{2—22}$$

we can write

$$s_{ij}=\begin{pmatrix}s_{xx} & s_{xy} & s_{xz}\\ s_{yx} & s_{yy} & s_{yz}\\ s_{zx} & s_{zy} & s_{zz}\end{pmatrix}. \tag{2—23}$$

The principal directions are the same for the stress deviator tensor and for the original stress tensor because the subtraction of a constant normal stress in all directions will not change the principal directions. Similarly, as was described in Section 2.1.2, the principal normal stresses of the deviator tensor denoted by s_{I}, s_{II}, s_{III} can be obtained from the following equation

$$s_k^3-K_1s_k^2-K_2s_k-K_3=0 \tag{2—24}$$

where

$$\left.\begin{aligned} &K_1=s_{xx}+s_{yy}+s_{zz}=0,\\ &K_2=-\begin{vmatrix}s_{xx} & s_{xy}\\ s_{yx} & s_{yy}\end{vmatrix}-\begin{vmatrix}s_{yy} & s_{yz}\\ s_{zy} & s_{zz}\end{vmatrix}-\begin{vmatrix}s_{xx} & s_{xy}\\ s_{zx} & s_{zz}\end{vmatrix},\\ &K_3=\begin{vmatrix}s_{xx} & s_{xy} & s_{xz}\\ s_{yx} & s_{yy} & s_{yz}\\ s_{zx} & s_{zy} & s_{zz}\end{vmatrix}.\end{aligned}\right\} \tag{2—25}$$

Here again K_1, K_2, K_3 do not depend on the coordinate axes chosen; therefore, they are the first, second and third *invariants* of the stress deviator tensor. Making use of eqs (2—22), K_2 can also be written as

$$K_2 = \frac{1}{6}[(\sigma_{xx}-\sigma_{yy})^2+(\sigma_{yy}-\sigma_{zz})^2+(\sigma_{zz}-\sigma_{xx})^2]+\sigma_{xy}^2+\sigma_{yz}^2+\sigma_{xz}^2 =$$

$$= \frac{1}{6}[(\sigma_I-\sigma_{II})^2+(\sigma_{II}-\sigma_{III})^2+(\sigma_{III}-\sigma_I)^2] \qquad (2—26)$$

or since $K_1 = 0$

$$K_2 = K_2 + \frac{1}{2}K_1^2 = \frac{1}{2}(s_{xx}^2+s_{yy}^2+s_{zz}^2)+s_{xy}^2+s_{yz}^2+s_{xz}^2 =$$

$$= \frac{1}{2}(s_I^2+s_{II}^2+s_{III}^2) = \frac{1}{2}s_{ij}s_{ij}. \qquad (2—27)$$

Finally, comparing eqs (2—16) and (2—26) the invariant K_2 can also be expressed in terms of the octahedral shear stress

$$K_2 = \frac{3}{2}\tau_{oct}^2. \qquad (2—28)$$

In the same way as for to the stress tensor, the components of the stress deviator tensor can also be written in a diagonal form when referred to coordinate axes coinciding with the principal directions

$$s_{ij} = \begin{pmatrix} s_I & 0 & 0 \\ 0 & s_{II} & 0 \\ 0 & 0 & s_{III} \end{pmatrix}.$$

2.1.5. GRAPHICAL REPRESENTATION OF THE STRESS STATE. MOHR'S CIRCLE

The state of stress at a point in a body can be graphically illustrated by the use of *Mohr's circles*. Let us take the principal directions as the coordinate axes and consider the normal and shear stress components σ_n and τ_n of the stress vector $p_i^{(n)}$ acting on the section with orientation defined by the unit normal vector n_i. Then, making use of eqs (2—4) and (2—11), σ_n and τ_n can be expressed as

$$\left.\begin{aligned} \sigma_n &= n_i p_i = n_i\sigma_{ij}n_j = \sigma_I n_1^2+\sigma_{II}n_2^2+\sigma_{III}n_3^2, \\ \tau_n &= (p_i^2-\sigma_n^2)^{1/2} = (\sigma_I^2 n_1^2+\sigma_{II}^2 n_2^2+\sigma_{III}^2 n_3^2-\sigma_n^2)^{1/2}. \end{aligned}\right\} \qquad (2—29)$$

Considering in addition the identity $n_1^2+n_2^2+n_3^2=1$, the three equations can be solved for n_1^2, n_2^2 and n_3^2. The solution is found to be

$$n_1^2=\left|\frac{\tau_n^2+(\sigma_n-\sigma_{II})(\sigma_n-\sigma_{III})}{(\sigma_I-\sigma_{II})(\sigma_I-\sigma_{III})}\right|,$$

$$n_2^2=\left|\frac{\tau_n^2+(\sigma_n-\sigma_{III})(\sigma_n-\sigma_I)}{(\sigma_{II}-\sigma_{III})(\sigma_{II}-\sigma_I)}\right|,$$

$$n_3^2=\left|\frac{\tau_n^2+(\sigma_n-\sigma_I)(\sigma_n-\sigma_{II})}{(\sigma_{III}-\sigma_I)(\sigma_{III}-\sigma_{II})}\right|.$$

Since we assumed that the relationship $\sigma_I\geq\sigma_{II}\geq\sigma_{III}$ holds and, at the same time, $n_1^2\geq 0$, $n_2^2\geq 0$ and $n_3^2\geq 0$, from these equations it follows that

$$\tau_n^2+(\sigma_n-\sigma_{II})(\sigma_n-\sigma_{III})\geq 0,$$

$$\tau_n^2+(\sigma_n-\sigma_{III})(\sigma_n-\sigma_I)\leq 0,$$

$$\tau_n^2+(\sigma_n-\sigma_I)(\sigma_n-\sigma_{II})\geq 0.$$

Rearranging the above inequalities we find

$$\left.\begin{aligned}
&\tau_n^2+\left(\sigma_n-\frac{\sigma_{II}+\sigma_{III}}{2}\right)^2\geq\left(\frac{\sigma_{II}-\sigma_{III}}{2}\right)^2,\\
&\tau_n^2+\left(\sigma_n-\frac{\sigma_I+\sigma_{III}}{2}\right)^2\leq\left(\frac{\sigma_I-\sigma_{III}}{2}\right)^2,\\
&\tau_n^2+\left(\sigma_n-\frac{\sigma_I+\sigma_{II}}{2}\right)^2\geq\left(\frac{\sigma_I-\sigma_{II}}{2}\right)^2.
\end{aligned}\right\}\qquad(2—30)$$

If the equality sign is used in relations (2—30) the equations obtained represent three circles in the τ_n, σ_n plane that are called *Mohr's circles* (Fig. 2—4). The centres of these circles are on the σ_n axis at distances

$$\frac{\sigma_{II}+\sigma_{III}}{2},\quad\frac{\sigma_I+\sigma_{III}}{2},\quad\frac{\sigma_I+\sigma_{II}}{2}$$

from the origin. The circles have the radii

$$\frac{\sigma_{II}-\sigma_{III}}{2},\quad\frac{\sigma_I-\sigma_{III}}{2},\quad\frac{\sigma_I-\sigma_{II}}{2}.$$

Considering eqs (2—14) and (2—13), the radii and distances given above are equal to the principal shear stresses and the corresponding normal stresses, respectively. Consequently, the radius of the largest circle gives the maximum shear stress and the intersection points of the circles with the axis σ_n define the principal stresses.

It follows from eq. (2—30) that the feasible values of σ_n and τ_n lie in the shaded region bounded by the three circles shown in Fig. 2—4. In the special case when the normal vector n_i under consideration is perpendicular to one of the principal axes, the corresponding stress vector $p_i^{(n)}$ will also be perpendicular to this axis. Then, the point

which represents the components σ_n and τ_n of the stress vector $p_i^{(n)}$ lies on the circle which is defined by the principal stresses of the other two principal directions.

Additional properties and applications of *Mohr's circles* will be described in Section 5.2.2.

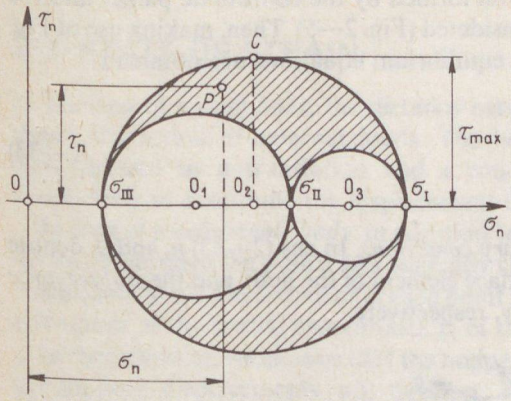


Fig. 2–4

2.1.6. EQUILIBRIUM EQUATIONS

The state of stress in a body is a function of the coordinates: $\sigma_{ij} = \sigma_{ij}(x_i)$. The nine scalar functions of $\sigma_{ij}(x_i)$ are not independent; they have to satisfy relationships that can be derived by using equilibrium considerations.

It has already been mentioned that writing three *moment equilibrium equations* of the infinitesimal parallelepiped shown in Fig. 2—1(b) yields the relationships

$$\left.\begin{aligned} \sigma_{xy} &= \sigma_{yx} \\ \sigma_{yz} &= \sigma_{zy} \\ \sigma_{xz} &= \sigma_{zx} \end{aligned}\right\} \quad \sigma_{ij} = \sigma_{ji}. \tag{2—31}$$

Considering the *force equilibrium equations* of infinitesimal parallelepiped with infinitesimal changes in stress state in the three coordinate directions yields the three differential equations of equilibrium

$$\left.\begin{aligned} \frac{\partial \sigma_{xx}}{\partial x} + \frac{\partial \sigma_{xy}}{\partial y} + \frac{\partial \sigma_{xz}}{\partial z} + f_x &= 0 \\ \frac{\partial \sigma_{yx}}{\partial x} + \frac{\partial \sigma_{yy}}{\partial y} + \frac{\partial \sigma_{yz}}{\partial z} + f_y &= 0 \\ \frac{\partial \sigma_{zx}}{\partial x} + \frac{\partial \sigma_{zy}}{\partial y} + \frac{\partial \sigma_{zz}}{\partial z} + f_z &= 0 \end{aligned}\right\} \quad \sigma_{ij,j} + f_i = 0. \tag{2—32}$$

These are called *Cauchy's equilibrium equations* in which $f_i(f_x\, f_y\, f_z)$ designates the *body (volume) force* per unit volume.

Since the infinitesimal neighbourhood of a point on the surface of the body cannot in general be contained in a rectangular parallelepiped with sides normal to the coordinate axes, eqs (2—32) are not valid on the surface of the body. In order to investigate the equilibrium of a material point on the surface of the body, the equilibrium of an infinitesimal tetrahedron formed by the coordinate planes and the surface element of the body has to be considered (Fig. 2—5). Then, making use of Fig. 2—2 and eq. (2—3), the following force equilibrium equations are obtained

$$\left.\begin{aligned} &\sigma_{xx}n_x+\sigma_{xy}n_y+\sigma_{xz}n_z=q_x\\ &\sigma_{yx}n_x+\sigma_{yy}n_y+\sigma_{yz}n_z=q_y\\ &\sigma_{zx}n_x+\sigma_{zy}n_y+\sigma_{zz}n_z=q_z \end{aligned}\right\}\quad \sigma_{ij}n_j=q_i. \tag{2—33}$$

These are called *static (dynamic) boundary conditions.* In eqs (2—33) n_i and q_i denote the external unit normal vector of the surface element of the body and the *surface force* per unit surface area acting on the body, respectively.

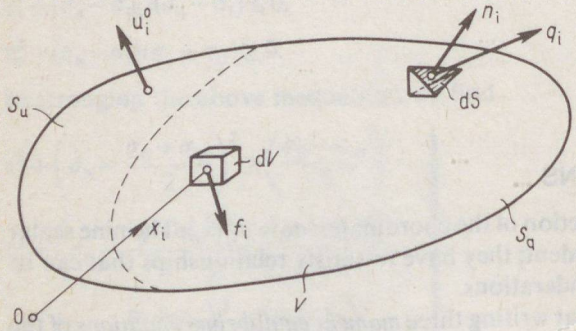


Fig. 2–5

In the case of *cylindrical coordinates* r, φ, z the equilibrium equations (2—32) have the form

$$\left.\begin{aligned} &\frac{\partial\sigma_{rr}}{\partial r}+\frac{1}{r}\frac{\partial\sigma_{r\varphi}}{\partial\varphi}+\frac{\partial\sigma_{rz}}{\partial z}+\frac{\sigma_{rr}-\sigma_{\varphi\varphi}}{r}+f_r=0,\\ &\frac{\partial\sigma_{r\varphi}}{\partial r}+\frac{1}{r}\frac{\partial\sigma_{\varphi\varphi}}{\partial\varphi}+\frac{\partial\sigma_{\varphi z}}{\partial z}+2\frac{\sigma_{r\varphi}}{r}+f_\varphi=0,\\ &\frac{\partial\sigma_{rz}}{\partial r}+\frac{1}{r}\frac{\partial\sigma_{\varphi z}}{\partial\varphi}+\frac{\partial\sigma_{zz}}{\partial z}+\frac{\sigma_{rz}}{r}+f_z=0. \end{aligned}\right\} \tag{2—34}$$

Using *spherical coordinates* r, φ, θ and considering only *point-symmetrical* problems, when $\varphi\equiv\theta$, $\sigma_{\varphi\varphi}\equiv\sigma_{\theta\theta}$ and $\sigma_{r\varphi}=\sigma_{\varphi\theta}=\sigma_{r\theta}=0$, eqs (2—32) take the form

$$\frac{d\sigma_{rr}}{dr}+\frac{2}{r}(\sigma_{rr}-\sigma_{\varphi\varphi})+f_r=0. \tag{2—35}$$

It can be seen, that the equilibrium equations are unrelated to the material's properties, and are therefore valid for bodies of any kind of material. In the three

equations (2—32) we have six unknown functions for the stress components; thus, the problem under consideration is statically indeterminate. To find further equations needed for the solution, we have to study the state of strain of the body and construct the stress–strain relationships as well.

2.2. STATE OF STRAIN

In the case of a *rigid body*, the distance between any pair of points does not change under the action of external loads. The body undergoes only rigid body motion characterized by a translation and a rotation vector and these two vectors are satisfactory to determine the displacement of any point.

In case of a *deformable body*, in addition to rigid body translation and rotation, the distances between the points will generally change under the action of external loads; consequently, the displacement of each point has to be described by a separate vector as a function of the spatial coordinates x_i of the point.*

In the following, we assume that the body has *continuous deformations* i.e. no gaps or overlapping displacements will develop. This means that the displacements are described by continuous functions of the coordinates. The derivation of the relationships that describe the deformed state of the body will be discussed next. As will be seen, these relationships are strictly geometric in nature and, therefore, are valid for bodies of any material.

2.2.1. RELATIVE DISPLACEMENT TENSOR

Let us consider two neighbouring points P_0 and P in the undeformed body (Fig. 2—6(a)). The absolute positions of these two points are defined by the vectors x_i^0 and x_i while their relative positions are characterized by the vector Δx_i. As a consequence of deformation and motion of the body, the points P_0 and P undergo displacements $u_i^0(x_i)$ and $u_i = u_i(x_i)$ and move to positions P_0' and P', respectively. Since the displacements are continuous functions of the coordinates we can expand them at P_0 in a Taylor series

$$\left.\begin{aligned} u_1 &= u_1^0 + \frac{\partial u_1}{\partial x_1}\Delta x_1 + \frac{\partial u_1}{\partial x_2}\Delta x_2 + \frac{\partial u_1}{\partial x_3}\Delta x_3 + \ldots, \\ u_2 &= u_2^0 + \frac{\partial u_2}{\partial x_1}\Delta x_1 + \frac{\partial u_2}{\partial x_2}\Delta x_2 + \frac{\partial u_2}{\partial x_3}\Delta x_3 + \ldots, \\ u_3 &= u_3^0 + \frac{\partial u_3}{\partial x_1}\Delta x_1 + \frac{\partial u_3}{\partial x_2}\Delta x_2 + \frac{\partial u_3}{\partial x_3}\Delta x_3 + \ldots, \end{aligned}\right\} \quad u_i = u_i^0 + u_{i,j}\Delta x_j + \ldots \qquad (2—36)$$

* Depending on whether the deformations are viewed as functions of the position of the point before or after deformations, two different but related formulations are possible. The difference is negligible for small deformations. In this text the relationships will be referred to coordinates prior to deformations (Lagrangian formulation), as prevails in studies in solid mechanics.

or

$$\Delta u_i = u_i - u_i^0 = u_{i,j}\Delta x_j + \dots \tag{2—37}$$

If we assume that Δx_j is small, the following approximation can be applied

$$\Delta u_i = u_{i,j}\Delta x_j. \tag{2—38}$$

Here $u_{i,j}$ is called the *relative displacement tensor*. The matrix of this tensor has the form

$$u_{i,j} = \begin{pmatrix} \frac{\partial u_1}{\partial x_1} & \frac{\partial u_1}{\partial x_2} & \frac{\partial u_1}{\partial x_3} \\ \frac{\partial u_2}{\partial x_1} & \frac{\partial u_2}{\partial x_2} & \frac{\partial u_2}{\partial x_3} \\ \frac{\partial u_3}{\partial x_1} & \frac{\partial u_3}{\partial x_2} & \frac{\partial u_3}{\partial x_3} \end{pmatrix} \tag{2—39}$$

The displacements u_i equally represent rigid body motions and deformations. Since rigid body motions do not play a role in our future investigations, it is convenient to eliminate them. The tensor $u_{i,j}$ already does not contain the translation of the infinitesimal elements, since it stands for *relative* displacements. To eliminate the rotations one has to remember that rigid body motion does not change the distance between the points P_0 and P, i.e. $(\Delta x_i)^2 = (\Delta x_i')^2$. Here

$$\Delta x_i' = \Delta x_i + (u_i - u_i^0) = \Delta x_i + \Delta u_i$$

is the distance between the points P_0' and P′ (see Fig. 2—6(a)).
Making use of this relationship we have

$$(\Delta x_i)^2 = (\Delta x_i')^2 = (\Delta x_i + \Delta u_i)^2 = (\Delta x_i)^2 + 2\Delta x_i \Delta u_i + (\Delta u_i)^2.$$

Considering only small displacements, the term $(\Delta u_i)^2$ can be neglected, and therefore using eq. (2—37) we obtain

$$\Delta x_i \Delta u_i = \Delta x_i u_{i,j} \Delta x_j = \frac{\partial u_1}{\partial x_1}(\Delta x_1)^2 + \left(\frac{\partial u_1}{\partial x_2} + \frac{\partial u_2}{\partial x_1}\right)\Delta x_1 + \Delta x_2 +$$

$$+\left(\frac{\partial u_1}{\partial x_3} + \frac{\partial u_3}{\partial x_1}\right)\Delta x_1 \Delta x_3 + \frac{\partial u_2}{\partial x_2}(\Delta x_2)^2 +$$

$$+\left(\frac{\partial u_2}{\partial x_3} + \frac{\partial u_3}{\partial x_2}\right)\Delta x_2 \Delta x_3 + \frac{\partial u_3}{\partial x_3}(\Delta x_3)^2 = 0.$$

This equation can be satisfied for all values of Δx_1, Δx_2, Δx_3 only, if

$$\left.\begin{aligned} &\frac{\partial u_1}{\partial x_1} = \frac{\partial u_2}{\partial x_2} = \frac{\partial u_3}{\partial x_3} = 0, \\ &\frac{\partial u_1}{\partial x_2} = -\frac{\partial u_2}{\partial x_1}, \quad \frac{\partial u_1}{\partial x_3} = -\frac{\partial u_3}{\partial x_1}, \quad \frac{\partial u_2}{\partial x_3} = -\frac{\partial u_3}{\partial x_2} \end{aligned}\right\} \; u_{i,j} = -u_{j,i}. \tag{2—40}$$

That is, for pure rigid body motion the tensor $u_{i,j}$ is *skew-symmetric*.

It is known (see Flügge 1972) that a second-order tensor can always be decomposed into a symmetric and skew-symmetric tensor. In our case we can write

$$u_{i,j} = \frac{1}{2}(u_{i,j} + u_{j,i}) + \frac{1}{2}(u_{i,j} - u_{j,i}) = \varepsilon_{ij} + \omega_{ij}.$$

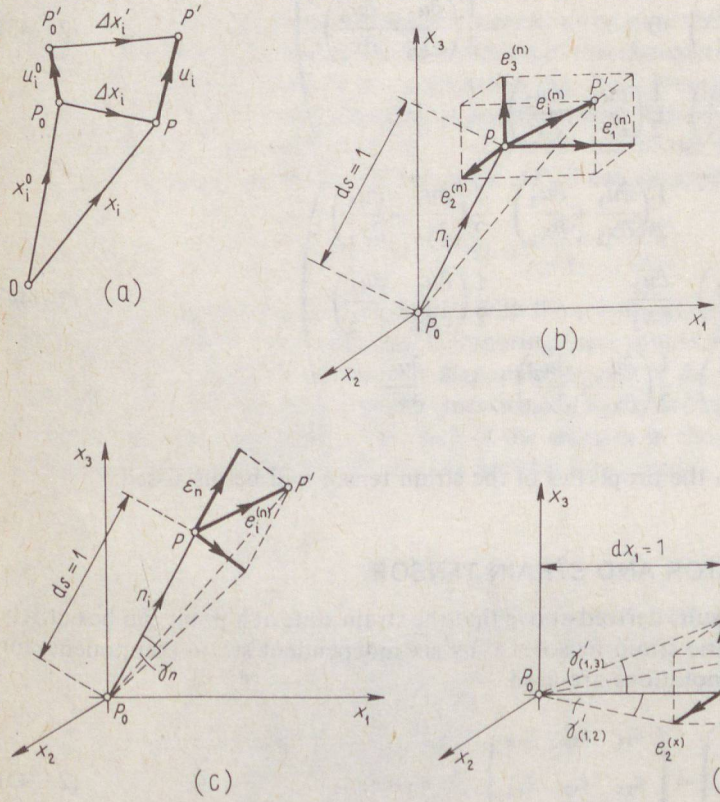


Fig. 2–6

Considering eq. (2—40) the skew-symmetric tensor

$$\omega_{ij} = -\omega_{ji} = \frac{1}{2}(u_{i,j} - u_{j,i}) \qquad (2—41)$$

corresponds to rigid body rotation and is called the *rotation tensor*. Consequently, the remaining symmetric tensor

$$\varepsilon_{ij} = \varepsilon_{ji} = \frac{1}{2}(u_{i,j} + u_{j,i}) \qquad (2—42)$$

corresponds to the pure deformation and is called the *strain tensor*. The matrices of the scalar components of these tensors are

$$\omega_{ij}=\begin{pmatrix} 0 & \frac{1}{2}\left(\frac{\partial u_1}{\partial x_2}-\frac{\partial u_2}{\partial x_1}\right) & \frac{1}{2}\left(\frac{\partial u_1}{\partial x_3}-\frac{\partial u_3}{\partial x_1}\right) \\ \frac{1}{2}\left(\frac{\partial u_2}{\partial x_1}-\frac{\partial u_1}{\partial x_2}\right) & 0 & \frac{1}{2}\left(\frac{\partial u_2}{\partial x_3}-\frac{\partial u_3}{\partial x_2}\right) \\ \frac{1}{2}\left(\frac{\partial u_3}{\partial x_1}-\frac{\partial u_1}{\partial x_3}\right) & \frac{1}{2}\left(\frac{\partial u_3}{\partial x_2}-\frac{\partial u_2}{\partial x_3}\right) & 0 \end{pmatrix} \tag{2—43}$$

$$\varepsilon_{ij}=\begin{pmatrix} \frac{\partial u_1}{\partial x_1} & \frac{1}{2}\left(\frac{\partial u_1}{\partial x_2}+\frac{\partial u_2}{\partial x_1}\right) & \frac{1}{2}\left(\frac{\partial u_1}{\partial x_3}+\frac{\partial u_3}{\partial x_1}\right) \\ \frac{1}{2}\left(\frac{\partial u_2}{\partial x_1}+\frac{\partial u_1}{\partial x_2}\right) & \frac{\partial u_2}{\partial x_2} & \frac{1}{2}\left(\frac{\partial u_2}{\partial x_3}+\frac{\partial u_3}{\partial x_2}\right) \\ \frac{1}{2}\left(\frac{\partial u_3}{\partial x_1}+\frac{\partial u_1}{\partial x_3}\right) & \frac{1}{2}\left(\frac{\partial u_3}{\partial x_2}+\frac{\partial u_2}{\partial x_3}\right) & \frac{\partial u_3}{\partial x_3} \end{pmatrix} \tag{2—44}$$

In the next section the properties of the strain tensor will be discussed.

2.2.2. STRAIN VECTOR AND STRAIN TENSOR

It follows from the results derived above that the strain state at a point can be entirely defined by a symmetric strain tensor, i.e. by six independent strain components for which the following notations are used

$$\varepsilon_{ij}=\begin{pmatrix} \varepsilon_{11} & \varepsilon_{12} & \varepsilon_{13} \\ \varepsilon_{21} & \varepsilon_{22} & \varepsilon_{23} \\ \varepsilon_{31} & \varepsilon_{32} & \varepsilon_{33} \end{pmatrix}=\begin{pmatrix} \varepsilon_{xx} & \varepsilon_{xy} & \varepsilon_{xz} \\ \varepsilon_{yx} & \varepsilon_{yy} & \varepsilon_{yz} \\ \varepsilon_{zx} & \varepsilon_{zy} & \varepsilon_{zz} \end{pmatrix}, \qquad \varepsilon_{ij}=\varepsilon_{ji}. \tag{2—45}$$

In order to illustrate the geometrical meanings of the strain components consider an infinitesimal line element between the points P_0 and P and assume that $\overline{P_0P}=1$ and that the direction of this element is defined by the unit vector n_i (Fig. 2—6(b)). Focussing our investigations only on the deformations the position of the point P_0 can be assumed to be fixed. Then, as a consequence of the deformation of the body, the point P moves to point P' and the deformation of the line element is described by the vector $e_i^{(n)}$, called the *strain vector*. As in the case of the stress vector, the strain vector can be determined by a similar transformation

$$\varepsilon_i^{(n)}=\varepsilon_{ij}n_j.$$

The strain vector can be decomposed into directions parallel and perpendicular to the vector n_i. Then, as shown in Fig. 2—6(c), the components ε_n and γ_n describe the

extension per unit length and the change of the direction of the line element, respectively. Since the change of angle is caused by shear, γ_n is called the *shear strain.*

Figure 2—6(d) shows the strain vector of a line element parallel to the axis x_1. Here $e_1^{(x)}$ denotes the strain in the direction of x_1 while the components $e_2^{(x)}=\gamma'_{(1,2)}$ and $e_3^{(x)}=\gamma'_{(1,3)}$ describe the change in the right angle between the axes x_1, x_2 and x_1, x_3, respectively, caused by the deformation of the line element.

Now let us consider an infinitesimal prismatic element in the neighbourhood of the point P_0 under consideration. The intersection of this element with the plane x_1, x_2—before and after the deformation—is shown in Fig. 2—7. Here the rigid body rotation, which has no influence on the strains, is not illustrated. Assuming small deformations and considering the notations of Fig. 2—7, the extensions per unit length of the edges P_0A and P_0B and the change of the angle AP_0B can be expressed as

$$\varepsilon_{11}=\frac{\partial u_1}{\partial x_1}, \quad \varepsilon_{22}=\frac{\partial u_2}{\partial x_2}, \quad \gamma_{(1,2)}=\gamma'_{(1,2)}+\gamma'_{(2,1)}=\frac{\partial u_1}{\partial x_2}+\frac{\partial u_2}{\partial x_1}. \tag{2—46}$$

Forming the intersections of the element with the coordinate planes x_2, x_3 and x_1, x_3, similar relationships can be derived. Comparing these results with the elements of the matrix (2—44) one can state that the diagonal elements of the strain tensor represent the extensions per unit length in the directions of the coordinate axes, while the off-diagonal elements are equal to the half of the changes in the right angles originally parallel to the coordinate axes, i.e. they are the shear strains.

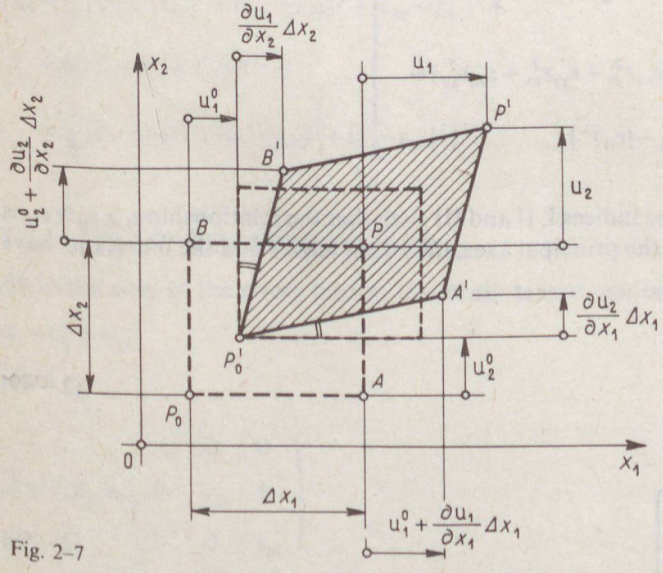


Fig. 2–7

The stress tensor and the strain tensor have different physical contents, but from the mathematical point of view they are equivalent. Consequently, by a suitable change of notations and names, all the results presented in Section 2.1. for the stress tensor are valid for the strain tensor as well. For the sake of completeness, these will now be summarized.

2.2.3. PRINCIPAL STRAINS. STRAIN INVARIANTS

At each point in a body at least three perpendicular axes can be found which do not change their directions during the deformation. These are the *principal directions* I, II, III of the strain state at that point. The corresponding strains ε_{I}, $\varepsilon_{\mathrm{II}}$, $\varepsilon_{\mathrm{III}}$ are called the *principal strains*. They can be determined from the equation

$$\varepsilon_k^3 - I'_1\varepsilon_k^2 - I'_2\varepsilon_k - I'_3 = 0, \tag{2—47}$$

where I'_1, I'_2, I'_3 are the *invariants of the strain tensor* and are given by the expressions

$$\left.\begin{aligned}
&I'_1 = \varepsilon_{xx} + \varepsilon_{yy} + \varepsilon_{zz} = \varepsilon_{ii},\\
&I'_2 = -\begin{vmatrix}\varepsilon_{xx} & \varepsilon_{xy}\\ \varepsilon_{yx} & \varepsilon_{yy}\end{vmatrix} - \begin{vmatrix}\varepsilon_{yy} & \varepsilon_{yz}\\ \varepsilon_{zy} & \varepsilon_{zz}\end{vmatrix} - \begin{vmatrix}\varepsilon_{xx} & \varepsilon_{xz}\\ \varepsilon_{zx} & \varepsilon_{zz}\end{vmatrix} =\\
&\quad = -(\varepsilon_{xx}\varepsilon_{yy} + \varepsilon_{yy}\varepsilon_{zz} + \varepsilon_{xx}\varepsilon_{zz}) + (\varepsilon_{xy}^2 + \varepsilon_{yz}^2 + \varepsilon_{zx}^2) =\\
&\quad = \frac{1}{2}[\varepsilon_{ij}\varepsilon_{ij} - (\varepsilon_{ii})^2],\\
&I'_3 = \begin{vmatrix}\varepsilon_{xx} & \varepsilon_{xy} & \varepsilon_{xz}\\ \varepsilon_{yx} & \varepsilon_{yy} & \varepsilon_{yz}\\ \varepsilon_{zx} & \varepsilon_{zy} & \varepsilon_{zz}\end{vmatrix} =\\
&\quad = \varepsilon_{xx}\varepsilon_{yy}\varepsilon_{zz} + 2\varepsilon_{xy}\varepsilon_{yz}\varepsilon_{zx} - (\varepsilon_{xx}\varepsilon_{yz}^2 + \varepsilon_{yy}\varepsilon_{zx}^2 + \varepsilon_{zz}\varepsilon_{xy}^2) =\\
&\quad = \frac{1}{6}[3\varepsilon_{ii}\varepsilon_{jk}\varepsilon_{jk} - 2\varepsilon_{ij}\varepsilon_{jk}\varepsilon_{ki} - (\varepsilon_{ii})^3].
\end{aligned}\right\} \tag{2—48}$$

It is customary to choose the indices I, II and III such that the relationship $\varepsilon_{\mathrm{I}} \geq \varepsilon_{\mathrm{II}} \geq \varepsilon_{\mathrm{III}}$ is satisfied. When referred to the principal axes, the strain tensor and the invariants have the simple forms

$$\varepsilon_{ij} = \begin{pmatrix}\varepsilon_{\mathrm{I}} & 0 & 0\\ 0 & \varepsilon_{\mathrm{II}} & 0\\ 0 & 0 & \varepsilon_{\mathrm{III}}\end{pmatrix}, \tag{2—49}$$

$$\left.\begin{aligned}
&I'_1 = \varepsilon_{\mathrm{I}} + \varepsilon_{\mathrm{II}} + \varepsilon_{\mathrm{III}},\\
&I'_2 = -(\varepsilon_{\mathrm{I}}\varepsilon_{\mathrm{II}} + \varepsilon_{\mathrm{II}}\varepsilon_{\mathrm{III}} + \varepsilon_{\mathrm{III}}\varepsilon_{\mathrm{I}}),\\
&I'_3 = \varepsilon_{\mathrm{I}}\varepsilon_{\mathrm{II}}\varepsilon_{\mathrm{III}}.
\end{aligned}\right\} \tag{2—50}$$

One can prove that the first invariant is equal to the change in volume per unit volume, i.e. the *dilatation*

$$e = I'_1 = \varepsilon_{xx} + \varepsilon_{yy} + \varepsilon_{zz} = \varepsilon_{ii}. \tag{2—51}$$

The quantity

$$\varepsilon_m = \frac{1}{3} I_1' = \frac{1}{3}(\varepsilon_{xx} + \varepsilon_{yy} + \varepsilon_{zz}) = \frac{1}{3}\varepsilon_{ii} \tag{2—52}$$

is called the *mean strain.*

2.2.4. PRINCIPAL SHEAR STRAINS. OCTAHEDRAL STRAINS

Similarly to the case of stresses, the shear strains, corresponding to the mutually perpendicular directions and bisecting the angles between the principal axes, are given by the equations

$$\gamma_I = (\varepsilon_{II} - \varepsilon_{III}),\ \gamma_{II} = (\varepsilon_I - \varepsilon_{III}),\ \gamma_{III} = (\varepsilon_I - \varepsilon_{II}). \tag{2—53}$$

These are called the *principal shear strains.* One of the principal shear strains is the *maximum shear strain* at the point under consideration. When $\varepsilon_I \geq \varepsilon_{II} \geq \varepsilon_{III}$ holds then

$$\gamma_{max} = \gamma_{II} = (\varepsilon_I - \varepsilon_{III}). \tag{2—54}$$

The shear strains corresponding to those directions which form equal angles with the principal directions are called *octahedral shear strains.* They have the magnitude

$$\begin{aligned}\gamma_{oct} = \frac{1}{3}[&(\varepsilon_{xx} - \varepsilon_{yy})^2 + (\varepsilon_{yy} - \varepsilon_{zz})^2 + (\varepsilon_{zz} - \varepsilon_{xx})^2 + \\ &+ 6(\varepsilon_{xy}^2 + \varepsilon_{yz}^2 + \varepsilon_{zx}^2)]^{1/2} = \\ &= \frac{1}{3}[(\varepsilon_I - \varepsilon_{II})^2 + (\varepsilon_{II} - \varepsilon_{III})^2 + (\varepsilon_I - \varepsilon_{III})^2]^{1/2}.\end{aligned} \tag{2—55}$$

2.2.5. STRAIN DEVIATOR TENSOR

As in the case of the stress tensor, the strain tensor can be separated into two parts

$$\varepsilon_{ij} = \varepsilon_{ij}^0 + e_{ij}. \tag{2—56}$$

Here

$$\varepsilon_{ij}^0 = \varepsilon_m \delta_{ij} = \begin{pmatrix} \varepsilon_m & 0 & 0 \\ 0 & \varepsilon_m & 0 \\ 0 & 0 & \varepsilon_m \end{pmatrix} \tag{2—57}$$

is the *spherical strain tensor* which describes the *volume change.* Introducing the notations

$$e_{xx} = \varepsilon_{xx} - \varepsilon_m,\quad e_{yy} = \varepsilon_{yy} - \varepsilon_m,\quad e_{zz} = \varepsilon_{zz} - \varepsilon_m,$$

$$e_{xy} = \varepsilon_{xy},\qquad e_{yz} = \varepsilon_{yz},\qquad e_{xz} = \varepsilon_{xz}$$

we can write the *strain deviator tensor*, which represents the *distortion*, as

$$e_{ij} = \varepsilon_{ij} - \varepsilon_m \delta_{ij} = \begin{pmatrix} e_{xx} & e_{xy} & e_{xz} \\ e_{yx} & e_{yy} & e_{yz} \\ e_{zx} & e_{zy} & e_{zz} \end{pmatrix}. \tag{2—58}$$

One can also determine the principal axes and the principal strains in the case of the strain deviator tensor. The principal axes of the strain deviator tensor simply coincide with those of the strain tensor. The principal strains e_I, e_{II}, e_{III} can be determined by the use of the invariants K'_1, K'_2, K'_3 of the strain deviator tensor. Their magnitude differs from the principal strains ε_I, ε_{II}, ε_{III} of the strain tensor only by the value of the mean strain ε_m.

Finally, it is apparent that the Mohr's circle representation of the stresses can be used for the strains in an identical fashion.

2.2.6. STRAIN INCREMENTS AND STRAIN RATES

It has already been mentioned in the Introduction that in the theory of plasticity the stress–strain relationships are expressed in terms of increments and therefore strain increments play an important role. Strain increments represent the infinitesimal change in the strains associated with an infinitesimal change in a certain parameter of the loading process. It can be the time, the load parameter or any other quantity characterizing the change of state of the body (e.g. the characteristic dimension of the plastic zone). For the *strain increment tensor* the following notation is used

$$d\varepsilon_{ij} = \begin{pmatrix} d\varepsilon_{xx} & d\varepsilon_{xy} & d\varepsilon_{xz} \\ d\varepsilon_{yx} & d\varepsilon_{yy} & d\varepsilon_{yz} \\ d\varepsilon_{zx} & d\varepsilon_{zy} & d\varepsilon_{zz} \end{pmatrix}. \tag{2—59}$$

It is apparent that for the strain increment tensor, all the relationships which have been described in case of the strain tensor are valid. For example, denoting by du_i the *displacement increments* eq. (2—42) has the modified form

$$d\varepsilon_{ij} = \frac{1}{2}(du_{i,j} + du_{j,i}). \tag{2—60}$$

The strain increment tensor can also be separated into spherical and deviator components

$$d\varepsilon_{ij} = d\varepsilon^0_{ij} + de_{ij}. \tag{2—61}$$

Relating the strain increments to the time increments we can formally pass from increments $d\varepsilon_{ij}$ to *strain rates* $\dot{\varepsilon}_{ij}$. The *strain rate tensor* has the form

$$\dot{\varepsilon}_{ij} = \frac{d\varepsilon_{ij}}{dt} = \begin{pmatrix} \dot{\varepsilon}_{xx} & \dot{\varepsilon}_{xy} & \dot{\varepsilon}_{xz} \\ \dot{\varepsilon}_{yx} & \dot{\varepsilon}_{yy} & \dot{\varepsilon}_{yz} \\ \dot{\varepsilon}_{zx} & \dot{\varepsilon}_{zy} & \dot{\varepsilon}_{zz} \end{pmatrix}. \tag{2—62}$$

Similarly, one can introduce the *velocity*

$$v_i = \frac{du_i}{dt} = \dot{u}_i \tag{2—63}$$

and then eq. (2—60) yields

$$\dot{\varepsilon}_{ij} = \frac{1}{2}(v_{i,j} + v_{j,i}). \tag{2—64}$$

Since time does not appear as an explicit variable in the fundamental equations of plasticity, in these equations increments and velocities can be used equivalently. We will mostly use strain increments, except in a few chapters where the use of strain rates and velocities is more convenient.

Finally, introducing strain increments and strain rates one has to deal with *stress increments* and *stress rates*, as well. For example, the *stress increment tensor* is of the form

$$d\sigma_{ij} = \begin{pmatrix} d\sigma_{xx} & d\sigma_{xy} & d\sigma_{xz} \\ d\sigma_{yx} & d\sigma_{yy} & d\sigma_{yz} \\ d\sigma_{zx} & d\sigma_{zy} & d\sigma_{zz} \end{pmatrix}. \tag{2—65}$$

2.2.7. KINEMATIC EQUATIONS. COMPATIBILITY EQUATIONS

As was shown in Section 2.2.1. the elements of the strain tensor are not independent from each other. The strain tensor is symmetric

$$\varepsilon_{ij} = \varepsilon_{ji} \tag{2—66}$$

and according to eq. (2—42) the strains and displacements have the following relationships

$$\left.\begin{aligned}
&\varepsilon_{xx}=\frac{\partial u_x}{\partial x},\quad \varepsilon_{yy}=\frac{\partial u_y}{\partial y},\quad \varepsilon_{zz}=\frac{\partial u_z}{\partial z},\\
&\varepsilon_{xy}=\frac{1}{2}\left(\frac{\partial u_x}{\partial y}+\frac{\partial u_y}{\partial x}\right),\\
&\varepsilon_{yz}=\frac{1}{2}\left(\frac{\partial u_y}{\partial z}+\frac{\partial u_z}{\partial y}\right),\\
&\varepsilon_{xz}=\frac{1}{2}\left(\frac{\partial u_x}{\partial z}+\frac{\partial u_z}{\partial x}\right),
\end{aligned}\right\}\qquad \varepsilon_{ij}=\frac{1}{2}(u_{i,j}+u_{j,i}). \tag{2—67}$$

These are called *strain–displacement* or *kinematic equations.**

On certain parts of the surface of the body under consideration the displacements u_i^0 may be prescribed (see Fig. 2—5). The displacements u_i then have to satisfy the *kinematic boundary conditions*

$$u_i=u_i^0. \tag{2—68}$$

In the case of *cylindrical coordinates* r, φ, z eqs (2—67) have the form

$$\left.\begin{aligned}
&\varepsilon_{rr}=\frac{\partial u_r}{\partial r},\quad \varepsilon_{\varphi\varphi}=\frac{u_r}{r}+\frac{\partial u_\varphi}{r\partial\varphi},\quad \varepsilon_{zz}=\frac{\partial u_z}{\partial z},\\
&\varepsilon_{r\varphi}=\frac{1}{2}\left(\frac{\partial u_r}{r\partial\varphi}+\frac{\partial u_\varphi}{\partial r}-\frac{u_\varphi}{r}\right),\\
&\varepsilon_{\varphi z}=\frac{1}{2}\left(\frac{\partial u_\varphi}{\partial z}+\frac{\partial u_z}{r\partial\varphi}\right),\quad \varepsilon_{rz}=\frac{1}{2}\left(\frac{\partial u_r}{\partial z}+\frac{\partial u_z}{\partial r}\right).
\end{aligned}\right\} \tag{2—67a}$$

Using *spherical coordinates* r, φ, θ and considering only *point-symmetrical* problems, when $\varphi\equiv\theta$ and $\varepsilon_{r\varphi}=\varepsilon_{\varphi\theta}=\varepsilon_{r\theta}=0$, eqs (2—32) become

$$\varepsilon_{rr}=\frac{\partial u_r}{\partial r},\quad \varepsilon_{\varphi\varphi}=\varepsilon_{\theta\theta}=\frac{u_r}{r}. \tag{2—67b}$$

It is obvious, that if the displacements are specified as continuous functions of the coordinates then the strains can be determined from eqs (2—67) uniquely. However, in the case of the reverse problem, i.e. when the strains are specified and the displacements are to be determined, two problems arise. Firstly, the solution cannot be unique since the strains do not represent rigid body motions which are included in the displacements. However, specifying the translation and rotation at some point in the body makes the solution, at least from this point of view, unique.

The second problem arises from the fact that there are six equations (2—67) for the three unknown displacement components u_x, u_y and u_z, and therefore these equations

* One has to emphasize that these relationships are valid only in the case of *small deformations*; this assumption was made clear in the introduction to this book.

do not have a unique solution for any arbitrarily chosen strains. To illustrate the physical content of this problem, assume that the body is divided into infinitesimal cubes. If the cubes are separated from each other and undergo arbitrary deformations we will not be able, in general, to fit all the cubes back together to produce a continuous body without any gaps. This shows that there must be some relationships between the strains in order for the body to remain continuous, i.e. for the displacements be continuous functions of the coordinates. These relationships can be obtained by eliminating the displacements from eqs (2—67). Omitting the details one obtains (see e.g. Sokolnikoff 1956):

$$
\left.
\begin{aligned}
&\frac{\partial^2 \varepsilon_{xx}}{\partial y^2} + \frac{\partial^2 \varepsilon_{yy}}{\partial x^2} = 2\frac{\partial^2 \varepsilon_{xy}}{\partial x \partial y} \\
&\frac{\partial^2 \varepsilon_{yy}}{\partial z^2} + \frac{\partial^2 \varepsilon_{zz}}{\partial y^2} = 2\frac{\partial^2 \varepsilon_{yz}}{\partial y \partial z} \\
&\frac{\partial^2 \varepsilon_{zz}}{\partial x^2} + \frac{\partial^2 \varepsilon_{xx}}{\partial z^2} = 2\frac{\partial^2 \varepsilon_{xz}}{\partial x \partial z} \\
&\frac{\partial}{\partial x}\left(-\frac{\partial \varepsilon_{yz}}{\partial x} + \frac{\partial \varepsilon_{zx}}{\partial y} + \frac{\partial \varepsilon_{xy}}{\partial z}\right) = \frac{\partial^2 \varepsilon_{xx}}{\partial y \partial z} \\
&\frac{\partial}{\partial y}\left(-\frac{\partial \varepsilon_{zx}}{\partial y} + \frac{\partial \varepsilon_{xy}}{\partial z} + \frac{\partial \varepsilon_{yz}}{\partial x}\right) = \frac{\partial^2 \varepsilon_{yy}}{\partial z \partial x} \\
&\frac{\partial}{\partial z}\left(-\frac{\partial \varepsilon_{xy}}{\partial z} + \frac{\partial \varepsilon_{yz}}{\partial x} + \frac{\partial \varepsilon_{zx}}{\partial y}\right) = \frac{\partial^2 \varepsilon_{zz}}{\partial x \partial y}.
\end{aligned}
\right\} \qquad (2—69)
$$

These relationships are called the *compatibility* or *continuity equations* and represent the necessary and sufficient conditions for the strains to yield continuous deformations.

Finally, it should be emphasized again that the kinematic and compatibility equations are independent of the material properties and therefore are valid for bodies made of any kind of material.

2.3. STRESS–STRAIN RELATIONS

It is evident from our investigations so far that the equilibrium equations (2—32) and the kinematic equations (2—67) do not determine uniquely the stresses, strains and displacements in a body. Further equations are needed to obtain unique solutions of the problem; we have to construct the *stress–strain relations*, usually called the *constitutive equations*. These equations depend on the material properties and therefore should be separately derived for elastic and elasto-plastic bodies. In the case of elasto-plastic bodies, a key problem is to define the ranges of validity both of the elastic constitutive equation and of the plastic constitutive equation. This can be done by introducing the concept of yield conditions. As will be shown, yield conditions also play a fundamental role in deriving the plastic constitutive equations.

2.3.1. CONSTITUTIVE EQUATIONS FOR LINEARLY ELASTIC, ISOTROPIC BODIES

The stress–strain relations of linearly elastic, isotropic bodies is described by the generalized *Hooke's Law*

$$\left.\begin{aligned}
\varepsilon_{xx} &= \frac{1}{E}[\sigma_{xx} - \nu(\sigma_{yy} + \sigma_{zz})] = \frac{1}{E}[(1+\nu)\sigma_{xx} - \nu s], \\
\varepsilon_{yy} &= \frac{1}{E}[\sigma_{yy} - \nu(\sigma_{xx} + \sigma_{zz})] = \frac{1}{E}[(1+\nu)\sigma_{yy} - \nu s], \\
\varepsilon_{zz} &= \frac{1}{E}[\sigma_{zz} - \nu(\sigma_{xx} + \sigma_{yy})] = \frac{1}{E}[(1+\nu)\sigma_{zz} - \nu s], \\
\varepsilon_{xy} &= \frac{1}{2G}\sigma_{xy}, \quad \varepsilon_{yz} = \frac{1}{2G}\sigma_{yz}, \quad \varepsilon_{xz} = \frac{1}{2G}\sigma_{xz},
\end{aligned}\right\} \tag{2—70}$$

or, in a briefer notation,

$$\varepsilon_{ij} = \frac{1}{E}[(1+\nu)\sigma_{ij} - \nu\sigma_{kk}\delta_{ij}].$$

Here E, G and ν are the *Young's modulus*, the *shear modulus* and the *Poisson's ratio* of the material, respectively, and $s = \sigma_{kk}$ is defined by eq. (2—18). E, G and ν are not independent of each other; they satisfy the relationship

$$G = \frac{E}{2(1+\nu)}. \tag{2—71}$$

Using the stress deviator and the strain deviator tensors, *Hooke's Law* can be expressed in a simpler form

$$\left.\begin{aligned}
e_{xx} &= \frac{1}{2G}s_{xx}, \quad e_{xy} = \frac{1}{2G}s_{xy}, \\
e_{yy} &= \frac{1}{2G}s_{yy}, \quad e_{yz} = \frac{1}{2G}s_{yz}, \\
e_{zz} &= \frac{1}{2G}s_{zz}, \quad e_{xz} = \frac{1}{2G}s_{xz},
\end{aligned}\right\} \quad e_{ij} = \frac{1}{2G}s_{ij}. \tag{2—72}$$

In addition, we have the relationship

$$\varepsilon_m = \frac{1-2\nu}{E}\sigma_m = \frac{\sigma_m}{3K}, \tag{2—73}$$

where

$$K = \frac{E}{3(1-2\nu)} \tag{2—71a}$$

is called the *bulk modulus*. Equation (2—73) makes possible the calculation of stresses and strains from the stress and strain deviator and hydrostatic components.

Sometimes it is convenient to consider the stress and strain components as the elements of a *stress vector* $\sigma_\alpha(\sigma_{xx}\,\sigma_{yy}\,\sigma_{zz}\,\sigma_{xy}\,\sigma_{yz}\,\sigma_{xz})$ and a *strain vector* $\varepsilon_\alpha(\varepsilon_{xx}\,\varepsilon_{yy}\,\varepsilon_{zz}\,\varepsilon_{xy}\,\varepsilon_{yz}\,\varepsilon_{xz})$. Then Hooke's Law has the form

$$\varepsilon_\alpha = H_{\alpha\beta}\sigma_\beta$$

or

$$\sigma_\alpha = (H_{\alpha\beta})^{-1}\varepsilon_\beta = D_{\alpha\beta}\varepsilon_\beta, \tag{2—70a}$$

where

$$H_{\alpha\beta} = \frac{1}{E}\begin{pmatrix} 1 & -\nu & -\nu & . & . & . \\ -\nu & 1 & -\nu & . & . & . \\ -\nu & -\nu & 1 & . & . & . \\ . & . & . & (1+\nu) & . & . \\ . & . & . & . & (1+\nu) & . \\ . & . & . & . & . & (1+\nu) \end{pmatrix} \tag{2—74}$$

$$D_{\alpha\beta} = \frac{\lambda}{\nu}\begin{pmatrix} (1-\nu) & \nu & \nu & . & . & . \\ \nu & (1-\nu) & \nu & . & . & . \\ \nu & \nu & (1-\nu) & . & . & . \\ . & . & . & (1-2\nu) & . & . \\ . & . & . & . & (1-2\nu) & . \\ . & . & . & . & . & (1-2\nu) \end{pmatrix} \tag{2—75}$$

and

$$\lambda = \frac{\nu E}{(1+\nu)(1-2\nu)} \tag{2—71b}$$

is the *Lamé's modulus* of the material.

Finally, it should be noted that in the most general case Hooke's Law can be expressed in the form

$$\varepsilon_{ij} = H_{ijkl}\sigma_{kl} \quad \text{or} \quad \sigma_{ij} = (H_{ijkl})^{-1}\varepsilon_{kl} = D_{ijkl}\varepsilon_{kl}, \tag{2—70b}$$

where H_{ijkl} and D_{ijkl} are fourth-order symmetric tensors.* In the case of isotropic materials D_{ijkl}, for example, has the form (see e.g. Hearmon (1961), Flügge (1972)):

$$D_{ijkl}=\frac{\lambda}{\nu}\left[\nu\delta_{ij}\delta_{kl}+\frac{1}{2}(1-2\nu)(\delta_{ik}\delta_{jl}+\delta_{il}\delta_{jk})\right]. \tag{2—75a}$$

Here δ_{ij} denotes the *Kronecker delta.*

2.3.2. YIELD CONDITIONS FOR PERFECTLY PLASTIC MATERIALS

In case of elasto-plastic materials, the validity of Hooke's Law is limited by the occurrence of plastic deformations. When the material starts to yield, Hooke's Law should be replaced by the constitutive equations of plastic bodies. It is a key problem in the theory of plasticity to construct mathematical criteria for defining the range of validities of Hooke's Law and the constitutive equations of plastic bodies. These criteria are called *yield criteria* or *yield conditions.*

In this chapter we will deal only with the yield conditions of *perfectly plastic materials.* The yield conditions of strain hardening and granular materials will be presented in sections 8.1. and 8.2.

2.3.2.1. GENERAL REMARKS

In case of a uniaxial state of stress at a point it is easy to define the stresses at which the material behaves elastically or starts to yield. Introducing the function

$$f=\sigma^2-\sigma_0^2$$

the conditions $f<0$ and $f=0$ define the elastic and plastic ranges of the material, respectively. In the case of perfectly plastic materials the *yield stress* σ_0 cannot be exceeded. Thus, a state of stress for which $f>0$ is considered physically impossible.

The multi-axial state of stress at a point is characterized by the six independent elements of the stress tensor σ_{ij}. When the stresses are small, the material behaves elastically but at certain levels and combinations of stresses plastic deformations occur. To distinguish between these two ranges, we have to construct a mathematical relationship which defines all the possible combinations of stresses delineating the ranges of elastic and plastic behaviour of the material. This relationship is called the *yield condition.*

The yield condition for multi-axial states of stress in perfectly plastic materials can be described by a *yield function* f such that

in the elastic range $\quad f<0,$

in the plastic range $\quad f=0$

and stress states for which $f>0$ are considered physically impossible.

* In the case of *anisotropic* materials these tensors contain 21 independent material constants (Sokolnikoff 1956). Considering *orthotropic* materials, the number of independent constants can be reduced to 9, while in the *isotropic* case we have only 2 independent material constants, as is shown above.

In the general case, the yield function can be expressed in the form

$$f = f(\sigma_{ij}, \varepsilon_{ij}, \dot{\sigma}_{ij}, \dot{\varepsilon}_{ij}, x_i, T, t),$$

where T and t denote the temperature and the time, respectively. In order to obtain relatively simple yield functions we have to introduce simplifying assumptions generally used in the theory of the strength of materials.

First, we assume that the body under consideration is homogeneous and its material properties are *time- and temperature-independent*. Consequently, the yield function does not depend on the coordinates x_i, the temperature T, the time t and the time derivatives $\dot{\sigma}_{ij}$ and $\dot{\varepsilon}_{ij}$ of stresses and strains, respectively.

Furthermore, we assume that the material properties of perfectly plastic bodies are independent of any elastic or plastic deformations which previously occurred: i.e. the yield function is *path-independent* and can be expressed merely in terms of the *instantaneous stresses* and an appropriate constant k representing the plastic properties of the material (e.g. the yield stress)

$$f = f(\sigma_{ij}, k). \tag{2—76}$$

If we assume that the material is *isotropic* then the material properties are the same in any direction and therefore the material constants are independent of the transformation of coordinates. Consequently, the yield function can be expressed simply in terms of the invariants of the stress tensor or in terms of the principal stresses

$$f = f(I_1, I_2, I_3) \quad \text{or} \quad f = f(\sigma_I, \sigma_{II}, \sigma_{III}). \tag{2—77}$$

According to experiments conducted with metals (Lode 1926), the hydrostatic compression or tension, at least up to the level of stresses that occur in most engineering problems, does not cause significant plastic deformation. Therefore the spherical component of the stress tensor can be omitted from the yield condition. Consequently, the yield function can be expressed in terms of the invariants $K_1 = 0$, K_2, K_3 of the stress deviator tensor

$$f = f(K_2, K_3, k). \tag{2—78}$$

In order to study the properties of the yield function above, consider the *three-dimensional principal stress space* shown in Fig. 2—8. In this space, the stress state is illustrated by a stress vector $\sigma_\alpha(\sigma_I\, \sigma_{II}\, \sigma_{III})$. The line OM making equal angles with the coordinate axes has the property that for every point on it the stress state is one for which $\sigma_I = \sigma_{II} = \sigma_{III} = \sigma_m$. Thus, every point on this line corresponds to a spherical (hydrostatic) stress state. Consider now the plane S passing through the origin perpendicular to the line OM. The equation of this plane is $\sigma_I + \sigma_{II} + \sigma_{III} = 0$, where $\sigma_I + \sigma_{II} + \sigma_{III}$ denotes the first invariant of the stress tensor. According to eq. (2—25), in the case of the stress deviator this invariant is equal to zero; therefore any point of the plane $\sigma_I + \sigma_{II} + \sigma_{III} = 0$ represents a deviatoric stress state. Now any arbitrary stress vector σ_α can be decomposed into a component σ_m parallel to the line OM and into another component σ_d in the plane S. These two components represent the spherical and deviatoric components of the stress state.

The yield condition $f(\sigma_I, \sigma_{II}, \sigma_{III}, k) = 0$ can now be represented in the principal stress space by a surface called the *yield surface*. The domain bounded by this surface is the

feasible domain of perfectly plastic materials. If the stress vector σ_α is inside this domain, the point in the body under consideration is in the elastic range. If the stress vector reaches the yield surface, plastic deformations may occur. Those stress states for which the stress vector passes through the yield surface are considered physically impossible.

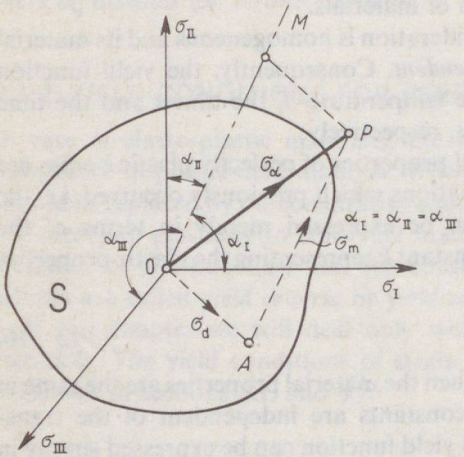


Fig. 2–8

Since it has been assumed that the yield condition is independent of the hydrostatic stress state, the addition of any hydrostatic stress state to the existing one does not influence the occurrence of yielding. Consequently, the yield surface must be open in the direction of the line OM, i.e. it is a *cylinder* with generators parallel to OM (Fig. 2—9(a)). This cylinder is entirely defined by the curve C obtained by the intersection of the cylinder with the plane S. This curve is called the *yield locus*. We will now study the properties of this locus.

Generally, the yield surface is *closed*. If we assume, however, that a special stress state does not cause plastic deformations, then the yield surface is open in the corresponding direction. This was the case that we studied above, when we assumed that the hydrostatic stress state does not play any role in the yield conditions. Even in these special cases, however, the yield locus must be a closed curve.

Figure 2—9(b) shows the yield locus and the projections of the axes σ_I, σ_{II}, σ_{III} upon the plane S. These projections, denoted by $\bar{\sigma}_I$, $\bar{\sigma}_{II}$ and $\bar{\sigma}_{III}$, make equal angles with each other, namely 120°. It can be shown that the yield locus has the same shape in each of the twelve 30° sectors as shown in Fig. 2—9(b). Because of the isotropy of the material the stresses σ_I, σ_{II} and σ_{III} are interchangeable; therefore the yield locus must be symmetric about the line a–a bisecting the angles between the axes $\bar{\sigma}_I$, $\bar{\sigma}_{II}$ and $\bar{\sigma}_{III}$. Furthermore, we have assumed that the yield stress is the same in tension and in compression. Therefore, a change in the sign of the stresses should not affect the plastic behaviour of the material. Consequently, the yield locus must have a symmetry about the lines b–o perpendicular to the axes $\bar{\sigma}_I$, $\bar{\sigma}_{II}$ and $\bar{\sigma}_{III}$. This leads to the conclusion that the twelve 30° sectors of the yield locus must have the same shape.

The yield surface and the yield locus have another important property: they are *convex*. This problem will be discussed in Section 2.3.3.

The determination of the yield loci and the yield conditions of different materials can be based on experimental results and theoretical considerations. A description of the great number of experiments conducted with different kinds of materials to investigate their plastic behaviour is beyond the scope of this book. In the next two sections, we will present only two yield conditions widely used in engineering practice for metals. Both are based on the assumptions described above and are called the *Huber–v. Mises–Hencky* and *Tresca yield conditions*. In Chapter 8 other yield conditions will also be presented.

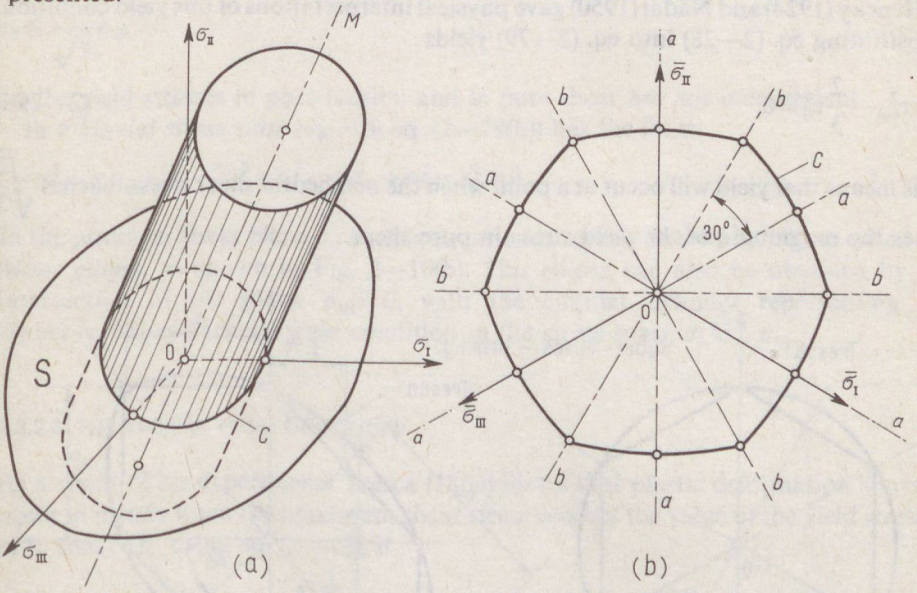


Fig. 2–9

2.3.2.2. THE HUBER—V. MISES—HENCKY YIELD CONDITION

Huber (1904), v. Mises (1913) and Hencky (1924) independently proposed a yield condition which can be defined as

$$f = K_2 - \tau_0^2 = 0. \tag{2—79}$$

Here τ_0 is the *yield stress in pure shear*.* Using eqs (2—26) and (2—27), this yield condition can be expressed in different forms

$$f = \frac{1}{6}[(\sigma_{xx}-\sigma_{yy})^2+(\sigma_{yy}-\sigma_{zz})^2+(\sigma_{xx}-\sigma_{zz})^2]+$$

$$+\sigma_{xy}^2+\sigma_{yz}^2+\sigma_{xz}^2-\tau_0^2=0, \tag{2—79a}$$

* Pure shear can be produced by the torsion of thin-walled tubes to determine the yield stess τ_0 experimentally.

$$f=\frac{1}{6}[(\sigma_{\mathrm{I}}-\sigma_{\mathrm{II}})^2+(\sigma_{\mathrm{II}}-\sigma_{\mathrm{III}})^2+(\sigma_{\mathrm{I}}-\sigma_{\mathrm{III}})^2]-\tau_0^2=0, \tag{2—79b}$$

$$f=\frac{1}{2}s_{ij}s_{ij}-\tau_0^2=0. \tag{2—79c}$$

The yield surface given by eq. (2—79(b)) in the principal stress space is a *circular cylinder*, and the yield locus is a *circle* with radius $r=\frac{\sqrt{3}}{2}\tau_0$, as it is shown in Fig. 2—10(a).

Hencky (1924) and Nádai (1950) gave physical interpretations of this yield condition. Substituting eq. (2—28) into eq. (2—79) yields

$$f=\tau_{\mathrm{oct}}^2-\frac{2}{3}\tau_0^2=0. \tag{2—79d}$$

This means that yield will occur at a point when the octahedral shear stress reaches $\sqrt{\frac{2}{3}}$ times the magnitude of the yield stress in pure shear.

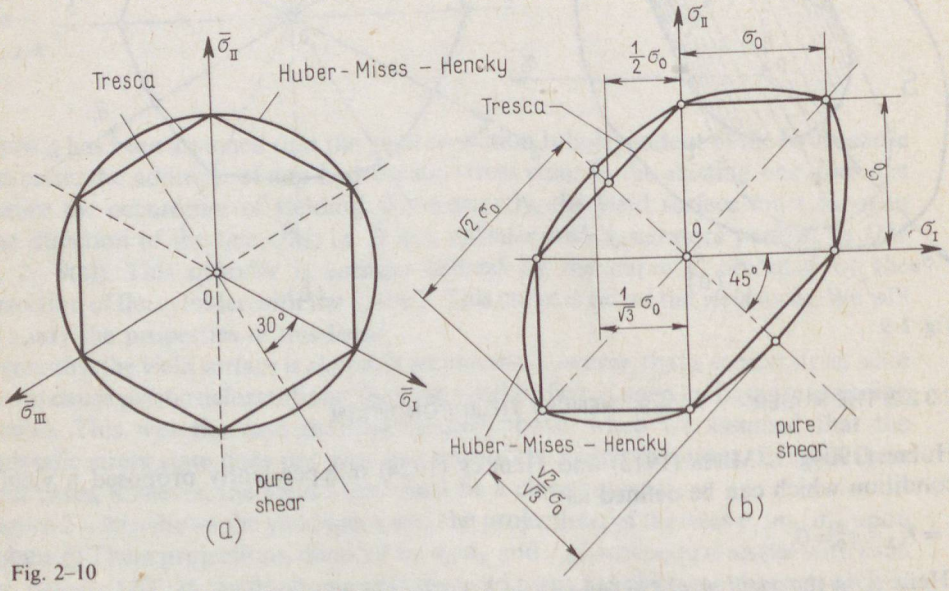


Fig. 2–10

Alternatively, the specific elastic distortion energy calculated from the components of the stress deviator tensor is equal to $U_{\mathrm{d}}=\frac{1}{2G}K_2$. Consequently, eq. (2—79) can be written as

$$f=U_{\mathrm{d}}-\frac{1}{2G}\tau_0^2=0. \tag{2—79e}$$

That is, yield will occur at a point when the specific elastic distortion energy reaches the value $\frac{1}{2G}\tau_0^2$. Hence, this theory is also called the *distortion energy theory.*

In a *uniaxial stress state* ($\sigma_{II}=\sigma_{III}=0$) the yield condition leads to

$$f=\sigma_I^2-3\tau_0^2=0. \tag{2—80}$$

In pure tension or compression, however, yield occurs when the stress reaches the yield stress in pure tension, i.e. $\sigma_I=\sigma_0$. Substituting this value in eq. (2—80), we obtain a relationship between the two yield stresses

$$\tau_0=\frac{1}{\sqrt{3}}\sigma_0, \tag{2—81}$$

i.e. the yield stresses in pure tension and in pure shear are not independent.

In a *biaxial stress state* ($\sigma_{III}=0$) eq. (2—79(b)) has the form

$$f=\sigma_I^2-\sigma_I\sigma_{II}+\sigma_{II}^2-3\tau_0^2=\sigma_I^2-\sigma_I\sigma_{II}+\sigma_{II}^2-\sigma_0^2=0. \tag{2—82}$$

In the principal stress plane σ_I, σ_{II} this equation is represented by an ellipse called the *Mises ellipse*, as shown in Fig. 2—10(b). This ellipse can also be obtained by the intersection of the plane $\sigma_{III}=0$, with the circular cylinder representing the Huber–v. Mises–Hencky yield condition in the stress space σ_I, σ_{II}, σ_{III}.

2.3.2.3. THE TRESCA YIELD CONDITION

As a result of his experiments Tresca (1864) found that plastic deformation starts to occur in metals when the maximum shear stress reaches the value of the yield stress in pure shear i.e., using eq. (2—15), if

$$f=|\tau_{max}|-\tau_0=\frac{1}{2}|\sigma_I-\sigma_{III}|-\tau_0=0. \tag{2—83}$$

Because of its physical content this theory is also called the *maximum shear stress theory.*

Equation (2—83) holds only in the case when the relationship $\sigma_I\leq\sigma_{II}\leq\sigma_{III}$ is satisfied. Generally, however, the sequence of magnitudes of the principal stresses is not known *a priori*; therefore using eqs (2—14) and eliminating the signs of absolute magnitude the Tresca yield condition assumes the following general form

$$\left.\begin{aligned} f_1&=(\sigma_{II}-\sigma_{III})^2-4\tau_0^2=0,\\ f_2&=(\sigma_I-\sigma_{III})^2-4\tau_0^2=0,\\ f_3&=(\sigma_I-\sigma_{II})^2-4\tau_0^2=0. \end{aligned}\right\} \tag{2—83a}$$

Plastic deformation will occur at a point in a body if at least one of eqs (2—83(a)) is satisfied. Formally, this condition can be expressed by a single yield condition

$$f=f_1f_2f_3=[(\sigma_{II}-\sigma_{III})^2-4\tau_0^2][(\sigma_I-\sigma_{III})^2-4\tau_0^2][(\sigma_I-\sigma_{II})^2-4\tau_0^2]. \tag{2—83b}$$

Finally, the Tresca yield condition can be expressed in terms of the invariants of the stress deviator tensor

$$4K_2^3-27K_3^2-36\tau_0^2K_2^2+96\tau_0^4K_2-64\tau_0^6=0. \tag{2—83c}$$

In the principal stress space the yield surface given by eqs (2—83a) is a *regular hexagonal cylinder* and the yield locus is a *regular hexagon*, as shown in Fig. 2—10(a).

In a *uniaxial stress state* ($\sigma_{II}=\sigma_{III}=0$), the yield condition becomes

$$f=\sigma_I^2-4\tau_0^2=0. \tag{2—84}$$

In pure tension or compression, however, yield occurs when the stress reaches the yield stress in pure tension, i.e. $\sigma_I=\sigma_0$. Substituting this value in eq. (2—84), we obtain a relationship between the yield stresses in pure tension and shear

$$\tau_0=\frac{1}{2}\sigma_0. \tag{2—85}$$

This result differs from that of the Huber–v. Mises–Hencky yield condition given by eq. (2—81). The discrepancy between the two theories can be decreased if the radius representing the Huber–v. Mises–Hencky yield condition is chosen to be the average value of the radii corresponding to the circles inscribing and circumscribing the Tresca hexagon. The discrepancy between the two theories for any possible stress state will then be less than 15.5%.

In a *biaxial stress state* ($\sigma_{III}=0$), by the use of relationship (2—85) eq. (2—83a) becomes

$$\left.\begin{aligned} f_1&=\sigma_{II}^2-\sigma_0=0,\\ f_2&=\sigma_I^2-\sigma_0=0,\\ f_3&=(\sigma_I-\sigma_{II})^2-\sigma_0=0. \end{aligned}\right\} \tag{2—86}$$

In the principal stress plane σ_I, σ_{II} this equation is represented by a hexagon called the *Tresca hexagon*, shown in Fig. 2—10(b). This hexagon can also be obtained as the intersection of the plane $\sigma_{III}=0$ with the hexagonal cylinder representing the Tresca yield condition in the stress space σ_I, σ_{II}, σ_{III}.

2.3.2.4. COMPARISON OF YIELD CONDITIONS

From a theoretical point of view, the main difference between the Huber–v. Mises–Hencky and Tresca yield conditions is the fact that in the former all three principal stresses play equal roles, while in the latter the intermediate principal stress has no effect on yielding. To study this problem Lode (1926) conducted the first experiments with steel, copper and nickel thin-walled tubes under various combinations of longitudinal tension and internal pressure. Briefly, (see e.g. Mendelson 1968) Lode found that experimental results favour the Huber–v. Mises–Hencky yield condition. Similar results were found by Taylor and Quinney (1931), who conducted experiments with steel and copper tubes under axial tension and torsion. A large number of other experimental studies can be found in the literature (see e.g. Nádai 1950).

Both in the theory of plasticity and in engineering practice, the Huber–v. Mises–Hencky and the Tresca yield conditions are equally used for the analysis of metals. The advantage of the Huber–v. Mises–Hencky yield condition is that it is described by a single function; its disadvantage is that this function is nonlinear. The Tresca yield condition, on the other hand, can be defined only by three functions which are, however, linear. In analytical solutions the use of three yield functions causes difficulties. There are, however, special problems where the orientation of the principal axes at each point are known *a priori* (e.g. in the case of rotational and point-symmetrical problems); then the Tresca yield condition involves relatively simple calculations. Finally, there are cases where the two yield conditions are identical as, for example, in the case of plane strain problems.

2.3.3. CONSTITUTIVE EQUATIONS FOR LINEARLY ELASTIC–PERFECTLY PLASTIC BODIES

2.3.3.1. GENERAL RELATIONSHIPS

We have already discussed conditions which define the stress states at which plastic flow begins and Hooke's Law is no longer valid. The next task is to derive the stress-strain relationships for material in the plastic range. These relationships will generally be nonlinear. Another problem arises from the fact that, whereas in the elastic range the strains are uniquely determined by the stresses, in the plastic range the strains depend on the history of loading. Because of this path-dependence, only plastic strain increments can be related to the instantaneous stresses; to obtain the total strains, the strain increments must be integrated throughout the whole loading history.

First, consider the problem of determining the conditions at a point where the plastic range has been reached. In a uniaxial tension, if $\sigma = \sigma_0$ and $d\sigma = 0$, then plastic strains can develop but, if $\sigma = \sigma_0$ and $d\sigma < 0$, this corresponds to unloading and, therefore, only elastic deformations will take place. These statements can be generalized to the case of triaxial state of stress. That is, if $f = 0$ and $df = 0$, then the point under consideration remains in the plastic range and consequently can undergo plastic deformations, however, if $f = 0$ and $df < 0$, only elastic deformations will develop. As stated before, the case $f = 0$ and $df > 0$ is physically impossible.

The results described above can be summarized as follows:

only *elastic deformations* arise, if	$f < 0$ (elastic range) or $f = 0$ and $df < 0$ (passive plastic range; unloading)
plastic deformations can arise, if	$f = 0$ and $df = 0$ (active plastic range)

In what follows, we will deal with the case in which plastic deformations can develop, i.e. when $f = 0$ and $df = 0$. To take a general case consider a six-dimensional stress space

σ_{ij} and describe the stress state at a point in this space by a six-dimensional *stress vector** σ_{ij} $(\sigma_{xx}\ \sigma_{yy}\ \sigma_{zz}\ \sigma_{xy}\ \sigma_{yz}\ \sigma_{xz})$. The yield condition $f(\sigma_{ij},k)=0$ is represented in this stress space by a six-dimensional surface, called the *yield hypersurface*. In Fig. 2—11 the yield hypersurface is illustrated by a curve. Generally, when there are no special stress states of which the yield condition is independent, the yield hypersurface is *closed* and divides the stress space into two domains.** The entire set of points which are inside or on the surface (i.e. for which $f\leq 0$) define the *feasible domain* of stress states. A point inside the surface represents an elastic range and a point on the surface corresponds to plastic range. The domain outside the yield surface (i.e. for which $f>0$) is physically impossible.

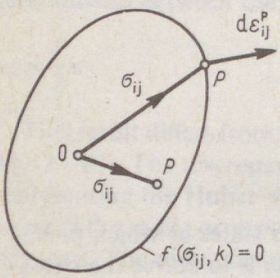


Fig. 2–11

Previously, in studying a uniaxial stress state, we decomposed the strain into elastic and plastic strain components: $\varepsilon=\varepsilon^e+\varepsilon^p$. It is a fundamental assumption of the theory of plasticity that this simplification can be generalized for three-dimensional states of strain. Hence, the strain tensor and the strain increment tensor can be decomposed into elastic and plastic strain components

$$\begin{aligned}\varepsilon_{ij}&=\varepsilon^e_{ij}+\varepsilon^p_{ij},\\ d\varepsilon_{ij}&=d\varepsilon^e_{ij}+d\varepsilon^p_{ij}.\end{aligned}\qquad(2—87)$$

Since the elastic stress-strain relationship is already known, our further investigations will be confined to the plastic component of the deformation.

As was done with stresses, consider a six-dimensional *strain space* coaxial with the stress space and describe the *plastic* strain state of a point in this space by a six-dimensional *plastic strain vector* ε^p_{ij} $(\varepsilon^p_{xx}\ \varepsilon^p_{yy}\ \varepsilon^p_{zz}\ \varepsilon^p_{xy}\ \varepsilon^p_{yz}\ \varepsilon^p_{xz})$. The *plastic strain increment vector* $d\varepsilon^p_{ij}$ $(d\varepsilon^p_{xx}\ d\varepsilon^p_{yy}\ d\varepsilon^p_{zz}\ d\varepsilon^p_{xy}\ d\varepsilon^p_{yz}\ d\varepsilon^p_{xz})$ can also be shown in this space, and as a free vector, can be attached to the end point of the corresponding *stress* vector. If $f<0$ no plastic deformations occur (i.e. $d\varepsilon^p_{ij}=0$): therefore plastic strain increment vectors correspond only to those stress vectors which touch the yield surface, as shown in Fig. 2—11.

* For convenience, the stress components will be considered to be the elements of a vector rather than the components of a tensor.

** It has already been mentioned that since the Huber–v.Mises–Hencky and the Tresca yield conditions are independent of the hydrostatic state of stress, they are illustrated by *open* cylinders.

To determine the increment vector $d\varepsilon_{ij}^{p}$, we have to return to the *stability postulate of materials* already discussed in the case of uniaxial stress (Drucker 1952a). Suppose we have a state of stress σ_{ij}^{A} statisfying the condition $f(\sigma_{ij}^{A},k)<0$; then some external agency applies an additional set of stresses and then removes it (Fig. 2—12(a)). During this action, the endpoint of the stress vector moves to points B and C on the yield surface and then returns to point A. According to the stability postulate, in the case of stable materials such as a perfectly plastic one, the net work done by the *additional* stresses $(\sigma_{ij}-\sigma_{ij}^{A})$ during the complete loading cycle A–B–C–A cannot be negative, i.e.

$$\oint(\sigma_{ij}-\sigma_{ij}^{A})d\varepsilon_{ij}=\oint(\sigma_{ij}-\sigma_{ij}^{A})d\varepsilon_{ij}^{e}+\oint(\sigma_{ij}-\sigma_{ij}^{A})d\varepsilon_{ij}^{p}\geqq 0. \qquad (2—88)$$

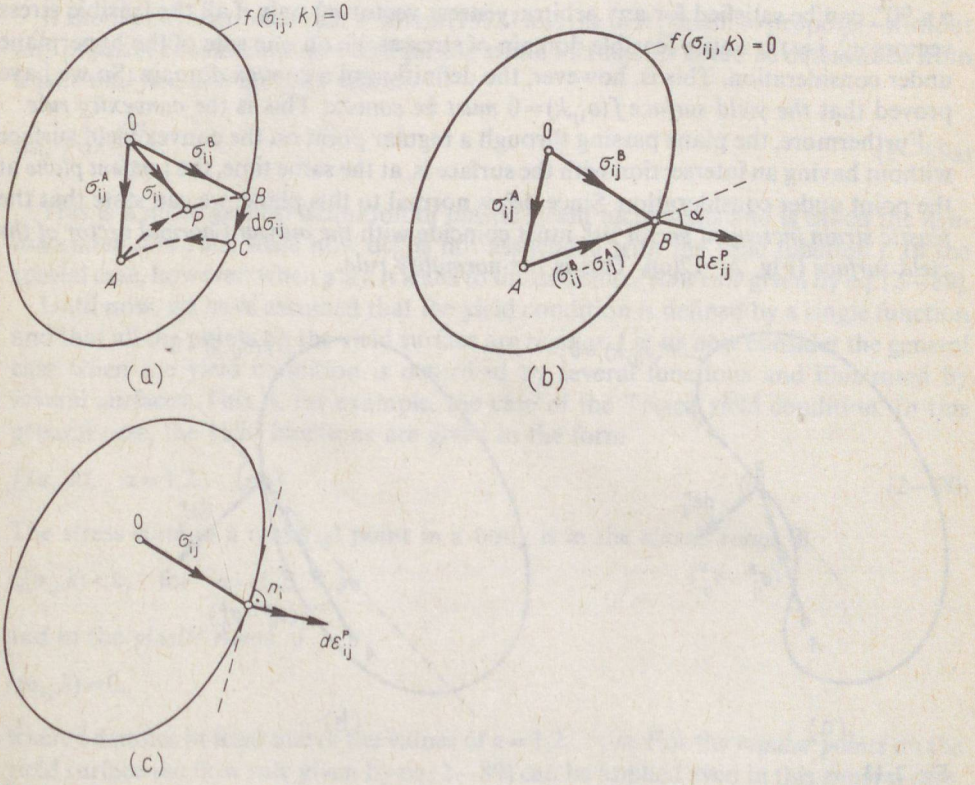


Fig. 2–12

In a complete loading cycle, however, the total elastic energy is restored and so the work done on the elastic deformations is equal to zero; therefore the first term can be omitted from the above equation. Plastic deformations, on the other hand, develop only in that range of stresses which is represented by the line BC on the yield surface. Let us suppose that the points B and C are *regular points* on the yield surface and that the distance between them, i.e. the stress increment $d\sigma_{ij}$, is infinitesimally small. Then the corresponding plastic strain increment vector $d\varepsilon_{ij}^{p}$ can be assumed constant and

also infinitesimal, and therefore the work $d\sigma_{ij}d\varepsilon^p_{ij}$ can be omitted from eq. (2—88) as negligibly small. Thus, the stability postulate can be expressed in the simple form

$$(\sigma^B_{ij}-\sigma^A_{ij})d\varepsilon^p_{ij}\geqq 0. \qquad (2—88a)$$

This means that the angle α between the vectors $(\sigma^B_{ij}-\sigma^A_{ij})$ and $d\varepsilon^p_{ij}$ cannot be larger than 90° (Fig. 2—12(b)). In our considerations the stress vector σ^B_{ij} has a given position. Since the material is path-independent, the plastic strain increment can depend only on the instantaneous stress σ^B_{ij} and therefore it is also represented by a fixed but still unspecified vector $d\varepsilon^p_{ij}$ at the point B. The stress vector σ^A_{ij}, however, can be anywhere in the feasible domain of stresses. Let us consider now a hyperplane passing through the point B normal to the vector $d\varepsilon^p_{ij}$. It is obvious that eq. (2—88a), i.e. the condition $\alpha\leq 90°$, can be satisfied for any arbitrary stress vector σ^A_{ij} only if all the feasible stress vectors σ^A_{ij}, i.e. the entire feasible domain of stresses, lie on one side of the hyperplane under consideration. This is, however, the definition of a convex domain. So we have proved that *the yield surface* $f(\sigma_{ij},k)=0$ *must be convex*. This is the *convexity rule*.

Furthermore, the plane passing through a regular point on the convex yield surface without having an intersection with the surface is, at the same time, the *tangent plane* at the point under consideration. Since $d\varepsilon^p_{ij}$ is normal to this plane, we can state that the *plastic strain increment vector* $d\varepsilon^p_{ij}$ must coincide with *the outward normal vector of the yield surface* (Fig. 2—12(c)). This is the *normality rule*.

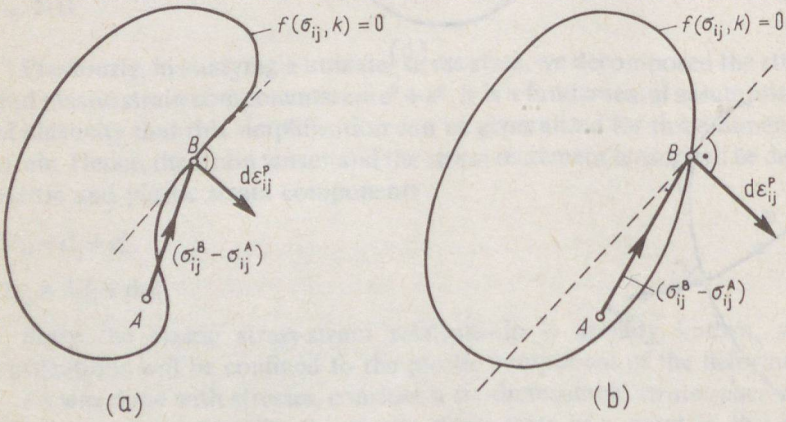


Fig. 2–13

Figures 2—13(a) and 2—13(b) show situations where the yield surface is not convex, or the vector $d\varepsilon^p_{ij}$ is not normal to the yield surface. It is obvious that these cases are impossible, since in both cases one can find points (e.g. points A in the Figures) for which the relation (2—88a) cannot be satisfied.

The outward normal vector n_i of the yield surface $f(\sigma_{ij},k)=0$ can be obtained as the gradient of the yield function

$$n_i=\frac{df}{\partial\sigma_{ij}}.$$

Consequently, the plastic strain increment vector can be expressed in the form

$$d\varepsilon_{ij}^{p} = d\lambda\, n_i = d\lambda \frac{\partial f}{\partial \sigma_{ij}}, \tag{2—89}$$

where $d\lambda$ is a *non-negative* unspecified scalar multiplier called the *plastic multiplier.*

Equation (2—89) is called the *flow rule* of plastic materials. According to this rule, *the yield function is the potential function of the plastic strain increments.* Because in eq. (2—89) $d\lambda$ is not specified, the flow rule does not uniquely define the plastic strain increment vector, but only gives its direction, i.e. the ratios of its components. The determination of the plastic multiplier $d\lambda$, which defines the magnitude of the plastic deformations, is a separate problem which will be presented later.

It should be mentioned that v. Mises (1928) was the first person to propose—without any physical considerations—that plastic strain increments could be determined from a *potential function* $g(\sigma_{ij})$ as follows

$$d\varepsilon_{ij}^{p} = d\lambda \frac{\partial g}{\partial \sigma_{ij}}. \tag{2—89a}$$

This is a more general definition of plastic strain increments and is called the *non-associated flow rule*, since now $d\varepsilon_{ij}^{p}$ is not associated with the yield function f. In the special case, however, when $g \equiv f$, it leads to the *associated flow rule* given by eq. (2—89).

Until now, we have assumed that the yield condition is defined by a single function and that all the points on the yield surface are *regular*. Let us now consider the general case when the yield condition is described by several functions and illustrated by several surfaces. This is, for example, the case of the Tresca yield condition. In this general case, the yield functions are given in the form

$$f_\alpha(\sigma_{ij}, k), \quad \alpha = 1,2,\ldots,m. \tag{2—90}$$

The stress state of a material point in a body is in the *elastic range*, if

$$f_\alpha(\sigma_{ij}, k) < 0, \quad \text{for} \quad \alpha = 1,2,\ldots,m$$

and in the *plastic range*, if

$$f_l(\sigma_{ij}, k) = 0,$$

where l denotes at least one of the values of $\alpha = 1,2,\ldots,m$. For the *regular points* on the yield surface the flow rule given by eq.(2—89) can be applied even in this general case. But now the yield surface has vertices and corners where the normal vector of the surface is not uniquely defined. Thus, at these *singular points*, the flow rule (2—98) cannot be used. This problem leads to the general formulation of the plastic flow rule (Koiter 1953) to be briefly presented next.

Let us consider a point S on a vertex formed by the intersection of two yield surfaces f_1 and f_2, as shown in a simplified manner in Fig. 2—14(a). When this singular point is approached along the surface f_1 then—until the point is reached—the relation

$$d\varepsilon_{ij1}^{p} = d\lambda_1 \frac{\partial f_1}{\partial \sigma_{ij}}, \quad d\lambda \geq 0$$

is valid. On the other hand, approaching the singular point along the surface f_2, the equation

$$d\varepsilon_{ij2}^p = d\lambda_2 \frac{\partial f_2}{\partial \sigma_{ij}}, \quad d\lambda_2 \geq 0$$

can be used. Since the plastic strain increment $d\varepsilon_{ij}^p$ corresponding to the state of stress defined by the point S must be independent of the loading path, both limit cases

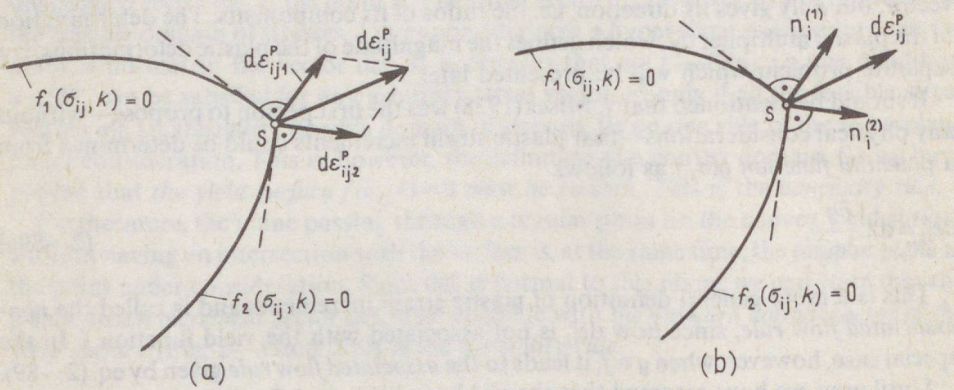


Fig. 2–14

described above must be incorporated into the general flow rule for the point S. This can be achieved if $d\varepsilon_{ij}$ is defined by the linear combination of these limit cases, i.e. if

$$d\varepsilon_{ij}^p = d\varepsilon_{ij1}^p + d\varepsilon_{ij2}^p = d\lambda_1 \frac{\partial f_1}{\partial \sigma_{ij}} + d\lambda_2 \frac{\partial f_2}{\partial \sigma_{ij}}, \quad d\lambda_1 \geq 0,\ d\lambda_2 \geq 0. \tag{2—91}$$

In the case of a hyper-corner formed by the intersection of several yield surfaces, the relationship eqs (2—91) can be generalized as*

$$d\varepsilon_{ij}^p = d\lambda_l \frac{\partial f_l}{\partial \sigma_{ij}}, \quad d\lambda_l \geqq 0. \tag{2—92}$$

In this generalized flow rule, the index l refers to the yield surfaces which contain the singular point, i.e. for which the condition

$$f_l(\sigma_{ij},k)=0 \tag{2—93}$$

is satisfied.

From a geometrical point of view, the generalized flow rule implies that at a singular point the plastic strain increment vector may have any direction, within the fan or hypercone formed by all the outward normals at all the points adjacent to the singular point. This is shown symbolically in Fig. 2—14(b).

* In eq.(2—92) the subscript l is repeated therefore the summation convention applies.

The flow rule presented above forms the fundamental basis for the derivation of the constitutive equations of perfectly plastic bodies. It can be associated with different yield conditions, so that several constitutive equations can be obtained. In the following, the most widely used constitutive equations which have been derived by Prandtl and Reuss and Lévy and Mises, respectively will be presented.

2.3.3.2. PRANDTL–REUSS AND LÉVY–V. MISES CONSTITUTIVE EQUATIONS

The constitutive equations of linearly elastic-perfectly plastic bodies, derived for plane problems by Prandtl (1924) and generalized for three dimensional problems by Reuss (1930) are based on the following assumptions:

(a) the material of the body is linearly elastic-perfectly plastic and obeys the Huber–v. Mises–Hencky yield condition (see eq. (2—79c))

$$f = \frac{1}{2} s_{ij} s_{ij} - \tau_0^2 = 0; \tag{2—94}$$

(b) the strains can be separated into elastic and plastic components

$$\varepsilon_{ij} = \varepsilon_{ij}^{e} + \varepsilon_{ij}^{p}; \tag{2—95}$$

(c) the permanent (plastic) change in volume is equal to zero

$$\varepsilon^{p} = 3\varepsilon_{m}^{p} = \varepsilon_{kk}^{p} = 0; \text{ and} \tag{2—96}$$

(d) the flow rule

$$\mathrm{d}\varepsilon_{ij}^{p} = \mathrm{d}\lambda \frac{\partial f}{\partial \sigma_{ij}} \tag{2—97}$$

applies to the derivation of the plastic strain increments.

Using these assumptions, the Prandtl–Reuss equations can be constructed as follows.

First, from eqs (2—51), (2—56) and (2—96), we obtain

$$\varepsilon_{ij}^{p} = e_{ij}^{p} + \frac{1}{3} \varepsilon_{kk}^{p} \delta_{ij} = e_{ij}^{p}.$$

Making use of this relationship, it can easily be shown that the flow rule (2—97) expressed in terms of the deviatoric components of stresses and strains has the form

$$\mathrm{d}e_{ij}^{p} = \mathrm{d}\lambda \frac{\partial f}{\partial s_{ij}}.$$

Substituting the yield condition eq. (2—94) into this relationship yields

$$\mathrm{d}e_{ij}^{p} = \mathrm{d}\lambda \frac{\partial f}{\partial s_{ij}} = \mathrm{d}\lambda s_{ij}. \tag{2—98}$$

For the elastic range of strains, Hooke's Law is valid, therefore applying eq. (2—72) to the elastic strain increments we obtain

$$de_{ij}^{e} = \frac{1}{2G} ds_{ij}. \tag{2—98a}$$

Finally, making use of the relationships eqs (2—98) and (2—98a) results in the following equation

$$de_{ij} = de_{ij}^{e} + de_{ij}^{p} = \frac{ds_{ij}}{2G} + d\lambda s_{ij} \tag{2—99}$$

or, in more detail,

$$\left.\begin{aligned} de_{xx} &= \frac{ds_{xx}}{2G} + d\lambda s_{xx}, \quad de_{xy} = \frac{ds_{xy}}{2G} + d\lambda s_{xy}, \\ de_{yy} &= \frac{ds_{yy}}{2G} + d\lambda s_{yy}, \quad de_{yz} = \frac{ds_{yz}}{2G} + d\lambda s_{yz}, \\ de_{zz} &= \frac{ds_{zz}}{2G} + d\lambda s_{zz}, \quad de_{xz} = \frac{ds_{xz}}{2G} + d\lambda s_{xz}. \end{aligned}\right\} \tag{2—99a}$$

In addition to these equations, a relationship can be derived for the mean stresses σ_m and mean strains ε_m which allows the calculation of the existing stresses and strains from their deviator components. To obtain this relationship, we simply have to consider eq. (2—96), which leads to $\varepsilon_m = \varepsilon_m^e + \varepsilon_m^p = \varepsilon_m^e$. Then eq. (2—73), derived for elastic strains, can be applied to the total strains and total strain increments

$$\varepsilon_m = \frac{\sigma_m}{3K}, \quad d\varepsilon_m = \frac{d\sigma_m}{3K}. \tag{2—100}$$

Equations (2—99) and (2—100) are *the Prandtl–Reuss constitutive equations of linearly elastic–perfectly plastic bodies.* On comparing these equations with the elastic stress-strain relationships, we can see that the main difference is that the Prandtl–Reuss equations are expressed in *incremental form* and are *nonlinear* because of the plastic multiplier $d\lambda$ (to be dicussed in the next section). They are, however, more general since they describe the elasto-plastic loading history of a body, as will be shown below.

(a) *In the elastic range* ($f < 0$) no plastic deformations develop therefore in eq. (2—99) $d\lambda = 0$. Then, by integration of the two sides of the equation the Hooke's Law can be obtained.

(b) *In the active plastic range* ($f = 0$ and $df = 0$) both elastic and plastic deformations can develop. Then $d\lambda$ can be expressed in terms of the current stresses or strains and eq. (2—99) can form the basis of the load history analysis of a body in the elasto-plastic range.

(c) *In the passive plastic range* (unloading) ($f = 0, df < 0$), no plastic deformations arise, therefore $d\lambda = 0$ in eq. (2—99). This again yields the incremental formulation of Hooke's Law. On integrating this equation, constants which represent the *permanent*

(*plastic*) *deformations* developed during the previous plastic states of the body should be introduced. To obtain the *total* deformation, an analysis of the entire loading history should be conducted.

Finally, we note that substituting $G \to \infty$ and $K \to \infty$ in the Prandtl–Reuss equations provides the constitutive equations of the rigid-perfectly plastic bodies. If $K \to \infty$, eq. (2—100) gives $\varepsilon_m = 0$, and this leads to $de_{ij} = d\varepsilon_{ij}$. Substituting this result and setting $G \to \infty$ in eq. (2—99), we obtain *the constitutive equations of rigid-perfectly plastic bodies*:

$$d\varepsilon_{ij} = d\lambda s_{ij}. \tag{2—99b}$$

These relationships are called the *Lévy–v. Mises constitutive equations* (Lévy 1870; v. Mises 1913).

2.3.3.3. THE PLASTIC MULTIPLIER $d\lambda$

In considering the plastic multiplier $d\lambda$, we have to emphasize that it is not a material constant but a scalar function which can be expressed in terms of the current stresses and strain increments at all points in the body, i.e. $d\lambda = d\lambda(\sigma_{ij}, d\varepsilon_{ij})$. Since the stresses and strains vary from point to point, and also change during the loading history, one can also say that $d\lambda$ is a function of the coordinates and some parameter which describes the loading procedure. This latter can be e.g. the intensity of the load or, in general, time. Then, one can write that $d\lambda = d\lambda(x_i, t)$.

It has already been shown that $d\lambda$ can then be non-zero only if

$$df = \frac{\partial f}{\partial \sigma_{ij}} d\sigma_{ij} = 0. \tag{2—101}$$

This equation forms the basis of the determination of $d\lambda$.

Starting with Hooke's Law, given by eq. (2—70b) we can express the stress increments in terms of the elastic strain increments

$$d\sigma_{ij} = D_{ijkl} d\varepsilon^e_{kl}.$$

Since $d\varepsilon^e_{ij} = d\varepsilon_{ij} - d\varepsilon^p_{ij}$, these two equations lead to

$$d\sigma_{ij} = D_{ijkl}(d\varepsilon_{kl} - d\varepsilon^p_{kl}).$$

Substituting the flow rule

$$d\varepsilon^p_{ij} = d\lambda \frac{\partial f}{\partial \sigma_{ij}}$$

into this equation we obtain

$$d\sigma_{ij} = D_{ijkl}\left(d\varepsilon_{kl} - d\lambda \frac{\partial f}{\partial \sigma_{kl}}\right). \tag{2—102}$$

Now, multiplying both sides of this equation by $\frac{\partial f}{\partial \sigma_{ij}}$, and considering eq. (2—101), we have

$$D_{ijkl}\frac{\partial f}{\partial \sigma_{ij}}d\varepsilon_{kl} - D_{ijkl}d\lambda\frac{\partial f}{\partial \sigma_{ij}}\frac{\partial f}{\partial \sigma_{kl}} = 0.$$

With the proper change of subscripts to prevent superfluous summations, this leads to

$$d\lambda = \frac{D_{ijkl}\frac{\partial f}{\partial \sigma_{ij}}d\varepsilon_{kl}}{D_{pqrs}\frac{\partial f}{\partial \sigma_{pq}}\frac{\partial f}{\partial \sigma_{rs}}}. \qquad (2—103)$$

This equation clearly shows that the scalar function $d\lambda$ is expressed in terms of the current stresses and strain increments at the point in the body under consideration.

Substituting eq. (2—103) into (2—102), a direct relationship can be obtained between the stress and the strain increments

$$d\sigma_{ij} = \left[D_{ijkl} - \alpha\frac{D_{ijrs}\frac{\partial f}{\partial \sigma_{rs}}D_{pqkl}\frac{\partial f}{\partial \sigma_{pq}}}{D_{pqrs}\frac{\partial f}{\partial \sigma_{pq}}\frac{\partial f}{\partial \sigma_{rs}}}\right]d\varepsilon_{kl}. \qquad (2—104)$$

Here $\alpha = 0$ or $\alpha = 1$, depending on whether $d\varepsilon_{ij}$ is purely elastic (i.e. $d\lambda = 0$) or contains plastic terms as well (i.e. $d\lambda > 0$). Considering the expression of $d\lambda$ given by eq. (2—103) this condition can be expressed as

$$\alpha = 0 \quad \text{if} \quad f < 0 \quad \text{or} \quad f = 0 \quad \text{and} \quad D_{ijkl}\frac{\partial f}{\partial \sigma_{ij}}d\varepsilon_{kl} \leq 0,$$

$$\alpha = 1 \quad \text{if} \quad f = 0 \quad \text{and} \quad D_{ijkl}\frac{\partial f}{\partial \sigma_{ij}}d\varepsilon_{kl} > 0.$$

Equation (2—104) can be expressed in a short form

$$d\sigma_{ij} = A_{ijkl}d\varepsilon_{kl}, \qquad (2—104a)$$

where the fourth-order tensor A_{ijkl} is a function of the current stresses as defined by eq. (2—104).

In the case of the *Prandtl–Reuss equations* (where $f = \frac{1}{2}s_{ij}s_{ij} - \tau_0^2$) eq. (2—103) leads to the following simple result

$$d\lambda = \frac{s_{ij}d\varepsilon_{ij}}{2\tau_0^2}, \qquad (2—103a)$$

and then eq. (2—104) has the form

$$ds_{ij} = 2G\left[\delta_{ij}\delta_{kl} - \alpha\frac{1}{2\tau_0^2}s_{ij}s_{kl}\right]de_{kl}. \qquad (2—104b)$$

Here again, $\alpha=0$ or $\alpha=1$ depending on whether de_{ij} is purely elastic (i.e. $d\lambda=0$) or contains plastic parts, as well (i.e. $d\lambda>0$). Considering the expression for $d\lambda$ given by eq. (2—103a) these conditions can be expressed as

$$\alpha=0 \quad \text{if} \quad \frac{1}{2}s_{ij}s_{ij}-\tau_0^2<0, \quad \text{or} \quad \frac{1}{2}s_{ij}s_{ij}-\tau_0^2=0 \quad \text{and} \quad s_{ij}d\varepsilon_{ij}\leq 0,$$

$$\alpha=1 \quad \text{if} \quad \frac{1}{2}s_{ij}s_{ij}-\tau_0^2=0 \quad \text{and} \quad s_{ij}d\varepsilon_{ij}>0.$$

The numerator of eq. (2—103a) represents an increment of work which can be expanded to give

$$dW=s_{ij}de_{ij}=s_{ij}(de_{ij}^{e}+de_{ij}^{p})=\frac{1}{2G}s_{ij}ds_{ij}+s_{ij}de_{ij}^{p}.$$

According to the Huber–v. Mises–Hencky yield condition, however, eq. (2—101) becomes

$$df=\frac{\partial f}{\partial s_{ij}}ds_{ij}=s_{ij}ds_{ij}=0$$

and therefore dW retains only the plastic part of the work: $dW=dW^{p}=s_{ij}de_{ij}^{p}$. Substituting this result into eq. (2—103a) yields

$$d\lambda=\frac{dW^{p}}{2\tau_0^2}=\frac{s_{ij}de_{ij}^{p}}{2\tau_0^2}. \qquad (2—103b)$$

From this equation one can see that since the work dW^{p} cannot be negative, therefore the plastic multiplier must satisfy the relationship $d\lambda\geq 0$.

Finally, substituting eq. (2—103b) into eq. (2—99), the Prandtl–Reuss equation can be expressed in a different form

$$de_{ij}=\frac{ds_{ij}}{2G}+\left(\frac{dW^{p}}{2\tau_0^2}\right)s_{ij}. \qquad (2—99c)$$

Equations (2—104b) and (2—99c) clearly illustrate that the Prandtl—Reuss equations are nonlinear.

2.3.3.4. THE HENCKY CONSTITUTIVE EQUATIONS

The Prandtl–Reuss and Lévy–v. Mises equations discussed above express incremental stress–strain relationships, therefore the theories based on these equations are called *incremental or flow theories.* In contrast, Hencky (1924) proposed a constitutive equation whereby the *total strains* are related to the current stresses. The theory based on these *Hencky equations* was later developed and applied by Ilyushin (1948) and Lenski (1967). This type of theories are called *deformation theories.*

To illustrate the main features of deformation theories consider first the stress–strain diagram shown in Fig. 2—15(a). The total strain ε caused by the stress σ can be

separated into elastic and plastic strains $\varepsilon = \varepsilon^e + \varepsilon^p$, as discussed earlier. We assume that the elastic strains are defined by the initial tangent of the stress–strain curve and that the remaining part stands for the plastic strains. Then, introducing the constant *Elastic modulus* $E = \tan\alpha$ and the variable *Plastic modulus* $\phi = \tan\varphi$ and *Secant modulus* $E' = \tan\beta$, the following relationship can be obtained

$$\varepsilon = \varepsilon^e + \varepsilon^p = \left(\frac{1}{E} + \frac{1}{\phi}\right)\sigma = \frac{\sigma}{E'}.$$

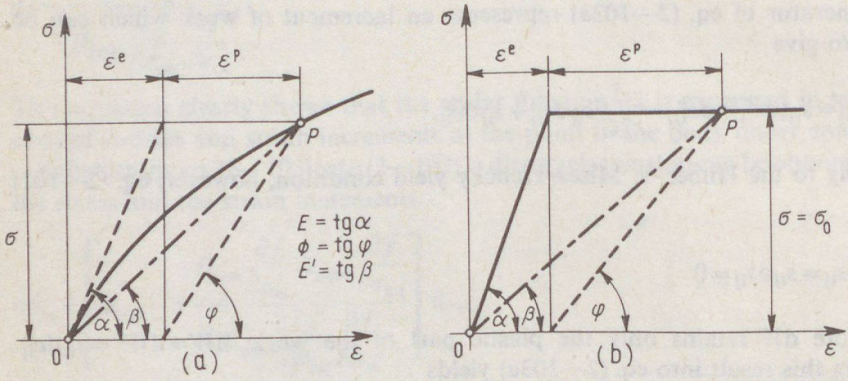


Fig. 2–15

During unloading no plastic deformations develop, therefore

$$d\varepsilon = \frac{d\sigma}{E}.$$

Hencky assumed that the above relationships can be generalized for a triaxial state of stress and strain in the following form

(a) in the case of *loading*

$$e_{ij} = e^e_{ij} + e^p_{ij} = \left(\frac{1}{2G} + \frac{1}{\psi}\right)s_{ij} = \frac{s_{ij}}{2G'}, \tag{2—105}$$

(b) in the case of *unloading*

$$de_{ij} = \frac{ds_{ij}}{2G}. \tag{2—106}$$

In addition, Hencky also assumed that the permanent (plastic) change in volume is zero

$$e^p = 3\varepsilon^p_m = \varepsilon^p_{kk} = 0, \quad \text{i.e.} \quad e^p_{ij} = \varepsilon^p_{ij}. \tag{2—107}$$

The determination of the plastic modulus ψ in eq. (2—105) needs further clarification, as presented below.

The Hencky equations—as a special case—can be applied to *linearly elastic–perfectly plastic bodies*, as well. In this case, the material has a well-defined yield point and therefore a yield condition $f(\sigma_{ij,k})=0$ has to be introduced. Figure 2—15(b) shows the stress–strain diagram and the corresponding notations for a uniaxial state of stress. In three-dimensional problems the expression (2—105) can be used on the following conditions:

(a) *In the elastic range* ($f<0$) no plastic deformations occur, therefore in eq. (2—105) $\frac{1}{\psi}=0$, i.e. $\frac{1}{G'}=\frac{1}{G}$ has to be substituted. Then eq. (2—105) leads to Hooke's Law.

(b) *In the active plastic range* ($f=0$, $\mathrm{d}f=0$) plastic deformations can develop, therefore $\frac{1}{\psi}\geq 0$.

(c) *In the passive plastic range* (unloading) ($f=0$, $\mathrm{d}f<0$) the incremental form (2—106) should be used.

It can be seen that the multiplier $\frac{1}{\psi}$ plays a similar role in the Hencky equations to that $\mathrm{d}\lambda$ in the Prandtl–Reuss relationships. $\frac{1}{\psi}$ is a scalar function which can be expressed in terms of the current stresses and plastic strains $\frac{1}{\psi}=F(s_{ij}, e^{p}_{ij})$. Since the stresses and strains vary from point to point and also change during loading, one can also say that $\frac{1}{\psi}$ is a function of the coordinates and some scalar parameter which describes the loading procedure. In general, this latter can be time and therefore one can write $\frac{1}{\psi}=F(x_i, t)$.

To determine the multiplier $\frac{1}{\psi}$, let us assume that the Huber–v. Mises–Hencky yield condition

$$f=\frac{1}{2}s_{ij}s_{ij}-\tau_0^2=0 \qquad (2—108)$$

holds. By making use of eq. (2—105) we can write the expression for the plastic work

$$W^{p}=s_{ij}e^{p}_{ij}=\frac{1}{\psi}s_{ij}s_{ij}. \qquad (2—109)$$

Comparing this expression with eq. (2—108) we obtain

$$\frac{1}{\psi}=\frac{W^{p}}{2\tau_0^2}. \qquad (2—110)$$

Since the work W^{p} cannot be negative, the relationship $\frac{1}{\psi}\geq 0$ must be satisfied.

Finally, substituting eq. (2—110) into eq. (2—105), the Hencky equation is expressed in the different form

$$e_{ij}=\left(\frac{1}{2G}+\frac{W^p}{2\tau_0^2}\right)s_{ij}. \tag{2—105a}$$

Because of the form of the plastic work W^p, the Hencky equations are also nonlinear. They, however, lead to much simpler calculations than the Prandtl–Reuss equations do, because in eq. (2—105) the *total strains*, rather than the strain increments, are involved.

To compare the two theories, let us write the expressions of plastic deformations and plastic work defined by eqs (2—105) and (2—109) in incremental form. Making use of the expression (2—110), we get

$$de_{ij}^p=d\left(\frac{s_{ij}}{\psi}\right)=\frac{ds_{ij}}{\psi}+d\left(\frac{1}{\psi}\right)s_{ij}=\left(\frac{W^p}{2\tau_0^2}\right)ds_{ij}+\left(\frac{dW^p}{2\tau_0^2}\right)s_{ij}$$

and

$$dW^p=d(s_{ij}e_{ij}^p)=ds_{ij}e_{ij}^p+s_{ij}de_{ij}^p.$$

Substituting the second equation into the first leads to

$$de_{ij}^p=\left(\frac{W^p}{2\tau_0^2}\right)ds_{ij}+\left(\frac{ds_{ij}e_{ij}^p}{2\tau_0^2}\right)s_{ij}+\left(\frac{s_{ij}de_{ij}^p}{2\tau_0^2}\right)s_{ij}. \tag{2—111}$$

In the case of the Prandtl–Reuss equations for de_{ij}^p, we obtained a different expression (see eq. (2—103b))

$$de_{ij}^p=d\lambda s_{ij}=\left(\frac{s_{ij}de_{ij}^p}{2\tau_0^2}\right)s_{ij}. \tag{2—112}$$

Since the Prandtl–Reuss theory is based on the normality rule, *the Hencky theory generally does not obey the normality rule* because of the difference between eqs (2—111) and (2—112), and, consequently, is in contradiction to the Drucker postulate.

Another contradiction in the Hencky theory is that in this theory the *total plastic strains* depend only on the current stresses, i.e. they are *path-independent*. Generally, however, as it was already demonstrated in Chapter 1 for the case of a uniaxial state of stress, the total plastic strains depend on the loading history. To illustrate this problem for three-dimensional cases, let us consider two loading paths *O–A–P* and *O–B–P* which result in the same state of stress σ_{ij}, as shown in Fig. 2—16. Because of the normality of the plastic strain increments and the convexity of the yield surface, the resultants ε_{ij1}^p and ε_{ij2}^p of the plastic strain increments in the cases of these two loading paths will generally be different, i.e. the *total plastic strain is path-dependent*.

Summarizing, we can state that in the case of general loading paths, the deformation theories do not lead to theoretically correct solutions.

Now let us consider a special case, called *the proportional stress change*. This is the case when all the stresses in the body are increasing proportionally—i.e. the *directions* of the stress vectors s_{ij} remain constant—and, consequently, at the points where $f=0$ and $df=0$ the stress vectors do not change at all (i.e. $ds_{ij}=0$). The first two terms of eq.

(2—111) now become zero and eqs (2—111) and (2—112) are identical. Hence, in this case, the contradictions to the deformation theory are automatically eliminated and the deformation and flow theories lead to the same solutions.

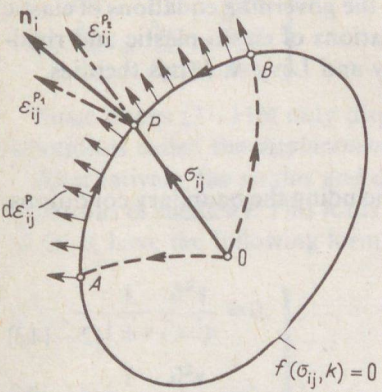


Fig. 2–16

From a practical point of view, in many engineering problems the stress change is not far from the proportional stress change and therefore, because of its simplicity, the Hencky theory has been successfully used in the solution of a great number of practical problems (see e.g. Sokolovski 1950, 1969; Rabotnov 1962; Ilyushin, Lenski 1967; Kachanov 1971; Martin 1975).

2.4. THE GOVERNING EQUATIONS FOR LINEARLY ELASTIC–PERFECTLY PLASTIC BODIES

In order to construct the governing equations of linearly elastic–perfectly plastic bodies we simply have to collect the equilibrium, kinematic and constitutive equations discussed in previous sections.

Consider a linearly elastic–perfectly plastic body with volume V and surface area S, loaded by volume (body) forces f_i in V and by surface forces q_i on S_q and subjected to prescribed displacements u_i^0 on S_u (see Fig.2—5).* The state of the body is characterized by the stress *tensor field* σ_{ij}, the *strain tensor field* ε_{ij} and the *displacement vector field* u_i. The corresponding *state variable functions* are as follows:

$$\sigma_{ij}(x_i) \ldots \begin{cases} \sigma_{xx}(x_i), & \sigma_{yy}(x_i), & \sigma_{zz}(x_i), \\ \sigma_{xy}(x_i), & \sigma_{yz}(x_i), & \sigma_{xz}(x_i), \end{cases}$$

$$\varepsilon_{ij}(x_i) \ldots \begin{cases} \varepsilon_{xx}(x_i), & \varepsilon_{yy}(x_i), & \varepsilon_{zz}(x_i), \\ \varepsilon_{xy}(x_i), & \varepsilon_{yz}(x_i), & \varepsilon_{xz}(x_i), \end{cases}$$

$$u_i(x_i) \ldots \{u_x(x_i), \quad u_y(x_i), \quad u_z(x_i).$$

* S_q and S_u contain all the points of the surface S, where q_i and u_i^0 have prescribed values, including the points where $q_i = 0$ or $u_i^0 = 0$. Points where both q_i and u_i^0 are prescribed are not allowed in our further investigations. Consequently, $S = S_q + S_u$.

To determine these 15 unknown functions we have derived 3 equilibrium, 6 kinematic and 6 constitutive equations, i.e. 15 equations in all, which provide the necessary and sufficient conditions for the solution of problems.*

For the sake of completeness, first we will present the governing equations of elastic bodies and then we will discuss the governing equations of elasto-plastic and rigid-plastic bodies based on the Prandtl–Reuss, Hencky and Lévy–v. Mises theories.

2.4.1. THE LINEARLY ELASTIC BODY

The governing equations of linearly elastic bodies, including the boundary conditions, can be summarized as follows:

(a) *Equilibrium equations*

$$\left.\begin{aligned} &\sigma_{ij,j}+f_i=0,\\ &\sigma_{ij}=\sigma_{ji}, \end{aligned}\right\} \quad \text{in } V \tag{2—113}$$

$$\sigma_{ij}n_j=q_i \qquad \text{on } S_q. \tag{2—113a}$$

(b) *Kinematic equations*

$$\varepsilon_{ij}=\frac{1}{2}(u_{i,j}+u_{j,i}) \quad \text{in } V, \tag{2—114}$$

$$u_i=u_i^0 \quad \text{on } S_u. \tag{2—114a}$$

(c) *Constitutive equations*

$$\varepsilon_{ij}=\frac{1}{E}[(1+\nu)\sigma_{ij}-\nu\sigma_{kk}\delta_{ij}], \tag{2—115}$$

or

$$e_{ij}=\frac{s_{ij}}{2G}, \quad \varepsilon_m=\frac{\sigma_m}{3K}. \tag{2—115a}$$

Two main possibilities are available to eliminate a certain group of the unknown functions and to reduce the number of equations. By suitable transformations the stresses and strains can be eliminated from the above equations and then we obtain the *Lamé–Navier equations*

$$\left.\begin{aligned} &\frac{1}{1-2\nu}\frac{\partial e}{\partial x}+\nabla^2 u_x+f_x=0\\ &\frac{1}{1-2\nu}\frac{\partial e}{\partial y}+\nabla^2 u_y+f_y=0\\ &\frac{1}{1-2\nu}\frac{\partial e}{\partial z}+\nabla^2 u_z+f_z=0 \end{aligned}\right\} \quad \frac{1}{1-2\nu}u_{k,ki}+u_{i,kk}+f_i=0. \tag{2—116}$$

* The investigation of the uniqueness of the solutions is beyond the scope of this book (see e.g. Martin 1975).

Here

$$\left.\begin{aligned} V^2 &= \frac{\partial^2}{\partial x^2} + \frac{\partial^2}{\partial y^2} + \frac{\partial^2}{\partial z^2}, \\ e &= \frac{\partial u_x}{\partial x} + \frac{\partial u_y}{\partial y} + \frac{\partial u_z}{\partial z}. \end{aligned}\right\} \tag{2—117}$$

Since in eqs (2—116) only displacements are involved, the method used for their solution is called the *displacement method.*

Alternatively, the strains and displacements can be eliminated from the governing equations of elasticity. This leads to the *Beltrami–Michell equations* which, in the case of $f_i = 0$, have the following form

$$\left.\begin{aligned} V^2\sigma_{xy} + \frac{1}{1+\nu}\frac{\partial^2 s}{\partial x \partial y} &= 0, \\ V^2\sigma_{yz} + \frac{1}{1+\nu}\frac{\partial^2 s}{\partial y \partial z} &= 0, \\ V^2\sigma_{xz} + \frac{1}{1+\nu}\frac{\partial^2 s}{\partial x \partial z} &= 0, \\ V^2\sigma_{xx} + \frac{1}{1+\nu}\frac{\partial^2 s}{\partial x^2} &= 0, \\ V^2\sigma_{yy} + \frac{1}{1+\nu}\frac{\partial^2 s}{\partial y^2} &= 0, \\ V^2\sigma_{zz} + \frac{1}{1+\nu}\frac{\partial^2 s}{\partial z^2} &= 0. \end{aligned}\right\} \qquad \sigma_{ij,kk} + \frac{1}{1+\nu}\sigma_{kk,ij} = 0. \tag{2—118}$$

Here $s = \sigma_{kk} = \sigma_{xx} + \sigma_{yy} + \sigma_{zz}$. Since in eqs (2—118) only stresses are involved, the method used for their solution is called the *force method.*

Many other methods and a great number of solutions to different problems can be found in the rich literature of elasticity (see e.g. Timoshenko and Goodier 1951; Muskelisvili 1953; Sokolnikoff 1956).

2.4.2. THE PRANDTL–REUSS ELASTO-PLASTIC BODY

The governing equations of linearly elastic–perfectly plastic bodies derived on the basis of the Prandtl–Reuss constitutive equations are as follows.*

(a) *Equilibrium equations*

$$\left.\begin{aligned} \sigma_{ij,j} + f_i &= 0, \\ \sigma_{ij} &= \sigma_{ji}, \end{aligned}\right\} \quad \text{in} \quad V \tag{2—119}$$

$$\sigma_{ij} n_j = q_i \quad \text{on} \quad S_q. \tag{2—119a}$$

* Since strain increments are involved in the constitutive equations, it is customary to write the kinematic equations also in terms of the strain and displacement increments.

(b) *Kinematic equations*

$$d\varepsilon_{ij} = \frac{1}{2}(du_{i,j} + du_{j,i}) \quad \text{in} \quad V, \tag{2—120}$$

$$u_i = u_i^0 \quad \text{on} \quad S_u. \tag{2—120a}$$

(c) *Constitutive equations*

$$de_{ij} = \frac{ds_{ij}}{2G} + d\lambda s_{ij}, \tag{2—121}$$

$$d\varepsilon_m = \frac{d\sigma_m}{3K}. \tag{2—122}$$

In general, a linearly elastic–perfectly plastic body subjected to external loads can be divided into three domains (Fig. 2—17).

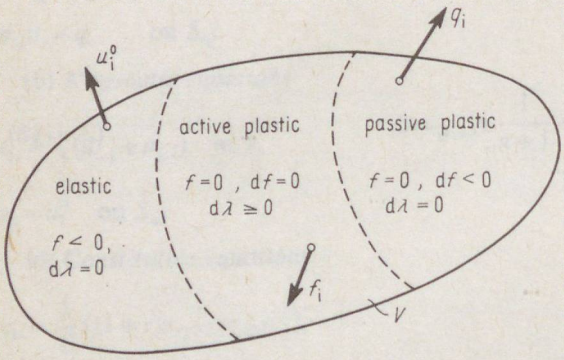


Fig. 2–17

(a) *In the elastic domain*, where

$$f = \frac{1}{2} s_{ij} s_{ij} - \tau_0^2 < 0,$$

only elastic deformations develop and therefore $d\lambda = 0$ and eq. (2—121) reduces to the incremental form of Hooke's Law.

(b) *In the active plastic domain*, where

$$f = \frac{1}{2} s_{ij} s_{ij} - \tau_0^2 = 0 \quad \text{and} \quad df = s_{ij} ds_{ij} = 0,$$

both elastic and plastic deformations can develop. The plastic multiplier $d\lambda \geq 0$ is then defined by eq. (2—103a). Alternatively, in the active domain eq. (2—121) can be replaced by eq. (2—104b).

(c) *In the passive plastic domain*, where

$$f = \frac{1}{2} s_{ij} s_{ij} - \tau_0^2 = 0 \quad \text{and} \quad df = s_{ij} ds_{ij} < 0,$$

unloading takes place and no plastic deformations develop, therefore $d\lambda = 0$. Then eq. (1—121) again reduces to the incremental form of Hooke's Law.

Considering the three possible domains of the body, the constitutive equations (2—121) and the associated subsidary conditions can be summarized as

$$\left.\begin{aligned} de_{ij} &= \frac{ds_{ij}}{2G} + d\lambda s_{ij}, \\ f &= \frac{1}{2} s_{ij} s_{ij} - \tau_0^2, \\ f\,d\lambda &= 0, \quad df\,d\lambda = 0. \end{aligned}\right\} \tag{2—123}$$

2.4.3. THE HENCKY ELASTO-PLASTIC BODY

Replacing the constitutive equations (2—121) in the governing equations of Prandtl–Reuss bodies by the relationships

$$\left.\begin{aligned} e_{ij} &= \left(\frac{1}{2G} + \frac{1}{\psi}\right) s_{ij} = \frac{s_{ij}}{2G'}, \\ f &= \frac{1}{2} s_{ij} s_{ij} - \tau_0^2, \\ f\left(\frac{1}{\psi}\right) &= 0, \quad df \cdot \left(\frac{1}{\psi}\right) = 0, \end{aligned}\right\} \tag{2—124}$$

leads to the governing equations of the Hencky elasto-plastic bodies. The determination of the plastic multiplier $\left(\frac{1}{\psi}\right) \geq 0$ has already been described in Section 2.3.3.4.

2.4.4. THE LÉVY–v. MISES RIGID-PLASTIC BODY

Replacing the constitutive equations (2—121) in the governing equations of Prandtl–Reuss bodies by the relationships

$$\left.\begin{aligned} d\varepsilon_{ij} &= d\lambda s_{ij}, \\ f &= \frac{1}{2} s_{ij} s_{ij} - \tau_0^2, \\ f\,d\lambda &= 0, \quad df\,d\lambda = 0, \end{aligned}\right\} \tag{2—125}$$

leads to the governing equations of the Lévy–v. Mises rigid — plastic bodies. The determination of the plastic multiplier $d\lambda$ has already been described in Section 2.3.3.3.

2.4.5. NOTES ON THE SOLUTION OF ELASTO-PLASTIC PROBLEMS

The solution of elasto-plastic problems is far more difficult than that of linear elastic problems.

Considering first the Prandtl–Reuss bodies, the main difficulties of the solution can be described as follows:

— The Prandtl–Reuss equations are expressed in *incremental form* and therefore describe the *state change* rather than the state of an elasto-plastic body.

— Because of the plastic multiplier $d\lambda$ and the yield function the governing equations are *nonlinear*.

— In the *elastic and plastic domains* of the body, the constitutive equations have different forms. The boundaries of these domains are generally not known and change their position during loading. At the boundary surfaces, certain *continuity conditions* have to be fulfilled and, on the other hand, in the plastic domains certain *discontinuity surfaces* can develop (see Chapter 3).

To decrease the difficulties certain simplifications can be introduced:

— If the elastic deformations are much smaller than the plastic ones, they can be neglected. Besides, there are problems (e.g. plastic limit analysis), where the elastic deformations do not play any role and can therefore be omitted. In both cases the Lévy–v. Mises equations of *rigid–perfectly plastic bodies* can be used, which reduce significantly the difficulties arising in the solution of plastic problems.

— The *linearization of the yield conditions* (using e.g. the Tresca yield condition) can also simplify the solution. But in general, using linearized yield conditions requires the plastic domain of the body to be subdivided into further domains with unspecified boundaries corresponding to the different planes of the yield surface, and this very often makes the solution of problems even more complicated (see e.g. the plane stress problems to be discussed in Section 5.3.).

In spite of the possible simplifications, the Prandtl–Reuss equations generally cannot be integrated and therefore in the theory of plasticity those analytical solutions which are common in the theory of elasticity cannot be used. Thus, in general, a complete *load history analysis* has to be conducted in order to obtain the solution. This needs a numerical procedure, to be described briefly below.

Let us consider a state of an elasto-plastic body under a given load where all the current stresses, strains and displacements are known. Then, the constitutive equation (2—121) specify a one-to-one relationship between the strain and stress increments; therefore on applying an additional incremental load the corresponding increments of stresses, strains and displacements can be calculated. This leads to a known subsequent state of the body. This step-by-step procedure can be continued until the required state is reached. To conduct this numerical procedure, the body has to be discretized (e.g. by using the finite element method) and computer programs have to be developed. This question will be briefly discussed in Section 5.4. in connection with plane problems, but a detailed presentation is beyond the scope of this book (see e.g. Argyris 1964, 1971; Zienkiewicz 1971).

The main difference between the Prandtl–Reuss and the Hencky equations is that, in the same way as for the elastic problems, the latter describes the state rather than the state change of an elasto-plastic body. Consequently, the analysis of a given state does

not require a step-by-step load history analysis but can be conducted directly by the use of the Hencky equations. Because of the plastic multiplier $\frac{1}{\psi}$ appearing in eqs (2—124), however, these equations are also *nonlinear* and therefore in most cases numerical methods have to be used. Still, the solution is much simpler than in the case of the Prandtl–Reuss equations and therefore, in spite of the inconsistencies described earlier, the Hencky deformation theory is widely used in theoretical investigations and also in engineering practice.

3. VARIATIONAL PRINCIPLES

In the first part of this chapter the principles of virtual work and complementary virtual work will be presented. These two principles form a basis for the derivation of other principles, both in elasticity and in plasticity. First the principles of stationary potential energy and minimum complementary energy will be derived for linearly elastic bodies, and a few other important energy principles will be briefly described. Then the variational principles associated with the following three basic problems in plasticity will be discussed: incremental load history analysis, limit analysis and shakedown analysis of linearly elastic–perfectly plastic bodies. From these, the static and kinematic principles of limit analysis play an especially important role in engineering practice. The last part of the chapter deals with the discontinuities of plastic stress and strain fields.

3.1. INTRODUCTORY REMARKS

Variational principles, often called work and energy principles, have great importance and wide application in solid mechanics. This is because a deformable body under external loads behaves in such a manner that some functionals expressing work or energy assume a stationary value.

In the previous chapter we found that the state or state change of a deformable body can be described by a set of (differential) equations. Using variational principles, this local description is replaced by an overall description and the state or state change of a deformable body is expressed in integral form. This integral formulation has several advantages, as will be briefly described below.

The functional subject to variation usually has a definite physical meaning (e.g. work, energy), which makes the mechanical behaviour of deformable bodies much easier to understand. These functionals are invariant during coordinate transformations, so that a transformation from one coordinate system to another is relatively simple: only the expression of the functional in terms of the new coordinates is needed for the variational procedure to be carried out.

Variational methods also provide approximate formulations which often lead to upper or lower bounds of the exact solution of problems (see e.g. the *Rayleigh–Ritz* or the *Galerkin method*).

Finally, the variational formulation provides a powerful tool for the derivation of the governing equations of discrete systems (see e.g. the finite element method).

In this chapter we will present the most important variational principles of the state of equilibrium of elastic and elasto-plastic bodies. A more detailed description of this field of solid mechanics can be found in the literature (see e.g. Kachanov 1971; Washizu 1975; Szabó 1977).

The variational principles of elastic and elasto-plastic bodies are usually based on imaginary stress and force fields or on imaginary strain and displacement fields which satisfy only a group of the governing equations. These are called *statically admissible stress and force fields* and *kinematically admissible strain and displacement fields*, respectively. In order to define these fields, let us consider a deformable body, with volume V and surface area S, in static equilibrium under the body forces f_i in V and the surface forces q_i on S_q together with the prescribed displacements u_i^0 on $S_u = S - S_q$. Then,

(a) the stress and force fields σ_{ij}^s, q_i, f_i which satisfy the *equilibrium equations*

$$\sigma_{ij,j}^s + f_i = 0, \quad \sigma_{ji}^s = \sigma_{ij}^s \quad \text{in} \quad V \tag{3—1}$$

and the *static boundary conditions*

$$\sigma_{ij}^s n_j = q_i \quad \text{in} \quad S_q \tag{3—2}$$

are called the *statically admissible stress and force fields*, and

(b) the strain and displacement fields ε_{ij}^k, u_i^k which satisfy the *kinematic equations*

$$\varepsilon_{ij}^k = \frac{1}{2}(u_{i,j}^k + u_{j,i}^k) \quad \text{in} \quad V \tag{3—3}$$

and the *kinematic boundary conditions*

$$u_i^k = u_i^0 \quad \text{on} \quad S_u \tag{3—4}$$

are called *kinematically admissible strain and displacement fields.*

Since the problem of deformable bodies is statically and kinematically indeterminate, in general an infinite set of statically admissible stress and force fields, and kinematically admissible strain and displacement fields can be constructed.

In general, the two different kinds of field are *independent* of each other. Making use of the constitutive equations (if they define a one-to-one relationship between the stresses and the strains, as in the case of elastic bodies) for each stress field σ_{ij}^s and strain field ε_{ij}^k a strain field ε_{ij}^s and a stress field σ_{ij}^k can be determined. These associated strain and stress fields, however, do not usually satisfy the kinematic equations (3—3) and (3—4) and the equilibrium equations (3—1) and (3—2), respectively. Nevertheless, one can always find a statically admissible stress field and a kinematically admissible strain field such that the associated strain fields and stress fields, respectively, satisfy the remaining group of the governing equations, and so give the actual solution of the problem. Variational principles define how one can select the actual stress and strain fields in a body from the set of statically admissible stress fields and from the set of kinematically admissible strain fields, respectively.

In Chapter 2 we have already introduced the *increments* of stresses, strains and diplacements caused by an incremental change in external forces (during an

incremental increase of time). Now we will define the *variations* of stresses, strains, forces and displacements. These variations describe the *virtual infinitesimal changes* of the state of a deformable body while the body forces f_i in V, the surface forces q_i on S_q and the displacements u_i^0 on S_u are kept unchanged, the displacements u_i in V and the surface forces $\bar{q}_i$ on S_u being, however, subject to variation.* Consequently, the functions f_i, q_i and u_i^0 are considered constant in our further variational procedure.

Let us introduce the following definitions:

(a) The variations $\delta\sigma_{ij}$ and $\delta\bar{q}_i$ of the statically admissible stress and force fields denoted by σ_{ij} and $\bar{q}_i$, which satisfy the equilibrium conditions

$$\delta\sigma_{ij,j}=0, \quad \delta\sigma_{ij}=\delta\sigma_{ji} \quad \text{in} \quad V, \tag{3—1a}$$

$$\delta\sigma_{ij}n_j=0 \quad \text{on} \quad S_q, \tag{3—2a}$$

$$\delta\sigma_{ij}n_j=\delta\bar{q}_i \quad \text{on} \quad S_u \tag{3—2b}$$

are called *virtual stresses and virtual forces*, and

(b) the variations $\delta\varepsilon_{ij}$ and δu_i of the kinematically admissible strain and displacement fields denoted by ε_{ij} and u_i, which satisfy the kinematic conditions

$$\delta\varepsilon_{ij}=\frac{1}{2}(\delta u_{i,j}+\delta u_{j,i}) \quad \text{in} \quad V, \tag{3—3a}$$

$$\delta u_i=0 \quad \text{on} \quad S_u \tag{3—4a}$$

are called *virtual strains and virtual displacements.***

We note that in the more general sense any statically admissible stress and force field or kinematically admissible strain and displacement field can be treated as virtual. For example, in certain problems instead of the variations we will apply the rates and velocities $\dot{\sigma}_{ij}^s$, $\dot{\bar{q}}_i^s$, $\dot{\varepsilon}_{ij}^k$ and $\dot{u}_i^k=v_i^k$. In the derivation of variational principles, however, the use of variations is more convenient.

3.2. PRINCIPLE OF VIRTUAL WORK AND COMPLEMENTARY VIRTUAL WORK

The principles of virtual work and complementary virtual work play a fundamental role in solid mechanics. These principles express in integral form the conditions of equilibrium and compatibility of deformable bodies, and provide a basis for the systematic derivation of several other principles which can be applied to the solution of different static and dynamic problems and to the analysis of bodies with material responses that can be elastic, plastic, viscous etc.

* $\bar{q}_i$ are unspecified forces which achieve the prescribed displacements u_i^0 on S_u and have to satisfy the boundary condition $\sigma_{ij}n_i=\bar{q}_j$ on S_u.

** For the sake of simplicity, in the notation of virtual stresses, forces, strains and displacements the indices s and k will be omitted because they are *by definition* statically and kinematically admissible, respectively.

3.2.1. VIRTUAL WORK AND COMPLEMENTARY VIRTUAL WORK

Consider the work W done by a force F_i on a displacement u_i. Then the *virtual work* is the variation in this work when the *displacement* is the subject of variation. That is,

$$\delta W = F_i \delta u_i.$$

The *complementary virtual work* is the variation of W when the *force* is the subject of variation

$$\delta \overline{W} = \delta F_i u_i.$$

Briefly, the virtual work can be viewed as the incremental work done during the virtual displacement, and the complementary virtual work can be viewed as the incremental work corresponding to the virtual change in force. Figure 3—1 illustrates the geometrical content of these two different types of virtual work for the one dimensional case.

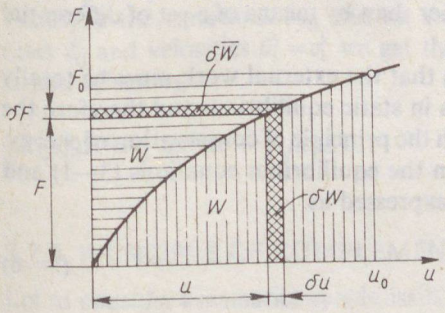


Fig. 3–1

Considering an entire deformable body, the internal virtual work and the internal complementary virtual work are defined as

$$\delta W = \int_V \sigma_{ij} \delta \varepsilon_{ij} \mathrm{d}V,$$

$$\delta \overline{W} = \int_V \varepsilon_{ij} \delta \sigma_{ij} \mathrm{d}V.$$

It is important to note that in these expressions the stress field σ_{ij} and the strain field ε_{ij} are, in general, *independent* of each other, i.e. they are not related to each other by the constitutive equations. The only requirement is that $\delta\sigma_{ij}$ and $\delta\varepsilon_{ij}$ must be statically and kinematically admissible, respectively.

3.2.2. PRINCIPLE OF VIRTUAL WORK

Let us consider a statically admissible stress and force field σ_{ij}^s and $\bar{q}_i^s$ in a body which maintain static equilibrium with the body and surface forces f_i and q_i. Independently, consider sets of *arbitrary* kinematically admissible strain and displacement fields ε_{ij}^k and

u_i^k and their variations $\delta\varepsilon_{ij}$ and δu_i which obey eqs (3—3a) and (3—4a). Then the *principle of virtual work* can be stated as follows:

The internal virtual work done by the statically admissible stresses on *any arbitrary* virtual strains is equal to the external virtual work done by the external forces on the displacements associated with the applied virtual strains* i.e.

$$\int_V \sigma_{ij}^s \delta\varepsilon_{ij} dV = \int_{S_q} q_i \delta u_i dS + \int_V f_i \delta u_i dV \tag{3—5a}$$

or

$$\int_V \sigma_{ij}^s \delta\varepsilon_{ij} dV - \int_{S_q} q_i \delta u_i dS - \int_V f_i \delta u_i dV = 0. \tag{3—5b}$$

Alternatively, stress fields that satisfy eq. (3—5) for *any arbitrary* virtual strains and displacements, and also satisfy the static boundary conditions (3—2), are statically admissible.

This is another definition of the statically admissible stresses which expresses the condition of equilibrium in integral form rather than by means of a set of differential equations.

The principle of virtual work simply states that the external work must be totally converted into strain energy since the body is in static equilibrium and therefore the kinetic energy is zero. This is in agreement with the principle of conservation of energy. The correct proof of the principle is based on the equilibrium equations (3—1) and (3—2) and Gauss' theorem. This theorem is expressed as

$$\int_V T_{j,j} dV = \int_S T_j n_j dS, \tag{3—6}$$

where $T_j(x_i)$ is a vector field, V is any region, S is the surface enclosing V and n_j is the outward vector normal to a small element dS on the surface S (see e.g. B. G. A. Korn, T. M. Korn 1968).

To prove the principle of virtual work, by making use of eq. (3—3a), let us express the internal virtual work as

$$\int_V \sigma_{ij}^s \delta\varepsilon_{ij} dV = \frac{1}{2} \int_V \sigma_{ij}^s (\delta u_{i,j} + \delta u_{j,i}) dV. \tag{3—7}$$

Since $\sigma_{ij}^s = \sigma_{ji}^s$ one can obtain

$$\frac{1}{2} \sigma_{ij}^s (\delta u_{i,j} + \delta u_{j,i}) = \sigma_{ij}^s \delta u_{i,j}.$$

This relationship together with the equilibrium equations (3—1) yields

$$\sigma_{ij}^s \delta u_{i,j} = (\sigma_{ij}^s \delta u_j)_{,j} - \sigma_{ij,j}^s \delta u_i = (\sigma_{ij}^s \delta u_j)_{,j} + f_i \delta u_i.$$

* The surface forces $\bar{q}_i^s$ do not appear in eqs (3—5a) and (3—5b) since on S_u $\delta u_i^0 = 0$ and therefore the virtual work done by $\bar{q}_i^s$ is zero.

The internal virtual work given by eq. (3—7) can now be expressed in a different form

$$\int_V \sigma_{ij}^s \delta\varepsilon_{ij} dV = \int_V (\sigma_{ij}^s \delta u_i)_j dV + \int_V f_i \delta u_i dV.$$

Applying Gauss' theorem defined by eq. (3—6) to the vector field $T_j = (\sigma_{ij}^s \delta u_i)$ results in

$$\int_V \sigma_{ij}^s \delta\varepsilon_{ij} dV = \int_V (\sigma_{ij}^s \delta u_i) n_j dS + \int_V f_i \delta u_i dV.$$

According to eqs (3—2) and (3—4a), however, $\sigma_{ij}^s n_j = q_i$ on S_q and $\delta u_i = 0$ on S_u so we obtain the final expression

$$\int_V \sigma_{ij}^s \delta\varepsilon_{ij} dV = \int_{S_q} q_i \delta u_i dS + \int_V f_i \delta u_i dV,$$

which is identical with eq. (3—5).

The principle of virtual work is also called the *principle of virtual displacements.* Finally, if the variations $\delta\varepsilon_{ij}$ and δu_i are replaced by kinematically admissible strain rates $\dot{\varepsilon}_{ij}^k$ and velocities $\dot{u}_i^k = v_i^k$ we get the *principle of virtual power* or the *principle of virtual velocities,*

$$\int_V \sigma_{ij}^s \dot{\varepsilon}_{ij}^k dV = \int_{S_q} q_i v_i^k dS + \int_V f_i v_i^k dV. \qquad (3—8)$$

3.2.3. PRINCIPLE OF COMPLEMENTARY VIRTUAL WORK

Let us consider kinematically admissible strain and displacement fields ε_{ij}^k and u_i^k in a body with prescribed kinematic boundary conditions $u_i = u_i^0$ on the surface S_u. Consider also independent sets of *arbitrary* statically admissible stress and force fields σ_{ij}^s and $\bar{q}_i^s$ and their variations $\delta\sigma_{ij}$, and $\delta\bar{q}_i$, which obey eqs (3—1a), (3—2a) and (3—2b). The *principle of complementary virtual work* can now be stated as follows:

The internal complementary virtual work done by *any arbitrary* virtual stresses on the kinematically admissible strains is equal to the external complementary virtual work done by the associated virtual surface forces on the prescribed displacements, i.e.

$$\int_V \varepsilon_{ij}^k \delta\sigma_{ij} dV = \int_{S_u} u_i^0 \delta\bar{q}_i dS \qquad (3—9)$$

or

$$\int_V \varepsilon_{ij}^k \delta\sigma_{ij} dV - \int_{S_u} u_i^0 \delta\bar{q}_i dS = 0. \qquad (3—9a)$$

Alternatively, strain and displacement fields such that satisfy eq. (3—9) for *any arbitrary* virtual stresses and forces, and also satisfy the kinematic boundary condition (3—4), are kinematically admissible.

This is another definition of the kinematically admissible strains and displacements which expresses the kinematic condition in integral form rather than by means of differential equations.

In eqs (3—9) and (3—9a) $\delta\bar{q}_i$ denotes the variation in the surface forces on S_u where the displacements u_i^0 are prescribed. If, however, $u_i^0 = 0$ on S_u the right-hand side of eq. (3—9) vanishes and the principle has a simpler form

$$\int_V \varepsilon_{ij}^k \delta\sigma_{ij} \mathrm{d}V = 0. \tag{3—9b}$$

The proof of the principle of complementary virtual work is analogous to that of the principle of virtual work described above, and therefore it will not be presented (see e.g. Washizu 1975).

The principle of complementary virtual work is often called the *principle of virtual forces*. The principle can also be expressed in terms of the stress and force rates and then has the following form

$$\int_V \varepsilon_{ij}^k \dot{\sigma}_{ij}^s \mathrm{d}V = \int_{S_u} u_i^0 \dot{\bar{q}}_i^s \mathrm{d}S. \tag{3—10}$$

This form is called the *principle of complementary virtual power.*

3.3. VARIATIONAL PRINCIPLES OF ELASTICITY

As we have already noted, the principle of virtual work and the principle of complementary virtual work are valid for deformable bodies with any material properties. In the following, making use of these principles and Hooke's Law, we will derive two special principles for linearly elastic bodies. These are called the *principle of stationary potential energy* and the *principle of minimum complementary energy.*

3.3.1. PRINCIPLE OF STATIONARY POTENTIAL ENERGY

The principle of stationary potential energy is a variational formulation of the condition of static equilibrium of linearly elastic bodies. It can be derived from the principle of virtual work.

Let us consider a linearly elastic body which is in static equilibrium under the volume and surface forces f_i and q_i, together with the prescribed surface displacements u_i^0. Considering sets of kinematically admissible strain and displacement fields ε_{ij}^k and u_{ij}^k, and using Hooke's Law for each strain field an associated stress field σ_{ij}^k can be specified

$$\sigma_{ij}^k = D_{ijkl} \varepsilon_{kl}^k. \tag{3—11}$$

Then, forming the variations $\delta\varepsilon_{ij}$ and δu_i of the kinematically admissible strains and displacements, the internal and external virtual work can be expressed as

$$\delta W^i = \int_V \sigma_{ij}^k \delta\varepsilon_{ij} \mathrm{d}V = \int_V D_{ijkl} \varepsilon_{kl}^k \delta\varepsilon_{ij} \mathrm{d}V = \delta\left[\frac{1}{2}\int_V \varepsilon_{ij}^k D_{ijkl} \varepsilon_{kl}^k \mathrm{d}V\right], \tag{3—12}$$

$$\delta W^e = \int_{S_q} q_i \delta u_i \mathrm{d}S + \int_V f_i \delta u_i \mathrm{d}V = \delta\left[\int_{S_q} q_i u_i^k \mathrm{d}S + \int_V f_i u_i^k \mathrm{d}V\right]. \tag{3—13}$$

In eq. (3—13) we have made use of the assumption that q_i and f_i are kept unchanged and are therefore not subject to variation.

The expression in the bracket of eq. (3—12) is called the *elastic strain energy* or *internal potential energy*

$$\Pi^{i}(\varepsilon_{ij}^{k}) = \frac{1}{2}\int_{V} \varepsilon_{ij}^{k} D_{ijkl} \varepsilon_{kl}^{k} \mathrm{d}V, \tag{3—14}$$

while the expression in the bracket of eq. (3—13) with opposite sign denotes the *external potential energy*

$$\Pi^{e}(u_i^k) = -\int_{S_q} q_i u_i^k \mathrm{d}S - \int_{V} f_i u_i^k \mathrm{d}V. \tag{3—15}$$

Thus, the *total potential energy* of the body has the following expression

$$\Pi(\varepsilon_{ij}^{k}, u_i^k) = \Pi^{i} + \Pi^{e} = \frac{1}{2}\int_{V} \varepsilon_{ij}^{k} D_{ijkl} \varepsilon_{kl}^{k} \mathrm{d}V - \int_{S_q} q_i u_i^k \mathrm{d}S - \int_{V} f_i u_i^k \mathrm{d}V. \tag{3—16}$$

Considering eqs (3—12) and (3—13), the variation in the total potential energy can be expressed as

$$\delta\Pi = \delta W^{i} - \delta W^{e} = \int_{V} \sigma_{ij}^{k} \delta\varepsilon_{ij} \mathrm{d}V - \int_{S_q} q_i \delta u_i \mathrm{d}S - \int_{V} f_i \delta u_i \mathrm{d}V. \tag{3—17}$$

Let us now suppose that ε_{ij}^{k} and u_i^k designate the *actual* strain and displacement fields of the body, i.e. $\varepsilon_{ij}^{k} \equiv \varepsilon_{ij}$ and $u_i^k \equiv u_i$. Then the associated stress field is also identical with the actual stress field, i.e. $\sigma_{ij}^{k} \equiv \sigma_{ij}$. Consequently, in this specific case the stress field under consideration is *statically admissible* and therefore according to the principle of virtual work (see eq. (3—5a)) the expression (3—17) vanishes, i.e. $\delta\Pi = 0$. This means that in a state of static equilibrium the total potential energy of an elastic body is stationary.

The *principle of stationary energy* can then be stated as follows:

Among all the kinematically admissible strain and displacement fields of a linearly elastic body, the actual strain and displacement fields, which also satisfy the equilibrium conditions make the functional

$$\Pi(\varepsilon_{ij}^{k}, u_i^k) = \frac{1}{2}\int_{V} \varepsilon_{ij}^{k} D_{ijkl} \varepsilon_{kl}^{k} \mathrm{d}V - \int_{S_q} q_i u_i^k \mathrm{d}S - \int_{V} f_i u_i^k \mathrm{d}V \tag{3—18}$$

of the total potential energy *stationary* i.e.

$$\delta\Pi = 0. \tag{3—19}$$

Alternatively, if a kinematically admissible strain and displacement field makes the total potential energy of an elastic body stationary and satisfies the static boundary conditions, then it is identical with the actual strain and displacement field.

This is the necessary and sufficient condition for static equilibrium of an elastic body. Depending on the second variation of the potential energy, three different states of equilibrium can be distinguished:

(a) the state of equilibrium is *stable*, if $\delta\Pi^2 > 0$, i.e. $\Pi =$ minimum;

(b) the state of equilibrium is *neutral*, if $\delta^2\Pi = 0$,

(c) the state of equilibrium is *unstable*, if $\delta^2\Pi < 0$, i.e. $\Pi =$ maximum.

Finally we note that the strain energy of a linearly elastic body expressed in terms of strains has the following expression:

$$\Pi^i = W^i = \frac{1}{2}\int_V \varepsilon_{ij} D_{ijkl} \varepsilon_{kl} \mathrm{d}V = \int_V \left[\frac{1}{2}\lambda(\varepsilon_{xx}+\varepsilon_{yy}+\varepsilon_{zz})^2 + \right.$$

$$\left. + G(\varepsilon_{xx}^2+\varepsilon_{yy}^2+\varepsilon_{zz}^2) + 2G(\varepsilon_{xy}^2+\varepsilon_{yz}^2+\varepsilon_{yz}^2) \right] \mathrm{d}V. \tag{3—20}$$

Here λ denotes *Lamé's modulus* defined by eq. (2—71b).

The variational principle defined by eqs (3—18) and (3—19) has an additional condition that the strain and displacement fields ε_{ij}^k and u_i^k have to satisfy the kinematic equations (3—3) and the kinematic boundary conditions (3—4).

The functional of the potential energy, however, can be formulated so as to contain the additional conditions as well. This generalized functional has the form

$$\Pi_G = \frac{1}{2}\int_V \varepsilon_{ij} D_{ijkl} \varepsilon_{kl} \mathrm{d}V - \int_V \sigma_{ij}\left[\varepsilon_{ij} - \frac{1}{2}(u_{i,j}+u_{j,i}) \right] \mathrm{d}V -$$

$$- \int_{S_q} q_i u_i \mathrm{d}S - \int_V f_i u_i \mathrm{d}V - \int_{S_u} \bar{q}_i (u_i - u_i^0) \mathrm{d}S. \tag{3—21}$$

Then, the generalized principle of stationary potential energy, called the *Hu–Washizu principle*, can be formulated as follows:

Among all the strain and displacement fields of a linearly elastic body the actual strain and displacement field, which satisfies both the equilibrium and kinematic equations and the boundary conditions, makes the generalized potential energy stationary, i.e.

$$\delta\Pi_G = 0. \tag{3—22}$$

Since in this generalized principle the kinematic conditions are already included, the strain and displacement fields in the generalized functional should not necessarily be kinematically admissible. In the functional Π_G, the nine elements of the tensor σ_{ij} and the vector $\bar{q}_i$ are *Lagrange multipliers*. They denote the stress components in the body and the surface forces on S_u where the displacements are prescribed. The derivation and a more detailed description of this generalized principle can be found in the literature (see e.g. Washizu 1975).

3.3.2. PRINCIPLE OF MINIMUM COMPLEMENTARY ENERGY

The principle of minimum complementary energy is a variational formulation of the kinematic conditions of a linearly elastic body. This principle can be derived from the principle of complementary virtual work, as will be shown below.

Let us consider a linearly elastic body which, under the volume and surface forces f_i and q_i together with the prescribed surface displacements u_i^0, is in static equilibrium. Considering the sets of statically admissible stress and force fields σ_{ij}^s and $\bar{q}_i^s$, by the use of Hooke's Law, for each stress field an associated strain field ε_{ij}^s can be specified

$$\varepsilon_{ij}^s = H_{ijkl}\sigma_{kl}^s. \tag{3—23}$$

Then, in terms of the variations $\delta\sigma_{ij}$ and $\delta\bar{q}_i$ of the statically admissible stresses and surface forces, the internal and external complementary virtual work can be expressed as follows

$$\delta\bar{W}^i = \int_V \varepsilon_{ij}^s \delta\sigma_{ij}\,dV = \int_V H_{ijkl}\sigma_{kl}^s \delta\sigma_{ij}\,dV =$$

$$= \delta\left[\frac{1}{2}\int_V \sigma_{ij}^s H_{ijkl}\sigma_{kl}^s\,dV\right], \tag{3—24}$$

$$\delta\bar{W}^e = \int_{S_u} u_i^0 \delta\bar{q}_i^s\,dS = \delta\left[\int_{S_u} \bar{q}_i^s u_i^0\,dS\right]. \tag{3—25}$$

The expression in the bracket of eq. (3—24) is called the *complementary elastic strain energy* or *internal complementary energy*

$$\bar{\Pi}^i(\sigma_{ij}^s) = \frac{1}{2}\int_V \sigma_{ij}^s H_{ijkl}\sigma_{kl}^s\,dV, \tag{3—26}$$

while the expression in the bracket of eq. (3—25) with opposite sign denotes the *external complementary energy*

$$\bar{\Pi}^e(\bar{q}_i^s) = -\int_{S_u} \bar{q}_i^s u_i^0\,dS. \tag{3—27}$$

Thus, the *total complementary energy* of the body has the following expression

$$\bar{\Pi}(\sigma_{ij}^s, \bar{q}_i^s) = \bar{\Pi}^i + \bar{\Pi}^e = \frac{1}{2}\int_V \sigma_{ij}^s H_{ijkl}\sigma_{kl}^s\,dV - \int_{S_u} \bar{q}_i^s u_i^0\,dS. \tag{3—28}$$

Considering eqs (3—24) and (3—25), the variation of the total complementary energy is

$$\delta\bar{\Pi} = \delta\bar{W}^i - \delta\bar{W}^e = \int_V \varepsilon_{ij}^s \delta\sigma_{ij}\,dV - \int_{S_u} u_i^0 \delta\bar{q}_i\,dS. \tag{3—29}$$

Let us suppose now that σ_{ij}^s and $\bar{q}_i^s$ denote the *actual* stress field of the body, i.e. $\sigma_{ij}^s \equiv \sigma_{ij}$ and $\bar{q}_i^s \equiv \bar{q}_i$. Then, the associated strain and displacement field is also identical with the actual strain and displacement field, i.e. $\varepsilon_{ij}^e \equiv \varepsilon_{ij}$ and $u_i^s \equiv u_i$. Consequently, in this special case, the strain and displacement field under consideration is kinematically admissible and therefore, according to the principle of complementary virtual work, (see eq. (3—9a)) the expression (3—29) vanishes, i.e. $\delta\bar{\Pi} = 0$. This means that the total complementary energy of an elastic body in a compatible state of deformation is stationary. It can be proved that the second variation of $\bar{\Pi}$ is always positive: thus, for a state of compatible deformation the total complementary energy is at a minimum.

The *principle of minimum complementary energy* can now be stated as follows:

Among all the statically admissible stress and force fields of a linearly elastic body, the actual stress and force field which also satisfies the compatibility conditions minimizes the functional

$$\bar{\Pi}(\sigma_{ij}^s, \bar{q}_i^s) = \frac{1}{2}\int_V \sigma_{ij}^s H_{ijkl}\sigma_{kl}^s \mathrm{d}V - \int_{S_u} \bar{q}_i^s u_i^0 \mathrm{d}S \tag{3—30}$$

of the total complementary energy, i.e.

$$\delta\bar{\Pi} = 0. \tag{3—31}$$

Alternatively, if a statically admissible stress and force field makes the total complementary energy of an elastic body a minimum and satisfies the kinematic boundary conditions, then it is identical with the actual stress and force field.

This last formulation states the necessary and sufficient condition for the compatibility of deformations of an elastic body.

In the special case, when

$$u_i^0 = 0 \quad \text{on} \quad S_u, \tag{3—32}$$

the external complementary energy is zero and the expression (3—30) has a simpler form. This leads to the *principle of minimum elastic strain energy or Castigliano's theorem.* This theorem states that if the surface displacements are specified to be zero on S_u, then among all the statically admissible stress fields of a linearly elastic body the actual stress field which satisfies the compatibility conditions minimizes the functional of the elastic strain energy

$$U^e = \frac{1}{2}\int_V \sigma_{ij}^s H_{ijkl}\sigma_{kl}^s \mathrm{d}V. \tag{3—33}$$

The strain energy of a linearly elastic body expressed in terms of stresses has the form

$$U^e = \frac{1}{2}\int_V \sigma_{ij} H_{ijkl}\sigma_{kl}\mathrm{d}V = \frac{1}{2E}\int_V \Big[(\sigma_{xx}^2 + \sigma_{yy}^2 + \sigma_{zz}^2) - 2\nu(\sigma_{xx}\sigma_{yy} + \sigma_{yy}\sigma_{zz} + \sigma_{zz}\sigma_{xx}) + 2(1+\nu)(\sigma_{xy}^2 + \sigma_{yz}^2 + \sigma_{zx}^2)\Big]\mathrm{d}V. \tag{3—34}$$

Let us consider another special case when the body on S_u is *elastically supported.* Then, on the surface S_u the displacements and the surface forces are linearly related

$$\left.\begin{aligned} &u_i = -C_{ij}\bar{q}_j, \\ &\text{or} \\ &\bar{q}_i = -D_{ij}u_j. \end{aligned}\right\} \tag{3—35}$$

Here the elements of the tensors C_{ij} and $D_{ij} = C_{ij}^{-1}$ are the spring coefficients of the elastic supports. The negative sign in eq. (3—35) is due to the fact that at the elastic supports the displacements and the reaction forces always have opposite directions. In this special case the external complementary virtual work has the form

$$\delta\bar{W}^e = \int_{S_u} u_i^s \delta\bar{q}_i^s \mathrm{d}S = -\int_{S_u} C_{ij}\bar{q}_j^s \delta\bar{q}_i^s \mathrm{d}S = -\delta\left[\frac{1}{2}\int_{S_u} \bar{q}_i^s C_{ij}\bar{q}_j^s \mathrm{d}S\right].$$

Comparing this result with eqs (3—25) and (3—30) the functional of the complementary energy is now expressed in the form

$$\bar{\Pi} = \frac{1}{2}\int_V \sigma_{ij}^s H_{ijkl}\sigma_{kl}^s \mathrm{d}V + \int_{S_u} \bar{q}_i^s C_{ij}\bar{q}_j^s \mathrm{d}S \tag{3—36}$$

and this functional takes its minimum in the case of the actual stresses and forces.

As in the case of the principle of stationary potential energy, the principle of minimum complementary energy can also be expressed in a more general form and this leads to the *Helliger–Reissner principle* (see e.g. Washizu 1975).

Finally, we note that the potential energy is expressed in terms of strains and displacements, while the complementary energy is written as function of stresses. Thus, depending on the nature of the boundary conditions in the problem to be solved, either the principle of stationary potential energy or the principle of minimum complementary energy may lead to more convenient calculations.

3.4. VARIATIONAL PRINCIPLES OF PLASTICITY

3.4.1. GENERAL REMARKS

Since the constitutive equation of elasto-plastic bodies are more complicated than those involved in the theory of elasticity, it may be expected that establishing variational principles in plasticity is more difficult. Nevertheless, in the framework of both the incremental and deformation theories a great many variational principles have been derived for different yield conditions and constitutive equations. A number of these principles have great practical importance, since in plasticity exact solutions are harder to obtain than in elasticity (see e.g. Hill 1950; Prager, Hodge 1951; Washizu 1975).

In the following, we will deal only with linearly elastic–perfectly plastic bodies which obey the constitutive equations of the incremental theory of plasticity and we will

present variational principles which can be applied to incremental load history analysis, to limit analysis and to the shakedown analysis of elasto-plastic bodies. These principles have already been very successfully used in the numerical solution of many engineering problems. The numerical formulation of these principles applicable to discretized systems will be presented in Section 6.

The principles of virtual work and of complementary virtual work are valid for elasto-plastic bodies as well, and it will be seen that they play an important role in the derivation and application of the variational principles of plasticity.

3.4.2. INCREMENTAL LOAD HISTORY ANALYSIS

3.4.2.1. INTRODUCTION

The problem of incremental load history analysis can be defined as follows.* Consider an elasto-plastic body which is in a state of static equilibrium under the surface forces q_i on S_q and displacements u_i^0 on S_u, and assume that the instantaneous states of stress and strain fields and their loading history are known. Now, external force increments dq_i on S_q and displacement increments du_i^0 on S_u are applied under quasi-static conditions. The problem is to determine the stress, strain and displacement increments $d\sigma_{ij}$, $d\varepsilon_{ij}$ and du_i induced in the body, assuming that the increments are infinitesimal. For convenience, the problem can also be stated in terms of rates. Then, the rates of application of the external forces $\dot{q}_i$ and the surface velocities v_i^0 are prescribed, and the problem is to find the stress and strain rates $\dot{\sigma}_{ij}$ and $\dot{\varepsilon}_{ij}$ and the velocities v_i induced in the body.

To construct the variational principles of incremental analysis the definitions presented in Section 3.1. (see eqs (3—1)–(3—4)) will now be modified:

(a) A stress rate and force rate field $\dot{\sigma}_{ij}^s$, $\dot{q}_i$, $\dot{\bar{q}}_i^s$ is called *statically admissible* if it satisfies the equilibrium conditions

$$\dot{\sigma}_{ij,j}^s = 0, \quad \dot{\sigma}_{ij}^s = \dot{\sigma}_{ji}^s \quad \text{in} \quad V, \tag{3—37}$$

$$\dot{\sigma}_{ij}^s n_j = \dot{q}_i \quad \text{on} \quad S_q, \tag{3—38}$$

$$\dot{\sigma}_{ij}^s n_j = \dot{\bar{q}}_i^s \quad \text{on} \quad S_u. \tag{3—39}$$

(b) A strain rate and velocity field $\dot{\varepsilon}_{ij}^k$, v_i^k, v_i^0 is called *kinematically admissible* if it satisfies the kinematic conditions

$$\dot{\varepsilon}_{ij}^k = \frac{1}{2}(v_{i,j}^k + v_{j,i}^k) \quad \text{in} \quad V, \tag{3—40}$$

$$v_i^k = v_i^0 \quad \text{on} \quad S_u. \tag{3—41}$$

* In the following, for convenience, the absence of body forces f_i will be assumed.

MAGYAR
TUDOMÁNYOS AKADÉMIA
KÖNYVTÁRA

3.4.2.2. PRINCIPLE OF MINIMUM COMPLEMENTARY ENERGY RATE

The principle of minimum complementary energy rate is stated as follows:
During the change of an instantaneous stress field σ_{ij} of a linearly elastic–perfectly plastic body under the action of the loads and displacements $\dot{q}_i$ and $\dot{u}_i^0$ among all statically admissible stress rate and force rate fields that will actually develop which minimizes the functional

$$\dot{\Pi}^s = \frac{1}{2}\int \dot{\sigma}_{ij}^s H_{ijkl}\dot{\sigma}_{ke}^s \mathrm{d}V - \int_{S_u} \dot{\bar{q}}_i^s v_i^0 \mathrm{d}S \tag{3—42}$$

of the complementary energy rate and at those points of the body where $f(\sigma_{ij}, k)=0$ satisfies the condition

$$\dot{f} = \frac{\partial f}{\partial \sigma_{ij}}\dot{\sigma}_{ij}^s \leq 0. \tag{3—43}$$

This inequality expresses the condition that the stresses $(\sigma_{ij}+\dot{\sigma}_{ij}^s)$ developed after the change of the external loads and displacements should also satisfy the yield condition i.e., $f[(\sigma_{ij}+\dot{\sigma}_{ij}^s), k]\leq 0$. The geometrical meaning of this condition is that the stress rate vector $\dot{\sigma}_{ij}^s$ attached to the end of the stress vector σ_{ij} should not pass through the yield surface.

Although this principle is formally similar to the principle of minimum complementary energy, two substantial differences should be noted:

(a) While the principle of minimum complementary energy defines the kinematically compatible *state* of a linearly elastic body, the principle of minimum complementary energy rate defines the kinematically compatible *change* in state of a linearly elastic–perfectly plastic body.

(b) In the case of the principle of minimum complementary energy rate, an additional condition given by eq. (3—43) has to be taken into consideration which in the case of elastic bodies obviously should not be introduced. Since this additional condition is expressed in the form of an inequality the analytical solution of elasto-plastic problems by the use of variational calculus is, in general, not possible.

As a special case, the principle of minimum complementary energy rate can be applied to the analysis of linearly elastic bodies. The additional condition (3—43) can then be omitted and, integrating the functional (3—42) with respect to time, we obtain the principle of minimum complementary energy given by eq. (3—31).

To prove the principle given above we must show that, for any statically admissible stress rate and force rate field $\dot{\sigma}_{ij}^s$, $\dot{\bar{q}}_i^s$, the complementary energy rate $\dot{\Pi}^s$ cannot be smaller than the complementary energy rate $\dot{\Pi}$ expressed in terms of the actual stress and force rates $\dot{\sigma}_{ij}$ and $\dot{\bar{q}}_i$. Assuming first, an arbitrary, statically admissible stress and force rate field and secondly, the actual stress and force rate field to be subject to variation and using the actual strain rates $\dot{\varepsilon}_{ij}$ and the velocities v_i^0, the principle of complementary virtual power (see eq. (3—10)) can be written as

$$\left.\begin{aligned} \int_V \dot{\varepsilon}_{ij}\dot{\sigma}_{ij}^s \mathrm{d}V &= \int_{S_u} v_i^0 \dot{\bar{q}}_i^s \mathrm{d}S, \\ \int_V \dot{\varepsilon}_{ij}\dot{\sigma}_{ij} \mathrm{d}V &= \int_{S_u} v_i^0 \dot{\bar{q}}_i \mathrm{d}S. \end{aligned}\right\} \tag{3—44}$$

Substituting the general form of the constitutive equation of linearly elastic–perfectly plastic materials (see eqs (2—70b) and (2—89))

$$\dot{\varepsilon}_{ij}=\dot{\varepsilon}_{ij}^{e}+\dot{\varepsilon}_{ij}^{p}=H_{ijkl}\dot{\sigma}_{kl}+\dot{\lambda}\frac{\partial f}{\partial \sigma_{ij}} \tag{3—45}$$

into these two equations and subtracting them from each other yields

$$\int_{S_u}(\dot{q}_i^s-\dot{\bar{q}}_i)v_i^0 dS=\int_V(\dot{\sigma}_{ij}^s-\dot{\sigma}_{ij})\left(H_{ijkl}\dot{\sigma}_{kl}+\dot{\lambda}\frac{\partial f}{\partial \sigma_{ij}}\right)dV=$$

$$=\int_V\left[\dot{\sigma}_{ij}^s H_{ijkl}\dot{\sigma}_{kl}-\dot{\sigma}_{ij}H_{ijkl}\dot{\sigma}_{kl}+\dot{\sigma}_{ij}^s\dot{\lambda}\frac{\partial f}{\partial \sigma_{ij}}\right]dV. \tag{3—46}$$

Here we made use of the last expression of eqs (2—123) according to which

$$\dot{\lambda}\dot{f}=\dot{\lambda}\frac{\partial f}{\partial \sigma_{ij}}\dot{\sigma}_{ij}=0. \tag{3—47}$$

This is due to the fact that in elastic and in passive plastic stages $\dot{\lambda}=0$ and in active plastic stages $\dot{f}=0$; thus $\dot{\lambda}\dot{f}$ always vanishes.

Next, we write the complementary energy rate in terms of the actual stresses and surface forces

$$\dot{\Pi}=\frac{1}{2}\int_V\dot{\sigma}_{ij}H_{ijkl}\dot{\sigma}_{kl}dV-\int_{S_u}\dot{\bar{q}}_i v_i^0 dS. \tag{3—48}$$

Then, making use of relationship (3—46), we find the difference between the functionals given by eqs (3—42) and (3—47), as follows:

$$\dot{\Pi}^s-\dot{\Pi}=\frac{1}{2}\int_V\left[(\dot{\sigma}_{ij}^s-\dot{\sigma}_{ij})H_{ijkl}(\dot{\sigma}_k^s-\dot{\sigma}_{ij})-2\dot{\lambda}\frac{\partial f}{\partial \sigma_{ij}}\dot{\sigma}_{ij}^s\right]dV. \tag{3—49}$$

If $\dot{\sigma}_{ij}^s\neq\dot{\sigma}_{ij}$, the first integrand represents the elastic strain energy due to the stress rates $(\dot{\sigma}_{ij}^s-\dot{\sigma}_{ij})$, which is always positive. At the points in the body where $f<0$, $\dot{\lambda}$ equals zero and the second integrand vanishes; and at the points where $f=0$ the second integrand cannot be negative because of the additional condition (3—43). Thus, if $\dot{\sigma}_{ij}^s\neq\dot{\sigma}_{ij}$, $\dot{\Pi}^s-\dot{\Pi}>0$.

If $\dot{\sigma}_{ij}^s=\dot{\sigma}_{ij}$, considering eq. (3—47), the total expression (3—49) vanishes, i.e. $\dot{\Pi}^s-\dot{\Pi}=0$. This is the proof of the principle of minimum complementary energy rate (Greenberg 1949).

In the special case when the surface displacements u_i^0 are unchanged during the loading procedure, i.e. if $v_i^0=0$, the functional defined by eq. (3—42) has a simpler form

$$\dot{\Pi}^s=\frac{1}{2}\int_V\dot{\sigma}_{ij}^s H_{ijkl}\dot{\sigma}_{kl}^s dV$$

and this functional takes its minimum value in the case of the actual stress rates.

Finally, we note that for *rigid-perfectly plastic bodies* a special principle can be derived in terms of the statically admissible stresses. Assuming that under constant surface forces q_i on S_q and given surface velocities v_i^0 on S_u the *entire* body is in a state of plastic flow, this principle can be stated as follows (Hill 1949):

In a state of plastic flow under constant external forces and prescribed surface velocities, among all the statically admissible stress fields of a rigid–perfectly plastic body the actual one makes the external plastic work

$$\int_{S_u} \bar{q}_i^s v_i^0 \mathrm{d}S = \int_{S_u} \sigma_{ij}^s n_j v_i^0 \mathrm{d}S \tag{3—50}$$

an absolute maximum.

This is called the *principle of maximum plastic work* or sometimes the *principle of maximum plastic resistance.*

3.4.2.3. PRINCIPLE OF MINIMUM POTENTIAL ENERGY RATE

The principle of minimum potential energy rate is stated as follows:

For a linearly elastic–perfectly plastic body in static equilibrium, among all kinematically admissible strain rate and velocity fields the actual one which also satisfies the equilibrium conditions minimizes the functional

$$\dot{\Pi} = \frac{1}{2}\int_V \dot{\sigma}_{ij}^k \dot{\varepsilon}_{ij}^k \mathrm{d}V - \int_{S_q} \dot{q}_i v_i^k \mathrm{d}S. \tag{3—51}$$

Here $\dot{\sigma}_{ij}^k$ denotes a stress rate field which is associated with the strain rate field $\dot{\varepsilon}_{ij}^k$ by means of the constitutive equation (2—104)

$$\dot{\sigma}_{ij}^k = \left[D_{ijkl} - \alpha \frac{D_{ijrs}\dfrac{\partial f}{\partial \sigma_{rs}} D_{pqkl}\dfrac{\partial f}{\partial \sigma_{pq}}}{D_{pqrs}\dfrac{\partial f}{\partial \sigma_{pq}}\dfrac{\partial f}{\partial \sigma_{rs}}} \right] \dot{\varepsilon}_{kl}^k \tag{3—52}$$

where

$$\begin{aligned} &\alpha = 0, \quad \text{if} \quad f<0 \quad \text{or} \quad f=0 \quad \text{and} \quad D_{ijkl}\frac{\partial f}{\partial \sigma_{ij}}\dot{\varepsilon}_{kl}^k \le 0, \\ &\alpha = 1, \quad \text{if} \quad f=0 \quad \text{and} \quad D_{ijkl}\frac{\partial f}{\partial \sigma_{ij}}\dot{\varepsilon}_{kl}^k > 0. \end{aligned} \tag{3—53}$$

Unfortunately, the substitution of eq. (3—52) into the functional (3—51) does not lead to simplifications such as it was possible in the derivation of the principle of minimum complementary energy rate. This is because in relationship (3—52) the elastic and the plastic strain rates do not appear separately. The application of the principle of minimum potential energy rate therefore leads to greater mathematical difficulties. The proof of this principle can be found elsewhere (e.g. Hill 1950; Prager, Hodge 1951).

In the case of *rigid-perfectly plastic bodies*, the variational principles expressed in terms of the kinematically admissible strain rates and velocity fields also have much simpler form. Using the Lévy–v. Mises constitutive equations, and assuming that under constant surface forces q_i on S_q and given surface velocities v_i^0 on S_u the *entire* body is in a state of plastic flow, the following principle can be derived (Markov 1947):

For a state of plastic flow under constant external forces and prescribed surface velocities, among all kinematically admissible strain rate and velocity fields of a Lévy–v. Mises rigid-plastic body the actual one minimizes the functional

$$\sqrt{2}\tau_0 \int_V \sqrt{\dot{\varepsilon}_{ij}^k \dot{\varepsilon}_{ij}^k} \mathrm{d}V - \int_{S_q} q_i v_i^k \mathrm{d}S. \tag{3—54}$$

3.4.3. LIMIT ANALYSIS

3.4.3.1. GENERAL REMARKS

One of the most successful applications of the variational formulations in the incremental theory of plasticity is the theory of limit analysis. The problem of limit analysis is formulated as follows.

Consider an elastic–perfectly plastic body subjected to given surface forces q_i on the surface S_q, while on the remaining surface S_u the surface displacements are zero ($u_i^0 = 0$), and assume that all the surface forces are continuously increased in such a manner as to preserve their positions, directions and ratios. This is called *proportional* or *one-parameter loading*, and can be defined in the form

$$q_i(x_i, t) = m(t)\, q_{i0}(x_i), \tag{3—55}$$

where the vector–vector function q_{i0} describes the positions and directions of the external forces and m is a monotonically increasing scalar parameter called the *load multiplier* or *load intensity*.

When the load intensity is sufficiently small, the entire body behaves elastically. At a certain load intensity m_e, one or maybe (simultaneously) more points in the body reach the plastic state. This load indicates the limit of applicability of the theory of elasticity and therefore the load $q_{ie} = m_e q_{i0}$ is called the *elastic limit load*. As m increases further, the plastic regions of the body gradually spread and at a well defined intensity m_p a state of *unrestricted plastic flow* will eventually be reached, such that an increase in plastic strains and displacements under *constant* external forces becomes possible for the first time during the loading process. The state when the entire elasto-plastic body or one or several parts of it undergo unrestricted plastic deformation under constant external load is called the *plastic limit state*. The corresponding multiplier m_p designates the *plastic limit load multiplier (collapse load multiplier)* and $q_{ip} = m_p q_{i0}$ is the *plastic limit load (collapse load)* of the body.

In the following, we will study only the *incipient plastic deformations* arising at the plastic limit state of the body, and therefore the statements and principles presented below will be confined to the region of *small displacements*. Besides, since at the plastic limit state the stresses and external forces can still maintain the *static equilibrium* of the body, the equilibrium equations will be applied.

The fundamental problem of limit analysis is to determine the plastic limit load multiplier and the stresses, strain rates and velocities at the plastic limit state of the body. This can always be achieved by conducting an incremental analysis which is, however, usually very time-consuming. The main advantage of the extremum principles to be presented lies in the fact that, without a study of the entire loading history, they directly provide the exact value or the upper and lower bounds of the plastic limit load multiplier. This is achieved merely by considering the sets of statically or kinematically admissible stress or strain rate fields of the body. Before discussing these extremum principles we will derive the *theorem of constant stress.*

3.4.3.2. THEOREM OF CONSTANT STRESS

Consider the plastic limit state of a body under the plastic limit load $q_{ip}=m_p q_{i0}$, and denote the stresses, strain rates and velocities* arising in this state by σ_{ij}, $\dot{\varepsilon}_{ij}$ and v_i. Then, *the theorem of constant stress* states, that at the plastic limit state of a linearly elastic–perfectly plastic body, the stresses remain unchanged during an increase in deformation, i.e.

$$\dot{\sigma}_{ij}=0. \tag{3—56}$$

At the plastic limit, the stresses σ_{ij} maintain with the plastic limit load q_{ip} a quasi-static state of equilibrium; thus, using the actual strain rates and velocities as kinematically admissible strain rate and velocity fields the principle of virtual velocities can be applied. To prove the above theorem, we will first assume that at the plastic limit state during an increase in deformation the stresses also increase, i.e. $\dot{\sigma}_{ij}\neq 0$, and then we will show that this is incompatible with the principle of virtual velocities.

Let us write the principle of virtual velocities for the actual stress rates, strain rates and velocities. Since at the plastic limit state by definition $\dot{q}_{ip}=\dot{m}_p q_{i0}=0$, we obtain

$$\int_V \dot{\sigma}_{ij}\dot{\varepsilon}_{ij}\mathrm{d}V=\int_{S_q}\dot{q}_{ip}v_i\mathrm{d}S=0. \tag{3—57}$$

Now, substituting the constitutive equations (3—45) of linearly elastic–perfectly plastic bodies into this relationship we can write

$$\int_V \dot{\sigma}_{ij}\dot{\varepsilon}_{ij}\mathrm{d}V=\int_V\left(\dot{\sigma}_{ij}H_{ijkl}\dot{\sigma}_{kl}+\dot{\lambda}\frac{\partial f}{\partial\sigma_{ij}}\dot{\sigma}_{ij}\right)\mathrm{d}V=\int_V(\dot{\sigma}_{ij}H_{ijkl}\dot{\sigma}_{kl})\mathrm{d}V=0. \tag{3—58}$$

Here we made use of the relationship

$$\dot{\lambda}\frac{\partial f}{\partial\sigma_{ij}}\dot{\sigma}_{ij}=\dot{\lambda}\dot{f}=0,$$

* Because of unrestricted plastic flow, the strains and displacements cannot be specified at the plastic limit state.

since in the elastic and in the passive plastic states $\dot{\lambda}=0$, and in the active plastic state $\dot{f}=0$. The expression (3—58) represents the rate of elastic strain energy of the body. This can vanish only, if at each point in the body $\dot{\sigma}_{ij}=0$. This is the proof of the theorem of constant stress. From this theorem significant conclusions can be drawn.

It is obvious that if $\dot{\sigma}_{ij}=0$ then $\dot{\varepsilon}^{e}_{ij}=H_{ijkl}\dot{\sigma}_{kl}=0$, i.e at the plastic limit state a body undergoes only *plastic* deformations, so that $\dot{\varepsilon}_{ij}=\dot{\varepsilon}^{p}_{ij}$. Consequently, in limit analysis the elastic material properties do not play any role and therefore the material of the body can be considered as *rigid–perfectly plastic.*

The plastic flow of a *rigid–perfectly plastic body* starts only when the plastic limit state is reached. Below this limit the body experiences no deformations. Consequently, the plastic limit state and the plastic limit load of a body are independent of the loading history.

3.4.3.3. STATIC PRINCIPLE

Consider the sets of statically admissible stress and external force fields σ^{s}_{ij} and $q_{is}=m_s q_{i0}$ of a rigid-perfectly plastic body, which satisfy the equilibrium conditions

$$\left.\begin{aligned} &\sigma^{s}_{ij,j}=0, \quad \sigma^{s}_{ij}=\sigma^{s}_{ji} \quad \text{in} \quad V,\\ &\sigma^{s}_{ij}n_j=m_s q_{i0} \quad \text{on} \quad S_u \end{aligned}\right\} \tag{3—59}$$

and define the load multipliers m_s in such a manner that at each point in the body the yield condition

$$f(\sigma^{s}_{ij},k)\leqq 0 \tag{3—60}$$

is also satisfied.

Then, the multipliers m_s are called *statically admissible stable load multipliers* and the *static principle* or *lower bound theorem of limit analysis* states that any statically admissible stable load multiplier is less than or equal to the plastic limit load multiplier

$$m_s\leqq m_p. \tag{3—61}$$

To prove this principle, let us consider the actual stress field σ_{ij} in a body which maintains a quasi-static equilibrium with the plastic limit load $q_{ip}=m_p q_{i0}$, and another arbitrary statically admissible stress and force field σ^{s}_{ij} and $q_{is}=m_s q_{i0}$ which satisfies the yield condition (3—60). Making use of the actual strain rates* $\dot{\varepsilon}_{ij}$ and velocities v_i which are kinematically admissible, the principle of virtual velocities can be applied for both the stress and the force fields under consideration

$$\int_V \sigma_{ij}\dot{\varepsilon}_{ij}\,dV=m_p\int_{S_q} q_{i0}v_i\,dS,$$

$$\int_V \sigma^{s}_{ij}\dot{\varepsilon}_{ij}\,dV=m_s\int_{S_q} q_{i0}v_i\,dS.$$

* Since in a rigid-plastic body $\varepsilon^{e}_{ij}=0$ and therefore $\varepsilon_{ij}=\varepsilon^{p}_{ij}$, in the following the plastic strain rates will be denoted, for convenience, by $\dot{\varepsilon}_{ij}$.

Subtracting these two equations yields

$$\int_V (\sigma_{ij} - \sigma^s_{ij})\dot{\varepsilon}_{ij} \mathrm{d}V = (m_p - m_s) \int_{S_q} q_{i0} v_i \mathrm{d}S. \tag{3—62}$$

According to the convexity of the yield surface and the normality rule, at every point in the body

$$(\sigma_{ij} - \sigma^s_{ij})\dot{\varepsilon}_{ij} \geqq 0, \tag{3—63}$$

as it is obvious from Fig. 3—2(a). Consequently, eq. (3—62) yields

$$(m_p - m_s) \int_{S_q} q_{i0} v_i \mathrm{d}S \geqq 0.$$

In this expression, the integral represents the work done by the external forces on the actual velocities of the body. As a consequence of the definition of the plastic limit state this work cannot be negative, consequently $m_s \leq m_p$, and the static principle has been proved.

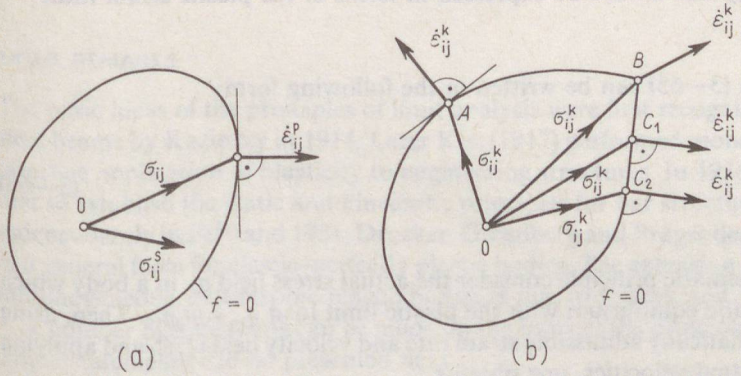


Fig. 3–2

3.4.3.4. KINEMATIC PRINCIPLE

Consider the sets of kinematically admissible plastic strain rate and velocity fields $\dot{\varepsilon}^k_{ij}$ and v^k_i in a rigid-perfectly plastic body which satisfy the kinematic conditions

$$\left.\begin{aligned} \dot{\varepsilon}^k_{ij} &= \frac{1}{2}(v^k_{i,j} + v^k_{j,i}) \quad \text{in} \quad V, \\ v^k_i &= 0 \quad \text{on} \quad S_u \end{aligned}\right\} \tag{3—64}$$

and define the associated load multipliers m_k in the following manner

$$m_k \int_{S_q} q_{i0} v^k_i \mathrm{d}S \geqq \int_V \sigma^k_{ij} \dot{\varepsilon}^k_{ij} \mathrm{d}V, \tag{3—65}$$

$$\int_{S_q} q_{i0} v^k_i \mathrm{d}S > 0. \tag{3—66}$$

Here σ_{ij}^k denotes the stresses associated with the kinematically admissible strain rates $\dot{\varepsilon}_{ij}^k$. The multipliers m_k are called *kinematically admissible unstable load multipliers.* The *kinematic principle* or *upper bound theorem of limit analysis* states that any kinematically admissible unstable load multiplier is greater than or equal to the plastic limit load multiplier:

$$m_k \geqq m_p. \tag{3—67}$$

To prove this principle, first we have to show that the expression (3—65) uniquely defines a load multiplier m_k for a given plastic strain rate and velocity field in the body. Considering the convexity of the yield surface and the normality of the plastic strain rate vector, we can see from Fig. 3—2(b) that for a given plastic strain rate vector $\dot{\varepsilon}_{ij}^k$ the yield locus, and consequently the associated stress vector σ_{ij}^k, can in general be uniquely determined (see points A or B). The only exception is when the vector $\dot{\varepsilon}_{ij}^k$ is normal to a flat part of the yield surface. Then, a set of stress vectors σ_{ij}^k can be associated with a given strain vector $\dot{\varepsilon}_{ij}^k$ (see points C_1 and C_2), but even in this case the scalar product $\sigma_{ij}^k \dot{\varepsilon}_{ij}^k$, i.e. the work done by σ_{ij}^k on $\dot{\varepsilon}_{ij}^k$, is uniquely determined. This means that the *specific dissipation of energy* can always be expressed in terms of the plastic strain rates

$$d = \sigma_{ij}^k \dot{\varepsilon}_{ij}^k = d(\dot{\varepsilon}_{ij}^k)$$

and the expression (3—65) can be written in the following form

$$m_k \geqq \frac{\int\limits_V d(\dot{\varepsilon}_{ij}^k) \mathrm{d}V}{\int\limits_{S_q} q_{i0} v_i^k \mathrm{d}S}. \tag{3—68}$$

To prove the kinematic principle consider the actual stress field σ_{ij} in a body which maintains quasi-static equilibrium with the plastic limit load $q_{ip} = m_p q_{i0}$. Then, using any arbitrary kinematically admissible strain rate and velocity field v_i^k, $\dot{\varepsilon}_{ij}^k$ and applying the principle of virtual velocities, one obtains

$$m_p \int\limits_{S_q} q_{i0} v_i^k \mathrm{d}S = \int\limits_V \sigma_{ij} \dot{\varepsilon}_{ij}^k \mathrm{d}V.$$

Subtracting this equation from eq. (3—65) yields

$$(m_k - m_p) \int\limits_{S_q} q_{i0} v_i^k \mathrm{d}S \geq \int\limits_V (\sigma_{ij}^k - \sigma_{ij}) \dot{\varepsilon}_{ij}^k \mathrm{d}V. \tag{3—69}$$

Here σ_{ij}^k is associated with $\dot{\varepsilon}_{ij}^k$ and satisfies the yield condition $f(\sigma_{ij}^k, k) = 0$ at each point in the body. Therefore, considering the convexity of the yield surface and the normality of the vector of the plastic strain rate, we can write

$$(\sigma_{ij}^k - \sigma_{ij}) \dot{\varepsilon}_{ij}^k \geqq 0,$$

as can be seen from Fig. 3—3. Consequently, eq. (3—69) results in

$$(m_k - m_p) \int\limits_{S_q} q_{i0} v_i^k \mathrm{d}S \geqq 0.$$

Here, because of eq. (3—66), the integral expression cannot be negative and therefore $m_k \geqq m_p$. Thus, the kinematic principle has been proved.

In the limit analysis of structures, the kinematically admissible strain rates and velocity fields, which also satisfy the condition (3—66), are called *yield mechanisms.*

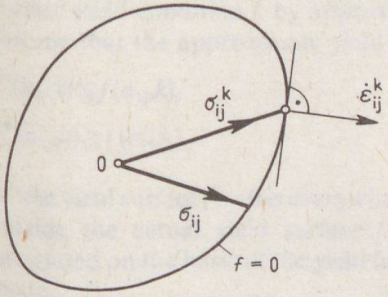


Fig. 3–3

3.4.3.5. REMARKS

The basic ideas of the principles of limit analysis were first recognized and applied to steel beams by Kazinczy in 1914. Later Kist (1917) performed pioneering work on the intuitive application of plasticity to engineering structures. In 1936 Gvozdev was the first to establish the static and kinematic principles for bar structures and plates and, independently in 1950 and 1951, Drucker, Greenberg and Prager derived the principles in a general form for elastic–perfectly plastic bodies. The extension of the principles to inhomogeneous, orthotropic plastic bodies is due to Olszak and Perzyna (1958).

A number of statements can be made on the basis of the principles of limit analysis. These statements will be presented next.

At the plastic limit state the stresses can maintain a static equilibrium with the plastic limit load and, at the same time, satisfy the yield condition at every point in the body. Thus, the plastic limit load multiplier is statically admissible and stable, i.e. $m_p = m_s$. On the other hand, at the plastic limit state the plastic limit load is just large enough to force the body to undergo plastic deformations and displacements. Thus, satisfying eqs (3—65), the plastic limit load multiplier is kinematically admissible and unstable, i.e. $m_p = m_k$. Briefly, the plastic limit load is the largest load which can be balanced by the stresses satisfying the yield conditions, and the smallest load which can convert the body into a yield mechanism.

Considering these statements and eqs (3—61) and (3—67) one can state that the plastic limit load multiplier is equal to the maximum statically admissible stable load multiplier

$$m_p = \max m_s. \tag{3—70}$$

The plastic limit load multiplier is also equal to the minimum kinematically admissible unstable load multiplier

$$m_p = \min m_k. \tag{3—71}$$

The plastic limit load multiplier is equal to that load multiplier which is, at the same time, statically admissible, stable and kinematically admissible, unstable

$$m_p = m = m_s = m_k. \tag{3—72}$$

The statements above are symbolically illustrated in Fig. 3—4.

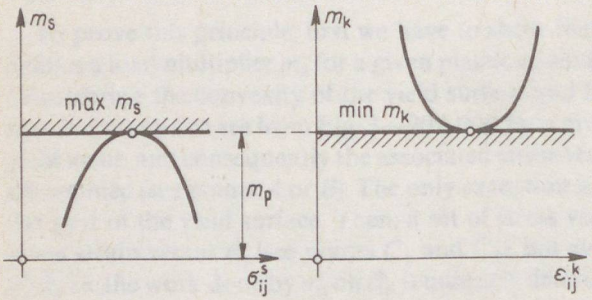


Fig. 3–4

Now it is obvious that there are three ways to determine the plastic limit load multiplier of a body:

- finding the maximum value of the statically admissible stable load multipliers,
- finding the minimum value of the kinematically admissible unstable load multipliers, and
- proving that a certain load multiplier is, at the same time, statically admissible, stable and also kinematically admissible, unstable.

The static and kinematic principles are very often used for the calculation of the approximate value of the plastic limit load multiplier. One can obviously state that any statically admissible, stable load multiplier is a lower bound and any kinematically admissible, unstable load multiplier is an upper bound for the plastic limit load multiplier

$$m_s \leq m_p \leq m_k. \tag{3—73}$$

By determining a lower and an upper bound, the "best" approximate value of the plastic limit load multiplier can be obtained as

$$m_p \approx \frac{1}{2}(m_s + m_k). \tag{3—74}$$

Using this value, the error to be expected in m_p is

$$\Delta m_p \leqq \frac{m_k - m_s}{2m_s}. \tag{3—75}$$

By repeated calculations of the load multipliers the lower and upper bounds can be improved until the error is less than a requested value.

On the basis of the static and kinematic principles other statements that are important in the practical applications of limit analysis can also be made. The

correctness of these statements is obvious, therefore they are presented here without proof.

Adding weightless material to a body does not decrease the plastic limit load.

Taking away weightless material from a body does not increase the plastic limit load.

The solution of many problems of limit analysis can be simplified by replacing the correct yield condition f, by approximate (usually linearized) yield conditions. Let us assume that the approximate yield functions f^{I} and f^{II} satisfy the relations

$$f^{\mathrm{I}}(\sigma_{ij},k) \leqq f(\sigma_{ij},k),$$

$$f^{\mathrm{II}}(\sigma_{ij},k) \geqq f(\sigma_{ij},k),$$

i.e. the yield surface $f^{\mathrm{I}}=0$ is everywhere inside, and the yield surface $f^{\mathrm{II}}=0$ is everywhere outside the actual yield surface $f=0$ (Fig. 3—5). Then, for the load multipliers calculated on the basis of the yield functions f^{I} and f^{II}, the following statements can be made.

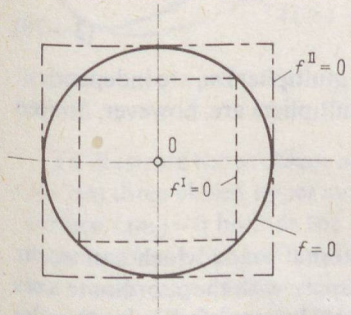


Fig. 3–5

Any statically admissible, stable load multiplier m_s^{I} calculated on the basis of a yield function $f^{\mathrm{I}} \leqq f$ is less than or equal to the plastic limit load multiplier m_p determined by the use of the yield function f

$$m_s^{\mathrm{I}} \leqq m_p. \tag{3—76}$$

Consequently, the plastic limit load multiplier m_p^{I} is a lower bound for m_p

$$m_p^{\mathrm{I}} \leqq m_p. \tag{3—76a}$$

Any kinematically admissible, unstable load multiplier m_k^{II} calculated on the basis of a yield function $f^{\mathrm{II}} \geqq f$ is greater than or equal to the plastic limit load multiplier m_p determined by the use of the yield function f

$$m_k^{\mathrm{II}} \geqq m_p. \tag{3—77}$$

Consequently, the plastic limit load multiplier m_p^{II} is an upper bound for m_p

$$m_p^{\mathrm{II}} \geqq m_p. \tag{3—77a}$$

The above statements express the obvious fact that decreasing and increasing the "yield strength" of the material cannot increase and decrease, respectively, the plastic limit load of a body.

Finally, bearing in mind that the plastic limit load does not depend on the loading path, one can state that initial and residual stresses and strains and changes in temperature have no influence on the plastic limit load of a body, provided that the yield condition is independent of these effects.

3.4.4. SHAKEDOWN ANALYSIS

3.4.4.1. INTRODUCTION

To define the fundamental problem of shakedown analysis, consider a linearly elastic–perfectly plastic body subjected to quasi-static *multiple loading* on the surface S_q, while on the remaining surface S_u the surface displacements are specified to be zero ($u_i^0 = 0$). We assume that the multiple loading consists of a set of one-parameter loads

$$q_i^{(l)} = m_l(t)\, q_{i0}^{(l)}(x_i), \quad (l = 1,2,\ldots r) \tag{3—78}$$

which can vary independently of each other, i.e. the load multipliers m_l are independent scalar functions of time.* The magnitudes of the load multipliers are, however, limited by the relationship

$$L(m_l) \leq 0.$$

This defines all the *possible combinations* of the external loads which can occur during the loading procedure. In an r-dimensional *load space* with the coordinate axes $m_1, m_2, \ldots m_r$ the function $L(m_l) = 0$ is illustrated by a closed hypersurface bounding the *domain of possible loads* and the curves inside this domain represent the *load paths*, as shown in Fig. 3—6. When monotonically increasing *proportional loading* is assumed, the ratios of m_l are kept unchanged during the loading process and the load path is illustrated by a *straight line* (e.g. line OA in Fig. 3—6). In the case of *cyclic loading*, the loads are applied repeatedly and their variation is represented by a *closed curve* in the load space (e.g. the curve O–B–C–O in Fig. 3—6 describes one cycle). Finally, the curve O–D–E–F etc. in Fig. 3—6 illustrates a *general loading* process.

In the case of cyclic loading, during each cycle *alternating plastic deformations* may arise which can lead after a certain amount of repetition to failure, through the appearance of localized fractures. During a general loading procedure, the body may also undergo plastic deformations several times. These plastic deformations may accumulate without limit and lead to *progressive plastic flow* or, in other words, to *incremental collapse*. Obviously, both alternating plastic flow and progressive plastic flow are phenomena which should be avoided in engineering practice.

* As in our previous notes in plasticity, the loading procedure and the state of the body can be expressed in terms of any monotonically increasing parameter. In the following, for the sake of simplicity, we will assume that this parameter is time.

In connection with the plastic deformations, however, residual stresses also arise and can result in such a *residual stress field* which prevents the body from undergoing any further plastic deformations during further repeated loading. When it occurs, this phenomenon is called the *shakedown* of the body.

The goal of *shakedown analysis* is to determine those conditions and bounds for a general loading process at which shakedown occurs.

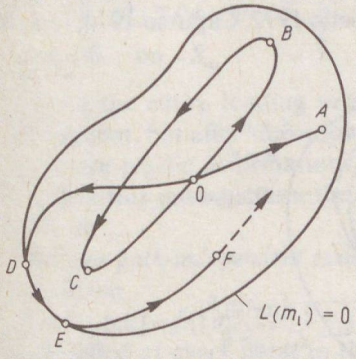


Fig. 3–6

To illustrate the problem of shakedown, let us consider again the load space. In Fig. 3—7(a) three closed hyper surfaces are shown symbolically. As in Fig. 3—6 the hyper surface $L(m_1)=0$ bounds the domain of possible loads. The domains bounded by the hyper surfaces $E(m_1)=0$ and $P(m_1)=0$ correspond to such maximum loads which do not cause any plastic deformations and do not exceed the plastic limit loads, respectively. Therefore the surfaces $E(m_1)=0$ and $P(m_1)=0$ are called *elastic limit surface* and *plastic limit surface*, respectively. Reaching these surfaces during the loading process a single point in the body starts to yield or the plastic limit of the body is reached, respectively. The surfaces $L(m_1)=0$ and $P(m_1)=0$ are path-independent. The surface $E(m_1)=0$, however, depends on the residual stresses and therefore is path-dependent. When the residual stresses change, the surface $E(m_1)=0$ moves and forms subsequent surfaces during the loading process. In Fig. 3—7(a) the virgin state of the surface $E(m_1)=0$ is illustrated, while in Fig. 3—7(b) some subsequent states are also shown.

If the domain L is included in the domain P, the body can maintain equilibrium with all possible loads. In addition, if the domain L is included in the domain E, the body will undergo only elastic deformations. When the domain L is only partially included in the domain E then, whenever the load-path exceeds the common part of the domains, the body will undergo plastic deformations which may lead to alternating or progressive plastic flow. The surface $E(m_1)=0$, however, may move and change because of the change in the residual stresses and it can happen that at a certain stage of the loading process the domain L will become a subset of the domain E (see the surface $E_{(t=T)}=0$ in Fig. 3—7(b)). After this stage, no further plastic deformations will arise during further repeated loading. This means that the body has shaked down.

To determine the plastic deformations to be expected and to analyse the possiblity of shakedown of a body, incremental analysis can always be used. This analysis, however,

is usually fairly time-consuming and very often cannot be conducted since in most practical cases the exact loading history is not known. To avoid these difficulties, variational principles can be derived which provide efficient tools for the analysis of the expected plastic deformations and shakedown of a body.

In the following, the static and kinematic principles of shakedown analysis, which can be used to predict the conditions at which shakedown will occur, will be presented. Other principles useful in determining the expected plastic deformations can be found in the literature (see e.g. Koiter 1960, König 1972, Vitiello 1972, Capurso 1974, Dorosz 1978).

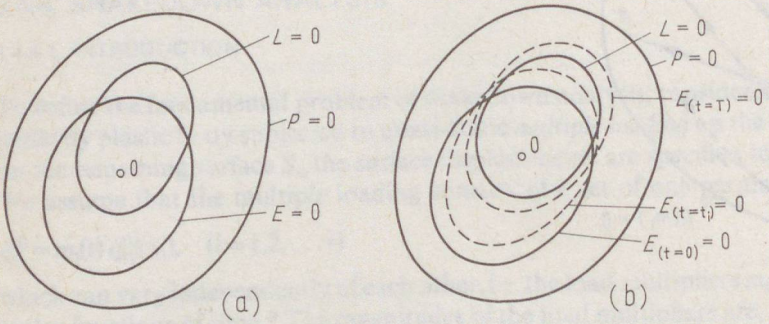


Fig. 3–7

3.4.4.2. STATIC PRINCIPLE

Consider a linearly elastic–perfectly plastic body subjected to quasi-static variable multiple loads on the surface S_q. Assume that on the surface S_u the surface displacements are specified to be zero and denote the *actual path-dependent stresses and strains* caused by the variable loads during the period $0 \leq t \leq T$ of the loading program by $\sigma_{ij}(x_i,t)$ and $\varepsilon_{ij}(x_i,t)$, respectively. In addition, to construct the static principle we have to define those *path-dependent elastic stresses and strains* which would occur during the loading program if the body were *perfectly elastic*. We will denote them by

$$\sigma_{ij}^{(e)}(x_i,t) \quad \text{and} \quad \varepsilon_{ij}^{(e)}(x_i,t) = H_{ijkl}\sigma_{kl}^{(e)}(x_i,t).$$

So long as the yield condition

$$f(\sigma_{ij}^{(e)},k) \leq 0$$

is satisfied at every point in the body, the actual stresses are identical with the elastic stresses, i.e. $\sigma_{ij} = \sigma_{ij}^{e}$. When, however, the elastic stresses would violate the yield condition they could not increase any further. Then, plastic deformations will occur which lead to the redistribution of the stresses. In this state, the actual stress field can be expressed as the sum of the elastic stress field and another stress field, called the *residual stress field*

$$\sigma_{ij}(x_i,t) = \sigma_{ij}^{(e)}(x_i,t) + \rho_{ij}(x_i,t). \tag{3—79}$$

Hence, the residual stresses

$$\rho_{ij}(x_i,t)=\sigma_{ij}(x_i,t)-\sigma_{ij}^{(e)}(x_i,t) \tag{3—80}$$

denote those *permanent stresses* which would remain in the body after unloading under *elastic* conditions. Thus, the residual stress field corresponds to zero external load and forms a *self-equilibrating system* which satisfies the equilibrium conditions*

$$\left.\begin{aligned} &\rho_{ij,i}=0 \quad \rho_{ij}=\rho_{ji} \quad \text{in} \quad V, \\ &\rho_{ij}n_j=0, \quad \text{on} \quad S_q \end{aligned}\right\} \tag{3—81}$$

during the entire loading procedure. The residual stresses are generally also path-dependent, but after shakedown has occurred they will not change any more because no more plastic deformations will arise.

After this introduction, the *static principle of shakedown analysis* can be stated as follows:

If any *path-independent* residual stress field $\bar{\rho}_{ij}(x_i)$ can be found such that the yield condition

$$f[\sigma_{ij}(x_i,t),k]=f\{[\sigma_{ij}^{(e)}(x_i,t)+\bar{\rho}_{ij}(x_i)],k\}\leq 0 \tag{3—82}$$

is satisfied at every point in the body for any possible loading case, then during the loading process this residual stress field or another one will develop and the body will shake down.

Alternatively, if any *path-independent* residual stress field can be found such that the corresponding domain of elastic limit loads includes the domain of possible loads then shakedown will occur during the loading process.

This last statement refers to the fact that for the determination of the occurrence of shakedown a knowledge of the complete loading history is not needed. It is enough to know only the *domain of possible loads*, i.e. the extreme values of the loads which are defined by the surface $L(m_l)=0$.

It is obvious that if a residual stress field which satisfies the condition defined in the static principle *really* does develop, then the body will shake down. On the other hand, it is also obvious that if such a residual stress field does not exist, shakedown cannot occur. However, it has to be proved that if there exists a residual stress field which satisfies the condition of shakedown, then this stress field or another one, which can also assure the shakedown of the body, will surely develop during the loading process.

Consider the current actual path-dependent residual stresses $\rho_{ij}(x_i, t)$ and the path-independent residual stresses $\bar{\rho}_{ij}(x_i)$ appearing in eq. (3—82) and write the *fictitious* elastic strain energy defined by the difference between these stresses

$$W=\frac{1}{2}\int_V (\rho_{ij}-\bar{\rho}_{ij})\, H_{ijkl}(\rho_{kl}-\bar{\rho}_{kl})\mathrm{d}V. \tag{3—83}$$

During plastic deformations the difference $(\rho_{ij}-\bar{\rho}_{ij})$ and consequently the work W changes, but when only elastic deformations occur it remains constant. Thus, the necessary and sufficient condition for shakedown can be stated by saying that during

* In a general sense, ρ_{ij} is also a fictitious stress field which does not necessarily satisfy the yield condition.

the loading procedure the work W has to tend to a constant value. If this value is zero, then ρ_{ij} tends to $\bar{\rho}_{ij}$ and shakedown will occur at the residual stresses $\bar{\rho}_{ij}$ stated in the principle. Otherwise, the residual stresses arising at shakedown will differ from $\bar{\rho}_{ij}$.

To prove the static principle we have to show that if a residual stress field $\bar{\rho}_{ij}$ satisfies the conditions (3—81) and (3—82) then W always tends to a constant value and consequently the energy *rate*

$$\dot{W}=\int_V (\rho_{ij}-\bar{\rho}_{ij})\dot{\varepsilon}^{e}_{ijR}\,dV \tag{3—84}$$

vanishes. Here $\varepsilon^{e}_{ijR}=H_{ijkl}\,\rho_{kl}$ denotes the elastic deformations associated with the current residual stresses. Let us express the actual strains of the body in the form

$$\varepsilon_{ij}=\varepsilon^{e}_{ij}+\varepsilon^{p}_{ij}=\varepsilon^{(e)}_{ij}+\varepsilon^{e}_{ijR}+\varepsilon^{p}_{ij},$$

where ε^{e}_{ij} are the actual elastic strains. Then, using these relationships, expression (3—84) becomes

$$\dot{W}=\int_V (\rho_{ij}-\bar{\rho}_{ij})\,(\dot{\varepsilon}_{ij}-\dot{\varepsilon}^{(e)}_{ij}-\dot{\varepsilon}^{p}_{ij})\,dV. \tag{3—85}$$

Now we apply the principle of virtual velocities to the statically admissible stresses $(\rho_{ij}-\bar{\rho}_{ij})$ and the kinematically admissible strain rates $(\dot{\varepsilon}_{ij}-\dot{\varepsilon}^{(e)}_{ij})$. Since both ρ_{ij} and $\bar{\rho}_{ij}$ are in a state of self-equilibrium we can write

$$\int_V (\rho_{ij}-\bar{\rho}_{ij})(\dot{\varepsilon}_{ij}-\dot{\varepsilon}^{(e)}_{ij})\,dV=0$$

and then eq. (3—85) becomes

$$\dot{W}=-\int_V (\rho_{ij}-\bar{\rho}_{ij})\,\dot{\varepsilon}^{p}_{ij}\,dV. \tag{3—86}$$

Considering eq. (3—80), the residual stresses can be expressed as

$$\begin{aligned}\rho_{ij}&=\sigma_{ij}-\sigma^{(e)}_{ij},\\ \bar{\rho}_{ij}&=\bar{\sigma}_{ij}-\sigma^{(e)}_{ij}.\end{aligned} \tag{3—87}$$

Here, according to eq. (3—82) the stresses $\bar{\sigma}_{ij}=\sigma^{(e)}_{ij}+\bar{\rho}_{ij}$, similarly to the actual stresses σ_{ij}, satisfy the yield condition

$$f(\bar{\sigma}_{ij},\,k)\leq 0$$

at every point in the body. Substituting eqs (3—87) in eq. (3—85) leads to

$$\dot{W}=-\int_V (\sigma_{ij}-\bar{\sigma}_{ij})\dot{\varepsilon}^{p}_{ij}\,dV. \tag{3—88}$$

According to Drucker's postulate (see eq. (2—88)), however,

$$(\sigma_{ij}-\bar{\sigma}_{ij})\dot{\varepsilon}^{p}_{ij}\geq 0$$

at every point in the body and therefore during the loading procedure $\dot{W}$ is negative (if plastic deformations occur) or zero (in the elastic state of the body). Hence

$$\dot{W}\leq 0.$$

Since the elastic strain energy W itself is always positive, we can conclude that during the entire loading procedure W is decreasing and—since it cannot be negative—tends to a non-negative value. This proves the static principle of shakedown analysis.

The condition for shakedown defined by eq. (3—82) can also be expressed in terms of the load multipliers m_l described in Section 3.4.4.1. Since the elastic stresses $\sigma_{ij}^{(e)}$ are linear functions of the load multipliers they can be written as

$$\sigma_{ij}^{(e)} = m_l (\sigma_{ij}^{(e)})_l \; ; \quad (l = 1, 2, \ldots, r). \tag{3—89}$$

Here, $(\sigma_{ij}^{(e)})_l$ denotes the time-independent elastic stress fields calculated from the loads $q_{io}^{(l)}(x_i)$ defined by eq. (3—78) and the multipliers m_l are functions of time.* Substituting eq. (3—89) in (3—82) yields

$$f\{[m_l(\sigma_{ij}^{(e)})_l + \bar{\rho}_{ij}], k\} \leqq 0. \tag{3—90}$$

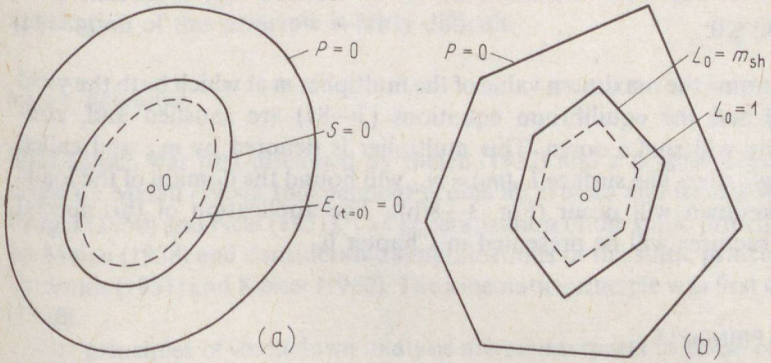


Fig. 3–8

Since in this expression only the multipliers m_l are path-dependent, it is evident that in eq. (3—90) only those extremal values of m_l which correspond to the boundary of the domain of possible loads, i.e. which satisfy the equation $L(m_l) = 0$, have to be taken into consideration. This leads to the statement already mentioned, that the shakedown analysis is independent of the loading history. To answer the question whether or not shakedown will occur a knowledge of the domain of possible loads is enough.

Using the shakedown condition (3—90), we can construct a *shakedown limit surface* $S(m_l) = 0$ such that if the load multipliers corresponding to the external loads are inside the domain bounded by the surface $S(m_l) = 0$, then the body will shake down (Fig. 3—8(a)).**

In order to achieve further simplifications, one can assume that the *shape* of the domain of possible loads is described by a given normalized equation

$$L_0(m_l) = 1, \tag{3—91}$$

* In eq. (3—89) the summation convention applies to the subscript l.

** It is to be noted that in the case of *statically determinate* problems the three surfaces $P(m_l) = 0$, $S(m_l) = 0$ and $E(m_l) = 0$ coincide, i.e. $P(m_l) = S(m_l) = E(m_l)$.

while the magnitude of the domain is defined by a scalar multiplier m such that the actual bounding surface is expressed in the form

$$L_0(m_1) = m. \tag{3—92}$$

In addition, in most engineering problems $L_0(m_1)$ is defined by several homogeneous, *linear* functions. Then the domain of possible loads is bounded by hyperplanes, and the parameter m defines the distances of these hyperplanes from the origin.

Considering this special case, let us denote the path-independent elastic stresses corresponding to the loads satisfying eq. (3—91) by $(\sigma_{ij}^{(e)})_L$. Then, the elastic stresses corresponding to the loads satisfying eq. (3—92) can be expressed as

$$\sigma_{ij}^{(e)} = m(\sigma_{ij}^{(e)})_L. \tag{3—93}$$

Substituting (3—93) in expression (3—82) yields

$$f\{[m(\sigma_{ij}^{(e)})_L + \bar{\rho}_{ij}], k\} \leqq 0. \tag{3—94}$$

One can now determine the maximum value of the multiplier m at which both the yield condition (3—94) and the equilibrium equations (3—81) are satisfied and, consequently, the body will shake down. This multiplier is denoted by m_{sh} and called *shakedown load multiplier*. The surface $L_0(m_1) = m_{sh}$ will bound the domain of the loads under which shakedown will occur (Fig. 3—8(b)). The application of this special solution to bar structures will be presented in Chapter 6.

3.4.4.3. KINEMATIC PRINCIPLE

Consider a linearly elastic–perfectly plastic body subjected to quasi-static multiple loading on the surface S_q and assume that on the surface S_u the displacements are zero. In addition, introduce the kinematically admissible plastic strain rates $\dot{\varepsilon}_{ij}^k(x_i, t)$ for $0 \leq t \leq T$ which are characterized by the property that for the time interval T the plastic strains

$$\Delta\varepsilon_{ij}^k = \int_0^T \dot{\varepsilon}_{ij}^k(x_i, t)\mathrm{d}t$$

constitute a kinematically admissible strain field together with the displacement field

$$\Delta u_i^k = \int_0^T \dot{u}_i^k \mathrm{d}t,$$

which, at the same time, satisfies the boundary condition

$$\Delta u_i^k = 0 \quad \text{on} \quad S_u.$$

Then, the *kinematic principle of shakedown analysis* states that

if *any* kinematically admissible plastic strain rate and velocity field can be found such that

$$\int_0^T \mathrm{d}t \int_{S_q} q_i \dot{u}_i^k \mathrm{d}S > \int_0^T \mathrm{d}t \int_V \sigma_{ik}^k \dot{\varepsilon}_{ij}^k \mathrm{d}V = \int_0^T \mathrm{d}t \int_V d(\dot{\varepsilon}_{ij}^k)\mathrm{d}V \tag{3—95}$$

then the body will not shake down during the loading procedure in the time interval $0 \leq t \leq T$.

Alternatively,

shakedown will occur during the loading procedure in the time interval $0 \leq t \leq T$ if for *all* possible kinematically admissible strain rate and velocity fields

$$\int_0^T \mathrm{d}t \int_{S_q} q_i \dot{u}_i^k \mathrm{d}S \leq \int_0^T \mathrm{d}t \int_V \sigma_{ij}^k \dot{\varepsilon}_{ij}^k \mathrm{d}V = \int_0^T \mathrm{d}t \int d(\dot{\varepsilon}_{ij}^k) \mathrm{d}V. \tag{3—96}$$

In expressions (3—95) and (3—96) the stress σ_{ij}^k is associated with the plastic strain rate $\dot{\varepsilon}_{ij}^k$ through the constitutive equations. It has been shown in Section 3.4.3.4. that σ_{ij}^k cannot be uniquely determined if the yield surface has flat regions; the *plastic energy dissipation* $d(\dot{\varepsilon}_{ij}^k) = \sigma_{ij}^k \dot{\varepsilon}_{ij}^k$, however, is always uniquely defined.

The proof of the kinematic principle can be found in the literature (see e.g. Koiter 1960; Martin 1975). Because of its very complex and general formulation, the application of this principle is fairly difficult.

3.4.4.4. REMARKS

Shakedown was first discussed by Bleich (1932) and a general proof for trusses was given by Melan (1936). Independent proofs for trusses and frames were presented by Prager (1950) and Neal (1951). The generalization of the static principle was presented by Melan (1938) and considerable simplifications of the static principle were given by Symonds (1951) and Koiter (1960). The kinematic principle was first derived by Koiter (1956).

The principles of shakedown analysis are counterparts to those of limit analysis in the sense that they provide static and kinematic approaches to the question of whether or not shakedown will occur for a body under multiple variable loading conditions. The principles of limit analysis provide static and kinematic approaches to the question of whether or not the plastic limit state will be reached by a body under proportional loading. The principles of shakedown analysis are, however, considerably more difficult to apply than those of limit analysis. In the application of the static theorem, an initial elastic analysis must be carried out. The application of the kinematic principle also requires difficult additional computations in order to evaluate the right-hand side of equation (3—95).

In spite of these difficulties, shakedown analysis is a vital and developing topic in plasticity and a great number of applications have been made, based mostly on the static principle. Among them the shakedown analysis of framed structures has been significantly developed, largely within the context of linear programming. The details of this application will be presented in Chapter 6.

3.5. DISCONTINUITY OF STRESS AND VELOCITY FIELDS

In the derivation and formulation of the principles above, we have assumed that the stresses and strains are continuous functions of coordinates. There are problems in plasticity, however, where the stresses and/or the strains vary in

a discontinuous manner. In the following, we will discuss how discontinuities in stress and strain fields can be taken in the solution of plastic problems into consideration.

3.5.1. DISCONTINUITY IN STRESS FIELD

Let us consider a statically admissible stress field σ_{ij}^{s} of a body which varies discontinuously across the surfaces $S_d (d = 1, 2, \ldots h)$. For the sake of simplicity, we will assume that the body is in a state of plane stress, so that the *discontinuity surfaces* can be represented by *discontinuity lines*. Figure 3—9(a) shows an element of a discontinuity line. Here we have assumed that the normal and shearing stresses N_1, N_2 and T on the two sides of the discontinuity line are different and are denoted by N_1', N_2', T' and N_1'',

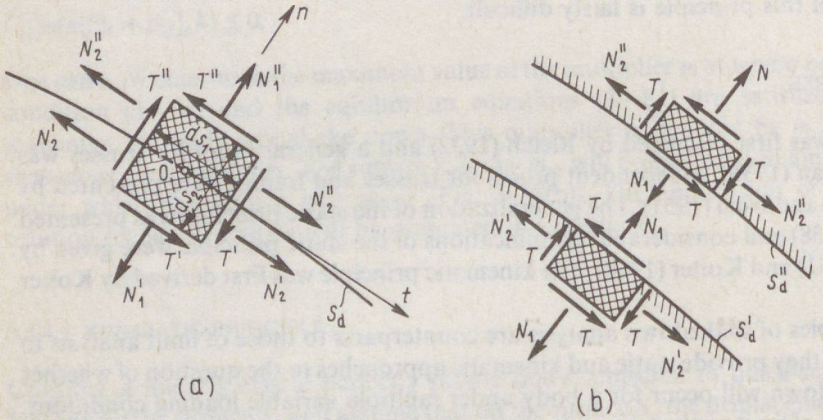


Fig. 3–9

N_2'', T'', respectively. Using equilibrium considerations, however, it will be shown that the *exterior components* of stress (N_1 and T) are always continuous across the discontinuity line and only the *interior component* N_2 may be discontinuous. From the moment equilibrium of the element it is obvious that $T' = T'' = T$. Then, the force equilibrium equations in the directions t and n yield

$$(N_1'' - N_1')ds_1 - \frac{\partial T}{\partial t} ds_1 ds_2 + g_t ds_1 ds_2 = 0,$$

$$\frac{\partial N_2'}{\partial t} ds_1 \frac{1}{2} ds_2 + \frac{\partial N_2''}{\partial t} ds_1 \frac{1}{2} ds_2 - \frac{\partial T}{\partial n} ds_1 ds_2 + g_n ds_1 ds_2 = 0.$$

Here g_t and g_n denote the components of the specific volume force. In the first equation, the last two terms are of higher order of magnitude than the first term and can be neglected. This leads to $N_1' = N_1'' = N_1$. In the second equation, however, all the terms have the same order of magnitude and therefore this equation can be satisfied if $N_2' \neq N_2''$. Thus, a discontinuity in the internal stress N_2 may occur.

Next, we will discuss how the stress discontinuities change the expression of the internal work appearing in the variational principles of plasticity. We suppose that the discontinuity surfaces divide the body into a finite number of subregions, such that in each of these subregions both the stresses and the strains are continuous functions of the coordinates. Then, the work for each subregion can be determined and the sum of the work gives the total internal work done on the body. This sum, however, contains not only the work done by the stresses acting inside the subregions but also the work of the stresses acting on the surfaces of the separated subregions. We will show, however, that the sum of the latter work vanishes. Figure 3—9(b) shows that an element of the discontinuity line always appears twice as portions of two neighbouring subregions. Since the exterior stresses are continuous, the stresses which these portions exert on one another across the discontinuity line are equal in magnitude but opposite in direction. Because the displacements are supposed to be continuous, the work done by the stresses acting on the surfaces of the neighbouring subregions will cancel each other out. Accordingly, the presence of the discontinuities in the stress field does not modify the expression for the internal work. The only difference is that, since the functions of the stress components are not continuous, the integral expression of the internal work can be evaluated only by subregions, but no additional terms have to be taken into consideration.

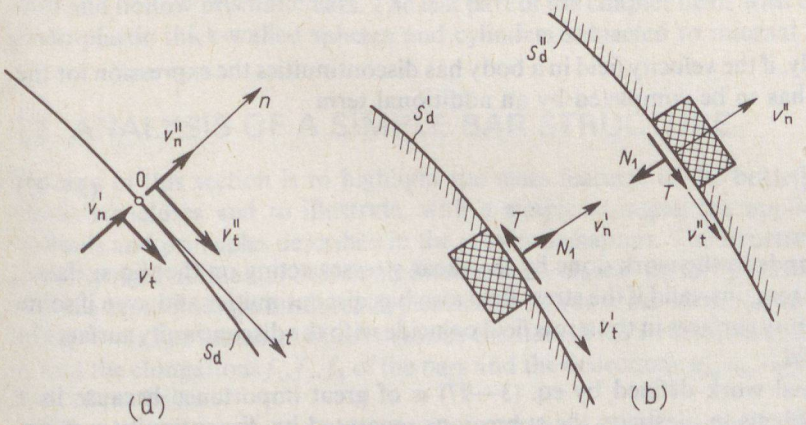


Fig. 3–10

3.5.2. DISCONTINUITY IN VELOCITY FIELD

Let us consider a velocity field v_i of a body which varies discontinuously across the surfaces $S_d (d = 1, 2, \ldots, h)$. For the sake of simplicity, we will assume that the body is in a state of plane strain so that the *discontinuity surfaces* can be represented by *discontinuity lines*. In Fig. 3—10(a) v_n', v_n'' and v_t', v_t'' denote the normal and tangential components of the velocities on the two sides of the discontinuity line. In the following, we consider the particular case when only the tangential components are discontinuous and the normal components vary continuously across the discontinuity

line, i.e. $v_t' \neq v_t''$ but $v_n' = v_n''$. These special kinds of discontinuity surfaces and lines are called *slip surfaces* and *slip lines*, respectively. Now we will discuss how the velocity discontinuities influence the expression for the internal work appearing in the variational principles of plasticity. We suppose that the discontinuity surfaces divide the body into a finite number of subregions, such that in each of these subregions both the stresses and the strains are continuous functions of the coordinates. Then, the work for each subregion can be determined and the sum of the work gives the total internal work done on the body. This sum, however, contains not only the work done by the stresses acting inside the subregions but also the work of the stresses acting on the surfaces of the separated subregions. For example, the work done by the stresses acting on the surfaces S_d' and S_d'' of the neighbouring subregions can be expressed as (see Fig. 3—10(b))

$$\int_{S_d} (N_1 v_n' - T v_t') \, dS,$$

$$\int_{S_d} (-N_1 v_n'' + T v_t'') \, dS.$$

Since $v_n' = v_n''$, the sum of these two expressions reduces to

$$\int_{S_d} T(v_t'' - v_t') \, dS.$$

Consequently, if the velocity field in a body has discontinuities the expression for the internal work has to be completed by an additional term

$$\sum_{d=1}^{h} \int_{S_d} T(v_t'' - v_t') \, dS \tag{3—97}$$

which corresponds to the work done by the shear stresses acting on the slip surfaces. This statement remains valid if the stress field also has discontinuities and even if some or all discontinuity surfaces in the stress field coincide with the discontinuity surfaces in the velocity field.

The additional work defined by eq. (3—97) is of great importance because in a number of problems in plasticity the subregions separated by discontinuity surfaces undergo only rigid body motion. In such cases only the shear stresses acting on the discontinuity surfaces produce internal work and then the expression for the internal work has only the term defined by eq. (3—97).

4. ELASTO-PLASTIC ANALYSIS OF SOME SIMPLE PROBLEMS

This chapter presents several simple applications of the principles and methods described in the previous chapters of the book.

First, in order to show the behaviour of elasto-plastic structures and to illustrate the application of the variational principles discussed in Chapter 3, the elastic, elasto-plastic, limit and shakedown analysis and optimal design of a simple bar structure will be presented. This will be followed by the analysis of elastic and elasto-plastic torsion of solid and hollow prismatic bars. The last part of the chapter deals with the problem of elasto-plastic thick-walled spheres and cylinders subjected to internal pressure.

4.1. ANALYSIS OF A SIMPLE BAR STRUCTURE

The aim of this section is to highlight the main features of the behaviour of elasto-plastic structures and to illustrate, with a simple example, the applications of the methods and principles described in the previous chapters. The structure consists of a perfectly rigid horizontal beam and three linearly elastic–perfectly plastic vertical bars with the same Young's modulus E, yield stress σ_0 and cross-sectional area A, as shown in Fig. 4—1. The variables which describe the state of the structure are the forces S_1, S_2, S_3 and the elongations f_1, f_2, f_3 of the bars and the deflections u_A, u_B, u_C at the points A, B, C of the beam.

First, the elastic, elasto-plastic and limit analysis of the structure will be discussed considering a single concentrated force acting on the beam. Then, two independently concentrated forces will be taken into consideration and the limit and the shakedown analysis will be conducted. Although, the problem to be studied is very simple its elementary analysis provides a clear insight into the behaviour of elasto-plastic structures and the phenomena observed. The conclusions can be generalized for more complex elasto-plastic problems.

4.1.1. ELASTIC ANALYIS

Let us assume that the external force F is small and that the structure shown in Fig. 4—1 is in the elastic range, i.e. $|S_i| < S_p$, $(i = 1, 2, 3)$, where $S_p = A\sigma_0$ denotes the *yield force* of the bars. The elastic solution of the problem can be obtained by the use of

the equilibrium and kinematic equations and Hooke's Law, or by the application of either the principle of minimum potential energy or the principle of complementary potential energy. In the following, these three methods of solution will be discussed.

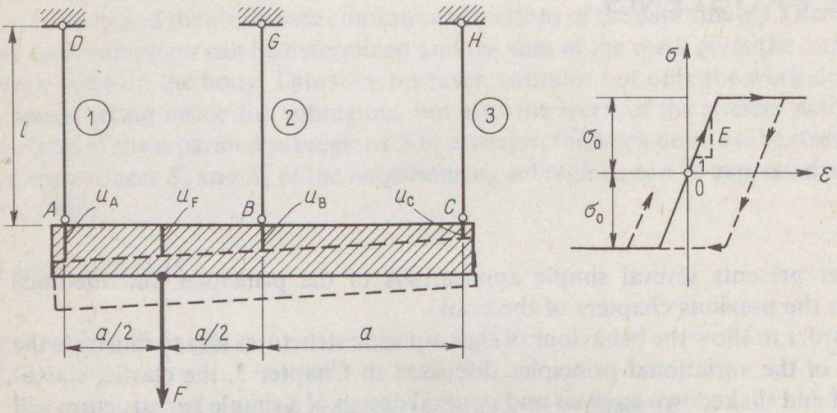


Fig. 4–1

4.1.1.1. SOLUTION BY THE USE OF FIELD EQUATIONS

The equations describing the elastic behaviour of the structure under consideration can be constructed as follows.

(a) The *equilibrium equations* have the form

$$S_1 a - S_3 a - \frac{1}{2} F a = 0,$$

$$-S_2 a - 2S_3 a + \frac{1}{2} F a = 0,$$

from which the relationships

$$\left.\begin{aligned} S_1 &= S_3 + \frac{1}{2} F, \\ S_2 &= -2S_3 + \frac{1}{2} F \end{aligned}\right\} \qquad (4—1)$$

can be obtained.

(b) The relationships between the displacements of the beam and the elongations of the bars are expressed by the *kinematic equations*

$$\left.\begin{aligned} &f_1 = u_A, \quad f_2 = u_B, \quad f_3 = u_C \\ &u_B = \frac{1}{2}(u_A + u_C). \end{aligned}\right\} \qquad (4—2)$$

Eliminating the displacements from these equations results in the *compatibility equation*

$$f_2 = \frac{1}{2}(f_1 + f_3). \tag{4—3}$$

(c) Finally, the *constitutive equations* (Hooke's Law) can be written as

$$f_1 = \frac{S_1 l}{EA}, \quad f_2 = \frac{S_2 l}{EA}, \quad f_3 = \frac{S_3 l}{EA}. \tag{4—4}$$

The solution of eqs (4—1), (4—3) and (4—4) leads to

$$\left.\begin{aligned} &S_1 = \frac{7}{12}F, \quad S_2 = \frac{4}{12}F, \quad S_3 = \frac{1}{12}F \\ &u_A = f_1 = \frac{7}{12}\frac{Fl}{EA}, \quad u_B = f_2 = \frac{4}{12}\frac{Fl}{EA}, \quad u_C = f_3 = \frac{1}{12}\frac{Fl}{EA}. \end{aligned}\right\} \tag{4—5}$$

This solution is valid if the forces in the bars are less than the yield force S_p, i.e. if $S_{max} = S_1 = \frac{7}{12}F < S_p$. The external force under which S_{max} reaches S_p is the *elastic limit load* of the structure

$$F_e = \frac{12}{7}S_p. \tag{4—6}$$

Using eqs (4—5) the corresponding forces and displacements are

$$\left.\begin{aligned} &S_{1e} = S_p, \quad S_{2e} = \frac{4}{7}S_p, \quad S_{3e} = \frac{1}{7}S_p, \\ &u_{Ae} = \frac{S_p l}{EA}, \quad u_{Be} = \frac{4}{7}\frac{S_p l}{EA}, \quad u_{Ce} = \frac{1}{7}\frac{S_p l}{EA}. \end{aligned}\right\} \tag{4—7}$$

When $F > F_e$, the structure becomes elasto-plastic. The analysis of this range will be discussed in Section 4.1.2. In the next section the elastic solution based on variational principles will be presented.

4.1.1.2. SOLUTION BY THE USE OF VARIATIONAL PRINCIPLES

(a) To find the elastic solution of the structure by the use of the *principle of minimum potential energy* one has to consider the *kinematically admissible strains and displacements* and *Hooke's Law* defined by eqs (4—2) and (4—4). Then, the potential energy of the structure has to be expressed in terms of the unknown displacements, say u_A and u_C. Using eq. (3—19) the expressions for external work and internal strain energy, respectively, can be written as

$$\Pi^e = -Fu_F = -\frac{1}{4}F(3u_A + u_C),$$

$$\Pi^{i}=\frac{1}{2}\left[\frac{EA}{l}u_A^2+\frac{EA}{l}u_B^2+\frac{EA}{l}u_C^2\right]=\frac{EA}{2l}\left[u_A^2+\frac{1}{4}(u_A+u_C)^2+u_C^2\right].$$

Hence, the total potential energy of the structure becomes

$$\Pi=\Pi^{e}+\Pi^{e}=-\frac{1}{4}F(3u_A+u_C)+\frac{EA}{2l}\left[u_A^2+\frac{1}{4}(u_A+u_C)^2+u_C^2\right]. \tag{4—8}$$

Among all kinematically admissible displacements u_A and u_C the ones that minimize the total potential energy will give rise to forces that satisfy the equilibrium equations, and are the actual displacements. Consequently, the conditions

$$\frac{\partial\Pi}{\partial u_A}=0,\quad \frac{\partial\Pi}{\partial u_C}=0 \tag{4—9}$$

have to be satisfied. This leads to the equations

$$5u_A+u_C=3\frac{lF}{EA},\quad u_A+5u_C=\frac{lF}{EA},$$

the solution of which is, of course, identical to the results given by eqs (4—5).

(b) To find the elastic solution of the structure by the use of the *principle of minimum complementary energy* one has to consider the *statically admissible internal forces* and Hooke's Law defined by eqs (4—1) and (4—4). Then, the complementary energy of the structure has to be expressed in terms of the unknown internal force, say S_3. Considering eq. (3—31) the external complementary energy vanishes, since at the supports D, G and H the diplacements are prescribed to be zero (i.e. $u_i^0=0$).* This means that the solution of the problem is reduced to an application of the *principle of minimum strain energy* defined by eq. (3—33). The elastic strain energy of the structure expressed as a function of the unknown force S_3 has the form:

$$U^{e}=\frac{1}{2}\left[\frac{S_1^2 l}{EA}+\frac{S_2^2 l}{EA}+\frac{S_3^2 l}{EA}\right]=\frac{l}{2EA}\left[(S_3+\frac{1}{2}F)^2+(-2S_3+\frac{1}{2}F)^2+S_3^2\right]. \tag{4—10}$$

Among all statically admissible values of S_3, the one that minimizes the elastic strain energy will give rise to the strains and displacements that satisfy the compatibility conditions, and is the actual solution. Consequently, the condition

$$\frac{dU^{e}}{dS_3}=0 \tag{4—11}$$

has to be satisfied. This leads to the solution $S_3=\frac{F}{12}$ which is, of course, identical to the result given by eq. (4—5).

* If at the supports vertical displacements u_D^0, u_G^0 and u_H^0 were prescribed, the external complementary energy would have the form $\Pi^{e}=-(S_1u_D^0+S_2u_G^0+S_3u_H^0)$ and using eq. (4—1) it should be expressed in terms of S_3.

4.1.2. ELASTO-PLASTIC ANALYSIS

When the force exceeds the elastic limit load $F_e = \frac{12}{7} S_p$, the structure becomes elasto-plastic. In the following, the incremental analysis of the loading, unloading and reloading process in the elasto-plastic range will be discussed.

4.1.2.1. LOADING

When the external force reaches the elastic limit $F_e = \frac{12}{7} S_p$ the bar 1 starts to yield and therefore the force $S_1 = S_p$ acting on this bar cannot be futher increased. The two other bars, however, are still in the elastic range and can support further external loads. Consequently, in this range the *increment* ΔF of the load will be carried by the statically determinate structure consisting of the bars 2 and 3. Since this structure is in the elastic range, for the force and *displacement increments* the equations derived in Section 4.1.1.1. are valid. Substituting $\Delta S_1 = 0$ in the incremental form of the equilibrium equations (4—1) lead to

$$\Delta S_3 = -\frac{1}{2}\Delta F, \quad \Delta S_2 = -2\Delta S_3 + \frac{1}{2}\Delta F = \frac{3}{2}\Delta F, \tag{4—12}$$

and then the kinematic equations (4—2) and Hooke's Law (4—4) result in

$$\Delta u_A = \frac{7}{2}\frac{\Delta F l}{EA}, \quad \Delta u_B = \frac{3}{2}\frac{\Delta F l}{EA}, \quad \Delta u_C = -\frac{1}{2}\frac{\Delta F l}{EA}. \tag{4—13}$$

These relationships are valid until one of the forces in bars 2 and 3 reaches the yield force S_p. Considering eqs (4—7) and (4—12), the forces caused by the external load $F = F_e + \Delta F$ become

$$\left.\begin{aligned} S_2 &= \frac{4}{7} S_p + \frac{3}{2}\Delta F, \\ S_3 &= \frac{1}{7} S_p - \frac{1}{2}\Delta F. \end{aligned}\right\} \tag{4—14}$$

Since $S_2 > S_3$, first bar 2 will start to yield when $S_2 = \frac{4}{7} S_p + \frac{3}{2}\Delta F = S_p$.

From this equation, the force increment which causes yielding in bar 2 is found to be $\Delta F_1 = \frac{2}{7} S_p$ and the corresponding total external force is equal to

$$F_1 = F_e + \Delta F_1 = \frac{12}{7} S_p + \frac{2}{7} S_p = 2S_p.$$

On reaching this load also bar 2 becomes plastic and the structure is converted into a *yield mechanism* which undergoes unrestricted plastic deformations and deflections under constant load. This is the *plastic limit state* of the structure and the force

$$F_p = 2S_p \tag{4—15}$$

is called the *plastic limit force*. The internal forces and the deflections arising at the instant when the load reaches the plastic limit force can be obtained from eqs (4—7), (4—13) and (4—14)

$$S_1 = S_2 = S_p, \quad S_3 = 0, \quad u_{A0} = 2\frac{S_p l}{EA}, \quad u_{B0} = \frac{S_p l}{EA}, \quad u_{C0} = 0. \tag{4—16}$$

The variation in the external and internal forces in terms of the vertical displacement u_A is illustrated in Fig. 4—2.*

4.1.2.2. UNLOADING AND RELOADING

(a) Let us assume that the structure, which has been loaded up to the plastic limit force $F_p = 2S_p$, will be unloaded. The unloading can be conducted by keeping the original force F_p and applying a force in the opposite direction with magnitude $F' = -F_p = -2S_p$. During unloading, the structure behaves elastically and therefore the forces and displacements corresponding to the load F' can be obtained by substituting $F = F' = -2S_p$ in eqs (4—5) derived for the elastic range

$$\left.\begin{aligned} S'_1 &= \frac{7}{12}F' = -\frac{7}{6}S_p, \quad S'_2 = \frac{4}{12}F' = -\frac{4}{6}S_p, \\ S'_3 &= \frac{1}{12}F' = -\frac{1}{6}S_p, \quad u'_A = \frac{7}{12}\frac{F'l}{EA} = -\frac{7}{6}\frac{S_p l}{EA}. \end{aligned}\right\} \tag{4—17}$$

Considering the forces and displacements induced in the structure during the loading procedure, the residual forces and the permanent displacements which remain after unloading become

$$\left.\begin{aligned} S_{1r} &= S_p + S'_1 = -\frac{1}{6}S_p, \quad S_{2r} = S_p + S'_2 = \frac{2}{6}S_p, \\ S_{3r} &= 0 + S'_3 = -\frac{1}{6}S_p, \quad u_{Ap} = 2\frac{S_p l}{EA} + u'_A = \frac{5}{6}\frac{S_p l}{EA}. \end{aligned}\right\} \tag{4—18}$$

The residual forces represent a self-equilibrating system and prestress the structure so that if it is reloaded no plastic deformations will arise until the plastic limit force F_p is reached. Indeed, if we apply the force F again the corresponding *elastic* forces $S_1 = \frac{7}{12}F$, $S_2 = \frac{4}{12}F$, $S_3 = \frac{1}{12}F$ (see eqs (4—5)) together with the residual forces given by eqs (4—18) will not reach S_p for $F < F_p$:

* This example shows that it is not necessary at the plastic limit state for all parts of the structure to be in the plastic range.

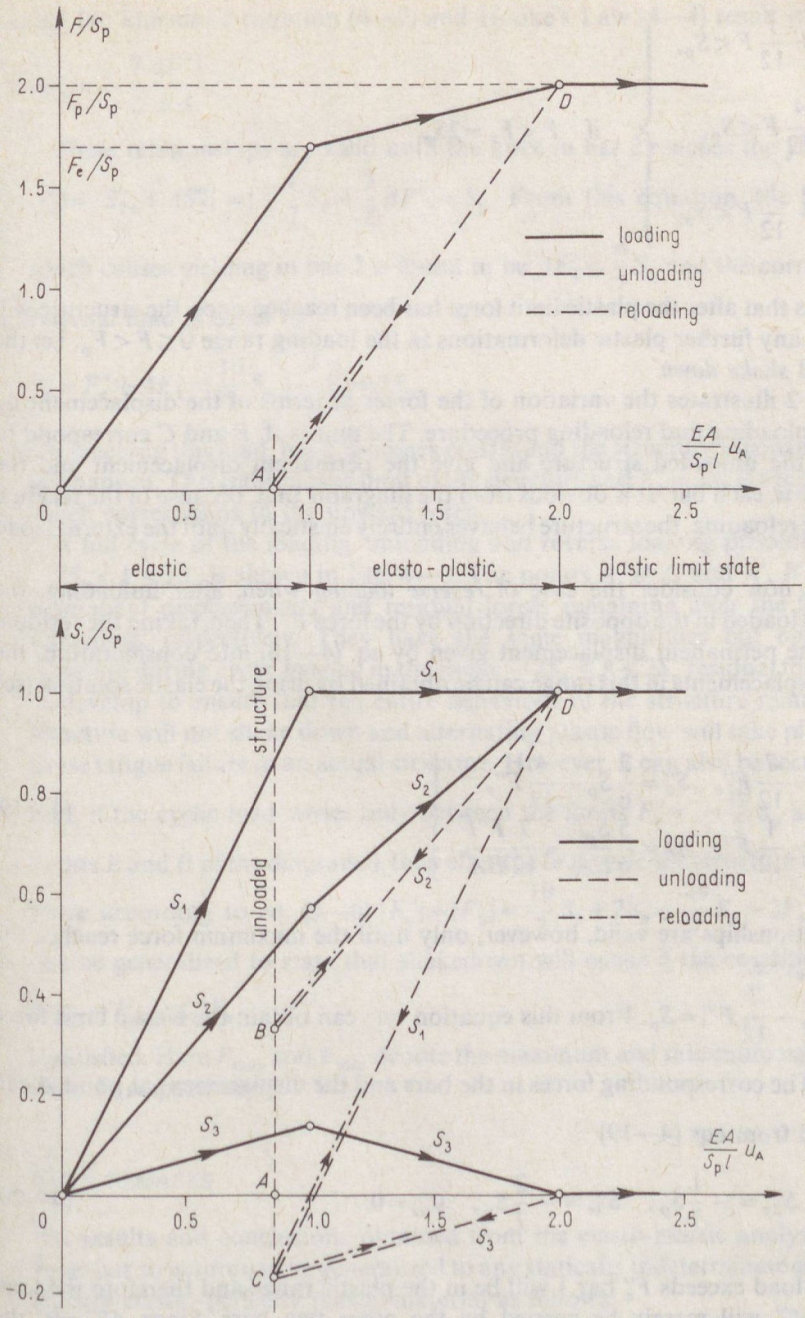

F/Sp
2.0
Fp/Sp
Fe/Sp
1.5
1.0
0.5
A
D
loading
unloading
reloading
EA/Sp l uA
0
0.5
1.0
1.5
2.0
2.5
elastic
elasto - plastic
plastic limit state
Si/Sp
structure
unloaded
S1
S2
S3
B
C
-0.2

Fig. 4–2

$$\left.\begin{aligned} S_1 &= -\frac{1}{6}S_p + \frac{7}{12}F < S_p, \\ S_2 &= \frac{2}{6}S_p + \frac{4}{12}F < S_p, \\ S_3 &= -\frac{1}{6}S_p + \frac{1}{12}F < S_p, \end{aligned}\right\} \quad \text{if} \quad F < F_p = 2S_p.$$

This means that after the plastic limit force has been reached once, the structure will not undergo any further plastic deformations in the loading range $0 \leq F < F_p$, i.e. the structure will *shake down*.

Figure 4—2 illustrates the variation of the forces in terms of the displacement u_A during the unloading and reloading procedure. The points A, B and C correspond to the state of the unloaded structure and give the permanent displacement and the residual force in each bar. It is obvious from the diagrams that, because of the residual forces during reloading, the structure behaves entirely elastically until the external load reaches $2S_p$.

(b) Let us now consider the case of *reverse loading* when, after unloading, the structure is reloaded in the opposite direction by the force F''. Then, taking the residual forces and the permanent displacement given by eq. (4—18) into consideration, the forces and displacements in this range can be obtained by using the elastic solution (see eq. (4—5))

$$\left.\begin{aligned} S_1'' &= -\frac{1}{6}S_p - \frac{7}{12}F'', \quad S_2'' = \frac{2}{6}S_p - \frac{4}{12}F'', \\ S_3'' &= -\frac{1}{6}S_p - \frac{1}{12}F'', \quad u_A'' = \frac{5}{6}\frac{S_p l}{EA} - \frac{7}{12}\frac{F'' l}{EA}. \end{aligned}\right\} \tag{4—19}$$

These relationships are valid, however, only until the maximum force reaches the yield force S_p, i.e.

$|S_1''| = |-\frac{1}{6}S_p - \frac{7}{12}F''| = S_p$. From this equation one can obtain the elastic limit force $F_e'' = \frac{10}{7}S_p$. The corresponding forces in the bars and the displacement at point A can be calculated from eqs (4—19)

$$S_{1e}'' = -S_p, \quad S_{2e}'' = -\frac{1}{7}S_p, \quad S_{3e}'' = -\frac{2}{7}S_p, \quad u_{Ae}'' = 0. \tag{4—20}$$

When the load exceeds F_e'' bar 1 will be in the plastic range and therefore the load increment $\Delta F''$ will merely be carried by the other two bars. Since $\Delta S_1'' = 0$, the equilibrium equations (4—1) become

$$\Delta S_3'' = \frac{1}{2}\Delta F'', \quad \Delta S_2'' = -2\Delta S_3'' - \frac{1}{2}\Delta F'' = -\frac{3}{2}\Delta F''$$

and the kinematic equation (4—2) and Hooke's Law (4—4) result in

$$\Delta u''_A = -\frac{7}{2}\frac{\Delta F'' l}{EA}.$$

These relationships are valid until the force in bar 2 reaches the yield force S_p, i.e. $|S''_2| = |S''_{2e} + \Delta S''_2| = |-\frac{1}{7}S_p - \frac{3}{2}\Delta F''| = S_p$. From this equation, the force increment which causes yielding in bar 2 is found to be $\Delta F''_1 = \frac{4}{7}S_p$ and the corresponding total external load is equal to

$$F''_p = F''_e + \Delta F_1 = \frac{10}{7}S_p + \frac{4}{7}S_p = 2S_p.$$

On reaching this load, bar 2 becomes plastic and the structure is converted into a yield mechanism. This is the plastic limit of the structure and $F''_p = 2S_p$ is the plastic limit load which corresponds to the upward force.

A full cycle of the loading, unloading and reverse loading procedure in the range $-2S_p \leq F \leq 2S_p$ is shown in Fig. 4—3. The points A, B, C and A', B', C' indicate the permanent displacements and residual forces remaining after the first and second unloading, respectively. They have the same magnitudes but *opposite sign* and therefore during *cyclic loading* in the range $-2S_p \leq F \leq 2S_p$ residual forces are not able to develop to ensure that the entire behaviour of the structure remains elastic. The structure will not shake down and alternating plastic flow will take place which could cause fatigue failure in an actual structure. However, it can also be seen from Fig. 4—3 that, if the cyclic load varies only between the limits $F''_e = -\frac{10}{7}S_p$ and $F_p = 2S_p$ (see points E and D of the diagrams), then after the first cycle the structure will shake down. Since according to eq. (4—6) $|F''_e| + |F_p| = \frac{10}{7}S_p + 2S_p = \frac{24}{7}S_p = 2F_e$, this statement can be generalized to state that shakedown will occur if the condition

$$(F_{max} - F_{min}) \leq 2F_e$$

is satisfied. Here F_{max} and F_{min} denote the maximum and minimum values of the cyclic force F, respectively.*

4.1.2.3. REMARKS

The results and conclusions obtained from the elasto-plastic analysis of the simple three-bar structure can be generalized to any statically indeterminate structure made of linearly elastic–perfectly plastic material as follows.

(a) The load-carrying capacity of a statically indeterminate elasto-plastic structure is not exhausted when one of its members starts to yield. The plastic deformations allow

* The correct proof of this general statement will be given in Section 6.

the redistribution of internal forces such that those members of the structure which are still elastic can be better utilized. Further increases in the load result in more and more members becoming plastic and not taking part in supporting the additional load increments. Consequently, the redundancy of the structure is reduced step by step. The load-carrying capacity will finally be exhausted only when the structure is converted into a yield mechanism which then undergoes unrestricted plastic flow under constant load. This is the *plastic limit state* of the structure and the corresponding load is the *plastic limit load.*

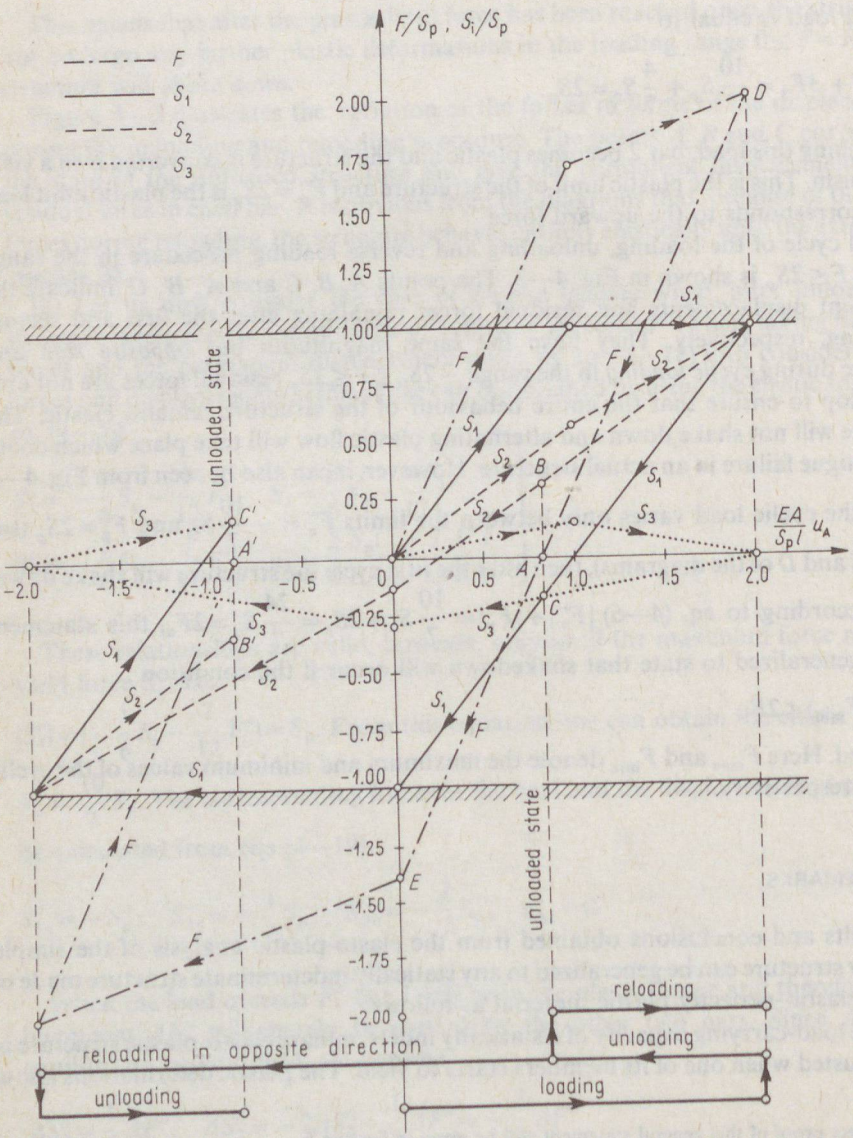


Fig. 4–3

(b) During unloading from the plastic limit state the structure behaves elastically. After complete unloading, permanent deformations and residual stresses remain in the structure. The residual stresses "prestress" the structure in such a way that reloading in the same sense will cause no plastic deformations.* This means that for cyclic loading in the range $0 \leq F < F_p$ the structure shakes down.

(c) In the case of reverse loading up to the plastic limit load, further plastic deformations will occur. Under cyclic loading alternating between the plastic limit loads, alternating plastic deformations will take place; i.e. the structure will not shake down. However, when the range of the magnitude of the cyclic load is not greater than twice the elastic limit load, shakedown will occur.

4.1.3. LIMIT ANALYSIS

The plastic limit load and the force and velocity distribution at the plastic limit state of the structure shown in Fig. 4—1 can be obtained by the use of the static and kinematic principles of limit analysis.

(a) Applying the *static principle* (see Section 3.4.3.3) one has to consider the statically admissible force distributions of the structure which satisfy the equilibrium equations (see eqs (4—1))

$$\left.\begin{aligned} S_1^s - S_3^s &= \frac{1}{2} F_s, \\ S_2^s + 2S_3^s &= \frac{1}{2} F_s, \end{aligned}\right\} \tag{4—21}$$

and the yield conditions

$$\left.\begin{aligned} -S_p \leq S_1^s \leq S_p, \\ -S_p \leq S_2^s \leq S_p, \\ -S_p \leq S_3^s \leq S_p. \end{aligned}\right\} \tag{4—22}$$

According to the static principle, any statically admissible stable load F_s defined by eqs (4—21) and (4—22) is less than or equal to the plastic limit load F_p. Hence, to determine F_p one has to maximize F_s. Briefly,

$$F_s = \max! \tag{4—23}$$

subject to the constraints given by eqs (4—21) and (4—22). This is a *linear programming* problem with the solution

$$F_p = 2S_p, \quad S_1 = S_2 = S_p, \quad S_3 = 0.$$

This is, of course, in agreement with the results obtained by elasto-plastic analysis (see eqs (4—15) and (4—16)).

* In cases when the plastic limit load is greater than twice the elastic limit load ($F_p > 2F_e$), during unloading further plastic deformations take place and therefore this statement is no longer valid (see Section 6).

(b) Applying the *kinematic principle* (see Section 3.4.3.4) one has to consider the kinematically admissible *plastic* strain rate and velocity distributions in the structure defined by eq. (4—2) and shown in Fig. 4—4.

$$\dot{f}_1^k = v_A^k, \quad \dot{f}_2^k = v_B^k, \quad \dot{f}_3^k = v_C^k, \tag{4—24}$$

$$v_B^k = \frac{1}{2}(v_A^k + v_C^k). \tag{4—25}$$

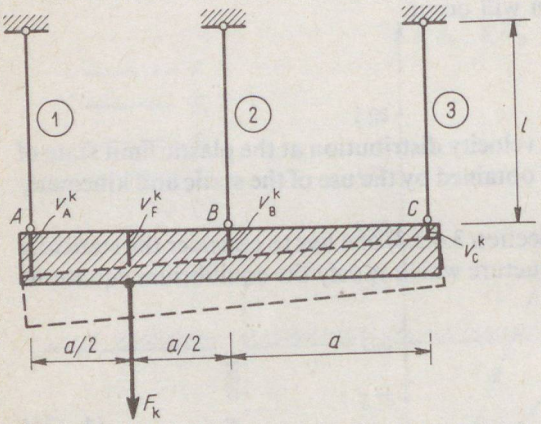


Fig. 4—4

To obtain the corresponding kinematically admissible, unstable loads F_k, one has to write the external and internal powers associated with the strain rates and velocities above. Using eq. (4—24) and considering the fact that the yield forces and strain rates of the bars have by definition the same signs, one can obtain these powers

$$F_k v_F^k = F_k \frac{1}{2}(v_A^k + v_B^k),$$

$$(|\dot{f}_1^k| + |\dot{f}_2^k| + |\dot{f}_3^k|) S_p = (|v_A^k| + |v_B^k| + |v_C^k|) S_p.$$

To eliminate the absolute values, the expression for the internal power can be written in the form

$$S_1 v_A^k + S_2 v_B^k + S_3 v_C^k,$$

where

$$\left.\begin{aligned} &|S_1| = |S_2| = |S_3| = S_p \\ &\text{and} \\ &S_1 v_A^k \geq 0, \quad S_2 v_B^k \geq 0, \quad S_3 v_C^k \geq 0. \end{aligned}\right\} \tag{4—26}$$

Substituting for the expressions of the external and internal powers in eqs (3—65) and (3—66) leads to

$$F_k = \frac{S_1 v_A^k + S_2 v_B^k + S_3 v_C^k}{\frac{1}{2}(v_A^k + v_B^k)}, \tag{4—27}$$

$$\frac{1}{2}(v_A^k + v_B^k) \geq 0. \tag{4—28}$$

Since at the plastic limit only the ratios of the velocities are defined and their magnitudes are unspecified, one can normalize the external power exerted by $F_k = 1$ such that

$$\frac{1}{2}(v_A^k + v_B^k) = 1. \tag{4—29}$$

Then eq. (4—27) becomes

$$F_k = S_1 v_A^k + S_2 v_B^k + S_3 v_C^k \tag{4—30}$$

and the inequality (4—28) which ensures that F_k is non-negative can be omitted. It is always fulfilled if eqs (4—26) and (4—29) are satisfied.

According to the kinematic principle, any kinematically admissible, unstable load defined by eqs (4—25), (4—26), (4—29) and (4—30) is greater than or equal to the plastic limit load F_p. Hence, to determine F_p one has to minimize F_k. Briefly,

$$F_k = S_1 v_A^k + S_2 v_B^k + S_3 v_C^k = \text{min!} \tag{4—31}$$

subject to the constraints given by eqs (4—25), (4—26) and (4—29). This is a *linear programming* problem with the solution

$$F_p = 2S_p, \quad v_A^k / v_B^k = 2, \quad v_C^k = 0.$$

This is, of course, in agreement with the results obtained by the elasto-plastic analysis (see eqs (4—15) and (4—16)).

The solution described above was based on the most general strain rate and velocity distribution, in which the possibility of yielding in any member of the structure was considered and the structure had two degrees of freedom. There is also another way to solve the problem. It is based on the analysis of special strain rate and velocity distributions which have only one degree of-freedom and are called *yield mechanisms*. Using the kinematic principle of limit analysis for any yield mechanism, a kinematically admissible unstable load multiplier can be determined and the smallest multiplier gives the plastic limit load of the structure.

Figure 4—5 shows all the possible yield mechanisms of the structure under consideration.* Since at the plastic limit state the magnitudes of the velocities are unspecified, for each yield mechanism the magnitude of one of the velocities can be assumed to be unit velocity. At this simple problem the general formulation of the

* Those yield mechanisms for which eq. (4—28) is not satisfied have been disregarded.

linear programming problem given by eq. (4—26) can be omitted. Then, using the notations of Fig 4—5 the equations for the external and internal powers and the corresponding kinematically admissible unstable loads can be obtained as below:

yield mechanism (*a*)

$$\frac{3}{4}F_k=\left(1+\frac{1}{2}\right)S_p;\quad F_k=2S_p,$$

yield mechanism (*b*)

$$\frac{1}{2}F_k=(1+1)S_p;\quad F_k=4S_p,$$

yield mechanism (*c*)

$$\frac{1}{4}F_k=\left(\frac{1}{2}+1\right)S_p;\quad F_k=6S_p.$$

From these results the plastic limit load and the corresponding velocities which define the collapse mechanism of the structure can be obtained as

$$F_p=\min(F_k)=2S_p,\quad v_A^k/v_B^k=2,\quad v_C^k=0.$$

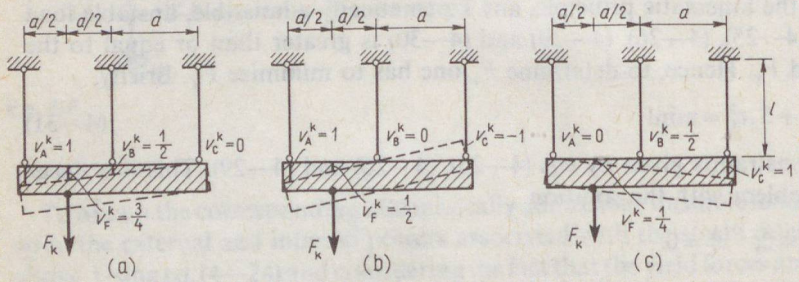


Fig. 4–5

4.1.4. TWO-PARAMETER LOADING

In the following, we will consider the problem where the structure shown in Fig. 4—1 is subjected to two *independent* external forces. We will first determine the magnitudes of these forces at which the plastic limit state occurs and we will then present the shakedown analysis of the structure.

4.1.4.1. LIMIT ANALYSIS

Let us consider the three-bar structure subjected simultaneously to two *independent* forces $F_1\geq 0$ and $F_2\geq 0$. Figures 4—6(a) and 4—6(b) show the *collapse mechanisms* of the structure when $F_1>F_2$ and $F_1<F_2$, respectively. The equality of the external and internal powers P_e and P_i, respectively, can then be expressed in a general form

$$P=P_e-P_i=F_1v_{F1}+F_2v_{F2}-(v_A+v_B+v_C)S_p=0, \qquad (4—32)$$

Assuming $v_A = 1$ and $v_C = 1$, respectively, this equation leads to the following special forms in the cases of the two collapse mechanisms:

$$\left.\begin{aligned} P_1 &= \frac{3}{4}F_1 + \frac{1}{4}F_2 - \frac{3}{2}S_p = 0, \\ P_2 &= \frac{1}{4}F_1 + \frac{3}{4}F_2 - \frac{3}{2}S_p = 0. \end{aligned}\right\} \qquad (4—33)$$

These equations define all the possible combinations of the forces $F_1 \geq 0$ and $F_2 \geq 0$ under which the structure will collapse, i.e. they represent the *yield condition for the structure*. This can be expressed in a general form

$$P_l(F_i, S_p) = 0; \quad [l = 1,2; \quad i = 1,2]. \qquad (4—34)$$

In the *force plane* F_1, F_2 the yield condition (4—33) is illustrated by two straight lines which, together with the lines $F_1 = 0$ and $F_2 = 0$, bound the feasible domain of the external forces $F_1 \geq 0$, $F_2 \geq 0$ which can be supported by the structure (see Fig. 4—6(c)).

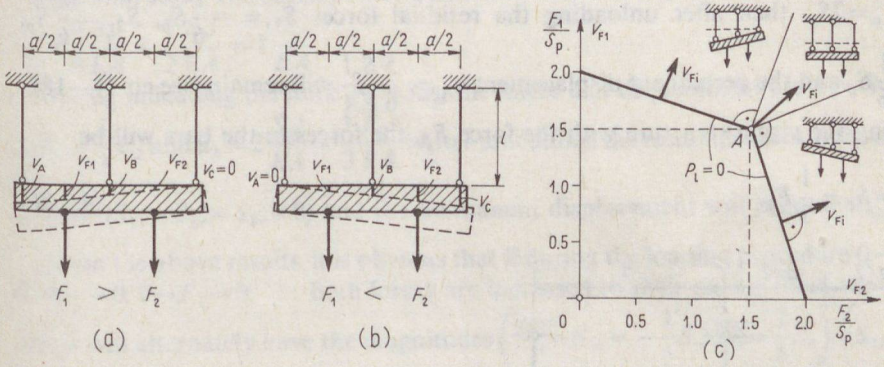


Fig. 4—6

In eq. (4—32) only the ratios of the velocities are specified and therefore a scalar multiplier, say $\dot{\Lambda}$, which would define the magnitude of the velocities, is unknown. Considering this, and differentiating the general expression (4—34) with respect to the external forces we can write

$$\left.\begin{aligned} v_{F1} &= \dot{\Lambda}\frac{\partial P_l}{\partial F_1}, \\ v_{F2} &= \dot{\Lambda}\frac{\partial P_l}{\partial F_2}. \end{aligned}\right\}$$

or shortly

$$v_{Fi} = \dot{\Lambda}\frac{\partial P_l}{\partial F_i}; \quad \dot{\Lambda} > 0, \quad (i = 1, 2). \qquad (4—35)$$

These relationships represent the *flow rule of the structure. Since* $\frac{\partial P_1}{\partial F_i}$ is the gradient of $P_1(F_i, S_p)=0$, one can state that the *generalized velocity vector* $v_{Fi}(v_{F1}v_{F2})$ of the structure coincides with the outer normal vector of the yield surface $P_1(F_i; S_p)=0$ at the point corresponding to the plastic limit state of the structure. Hence, the *normality rule* holds for the vector v_{Fi} and the yield surface $P_1(F_i, S_p)=0$. This rule can be extended to the singular points (vertices and edges) of the yield surface as described in Section 2.3.3.1. In addition, one can prove that $P_1(F_i, S_p)=0$ always represents a *convex* surface (see e.g. Hodge, 1963; Martin, 1975).

4.1.4.2. SHAKEDOWN ANALYSIS

Let us again consider the case where the three-bar structure is subjected to two independent forces $F_1 \geq 0$ and $F_2 \geq 0$, but suppose that now they cannot act simultaneously and study the conditions of shakedown (Fig. 4—7).

When the force F_1 is applied to the structure and increased up to the plastic limit load $F_{1p}=2S_p$, then after unloading the residual forces $S_{1r}=-\frac{1}{6}S_p$, $S_{2r}=\frac{2}{6}S_p$, $S_3=-\frac{1}{6}S_p$ and the permanent displacement $u_{AP}=\frac{5}{6}\frac{S_p l}{EA}$ will remain (see eq. (4—18)).

Loading the virgin structure with the force F_2, the forces in the bars will be

$$S_1=S_2=S_3=\frac{1}{3}F_2. \qquad (4—36)$$

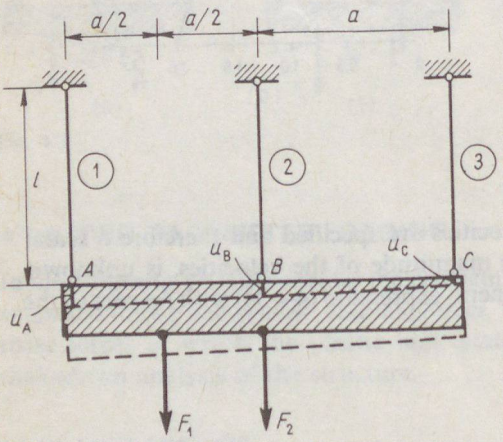


Fig. 4–7

Hence, the structure will reach its elastic and plastic limit state at the same magnitude of the external force $F_{2e}=F_{2p}=3S_p$, and after unloading no residual forces and permanent deflections remain. Consequently, in this case the entire loading and unloading process takes place elastically.

Let us assume now that the forces F_1 and F_2 are applied alternately and increased to heir plastic limit magnitudes $2S_p$ and $3S_p$, respectively.

After unloading the force $F_1 = 2S_p$ the residual forces and the permanent displacement are $S_{1r} = S_{3r} = -\frac{1}{6}S_p$, $S_{2r} = \frac{2}{6}S_p$ and $u_{Ap} = \frac{5}{6}\frac{S_p l}{EA}$, respectively. Next, applying now the force F_2, the forces in the bars become $S_1 = S_3 = -\frac{1}{6}S_p + \frac{1}{3}F_2$, $S_2 = \frac{2}{3}S_p + \frac{1}{3}F_2$. On reaching the force $F_2 = 2S_p$, the bar 2 starts to yield and the other two forces and the displacement will be $S_1 = S_3 = \frac{1}{2}S_p$ and $u_A = \frac{5}{6}\frac{S_p l}{EA} + \frac{2S_p l}{3EA} = \frac{9}{6}\frac{S_p l}{EA}$. Then, applying a force increment ΔF_2 the forces in the bars will be $S_2 = S_p$ and $S_1 = S_3 = \frac{1}{2}S_p + \frac{1}{2}\Delta F_2$. When the force increment $\Delta F_2 = S_p$ then the displacement increment $\Delta u_A = \frac{1}{2}\frac{S_p l}{EA}$ and the bars 1 and 3 also become plastic and the structure reaches the plastic limit state. The corresponding external force and displacement are $F_2 = 3S_p$ and $u_A = \frac{9}{6}\frac{S_p l}{EA} + \frac{1}{2}\frac{S_p l}{EA} = 2\frac{S_p l}{EA}$.

During unloading the force $F_2 = 3S_p$, the forces and displacement are $S_1 = S_2 = S_3 = S_p - \frac{1}{3}F_2$ and $u_A = 2\frac{S_p l}{EA} - \frac{1}{3}\frac{F_2 l}{EA}$. After unloading, the residual forces in the bars will be zero ($S_{1r} = S_{2r} = S_{3r} = 0$) and the permanent displacement will become $u_{Ap} = \frac{S_p l}{EA}$.

From the above results, it is obvious that if during the loading procedure $0 \to F_1 \to 0$; $0 \to F_2 \to 0$; $0 \to F_1 \to 0$; ... both forces are increased to their plastic limit, the residual forces will alternately have the magnitudes $\left(S_{1r} = S_{3r} = -\frac{1}{6}S_p, S_{2r} = \frac{2}{6}S_p\right)$; $\left(S_{1r} = S_{2r} = S_{3r} = 0\right)$; $\left(S_{1r} = S_{3r} = -\frac{1}{6}S_p, S_{2r} = \frac{2}{6}S_p\right)$ ... and the permanent displacements will monotonically increase having the values $\frac{5}{6}\frac{S_p l}{EA}$; $\frac{S_p l}{EA}$; $\left(1 + \frac{5}{6}\right)\frac{S_p l}{EA}$ ... Consequently, the structure will not shake down and the accumulating plastic deformations will lead to incremental collapse.

From the shakedown analysis presented in Section 3.4.4 it is known that by keeping the magnitude of the forces F_1 and F_2 below certain limits the shakedown of the structure can always be accomplished. Let us denote the *common* limit of those two external forces at which shakedown will occur by F_{sh}, and determine its magnitude.

Following the static principle of shakedown analysis presented in Section 3.4.4.2., and the method associated with eqs (3—91)–(3—94), we first have to determine the maximum values of the forces which arise in the elastic range in the bars under the action of the unit forces $F_1 = 1$ or $F_2 = 1$. According to eqs (4—5) and (4—36), these forces are

$$S_1^{max} = \frac{7}{12}, \quad S_2^{max} = \frac{1}{3}, \quad S_3^{max} = \frac{1}{3}.$$

Next, the self-equilibrating residual force distribution in the structure has to be constructed. This can be expressed in terms of the unspecified force S_0 arising in bar 2 as follows

$$S_{1r}=S_{3r}=-\frac{1}{2}S_0,\ S_{2r}=S_0.$$

According to the static principle of shakedown analysis, if the maximum forces together with the residual forces do not exceed the yield forces of the bars then the structure will shake down. This condition can be expressed in the form

$$\left.\begin{aligned}&\frac{7}{12}F_{sh}-\frac{1}{2}S_0\le S_p,\\&\frac{1}{3}F_{sh}+S_0\le S_p,\\&\frac{1}{3}F_{sh}-\frac{1}{2}S_0\le S_p.\end{aligned}\right\}\qquad(4—37)$$

Since we are looking for the maximum value of F_{sh} at which shakedown will occur, the problem is to maximize F_{sh}. Briefly

$$F_{sh}=\max!$$

subject to the constraints (4—37). This is a *linear programming* problem with the solution

$$F_{sh}=2S_p,\quad S_0=\frac{1}{3}S_p.$$

Hence, in order to maintain the shakedown of the structure the force F_1 can reach its plastic limit $F_{1p}=2S_p$ but the force F_2 cannot be fully utilized up to its plastic limit $F_{2p}=3S_p$; its magnitude should be kept below the limit $2S_p$.

The shakedown analysis of bar structures will be discussed in more detail in Section 6.

4.1.5. OPTIMAL DESIGN

In order to illustrate the idea of optimal (minimum weight) plastic design, let us consider the structure shown in Fig. 4—8. Now the length of bar 2 differs from that of the other two bars and is denoted by αl. Assume that the magnitude of the external force F is given and determine the plastic limit forces S_{1p}, S_{2p}, S_{3p} in the bars such that the structure is able to carry the external load and the total weight of the bars is minimum. In addition, we introduce the design constraint that the plastic limit forces should not be less than a given portion of the external force, i.e.

$$S_{1p}\ge\psi F,\quad S_{2p}\ge\psi F,\quad S_{3p}\ge\psi F,\qquad(4—38)$$

where the factor ψ will be specified later.

Since the cross-sectional areas of the bars are proportional to their plastic limit forces the *optimality condition* can be expressed as

$$W=(S_{1p}+\alpha S_{2p}+S_{3p})l=\min!\qquad(4—39)$$

In terms of the kinematic principle of limit analysis, it is obvious that if for all possible yield mechanisms the associated external power is less than or equal to the internal power then the structure will be able to support the external load. Considering the yield mechanisms of Fig. 4—5, this condition can be expressed in the following form

$$\left.\begin{aligned} \frac{3}{4}F &\le S_{1p}+\frac{1}{2}S_{2p},\\ \frac{1}{2}F &\le S_{1p}+S_{3p},\\ \frac{1}{4}F &\le \frac{1}{2}S_{2p}+S_{3p}. \end{aligned}\right\} \qquad (4—40)$$

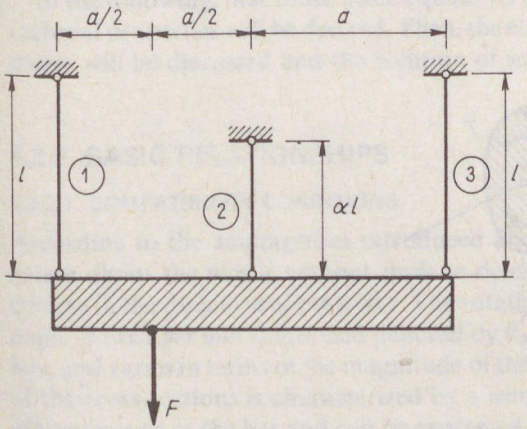


Fig. 4–8

Table 4—1

ψ	α	S_{1p}/F	S_{2p}/F	S_{3p}/F	W/Fl
0	$\frac{1}{2}$	0.50	0.50	0	0.75
	$\frac{1}{3}$	0.50	0.50	0	0.65
0.10	$\frac{1}{2}$	0.60	0.30	0.10	0.85
	$\frac{1}{3}$	0.60	0.30	0.10	0.80

The minimum condition (4—39) together with the constraints (4—38) and (4—40) is a *linear programming* problem. The solution for different values of α and ψ is given in Table 4—1.

The optimal design of structures will be discussed in more detail in Chapters 6 and 7.

4.2. TORSION OF PRISMATIC BARS

4.2.1. NOTATIONS AND ASSUMPTIONS

Let us consider a linearly elastic–perfectly plastic weightless prismatic bar in torsion, and choose the z axis of a system of rectangular Cartesian coordinates to be parallel with the generators of the prismatic surface of the bar (Fig. 4—9). The length of the bar is l and the shape C of the contour of the cross-section is defined by the function $y=\psi(x)$ (Fig. 4—10). The torques acting at the ends of the bar are denoted by T. To simplify the discussion we shall first restrict it to bars with simply connected cross-sections.

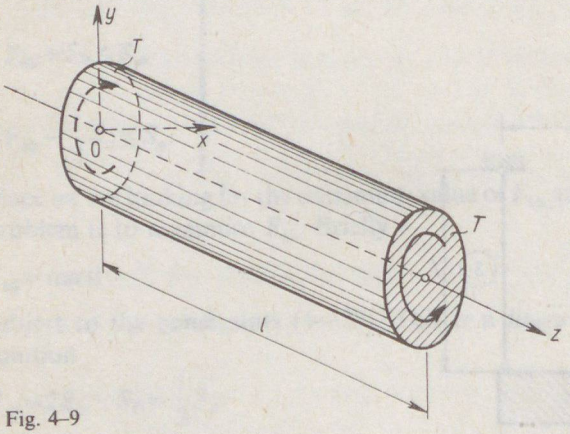


Fig. 4–9

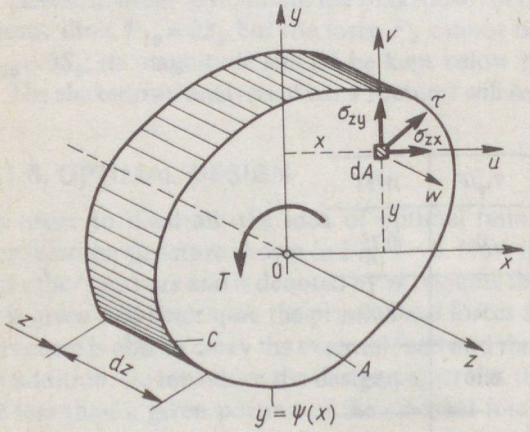


Fig. 4–10

Following de Saint-Venant's treatment of torsion problems (1856), our study will be based on the following assumptions.

(a) The planes of the cross-sections have no in-plane deformations but can freely deform in the direction of the axis of the bar. This deformation of the cross-sections is called *warping* and this specific problem is called the *free torsion problem.*

(b) The torque is applied in the form of shear stresses on the ends of the bar. The distribution of these shear stresses is not specified, but is supposed to be identical with that of the shear stresses to be determined in the internal cross-sections of the bar.

(c) The material of the bar obeys the Prandtl–Reuss constitutive equations.

It is obvious that as a consequence of the assumptions stated above the state of stress and strain is identical at every cross-section of the bar, and therefore the solution of the problem is independent of the coordinate z.

If the warping of the cross-sections cannot freely develop (e.g. because of some constraints applied at the ends of the bar) normal stresses will arise in the direction of the axis of the bar. In particular, in the case of thin-walled bars with open cross-sections, these normal stresses are of considerable magnitude and can significantly change the magnitudes and distribution of the shear stresses calculated on the assumption of free warping.

In the following, first those basic equations of torsion which are independent of the material properties will be derived. Then, the elastic, elasto-plastic and perfectly plastic stages will be discussed and the solution of some simple problems will be presented.

4.2.2. BASIC RELATIONSHIPS

4.2.2.1. COMPATIBILITY CONDITIONS

According to the assumptions introduced above, the cross-sections of a twisted bar rotate about the axis z without inplane deformations and, at the same time, freely deform in the direction of the axis z. The rotation of the cross-sections is defined by the *angle of twist per unit length* and denoted by θ_0, which is constant along the axis of the bar, and varies in terms of the magnitude of the torque applied to the bar. The warping of the cross-sections is characterized by a *warping function*, w, which is also constant along the axis of the bar and can be expressed in terms of the coordinates x, y and the angle of twist: $w = w(x,y,\theta_0)$.

In order to eliminate the rigid body motion, let us assume that one end of the bar is fixed against rotation. Then the rotation of another cross-section at a distance z from the fixed end is equal to $\theta = z\theta_0$ and, according to Fig. 4—11, the displacements of a point P at this cross-section can be expressed as

$$u = -\theta_0 zy, \quad v = \theta_0 zx, \quad w = w(x,y,\theta_0). \tag{4—41}$$

Making use of these relationships and the kinematic equations (2—67) the strain components can be obtained

$$\left.\begin{aligned}
&\varepsilon_{xx} = u_{,x} = 0, \quad \varepsilon_{yy} = v_{,y} = 0, \quad \varepsilon_{zz} = w_{,z} = 0,\\
&\varepsilon_{xy} = \frac{1}{2}(u_{,y} + v_{,x}) = \frac{1}{2}(-\theta_0 z + \theta_0 z) = 0,\\
&\varepsilon_{xz} = \frac{1}{2}(u_{,z} + w_{,x}) = \frac{1}{2}(-\theta_0 y + w_{,x}),\\
&\varepsilon_{yz} = \frac{1}{2}(v_{,z} + w_{,y}) = \frac{1}{2}(\theta_0 x + w_{,y}).
\end{aligned}\right\} \tag{4—42}$$

Here the last two equations lead to the *compatibility equations* of the torsion problem

$$\varepsilon_{zy,x}-\varepsilon_{zx,y}=\theta_0. \tag{4—43}$$

Using strain increments eqs (4—42) and (4—43) have the form

$$\left.\begin{aligned} &d\varepsilon_{xx}=d\varepsilon_{yy}=d\varepsilon_{zz}=d\varepsilon_{xy}=0,\\ &d\varepsilon_{zy,x}-d\varepsilon_{zx,y}=d\theta_0. \end{aligned}\right\} \tag{4—44}$$

We have only one geometrical constraint, namely one end of the bar fixed against rotation. This has already been taken into consideration in writing eqs (4—41) and therefore no further kinematic boundary conditions have to be satisfied.

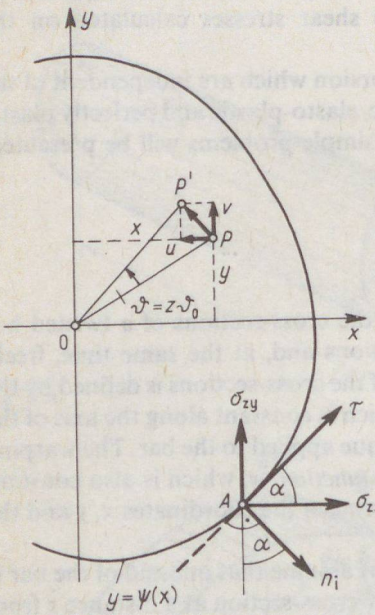


Fig. 4–11

4.2.2.2. EQUILIBRIUM CONDITIONS

The equilibrium equations (2—32) and (2—33) take on simpler forms when one considers that, similarly to the strains, a number of the stress components are also zero. Considering the first four relationships of eqs (4—42) and (4—44), Hooke's Law (2—70) and the Prandtl–Reuss constitutive equations (2—99a), one can state that in both the elastic and the plastic ranges

$$\sigma_{xx}=\sigma_{yy}=\sigma_{zz}=\sigma_{xy}=0. \tag{4—45}$$

Then, the equilibrium equations (2—32) become

$$\left.\begin{aligned} &\sigma_{xz,z}=0,\\ &\sigma_{yz,z}=0,\\ &\sigma_{xz,x}+\sigma_{zy,y}=0. \end{aligned}\right\} \tag{4—46}$$

According to the first two equations, σ_{zx} and σ_{zy} are independent of the coordinate z, which corresponds to our former statement. Then, the third equation can be identically satisfied by introducing a *stress function* $\phi = \phi(x,y,\theta_0)$ defined as

$$\sigma_{zx} = \frac{\partial \phi}{\partial_y}, \quad \sigma_{zy} = -\frac{\partial \phi}{\partial_x}. \tag{4—47}$$

The use of the stress function, together with the relationships (4—47) ensures the satisfaction of the equilibrium equations. This can be readily proved by substituting eqs (4—47) in eq. (4—46).

The stress function $\phi = \phi(x,y,\theta_0)$ can be represented by a surface. According to relationships (4—47) the slope of this surface in the x and y directions is equal to the magnitude of the shear stress components acting in the y and x directions, respectively. In addition, the magnitude of the resultant shear stress τ is equal to the magnitude of the *gradient* of the stress function

$$\tau = (\sigma_{zx}^2 + \sigma_{zy}^2)^{1/2} = \left[\left(\frac{\partial \phi}{\partial_y} \right)^2 + \left(\frac{\partial \phi}{\partial_x} \right)^2 \right]^{1/2} = |\text{grad } \phi|. \tag{4—48}$$

Let us write the total differential of the function ϕ and substitute it into the relationships (4—47). We then get

$$\mathrm{d}\phi = \frac{\partial \phi}{\partial_x} \mathrm{d}x + \frac{\partial \phi}{\partial_y} \mathrm{d}y = -\sigma_{zx} \mathrm{d}x + \sigma_{zy} \mathrm{d}y.$$

For the contour lines of the surface $\phi(x,y,\theta_0) =$ constant, consequently $\mathrm{d}\phi = 0$, and therefore

$$\frac{\sigma_{zy}}{\sigma_{zx}} = \frac{\mathrm{d}y}{\mathrm{d}x}. \tag{4—49}$$

This means that at every point in the cross-sections the resultant shear vector τ is directed along the tangent of the contour line of the surface ϕ. The lines $\phi =$ constant are therefore called the *stress trajectories.*

Next, we will formulate the *static boundary conditions* on the lateral surface and at the ends of the bar.

(a) The lateral surface of the bar is free from stresses, therefore in equation (2—33) of the static boundary condition $q_i = 0$. Considering (Fig. 4—11), the outer normal vector at a point A of the lateral surface is $n_i(\sin\alpha - \cos\alpha\ 0)$. Hence, making use of relationships (4—45) we find that in the first two equations of the static boundary condition (2—33) all terms vanish, and the third equation yields $\sigma_{zx} \sin\alpha - \sigma_{zy} \cos\alpha = 0$, i.e.

$$\frac{\sigma_{zy}}{\sigma_{zx}} = \tan\alpha = \frac{\mathrm{d}y}{\mathrm{d}x}.$$

This means that at every point in the contour C of the cross-section the resultant stress vector τ must be directed along the tangent of the contour C. According to eq. (4—49), however, the stress vector τ has the same relationship to the tangent of the contour lines $\phi =$ constant of the surface $\phi = \phi(x,y,\theta_0)$. Consequently, along the

contour C of the cross-section the stress function ϕ must be constant. Since the stress components are equal to the first derivatives of the stress function, we may take ϕ to be zero on the contour of a simply-connected cross-section*, i.e.

$$\phi = 0 \quad \text{on} \quad C. \tag{4—50}$$

(b) The resultant of the shear stresses acting on the ends of the bar must be identical with the torque T. Thus, considering Fig. 4—10 one can write

$$\left.\begin{aligned} &\int \sigma_{zx} \mathrm{d}A = 0. \\ &\int \sigma_{zy} \mathrm{d}A = 0, \\ &\int (\sigma_{zx} y - \sigma_{zy} x)\, \mathrm{d}A = T. \end{aligned}\right\} \tag{4—51}$$

Let us denote the intersection points of the contour line of the cross-section with the axis x by $A(x_1,0)$ and $B(x_2,0)$, and the functions of the curves of the contour line lying above and below the axis x by $y=\psi_1(x)$ and $y=\psi_2(x)$. Then, using relationships (4—47), the first expression of eqs (4—51) can be written as

$$\int \sigma_{zx} \mathrm{d}A = \int\int \frac{\partial \phi}{\partial y} \mathrm{d}x\mathrm{d}y = \int_{x_1}^{x_2} \left[\int_{\psi_1(x)}^{\psi_2(x)} \frac{\partial \phi}{\partial y} \mathrm{d}y \right] \mathrm{d}x =$$

$$= \int_{x_1}^{x_2} \{\phi[x,\psi_2(x)] - \phi[x,\psi_1(x)]\} \mathrm{d}x = 0. \tag{4—52}$$

Because of eq. (4—50), the functions $\phi[x,\psi_2(x)]$ and $\phi[x,\psi_1(x)]$ are identically equal to zero, and therefore eq. (4—52) will be automatically satisfied. A similar statement can be made for the second expression of eqs (4—51).

The third equation of (4—51) can be expressed as

$$\int \left(\frac{\partial \phi}{\partial y} y + \frac{\partial \phi}{\partial x} x \right) \mathrm{d}A = -T. \tag{4—53}$$

Considering the relationship

$$\frac{\partial (\phi y)}{\partial y} = \frac{\partial \phi}{\partial y} y + \phi,$$

integrating by parts and making use again of the boundary condition (4—51) the first term of the integral becomes

$$\int \frac{\partial \phi}{\partial y} y \, \mathrm{d}A = \int \left[\frac{\partial (\phi y)}{\partial y} - \phi \right] \mathrm{d}A = \int \phi \mathrm{d}A.$$

The same result can be obtained for the second term of the integral in eq. (4—53) and therefore eq. (4—53) finally results in

$$T = 2 \int \phi \mathrm{d}A. \tag{4—54}$$

* The case of multiply-connected cross-section will be discussed in Section 4.1.7.

Hence, the double volume of the "hill" constructed by the surface of the stress function over the cross section has to be equal to the magnitude of the torque.

After deriving the compatibility and equilibrium equations we will discuss the elastic, elasto-plastic and fully plastic ranges of a bar under torsion.

4.2.3. ELASTIC TORSION

At lower magnitudes of the torque every point in the bar is in the elastic range, i.e. at every point $f<0$, where f is the Huber–v. Mises–Hencky yield function defined by eq. (2—79a). Since now $\sigma_{xx}=\sigma_{yy}=\sigma_{zz}=\sigma_{xy}=0$ this condition has the simple form

$$f=\sigma_{zx}^2+\sigma_{zy}^2-\tau_0^2<0,$$

or making use of relationship (4—48)

$$\tau=(\sigma_{zx}^2+\sigma_{zy}^2)^{1/2}=\left[\left(\frac{\partial\phi}{\partial x}\right)^2+\left(\frac{\partial\phi}{\partial y}\right)^2\right]^{1/2}=|\text{grad }\phi|<\tau_0. \tag{4—55}$$

Considering eq. (2—83), one notices that in the case of free torsion the Huber–v. Mises–Hencky and the Tresca yield conditions have the same form.

On increasing the torque at a certain point in the cross-section the shear stress will reach the yield stress τ_0. This is the limit of the elastic range of the bar, and therefore the corresponding torque denoted by T_e is called the *elastic limit torque*. In the following we will consider the case when $T\leq T_e$.

4.2.3.1. ANALYTICAL SOLUTION

Using Hooke's Law and relationship (4—48) one can write

$$\varepsilon_{zx}=\frac{\sigma_{zx}}{2G}=\frac{1}{2G}\frac{\partial\phi}{\partial y},$$

$$\varepsilon_{zy}=\frac{\sigma_{zy}}{2G}=-\frac{1}{2G}\frac{\partial\phi}{\partial x}.$$

The substitution of these relationships into the compatibility equation (4—43) leads to the governing equation of elastic torsion

$$\frac{\partial^2\phi}{\partial x^2}+\frac{\partial^2\phi}{\partial y^2}=\Delta\phi=-2G\theta_0, \tag{4—56}$$

where

$$\Delta=\left(\frac{\partial^2}{\partial x^2}+\frac{\partial^2}{\partial y^2}\right).$$

Since the stress function $\phi=\phi(x, y, \theta_0)$ is a homogeneous, linear function of θ_0 and G, therefore it can be written in the form

$$\phi(x, y, \theta_0)=G\theta_0\phi_0(x, y). \tag{4—57}$$

Using this relationship (4—56) becomes

$$\frac{\partial^2 \phi_0}{\partial x^2} + \frac{\partial^2 \phi_0}{\partial y^2} = \Delta \phi_0 = -2. \tag{4—56a}$$

The problem of elastic torsion is to solve the *Poisson's differential equation* (4—56) together with the boundary conditions

$\phi = 0$ on C

and

$$T = 2 \int \phi \mathrm{d}A.$$

Substituting eq. (4—57) in the later boundary condition one can obtain a relationship between the torque and the angle of twist per unit length

$$T = 2G\theta_0 \int \phi_0 \mathrm{d}A = G\theta_0 J_T \text{ or } \theta_0 = \frac{T}{GJ_T}, \tag{4—58}$$

where

$$J_T = 2 \int \phi_0 \mathrm{d}A \tag{4—59}$$

is the *torsional moment of inertia* of the cross-section. Then, using relationship (4—58), the stress function can be expressed in the form

$$\phi = \frac{T}{J_T} \phi_0(x,y)$$

and the expressions (4—47) for the stresses are reduced to

$$\sigma_{zx} = \frac{T}{J_T} \frac{\partial \phi_0}{\partial y}, \quad \sigma_{zy} = -\frac{T}{J_T} \frac{\partial \phi_0}{\partial x}. \tag{4—60}$$

4.2.3.2. MEMBRANE ANALOGY

The elastic torsion problem can be experimentally solved and visualized by means of the *membrane analogy* suggested by Prandtl (1903). Consider a plate and a hole in it with the shape of the cross-section of the twisted bar, and stress a membrane with constant surface tension s per unit length of its boundary across this hole. On applying a small overpressure p to one side of the membrane, the small vertical displacements z of the membrane satisfy the differential equation

$$\frac{\partial^2 z}{\partial x^2} + \frac{\partial^2 z}{\partial y^2} = -\frac{p}{s} \tag{4—61}$$

and the boundary condition

$z = 0$ on C.

Comparison of the boundary value problems for z and ϕ defined by eqs (4—61) and (4—56) shows that the deflection z of the membrane will be proportional to the stress function ϕ, and if $2G\theta_0$ is equal to p/s then z is equal to ϕ. In this manner, the surface of the stress function can be obtained as the deformed shape of a membrane which has the same contour line as the twisted cross-section and is subjected to a pressure p satisfying the relationship $\frac{p}{s}=2G\theta_0$. The maximum slope of the membrane at any point is proportional to the resultant shear stress at the point, and the volume between the membrane and the $z=0$ plane is proportional to the torque producing the angle of twist θ_0 per unit length.

The *membrane analogy*, also called the *soap film analogy*, is useful for determining the stress function for complicated shapes. In addition, it furnishes a basis for an intuitive and qualitative discussion of torsional problems. As will be shown, the analogy can be extended to multiply-connected cross-sections and to the elasto-plastic and perfectly plastic stages of twisted bars, as well.

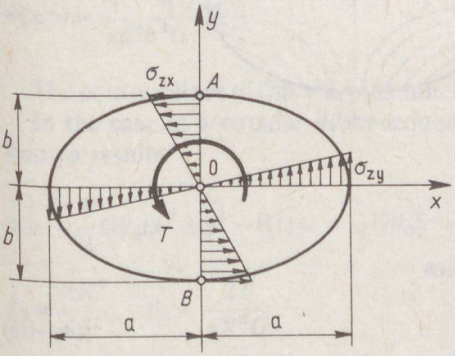


Fig. 4–12

4.2.3.3. BAR WITH ELLIPTICAL CROSS-SECTION

To illustrate the solution of elastic torsion, consider a bar with an elliptical cross-section (Fig. 4—12). The equation of the boundary curve is

$$\frac{x^2}{a^2}+\frac{y^2}{b^2}=1.$$

Let us choose the stress function in the form

$$\phi=K\left(\frac{x^2}{a^2}+\frac{y^2}{b^2}-1\right). \tag{4—62}$$

This function satisfies the boundary condition $\phi=0$ on the boundary of the cross-section, and the differential equation (4—56) is also satisfied if the constant K has the value

$$K=-\frac{a^2b^2}{a^2+b^2}G\theta_0.$$

Then, the stress function has the form

$$\phi = G\theta_0\phi_0 = -G\theta_0 \frac{a^2b^2}{a^2+b^2}\left(\frac{x^2}{a^2}+\frac{y^2}{b^2}-1\right). \tag{4—63}$$

The contour lines of the surface of the stress function are illustrated in Fig. 4—13(a). Using relationship (4—59) the torsional moment of inertia of the cross-section is

$$J_T = \int \phi_0 dA = -2\frac{a^2b^2}{a^2+b^2}\iint\left(\frac{x^2}{a^2}+\frac{y^2}{b^2}-1\right)dxdy = \frac{\pi a^3b^3}{a^2+b^2},$$

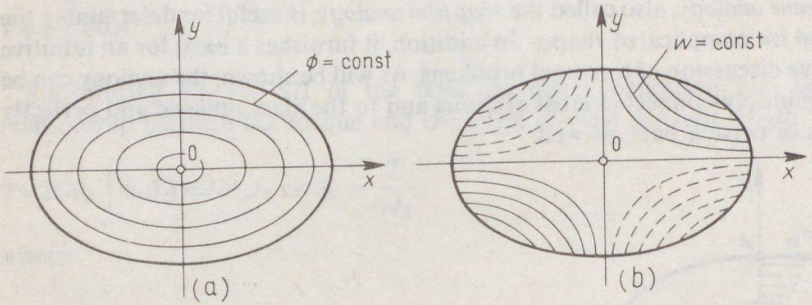


Fig. 4–13

and the angle of twist per unit length becomes

$$\theta_0 = \frac{T}{J_T G} = \frac{a^2+b^2}{\pi a^3 b^3 G}T. \tag{4—64}$$

Finally, using eqs (4—60), the shear stresses have the form

$$\left.\begin{aligned}
\sigma_{zx} &= \frac{T}{J_T}\frac{\partial\phi_0}{\partial y} = -\frac{2T}{\pi ab^3}y,\\
\sigma_{zy} &= -\frac{T}{J_T}\frac{\partial\phi_0}{\partial x} = \frac{2T}{\pi a^3 b}x,\\
\tau &= (\sigma_{zx}^2+\sigma_{zy}^2)^{1/2} = \frac{2T}{\pi ab}\left(\frac{x^2}{a^2}+\frac{y^2}{b^2}\right)^{1/2}.
\end{aligned}\right\} \tag{4—65}$$

The maximum stress will occur on the boundary at the point closest to the axis of the bar, i.e. if $a \geq b$, then at $x=0$, $y=b$

$$\tau_{max} = \frac{2T}{\pi ab^2}. \tag{4—66}$$

The *elastic limit torque* will be reached if $\tau_{max} = \tau_0$. Hence,

$$T_e = \frac{\pi ab^2}{2}\tau_0. \tag{4—67}$$

By the use of Hooke's Law and the geometrical equations (4—42) the warping function can also be determined. Making use of the results given by eqs (4—65) one can obtain

$$\frac{\partial w}{\partial x} = \theta_0 y + 2\varepsilon_{zx} = \frac{b^2 - a^2}{\pi a^3 b^3 G} Ty,$$

$$\frac{\partial w}{\partial y} = -\theta_0 x + 2\varepsilon_{zy} = \frac{b^2 - a^2}{\pi a^3 b^3 G} Tx.$$

Hence, the warping function is

$$w(x,y) = \frac{(b^2 - a^2)}{\pi a^3 b^3 G} Txy + \text{constant}.$$

If we assume that $w\,(0,0) = 0$, then

$$w(x,y) = \frac{(b^2 - a^2)}{\pi a^3 b^3 G} Txy. \tag{4—68}$$

The contour lines of this warping function are hyperbolic, as shown in Fig. 4—13(b).

In the case of a circular cross-section $a = b = R$ which leads to the following well known results:

$$\left.\begin{aligned}
&\phi = -\frac{1}{2} G\theta_0 (x^2 + y^2 - R^2) = -\frac{1}{2} G\theta_0 (r^2 - R^2), \\
&J_T = \frac{\pi R^4}{2}, \quad \theta_0 = \frac{2T}{\pi R^4 G}, \\
&\sigma_{zx} = -\frac{2T}{\pi R^4} y, \quad \sigma_{zy} = \frac{2T}{\pi R^4} x, \\
&\tau = \frac{2T}{\pi R^4} (x^2 + y^2)^{1/2} = \frac{2T}{\pi R^4} r, \quad \tau^{\max} = \frac{2T}{\pi R^3}, \\
&T_e = \frac{\pi R^3}{2} \tau_0, \quad w = 0.
\end{aligned}\right\} \tag{4—69}$$

The result $w = 0$ shows that in this special case the plane sections remain plane during the deformation of the twisted bar.

4.2.4. ELASTO-PLASTIC TORSION

4.2.4.1. ANALYTICAL SOLUTION

When the torque exceeds the elastic limit torque, i.e. $T > T_e$, one or more plastic zones will start to develop at some points on the boundary and spread towards the interior as the torque is increased (Fig. 4—14).

In the *elastic range*, denoted by A_e, at every point $\tau < \tau_0$ and the stress function ϕ_e has to satisfy the differential equation

$$\frac{\partial^2 \phi_e}{\partial x^2} + \frac{\partial^2 \phi_e}{\partial y^2} = -2G\theta_0. \tag{4—70}$$

In the *plastic range*, denoted by A_p, at every point $\tau = \tau_0$.

Since the relationships (4—55) between the shear stresses and the stress function have been derived from the equilibrium equations, the concept of the stress function and eqs (4—55) can be used in the plastic range, as well. Considering, however, the yield condition $\tau = (\sigma_{zx}^2 + \sigma_{zy}^2)^{1/2} = \tau_0$, the stress function ϕ_p now has to satisfy the differential equation

$$\left[\left(\frac{\partial \phi_p}{\partial x}\right)^2 + \left(\frac{\partial \phi_p}{\partial y}\right)^2\right]^{1/2} = |\text{grad } \phi_p| = \tau_0. \tag{4—71}$$

The boundary conditions (4—50) and (4—54) derived from purely static considerations are valid for both the elastic and the plastic zones of the cross-section. Thus,

$$\left.\begin{aligned} &\phi_e = 0 \quad \text{on} \quad C_e, \quad \phi_p = 0 \quad \text{on} \quad C_p, \\ &T = 2\left[\int_{A_e} \phi_e \mathrm{d}A + \int_{A_p} \phi_p \mathrm{d}A\right]. \end{aligned}\right\} \tag{4—72}$$

Here C_e and C_p denote those parts of the contour lines of the cross-section which belong to the elastic and the plastic zone, respectively. Finally, the stress functions ϕ_e and ϕ_p have to satisfy certain continuity conditions along the boundaries C_{ep} of the elastic and plastic zones that will be described latter.

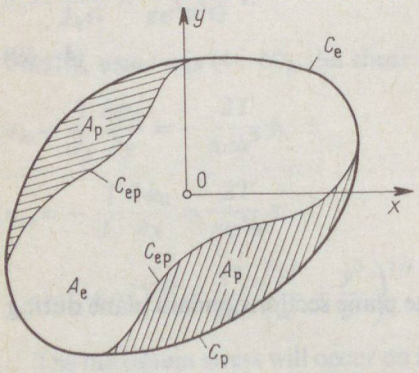


Fig. 4–14

Let us start with the solution of the elasto-plastic torsion problem in the plastic range of the cross-section. The parabolic partial differential equation (4—71) expresses the simple fact that at every point in the plastic range the maximum slope of the surface of the stress function is constant and is equal to the magnitude of the yield stress. This makes possible the construction of the surface of the stress function ϕ_p above the plastic

zone. Let us assume that the portion of the boundary curve of the cross-section which belongs to the plastic zone is already known, as illustrated in Fig. 4—15(a) by the curve C_p between the points A and B. Because ϕ_p must be zero on C_p, the curve between the points A and B represents the contour line with level zero of the surface of the stress function ϕ_p. The planes which contain the tangents of the curve C_p with a constant slope $\tan \phi = \tau_0$ will bound the surface of the stress function. The straight generators of this developable surface are its lines with the steepest descent; they have the slope τ_0 with respect to the plane of the cross-section and their orthogonal projections to this plane are the normals of the curve C_p. The contour lines of the surface ϕ_p, i.e. the stress trajectories, are orthogonal to these normals and hence, curves parallel to C_p.

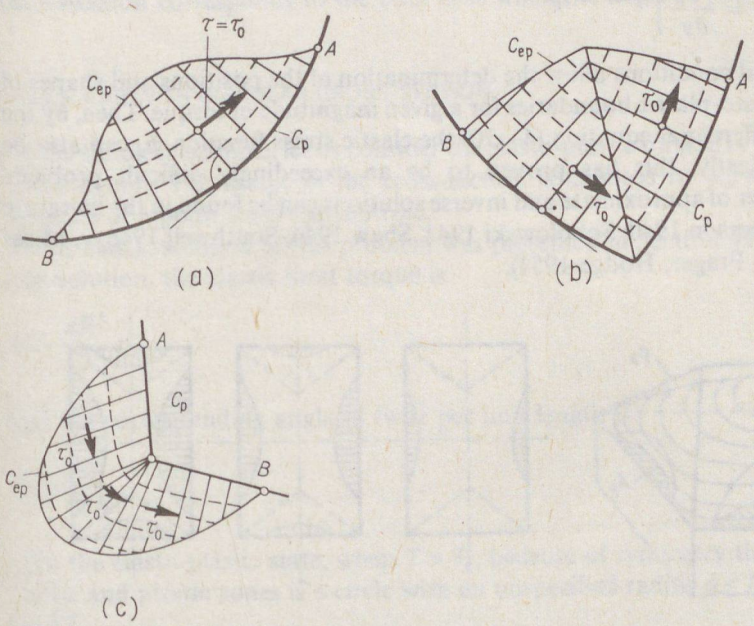


Fig. 4–15

For a boundary curve with corners, certain difficulties arise. They may be solved, however, by considering the boundary curve with corners as a limiting case of a curve with continuously turning tangents. Then, a convex corner causes the surface of the stress function to have an *edge* and a line of discontinuity in the direction of the shear stresses will occur, as shown in Fig. 4—15(b). In the case of a re-entrant corner, an edge cannot occur, but a conical portion will provide a smooth transition of the surface of the stress function (Fig. 4—15(c)). Finally, along the intersection of the conical surfaces a *ridge* can be formed which also corresponds to a line of discontinuity in the direction of the shear stresses.

It is obvious that discontinuities in the stress distribution are physically not feasible. Still, they cannot be avoided if we assume that at the plastic limit state the entire cross-section becomes plastic. We must therefore conclude that the fully plastic stress distribution represents only a limiting case which can never actually be reached.

As was shown, whenever we know the boundaries of the plastic zones the surface of the plastic stress function can be constructed. The boundaries C_p and C_{ep} are, however, unknown and their position and shape change with the magnitude of the torque. In order to make this problem determinate and to obtain the elastic stress function, we have to take the continuity conditions along the elasto-plastic boundary C_{ep} into consideration. It can be proved, by using equilibrium and strain compatibility considerations (see e.g. Prager, Hodge 1951), that the stress functions and their first derivatives must be continuous across the elastic–plastic boundary, i.e.

$$\left.\begin{aligned} &\phi_e = \phi_p, \\ &\frac{\partial \phi_e}{\partial x} = \frac{\partial \phi_p}{\partial x}, \quad \frac{\partial \phi_e}{\partial y} = \frac{\partial \phi_p}{\partial y} \end{aligned}\right\} \text{ on } \quad C_{ep}. \tag{4—73}$$

These additional conditions allow the determination of the positions and shapes of the plastic and elasto-plastic boundaries for a given magnitude of torque. Then, by the solution of the differential equation (4—70) the elastic stress function ϕ_e can also be obtained. Analytically, this has proved to be an exceedingly difficult problem. However, a number of approximate and inverse solutions can be found in the literature (see e.g. Christopherson 1940; Sokolowski 1942; Shaw 1944; Southwell 1946; v. Mises 1949; Galin 1949; Prager, Hodge 1951).

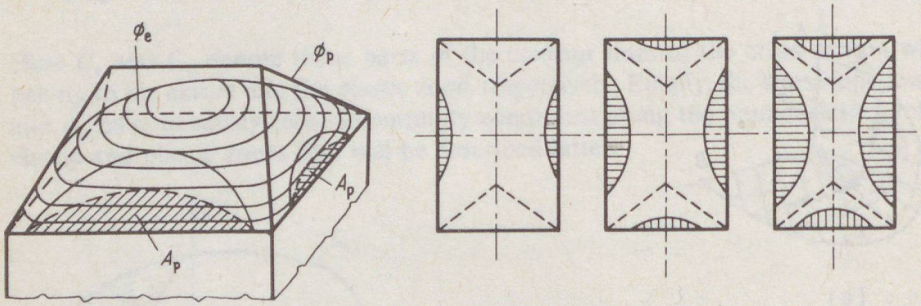


Fig. 4–16

4.2.4.2. MEMBRANE ANALOGY

The membrane analogy described for elastic torsion in Section 4.2.3.2. was extended by Nádai (1950) to elasto-plastic torsion.

Consider again a closed plane curve, forming a frame, with the shape of the cross-section of the twisted bar. Stress a membrane across this frame and also construct a rigid "roof" over the frame which represents the stress function for the fully plastic range. The steepest slope of this roof is equal to τ_0 at every point of the cross-section.

Figure 4—16 shows the case of a rectangular cross-section. Let us apply overpressure to the membrane. For smaller values of the overpressure the deflections of the membrane will not be affected by the roof. This stage corresponds to entirely elastic behaviour. For larger values of the overpressure, however, a part of the membrane will

be pressed against the roof. This constrained portion of the membrane will satisfy all the conditions for the plastic stress function and the free portion of the membrane will satisfy the conditions for the elastic stress function. In addition, along the boundary of these portions the continuity conditions of eq. (4—73) will be also satisfied. Thus, the free and constrained portions of the membrane represent the stress functions for a problem of elasto-plastic torsion.

As the pressure is increased, more portions of the membrane are pressed against the roof. At finite pressure, however, the membrane will always have round surfaces along the edges of the roof, which corresponds to our statement that for a finite angle of twist some parts of the cross-section will always remain elastic. The fully plastic state of the cross-section corresponds to the limit case when the angle of twist tends to infinity.

4.2.4.3. BAR WITH CIRCULAR CROSS-SECTION

As the simplest example, let us consider the elasto-plastic torsion of a bar with circular cross-section. The radius of the cross-section is denoted by R, while r defines the distance of a point from the centroid.

The elastic solution of this problem was presented in Section 4.2.3.3. According to this solution, the elastic limit torque is

$$T_e = \frac{\pi R^3}{2} \tau_0$$

and the corresponding angle of twist per unit length is

$$\theta_{0e} = \frac{\tau_0}{GR}.$$

In the elasto-plastic state, when $T > T_e$, because of symmetry the boundary of the elastic and plastic zones is a circle with an unspecified radius $\rho \leq R$, as shown in Fig. 4—17.

In the elastic zone ($r < \rho$), the stress function

$$\phi_e = -\frac{1}{2} G\theta_0 r^2 + K$$

satisfies the differential equation (4—70), while in the plastic zone ($r \geq \rho$) the stress function

$$\phi_p = \tau_0 (R - r)$$

satisfies the differential equation (4—71) and the boundary condition $\phi_p(R) = 0$. The constant K and the radius ρ can be obtained from the compatibility conditions along the elasto-plastic boundary

$$\phi_e(\rho) = \phi_p(\rho), \quad \left[\frac{d\phi_e}{dr}\right]_\rho = \left[\frac{d\phi_p}{dr}\right]_\rho.$$

These two equations lead to

$$\rho = \frac{\tau_0}{G\theta_0} = \frac{\theta_{0e}}{\theta_0} R, \quad K = \tau_0(R-\rho) + \frac{1}{2} G\theta_0 \rho^2. \tag{4—74}$$

Finally, from the last equation of (4—72) a relationship can be obtained between the magnitude of twist and the angle of twist

$$T = 2\left[\int \phi_e \mathrm{d}A + \int \phi_p \mathrm{d}A\right] = \frac{2\pi}{3}\left[1 - \frac{1}{4}\left(\frac{\rho}{R}\right)^3\right] R^3 \tau_0 =$$

$$= \frac{2\pi}{3}\left[1 - \frac{1}{4}\left(\frac{\theta_{0e}}{\theta_0}\right)^3\right] R^3 \tau_0. \tag{4—75}$$

One can see from relationship (4—74) that if $\theta_0 \to \infty$, then $\rho \to 0$, which corresponds to the fully plastic state of the cross-section.

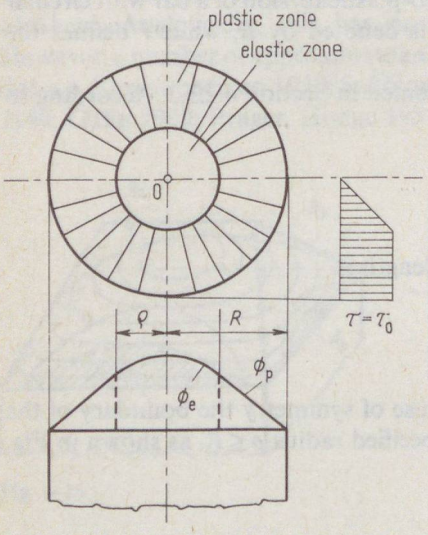


Fig. 4–17

According to eq. (4—75) the corresponding *plastic limit torque* is

$$T_p = \frac{2\pi}{3} R^3 \tau_0 = \frac{4}{3} T_e. \tag{4—76}$$

This is only a limit value of the torque, which cannot be reached in reality. Still, at a relatively low magnitude of θ_0 the corresponding torque very closely approaches the asymptotic value T_p, therefore in practical calculations T_p can be considered the plastic carrying capacity of the cross-section in torsion. For example, if $\theta_0 = 2\theta_{0e}$ the corresponding torque according to eq. (4—75) is $T = 0.969\ T_p$.

4.2.5. FULLY PLASTIC TORSION

4.2.5.1. ANALYTICAL SOLUTION

On increasing the torque in the range when $T > T_e$, more and more parts of the cross-section become plastic, and in the limiting case the torque tends to an asymptotic value T_p as discussed earlier. At the same time, θ_0 tends to infinity and the entire cross-section starts to yield. Determining the stress distribution in this fully plastic state means finding the plastic stress function which satisfies both the differential equation

$$\left[\left(\frac{\partial \phi_p}{\partial x}\right)^2 + \left(\frac{\partial \phi_p}{\partial y}\right)^2\right]^{1/2} = \tau_0$$

over the entire cross-section and also the boundary condition $\phi_p = 0$ along the whole length of the boundary. As was shown earlier, this stress function is represented by a "roof" constructed over the cross-section such that the steepest descent at every point is equal to τ_0. Then, the plastic limit torque is equal to

$$T_p = 2 \int \phi_p \mathrm{d}A. \tag{4—77}$$

4.2.5.2. SAND HILL ANALOGY

As was described in Section 4.2.4.2., the fully plastic state of a twisted bar can be described by the membrane analogy as a limiting case when the membrane is in contact with the whole roof. However, as Nádai (1950) pointed out, the stress function of the fully plastic state can also be obtained by simply pouring dry sand onto a horizontal plate whose shape is identical with the cross-section of the bar. If the coefficient of internal friction of the sand is equal to the magnitude of the yield stress τ_0 then the surface of the sand hill will give the stress function and the plastic limit torque will be equal to twice the volume of the sand. This *sand hill analogy* allows the illustration of the fully plastic stress distribution of a twisted bar, and the simple calculation of the plastic limit torque.

To illustrate the application of the sand hill analogy let us consider Fig. 4—18 where the sand hills of circular, triangular and rectangular cross-sections are shown. The heights of the hills have to be fixed that the slope of the hills is equal to τ_0. Then, the plastic limit torques of the cross-sections are as follows:

(a) *Circular cross-section*

$$h = a\tau_0; \quad T_p = 2\left[\frac{1}{3}\pi a^2 h\right] = \frac{2}{3}\pi a^3 \tau_0. \tag{4—78}$$

(b) *Equilateral triangular cross-section*

$$h = \frac{a}{\sqrt{3}}\tau_0; \quad T_p = 2\left[\frac{1}{2} 2a\sqrt{3}a \frac{h}{3}\right] = \frac{2}{3}a^3\tau_0. \tag{4—79}$$

(c) *Rectangular cross-section* ($a \leq b$)

$$h = \frac{a}{2}\tau_0; \quad T_p = 2\left[(b-a)a\frac{h}{2} + \frac{1}{3}a^2 h\right] = \frac{a^2 b}{6}\left(3 - \frac{a}{b}\right)\tau_0. \tag{4—80}$$

If the rectangular cross-section is narrow, i.e. $a \ll b$, then

$$T_p \approx \frac{a^2 b}{3} \tau_0. \tag{4—81}$$

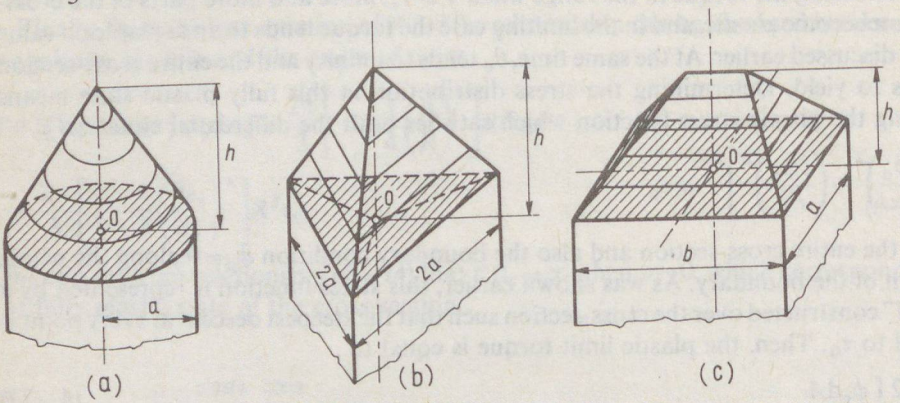


Fig. 4–18

4.2.6. TORSION OF HOLLOW BARS

In our previous investigations, we have assumed that the cross-section of the twisted bar has a simply-connected domain. In the following, we will discuss the problem of torsion of multiply-connected cross-sections. In deriving the governing equations of elastic and elasto-plastic torsion we made use of the fact that the cross-section was simply-connected only in the derivation of the static boundary conditions. Therefore all the equations presented above are valid for multiply connected cross-sections, as well, and only the boundary conditions (4—72) must be modified.

To illustrate the problem, let us consider the elastic torsion of a hollow bar with outer and inner contour lines C_0 and C_1, respectively, as shown in Fig. 4—19. The areas bounded by C_0 and C_1 are designated by A_0 and A_1, respectively, such that the actual area of the cross-section is $A = A_0 - A_1$. It follows from the derivation of the boundary condition (4—50) that the stress function must be constant along each boundary, but now one of these constants cannot be chosen arbitrarily. Denoting the constants by ϕ_0 and ϕ_1, we assume that $\phi_0 = 0$ along the outer boundary. Then the other constant can be determined in a manner as to make the displacements single-valued (see e.g. Sokolnikoff 1956; Timoshenko, Goodier 1971). Omitting the details of derivation, this condition reduces to

$$\oint \tau \mathrm{d}s = \oint \frac{\partial \phi}{\partial n} \mathrm{d}s = 2G\theta_0 A_1. \tag{4—82}$$

Here the left-hand side denotes line integrals along the boundary C_1, $\tau = \dfrac{\partial \phi}{\partial n}$ is the shear stress and n is the normal direction of this boundary. This equation allows the determination of the constant ϕ_1.

Considering now eq. (4—53) and integrating by parts, we find that

$$T=2[A_1\phi_1+\int_A \phi \mathrm{d}A]. \qquad (4—83)$$

Thus, the torque is given by twice the volume bounded by the surface of the stress function, the plane in height ϕ_1 and the cross-section, as shown in Fig. 4—19(b).

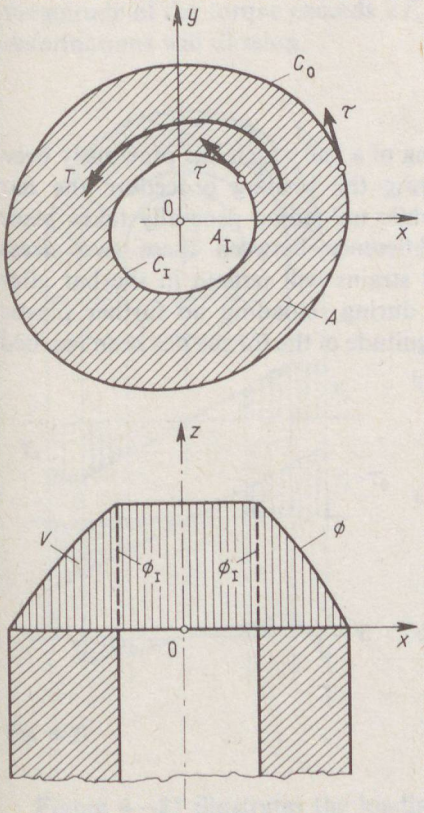


Fig. 4–19

The solution is much simpler in the special case where the inner boundary of the cross-section coincides with one of the stress trajectories of the *solid* bar. Then, considering the torsion of the solid bar, we can imagine the inner portion corresponding to the hole removed without changing the stress distribution in the other portion of the bar. Hence, the stress function of the solid bar applies to the hollow bar as well. For a given angle θ_0 of twist, the stresses in the hollow bar are the same as in the corresponding solid bar, but the torque will be smaller by the amount which is carried in the case of the solid bar by the portion of the cross-section corresponding to the hole. Thus, in this case in relationship (4—83) ϕ denotes the stress function of the solid bar.

The membrane analogy can also be extended to hollow bars. Now the middle portion of the membrane corresponding to the hole must be replaced by a horizontal weightless plate which is mounted on a vertical sliding column. On applying overpressure to the membrane and the plate the shape of the membrane will give the surface of the stress function of the hollow bar.

The analysis of the elasto-plastic torsion of hollow bars, apart from a few special cases, is very complicated. The treatment of these problems is outside the scope of this text.

4.2.7. UNLOADING

As our last problem, let us discuss the unloading of a bar which has previously been loaded beyond the elastic limit torque. During the loading procedure the bar undergoes elastic and plastic deformations, while unloading generally takes place purely elastically. Hence, because of the difference between these two stress distributions, residual stresses and permanent strains will remain in the bar after unloading. The residual stresses ensure that during reloading no further plastic deformations will develop until the original magnitude of the torque has been reached again.

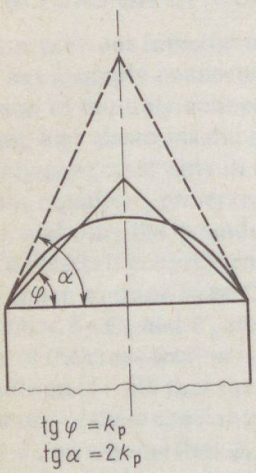


Fig. 4–20

To illustrate the problem, consider a circular bar loaded to the plastic limit torque T_p. The corresponding stress function is illustrated by a cone with slope k_p, while the stress function of the elastic unloading is represented by a rotational paraboloid, as shown in Fig. 4—20. The volumes bounded by the cone and the rotational paraboloid must be equal, since both stress functions correspond to the same magnitude of torque T_p. At every point the slopes k_p and k_e of the two surfaces are equal to the shear stresses, therefore the residual stresses remaining after unloading the bar are equal to the

differences between these slopes: $k_r = k_e - k_p$. The residual stresses cannot, however, be greater than the yield stress, i.e. $k_r = |k_e - k_p| \leq k_p$. Therefore the condition of fully elastic unloading is that $|k_e| \leq 2k_p$, i.e. the surface of the stress function corresponding to elastic unloading must be below the cone with slope $2k_p$. It is obvious that this condition is satisfied if $T_p \leq 2T_e$. This is the case for a circular cross-section where $T_p = \frac{4}{3} T_e < 2T_e$. For those cross-sections, however, for which $T_p > 2T_e$ and the magnitude of the torque exceeds $2T_e$, at each loading and unloading further plastic deformations will develop.

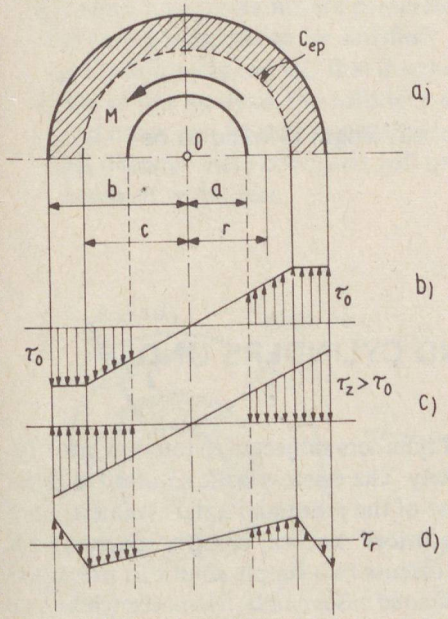


Fig. 4–21

Figure 4—21 illustrates the loading and unloading of an annular circular cross-section with inner and outer radii a and b, respectively. The torque and the angle of twist per unit length corresponding to the elasto-plastic stress distribution shown in Fig. 4—21(b) are equal to

$$\left.\begin{aligned} T = 2\pi \int_a^b \tau r^2 \mathrm{d}r = \frac{2\pi b^3}{3} \beta \tau_0 \quad \text{and} \quad \theta_0 = \frac{\tau_0}{cG}, \\ \text{where} \\ \beta = \left[1 - \frac{1}{4}\left(\frac{c}{b}\right)^3 - \frac{3}{4}\frac{a}{c}\alpha^3 \right], \quad \alpha = \frac{a}{b} \end{aligned}\right\} \qquad (4—84)$$

and c denotes the radius of the elasto-plastic boundary. If T is given c can be determined from the first relationship of eqs (4—84). The stress distribution and the

angle of twist per unit length corresponding to the elastic unloading can be obtained from the following formulae (see Fig. 4—21(c)):

$$\tau_e = \frac{2T}{\pi b^4(1-\alpha^4)} r, \quad \theta_{0e} = \frac{2T}{\pi b^4(1-\alpha^4)G}.$$

Finally, the residual stresses that remain after unloading can be obtained as the difference between the elasto-plastic and purely elastic stress distributions (see Fig. 4—21(d)). They have the forms

$$\text{if} \quad c \le r \le b, \quad \tau_r = \left[1 - \frac{4\beta r}{3b(1-\alpha^4)}\right]\tau_0,$$

$$\text{if} \quad a \le r \le c, \quad \tau_r = \frac{r}{c}\left[1 - \frac{4\beta c}{3b(1-\alpha^4)}\right]\tau_0.$$

Similarly, the permanent angle of twist per unit length is found to be

$$\theta_{0r} = \left[1 - \frac{4\beta c}{3b(1-\alpha^4)}\right]\frac{\tau_0}{cG}.$$

4.3. THICK-WALLED SPHERES AND CYLINDERS UNDER INTERNAL PRESSURE

The elastic analysis of thick-walled spheres and cylinders subjected to internal pressure is a much discussed, classical problem of elasticity. The elasto-plastic solution of these problems is also relatively simple since, because of the point and axial symmetry, the shapes of the elasto-plastic boundaries are "a priori" known, being a sphere and a cylinder, respectively. In the following we will discuss two simple solutions presented by Reckling (1967). The analysis of more complicated cases can be found elsewhere (see e.g. Prager, Hodge 1951; Johnson, Mellor 1962).

4.3.1. THICK-WALLED SPHERES

4.3.1.1. BASIC RELATIONSHIPS

Consider a thick-walled sphere with interior radius a and exterior radius b subjected to an internal pressure p (Fig. 4—22). To describe the stresses and strains produced by this pressure, we will use a system of spherical coordinates r, φ, θ. Because of point symmetry, the stresses $\sigma_{r\varphi}$, $\sigma_{r\theta}$, $\sigma_{\varphi\theta}$, the strains $\varepsilon_{r\varphi}$, $\varepsilon_{r\theta}$, $\varepsilon_{\varphi\theta}$, and the displacements u_φ, u_θ vanish and the remaining stresses σ_{rr} and $\sigma_{\varphi\varphi} = \sigma_{\theta\theta} = \sigma_{tt}$, strains ε_{rr} and $\varepsilon_{\varphi\varphi} = \varepsilon_{\theta\theta} = \varepsilon_{tt}$ and displacement $u_r = u$ are independent of the coordinates φ and θ.

The *equilibrium equation* of an infinitesimal element reduces (see eq. (2—35)) to

$$\frac{d\sigma_{rr}}{dr} + \frac{2}{r}(\sigma_{rr} - \sigma_{tt}) = 0. \tag{4—85}$$

The static boundary conditions have the form

$$\sigma_{rr}(a) = -p, \quad \sigma_{rr}(b) = 0. \tag{4—86}$$

The *kinematic equations* yield the simple form

$$\varepsilon_{rr} = \frac{du}{dr}, \tag{4—87}$$

$$\varepsilon_{tt} = \frac{u}{r}, \tag{4—88}$$

and, since no constraints are prescribed for the displacements, there are no kinematic boundary conditions to be satisfied.

In the following, we will first discuss the elasto-plastic state of the sphere. From the results of this analysis, the solutions of the purely elastic and purely plastic states, as special cases, can be readily obtained. In the derivation of the equations the Huber–v. Mises–Hencky yield condition will be used and the permanent change of volume will be assumed to be zero.

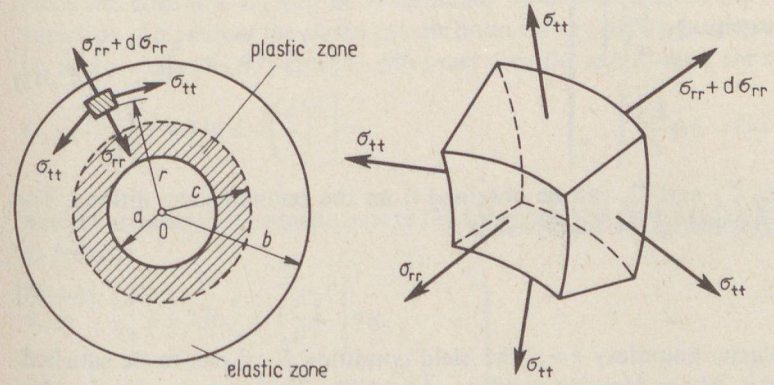


Fig. 4–22

4.3.1.2. ELASTO-PLASTIC STATE

In the elasto-plastic state the inner portion of the sphere bounded by a spherical surface with an unspecified radius c is plastic and the outer portion is elastic.

(a) In the *elastic part* of the sphere ($c \leq r \leq b$) Hooke's Law and eq. (4—88) reduce to

$$\varepsilon_{rr} = \frac{du}{dr} = \frac{1}{E}(\sigma_{rr} - 2\nu\sigma_{tt}),$$
$$\varepsilon_{tt} = \frac{u}{r} = \frac{1}{E}[\sigma_{tt}(1-\nu) - \nu\sigma_{rr}]. \tag{4—89}$$

Solving these equations for the stresses, we obtain

$$\left.\begin{aligned}\sigma_{rr}&=\frac{\lambda}{\nu}\left[(1-\nu)\frac{du}{dr}+2\nu\frac{u}{r}\right],\\ \sigma_{tt}&=\frac{\lambda}{\nu}\left[\nu\frac{du}{dr}+\frac{u}{r}\right],\end{aligned}\right\} \tag{4—90}$$

where λ is Lamé's modulus defined by eq. (2—71b). Let us substitute these two relationships into the equilibrium equation (4—85) and obtain the differential equation

$$\frac{d^2u}{dr^2}+\frac{2}{r}\frac{du}{dr}-\frac{2}{r^2}u=0. \tag{4—91}$$

The solution is found to be

$$u=C_1r+\frac{C_2}{r^2}. \tag{4—92}$$

Substituting this result into eqs (4—90) yields

$$\left.\begin{aligned}\sigma_{rr}&=\frac{\lambda}{\nu}\left[(1+\nu)C_1-2(1-2\nu)\frac{C_2}{r^3}\right],\\ \sigma_{tt}&=\frac{\lambda}{\nu}\left[(1+\nu)C_1+(1-2\nu)\frac{C_2}{r^3}\right].\end{aligned}\right\} \tag{4—93}$$

Here the constants C_1 and C_2 can be obtained from the boundary conditions. The condition $\sigma_{rr}(b)=0$ leads to the relationship

$$C_2=\frac{1+\nu}{2(1-2\nu)}b^3C_1. \tag{4—94}$$

At the elasto-plastic boundary $r=c$, the yield condition $f=0$ has to be satisfied. Using the Huber–v. Mises–Hencky yield condition (2—79a) and the relationship $\tau_0=\dfrac{\sigma_0}{\sqrt{3}}$ we can write*

$$f=(\sigma_{tt}-\sigma_{rr})^2-\sigma_0^2=0.$$

Supposing that at every point $\sigma_{tt}\geq\sigma_{rr}$ one can write

$$(\sigma_{tt}-\sigma_{rr})=\sigma_0. \tag{4—95}$$

Substituting eqs (4—93) and $r=c$ into this relationship reduces it to

$$C_2=\frac{1+\nu}{3}\frac{\sigma_0}{E}c^3. \tag{4—96}$$

* It can be seen that in this problem the Huber–v. Mises–Hencky and the Tresca yield conditions lead to the same relationship, as long as the yield stress σ_0 is assumed to have the same magnitude in both theories.

Finally, making use of eqs (4—93), (4—94) and (4—96) the stresses in the elastic part of the sphere can be expressed in terms of the radius c of the elasto-plastic boundary

$$\left.\begin{aligned}\sigma_{rr} &= -\frac{2}{3}\left(\frac{c}{b}\right)^3\left[\left(\frac{b}{r}\right)^3 - 1\right]\sigma_0,\\ \sigma_{tt} &= \frac{2}{3}\left(\frac{c}{b}\right)^3\left[\frac{1}{2}\left(\frac{b}{r}\right)^3 + 1\right]\sigma_0.\end{aligned}\right\} \tag{4—97}$$

(b) In the *plastic part* of the sphere ($a \leq r \leq c$) the equilibrium equation (4—85) together with the yield condition (4—95) leads to the differential equation

$$\frac{d\sigma_{rr}}{dr} - \frac{2}{r}\sigma_0 = 0, \tag{4—98}$$

with the following solution

$$\sigma_{rr} = 2\sigma_0 \ln r + C_3. \tag{4—99}$$

Here the constant C_3 can be determined by making use of the condition that the variation of σ_{rr} across the elasto-plastic boundary must be continuous (see Section 3.5.), i.e. at $r = c$ eqs (4—97) and (4—99) must give the same result for σ_{rr}. Hence,

$$C_3 = -\frac{2}{3}\left[1 + 3\ln c - \left(\frac{c}{b}\right)^3\right]\sigma_0$$

and the stresses in the plastic part of the sphere can be expressed in terms of the radius c as follows

$$\left.\begin{aligned}\sigma_{rr} &= -\frac{2}{3}\left[1 + 3\ln\frac{c}{r} - \left(\frac{c}{b}\right)^3\right]\sigma_0,\\ \sigma_{tt} &= \sigma_{rr} + \sigma_0 = \frac{2}{3}\left[\frac{1}{2} - 3\ln\frac{c}{r} + \left(\frac{c}{b}\right)^3\right]\sigma_0.\end{aligned}\right\} \tag{4—100}$$

Finally, we have to determine the radius c of the elasto-plastic boundary, which depends on the magnitude of the internal pressure and can be obtained from the boundary condition $\sigma_{rr}(a) = -p$. Using eq. (4—100) this condition leads to

$$p = \frac{2}{3}\left[1 + 3\ln\frac{c}{a} - \left(\frac{c}{b}\right)^3\right]\sigma_0. \tag{4—101}$$

The case when $c = a$ corresponds to the elastic limit and gives the *elastic limit pressure* for the sphere

$$p_e = \frac{2}{3}\left[1 - \left(\frac{a}{b}\right)^3\right]\sigma_0. \tag{4—102}$$

When, on the other hand, $c=b$ the whole sphere is in the plastic state and the corresponding *plastic limit pressure* becomes

$$p_p = 2\sigma_0 \ln \frac{b}{a}. \tag{4—103}$$

4.3.1.3. ELASTIC STATE

In the purely elastic state ($p < p_e$), the stress distribution in the sphere is described by the same functions as were found in the elasto-plastic analysis of the elastic part of the sphere, but the condition $(\sigma_{tt} - \sigma_{rr}) = \sigma_0$ for $r=c$ has to be replaced by the boundary condition $\sigma_{rr}(a) = -p$. This leads to

$$C_1 = \frac{1-2\nu}{E} \frac{a^3}{b^3 - a^3} p.$$

Substituting this relationship and eq. (4—94) in eqs (4—93) gives the stress distribution in the elastic sphere

$$\left.\begin{aligned} \sigma_{rr} &= -\frac{a^3}{b^3 - a^3}\left[\left(\frac{b}{r}\right)^3 - 1\right] p, \\ \sigma_{tt} &= \frac{a^3}{b^3 - a^3}\left[\frac{1}{2}\left(\frac{b}{r}\right)^3 + 1\right] p. \end{aligned}\right\} \tag{4—104}$$

4.3.1.4. FULLY PLASTIC STATE

On increasing the magnitude of the internal pressure up to the plastic limit pressure given by eq. (4—103) the entire sphere will become plastic. Then, substituting $c=b$ in eqs (4—100) yields the fully plastic stress distribution

$$\left.\begin{aligned} \sigma_{rr} &= -2\sigma_0 \ln \frac{b}{r}, \\ \sigma_{tt} &= \sigma_0\left(1 - 2\ln \frac{b}{r}\right). \end{aligned}\right\} \tag{4—105}$$

4.3.1.5. DISPLACEMENTS

Let us consider the elasto-plastic state of the sphere. To obtain the radial displacements u in the elastic part, one has to substitute the expressions for the constants C_1 and C_2 given by eqs (4—94) and (4—96) into eq. (4—91). Then the solution of this differential equation leads to

$$u = \frac{\sigma_0 c}{3E}\left[2(1-2\nu)\frac{rc^2}{b^3} + (1+\nu)\frac{c^2}{r^2}\right] \tag{4—106}$$

where c is defined by eq. (4—61).

Making use of the assumption that the permanent change in volume is zero (see eq. (2—101)), for the *plastic part* of the sphere the following relationship can be obtained

$$\varepsilon_{rr}+\varepsilon_{tt}=\frac{1-2\nu}{E}(\sigma_{rr}+2\sigma_{tt}).$$

Substituting eqs (4—87), (4—88) and (4—100) into this relationship results in the differential equation

$$\frac{du}{dr}+2\frac{u}{r}=-\frac{2(1-2\nu)}{E}\left[3\ln\frac{c}{r}-\left(\frac{c}{b}\right)^3\right]\sigma_0$$

with the solution

$$u=\frac{C_4}{r^2}-\frac{2(1-2\nu)\sigma_0}{E}r\left[\ln\frac{c}{r}+\frac{1}{3}\left(1-\frac{c^3}{b^3}\right)\right]. \tag{4—107}$$

Here the constant C_4 can be obtained from the condition that the displacements must vary continuously throughout the boundary $r=c$, i.e. at $r=c$ eqs (4—106) and (4—107) have to give the same values for u. Hence,

$$C_4=(1-\nu)\frac{\sigma_0}{E}c^3$$

and eq. (4—107) then assumes the form

$$u=\frac{\sigma_0}{E}r\left\{(1-\nu)\left(\frac{c}{r}\right)^3-\frac{2}{3}(1-2\nu)\left[1+3\ln\frac{c}{r}-\left(\frac{c}{b}\right)^3\right]\right\}. \tag{4—108}$$

Here c can be obtained from eq. (4—101).

The maximum radial displacement will occur at the interior surface of the sphere. Let us calculate this displacement for the cases when the internal pressure reaches the values p_e and p_p.

At the elastic limit pressure p_e, $c=a$ and eq. (4—108) for $r=a$ becomes

$$u_e(a)=\frac{\sigma_0 a}{E}\left[(1+\nu)+2(1-2\nu)\left(\frac{a}{b}\right)^3\right]. \tag{4—109}$$

Reaching the plastic limit pressure p_p, $c=b$ and eq. (4—108) for $r=a$ gives

$$u_p(a)=\frac{\sigma_0 a}{E}\left[(1-\nu)\left(\frac{b}{a}\right)^3-2(1-2\nu)\ln\frac{b}{a}\right]. \tag{4—110}$$

Then, under the constant pressure $p=p_p$, the sphere will undergo unrestricted plastic deformations.

4.3.1.6. UNLOADING AND RELOADING

Let us consider the unloading of a sphere which has previously been loaded beyond the elastic limit ($p>p_e$). The residual stresses after unloading are equal to the difference between the elasto-plastic and the perfectly elastic stresses both calculated from the pressure p. Thus, using eqs (4—94), (4—100) and (4—104) we obtain

in the part $a \leq r \leq c$:

$$\left.\begin{aligned} \sigma_{rr}^{r} &= -\frac{2}{3}\left[1+3\ln\frac{c}{r}-\left(\frac{c}{b}\right)^3\right]\sigma_0+\frac{a^3}{b^3-a^3}\left[\left(\frac{b}{r}\right)^3-1\right]p, \\ \sigma_{tt}^{r} &= \frac{2}{3}\left[\frac{1}{2}-3\ln\frac{c}{r}+\left(\frac{c}{b}\right)^3\right]\sigma_0-\frac{a^3}{b^3-a^3}\left[\frac{1}{2}\left(\frac{b}{r}\right)^3+1\right]p, \end{aligned}\right\} \quad (4—111a)$$

and in the part $c \leq r \leq b$:

$$\left.\begin{aligned} \sigma_{rr}^{r} &= -\frac{2}{3}\left(\frac{c}{b}\right)^3\left[\left(\frac{b}{r}\right)^3-1\right]\sigma_0+\frac{a^3}{b^3-a^3}\left[\left(\frac{b}{r}\right)^3-1\right]p, \\ \sigma_{tt}^{r} &= \frac{2}{3}\left(\frac{c}{b}\right)^3\left[\frac{1}{2}\left(\frac{b}{r}\right)^3+1\right]\sigma_0-\frac{a^3}{b^3-a^3}\left[\frac{1}{2}\left(\frac{b}{r}\right)^3+1\right]p. \end{aligned}\right\} \quad (4—111b)$$

Here the radius c of the elastic–plastic boundary is defined by eq. (4—101).

Equations (4—111a) and (4—111b) are valid, however, only while no plastic deformations occur during unloading, i.e. while at each point of the sphere $[\sigma_{tt}^{r}-\sigma_{rr}^{r}]<$ $<\sigma_0$. This condition is satisfied if the pressure does not exceed twice the elastic limit pressure, i.e. if $p \leq 2p_e$. According to eqs (4—102) and (4—103), if $\frac{b}{a} \leq 1.68$ then $p_p \leq 2p_e$ and therefore p cannot be greater than $2p_e$. Consequently, in spheres with ratios $\frac{b}{a}<$ <1.68 no plastic deformations occur during unloading. When the sphere is reloaded again, it will undergo only elastic deformations for pressures less than those applied earlier, consequently say the sphere will shake down.

In spheres with ratios $\frac{b}{a}>1.68$, however, $p_p > 2p_e$ and therefore the magnitude of the pressure may exceed $2p_e$. In such cases, during the subsequent loading and unloading process cyclic plastic deformations will develop which may lead to rupture. To avoid this, the plastic carrying capacity of the sphere should not be utilized, and the magnitude of the pressure should be kept below $2p_e$.

4.3.2. THICK-WALLED CYLINDERS

4.3.2.1. BASIC RELATIONSHIPS

Consider a thick-walled cylinder with interior radius a and exterior radius b subjected to an internal pressure p (Fig. 4—23). To describe the stresses and strains produced by the pressure, we will use a system of cylindrical coordinates r, φ, z. We assume that the stresses and strains are independent of the coordinate z and because of the axial symmetry, the stresses $\sigma_{r\varphi}$, $\sigma_{\varphi z}$, σ_{rz}, the strains $\varepsilon_{r\varphi}$, $\varepsilon_{\varphi z}$, ε_{rz} and the displacements u_φ all vanish. The remaining stresses σ_{rr}, $\sigma_{\varphi\varphi}=\sigma_{tt}$, σ_{zz}, strains ε_{rr}, $\varepsilon_{\varphi\varphi}=\varepsilon_{tt}$, ε_{zz} and the displacement $u_r=u$ are independent of the coordinates φ and z. The axial displacement $u_z=w$, on the other hand, varies only in terms of the coordinates r and z.

The elasto-plastic analysis of a thick-walled cylinder is more complicated than that of a thick-walled sphere. In a thick-walled sphere, only two stress and strain components and one displacement have to be determined, while in a thick-walled cylinder, three stress and strain components and two displacements are unknown. Therefore a closed form general solution for elasto-plastic cylinders cannot be obtained. To simplify the analysis certain assumptions have to be introduced. The solution becomes much simpler if it is assumed that the cylinder is in a state of plane strain ($\varepsilon_{zz}=0$) or in a state of plane stress ($\sigma_{zz}=0$) (see e.g. Prager, Hodge 1951; Johnson, Mellor 1962). Significant simplifications can also be achieved by the assumption that at every point in the cylinder the axial stress is equal to the mean value of the other two normal stresses, i.e.

$$\sigma_{zz}=\frac{1}{2}(\sigma_{rr}+\sigma_{tt}). \tag{4—112}$$

This assumption corresponds to the important practical problem which occurs when the cylinder is closed at its ends by two plates and the total pressure acting on these plates is carried by the cylinder in axial tension. The elasto-plastic analysis of this problem was presented by Reckling (1967) and will be discussed in the following sections.

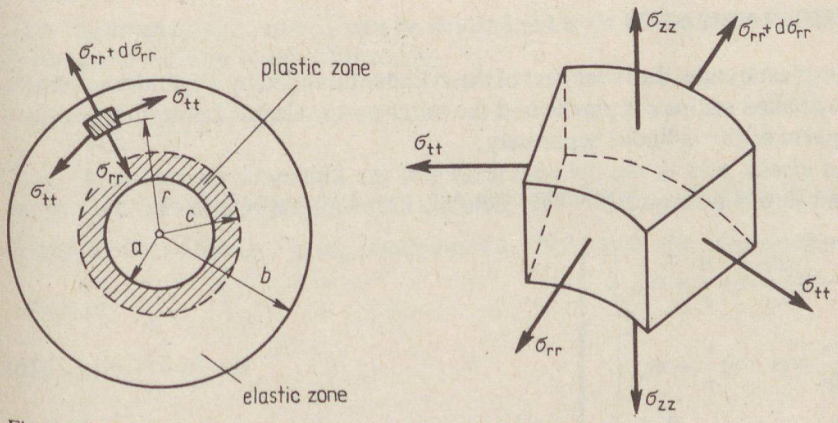


Fig. 4–23

The *equilibrium equation* of an infinitesimal element reduces to

$$\frac{d\sigma_{rr}}{dr}+\frac{1}{r}(\sigma_{rr}-\sigma_{tt})=0 \tag{4—113}$$

and the static boundary conditions have the form

$$\sigma_{rr}(a)=-p, \quad \sigma_{rr}(b)=0. \tag{4—114}$$

The *kinematic equations* lead to

$$\varepsilon_{rr}=\frac{du}{dr}, \quad \varepsilon_{tt}=\frac{u}{r}, \quad \varepsilon_{zz}=\frac{dw}{dz} \tag{4—115}$$

and there are no kinematic boundary conditions to be satisfied.

First, to prove that the assumption (4—112) corresponds to the case when the cylinder is closed by two plates at its ends, let us calculate the resultant of the axial stresses σ_{zz}. By making use of eqs (4—112)–(4—114) we have

$$N = 2\pi \int_a^b \sigma_{zz} r \mathrm{d}r = \pi \int_a^b (\sigma_{rr} + \sigma_{tt}) r \mathrm{d}r =$$

$$= \pi \int_a^b \left(2r\sigma_{rr} + r^2 \frac{\mathrm{d}\sigma_{rr}}{\mathrm{d}r} \right) \mathrm{d}r = \pi \int_a^b \frac{\mathrm{d}}{\mathrm{d}r} (r^2 \sigma_{rr}) \mathrm{d}r = \pi [r^2 \sigma_{rr}]_a^b = \pi a^2.$$

It can be seen that this force is indeed equal to the total pressure acting on the closing end plates.

In the following, we will first discuss the case when the cylinder is in the elasto-plastic state. From the results of this analysis, the solutions of the purely elastic and purely plastic states can be readily obtained as special cases.

In the derivation of these equations, the Huber–v. Mises–Hencky yield condition will be used and the permanent change of volume will be assumed to be zero.

4.3.2.2. ELASTO-PLASTIC STATE

In the elasto-plastic state, the inner part of the cylinder bounded by a cylindrical surface with an unspecified radius c is plastic and the outer part is elastic. Let us first consider these two parts of the cylinder separately.

(a) In the *elastic part of the cylinder* ($c \leq r \leq b$) the kinematic equations (4—115), Hooke's Law and relationship (4—112) yield the following expressions for the stresses

$$\left.\begin{aligned} \sigma_{rr} &= \frac{\lambda}{\nu} \left[(1-\nu) \frac{\mathrm{d}u}{\mathrm{d}r} + \nu \frac{u}{r} + \nu \varepsilon_{zz} \right], \\ \sigma_{tt} &= \frac{\lambda}{\nu} \left[\nu \frac{\mathrm{d}u}{\mathrm{d}r} + (1-\nu) \frac{u}{r} + \nu \varepsilon_{zz} \right], \\ \sigma_{zz} &= \frac{\lambda}{2\nu} \left[\frac{\mathrm{d}u}{\mathrm{d}r} + \frac{u}{r} + 2\nu \varepsilon_{zz} \right], \end{aligned}\right\} \qquad (4—116)$$

where λ is Lamé's modulus defined by eq. (2—71b).

Substituting these expressions into the equilibrium equation (4—113), the differential equation

$$\frac{\mathrm{d}^2 u}{\mathrm{d}r^2} + \frac{1}{r} \frac{\mathrm{d}u}{\mathrm{d}r} - \frac{u}{r^2} = 0$$

is obtained with the solution

$$u = C_1 r + \frac{C_2}{r}. \qquad (4—117)$$

In eqs (4—116) and (4—117) ε_{zz}, C_1 and C_2 are constants. First, to eliminate ε_{zz} let us make use of eq. (4—112) and write Hooke's Law in the form

$$\varepsilon_{zz}=\frac{1}{E}[\sigma_{zz}-\nu(\sigma_{rr}+\sigma_{tt})]=\frac{1-2\nu}{E}\sigma_{zz}.$$

Substituting this relationship together with eq. (4—117) into the last relationship of eqs (4—116) gives $\varepsilon_{zz}=C_1$. On making use of this result and eq. (4—117), the expressions for the stresses given by eqs (4—116) assume the form

$$\left.\begin{aligned}\sigma_{rr}&=\frac{\lambda}{\nu}\left[(1+\nu)C_1-(1-2\nu)\frac{C_2}{r^2}\right],\\ \sigma_{tt}&=\frac{\lambda}{\nu}\left[(1+\nu)C_1+(1-2\nu)\frac{C_2}{r^2}\right],\\ \sigma_{zz}&=\frac{E}{1-2\nu}C_1.\end{aligned}\right\} \qquad (4—118)$$

Here the constants C_1 and C_2 can be determined from the boundary conditions. The boundary condition $\sigma_{rr}(b)=0$ leads to

$$C_2=\frac{1+\nu}{1-2\nu}b^2C_1. \qquad (4—119)$$

At the elasto-plastic boundary $r=c$, the yield condition $f=0$ has to be satisfied. The Huber–v.Mises–Hencky yield condition (2—79a) and the relationship $\tau_0=\dfrac{\sigma_0}{\sqrt{3}}$ reduce to

$$f=(\sigma_{tt}-\sigma_{rr})^2-\sigma_0^2=0$$

or supposing that at every point $\sigma_{tt}\geq\sigma_{rr}$, one can write*

$$(\sigma_{tt}-\sigma_{rr})=\sigma_0. \qquad (4—120)$$

Substituting eqs (4—118) and $r=c$ in this relationship results in the expression

$$C_2=\frac{1+\nu}{\sqrt{3}}\frac{\sigma_0}{E}c^2. \qquad (4—121)$$

* It can be seen that for this problem the Huber–v. Mises–Hencky and the Tresca yield conditions lead to the same relationship as long as the yield stress σ_0 is assumed to have the same magnitude in both theories.

Finally, making use of eqs (4—118), (4—119) and (4—121) the stresses in the elastic part of the cylinder can be expressed in terms of the radius c of the elasto-plastic boundary

$$\left.\begin{aligned}\sigma_{rr} &= -\frac{1}{\sqrt{3}}\left(\frac{c}{b}\right)^2\left[\left(\frac{b}{r}\right)^2-1\right]\sigma_0,\\ \sigma_{tt} &= \frac{1}{\sqrt{3}}\left(\frac{c}{b}\right)^2\left[\left(\frac{b}{r}\right)^2+1\right]\sigma_0,\\ \sigma_{zz} &= \frac{1}{\sqrt{3}}\left(\frac{c}{b}\right)^2\sigma_0.\end{aligned}\right\} \tag{4—122}$$

(b) In the *plastic part of the cylinder* ($a \leq r \leq c$) the equilibrium equation (4—113) together with the yield condition (4—120) gives the differential equation

$$\frac{d\sigma_{rr}}{dr} - \frac{2\sigma_0}{\sqrt{3}}\frac{1}{r} = 0 \tag{4—123}$$

with the solution

$$\sigma_{rr} = \frac{2\sigma_0}{\sqrt{3}}\ln r + C_3. \tag{4—124}$$

Here the constant C_3 can be determined by expressing the condition that σ_{rr} must vary continously across the elasto-plastic boundary (see Section 3.5), i.e. at $r=c$ eqs (4—122) and (4—124) must give the same value for σ_{rr}. Then, making use of relationships (4—112) and (4—120), the stresses in the plastic part of the cylinder can be expressed in terms of the radius c of the elasto-plastic boundary

$$\left.\begin{aligned}\sigma_{rr} &= -\frac{1}{\sqrt{3}}\left[1+2\ln\frac{c}{r}-\left(\frac{c}{b}\right)^2\right]\sigma_0,\\ \sigma_{tt} &= \frac{1}{\sqrt{3}}\left[1-2\ln\frac{c}{r}+\left(\frac{c}{b}\right)^2\right]\sigma_0,\\ \sigma_{zz} &= \frac{1}{\sqrt{3}}\left[\left(\frac{c}{b}\right)^2-2\ln\frac{c}{r}\right]\sigma_0.\end{aligned}\right\} \tag{4—125}$$

Finally, we have to determine the radius c of the elasto-plastic boundary. It depends on the magnitude of the internal pressure and can be obtained from the boundary condition $\sigma_{rr}(a) = -p$. Using eq. (4—125) this condition leads to

$$p = \frac{1}{\sqrt{3}}\left[1+2\ln\frac{c}{a}-\left(\frac{c}{b}\right)^2\right]\sigma_0. \tag{4—126}$$

The case when $c=a$ corresponds to the elastic limit state and gives the *elastic limit pressure* of the cylinder

$$p_e=\frac{1}{\sqrt{3}}\left[1-\left(\frac{a}{b}\right)^2\right]\sigma_0. \tag{4—127}$$

When, on the other hand, $c=b$ the whole cylinder is in plastic state and the corresponding *plastic limit pressure* becomes

$$p_p=\frac{2}{\sqrt{3}}\sigma_0 \ln\frac{b}{a}. \tag{4—128}$$

Next, let us determine the purely elastic and the fully plastic stress distributions in the cylinder.

4.3.2.3. ELASTIC STATE

In the purely elastic state ($p<p_e$) the stress distribution in the cylinder is described by the same functions as were found in the elasto-plastic analysis of the elastic part of the cylinder, but now the condition $(\sigma_{tt}-\sigma_{rr})=\sigma_0$ for $r=c$ has to be replaced by the boundary condition $\sigma_{rr}(a)=-p$. This leads to

$$C_1=\frac{1-2\nu}{E}\frac{a^2}{b^2-a^2}p.$$

Substituting this relationship and eq. (4—121) in eqs (4—122) gives the stress distribution in the purely elastic cylinder

$$\left.\begin{aligned}
\sigma_{rr}&=-\frac{a^2}{b^2-a^2}\left[\left(\frac{b}{r}\right)^2-1\right]p,\\
\sigma_{tt}&=\frac{a^2}{b^2-a^2}\left[\left(\frac{b}{r}\right)^2+1\right]p,\\
\sigma_{zz}&=\frac{a^2}{b^2-a^2}p.
\end{aligned}\right\} \tag{4—129}$$

4.3.2.4. FULLY PLASTIC STATE

On increasing the magnitude of the internal pressure to the plastic limit pressure given by eq. (4—128), the entire cylinder will become plastic. Then, substituting $c=b$ in eqs (4—125) gives the fully plastic stress distribution

$$\left.\begin{aligned}
\sigma_{rr}&=-\frac{2}{\sqrt{3}}\sigma_0\ln\frac{b}{r},\\
\sigma_{tt}&=\frac{2}{\sqrt{3}}\sigma_0\left(1-\ln\frac{b}{r}\right),\\
\sigma_{zz}&=\frac{1}{\sqrt{3}}\sigma_0\left(1-2\ln\frac{b}{r}\right).
\end{aligned}\right\} \tag{4—130}$$

4.3.2.5. DISPLACEMENTS

Let us consider the elasto-plastic state of the cylinder. To determine the radial displacements u in the elastic part, one has to substitute the constants C_1 and C_2 given by eqs (4—119) and (4—121) in eq. (4—117). This leads to

$$u=\frac{\sigma_0 c}{\sqrt{3}E}\left[(1-2\nu)\frac{rc}{b^2}+(1+\nu)\frac{c}{r}\right] \tag{4—131}$$

where c is defined by eq. (4—126).

Making use of the assumption that the permanent change in volume is zero (see eq. (2—100)) and considering eq. (4—112), for the plastic part of the cylinder ($a\leq r\leq c$) the following relationship can be obtained

$$\varepsilon_{rr}+\varepsilon_{tt}+\varepsilon_{zz}=\frac{1-2\nu}{E}(\sigma_{rr}+\sigma_{tt}+\sigma_{zz})=\frac{3(1-2\nu)}{E}\sigma_{zz}.$$

Substituting eqs (4—115) and (4—125) and the result $\varepsilon_{zz}=\frac{1-2\nu}{E}\sigma_{zz}$ into this relationship leads to the differential equation

$$\frac{du}{dr}+\frac{u}{r}=\frac{2(1-2\nu)\sigma_0}{\sqrt{3}E}\left[\left(\frac{c}{b}\right)^2-3\ln\frac{c}{r}\right]$$

with the solution

$$u=\frac{C_4}{r}-\frac{(1-2\nu)\sigma_0}{\sqrt{3}E}\left[3\ln\frac{c}{r}+\frac{3}{2}-\left(\frac{c}{b}\right)^2\right]r. \tag{4—132}$$

Here the constant C_4 can be obtained from the condition that the displacements must vary continuously across the elastic–plastic boundary, i.e. at $r=c$ eqs (4—131) and (4—132) have to give the same values. Determining C_4 and substituting in eq. (4—132) we obtain

$$u=\frac{\sigma_0 r}{2\sqrt{3}E}\left\{(5-4\nu)\left(\frac{c}{r}\right)^2-(1-2\nu)\left[6\ln\frac{c}{r}+3-2\left(\frac{c}{b}\right)^2\right]\right\}. \tag{4—133}$$

Here c can be obtained from eq. (4—126).

The maximum radial displacement will take place at the interior surface of the cylinder. Let us calculate this displacement when the interior pressure reaches the values p_e and p_p.

At the elastic limit pressure p_e, $c=a$ and for $r=a$ eq. (4—131) becomes

$$u_e(a)=\frac{\sigma_0 a}{\sqrt{3}E}\left[1+\nu+(1-2\nu)\left(\frac{a}{b}\right)^2\right]. \tag{4—134}$$

On reaching the plastic limit pressure p_p, $c=b$ and eq. (4—133) yields for $r=a$

$$u_p(a)=\frac{\sigma_0 a}{2\sqrt{3}E}\left[(5-4\nu)\left(\frac{b}{a}\right)^2-(1-2\nu)\left(1+6\ln\frac{b}{a}\right)\right]. \qquad (4—135)$$

Then, under the constant pressure $p=p_p$, the cylinder will undergo unrestricted plastic deformations.

4.3.2.6. UNLOADING AND RELOADING

The statements presented in Section 4.3.1.6. concerning the unloading and reloading of spheres are also valid for cylinders under internal pressure, however, the numerical values are different. In the case of cylinders $b/a=2.22$ is the limit ratio at which $p_p=2p_e$. Consequently, for cylinders with ratios $b/a<2.22$ p cannot be larger than $2p_e$ and therefore during unloading no plastic deformations occur. If the cylinder is reloaded again, then below the magnitude of the pressure applied previously it will undergo only elastic deformations and the cylinder will shake down.

In cylinders with the ratios $b/a>2.22$, however, $p_p>2p_e$ and therefore the pressure may exceed the magnitude $2p_e$. In such cases, during the subsequent loading and unloading process cyclic plastic deformations will develop which could lead to rupture. To avoid this phenomenon, the plastic carrying capacity of the cylinder should not be utilized and the magnitude of the pressure should be kept below $2p_e$.

5. PLASTIC ANALYSIS OF PLANE STRAIN AND PLANE STRESS PROBLEMS

After a brief presentation of the governing equations of plane problems of elasticity the first part of this chapter deals with the theory and applications of plane plastic flow. First, the basic equations of plane plastic flow are derived and the properties of shear lines which form the basis of the shear line theory are discussed. Next, the application of the shear line theory and the static and kinematic principles of limit analysis are illustrated by the exact and approximate solutions of several plane strain problems.

The second part of the chapter deals with the plane stress problem of plasticity. The basic equations based on both the Huber–v. Mises–Hencky and the Tresca yield conditions are presented, and methods of solution and some applications are briefly discussed.

In the last part of the chapter, a brief review of the application of the finite element method to plane plastic problems is given.

5.1. BASIC RELATIONSHIPS

5.1.1. INTRODUCTION

Consider the special states of a body when a system of rectangular coordinates x, y, z can be chosen such that the stress and strain fields are independent of one of these coordinates, say z, and the shear stresses and shear strains corresponding to this coordinate vanish, i.e.

$$\left.\begin{aligned} &\sigma_{xx}=\sigma_{xx}(x,y), \quad \sigma_{yy}=\sigma_{yy}(x,y), \quad \sigma_{zz}=\sigma_{zz}(x,y),\\ &\sigma_{xy}=\sigma_{xy}(x,y), \quad \sigma_{zx}=0, \quad \sigma_{zy}=0,\\ &\varepsilon_{xx}=\varepsilon_{xx}(x,y), \quad \varepsilon_{yy}=\varepsilon_{yy}(x,y), \quad \varepsilon_{zz}=\varepsilon_{zz}(x,y),\\ &\varepsilon_{xy}=\varepsilon_{xy}(x,y), \quad \varepsilon_{zx}=0, \quad \varepsilon_{zy}=0. \end{aligned}\right\} \tag{5—1}$$

In these states σ_{zz} and ε_{zz} are the principal stresses and principal strains, respectively, at every point in the body. When, in addition, one of these vanishes throughout the entire body, we have a plane stress or a plane strain problem.

In a *state of plane strain*, in addition to eqs (5—1),

$$\varepsilon_{zz}=0, \tag{5—2}$$

which can be achieved by the suitable choice of the boundary conditions. If a prismatic body is infinitely long, or if its displacements in the z direction are restrained, and in both cases the external load acting solely in the x, y plane is independent of the coordinate z, then the body is in a state of plane strain (Fig. 5—1(a)).

In a *state of plane stress*, in addition to eqs (5—1),

$$\sigma_{zz}=0. \tag{5—3}$$

This condition is approximately satisfied in thin plates which are loaded in their middle plane, as shown in Fig. 5—1(b).

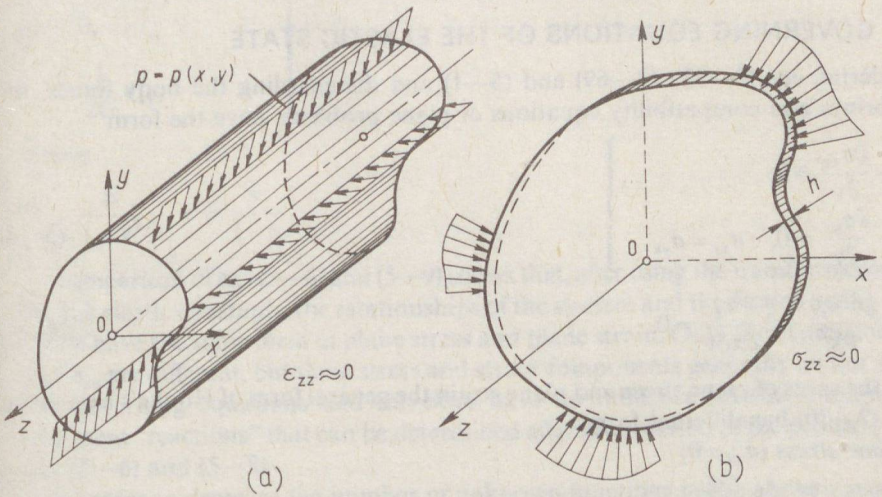


Fig. 5–1

In the case of elastic bodies, except in some special problems, there is no significant difference between the analyses of plane strain and plane stress problems. In the case of plastic bodies, however, the governing equations of plane strain and plane stress problems are different. In plane strain, the magnitude of the stress σ_{zz} is always equal to the mean value of the other two principal stresses therefore the plane of the maximum shear stresses is normal to the x, y plane at every point in the body. In plane stress, however, a similar "a priori" statement cannot be made, and therefore the governing equations have a different form and their solution is more complicated. This is the reason why the analysis of plane strain problems is a very well-developed field of plasticity, while for plane stress problems relatively few solutions can be found in the literature.

In spite of the simplifications which can be achieved by the assumption of plane strain or plane stress states, the elasto-plastic analysis of a body is very complicated and in most cases only numerical solutions can be obtained. The difficulties can be significantly decreased by assuming rigid–perfectly plastic material behaviour. Then, the governing equations of the plastic domains of the body are relatively simple and their solution provides reliable information about the plastic limit state of the body. These results are of practical importance in the study of metal-forming processes

where, because of large deformations, the elastic deformations are negligible. Rigid-plastic analysis, however, does not provide any information about the state of stress and strain in the rigid domains of the body. In many cases, it cannot even be proved that in the rigid domains there exists a statically admissible stress field that does not violate the yield condition. Thus, in terms of the extremum principles of limit analysis, these solutions which provide an upper bound for the external load necessary to cause unrestricted plastic flow can only be considered as approximate.

Before discussing the plane strain and stress problems of plasticity we will briefly summarize the governing equations of the plane state of elastic bodies.

5.1.2. GOVERNING EQUATIONS OF THE ELASTIC STATE

Considering eqs (2—32), (2—69) and (5—1) and disregarding the body forces, the equilibrium and compatibility equations of plane problems have the form

$$\left.\begin{aligned} &\frac{\partial \sigma_{xx}}{\partial x}+\frac{\partial \sigma_{xy}}{\partial y}=0, \\ &\frac{\partial \sigma_{yx}}{\partial x}+\frac{\partial \sigma_{yy}}{\partial y}=0, \quad \sigma_{xy}=\sigma_{yx}, \end{aligned}\right\} \tag{5—4}$$

$$\frac{\partial^2 \varepsilon_{xx}}{\partial y^2}+\frac{\partial^2 \varepsilon_{yy}}{\partial x^2}-2\frac{\partial^2 \varepsilon_{xy}}{\partial x \partial y}=0. \tag{5—5}$$

For the cases of plane stress and plane strain the general form of Hooke's Law given by eq. (2—70) has different forms.

For *plane stress* ($\sigma_{zz}=0$)

$$\left.\begin{aligned} \varepsilon_{xx}&=\frac{1}{2}(\sigma_{xx}-\nu\sigma_{yy}), \\ \varepsilon_{yy}&=\frac{1}{E}(\sigma_{yy}-\nu\sigma_{xx}), \\ \varepsilon_{zz}&=-\frac{\nu}{E}(\sigma_{xx}+\sigma_{yy}), \\ \varepsilon_{xy}&=\frac{1}{2G}\sigma_{xy}, \end{aligned}\right\} \tag{5—6}$$

while for *plane strain* ($\varepsilon_{zz}=0$)

$$\left.\begin{aligned} \varepsilon_{xx}&=\frac{1}{E}[\sigma_{xx}-\nu(\sigma_{yy}+\sigma_{zz})], \\ \varepsilon_{yy}&=\frac{1}{E}[\sigma_{yy}-\nu(\sigma_{xx}+\sigma_{zz})], \\ \varepsilon_{zz}&=\frac{1}{E}[\sigma_{zz}-\nu(\sigma_{xx}+\sigma_{yy})]=0, \\ \varepsilon_{xy}&=\frac{1}{2G}\sigma_{xy}. \end{aligned}\right\} \tag{5—7}$$

From the third expression of eqs (5—7), we obtain

$$\sigma_{zz} = \nu(\sigma_{xx} + \sigma_{yy}) \tag{5—8}$$

which together with eqs (5—7) leads to

$$\left.\begin{aligned} \varepsilon_{xx} &= \frac{1}{E'}(\sigma_{xx} - \nu'\sigma_{yy}), \\ \varepsilon_{yy} &= \frac{1}{E'}(\sigma_{yy} - \nu'\sigma_{xx}), \\ \varepsilon_{zz} &= 0, \\ \varepsilon_{xy} &= \frac{1}{2G}\sigma_{xy}, \end{aligned}\right\} \tag{5—9}$$

where

$$E' = \frac{E}{1-\nu^2}, \quad \nu' = \frac{\nu}{1-\nu}. \tag{5—10}$$

Comparison of eqs (5—6) and (5—9) shows that, after using the transformation (5—10) for the elastic constants, the relationships of the stresses and the strains acting in the xy plane have the same form in plane stress and plane strain. Only the expressions for σ_{zz} and ε_{zz} are different, but these stress and strain components generally do not appear in the governing equations and therefore have no influence on the solution.* They represent "reactions" that can be determined after the solution of the problem by using eqs (5—6) and (5—8).

In order to decrease the number of unknown functions in the above equations, we have to substitute eqs (5—6) or (5—9) into the compatibility equation (5—5). Then, by making use of one of the equilibrium equations (5—4), we can eliminate the shear stress σ_{xy} and obtain the following relationship

$$\left(\frac{\partial^2}{\partial x^2} + \frac{\partial^2}{\partial y^2}\right)(\sigma_{xx} + \sigma_{yy}) = \Delta(\sigma_{xx} + \sigma_{yy}) = 0. \tag{5—11}$$

To satisfy the remaining equilibrium equation, it is convenient to introduce a *stress function* ϕ, often called *Airy's stress function*, defined as follows

$$\sigma_{xx} = \frac{\partial^2\phi}{\partial y^2}, \quad \sigma_{yy} = \frac{\partial^2\phi}{\partial x^2}, \quad \sigma_{xy} = -\frac{\partial^2\phi}{\partial x \partial y}. \tag{5—12}$$

It is easy to check that using eqs (5—12) the equilibrium equations (5—4) are identically satisfied: thus, substituting eqs (5—12) into eq. (5—11) we obtain the *governing equation of plane problems of elasticity*

$$\frac{\partial^4\phi}{\partial x^4} + 2\frac{\partial^4\phi}{\partial x^2 \partial y^2} + \frac{\partial^4\phi}{\partial y^4} = \Delta^2\phi = 0. \tag{5—13}$$

* This statement may require modification in the case of multiply-connected bodies and in problems where both static and kinematic boundary conditions are prescribed (see e.g. Timoshenko, Goordier (1970)).

When only static boundary conditions are prescribed, these can easily be expressed in terms of the stress function, and then the biharmonic differential equation (5—13) can be solved. After determining the stress function and the stresses, the strains and the displacements can be obtained from eqs (5—6) and (2—67).

The solution is more complicated when kinematic boundary conditions are also prescribed, since these conditions cannot be expressed in a simple form in terms of the stress function. In these cases, the strains and displacements also have to be involved in the solution, and therefore it is more convenient to derive the governing equations on the basis of eqs (5—4)–(5—6), in which the displacements are the unknown functions. Discussions of this method and a great number of solutions to different problems can be found in the literature (see e.g. Muskelisvili 1953; Sokolnikoff 1956; Timoshenko, Goordier 1970).

5.2. PLANE PLASTIC FLOW

5.2.1. GENERAL REMARKS

Let us consider a *rigid–perfectly plastic body* in a *state of plane strain.* As the loads are slowly applied, the body initially does not undergo any deformations but at a certain magnitude of the load in the entire body or in a part of it unrestricted plastic deformations start to develop. Because of the state of plane strain the displacements and velocities of the points in the body can be characterized in the form

$$u_x = u_x(x,y), \quad u_y = u_y(x,y), \quad u_z = 0, \tag{5—14}$$

$$v_x = v_x(x,y), \quad v_y = v_y(x,y), \quad v_z = 0. \tag{5—15}$$

Since the behaviour of the plastic regions of the body is similar to the plane flow of fluids, this state is called *plane plastic flow.*

In the following, the Prandtl–Reuss constitutive equations (2—99a) will be used, which in the case of rigid-plastic material can be expressed in terms of strain rates in the following form*

$$\left.\begin{aligned} \dot{\varepsilon}_{xx} &= \dot{\lambda} s_{xx}, \\ \dot{\varepsilon}_{yy} &= \dot{\lambda} s_{yy}, \\ \dot{\varepsilon}_{zz} &= \dot{\lambda} s_{zz}, \\ \dot{\varepsilon}_{xy} &= \dot{\lambda} s_{xy}. \end{aligned}\right\} \tag{5—16}$$

Since in plane strain $\dot{\varepsilon}_{zz} = 0$, the third relationship of eqs (5—16) yields

$$s_{zz} = \sigma_{zz} - \sigma_m = \sigma_{zz} - \frac{1}{3}(\sigma_{xx} + \sigma_{yy} + \sigma_{zz}) = 0,$$

from which an important relationship can be obtained

$$\sigma_{zz} = \sigma_m = \frac{1}{2}(\sigma_{xx} + \sigma_{yy}). \tag{5—17}$$

* These equations are identical with the Lévy–v. Mises equations (2—93).

It follows that, in plane plastic flow the normal stress σ_{zz} is equal to the mean value of the other two normal stresses and identical to the mean normal stress $\sigma_m = \frac{1}{3}(\sigma_{xx}+\sigma_{yy}+\sigma_{zz})$. Since in plane strain $\sigma_{zx}=\sigma_{zy}=0$, σ_{zz} also represents a principal stress and therefore the other two principal stresses are always parallel to the x,y plane. Then, relationship (5—17) can be written as

$$\sigma_{zz}=\sigma_{II}=\frac{1}{2}(\sigma_I+\sigma_{III}). \tag{5—18}$$

Using eq. (5—17) and (2—22) the constitutive equation (5—16) assumes the form

$$\left.\begin{aligned}\dot{\varepsilon}_{xx}&=\frac{1}{2}\dot{\lambda}(\sigma_{xx}-\sigma_{yy}),\\ \dot{\varepsilon}_{yy}&=\frac{1}{2}\dot{\lambda}(\sigma_{yy}-\sigma_{xx}),\\ \dot{\varepsilon}_{xy}&=\dot{\lambda}\sigma_{xy},\end{aligned}\right\} \tag{5—16a}$$

and on eliminating $\dot{\lambda}$ it becomes

$$\left.\begin{aligned}\frac{\dot{\varepsilon}_{xx}-\dot{\varepsilon}_{yy}}{\dot{\varepsilon}_{xy}}&=\frac{\sigma_{xx}-\sigma_{yy}}{\sigma_{xy}},\\ \dot{\varepsilon}_{xx}+\dot{\varepsilon}_{yy}&=0.\end{aligned}\right\} \tag{5—16b}$$

Here, in correspondence with eq. (2—95), the second equation expresses the incompressibility of the material.

Making use of eqs (5—1) and (5—17), the Huber–v. Mises–Hencky yield condition (2—79a) reduces to

$$f=\frac{1}{4}(\sigma_{xx}-\sigma_{yy})^2+\sigma_{xy}^2-\tau_0^2=0 \tag{5—19}$$

and together with the equilibrium equations

$$\left.\begin{aligned}\frac{\partial\sigma_{xx}}{\partial x}+\frac{\partial\sigma_{xy}}{\partial y}&=0,\\ \frac{\partial\sigma_{yx}}{\partial x}+\frac{\partial\sigma_{yy}}{\partial y}&=0,\end{aligned}\right\} \tag{5—20}$$

provides three equations for the determination of the stresses $\sigma_{xx}, \sigma_{yy}, \sigma_{xy}$. Hence, if only static boundary conditions are prescribed, the determination of the stresses in the plastic domains is statically determinate. Equations (5—19) and (5—20) construct a set of *hyperbolic differential equations* and can be solved by the *method of characteristics*. It will be shown that the characteristics of the above differential equations have a mechanical meaning, since they coincide with the *shear lines* of the plastic domain, along which the shear stresses assume maximum values and only shear deformations occur. These properties of the characteristics simplify the solution of the problems of plane plastic flow.

When kinematic boundary conditions are also prescribed, the strains and displacements and, consequently, the compatibility and constitutive equations also have to be taken into consideration. This circumstance complicates the solution of this class of problem.

5.2.2. STRESS RELATIONSHIPS

In order to allow the solution of eqs (5—19) and (5—20), we have to derive some special stress relationships for the state of plane plastic flow. Considering eqs (2—8) and (5—1) in the case of plane stress or plane strain, the principal stresses and principal directions can be determined from the equations

$$\left.\begin{aligned}(\sigma_{xx}-\sigma_k)\,l_x+\sigma_{xy}l_y=0,\\ \sigma_{yx}l_x+(\sigma_{yy}-\sigma_k)\,l_y=0.\end{aligned}\right\} \tag{5—21}$$

These lead to the condition

$$\begin{vmatrix}(\sigma_{xx}-\sigma_k) & \sigma_{xy}\\ \sigma_{yx} & (\sigma_{yy}-\sigma_k)\end{vmatrix}=0$$

and to the characteristic equation

$$\sigma_k^2-(\sigma_{xx}+\sigma_{yy})\sigma_k+(\sigma_{xx}\sigma_{yy}-\sigma_{xy}^2)=0.$$

The solution of this equation together with relationship (5—18) is found to be

$$\left.\begin{aligned}\sigma_I&=\frac{1}{2}(\sigma_{xx}+\sigma_{yy})+\sqrt{\frac{1}{4}(\sigma_{xx}-\sigma_{yy})^2+\sigma_{xy}^2},\\ \sigma_{II}&=\sigma_m=\frac{1}{2}(\sigma_{xx}+\sigma_{yy})=\frac{1}{2}(\sigma_I+\sigma_{III}),\\ \sigma_{III}&=\frac{1}{2}(\sigma_{xx}+\sigma_{yy})-\sqrt{\frac{1}{4}(\sigma_{xx}-\sigma_{yy})^2+\sigma_{xy}^2}.\end{aligned}\right\} \tag{5—22}$$

Then, according to eq. (2—15), the *maximum shear stress* becomes

$$\tau_{max}=\frac{1}{2}(\sigma_I-\sigma_{III})=\sqrt{\frac{1}{4}(\sigma_{xx}-\sigma_{yy})^2+\sigma_{xy}^2}. \tag{5—23}$$

Comparing this result with eq. (5—19), one can see that in plane plastic flow the Huber–v. Mises–Hencky and the Tresca yield conditions have identical forms. This means that *at every point in the plastic domain the maximum shear stress is equal to the yield stress in shear*. Considering this result and eqs (5—22) and (5—23) the principal stresses may be written as

$$\left.\begin{aligned}\sigma_I&=\sigma_m+\tau_0,\\ \sigma_{II}&=\sigma_m,\\ \sigma_{III}&=\sigma_m-\tau_0.\end{aligned}\right\} \tag{5—24}$$

Let us denote the angle of the first principal direction, measured from the x axis by φ and assume its positive sense in the counter-clockwise direction. Then, substituting the elements $l_x = \cos\varphi$, $l_y = \sin\varphi$ of the corresponding unit normal vector into eq. (5—21) results in

$$\tan 2\varphi = \frac{2\sigma_{xy}}{\sigma_{xx} - \sigma_{yy}}. \tag{5—25}$$

The two roots of this equation in the range $0 \leq \varphi \leq 360°$ differ by 90° from each other, and provide the directions of the two principal axes I and III.

The stress state for plane plastic flow at a generic point can be illustrated by *Mohr's circles*. Figure 5—2(a) shows the *physical plane* and the sign convention used for the stress components while, making use of the results of Section 2.1.5., Mohr's circles are plotted on the *stress plane*, shown in Fig. 5—2(c). The points on the circumference of the circle with coordinates

$$\sigma_m = \frac{1}{2}(\sigma_{xx} + \sigma_{yy}) \text{ and } 0 \text{ of its centre and radius } \tau_0 = \sqrt{\frac{1}{4}(\sigma_{xx} - \sigma_{yy})^2 + \sigma_{xy}^2}$$

represent the normal and shear stresses acting on the surface elements which are perpendicular to the plane of flow. The other two circles inside this circle can be omitted in our further investigations.

There is a simple relationship between the physical and stress planes: the points on the circumference of the circle follow each other in the same sense of rotation as the corresponding normal vectors do in the x,y plane, and the central angle defined by two arbitrary points on the circumference of the circle is twice the angle between the corresponding two normal vectors.

Consider now the two sections of the maximum shear stresses where, according to Fig. 5—2(c), the shear and normal stresses are equal to τ_0 and σ_m, respectively. These two sections are perpendicular to each other and to the x,y plane as well, and intersect the principal axes I and III at 45°. One of the normal vectors of these sections, obtained from the principal direction I by a counter-clockwise rotation through 45°, defines the *first shear direction* and is denoted by α, while the direction of the other normal vector which is perpendicular to α is called the *second shear direction* and is denoted by β (see Fig. 5—2(b)). The angle θ of the first shear direction, measured from the x axis, is considered positive in the counter-clockwise direction. Introducing the above notations and using eq. (5—25), the following relationships can be obtained

$$\theta = \phi + 45°, \quad \tan 2\theta = -\frac{1}{\tan 2\varphi} = \frac{\sigma_{yy} - \sigma_{xx}}{\sigma_{xy}}.$$

Hence

$$\cos 2\theta = \frac{\sigma_{xy}}{\tau_0}, \quad \sin 2\theta = \frac{\sigma_{yy} - \sigma_{xx}}{\tau_0}. \tag{5—26}$$

At every point in the plastic domain of the body, the angles of the shear directions are defined by eq. (5—26). If curves are now drawn in the x,y plane such that at every point the tangent of these curves coincides with one of the shear directions then two families

of curves, called *shear lines*, will be obtained. Since the two shear directions are perpendicular to each other, the two families of shear lines form an *orthogonal set* and will be called α *lines* and β *lines*, respectively (Fig. 5—3(a)). These two lines can be considered curvilinear coordinates along which the corresponding shear and normal stresses have special values, namely

$$\left.\begin{aligned}\sigma_{\alpha\alpha}=\sigma_{\beta\beta}=\frac{1}{2}(\sigma_{\mathrm{I}}+\sigma_{\mathrm{III}})=\sigma_{\mathrm{m}},\\ \sigma_{\alpha\beta}=\frac{1}{2}(\sigma_{\mathrm{I}}-\sigma_{\mathrm{III}})=\tau_0,\end{aligned}\right\} \tag{5—27}$$

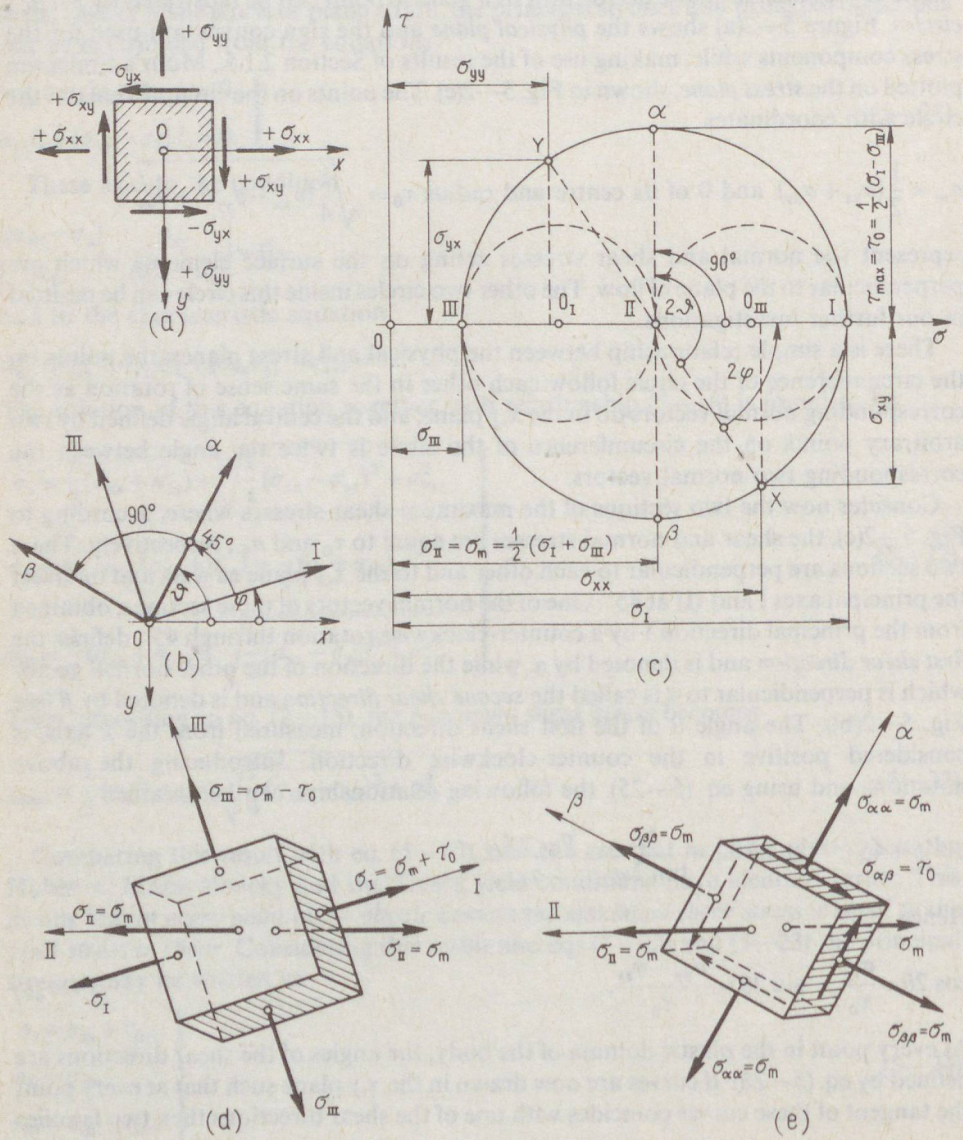


Fig. 5–2

as shown in Figs 5—2(b) and 5—3(e). This means that if the angle θ of the first shear direction were known, the state of stress at a point in the plastic domain could be uniquely defined by the mean normal stress σ_m. Therefore, in the following, we will express the stresses in terms of the variables θ and σ_m. This can be achieved by using eqs (5—17) and (5—26) and then the relationships

$$\sigma_{xx}=\sigma_m-\tau_0 \sin 2\theta,$$

$$\sigma_{yy}=\sigma_m+\tau_0 \cos 2\theta,$$

$$\sigma_{xy}=\tau_0 \cos 2\theta,$$

$$\sigma_{zz}=\sigma_m$$

can be obtained. Substituting these relationships into the equilibrium equations (5—20) results in

$$\left.\begin{aligned}\frac{\partial \sigma_m}{\partial x}-2\tau_0\left(\frac{\partial \theta}{\partial x}\cos\theta+\frac{\partial \theta}{\partial y}\sin 2\theta\right)=0,\\ \frac{\partial \sigma_m}{\partial y}+2\tau_0\left(\frac{\partial \theta}{\partial y}\cos 2\theta-\frac{\partial \vartheta}{\partial x}\sin 2\theta\right)=0,\end{aligned}\right\} \tag{5—28}$$

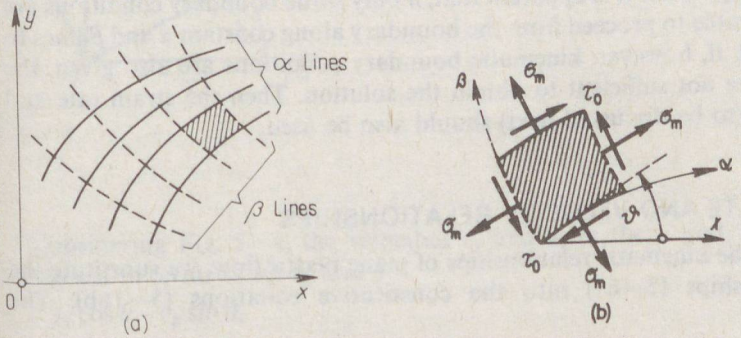


Fig. 5–3

or introducing the dimensionless magnitude of the mean normal stress

$$\omega=\frac{\sigma_m}{2\tau_0} \tag{5—29}$$

we obtain

$$\left.\begin{aligned}\frac{\partial \omega}{\partial x}-\cos 2\theta\frac{\partial \theta}{\partial x}-\sin 2\theta\frac{\partial \theta}{\partial y}=0,\\ \frac{\partial \omega}{\partial y}-\sin 2\theta\frac{\partial \theta}{\partial x}+\cos 2\theta\frac{\partial \theta}{\partial y}=0.\end{aligned}\right\} \tag{5—30}$$

To show the physical content of the above equations, let us choose the x and y axes at a given point to coincide with the α and β directions. Then,

$\theta=0$, $\dfrac{\partial}{\partial x}=\dfrac{\partial}{\partial \alpha}$, $\dfrac{\partial}{\partial y}=\dfrac{\partial}{\partial \beta}$ and eqs (5—30) results in

$$\left.\begin{aligned}\frac{\partial \omega}{\partial \alpha}-\frac{\partial \theta}{\partial \alpha}&=\frac{\partial}{\partial \alpha}(\omega-\theta)=0,\\ \frac{\partial \omega}{\partial \beta}+\frac{\partial \theta}{\partial \beta}&=\frac{\partial}{\partial \beta}(\omega+\theta)=0.\end{aligned}\right\} \qquad (5—31)$$

Hence

$$\left.\begin{aligned}(\omega-\theta)&=C_1 \text{ along an } \alpha \text{ line},\\ (\omega+\theta)&=C_2 \text{ along a } \beta \text{ line},\end{aligned}\right\} \qquad (5—32)$$

where C_1 and C_2 denote constants. This means that *along an α line $(\omega-\theta)$ is constant and along a β line $(\omega+\theta)$ is constant.*

The eqs (5—31) and (5—32) which contain the equilibrium equations (5—20) and the yield condition (5—19) as well are called *compatibility equations of stresses* (Hencky 1923). From these equations it is apparent that, if only static boundary conditions are prescribed, it is possible to proceed from the boundary along constant α and β lines to determine ω and θ. If, however, kinematic boundary conditions are also given, the above equations are not sufficient to obtain the solution. Then the strain rate and velocity equations (to be discussed next) should also be used.

5.2.3. STRAIN RATE AND VELOCITY RELATIONSHIPS

In order to derive the kinematic relationships of plane plastic flow, we substitute the kinematic relationships (2—67) into the constitutive equations (5—16b). The relationships

$$\left.\begin{aligned}\frac{\dfrac{\partial v_x}{\partial x}-\dfrac{\partial v_y}{\partial y}}{\dfrac{\partial v_x}{\partial y}+\dfrac{\partial v_y}{\partial x}}&=\frac{\sigma_{xx}-\sigma_{yy}}{\sigma_{xy}},\\ \frac{\partial v_x}{\partial x}+\frac{\partial v_y}{\partial y}&=0\end{aligned}\right\} \qquad (5—16c)$$

are then obtained. These two equations contain the kinematic and compatibility equations and, together with the equilibrium equations (5—20) and the yield condition (5—19), form the governing equations of plane plastic flow. In these five equations three stresses and two velocities are unknown. From a mathematical point of view, the problem is the simultaneous solution of these equations. To simplify this extremely

difficult problem let us discuss, as we did for the stress relationships, the geometrical content of eqs (5—16c).

Because in the constitutive equations (5—16) the strain rates are proportional to the stress deviators, the shear lines indicate not only the directions of the maximum shear stress but also the directions of maximum strain rate in shear. The strain rates corresponding to the directions normal to the shear lines are also equal to the mean strain rates and, therefore, considering eqs (5—16b) and (5—27), become

$$\dot{\varepsilon}_{\alpha\alpha}=\dot{\varepsilon}_{\beta\beta}=\dot{\varepsilon}_{\mathrm{m}}=\frac{1}{2}(\dot{\varepsilon}_{xx}+\dot{\varepsilon}_{yy})=0. \tag{5—33}$$

Consequently, *in the direction of shear lines the rate of extension vanishes and only pure shear deformations take place. That is why they are called shear lines. Hence, the shear lines can be considered as inextensional fibres.*

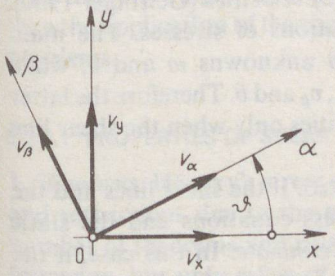


Fig. 5–4

Considering Fig. 5—4, the velocities v_x and v_y in the x and y directions can be expressed in terms of v_α, v_β and θ

$$\begin{aligned} v_x &= v_\alpha \cos\theta - v_\beta \sin\theta, \\ v_y &= v_\alpha \sin\theta + v_\beta \cos\theta. \end{aligned} \tag{5—34}$$

Choosing at a given point the x and y axes to coincide with the α and β directions, eq. (5—33) results in

$$\left.\begin{aligned} \dot{\varepsilon}_{\alpha\alpha} &= \frac{\partial v_x}{\partial x}=0, \\ \dot{\varepsilon}_{\beta\beta} &= \frac{\partial v_y}{\partial y}=0. \end{aligned}\right\} \tag{5—35}$$

Substituting relationships (5—34) and $\theta=0$ into these equations leads to

$$\left.\begin{aligned} \frac{\partial v_\alpha}{\partial x} - v_\beta \frac{\partial \theta}{\partial x} &= 0, \\ v_\alpha \frac{\partial \theta}{\partial y} + \frac{\partial v_\beta}{\partial y} &= 0. \end{aligned}\right\} \tag{5—36}$$

Also, since the directions of x and y are the same as the directions of α and β, respectively, these equations can be expressed in the form

$$\left.\begin{aligned} \frac{\partial v_\alpha}{\partial \alpha} - v_\beta \frac{\partial \theta}{\partial \alpha} = 0, \\ \frac{\partial v_\beta}{\partial \beta} + v_\alpha \frac{\partial \theta}{\partial \beta} = 0. \end{aligned}\right\} \tag{5—37}$$

If β is kept constant in the first equation and α in the second equation, i.e. if we proceed along the α and β line, respectively, we can write

$$\left.\begin{aligned} &dv_\alpha - v_\beta d\theta = 0 \text{ along an } \alpha \text{ line}, \\ &dv_\beta + v_\alpha d\theta = 0 \text{ along a } \beta \text{ line}. \end{aligned}\right\} \tag{5—38}$$

These equations contain the compatibility and incompressibility conditions of plastic strains and are called the *compatibility equations of velocities* (Geiringer 1930). These equations are similar to the compatibility equations of stresses. The main difference is that Hencky's stress equations relate two unknowns ω and θ, while Geiringer's velocity equations contain three unknowns v_α, v_β and θ. Therefore the latter equations can be used for the determination of the velocities only when the shear line field (i.e. θ) is already known.

The results previously obtained can now be summarized. If the shear lines and the stresses can be determined by the use of Hencky's stress equations and the static boundary conditions, then the problem is *statically determinate*. In this case, if the stresses and shear lines are known, the velocities can be independently computed from eqs (4—38) and from the kinematic boundary conditions. If, however, Hencky's stress equations and the static boundary conditions are insufficient to obtain the stress and shear line field, then the problem is *statically indeterminate*. Then, Hencky's stress equations and Geiringer's velocity equations must be solved simultaneously using both the static and kinematic boundary conditions. This is, in general, a very difficult problem and must usually be done by trial and error. First, a shear line field satisfying all stress conditions has to be constructed. Then, the velocities have to be computed from eq. (5—38) and a check has to be made to see if the kinematic boundary conditions are satisfied. It they are not, the shear line field has to be modified and the procedure has to be repeated until all the equations and boundary conditions are satisfied.

In terms of the static and kinematic principles of limit analysis, solutions which satisfy either only Hencky's stress equations and the static boundary conditions, or only Geiringer's velocity equations and the kinematic boundary conditions, provide only lower or upper bounds for the limit load necessary to produce unrestricted plastic flow.

5.2.4. SHEAR LINE THEORY

The partial differential equations (5—30) and (5—37) of plane plastic flow are *hyperbolic*. The solution of two hyperbolic partial differential equations with two variables can be reduced to the solution of two ordinary differential equations. One of

these differential equations defines a family of curves and the other describes the variation of the unknown functions along the characteristics. If the two differential equations are independent of each other the solution is relatively simple. In the general case, however, the two equations have to be solved simultaneously.

It can be shown (see e.g. Mendelson 1968; Kachanov 1971) that *the shear lines are identical with the characteristics of the hyperbolic partial differential equations* (5—30) *defining the problem*: therefore the theory based on the properties of characteristics is called *shear line theory*.

It has been shown that along the shear lines only pure shear deformations occur; therefore they are often called *slip lines*. We have to note that the variation in the shear deformations across the shear lines is, in general, continuous hence the shear lines are not identical with the discontinuity lines of velocitites discussed in Section 3.5. In particular cases, however, a shear line can, at the same time, be a discontinuity line in the velocity field.

In the following, first the geometric properties of shear lines will be discussed and then the application of the shear line theory will be illustrated by the solution of several problems.

5.2.4.1. PROPERTIES OF SHEAR LINE FIELDS

1. *Theorems.* Hencky's stress equations (5—32) express relatively simple relationships and restrictions due to the geometry of shear line fields and stresses, from which a number of theorems and rules can be derived. Some of these will be presented in the following, but only a few of them will be proved. More details can be found in the literature (see e.g. Prager, Hodge 1951; Geiringer 1953; Mendelson 1968; Kachanov 1971).

(a) *The angle formed by the tangents of two fixed shear lines of one family at their intersection points with a shear line of the other family is constant along the fixed shear lines under consideration.* This is called *Hencky's first theorem* and, using the notation of Fig. 5—5, means that $\theta_1 = \theta_2$. To prove this theorem we can write that, according to eqs (5—32), along the shear line α_1

$$\omega_A - \theta_A = \omega_D - \theta_D \tag{5—39}$$

and along the shear line β_2,

$$\omega_D + \theta_D = \omega_C + \theta_C. \tag{5—40}$$

From these two equations one can obtain

$$\omega_C - \omega_A = 2\theta_D - \theta_A - \theta_C. \tag{5—41}$$

Similarly, for the shear lines α_2 and β_1, the relation

$$\omega_C - \omega_A = -2\theta_B + \theta_A + \theta_C \tag{5—42}$$

can be derived. This relationship together with eq. (5—41) leads to

$$\theta_A - \theta_B = \theta_D - \theta_C. \tag{5—43}$$

Finally, since $\theta_A - \theta_B = \theta_1$ and $\theta_D - \theta_C = \theta_2$ eq. (5—43) proves the above theorem.

(b) *If one α line (β line) is straight between two β lines (α lines) then all α lines (β lines) are straight between these two β lines (α lines).*

To prove this theorem, assume that the part AD of the α_1 line between the lines β_1 and β_2 is straight (see Fig. 5—5). Then $\theta_D - \theta_A = 0$ and using eq. (5—43)

$$\theta_D - \theta_A = \theta_C - \theta_B = 0,$$

i.e. the part BC of the α_2 line is also a straight line. Following this argument it is apparent that all the α lines between the β_1 and β_2 lines must be straight.

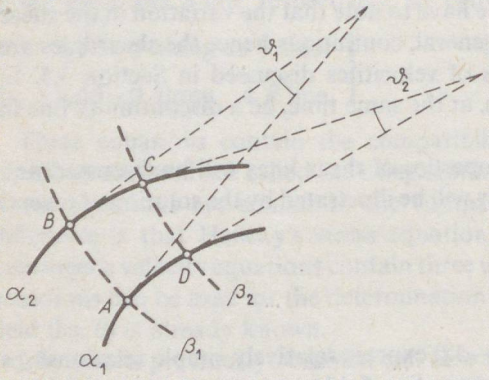


Fig. 5–5

(c) *If a family of shear lines contains a straight line, it consists entirely of straight lines.* Considering theorem (b), the truth of this theorem is obvious.

(d) *Along a straight shear line the state of stress is constant.* Let us assume e.g. that α_1 is a straight shear line. Then, according to Fig. 5—5, $\theta_D - \theta_A = 0$, which by the use of eq. (5—39) leads to $\omega_A = \omega_D$, i.e. $\sigma_m^A = \sigma_m^D$. This proves the above theorem.

2. *Simple shear line fields.* Next, shear line fields in which at least one of the families consists of straight lines will be discussed.

(a) When one family of shear lines consists of *parallel straight lines* then, because of the orthogonality, the other family also consists of parallel straight lines and the shear line field is a *quadratic net*, as shown in Fig. 5—6(a). In terms of theorem (d), one can state that *in the region where the shear lines form a quadratic net, the state of stress is constant, i.e.*

$$\sigma_{\alpha\alpha} = \sigma_{\beta\beta} = \sigma_m = \text{const}, \quad \sigma_{\alpha\beta} = \tau_0. \tag{5—44}$$

Since θ is constant throughout the quadratic net, eq. (5—38) shows that

$$\left.\begin{aligned} v_\alpha &= \text{constant along an } \alpha \text{ line}, \\ v_\beta &= \text{constant along a } \beta \text{ line}. \end{aligned}\right\} \tag{5—45}$$

Thus, the velocity field is defined as

$$v_\alpha = v_\alpha(\beta), \; v_\beta = v_\beta(\alpha). \tag{5—46}$$

This field may be obtained by the superposition of the following two fields

$$\left.\begin{aligned} v_\alpha &= v_\alpha(\beta), \quad v_\beta = 0; \\ v_\alpha &= 0, \quad v_\beta = v_\beta(\alpha). \end{aligned}\right\} \tag{5—46a}$$

The first field represents a shear flow in the α direction with the velocity profile $v_\alpha(\beta)$, while the second field represents a shear flow in the β direction with the velocity profile $v_\beta(\alpha)$.

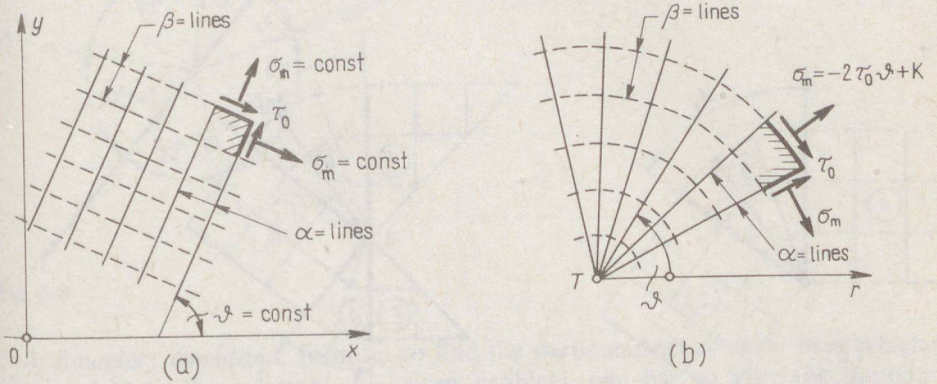


Fig. 5–6

Comparing eqs (5—44) and (5—46) one can see that Hencky's stress equations express more restrictions on the stress field than the Geiringer's velocity equations do on the velocity field.

(b) Consider a shear line field in which one family consists of straight lines originating from a point. Then, because of orthogonality, the lines of the other family are concentric circles and together with the straight lines form a *centred fan*, as shown in Fig. 5—6(b). In terms of theorem (d), σ_m is constant along the radial straight lines and therefore the second relationship of eq. (5—32) leads to

$$\sigma_{\alpha\alpha} = \sigma_{\beta\beta} = \sigma_m = -2\tau_0\theta + K, \tag{5—47}$$

where K denotes a constant which can be determined from the boundary conditions. The centre T of the fan is a singular point in the stress field. Hence we can state that *in a centred fan the mean normal stress is constant along the radii and varies linearly in terms of the direction of the radii.*

(c) Figure 5—7 shows two examples of the construction of more complex shear line fields by the use of rectangular nets and centred fans. In Fig. 5—7(a), two regions of constant state are interconnected by a centred fan in which the mean normal stress varies linearly along the circular shear lines. Due to the results of Section 3.5.1. no discontinuity can occur along the boundaries of the three regions, therefore eq. (5—47) provides the following relationship between the stresses acting in regions A and C

$$\sigma_m^C = \sigma_0^A + 2\tau_0\theta_B. \tag{5—48}$$

Similarly, the following relationships can be obtained in the case of the shear line field shown in Fig. 5—7(b):

$$\sigma_m^C = \sigma_m^A + 2\tau_0\theta_B,$$

$$\sigma_m^E = \sigma_m^C + 2\tau_0\theta_D = \sigma_m^A + 2\tau_0(\theta_B + \theta_D).$$

3. *Discontinuity lines.* It has already been mentioned that, though shear lines are not discontinuity lines, stress and velocity discontinuities may occur in plane plastic flow problems.

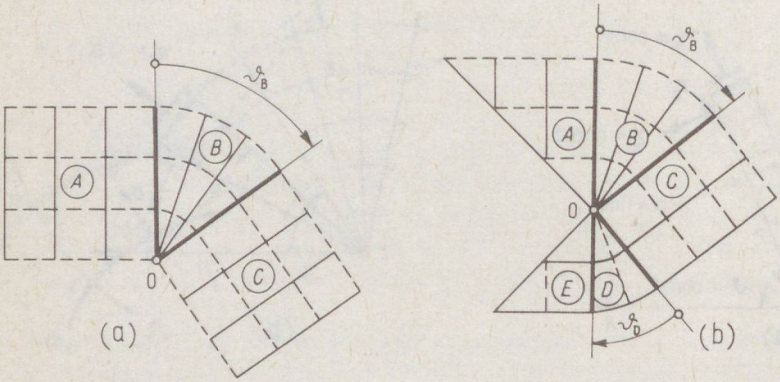


Fig. 5–7

In Section 3.5.1, we showed that across a *discontinuity line in the stress field* the exterior stresses must vary continuously and only the interior stresses can have discontinuities. On the basis of this result one can prove (see e.g. Prager, Hodge 1951; Kachanov 1971), that *across a discontinuity line of stress, the slope of the shear lines varies discontinuously* so *that the line of discontinuity bisects the angle formed by the shear lines of the adjacent fields*, as shown in Fig. 5—8. The line of stress discontinuity is considered as an elastic layer separating two plastic regions. This layer is inextensible but perfectly flexible.

Across the *discontinuity line in the velocity field* only the velocity component v_t, tangential to this line, may vary in a discontinuous manner. It can be proved (see e.g. Prager, Hodge 1951; Kachanov 1971) that *the discontinuity line in the velocity field is either a shear line or the envelope of shear lines, and along a discontinuity line the jump in the tangential component of the velocity is constant.* Similarly to the discontinuity lines in the stress field, a discontinuity line in the velocity field is considered to be the limiting case of a thin elastic layer producing a continuous transition from one velocity field to another, as shown in Fig. 5—9. The jump in the shear rate $\Delta\dot{\gamma}$ in this transition layer is obtained by dividing the difference $\Delta v_t = v'' - v'_t$ by the thickness of the layer. Since, according to the constitutive equations (5—16), the shear stress τ, acting along a line of discontinuity and the shear rate Δ_j have the same sense, it follows that $\tau(v''_t - v'_t)$ must be positive. The discontinuity line in the velocity field is, however, always a

shear line or the envelope of shear lines, therefore $\tau = \tau_0$. Hence, one can state that the power of the shear stresses on the discontinuous velocities is always positive and equal to $\tau_0 (v_t'' - v_t')$.

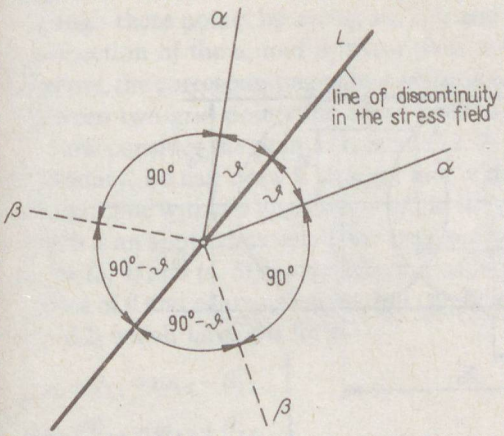


Fig. 5–8

4. *Boundary conditions.* In order to find the particular net of shear lines which is appropriate to the solution of a given problem, one has to take the boundary conditions into consideration. Let us assume that at the point A in the boundary of a plastic domain the static boundary condition is prescribed by the stress vector $p_i^{(n)}(\sigma_n \tau_n)$, as shown in Fig. 5—10. This vector is represented in the stress plane σ, τ by the point N. The Mohr's circle which describes the state of stress at the point A must pass through the point N and, at the same time, because of plastic flow, must be

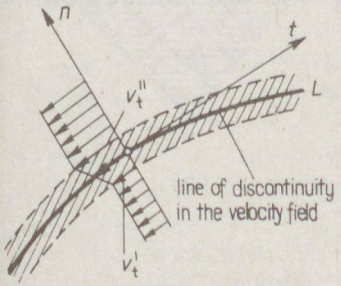


Fig. 5–9

tangential to the lines $\tau = \pm \tau_0$. According to Fig. 5—10, there are two circles which satisfy these conditions and therefore the state of stress at the points on the boundary cannot be uniquely determined from the static boundary conditions. This is due to the quadratic form of the yield condition. The solution leading to a smaller normal stress σ_m'' and a greater normal stress σ_m' are called the "weak" and "strong" solutions,

respectively. Although the local conditions do not uniquely determine the state of stress at a point on the boundary, considering the entire boundary it usually makes the selection of the appropriate solution possible. This will be shown by solving particular problems.

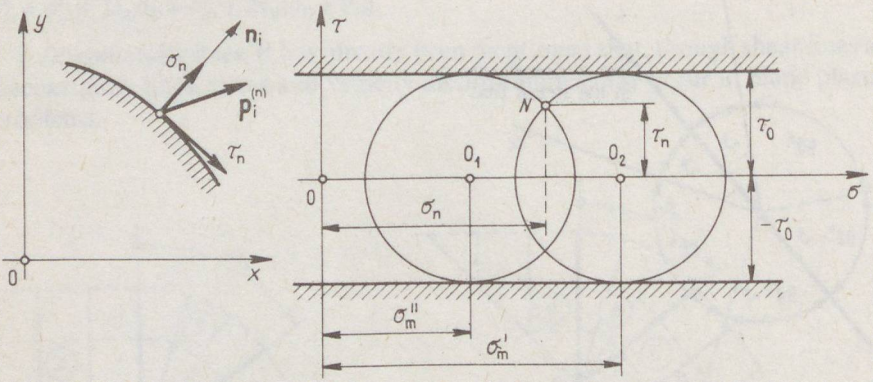


Fig. 5–10

5.2.4.2. NUMERICAL AND GEOMETRICAL SOLUTIONS

The analytical solution of the governing equations of plane plastic flow is not possible except in the case of some simple problems. In most cases, the application of numerical and graphical methods is necessary. In the following, a brief description of the main ideas of these methods will be presented. A more detailed discussion of this problem can be found in the literature (see e.g. Prager, Hodge 1951; Mendelson 1968; Kachanov 1971).

The three basic types of boundary value problems of plane plastic flow are shown in Fig. 5—11 and 5—13.

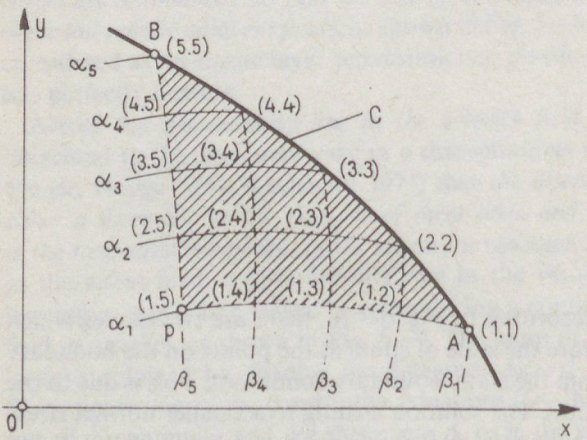


Fig. 5–11

(a) Figure 5—11 shows *Cauchy's boundary value problem* where between the points A and B of the boundary C the values of ω and θ are given and the boundary does not coincide with a shear line. In order to construct the shear line field inside the plastic domain, we choose a number of points on the line C and denote the shear lines passing through these points by $\alpha_1, \alpha_2, \alpha_3, \ldots$ and $\beta_1, \beta_2, \beta_3, \ldots$, respectively. The points of intersection of the α_i and β_j shear lines will be designated by (i, j) and, in a similar manner, the corresponding values of θ and ω will have the subscript ij. We assume that between two grid points the shear lines can be replaced by straight lines.

Now consider the points (1, 1) and (2, 2) on the curve C. Since θ is given along the boundary, we can draw a straight line with angle θ_{11} at the point (1, 1) and another straight line with the angle $\theta_{22}+\pi/2$ at the point (2, 2). The two lines intersect at (1, 2), which is an approximation to the true intersection point of the α and β lines. The points (2, 3), (3, 4) and (4, 5) can be determined in the same way. At these interior points, the values of θ and ω are unknown but can be calculated by applying Hencky's equations (5—32) which have the form

$$\left.\begin{aligned}\omega_{11}-\theta_{11}&=\omega_{12}-\theta_{12},\\ \omega_{22}+\theta_{22}&=\omega_{12}+\theta_{12}.\end{aligned}\right\} \qquad (5—49)$$

From these two equations, ω_{12} and θ_{12} can be determined and in the same way ω_{23}, $\theta_{23}, \omega_{34}, \theta_{34}, \ldots$ can also be found. Repeating this procedure, the shear line field and the stresses in the entire triangular region defined by the points A, B and P can be calculated, but the solution cannot be carried beyond this region. Hence, the region ABP is called the *region of influence* of the boundary AB.

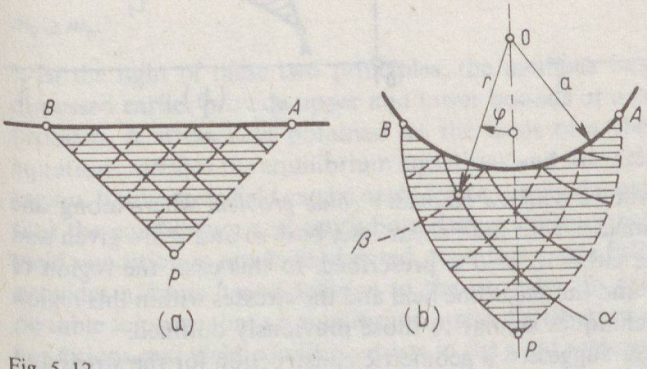


Fig. 5–12

As a special case, consider a boundary which is free of external stresses. Then, at every point on this *unloaded boundary*, the normal vectors denote principal directions and therefore the shear lines must intersect with the boundary at every point at an angle of 45°. It is then easy to prove that if the boundary is a *straight line* then the shear line field of the corresponding region of influence is a quadratic net, as it is shown in Fig. 5—12(a). It can also be proved (see e.g. Kachanov 1971) that if the unloaded boundary is a *circular arc* the shear line field of the region of influence is then formed by *logarithmic spirals*, as shown in Fig. 5—12(b).

(b) Figure 5—13(a) shows the *Riemann's boundary value problem*, when along two boundary lines C_1 and C_2 which coincide with one of the α and β shear lines, respectively, ω and θ are given. Then, from the points (0.1) and (1.0), part of the shear lines α and β can be drawn and by using eq. (5—32) the values of ω_{11} and θ_{11} belonging to the intersection point (1.1) can be obtained from the following equations

$$\left.\begin{aligned}\omega_{10}-\theta_{10}&=\omega_{11}-\theta_{11},\\ \omega_{01}+\theta_{01}&=\omega_{11}+\theta_{11}.\end{aligned}\right\} \qquad (5—50)$$

Assuming that ω and θ are given between the points A and B and A and D of the boundary, we may proceed in this manner and determine the shear line field and the stresses within the quadrilateral $ABPD$. The solution can not be extended, however, beyond this region therefore the quadrilateral $ABPD$ is the region of influence of the boundary value problem under consideration.

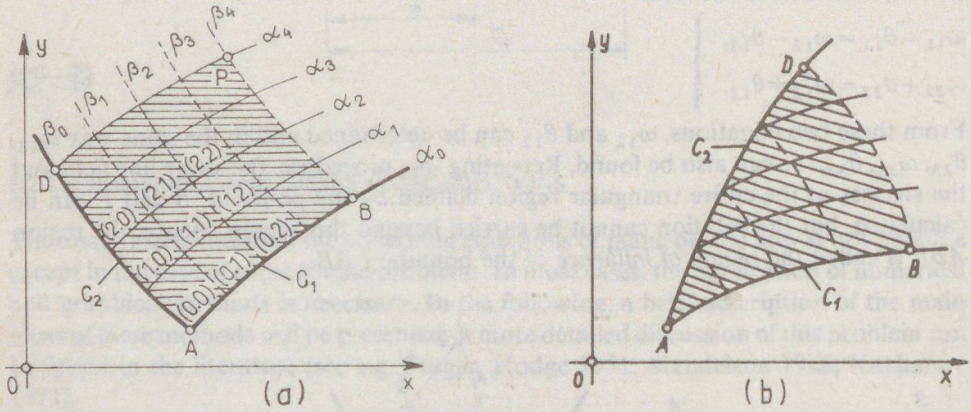


Fig. 5–13

(c) Finally, Fig. 5—13(b) shows a *mixed boundary value problem* where along one boundary line C_1, which coincides with an α shear line, both ω and θ are given and along another boundary line either ω or θ is prescribed. In this case, the region of influence is the triangle ABD and the shear line field and the stresses within this region can be obtained by using techniques similar to those previously outlined.

It is to be noted that Prager suggested a geometric construction for the stress and velocity fields which is based on the relationships derived between the properties of Mohr's circle and those of the shear lines and velocities (Prager 1959). This method is often useful and leads to a good insight into the principles of shear line theory.

5.2.4.3. APPROXIMATE SOLUTIONS

A very frequent and important problem in engineering practice is to determine the magnitude of a load necessary to produce unrestricted plastic flow. In structural problems this plastic limit load gives the load carrying capacity of a structure, and in

the case of metal forming processes makes it possible to predict the work necessary to produce certain prescribed plastic deformations. The static and kinematic principles of limit analysis can be very efficiently used to determine the approximate or exact value of the plastic limit load. In the following, we will briefly outline these principles as they are applied to problems of plane plastic flow.

The *static principle* of limit analysis states that any *statically admissible stable load multiplier* m_s, associated with a stress field σ_{ij}^s which satisfies the static boundary conditions and the equilibrium and yield conditions throughout the entire body, is a *lower bound for the plastic limit load multiplier* m_p, i.e.

$$m_s \leq m_p.$$

According to the *kinematic principle* of limit analysis, any *kinematically admissible unstable load multiplier* m_k, associated with a plastic strain rate and velocity field $\dot{\varepsilon}_{ij}^k$, v_i^k which satisfies the kinematic boundary conditions and the compatibility conditions throughout the entire body, and calculated from the relationship*

$$\left.\begin{aligned} m_k &= \frac{\int_V \sigma_{ij}^k \dot{\varepsilon}_{ij}^k \mathrm{d}V + \sum_{d=1}^{h} \tau_0 (v_t'' - v_t') \mathrm{d}S}{\int_{S_q} q_{i0} v_i^k \mathrm{d}S}, \\ \int_{S_q} q_{i0} v_i^k \mathrm{d}S &> 0 \end{aligned}\right\} \qquad (5\text{—}51)$$

is an *upper bound for the plastic limit load multiplier* m_p, i.e.

$$m_k \geq m_p.$$

In the light of these two principles, the methods based on the shear line theory discussed earlier provide upper and lower bounds or a complete (exact) solution to a problem. A stress field obtained on the basis of a shear line field from Hencky's equations satisfies the equilibrium equations and the yield condition inside the plastic region. If this stress field can be extended to the rigid regions of the body, and provided that the equilibrium and static boundary conditions there are also satisfied and the yield condition is nowhere violated, then this stress field is statically admissible and provides a *lower bound solution* to the problem. In many cases, however, it is not possible to prove that an equilibrium stress distribution satisfying the static boundary conditions and yield condition exists in the rigid regions. Then the solution based on the shear line theory leads only to an *approximate solution.*

A velocity field obtained on the basis of a shear line field from Geiringer's equations satisfies the compatibility conditions inside the plastic region. If this velocity field can be extended to the rigid regions of the body, and provided that the kinematic boundary conditions are also satisfied then this velocity field is kinematically admissible and provides an *upper bound solution* to the problem. The extension of the velocity field to the rigid regions is very simple, since they undergo only rigid body motion, and

* In the formula for m_k, the summation term expresses the power of the shear stresses acting along the lines $d = 1,2,\ldots h$ of velocity discontinuity.

therefore in most cases it is easy to check whether the kinematic boundary conditions are satisfied along the boundaries of the rigid regions. If this condition is not satisfied, the kinematic solution based on a shear line field provides only an *approximate solution.*

Finally, the shear line theory can provide a *complete* (exact) *solution* to a problem. In this case, one has to prove that both the stress field and the velocity field associated with a shear line field can be extended to the rigid regions of the body, and that all the necessary conditions are satisfied in these regions.

5.2.5. APPLICATIONS

The application of the shear line theory to different engineering problems has often been described in the literature (see e.g. Hoffman, Sachs 1953; Johnson, Mellor 1962; Lippmann, Mahrenholz 1977; Ismar, Mahrenholz 1979; Lippmann 1981). To illustrate the application, solutions to several problems will be shown next. It will be assumed for all the problems that the body under consideration is in a state of plane strain.

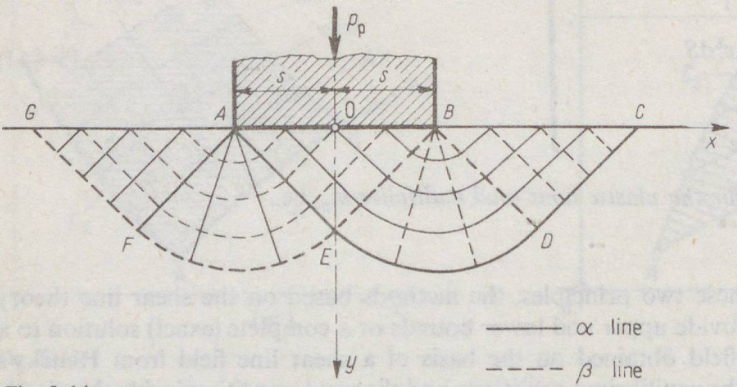


Fig. 5–14

(1) *Indentation by a punch.* Let us study the indentation of a semi-infinite rigid–plastic body by a flat rigid punch in the form of an infinite strip, as shown in Fig. 5—14. We will only consider a layer of the body and of the punch both with unit thickness in the z direction and assume that the surfaces of the body and the punch are perfectly smooth, so that there is no friction between them. On increasing the load acting on the punch, plastic regions begin to form at the points A and B, but the rigidity of the material between these local plastic regions rules out any plastic deformation in the plastic regions. Only when a plastic region extends below the entire bottom of the punch does indentation become possible. In the following, we will study the state of *incipient state of plastic flow* and determine the corresponding stress and velocity fields and the plastic limit load p_p. As the indentation proceeds, the material is pushed upwards at the sides of the punch and an unsteady plastic flow occurs, for which the boundary conditions at the deformed surface must be satisfied. This is a very difficult problem, and therefore our investigation will be restricted to the state of incipient plastic flow. We will first construct the shear line field in the neighbourhood of the punch, and determine the

stress field which satisfies the static boundary conditions. This solution will provide the magnitude of the external load. We will then prove that, on the basis of the assumed shear line field, a velocity field can be obtained which satisfies the compatibility and the kinematic boundary conditions. In this manner, we will establish the *complete solution* to the problem.

To find the shear line and stress fields in the neighbourhood of the punch, we start from the surface of the semi-infinite body. Since at every point of this surface the shear stress vanishes, the x and y axes are principal directions and the shear lines must intersect with the x axis at 45°. Then, considering the results obtained in connection with Fig. 5—12(a), we can predict that in the regions of influence of the boundaries CA, AB and BC the shear lines form quadratic nets, and we may assume that the transition between these triangular regions is a centred fan, as shown in Fig. 5—14.

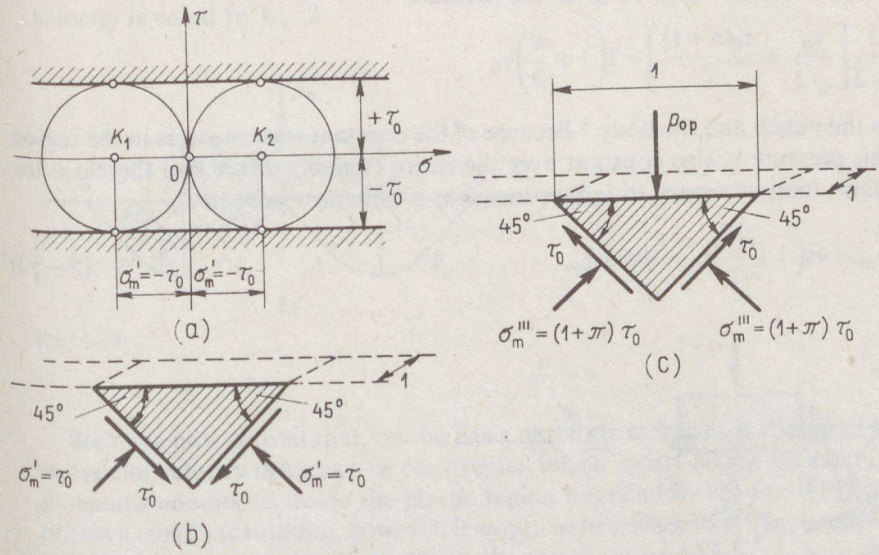


Fig. 5–15

The state of stress at an arbitrary point in the free surface AG is shown in Figs 5—15(a) and 5—15(b). Since it is very likely that a compressive stress will arise in the horizontal direction, we can try to solve the problem by using the "weak" solution $\sigma'_m = -\tau_0$. Inside the entire triangular domain AGF the normal stress is constant but, according to eq. (5—47) in the centred fan varies linearly with the angle θ, i.e.

$$\sigma''_m = -2\tau_0\theta + K.$$

Since across the line AF the stresses must vary continuously,* we can write

$$[\sigma''_m]_{\theta=0} = K = \sigma'_m = -\tau_0.$$

* According to Section 5.2.4.1. the shear lines have a discontinuous change in their slopes at a line of discontinuity in stresses. Since along the line AF the slope of the shear lines has no discontinuity, the variation in stresses must also be continuous.

Hence

$$\sigma''_m = -\tau_0(2\theta + 1)$$

and the normal stress acting along the line AE becomes

$$[\sigma''_m]_{\theta=\frac{\pi}{2}} = -\tau_0(\pi + 1).$$

This stress is constant inside the region ABE and therefore at points on the line AB we find

$$\sigma''_m = [\sigma''_m]_{\theta=\frac{\pi}{2}} = -\tau_0(\pi + 1).$$

Figure 5—15(c) shows the state of stress at an arbitrary point along the boundary AB. The equilibrium equation gives the pressure

$$p_{0p} = \frac{2}{\sqrt{2}}\left[\frac{\tau_0}{\sqrt{2}} + \frac{\tau_0(\pi+1)}{2}\right] = 2\left(1 + \frac{\pi}{2}\right)\tau_0$$

between the punch and the body.* Because of the constant state of stress in the region ABE, this pressure is also constant over the entire contact surface and therefore the plastic limit load necessary to induce incipient plastic flow becomes

$$p_p = 2sp_{0p} = 4s\left(1 + \frac{\pi}{2}\right)\tau_0 = 10.28s\tau_0. \qquad (5—52)$$

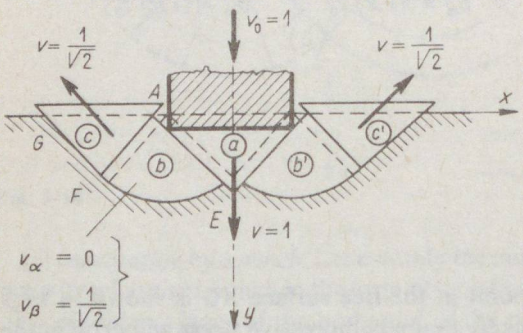


Fig. 5–16

Next, we will determine the velocity field associated with the assumed shear line field. Let us suppose that the plastic region a, together with the punch moves as a rigid body in the vertical direction with velocity $v = 1$, as shown in Fig. 5—16. Then, in accordance with eq. (5—48), we can assume that at every point in region b the velocity is constant and perpendicular to the radii, i.e. $v_\alpha = 0$ and $v_\beta = C$. Finally, the region c slips along the

* It is easy to show that using the "strong" solution $\sigma_m = \tau_0$ along the boundary AG leads to a smaller value for the pressure ($p_{0p} = \pi\tau_0$). Since the static solution described above gives a lower bound or the exact value of the plastic limit load, it is obvious that the "weak" solution provides a higher lower bound or the correct solution to the problem.

line GF as a rigid body with velocity $v = C$. The material below the line EFG remains at rest but this does not mean that it is not in a plastic state.

The velocity field described above satisfies Geiringer's equations and the kinematic boundary condition on the contact surface of the punch, but contains discontinuities along the lines AE, AF, EF and FG. According to the results of Section 5.2.4.1., the discontinuity line must coincide with a shear line and only the tangential velocity component can vary discontinuously across it. The first requirement is satisfied for all the discontinuity lines under consideration. Also, if we choose $C = 1/\sqrt{2}$ in the above relationships, then all along the lines AE and AF the normal component of the velocity will vary continuously and the jump in the tangential component of the velocity will be $1/\sqrt{2}$. Finally, along the line EFG $v_\alpha = 0$ and thus the continuity of the normal component of velocity is also satisfied here. The jump in the tangential component of velocity is equal to $1/\sqrt{2}$.

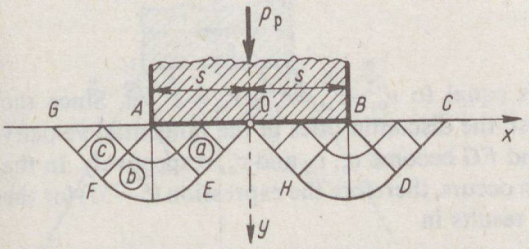


Fig. 5–17

We have now proved that, on the basis of the shear line field shown in Fig. 5—14, stress and velocity fields can be constructed which satisfy all the necessary static and kinematic conditions inside the plastic region bounded by the line EFG. In order to obtain a complete solution, however, it would be necessary to prove that the stress field outside this plastic region also satisfies the equilibrium and boundary conditions and nowhere violates the yield condition. The extension of the velocity field outside the plastic region is not necessary, because the material below the line EFG remains at rest. The exact proof of the fulfilment of the conditions due to the stress field, however, would need the complete elasto-plastic solution to the problem, which is extremely difficult. In the case presented above, however, it is very likely that the proof would be successful, and therefore the results derived above can be considered the complete (exact) solution to the problem.

The solution discussed above is due to Prandtl (1920). An alternative solution given by Hill (1949) is based on the shear line field shown in Fig. 5—17. For the stress field of the plastic regions and for the plastic limit load this shear line field provides the same solution as was obtained by *Prandtl*, but the velocity field is different. It is worth noting that the solutions given by *Prandtl* and *Hill* are only limit cases, between which an infinite number of solutions can be obtained. This is due to the fact that the solutions to problems of plasticity are very often not unique. In order to obtain a unique solution, a complete elasto-plastic incremental analysis should be conducted.

To illustrate the *upper bound solution* to the indentation problem presented above, consider the shear line field shown in Fig. 5—18. In accordance with eq. (5—46) we assume that the plastic regions *a*, *b* and *c* slip along the lines *OEFG* as rigid bodies with velocities v_a, v_b and v_c, respectively. If the vertical velocity of the punch is $v_0 = 1$, then $v_a = v_b = v_c = 2/\sqrt{3}$ and the jump in the tangential components of the velocities along

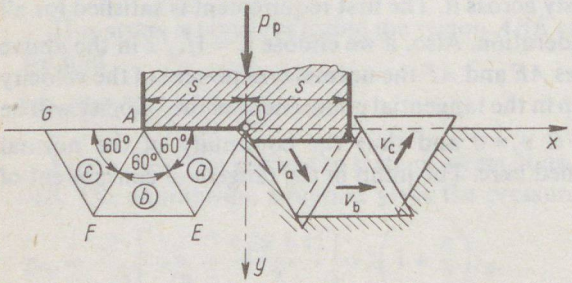


Fig. 5–18

the discontinuity lines *AE* and *AF* is equal to $v''_{bt} - v'_{at} = v''_{ct} - v'_{bt} = 2/\sqrt{3}$. Since the material below the line *OEFG* is at rest, the discontinuities in the tangential velocity components along the lines *OE*, *EF* and *FG* become v_a, v_b and v_c, respectively. In the plastic regions themself no deformation occurs, therefore the expression (5—51) for the *kinematically admissible unstable load* results in

$$p_k = 2s\tau_0[(v''_{bt} - v'_{at}) + (v''_{ct} - v'_{bt}) + v_a + v_b + v_c] = 11.56s\tau_0. \qquad (5—53)$$

This *upper bound* is 12.5% higher than the plastic limit load given by eq. (5—52).

Figure 5—19 shows a couple of problems, with their solutions readily obtainable by making use of the results derived above. In the Figure, the full lines and the dashed lines correspond to the shear line fields suggested by Prandtl and Hill, respectively. Following the derivation of the plastic limit load for the indentation problem, we can see that the term $\pi/2$ in eq. (5—52) corresponds to the right angle *FAE* of the fan shown in Fig. 5—14, and that in cases of Fig. 5—19 this angle is equal to $(\gamma - \pi/2)$, but apart from this difference, the solutions to these latter problems would need exactly the same procedure. Therefore the expression for their plastic limit load could be obtained merely by replacing $\frac{\pi}{2}$ by $(\gamma - \pi/2)$ in eq. (5—52):

$$p_p = 4s\left(1 + \gamma - \frac{\pi}{2}\right)\tau_0. \qquad (5—54)$$

This result is valid, however, only if $\gamma < \pi/2$. If $\gamma \geq \pi/2$, the centred fan degenerates to a straight line. It will be shown in connection with another problem that along this line the stresses are discontinuous, and therefore the solution to this problem must be derived in a different manner.

(2) *Wedge under unilateral pressure.* Figure 5—20 shows an obtuse and also a narrow wedge subjected to a uniformly distributed pressure p_0 over the portion *AB* of one flank.

The shear line field for the *obtuse wedge* ($\gamma \geq \pi/2$) is of the same nature as that of the region $ABCDE$ in Fig. 5—19(a). In addition, we found a uniformly distributed pressure under the punch and therefore the plastic limit pressure of the obtuse wedge can be obtained simply by dividing the plastic limit load given by eq. (5—54) by $2s$

$$p_{0p} = 2\left(1 + \gamma - \frac{\pi}{2}\right)\tau_0, \quad \gamma \geq \frac{\pi}{2}. \tag{5—55}$$

In the case of a *narrow wedge* $\left(\gamma < \frac{\pi}{2}\right)$ the centred fan degenerates to a line AD along which there is a jump in the slope of the shear lines, consequently the stresses also vary discontinuously across this line (Fig. 5—20(b)). Starting at the unloaded side of the

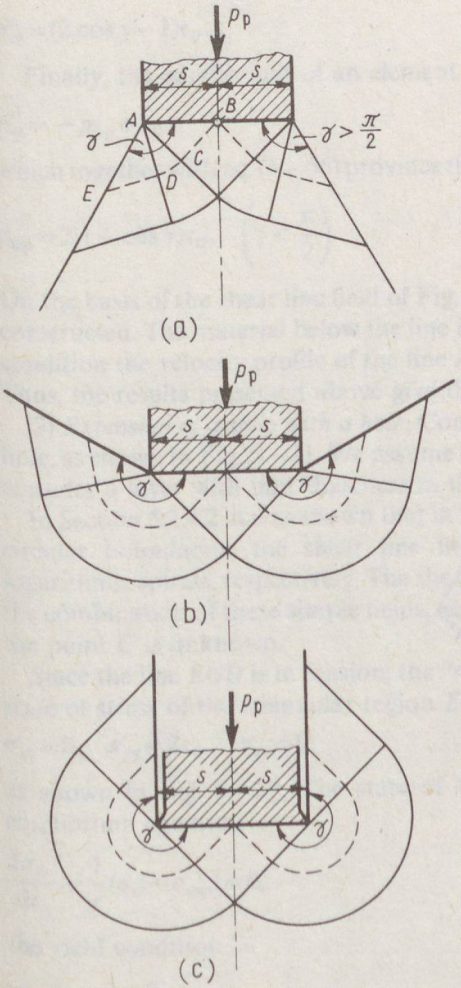


Fig. 5–19

wedge, it is obvious that the line AC is in compression, and therefore, the "weak" solution $\sigma'_m = -\tau_0$ leads to the correct solution to the problem. This normal stress σ'_m is constant in the region ACD.

Let us now consider a deltoid element in the neighbourhood of the discontinuity line.

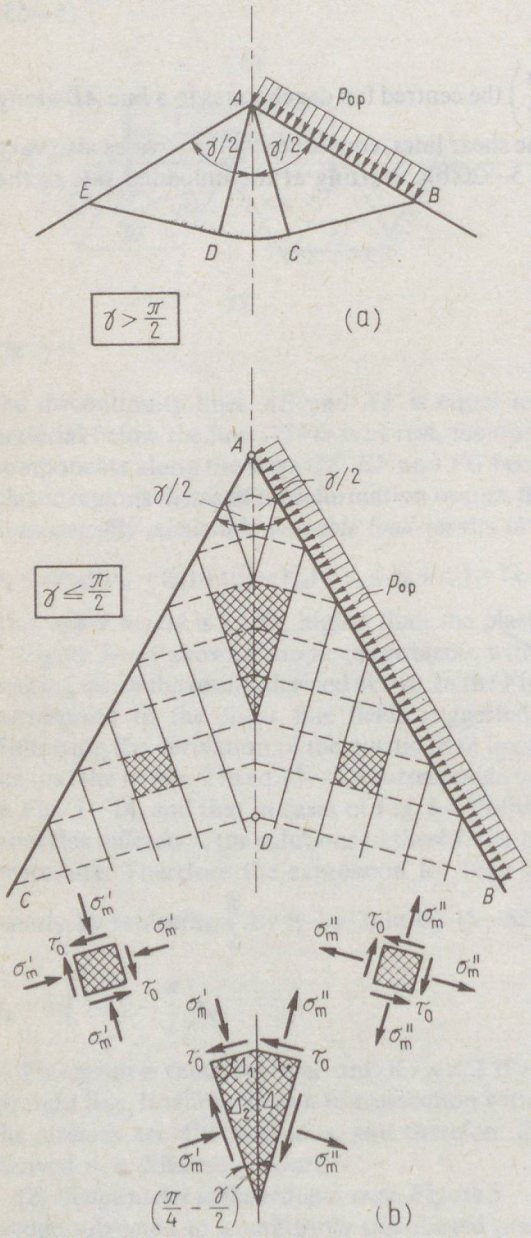


Fig. 5–20

The force equilibrium equation is found to be

$$\left[(\sigma'_m+\sigma''_m)\sin\left(\frac{\pi}{4}-\frac{\gamma}{2}\right)-2\tau_0\cos\left(\frac{\pi}{4}-\frac{\gamma}{2}\right)\right]\Delta_1+$$

$$+\left[(\sigma'_m+\sigma''_m)\cos\left(\frac{\pi}{4}-\frac{\gamma}{2}\right)-2\tau_0\sin\left(\frac{\pi}{4}-\frac{\gamma}{2}\right)\right]\Delta_2=0,$$

where

$$\Delta_1=\Delta\sin\left(\frac{\pi}{4}-\frac{\gamma}{2}\right) \quad \text{and} \quad \Delta_2=\Delta\cos\left(\frac{\pi}{4}-\frac{\gamma}{2}\right).$$

Substituting these relationships into the equilibrium equation gives the normal stress in the region *ABD*

$$\sigma''_m=(2\cos\gamma-1)\tau_0. \tag{5—56}$$

Finally, the equilibrium of an element of the line *AB* results in

$$\sigma''_m=-p_{0p}+\tau_0,$$

which together with eq. (5—56) provides the plastic limit pressure for the narrow wedge

$$p_{0p}=2(1-\cos\gamma)\tau_0, \quad \left(\gamma<\frac{\pi}{2}\right). \tag{5—57}$$

On the basis of the shear line field of Fig. 5—20(b), an associated velocity field can be constructed. The material below the line *BDC* remains at rest and from this boundary condition the velocity profile of the line *AD* can be derived (see e.g. Kachanov 1971). Thus, the results presented above give the complete solution to the problem.

(3) *Extension of a strip with a hole.* Consider the extension of a strip with a circular hole, as shown in Fig. 5—21. We assume that the strip is in a state of plane strain, and consider a layer with unit thickness in the direction z.

In Section 5.2.4.2. it was shown that in the neighbourhood of unloaded straight and circular boundaries, the shear line field consists of parallel straight lines and logarithmic spirals, respectively. The shear line field of the strip may be constructed by the combination of these simple fields, as shown in Fig. 5—21(a). Here the position of the point C is unknown.

Since the line *EGD* is in tension, the "strong" solution $\sigma'_m=\tau_0$ will be used, and the state of stress of the triangular region *ECD* is then equal to

$$\sigma'_{xx}=0, \quad \sigma'_{yy}=2\tau_0, \quad \sigma'_{xy}=0, \tag{5—58}$$

as shown in Fig. 5—22. The state of stress in the region *ACB* is defined by the equilibrium equation

$$\frac{d\sigma_{rr}}{dr}+\frac{1}{r}(\sigma_{rr}-\sigma_{\varphi\varphi})=0,$$

the yield condition

$$(\sigma_{\varphi\varphi}-\sigma_{rr})=2\tau_0$$

and the boundary condition

$$\sigma_{rr}(a)=0.$$

The solution to this problem leads to

$$\left.\begin{aligned}\sigma_{rr}&=2\tau_0\ln\frac{r}{a},\\ \sigma_{\varphi\varphi}&=2\tau_0\left(\ln\frac{r}{a}+1\right),\\ \sigma_{r\varphi}&=0.\end{aligned}\right\} \tag{5—59}$$

The stress components acting along the line CF are then found to be

$$\left.\begin{aligned}\sigma''_{xx}&=\sigma_{rr}=2\tau_0\ln\frac{r}{a},\\ \sigma''_{yy}&=\sigma_{\varphi\varphi}=2\tau_0\left(\ln\frac{r}{a}+1\right),\\ \sigma''_{xy}&=0.\end{aligned}\right\} \tag{5—60}$$

Finally, the integration of the normal stresses σ'_{yy} and σ''_{yy} provides the plastic limit load per unit thickness of the strip

$$p_p=2\left[\int_a^{r_c}\sigma''_{yy}dr+\int_{r_c}^{b}\sigma'_{yy}dr\right]=4\tau_0(b-a)+4\tau_0\int_a^{r_c}\ln\frac{r}{a}\,dr. \tag{5—61}$$

In this expression the upper limit r_c of integration is unknown and its calculation needs further considerations.

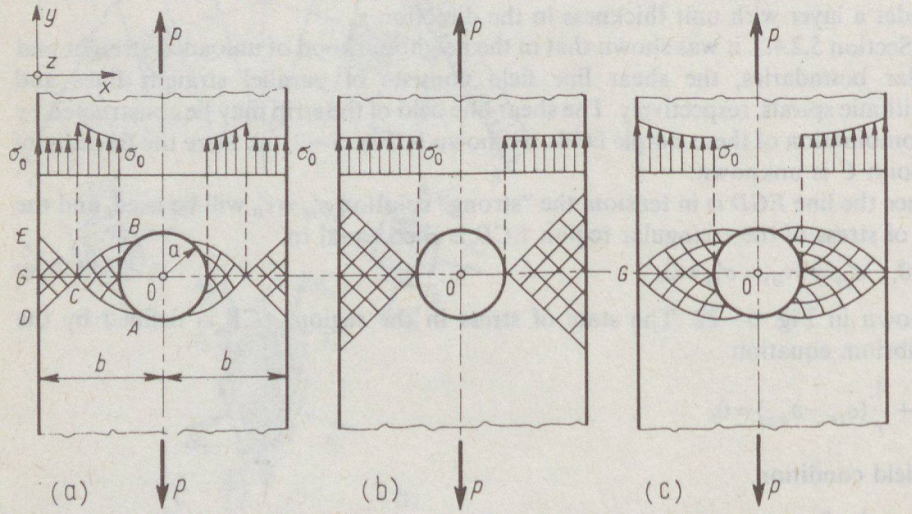


Fig. 5–21

Considering the velocity field in the plastic limit state, the rigid parts of the body move up and down, respectively, with constant velocity. From this the continuous normal and discontinuous tangential components of the velocities along the lines BCE and ACD can easily be determined. Then, the velocity fields in the plastic regions can also be uniquely obtained by solving the initial characteristic problem discussed in Section 5.2.4.2. Hence, the shear line field shown in Fig. 5—21(a) satisfies all the kinematic conditions, independently of the magnitude of r_c. This means that

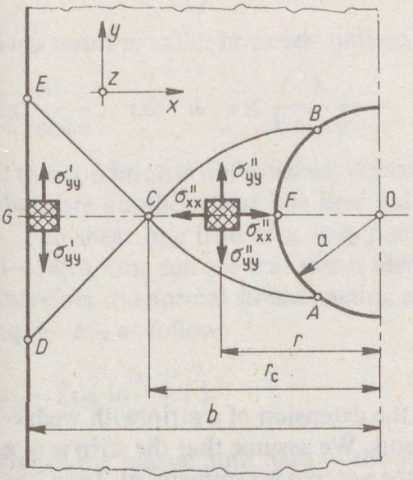


Fig. 5–22

depending on the choice of the point C, there is an infinite number of solutions and to each solution corresponds a particular plastic limit load. Since in eq. (5—61) the integrand is non-negative and is a monotonically increasing function of r_c, for $r_c = a$ the load $p_p = 4(b-a)\tau_0$ is a minimum and for $r_c = b$ it is a maximum. The corresponding shear line fields are shown in Figs 5—21(b) and 5—21(c). All the solutions between these limiting cases are kinematically admissible, and provide an upper bound solution. It is obvious that the best upper bound corresponds to the minimum value of the load, i.e. when $r_c = a$. That gives

$$p_p = 4(b-a)\tau_0, \tag{5—62}$$

or, making use of the relationship $\sigma_0 = 2\tau_0$,

$$p_p = 2(b-a)\sigma_0. \tag{5—63}$$

The corresponding shear line field is shown in Fig. 5—21(b). Everywhere along the horizontal line across the hole the normal stress is equal to σ_0, which is identical to the elementary strength of materials solution. It is easy to show that this stress distribution can be extended to the entire body without violating the yield conditions and static boundary conditions. This extended stress field is shown in Fig. 5—23, where the shaded region is free of stresses and in the remaining part of the body we have pure

tension, i.e. $\sigma_{xx}=\sigma_0$ and $\sigma_{xx}=\sigma_{xy}=0$. The external load corresponding to this stress field is obviously identical to the load given by eq. (5—63); thus the results presented above represent the complete solution to the problem.

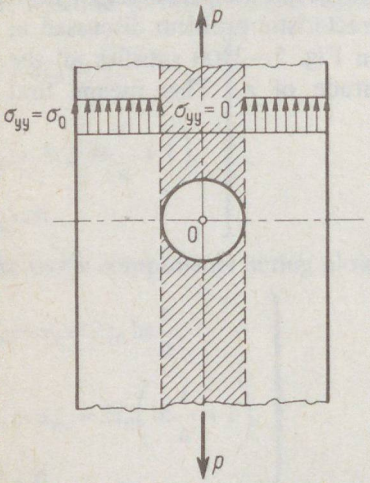


Fig. 5–23

(4) *Extension of a strip with notches.* Consider the extension of a strip with wedge-shaped notches and with notches with circular roots. We assume that the strip is in a state of plane strain and that the arrangement of the notches is symmetrical. Then, the study of one side of the strip shown in Fig. 5—24 is sufficient. As will be shown the

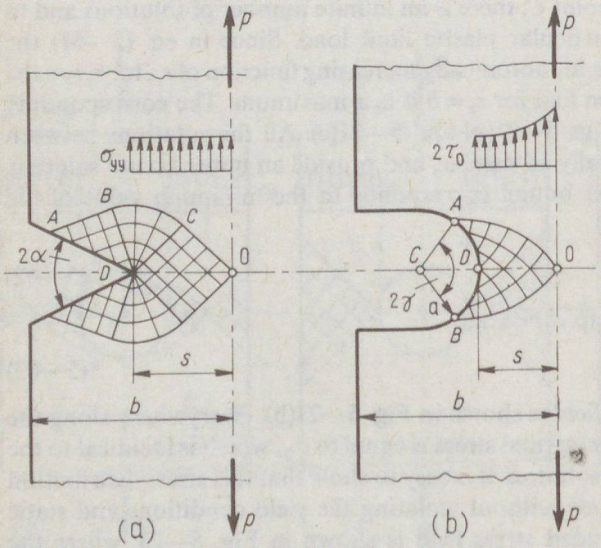


Fig. 5–24

plastic limit load for both cases can easily be derived using the results derived previously.

The shear line field in the *strip with wedge-shaped notches* is shown in Fig. 5—24a. One can see that the patterns of the shear lines in the region *ABCOD* are exactly the same as in the problem shown in Fig. 5—19(a). Consequently, replacing the angle γ by $(\pi-\alpha)$, eq. (5—54) provides the plastic limit load of the strip with wedge-shaped notches

$$p_p=4s\left(1+\frac{\pi}{2}-\alpha\right)\tau_0=2s\left(1+\frac{\pi}{2}-\alpha\right)\sigma_0. \tag{5—64}$$

This result is valid, however, only in the case where

$$s\leq\frac{b-s}{\cos\alpha}, \quad \text{i.e. if} \quad s\leq\frac{b}{1+\cos\alpha}.$$

If this condition is not satisfied, the shear line field of Fig. 5—24(a) cannot develop and therefore another shear line field has to be considered to solve the problem.

The shear line field of a *strip having notches with circular roots* is shown in Fig. 5—24(b). One can see that this is identical to the shear line field of Fig. 5—21(c), and therefore the normal stresses acting at points on the line *OD* can be determined from eq.(5—60) as follows

$$\sigma_{yy}=2\tau_0\left(\ln\frac{r}{a}+1\right).$$

Hence the plastic limit load of the strip becomes

$$p_p=4\tau_0\int_a^{a+s}\left(\ln\frac{r}{a}+1\right)dr=4s\left(1+\frac{a}{s}\right)\left(1+\frac{s}{a}\right)\tau_0. \tag{5—65}$$

The shear line field shown in Fig. 5—24(b) can develop only if the angle γ is less than $\frac{\pi}{2}$. Since γ and s are related by the equation $\gamma=\ln\left(1+\frac{s}{a}\right)$, the above condition leads to the restriction that eq. (5—65) can be applied only if $\frac{s}{a}\leq 3.81$.

(5) *Extrusion of a sheet.* In the problems discussed above we studied the cases of *incipient plastic flow* and determined the stress and velocity fields in a body at the instant when the monotonically increasing external load reached its plastic limit value. In these problems, during the more advanced phases of plastic flow, the boundaries and the stress and velocity fields change significantly, and therefore our study was not extended to the investigation of these later phases.

In several problems, however, under the action of the plastic limit load, *steady plastic flow*, similar to the steady flow of fluids, develops. In these cases the stresses and velocities of the individual particles of plastic material will change during their motion, but at a fixed location the moving material will always have the same state of stress and velocity. This means that the problem of steady plastic flow can be solved on the basis of a *fixed* stress and velocity field. The metal-forming processes such as rolling, drawing, machining and extrusion provide typical examples of steady plastic flow.

As an example, consider the frictionless extrusion of a sheet when the reduction in thickness is 50%. Figure 5—25(a) shows the die used in this extrusion process, and the assumed shear line field which consists of two centred fans OAB and $OA'B'$. This pattern fulfils the condition that the shear lines must intersect with the walls and the axis of symmetry at 45°, because no shear stress can be transmitted across the walls or across the axis of symmetry. This means that the assumed shear line field satisfies the static boundary conditions.

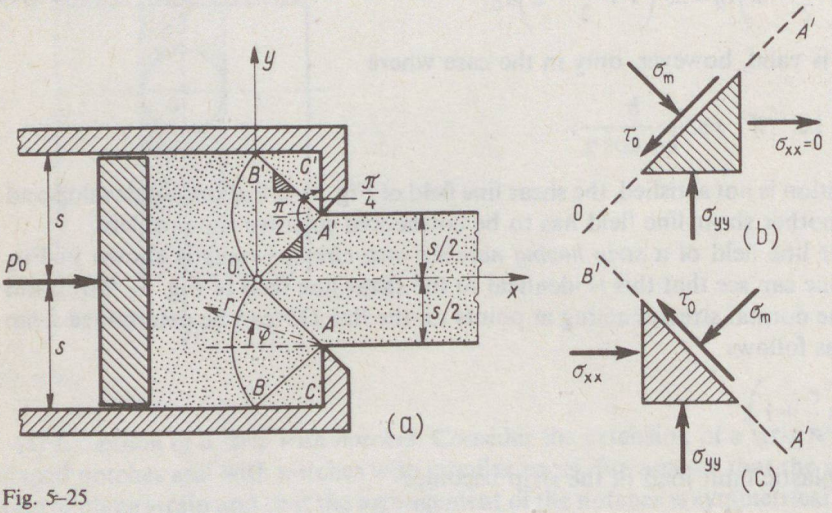


Fig. 5–25

To determine the stress field associated with the shear line field, we start from the condition that the resultant of the stresses transmitted across the line AOA' must vanish, because the extruded sheet to the right of this line is unloaded and is in equilibrium. Since the state of stress is constant along the line AOA' this condition requires σ_{xx} to vanish along these shear lines. Similarly, σ_{xy} must also be zero at every point on these lines, because the x axis forms an angle of 45° with the shear lines, and is therefore a principal axis of stresses. In accordance with these results Fig. 5—25(b) shows the state of stress in an infinitesimal element at an arbitrary point on the line OA'. It is obvious that in the y direction there is a compression, and therefore σ_{yy} should be obtained from the "weak" solution $\sigma_{yy}=-2\tau_0$. Then, the equilibrium of the infinitesimal element under consideration results in $\sigma_m=-\tau_0$. The variation of σ_m in the region $A'OB'$ is described by eq. (5—47). Measuring the angle θ from the line OA' the constant K in eq. (5—47) becomes $K=-\tau_0$, and along line $A'B'$, where $\theta=45°$, the normal stress is

$$\sigma_m=-(1+\pi)\tau_0. \qquad (5—66)$$

Now, considering an element at an arbitrary point on the line $A'B'$, the normal stresses can be derived from the equilibrium equations to obtain

$$\sigma_{xx}=-(2+\pi)\tau_0, \quad \sigma_{yy}=-\pi\tau_0. \qquad (5—67)$$

The extrusion pressure p_0 is equal to the resultant of the stresses acting along the shear lines $BAOA'B'$. Since the resultant of the stresses transmitted across AOA' vanishes from eq. (5—67) we obtain

$$p_0 = s\sigma_{xx} = s(2+\pi)\tau_0. \tag{5—68}$$

Considering the velocity field we can state that the material outside the fans OAB and $OA'B'$ remains rigid. If the material to the left of the fans moves with unit velocity to the right, then the incompressibility and continuity conditions require that the material to the right of AOA' moves with twice the unit velocity. The material in the corners ABC and $A'B'C'$ must remain at rest (as "dead" material).

Considering the above results one can now construct the velocity fields in the fans. The boundaries of the fans may be lines of discontinuity in the velocity field, therefore only the normal velocity components should be continuous across these boundaries. Thus, with respect to the polar coordinates r, φ, shown in Fig. 5—25(a), the following relationships can be obtained

$$\left.\begin{aligned} &\text{along the line } OA \quad v_\varphi = \sqrt{2}, \\ &\text{along the line } AB \quad v_\varphi = 0, \\ &\text{along the line } OB \quad v_r = -\cos\varphi. \end{aligned}\right\} \tag{5—69}$$

It follows from eqs (5—38) that the velocities inside the region OAB have to satisfy the equations

$$v_r = -\frac{\mathrm{d}f(\varphi)}{\mathrm{d}\varphi}, \quad v_\varphi = f(\varphi) + g(r) \tag{5—70}$$

where $f(\varphi)$ and $g(r)$ are unknown functions. This together with the boundary conditions, leads to the solution

$$v_r = -\cos\varphi, \quad v = \frac{1}{\sqrt{2}} + \sin\varphi. \tag{5—71}$$

We have proved that, associated with the assumed shear line field, a kinematically admissible velocity field can be constructed; therefore, the above results provide the complete solution to the problem.*

If the reduction in the sheet thickness differs from 50%, the shear line pattern and the solution become somewhat more complicated (see e.g. Prager, Hodge 1951; Johnson, Mellor 1962; Lippmann 1981).

* One can prove that a statically admissible stress field can be extended to the rigid regions without violating the yield conditions.

5.3. PLANE STRESS PROBLEMS

5.3.1. BASIC RELATIONSHIPS

In the state of plane stress, the stresses σ_{zz}, σ_{zx} and σ_{zy}, corresponding to the sections normal to the z axis, are equal to zero at every point in the body. Then, disregarding the volume forces the remaining stresses σ_{xx}, σ_{yy} and σ_{xy} have to satisfy the equilibrium equations

$$\left.\begin{aligned} \frac{\partial \sigma_{xx}}{\partial x}+\frac{\partial \sigma_{xy}}{\partial y}&=0,\\ \frac{\partial \sigma_{yx}}{\partial x}+\frac{\partial \sigma_{yy}}{\partial y}&=0 \end{aligned}\right\} \tag{5—72}$$

and the yield condition. Since the z axis is a principal axis and the corresponding principal stress vanishes ($\sigma_{zz}=\sigma_{III}=0$), the Huber–v. Mises–Hencky and the Tresca yield conditions (see eqs (2—82) and (2—86)) become

$$f=\sigma_I^2-\sigma_I\sigma_{II}^2+\sigma_{II}^2-\sigma_0^2\leq 0, \tag{5—73}$$

and

$$\left.\begin{aligned} f_1&=\sigma_{II}^2-\sigma_0^2\leq 0,\\ f_2&=\sigma_I^2-\sigma_0^2\leq 0,\\ f_3&=(\sigma_I-\sigma_{II})^2-\sigma_0^2\leq 0. \end{aligned}\right\} \tag{5—74}$$

The yield condition (5—73) can also be expressed in terms of the stresses σ_{xx}, σ_{yy} and σ_{xy} in a general form (see eq. (2—79a))

$$f=\sigma_{xx}^2+\sigma_{yy}^2-\sigma_{xx}\sigma_{yy}+3\sigma_{xy}^2-\sigma_0^2\leq 0. \tag{5—75}$$

We assume that the material is *rigid-perfectly plastic* and therefore in the domains where $f=0$, the body undergoes only plastic deformations. If we eliminate the plastic multiplier $d\lambda$ from the constitutive equation (2—89) and assume that the material is incompressible (see eq. (2—96)) then for the plastic strain rates the following relationships can be obtained

$$\left.\begin{aligned} &\frac{\dot{\varepsilon}_{xx}}{\partial f/\partial \sigma_{xx}}=\frac{\dot{\varepsilon}_{yy}}{\partial f/\partial \sigma_{yy}}=\frac{\dot{\varepsilon}_{xz}}{\partial f/\partial \sigma_{xz}},\\ &\dot{\varepsilon}_{xx}+\dot{\varepsilon}_{yy}+\dot{\varepsilon}_{zz}=0. \end{aligned}\right\} \tag{5—76}$$

Also, making use of the geometrical equations (2—64), these relationships can be expressed in terms of the velocities as below

$$\left.\begin{aligned} &\frac{\partial v_x/\partial x}{\partial f/\partial \sigma_{xx}}=\frac{\partial v_y/\partial y}{\partial f/\partial \sigma_{yy}}=\frac{1}{2}\frac{\partial v_x/\partial y+\partial v_y/\partial x}{\partial f/\partial \sigma_{xy}},\\ &\frac{\partial v_x}{\partial x}+\frac{\partial v_y}{\partial y}+\frac{\partial v_z}{\partial z}=0. \end{aligned}\right\} \tag{5—77}$$

Equations (5—72) and (5—77), together with the yield condition, provide six equations which contain six unknown functions σ_{xx}, σ_{yy}, σ_{xy}, v_x, v_y, v_z. If only static boundary conditions are prescribed, the stresses can be separately obtained from the equilibrium equations and the yield condition. Then, from eqs (5—76) and (5—77), the strain rates and velocities can also be determined. In the general case, however, the six equations must be solved simultaneously leading to serious difficulties. In this case a semi-inverse method can be applied: first we determine the stresses from the equilibrium equations, the static boundary conditions and the yield condition, and then we check whether the corresponding velocities satisfy the kinematic boundary conditions. If they do not the procedure has to be repeated until all the equations are simultaneously satisfied.

Comparing the governing equations of plane strain and plane stress problems the main difference is found to be associated with the yield conditions. While in plane strain the Huber–v. Mises–Hencky and the Tresca yield conditions are identical, in plane stress they are not. In addition, in plane strain the principal stress σ_{II} corresponding to the z axis obeys the relationship $\sigma_{II} = \frac{1}{2}(\sigma_I + \sigma_{III})$ therefore the sections corresponding to the maximum and minimum principal stresses are normal to the xy plane at every point in the body. In plane stress, however, depending on the sign of the non-zero principal stresses, the sections of the maximum and minimum principal stresses can be either normal or parallel to the xy plane. Consequently, the Tresca yield condition (5—74) will have different forms and the corresponding governing differential equations will be of hyperbolic, parabolic or elliptical type in different domains of the body. Similar problems arise in the case of the Huber–v. Mises–Hencky yield condition. In plasticity, therefore, the solution to a plane stress problem is much more complicated than that to a plane strain problem, where the state of the entire body is described by hyperbolic differential equations.

5.3.2. SOLUTION BASED ON THE HUBER–V. MISES–HENCKY YIELD CONDITION

5.3.2.1. BASIC RELATIONSHIPS

The derivation of the governing equations of plane stress problems is similar to that of plane plastic flow. First, we will introduce two new independent variables; then, making use of the yield condition and the equilibrium equations (5—72) we will obtain two differential equations similar to eqs (5—30). Their solution, however, is more complicated because, depending on the magnitude of the principal normal stresses, they are of elliptical, parabolic or hyperbolic type.

In the case of plane stress, the Huber–v. Mises–Hencky yield condition is illustrated by an ellipse and can be expressed in the following parametric form*

* The correctness of these expressions can easily be proved by substituting them in eq. (5—73).

$$\left.\begin{aligned}\sigma_{\mathrm{I}} &= 2\tau_0 \cos\left(\psi - \frac{\pi}{6}\right),\\ \sigma_{\mathrm{II}} &= 2\tau_0 \cos\left(\psi + \frac{\pi}{6}\right).\end{aligned}\right\} \tag{5—78}$$

Using the relatioship $\sigma_{\mathrm{m}} = \frac{1}{2}(\sigma_{\mathrm{I}} + \sigma_{\mathrm{II}})$, the parameter ψ can be expressed in terms of the mean normal stress

$$\cos\psi = \frac{\sqrt{3}}{2\tau_0}\sigma_{\mathrm{m}}. \tag{5—79}$$

The geometric meaning of the parameter ψ and the significant points of the ellipse are shown in Fig. 5—26. In the following, in correspondence with the Huber–v. Mises–Hencky yield condition, the relation $\sigma_0 = \sqrt{3}\tau_0$ will be used.

Considering the Mohr's circle shown in Fig. 5—2 the stresses σ_{xx}, σ_{yy}, σ_{xy} can be expressed in terms of the principal stresses and of the angle ϕ formed by the principal axis I and the x axis as follows

$$\left.\begin{aligned}\left.\begin{matrix}\sigma_{xx}\\ \sigma_{yy}\end{matrix}\right\} &= \frac{1}{2}(\sigma_{\mathrm{I}} + \sigma_{\mathrm{II}}) \pm \frac{1}{2}(\sigma_{\mathrm{I}} - \sigma_{\mathrm{II}})\cos 2\phi,\\ \sigma_{xy} &= \frac{1}{2}(\sigma_{\mathrm{I}} - \sigma_{\mathrm{II}})\sin 2\phi.\end{aligned}\right\}$$

Also, using eqs (5—78) these expressions can be written in the form

$$\left.\begin{aligned}\left.\begin{matrix}\sigma_{xx}\\ \sigma_{yy}\end{matrix}\right\} &= \tau_0(\sqrt{3}\cos\psi \pm \sin\psi\cos 2\phi),\\ \sigma_{xy} &= \tau_0 \sin\psi \sin 2\phi.\end{aligned}\right\} \tag{5—80}$$

Substituting these relations into the equilibrium equations (5—72) leads to the differential equations

$$\left.\begin{aligned}&\left(\sqrt{3}\sin\psi - \cos\psi\cos 2\phi\right)\frac{\partial\psi}{\partial x} - \cos\psi\sin 2\phi\frac{\partial\psi}{\partial\psi} +\\ &\quad + 2\sin\psi\left(\sin 2\phi\frac{\partial\phi}{\partial x} - \cos 2\phi\frac{\partial\phi}{\partial y}\right) = 0,\\ &\cos\psi\sin 2\phi\frac{\partial\psi}{\partial x} - \left(\sqrt{3}\sin\psi + \cos\psi\cos 2\phi\right)\frac{\partial\psi}{\partial y} +\\ &\quad + 2\sin\psi\left(\cos 2\phi\frac{\partial\phi}{\partial x} + \sin 2\phi\frac{\partial\phi}{\partial y}\right) = 0,\end{aligned}\right\} \tag{5—81}$$

which describe the state of plane stress of plastic bodies. In these equations $\psi(x, y)$ and $\phi(x, y)$ are unknown functions. Considering the above equations in more detail, three different cases can be distinguished (see e.g. Kachanov 1971).

(a) If $\frac{\pi}{6} \leq \psi \leq \frac{5\pi}{6}$ or $\frac{7\pi}{6} \leq \psi \leq \frac{11\pi}{6}$, i.e. if the point corresponding to the state of stress is on the full lines AB or CD of the ellipse shown in Fig. 5—26, then the system of differential equations (5—81) is *hyperbolic* and has two families of real characteristics.

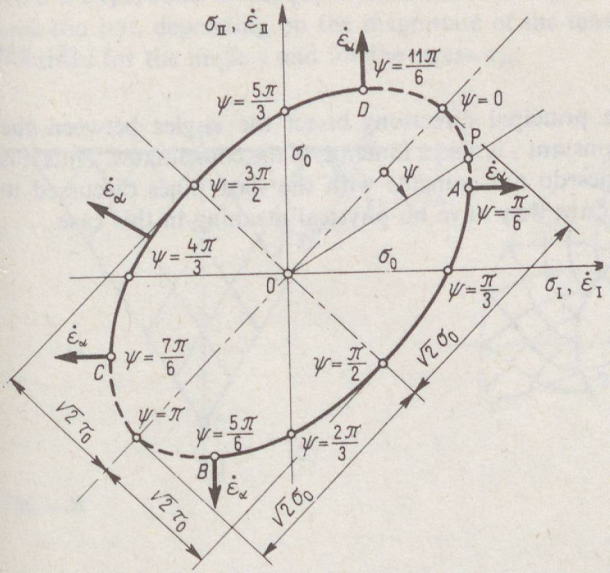


Fig. 5–26

(b) If ψ is equal to one of the values $\frac{\pi}{6}, \frac{5\pi}{6}, \frac{7\pi}{6}$ or $\frac{11\pi}{6}$, i.e. if the state of stress is illustrated by the points A, B, C or D of the ellipse, then the system of differential equations is *parabolic* and has only one family of real characteristics.

(c) If $\frac{5\pi}{6} \leq \psi \leq \frac{7\pi}{6}$ or $-\frac{\pi}{6} \leq \psi \leq \frac{\pi}{6}$, i.e. if the state of stress is illustrated by a point lying on the dashed line BC or DA of the ellipse, then the system of differential equations is *elliptic* and has no real characteristics.

Considering the normality rule (see eq. (2—89)) the strain rate vectors $\dot{\varepsilon}_\alpha(\dot{\varepsilon}_I\, \dot{\varepsilon}_{II})$ can also be illustrated in the stress space σ_I, σ_{II} shown in Fig. 5—26. One can notice, that the strain rate vectors corresponding to the parabolic points A, B, C and D are parallel to the $\dot{\varepsilon}_I$ or $\dot{\varepsilon}_{II}$ axes. Hence, the signs of the strain rates $\dot{\varepsilon}_I$ and $\dot{\varepsilon}_{II}$ belonging to the full lines and dashed lines of the ellipse have opposite and equal signs, respectively. Briefly,

(a) in *hyperbolic* domains $\dot{\varepsilon}_I \dot{\varepsilon}_{II} < 0$,

(b) in *parabolic* domains $\dot{\varepsilon}_I\, \dot{\varepsilon}_{II} = 0$,

(c) in *elliptical* domains $\dot{\varepsilon}_I\, \dot{\varepsilon}_{II} > 0$.

In the general case all three types of domain can occur in a body with their boundaries unknown, therefore the solutions are very complicated. In the following, we will briefly discuss the physical and geometrical properties of the different domains and will illustrate the application by the solution to a simple problem.

5.3.2.2. HYPERBOLIC DOMAIN

In the case of plane stress, characteristics of hyperbolic domains are different from those for plane strain (see e.g. Kachanov 1971). In plane stress the characteristics form a *non-orthogonal* net of curves and intersect at an angle

$$2\gamma = \pi - \arccos \frac{\cot \psi}{\sqrt{3}}, \tag{5—82}$$

as shown in Fig. 5—27. The principal directions bisect the angles between the characteristics. Since ψ is not constant γ is also a function of the coordinates. Thus it is apparent that the characteristics do not coincide with the shear lines discussed in connection with plane plastic flow; they have no physical meaning in this case.

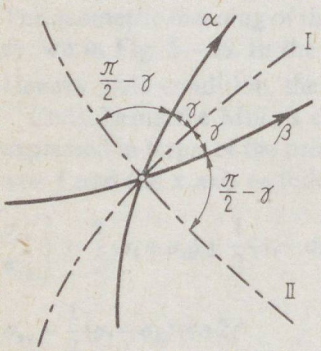


Fig. 5–27

Our further studies will be restricted to homogeneous and axisymmetric states of stress.

(1) *Homogeneous state of stress*

Consider the plane state of stress of a domain which is adjacent to a straight unloaded boundary, as shown in Fig. 5—28(a). Assuming the x axis to be parallel with the boundary, at points on the boundary line AB we have $\sigma_{yy} = \sigma_{xy} = 0$ and σ_{xx} is a principal stress. Then, according to the yield condition (5—75), $\sigma_{xx} = \pm\sigma_0$ and, depending on the sign of σ_{xx}, one can obtain from eq. (5—78) the values $\frac{\pi}{3}$ or $\frac{4\pi}{3}$ for ψ. This means that the domain in the neighbourhood of a straight unloaded boundary is hyperbolic. Considering the case of tension, when $\sigma_{xx} = \sigma_0$ and $\psi = \frac{\pi}{3}$, eq. (5—82) yields $\gamma = 54°44'$. Because the straight boundary line now coincides with the first principal direction ($\phi = 0$), the characteristics intersect with the boundary at an angle of 54°44'. Using the method presented in Section 5.2.4.2., it can be shown that in the region of influence ABC the characteristics form two families of parallel straight lines which intersect each other at an angle $2\gamma = 109°28'$. Hence, in the region ABC there is a homogeneous state of stress given by the stresses $\sigma_{xx} = \sigma_0$, $\sigma_{yy} = \sigma_{xy} = 0$.

Consider the case where the straight boundary is subjected to a uniformly distributed traction p, acting normal to the boundary. Then, along the boundary $\sigma_{yy} = \sigma_1 = p$, $\sigma_{xy} = 0$ and making use of eq. (5—78), the parameter ψ can be determined. If the corresponding point is on the hyperbolic region of the yield ellipse, then the domain ABC is hyperbolic. Consequently, the statements presented above will be valid in this case too but, depending on the magnitude of the tension p, different results can be obtained for the angle γ and for the stress σ_{xx}.

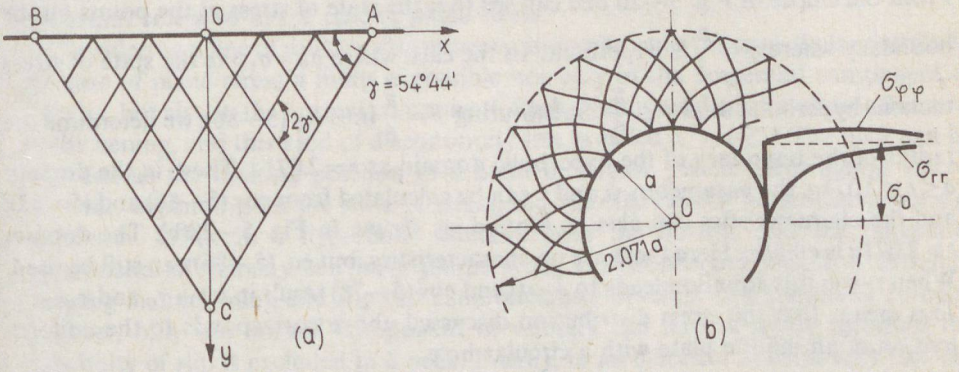


Fig. 5–28

(2) *Axisymmetric state of stress*

Consider an axisymmetric state of plane stress which is characterized by the stresses $\sigma_{rr}, \sigma_{\varphi\varphi}, \sigma_{\varphi r} = 0$ in the system of polar coordinates r, φ. Then, the equilibrium equation has the form

$$\frac{d\sigma_{rr}}{dr} + \frac{\sigma_{rr} - \sigma_{\varphi\varphi}}{r} = 0. \tag{5—83}$$

Assuming $\sigma_{\varphi\varphi} > \sigma_{rr}$, i.e. $\sigma_{\varphi\varphi} = \sigma_I$ and $\sigma_{rr} = \sigma_{II}$, eqs (5—78) become

$$\left.\begin{aligned} \sigma_{\varphi\varphi} &= 2\tau_0 \cos\left(\psi - \frac{\pi}{6}\right), \\ \sigma_{rr} &= 2\tau_0 \cos\left(\psi + \frac{\pi}{6}\right). \end{aligned}\right\} \tag{5—84}$$

Substituting these relations in eq. (5—83) leads to the differential equation

$$(\sqrt{3} + \cot\psi)\frac{d\psi}{dr} + 2r = 0,$$

the solution of which is

$$r^2 = \frac{C}{\sin\psi} e^{-\sqrt{3}\psi}. \tag{5—85}$$

Here the constant C is determined by the boundary condition.

Consider a region in the neighbourhood of an unloaded circular boundary shown in Fig. 5—28(b). Along the boundary $r=a$ $\sigma_{rr}=0$, and from the eqs (5—84) we obtain $\psi=\frac{\pi}{3}$. This makes possible the determination of the constant C. Then eq. (5—85) becomes

$$\left(\frac{r}{a}\right)^2=\frac{\sqrt{3}}{2}\frac{1}{\sin\psi}e^{\sqrt{3}\left(\frac{\pi}{3}-\psi\right)}. \tag{5—86}$$

From the ellipse of Fig. 5—26 one can see that the state of stress at the points on the boundary where $\psi=\frac{\pi}{3}$ is hyperbolic. In the case where $\sigma_\varphi=\sigma_1>0$, the state of stress remains hyperbolic until $\psi\leq\frac{\pi}{6}$. Substituting $\psi=\frac{\pi}{6}$ into eq. (5—86), we determine the radius of the boundary of the hyperbolic domain as $r=2.071a$. Then, in the domain $a\leq r\leq 2.071a$, the parameters ψ and γ can be calculated from eqs (5—86) and (5—82), and the characteristics can also be plotted, as shown in Fig. 5—28(b). The domain $r>2.071a$ is elliptic. Here there are no characteristics, but eq. (5—86) can still be used. When $r\to\infty$ this equation leads to $\psi\to 0$ and eqs (5—78) result in $\sigma_{rr}\to\sigma_0$ and $\sigma_\varphi\to\sigma_0$. This means that the stress distribution discussed above corresponds to the uniform tension of an infinite plate with a circular hole.

5.3.2.3. PARABOLIC AND ELLIPTICAL DOMAINS

(1) In a *parabolic domain* ψ is equal to one of the values $\frac{\pi}{6},\frac{5\pi}{6},\frac{7\pi}{6}$ or $\frac{11\pi}{6}$ and eqs (5—82) and (5—81) lead to $\gamma=0$ and $\phi=$constant. Consequently, the two families of characteristics now coincide and consist of straight lines. The domain has a homogeneous state of stress defined by the single variable ϕ, which can be determined from the boundary conditions.

(2) In an *elliptical domain* there are no real characteristics and the solution of the system of nonlinear differential equations (5—81) is very difficult. No general methods are available, and until now only axially symmetrical problems have been solved.

5.3.2.4. DETERMINATION OF THE VELOCITY FIELD

Substituting the yield condition (5—75) into the geometrical equations (5—77) leads to a system of linear differential equations with variable coefficients.*

$$\left.\begin{aligned}\left(2\sigma_{xx}-\sigma_{yy}\right)\frac{\partial v_y}{\partial y}&=\left(2\sigma_{yy}-\sigma_{xx}\right)\frac{\partial v_x}{\partial x},\\ \left(2\sigma_{xx}-\sigma_{yy}\right)\left(\frac{\partial v_x}{\partial v_y}+\frac{\partial v_y}{\partial v_x}\right)&=6\sigma_{xy}\frac{\partial v_x}{\partial x}.\end{aligned}\right\} \tag{5—87}$$

* The third equation of eqs (5—77) can be treated separately. After determining v_x and v_y from eqs (5—87) v_z can also be calculated.

Assuming the state of stress to be known, the velocities v_x and v_y can be determined from these two equations. It can be proved that in the hyperbolic domain of stress eqs (5—81) and (5—87) will also be hyperbolic and the characteristics of both systems will coincide.

5.3.2.5. LINES OF DISCONTINUITY

As in the case of plane strain, the discontinuities in the velocity and stress fields play an important role also in the case of plane stress.

Considering a line of *velocity discontinuity*, in constrast to the case of plane strain in the case of plane stress a jump is possible not only in the tangential component of velocity, but also in the normal component. Such a jump results in an abrupt thinning or thickening, and this kind of discontinuity line is called a "*neck*".* The neck can be regarded as the limiting position of a band of intense plastic deformation where, however, depending on the state of stress, the velocity cannot be arbitrary (see e.g. Kachanov 1971). In a hyperbolic domain, both the normal and the tangential components of velocity can have jumps along a discontinuity line, and therefore thinning or thickening and slip can simultaneously develop. In a parabolic domain, however, only the normal component of velocity can have a jump; therefore the possibility of slip is excluded in a neck. Finally, in an elliptical domain only slip can occur along a line of discontinuity.

In the case of plane stress, a line of *stress discontinuity* has the same properties as it has in plane strain. Hence, only the exterior normal stresses can be dicontinuous along a line of discontinuity causing a jump in the slope of the characteristics. In contrast to the case of plane strain, in the case of plane stress the lines of velocity and stress discontinuities cannot coincide.

5.3.2.6. EXTENSION OF NOTCHED PLATES

To illustrate the application, consider the extension of a plate with notches that have circular roots of radius a, as shown in Fig. 5—29. The stress field arising near the circular part of the contour is axisymmetric and the characteristics and the stresses are completely determined by the boundary conditions along the circle and by eqs (5—84) and (5—86). According to Fig. 5—28(b), however, these fields may be continued only through a distance not more than $r = 2.071a$. In this limiting case, the angular span of the circular part of the arc AB is $38°56'$.

(a) First, consider the case when $s \leq 1.071a$ and the fields spreading from the two notches meet at a point (see Fig. 5—29(a)). Then, the plastic limit load corresponding to this stress distribution can be obtained from the equation

$$P_p = 2 \int_a^{a+s} \sigma_{\varphi\varphi} \, dr. \qquad (5—88)$$

* It is obvious that this kind of discontinuity cannot develop in the case of plane strain, since this would be in contradiction to the condition $\dot{\varepsilon}_z = 0$.

Here, the stress σ_φ is defined by eqs (5—84) and (5—86) and the complicated result obtained after integration can be approximated by the following simple expression (see Kachanov 1971)

$$P_p \approx 2\left(1+0.23\frac{s/a}{1+s/a}\right)s\sigma_0; \quad s \leq 1.071a. \tag{5—89}$$

According to elementary strength of materials the plastic limit load of the notched plate under consideration is $P_p = 2s\sigma_0$. Hence, the factor in the parenthesis of eq. (5—89) expresses the increase of the plastic limit load obtained by the application of a more refined theory.

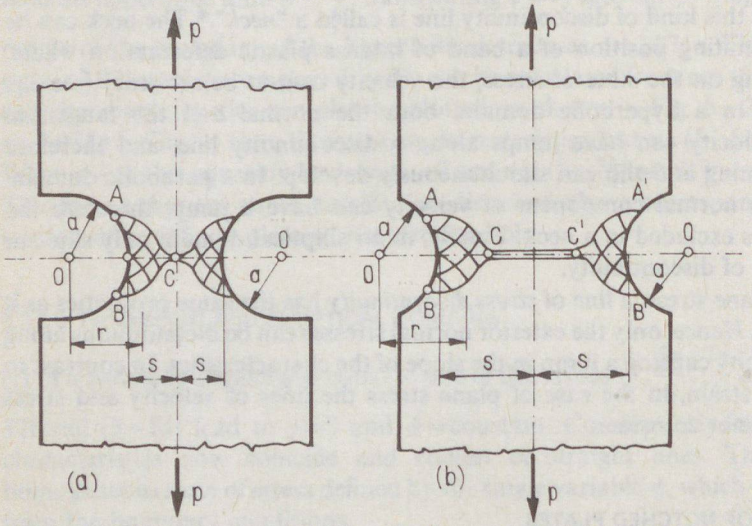


Fig. 5–29

(b) If $s > 1.071a$, the stress field in the domains ABC and $A'B'C'$ shown in Fig. 5—29(b) is also axisymmetric and along the line CC' a neck will develop. The state of stress at points on this line is defined by the parabolic point A on the yield ellipse shown in Fig. 5—26 and is characterized by the components $\sigma_{rr} = \tau_0$, $\sigma_{\varphi\varphi} = 2\tau_0$. The plastic limit load can then be determined by the use of the integral (5—88), and has the approximate formula

$$P_p \approx \left(1.25-\frac{0.04}{s/a}\right)s\sigma_0; \quad s \geq 1.071a. \tag{5—90}$$

The plastic limit loads given by formulae (5—89) and (5—90) are illustrated in Fig. 5—30.

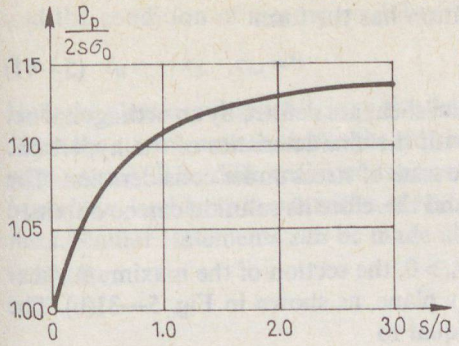


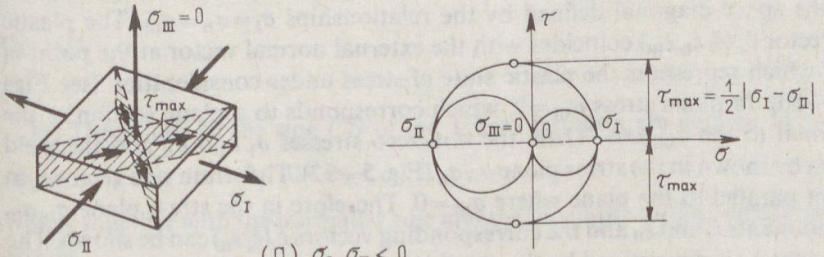
Fig. 5–30

5.3.3. SOLUTION BASED ON THE TRESCA YIELD CONDITION

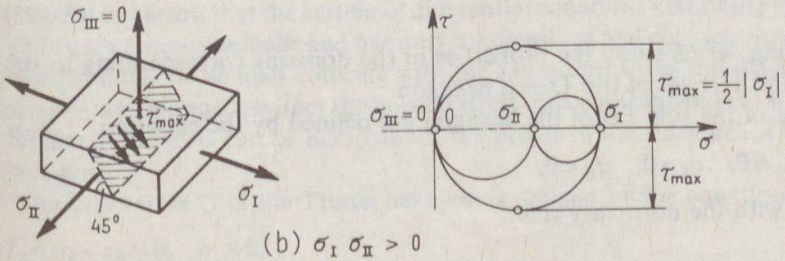
Depending on the signs of the principal stresses σ_I and σ_{II}, the Tresca yield condition has different forms and the governing equations are of different types.

(a) If σ_I and σ_{II} have *different signs* i.e. $\sigma_I \sigma_{II} < 0$, then the two sections of the maximum shear stresses are normal to the xy plane, as it is shown in Fig. 5—31(a). The maximum shear stress is equal to

$$\tau_{max} = \frac{1}{2}|\sigma_I - \sigma_{II}| = \frac{1}{2}\sqrt{(\sigma_{xx}-\sigma_{yy})^2 + 4\sigma_{xy}^2}$$



(a) $\sigma_I\ \sigma_{II} < 0$



(b) $\sigma_I\ \sigma_{II} > 0$

Fig. 5–31

and, considering eqs (5—74), the yield condition has the form

$$f_3=(\sigma_I-\sigma_{II})^2-\sigma_0^2\leq 0;\ \sigma_I\sigma_{II}<0. \tag{5—91}$$

The directions of the sections of the maximum shear are defined by an orthogonal net of shear lines, and the shear lines coincide with the characteristics of the hyperbolic system of differential equations describing the state of stress under consideration. The problem is similar to the case of plane strain and therefore its solution can be obtained in a similar manner.

(b) If σ_I and σ_{II} have *identical signs*, i.e. $\sigma_I\sigma_{II}>0$, the section of the maximum shear stress is inclined at an angle of 45° to the xy plane, as shown in Fig. 5—31(b). The magnitude of the maximum shear stress is equal to

$$\tau_{max}=\frac{1}{2}|\sigma_I| \quad \text{or} \quad \tau_{max}=\frac{1}{2}|\sigma_{II}|.$$

The yield condition then becomes

$$\left.\begin{aligned} f_2&=\sigma_I^2-\tau_0^2\leq 0, \quad \text{if} \quad \sigma_I\sigma_{II}>0 \quad \text{and} \quad |\sigma_I|>|\sigma_{II}|,\\ f_1&=\sigma_{II}^2-\tau_0^2\leq 0, \quad \text{if} \quad \sigma_I\sigma_{II}>0 \quad \text{and} \quad |\sigma_I|<|\sigma_{II}|. \end{aligned}\right\} \tag{5—92}$$

In this case the directions of the sections of the maximum shear stresses define only one family of shear lines in the xy plane, and the corresponding system of differential equations is parabolic.

In order to study the physical properties of the domains of different types, we have to take the plastic strain rates into consideration. In the principal stress space σ_I, σ_{II}, σ_{III} the general Tresca yield condition is illustrated by a hexagonal cylinder with generators parallel to the space diagonal defined by the relationships $\sigma_I=\sigma_{II}=\sigma_{III}$. The plastic strain rate vector $\dot{\varepsilon}_\alpha$ ($\dot{\varepsilon}_I\ \dot{\varepsilon}_{II}\ \dot{\varepsilon}_{III}$) coincides with the external normal vector at the point of the cylinder which represents the plastic state of stress under consideration (see Figs 2—9 and 2—10). In plane stress $\sigma_{III}=0$, which corresponds to a plane section of the cylinder normal to the σ_{III} axis. Then, the non-zero stresses σ_I and σ_{II} and the yield condition can be shown in the stress plane σ_I, σ_{II} (Fig. 5—32). The strain rate vector $\dot{\varepsilon}_\alpha$ in general is not parallel to the plane where $\sigma_{III}=0$. Therefore in the stress plane σ_I, σ_{II}, only the components $\dot{\varepsilon}_I$ and $\dot{\varepsilon}_{II}$ and the corresponding vectors $\dot{\varepsilon}_\alpha(\dot{\varepsilon}_I\ \dot{\varepsilon}_{II})$ can be shown. The third component $\dot{\varepsilon}_{III}$ is determined by the condition of incompressibility, which has the form

$$\dot{\varepsilon}_I+\dot{\varepsilon}_{II}+\dot{\varepsilon}_{III}=0. \tag{5—93}$$

In the following, let us study the properties of the domains corresponding to the different sides and vertices of the Tresca hexagon.

(a) The points of the side ED of the hexagon are defined by the equation

$$f_3=(\sigma_I-\sigma_{II})-\sigma_0=0, \quad \sigma_I>0, \quad \sigma_{II}<0,$$

which together with the normality rule

$$\dot{\varepsilon}_{ij}=\lambda_k\frac{\partial f_k}{\partial \sigma_{ij}}$$

and the condition of incompressibility (5—93) leads to the strains

$$\dot{\varepsilon}_{\mathrm{I}}=\dot{\lambda}_3, \quad \dot{\varepsilon}_{\mathrm{II}}=-\dot{\lambda}_3, \quad \dot{\varepsilon}_{\mathrm{III}}=0.$$

Here the plastic multiplier $\dot{\lambda}_3(x, y, t) \geqq 0$ denotes the magnitude of the strain rate vector. Since the strains now vanish in the z direction, this case corresponds to the problem of plane strain. The differential equations describing the state of stress and strain are *hyperbolic*, and have two families of real characteristics which coincide with the shear lines. Similar statements can be made about the internal points of the side AB of the hexagon.

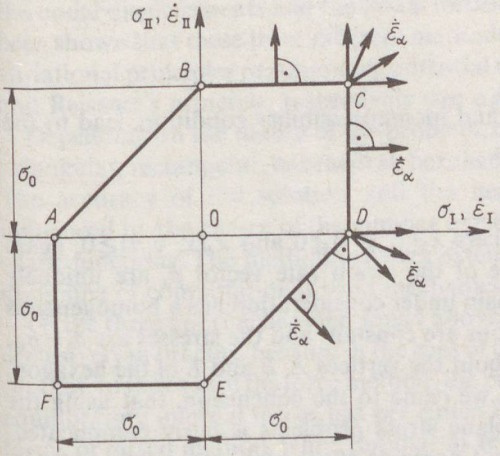


Fig. 5–32

(b) The points of the side CD of the Tresca hexagon are defined by the equations

$$f_2=\sigma_{\mathrm{I}}-\sigma_0=0, \quad \sigma_{\mathrm{I}}>0, \quad 0<\sigma_{\mathrm{II}}<\sigma_0,$$

which, together with the normality rule and the incompressibility condition, lead to the strains

$$\dot{\varepsilon}_{\mathrm{I}}=\dot{\lambda}_2, \quad \dot{\varepsilon}_{\mathrm{II}}=0, \quad \dot{\varepsilon}_{\mathrm{III}}=-\dot{\lambda}_2.$$

It can be shown that the system of differential equations describing the state of stress and strain is now *parabolic* and has only one family of real characteristics, consisting of straight lines. These lines coincide with the second principal directions of the normal stresses, and along these lines the normal stress σ_{II} is constant and the strain rate is zero. Similar statements can be made about the points of the sides BC, AF and FE of the hexagon.

(c) The vertex C of the Tresca hexagon is defined by the equations

$$f_2=\sigma_{\mathrm{I}}-\sigma_0=0, \quad \sigma_{\mathrm{I}}>0,$$

$$f_1=\sigma_{\mathrm{II}}-\sigma_0=0, \quad \sigma_{\mathrm{II}}>0,$$

which, together with the normality rule and the incompressibility condition, result in

$$\dot{\varepsilon}_{\mathrm{I}}=\dot{\lambda}_2, \quad \dot{\varepsilon}_{\mathrm{II}}=\dot{\lambda}_1, \quad \dot{\varepsilon}_{\mathrm{III}}=-\dot{\lambda}_1-\dot{\lambda}_2.$$

Here $\dot{\lambda}_1(x, y, t)\geq 0$ and $\dot{\lambda}_2(x, y, t)\geq 0$ denote two unknown plastic multipliers. Hence, in this case neither the direction nor the magnitude of the strain rate vector $\dot{\varepsilon}_\alpha$ are uniquely determined. The domain under consideration has a homogeneous state of stress, where in the xy plane each direction is a principal direction and the stresses are $\sigma_{xx}=\sigma_0$, $\sigma_{yy}=\sigma_0$, $\sigma_{xy}=0$. The system of differential equations which describes the state of stress and strain has no real characteristics. Similar statements can be made about the vertex F of the hexagon.

(d) The vertex D of the Tresca yield hexagon is defined by the equations

$$f_2=\sigma_{\mathrm{I}}-\sigma_0=0,$$

$$f_3=(\sigma_{\mathrm{I}}-\sigma_{\mathrm{II}})-\sigma_0=0, \quad \sigma_{\mathrm{I}}>0,$$

which, together with the normality rule and incompressibility condition, lead to the strain rates

$$\dot{\varepsilon}_{\mathrm{I}}=\dot{\lambda}_2+\dot{\lambda}_3, \quad \dot{\varepsilon}_{\mathrm{II}}=-\dot{\lambda}_2, \quad \dot{\varepsilon}_{\mathrm{III}}=-\dot{\lambda}_3.$$

Because of the unknown plastic multipliers $\dot{\lambda}_2(x, y, t)\geqq 0$ and $\dot{\lambda}_3(x, y, t)\geqq 0$, again neither the direction nor the magnitude of the strain rate vector $\dot{\varepsilon}_\alpha$ are uniquely determined. Similarly to case (*c*), the domain under consideration has a homogeneous state of stress where the principal directions are constant and the stresses are $\sigma_{\mathrm{I}}=\sigma_0$, $\sigma_{\mathrm{II}}=0$. Similar statements can be made about the vertices A, B and E of the hexagon.

After the brief study presented above, we came to the conclusion, that using the Tresca yield condition the analysis of plane stress problems is fairly complicated. Depending on the state of stress in different domains of the body, the yield condition has different forms and as a consequence of this the system of differential equations describing the state of stress and strain is hyperbolic, parabolic or elliptical. The boundaries of these domains are not known "a priori", which makes the solution even more difficult.

5.4. APPLICATION OF THE FINITE ELEMENT METHOD

5.4.1. INTRODUCTORY REMARKS

During the past quarter of this century the finite element method, as a very valuable and efficient method for the analysis of problems in structural and continuum mechanics, has evolved to become the most widely used tool in engineering practice. A large number of textbooks are available which deal with the mathematical and mechanical foundations and the wide range of applications of the finite element method (see e.g. Zienkiewicz 1971; 1974; Oden 1972; Chen 1975; Hinton–Owen 1979; Owen–Hinton 1980). In this section a brief review will be presented describing the basic concepts of the method and its application to plane plastic problems.

The basic *physical* concept of the finite element method is that the continuum or the structure is divided into distinct regions known as *finite elements* which are connected

at a discrete number of points along their periphery, called *nodal points*. Using properly chosen *shape functions* for the description of the displacements of the elements, the strains, the stresses and the *nodal forces* can be expressed in terms of the *nodal displacements*. Then the *global stiffness matrix* of the continuum or structure, which defines the relationship between the external forces and the nodal displacements, can be constructed. Finally, solving the resulting system of simultaneous equations for the unknown nodal displacements, the stresses, strains and nodal forces can be evaluated for each element.

The approach described above is called the *finite element stiffness (displacement) method*. In the case of the *flexibility (force) method*, all the variables are expressed in terms of the unknown *nodal forces*, while using the *mixed method* certain groups of both the nodal displacements and the nodal forces are treated as unknown variables. It has been shown that these three different methods can be derived by the application of the variational principles of stationary potential energy, minimum complementary energy and Reissner's principle, respectively (see e.g. Gallagher 1975).

Depending on the nature of the problem, elements with different types of geometry (triangular, rectangular, tetrahedral, hexahedral etc.) and shape functions can be used. The accuracy of the solution and the necessary computational time are highly influenced by the choice of the number of elements and nodes and by the form of the shape functions. The method involves extensive computation, giving rise to the new discipline of computational solid mechanics.

Of the three approaches mentioned above, the displacement method is used almost exclusively in practice because of the ease of organising and programming the solution process. In the case of the force method, the problem of selecting an optimum set of self-equilibrating internal forces has prevented it from attaining popularity. The various forms of mixed method, while popular as research topics, have yet to become widely used in practice despite potential advantages in accuracy and convergence properties. In this section only the displacement method will be briefly outlined. In the literature many approaches are detailed to introduce and derive the displacement method with varying degrees of mathematical rigour and formality. Here we employ a level of treatment appropriate to applications, and refer the reader to the literature for more rigorous treatment. In our presentation, for convenience, vector and matrix notation will be used.

5.4.2. FUNDAMENTAL EQUATIONS

Applying the finite element *stiffness (displacement) method*, one has to construct a relationship between the nodal displacements $\mathbf{q}$ and the nodal forces $\mathbf{Q}$ of the elements. To obtain this relationship, we first assume a kinematically admissible displacement function $\mathbf{u}$ for each element and, by the use of this *shape function* and the geometrical and constitutive equations, we express the strains $\boldsymbol{\varepsilon}$ and stresses $\boldsymbol{\sigma}$ of the elements in terms of the nodal displacements. Then, writing the equilibrium equations, one can derive a direct relationship between the nodal forces and the nodal displacements in the form

$$\mathbf{Q} = \mathbf{K}_t \mathbf{q}, \tag{5—94}$$

where $\mathbf{K}_l$ is the *stiffness matrix* of the element l under consideration. In the case of incremental analysis of elasto-plastic problems, the incremental variables $\mathrm{d}\mathbf{q}$, $\mathrm{d}\mathbf{Q}$, $\mathrm{d}\varepsilon$ and $\mathrm{d}\sigma$ have to be introduced and then the above relationship becomes

$$\mathrm{d}\mathbf{Q} = \mathbf{K}_l \mathrm{d}\mathbf{q}. \tag{5—95}$$

In the following we will deal only with plane strain and plane stress problems and will use triangular elements, as shown in Fig. 5—33. Denoting by i, j, m the nodes of a triangular element, the vectors of the increments in the nodal displacements and forces have the form*

$$\mathrm{d}\mathbf{q}^{\mathrm{T}}[\mathrm{d}q_{\mathrm{ix}}\ \mathrm{d}q_{\mathrm{iy}}\ \mathrm{d}q_{\mathrm{jx}}\ \mathrm{d}q_{\mathrm{jy}}\ \mathrm{d}q_{\mathrm{mx}}\ \mathrm{d}q_{\mathrm{my}}],$$

$$\mathrm{d}\mathbf{Q}^{\mathrm{T}}[\mathrm{d}Q_{\mathrm{ix}}\ \mathrm{d}Q_{\mathrm{iy}}\ \mathrm{d}Q_{\mathrm{jx}}\ \mathrm{d}Q_{\mathrm{jy}}\ \mathrm{d}Q_{\mathrm{mx}}\ \mathrm{d}Q_{\mathrm{my}}].$$

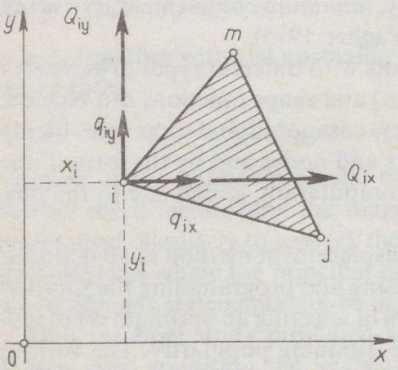


Fig. 5–33

Since each element has six degrees of freedom, six unknown coefficients $\alpha_1, \alpha_2, \ldots \alpha_6$ are required in the polynomial representing the shape function $\mathbf{u}\ (x, y)$ and the increment $\mathrm{d}\mathbf{u}\ (x, y)$ of this function. For the sake of simplicity, we choose the simplest representation of the shape function, which is given by two linear polynomials

$$\left.\begin{aligned} \mathrm{d}u_x &= \alpha_1 + \alpha_2 x + \alpha_3 y, \\ \mathrm{d}u_y &= \alpha_4 + \alpha_5 x + \alpha_6 y, \end{aligned}\right\} \tag{5—96}$$

or in matrix form

$$\mathrm{d}\mathbf{u} = [f(x, y)]\boldsymbol{\alpha}, \tag{5—97}$$

where

$$[f(x, y)] = \begin{bmatrix} 1 & x & y & 0 & 0 & 0 \\ 0 & 0 & 0 & 1 & x & y \end{bmatrix} \quad \text{and} \quad \boldsymbol{\alpha}^{\mathrm{T}}[\alpha_1\ \alpha_2\ \alpha_3\ \alpha_4\ \alpha_5\ \alpha_6].$$

* The superscript T indicates the transpose of a vector or a matrix.

At the nodes, $\mathbf{du}$ must be identical with $\mathbf{dq}$ and therefore, for example, at the node i with the coordinates x_i, y_i, the following relationships have to be satisfied

$$\alpha_1 + \alpha_2 x_i + \alpha_3 y_i = dq_{ix},$$

$$\alpha_4 + \alpha_5 x_i + \alpha_6 y_i = dq_{iy}.$$

Writing similar equations for the nodes j and m, the six linear equations obtained in this manner have the matrix form

$$\mathbf{A}\boldsymbol{\alpha} = \mathbf{dq},$$

where

$$\mathbf{A} = \begin{bmatrix} 1 & x_i & y_i & 0 & 0 & 0 \\ 0 & 0 & 0 & 1 & x_i & y_i \\ 1 & x_j & y_j & 0 & 0 & 0 \\ 0 & 0 & 0 & 1 & x_j & y_j \\ 1 & x_m & y_m & 0 & 0 & 0 \\ 0 & 0 & 0 & 1 & x_m & y_m \end{bmatrix}$$

and (x_i, y_i), (x_j, y_j) and (x_m, y_m) denote the coordinates of the nodes of the element under consideration.

Inverting the matrix A, the unknown polynomial coefficients $\boldsymbol{\alpha}$ can be obtained as a function of $\mathbf{dq}$ in the form

$$\boldsymbol{\alpha} = \mathbf{A}^{-1}\mathbf{dq}. \tag{5—98}$$

Substituting this expression into eq. (5—97), the displacement increments $\mathbf{du}$ can also be expressed in terms of the nodal displacement increments

$$\mathbf{du} = [f(x, y)]\mathbf{A}^{-1}\mathbf{dq}. \tag{5—99}$$

According to the *strain—displacement relationships* (2—60) the strain increments $\mathbf{d\varepsilon}$ and the function $\mathbf{du}$ have the following relationships

$$d\varepsilon_{xx} = \frac{\partial(du_x)}{\partial x}, \quad d\varepsilon_{yy} = \frac{\partial(du_y)}{\partial y}, \quad d\varepsilon_{xy} = \frac{1}{2}\left[\frac{\partial(du_x)}{\partial y} + \frac{\partial(du_y)}{\partial x}\right].$$

Substituting eqs (5—96) into these relationships leads to

$$d\varepsilon_{xx} = \alpha_2, \quad d\varepsilon_{yy} = \alpha_6, \quad d\varepsilon_{xy} = \frac{1}{2}(\alpha_3 + \alpha_5)$$

or, in matrix form,

$$\mathbf{d\varepsilon} = \mathbf{C}\boldsymbol{\alpha},$$

where

$$\mathbf{C}=\begin{bmatrix} 0 & 1 & 0 & 0 & 0 & 0 \\ 0 & 0 & 0 & 0 & 0 & 1 \\ 0 & 0 & \frac{1}{2} & 0 & \frac{1}{2} & 0 \end{bmatrix}.$$

Finally, making use of eq. (5—98), the strain increments can be expressed in terms of the nodal displacement increments

$$\mathrm{d}\boldsymbol{\varepsilon}=\mathbf{C}\mathbf{A}^{-1}\mathrm{d}\mathbf{q}=\mathbf{B}\mathrm{d}\mathbf{q}, \tag{5—100}$$

where

$$\mathbf{B}=\frac{1}{2\Delta}\begin{bmatrix} (y_j-y_m) & 0 & (y_m-y_i) & 0 & (y_i-y_j) & 0 \\ 0 & (x_m-x_j) & 0 & (x_i-x_m) & 0 & (x_j-x_i) \\ (x_m-x_j) & (y_j-y_m) & (x_i-x_m) & (y_m-y_i) & (x_j-x_i) & (y_i-y_j) \end{bmatrix}$$

and

$$2\Delta=(x_j y_m-x_m y_j)+(x_i y_m-x_m y_i)+(x_i y_j-x_j y_i).$$

Using the *constitutive equations*, the stress and strain increments have the following general relationship

$$\mathrm{d}\boldsymbol{\sigma}=\mathbf{D}\mathrm{d}\boldsymbol{\varepsilon} \tag{5—101}$$

and substituting relation (5—100) we obtain

$$\mathrm{d}\boldsymbol{\sigma}=\mathbf{D}\mathbf{B}\mathrm{d}\mathbf{q}. \tag{5—102}$$

Here in the case of *elastic* plane stress and strain problems the matrix **D** has the simple forms (see eqs (2—74) and (2—75))

$$\mathbf{D}=\frac{E}{1-\nu^2}\begin{bmatrix} 1 & \nu & 0 \\ \nu & 1 & 0 \\ 0 & 0 & 1-\nu \end{bmatrix},$$

$$\mathbf{D}=\frac{E}{(1+\nu)(1-2\nu)}\begin{bmatrix} 1-\nu & \nu & 0 \\ \nu & 1-\nu & 0 \\ 0 & 0 & 1-2\nu \end{bmatrix}.$$

In *elasto-plastic* problems, these relationships are expressed in terms of the instantaneous stresses, as will be shown later.

Finally, to derive a relationship between the nodal forces and displacements and to obtain the stiffness matrix of the element, the *equilibrium* of the element has to be taken into consideration. Using the virtual strains $\delta\boldsymbol{\varepsilon}_k$ and the virtual nodal displacements $\delta\mathbf{q}_k$, the equilibrium of the nodal forces $\mathrm{d}\mathbf{Q}$ and stresses $\mathrm{d}\boldsymbol{\sigma}$ can be expressed by writing the principle of virtual work

$$\delta\mathbf{q}_k^T\mathrm{d}\mathbf{Q}=\int\delta\boldsymbol{\varepsilon}_k^T\mathrm{d}\boldsymbol{\sigma}\mathrm{d}A.$$

Here the integral is extended to the entire area of the element* and, using eqs (5—100) and (5—102), can be written as

$$\delta\mathbf{q}_k^T\mathrm{d}\mathbf{Q}=\delta\mathbf{q}_k^T\left[\int\mathbf{B}^T\mathbf{D}\mathbf{B}\mathrm{d}A\right]\mathrm{d}\mathbf{q}.$$

This equation has to be fulfilled for any arbitrary virtual displacement field $\delta\mathbf{q}_k$, therefore the equation

$$\mathrm{d}\mathbf{Q}=\mathbf{K}_l\mathrm{d}\mathbf{q}$$

must be satisfied. Here

$$\mathbf{K}_l=\int\mathbf{B}^T\mathbf{D}\mathbf{B}\mathrm{d}A \tag{5—103}$$

is the *stiffness matrix* of the element l. In the case of linear elastic bodies, this matrix is a constant; in elasto-plastic problems, however, it is a function of the instantaneous stresses. Using the Prandtl–Reuss constitutive equations of *linear elastic–perfectly plastic* bodies, the matrix $\mathbf{D}$ can be expressed in the following form (Chen 1975).

(a) In the case of *plane stress*:

$$\mathbf{D}=\frac{E}{1-\nu^2}\begin{bmatrix}1-\omega\phi_{11} & \nu-\omega\phi_{12} & -\omega\phi_{13}\\ \nu-\omega\phi_{21} & 1-\omega\phi_{22} & -\omega\phi_{23}\\ -\omega\phi_{31} & -\omega\phi_{32} & 1-\nu-\omega\phi_{33}\end{bmatrix}, \tag{5—104}$$

where

$$\left.\begin{aligned}
&\omega=\frac{\langle f\rangle}{2(1-\nu)K_2-(1-2\nu)s_{zz}^2},\\
&\phi_{11}=[(1-\nu)s_{xx}-\nu s_{zz}]^2,\\
&\phi_{12}=\phi_{21}=[(1-\nu)s_{xx}-\nu s_{zz}][(1-\nu)s_{yy}-\nu s_{zz}],\\
&\phi_{13}=\phi_{31}=2[(1-\nu)s_{xx}-\nu s_{zz}][(1-\nu)s_{xy}],\\
&\phi_{22}=[(1-\nu)s_{yy}-\nu s_{zz}]^2,\\
&\phi_{23}=\phi_{32}=2[(1-\nu)s_{yy}-\nu s_{zz}][(1-\nu)s_{xy}],\\
&\phi_{33}=2[(1-\nu)s_{xy}]^2,\\
&\langle f\rangle\begin{cases}=1, & \text{if } f=0 \text{ and } \mathrm{d}f=0,\\ =0, & \text{if } f<0 \text{ or } f=0 \text{ and } \mathrm{d}f<0,\end{cases}
\end{aligned}\right\} \tag{5—105}$$

* We assume that the thickness of the element is equal to the unit.

and f and K_2 denote the Huber–v. Mises–Hencky yield condition and the second invariant of the stress deviator tensor, respectively (see eqs (2—25) and (2—79)).

(b) In the case of *plain strain*:

$$\mathbf{D}=\frac{E}{(1+\nu)(1-2\nu)}\begin{bmatrix} 1-\nu-\omega\phi_{11} & \nu-\omega\phi_{12} & -\omega\phi_{13} \\ \nu-\omega\phi_{21} & 1-\nu-\omega\phi_{22} & -\omega\phi_{23} \\ -\omega\phi_{31} & -\omega\phi_{32} & 1-2\nu-\omega\phi_{33} \end{bmatrix}, \tag{5—106}$$

where

$$\left.\begin{aligned} \omega &= \frac{\langle f\rangle}{2(1-2\nu)K_2}, \\ \phi_{11} &= (1-2\nu)^2 s_{xx}^2, \\ \phi_{12} &= \phi_{21} = (1-2\nu)^2 s_{xx}s_{yy}, \\ \phi_{13} &= \phi_{31} = 2(1-2\nu)^2 s_{xx}s_{xy}, \\ \phi_{22} &= (1-2\nu)s_{yy}^2, \\ \phi_{23} &= \phi_{32} = 2(1-2\nu)^2 s_{yy}s_{xy}, \\ \phi_{33} &= 2(1-2\nu)^2 s_{xy}^2, \end{aligned}\right\} \tag{5—107}$$

and f, $\langle f\rangle$ and K_2 have the same meaning as in the case of plane stress.

We note that the matrix **B**, appearing in the expression (5—103) for the stiffness matrix $\mathbf{K}_1$, depends only on the shape of the triangular element and on the form of the shape function $\mathbf{u}(x, y)$.

Whenever the stiffness matrices of the elements are known, the global stiffness matrix **K** of the continuum or structure can be constructed, and then the relationship between the increments in the external loads d**p** and the nodal displacements d**q** can be expressed in the form

$$\mathrm{d}\mathbf{p}=\mathbf{K}\mathrm{d}\mathbf{q}. \tag{5—108}$$

In the elasto-plastic state the global stiffness matrix is a function of the instantaneous stress field, and therefore in the incremental analysis of an elasto-plastic continuum or structure it has to be modified after each step. More details of this numerical procedure will be presented below. A systematic and comprehensive description of the application of the finite element method to elasto-plastic and visco-plastic problems, together with detailed algorithms, can be found in the literature (Owen–Hinton 1980).

5.4.3. INCREMENTAL ELASTO-PLASTIC ANALYSIS

In the *elastic state* of a continuum, when in every element the condition $f<0$ is satisfied, the global stiffness matrix is constant and from the linear equation

$$\mathbf{p}=\mathbf{K}\mathbf{q} \tag{5—109}$$

the nodal displacements and then the stresses and strains for each element can be determined. If the external load is increased beyond the elastic limit, several elements start to yield; therefore in this *elasto-plastic state* a step–by–step procedure has to be conducted to calculate the stresses and strains. In the following, two numerical methods of this incremental analysis will be briefly presented.

(1) *The tangential stiffness method.* Let us assume that, at an instant during the elasto-plastic state of a continuum subjected to the external loads $\mathbf{p}_0$, the nodal displacements, stresses and strains $\mathbf{q}_0$, $\boldsymbol{\sigma}_0$ and $\boldsymbol{\varepsilon}_0$ are known. Then, using eqs (5—100)–(5—107), the global stiffness matrix $\mathbf{K}_0$ corresponding to this state of the continuum can be calculated. $\mathbf{K}_0$ is equal to the *local gradient* of the force–displacement relationship of the continuum at any point and is called the *tangential stiffness matrix*. Increasing the external loads by $\Delta\mathbf{p}_0$ and using the tangential stiffness matrix $\mathbf{K}_0$, the approximate values of the corresponding displacement, stress and strain increments $\Delta\mathbf{q}_0$, $\Delta\boldsymbol{\sigma}_0$ and $\Delta\boldsymbol{\varepsilon}_0$ can be determined. These lead to the approximate results $\mathbf{q}_1 = \mathbf{q}_0 + \Delta\mathbf{q}_0$, $\boldsymbol{\sigma}_1 = \boldsymbol{\sigma}_0 + \Delta\boldsymbol{\sigma}_0$ and $\boldsymbol{\varepsilon}_1 = \boldsymbol{\varepsilon}_0 + \Delta\boldsymbol{\varepsilon}_0$ which correspond to the load $\mathbf{p}_1 = \mathbf{p}_0 + \Delta\mathbf{p}_0$. To improve this solution, another tangential stiffness matrix $\mathbf{K}_1$ can be calculated from these variables and, using eq. (5—109) the unbalanced forces

$$\Delta\mathbf{p}_0^r = \mathbf{K}_1\mathbf{q}_1 - \mathbf{p}_1 \tag{5—110}$$

can be determined. These forces can be interpreted as *residual forces*, which indicate the measure of the departure from the exact solution. Applying these forces as load increments, the step described above has to be repeated until the iterative process converges to the solution, indicated by the disappearance of the residual forces.

On finishing the iteration, the external load $\mathbf{p}_1$ may be increased again by $\Delta\mathbf{p}_1$ and the above iteration then has to be repeated. Applying further load increments, the requested magnitude of the external load can be reached.

The iterative process sometimes referred to as the generalized *Newton–Raphson method*, is illustrated for a single variable in Fig. 5—34(a).

(2) *The initial stiffness method.* In the case of the tangential stiffness method, in each step of the iterative process a new stiffness matrix has to be calculated and a complete solution has to be obtained, which needs a great deal of computational work. The idea of the initial stiffness method is to replace the tangential stiffness matrix in the global equation by the stiffness matrix corresponding to the *initial* step of the process in all steps of the iterations. In this way the solution of equation $\mathbf{K}d\mathbf{q} = d\mathbf{p}$ for $d\mathbf{q}$ has only to be performed for the first step of iteration, because the subsequent solutions merely necessitate the proportional reduction of the solution obtained from the first step. In determining the residual forces defined by eq. (5—110) even in this case the tangential stiffness matrix has to be used, but this calculation does not involve the inversion of the stiffness matrix.

It can be seen that the main advantage of the initial stiffness method is that the stiffness matrix has to be converted only once in the iteration process. This significantly reduces the computing time per iteration, but decreases the convergence rate. The most economical algorithm is generally provided by the combination of the two methods, in which the stiffness matrix is changed only at selected steps of the iterative process.

The solution algorithm of the initial stiffness method is illustrated for a single variable function in Fig. 5—34(b).

To examine the calculation of the residual forces, which play an important role in the iterations described above, let us assume that the stress and strain increments $\Delta\boldsymbol{\sigma}_0$ and $\Delta\boldsymbol{\varepsilon}_0$ calculated from the load increment $\Delta\mathbf{p}_0$ by the use of the stiffness matrix $\mathbf{K}_0$, are known. Then, the first approximation for the stresses caused by the load $\mathbf{p}_1=\mathbf{p}_0+\Delta\mathbf{p}_0$ is $\boldsymbol{\sigma}_1=\boldsymbol{\sigma}_0+\Delta\boldsymbol{\sigma}_0$. Now, depending on the satisfaction of the yield condition, three different kinds of elements can be distinguished.

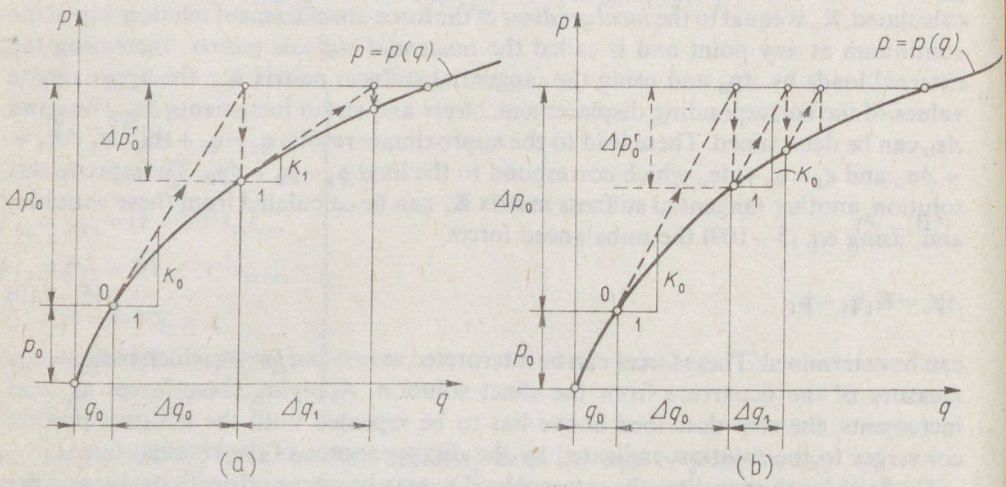


Fig. 5–34

(a) In the elements where $f(\boldsymbol{\sigma}_0)\leq 0$ and $f(\boldsymbol{\sigma}_1)\leq 0$, the correction of the stresses $\Delta\boldsymbol{\sigma}_0$ is not needed because here the yield conditions are not violated.

(b) In the elements where $f(\boldsymbol{\sigma}_0)=0$ and $f(\boldsymbol{\sigma}_1)>0$, the stresses have to be reduced in order to satisfy the yield condition, i.e. the point B shown in Fig. 5—35(a) must be brought onto the yield surface by allowing plastic deformation to occur. The stress increment $\Delta\boldsymbol{\sigma}'_0$ corresponding to the strain increment $\Delta\boldsymbol{\varepsilon}_0$ can be obtained from the elasto-plastic constitutive equation

$$\Delta\boldsymbol{\sigma}'_0=\mathbf{D}\Delta\boldsymbol{\varepsilon}_0, \tag{5—111}$$

where, using eqs (5—104)–(5—107), the matrix $\mathbf{D}$ is calculated on the basis of the stresses $\boldsymbol{\sigma}_1$. Then, the (residual) stresses which have to be removed from the element in order to satisfy the yield condition are obtained from the relationship

$$\Delta\boldsymbol{\sigma}^{\mathrm{r}}_0=\Delta\boldsymbol{\sigma}_0-\Delta\boldsymbol{\sigma}'_0. \tag{5—112}$$

(c) In the elements where $f(\boldsymbol{\sigma}_0)<0$ and $f(\boldsymbol{\sigma}_1)>0$, that portion of the stress increment $\Delta\boldsymbol{\sigma}_0$ which violates the yield condition has first to be calculated. According to Fig. 5—35(b), this portion is equal to $\dfrac{AB}{AC}\Delta\boldsymbol{\sigma}_0$. Considering this stress increment, the

problem is reduced to case (b) and the corresponding residual stresses can be determined from eqs (5—100) and (5—112).

When the residual stresses $\Delta\boldsymbol{\sigma}_0^r$ are known, the equivalent nodal forces on the elements can be calculated from eqs (5—102) and (5—103) as below

$$\Delta\mathbf{Q}_0^r = \int \mathbf{B}^T \Delta\boldsymbol{\sigma}_0^r \mathrm{d}A. \tag{5—113}$$

The assembly of these nodal forces provides the unbalanced external forces $\Delta\mathbf{p}_0^r$ which form the basis of the next step of the iterative process.

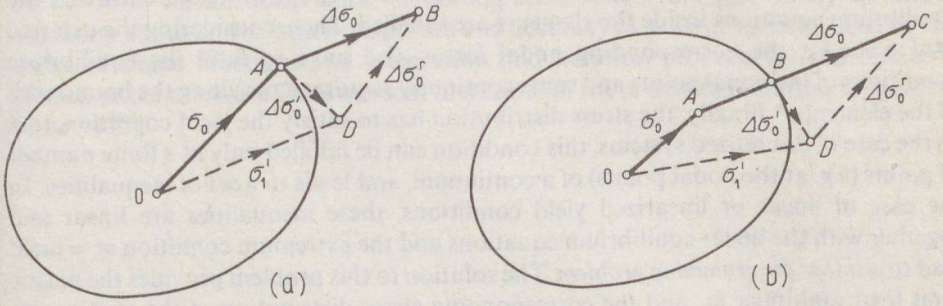


Fig. 5–35

If relatively large load increments are applied, the stress point D shown in Fig. 5—35, and obtained after the reduction of the stress increment $\Delta\boldsymbol{\sigma}_0$, may depart significantly from the yield surface. In order to remove the excess stress violating the yield condition, further reductions should be applied. This can be achieved by simply scaling the vector $\boldsymbol{\sigma}_1'$ or by using further iteration (see e.g. Owen–Hinton 1980).

Finally, it is to be noted that the incremental analysis of an elasto-plastic continuum or structure modelled by the finite element method can be based on the use of mathematical programming methods (see e.g. Grierson, Gladwell 1971; Maier, Giacomini, Paterlini 1976; Cohn, Maier 1977).

5.4.4. LIMIT ANALYSIS

The finite element method can also be used for the plastic limit analysis of continua and structures. One method of solution is to conduct an incremental analysis and find the load at which a small (theoretically zero) increase in the load causes very large (theoretically unrestricted) plastic deformations and deflections.* The corresponding solution will then give approximate values for the plastic limit load and the stresses, strains and displacements arising in the plastic limit state of the continuum or structure.

* The plastic limit state of the continuum or structure cannot be reached, because in this state the stiffness matrix $\mathbf{K}$ becomes singular.

Limit analysis can also be based on the lower or upper bound theorems of plasticity. Some details of this analysis connected with the finite element method will be presented below.

5.4.4.1. LOWER BOUND SOLUTION

The application of the lower bound theorem of limit analysis is based on the finite element *force method*. To construct *statically admissible stress and force fields* first, the stress distribution in the elements has to be defined by shape functions such that the equilibrium equations inside the elements are satisfied. Then, considering the external load $\mathbf{p} = m_s \mathbf{p}_0$, the corresponding nodal forces also have to fulfil the equilibrium conditions of the nodal points and some continuity requirements along the boundaries of the elements.* Finally, the stress distribution has to satisfy the yield condition, too. In the case of discretized systems, this condition can be fulfilled only at a finite number of points (e.g. at the nodal points) of a continuum, and leads to a set of inequalities. In the case of linear or linearized yield conditions, these inequalities are linear and together with the linear equilibrium equations and the extremum condition $m_s = \max!$ lead to a *linear programming problem*. The solution to this problem provides the plastic limit load multiplier m_p and the corresponding stress distribution of the continuum. More details of the numerical procedure can be found elsewhere (see e.g. Livesley 1966; Tottenham, Brebbia 1970; Peano 1977).

In plane problems it is convenient to derive the statically admissible stresses in the elements by making use of *Airy's stress function* (see Section 5.1.2.). Besides, stress resultants (normal and shear forces and couples) acting on the boundaries of the elements rather than the nodal forces, may be introduced as the unknown variables. This formulation of the problem automatically ensures the continuity of stresses along the boundaries of the elements, and using a linear or linearized yield condition also leads to a linear programming problem (Kaliszky 1979).

5.4.4.2. UPPER BOUND SOLUTION

The application of the upper bound theorem of limit analysis is based on the finite element *displacement method*. To construct *kinematically admissible strain rate and velocity fields*, first the strain rate distributions of the elements have to be defined by shape functions such that the strain–displacement relationships inside the elements are satisfied. The corresponding nodal velocities also have to fulfil the kinematic boundary conditions and the continuity requirements along the boundaries of the elements.** Finally, using eqs (3—65) and (3—66) and the plastic flow rule, the kinematically admissible load multiplier m_k can be expressed in terms of the nodal velocities. In the

* It has been shown in Section 3.5.1. that in plasticity certain discontinuities in the stress field are permitted.

** It was shown in Section 3.5.2. that in plasticity certain discontinuities of the strain rate and velocity fields are permitted.

case of a linear or linearized yield condition this expression will also be linear. Then, the kinematic equations of the nodal velocities together with the minimum condition m_k = min! lead to a *linear programming problem*, from which the plastic limit load multiplier m_p and the corresponding nodal velocities can be determined.

More details about the application of linear programming to the analysis of discretized structures are given in Section 6.

The above presentation was intended to give a brief introduction to the extension of finite element techniques to plasticity. This area is still in development; the topics of constitutive modelling for anisotropic materials, cyclic loading and temperature effects are far from an adequate state of development. There are also many questions remaining about convergence properties and accuracy in general, as influenced by the choice of shape functions and integration and iteration procedures. The reader is referred to the extensive finite element literature for more detailed information (Oden, Bathe 1978).

6. PLASTIC ANALYSIS AND DESIGN OF BAR STRUCTURES

The main subject of this chapter is the application of the general theorems presented in Chapter 3 to the plastic analysis and design of bar structures, and the illustration of the details of application by the solution of several simple problems.

The first part of the chapter deals with the yield conditions of bar members and the concept of plastic hinges. The elasto-plastic analysis of simply supported and continuous beams and the incremental elasto-plastic analysis of frames are then discussed.

The next part of the chapter is devoted to the application of the lower and upper bound theorems of limit analysis to bar structures. The solutions are illustrated by several examples, including the case where the structure is subjected to distributed loads. Next, the principles and methods of limit analysis are generalized for structures subjected to general (multi-parameter) loading conditions, and the effect of the interaction of internal forces on the collapse load is discussed.

In the plastic analysis of structures, deflections can play an important role. The chapter therefore presents a method for estimating deflections at the point of collapse, and discusses in detail the problems of alternating and progressive plastic flow. In connection with these problems, the static theorem of shakedown analysis is applied to bar structures. Finally, the effect of deflections on the collapse load is also briefly described.

The next part of the chapter deals with the optimal plastic design of bar structures. After a summary of the general principles, the optimal design methods for structures with piece-wise constant and with continuously variable cross-sections are presented.

The last part of the chapter deals with the application of mathematical programming to the incremental, limit and shakedown analysis and the optimal design of bar structures.

6.1. INTRODUCTORY REMARKS

The plastic methods of structural analysis are widely used in the analysis and design of steel and reinforced concrete beams and frames. They lead to rational and economical solutions, and have the advantage of simplicity.

The objective of *plastic analysis* is to predict the load at which a structure will collapse through the development of excessive plastic deformations, while in the case of

plastic design the dimensions of a structure are to be determined so that collapse is avoided. In addition, it both cases some additional investigations may be necessary to predict the permanent deformations developing and accumulating during the expected loading procedure for the structure.

To illustrate the problem, let us consider an elasto-plastic (e.g. steel) structure loaded by monotonically increasing external forces. First, let us assume that the overall and local instability effects, and the influence of deflections on the stress distribution, are negligibly small and therefore, that *small deflection theory* can be used for the analysis of the structure. Then, the relationship between the intensity of the load (m) and the deflection of a characteristic point in the structure (e) has a typical shape, as shown by the continuous line in Fig. 6—1.

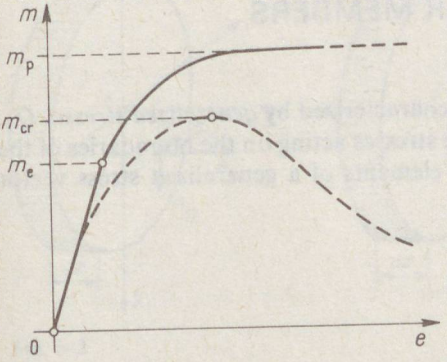


Fig. 6–1

Before reaching the *elastic limit load* m_e, the structure is in a purely elastic state. On increasing the load, plastic deformations start to develop and at the *plastic limit load* m_p, the deflections begin to increase very rapidly for small increases in the load. This indicates that the *plastic collapse* of the structure is being approached. Idealizing this phenomenon, we assume that in this state of plastic collapse *the structure undergoes unrestricted plastic deformations and deflections under a constant load.* This assumption can be applied, however, only to the incipient state of plastic collapse. When larger deformations develop, second order effects can be significant and the equilibrium of a structure can be maintained only at decreasing ("strain softening" structure) or increasing ("strain hardening" structure) external loads. The determination of the plastic limit load is the subject of *limit analysis.*

In those cases where the influence of changes in geometry on the stress distribution within the structure is already significant at lower loads, collapse may occur because of *loss of stability*, and therefore the load–displacement relationship has a different character, as shown in Fig. 6—1 by the dashed line. Then, depending on the slenderness of the structure, the corresponding *critical load* m_{cr} may be much lower than the plastic limit load m_p and can be determined by *large deflection theory.*

When a structure is loaded beyond the elastic limit, plastic deformations develop and permanent deflections remain after unloading. If plastic deformations accumulate

without limits, they lead to *progressive plastic flow*, called *incremental collapse*. On the other hand, in the case of cyclic loading *alternating plastic flow* may occur, which can cause failure. These phenomena can be prevented, however, if the magnitudes of the loads are kept below certain limits which are determined by *shakedown analysis*.

The major part of this chapter will deal with the limit analysis and plastic design of bar structures based on small deflection theory. In addition, the methods of calculation of the elasto-plastic and permanent deflections and the application of shakedown analysis will also be presented* and the influence of large deflections on the load-carrying capacity will be briefly discussed. Since all these investigations are based on the plastic properties of the individual bar members of the structure, the yield conditions of the bar members will first be discussed.

6.2. YIELD CONDITIONS FOR BAR MEMBERS

6.2.1. GENERAL RELATIONSHIPS

(1) The state of stress of a *bar member* can be characterized by *generalized stresses* Q_1, $Q_2, \ldots, Q_n$ obtained by the integration of the stresses acting on the boundaries of the member. They will be considered to be the elements of a generalized stress vector $Q_i(Q_1, Q_2 \ldots Q_n)$, and they represent the

axial force $N = \int_{(A)} \sigma_{zz} dA,$

shear forces $S_x = \int_{(A)} \sigma_{zx} dA,$

$S_y = \int_{(A)} \sigma_{zy} dA,$

bending moments $M_x = \int_{(A)} \sigma_{zz} y dA,$

$M_y = \int_{(A)} \sigma_{zz} x dA$

and torque $T = \int_{(A)} (x\sigma_{zy} - y\sigma_{zx}) dA$

acting on the cross-sections, as shown in Fig. 6—2.

Sometimes it is convenient to introduce the dimensionless magnitudes of the generalized stresses

$$\bar{Q}_i = \frac{Q_i}{Q_{ip}}; \quad (i = 1,2,\ldots n), \tag{6—1}$$

where Q_{ip} denotes that magnitude of Q_i which causes a fully plastic state in the member while all the other generalized stresses are zero. For example, if Q_1 denotes a bending moment M, then $\bar{Q} = \frac{M}{M_p}$, where M_p is the *fully plastic moment* of the cross-section.

* These concepts have already been briefly illustrated in connection with the analysis of a simple bar structure in Section 4.1.

(2) The state of strain of a bar member can be characterized by *generalized strains* q_1, q_2, ... q_n which describe the relative displacements between the boundaries of the member. They are considered to be elements of a generalized strain vector q_i (q_1 q_2 ... q_n), and defined such that the scalar product of Q_i and q_i gives the *specific strain energy* of a member

$$d = Q_i q_i = Q_1 q_1 + Q_2 q_2 + \ldots Q_n q_n. \tag{6—2}$$

Following the basic assumption of plasticity, the generalized strains can be decomposed into elastic and plastic parts

$$q_i = q_i^e + q_i^p. \tag{6—3}$$

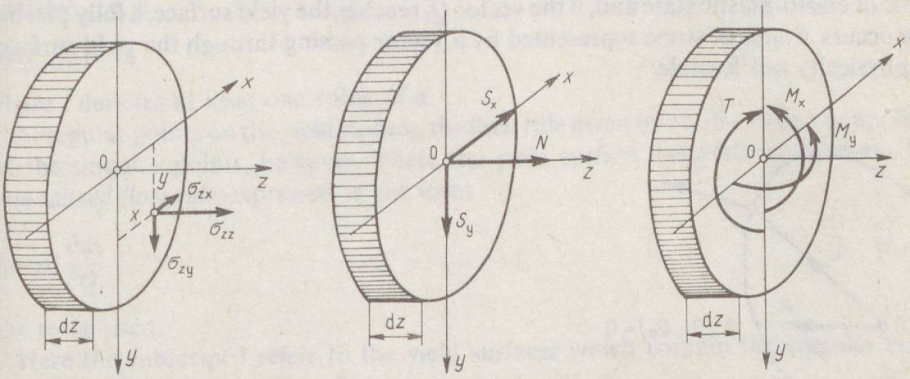


Fig. 6–2

In *rigid-plastic structures*, the elastic part vanishes and $q_i = q_i^p$. The increments in the generalized strains and the generalized strain rates will be denoted by dq_i and $\dot{q}_i$, respectively.

In the following, only those stress resultants which appear in the equation (6—2) for the strain energy will be called generalized stresses. If, for example, the shear deformation of a member is neglected, then the corresponding term in equation (6—2) will vanish and the corresponding shear force will not be considered as a generalized stress; it will be considered as a *reaction*.

(3) At lower magnitudes of the generalized stresses, a bar member is in a purely elastic state. Increasing the generalized stresses, however, more and more parts of the member start to yield and finally it becomes fully plastic. Under constant stresses unrestricted plastic deformations can then develop, which indicate the onset of the plastic limit of the member. The mathematical relationship which defines all those combinations and magnitudes of the generalized stresses which cause a fully plastic state is called the *yield condition* of the member. This yield condition is expressed in the general form

$$\phi(Q_i, Q_0) \leq 0. \tag{6—4}$$

The case $\phi < 0$ corresponds to the elastic or elasto-plastic state, while, if $\phi = 0$ and $\dot{\phi} = 0$, unrestricted plastic deformations can develop. When $\phi \leq 0$ and $\dot{\phi} < 0$ the member is being unloaded, and the case $\dot{\phi} > 0$ is physically not feasible.

In the yield condition (6—4) Q_0 denotes a constant containing the yield stress of the material and the dimensions of the member (e.g. it might be the fully plastic moment of the cross-section). Note that the yield condition is expressed in terms of the generalized stresses; the reaction-type stress resultants defined above do not play a role in the yield condition of the members, and therefore have no direct influence on the load-carrying capacity of a structure.

(4) In an n-dimensional *stress space* the state of stress of a bar member can be represented by the generalized stress vector Q_i, while the yield condition $\phi(Q_i, Q_0)=0$ is illustrated by a hypersurface, called the *yield surface* (Fig. 6—3). In the case of a perfectly plastic material, the yield surface is *convex* (Hodge 1959). When the tip of the stress vector Q_i is inside the domain bounded by the yield surface, the member is in an elastic or elasto-plastic state and, if the vector Q_i reaches the yield surface, a fully plastic state occurs. States of stress represented by a vector passing through the yield surface are physically not feasible.

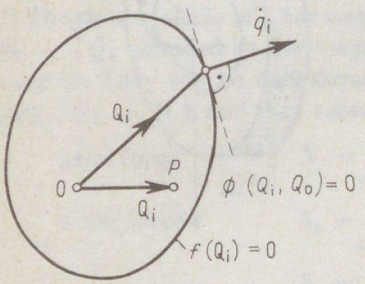


Fig. 6–3

(5) In the following, we are going to study only the plastic limit state of the bar members, and therefore in accordance with the theorem of constant stresses (see Section 3.4.3.2.) we will assume that the material is *rigid-perfectly plastic*. Hence, the total generalized strain and strain rate are identical with the plastic strain and strain rate, respectively, i.e. $q_i=q_i^p$ and $\dot{q}_i=\dot{q}_i^p$.

In an n-dimensional *strain space* coaxial with the stress space, the state of strain of a rigid-perfectly plastic bar member is represented by the generalized plastic strain rate vector $\dot{q}_i$. If $\phi<0$, the vector $\dot{q}_i$ vanishes. If $\phi=0$, $\dot{q}_i$ can be different from zero and, for convenience, might be attached to the tip of the stress vector Q_i inducing the fully plastic state of the bar member. Making use of eq. (2—89) it can be proved that the vector $\dot{q}_i$ coincides with the outward normal at the corresponding point on the yield surface (Hodge 1959). Hence, similarly to the plastic strain rates for a particle of a body, the *normality rule* is also valid for the generalized plastic strain rates and is expressed by the *flow rule*

$$\dot{q}_i=\lambda\frac{\partial\phi}{\partial Q_i}. \tag{6—5}$$

Here $\dot{\Lambda}$ is an unspecified *plastic multiplier*, which defines the magnitude of the plastic strain rate vector.

If $\phi<0$ or $\phi=0$ and $\dot{\phi}<0$, then $\dot{\Lambda}=0$,

if $\phi=0$ and $\dot{\phi}=0$, then $\dot{\Lambda}\geq 0$.

In many cases the yield condition for a bar member is defined by several yield functions in the form

$$f_\alpha(Q_i,Q_0)\leq 0, \quad (\alpha=0,1,2,\ldots m). \tag{6—6}$$

The member is in the plastic limit state if at least one of the yield functions in eq. (6—6) vanishes, i.e. if

$$\phi_l(Q_i,Q_0)=0,$$

where l denotes at least one value of α.

At regular points on the yield surface, the flow rule given by eq. (6—5) can be applied. At the singular points, however, where the yield surface has vertices (corners), the *generalized flow rule* expressed in the form

$$\dot{q}_i=\dot{\Lambda}_l\frac{\partial\phi_l}{\partial Q_i} \tag{6—7}$$

has to be used.

Here the subscript l refers to the yield surfaces which contain the singular point under consideration, i.e. for which

$$\phi_l(Q_i,Q_0)=0.$$

From a geometrical point of view, the generalized flow rule expresses the fact that, at a singular point on the yield surface, the generalized plastic strain rate vector may have any direction within the fan or cone formed by the outward normals at all points adjacent to the singular point. This is shown symbolically in Fig. 6—4.

The yield condition for a bar member can be expressed in terms of the dimensionless generalized stresses $\bar{Q}_i=\dfrac{Q_i}{Q_{ip}}$ defined by eq. (6—1). Then, the yield condition has the general form

$$\phi(\bar{Q}_i)\leq 0$$

and the flow rule assumes a modified expression

$$\dot{q}_i=\dot{\Lambda}\frac{\partial\phi}{\partial Q_i}=\dot{\Lambda}\frac{\partial\phi}{\partial\bar{Q}_i}\frac{\partial\bar{Q}_i}{\partial Q_i}=\frac{1}{Q_{ip}}\dot{\Lambda}\frac{\partial\phi}{\partial\bar{Q}_i}. \tag{6—8}$$

Then, introducing the *reduced generalized strain rates* $\dot{\bar{q}}_i=Q_{ip}\dot{q}_i$, eq. (6—8) becomes*

$$\dot{\bar{q}}_i=\dot{\Lambda}\frac{\partial\phi}{\partial\bar{Q}_i}. \tag{6—9}$$

* For this expression the summation convention is not applied.

Hence, if the yield condition is expressed in terms of the dimensionless generalized stresses $\bar{Q}_i$, the normality rule holds for the reduced generalized plastic strain rates $\dot{\bar{q}}_i$.

(6) In plastic analysis and design, the *specific dissipation of energy* $d = Q_i \dot{q}_i$ plays an important role. A common problem is that only the generalized strain rates are known, and from these the dissipation of energy has to be determined. Considering the convexity and normality rule, for a given generalized strain rate vector $\dot{q}_i$ the yield locus and, consequently, the associated generalized stress vector Q_i, in general, can be uniquely determined and the energy $d = Q_i \dot{q}_i$ can also be calculated. The only exception occurs, when the vector $\dot{q}_i$ is normal to a flat part of the yield surface (see Fig. 6—4).

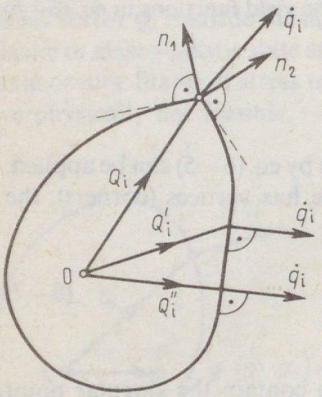


Fig. 6–4

Then, with a given vector $\dot{q}_i$ a set of stress vectors can be associated but even in this case the scalar product $Q_i \dot{q}_i$ is uniquely defined. Hence, we can state that *the specific dissipation of energy can always be uniquely expressed in terms of the generalized plastic strain rates*

$$d = Q_i \dot{q}_i = d(\dot{q}_i). \tag{6—10}$$

Next, we will derive the yield conditions for bar members under different combined loadings and will then discuss the elasto-plastic and fully plastic states of bar members subjected to pure bending.

6.2.2. MEMBERS UNDER COMBINED LOADING

6.2.2.1. BENDING AND TENSION OR COMPRESSION

(1) Let us consider a bar member whose cross-section has one axis of symmetry denoted by y. The member is subjected to a centric axial force N acting at the centroid of the cross-section and to a bending moment M acting in the plane of symmetry of the bar member (Fig. 6—5). We assume that during the elastic and plastic deformations the cross-section remains plane and perpendicular to the bent axis of the bar (*Bernoulli–Navier hypothesis*). Then, the variation in the strains in the member is linear and the

neutral surface, along which the strains are zero, is perpendicular to the plane of symmetry (Fig. 6—5(a)).

At lower magnitudes of the axial force and bending moment, the entire bar member is in an elastic state. On increasing the axial force and/or the bending moment, more and more parts of the member start to yield and at certain magnitudes of N and M the entire member becomes plastic, i.e. at every point $|\sigma| = \sigma_0$ (Fig. 6—5d). The axial force and the bending moment corresponding to this fully plastic state are expressed

$$\left.\begin{aligned} N &= \int_{(A)} \sigma \, dA = -\sigma_0 \int_{(A_1)} dA + \sigma_0 \int_{(A_2)} dA = (A_2 - A_1)\sigma_0, \\ M &= \int_{(A)} \sigma y \, dA = -\sigma_0 \int_{(A_1)} y \, dA + \sigma_0 \int_{(A_2)} y \, dA = (S_{x2} - S_{x1})\sigma_0. \end{aligned}\right\} \qquad (6—11)$$

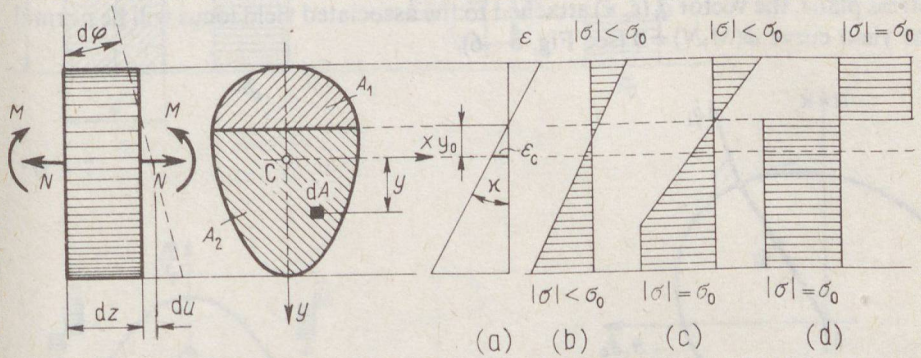


Fig. 6–5

Here A_1 and A_2 denote the areas of the parts of the cross-section separated by the neutral axis and S_{x1} and S_{x2} are the first (static) moments of these parts about the x axis. These areas and first moments are functions of the distance y_0 of the neutral axis from the x axis, therefore eqs (6—11) define the axial forces and moments corresponding to the fully plastic state in parametric form: $N = N(y_0)$ and $M = M(y_0)$. Eliminating y_0 from these equations, the yield condition of the bar member can be obtained

$$\phi(M,N) = 0.$$

This yield condition is represented in the stress plane N, M by a *closed, convex curve*, shown in Fig. 6—6.

The state of strain in the member under consideration is characterized by the relative displacement du and relative rotation $d\varphi$ of the boundary cross-sections, or by their value per unit length $\varepsilon_c = \dfrac{du}{dz}$ and $\kappa = \dfrac{d\varphi}{dz}$. The latter also gives the *curvature* of the

member. In the fully plastic state, the velocities $\dot{\varepsilon}_c$ and $\dot{\kappa}$ are defined by the flow rule given by eq. (6—9)

$$\dot{\kappa}=\dot{\Lambda}\frac{\partial\phi}{\partial M},\quad \dot{\varepsilon}_c=\dot{\Lambda}\frac{\partial\phi}{\partial N}. \tag{6—12}$$

Eliminating the unknown plastic multiplier $\dot{\Lambda}$, the direction of the generalized plastic strain rate vector $\dot{q}_i$ $(\dot{\varepsilon}_c\ \dot{\kappa})$ is defined by the relationship

$$\frac{\dot{\varepsilon}_c}{\dot{\kappa}}=\frac{\dfrac{\partial\phi}{\partial N}}{\dfrac{\partial\phi}{\partial M}}.$$

Illustrating the strain rates in a system of coordinates coaxial with the axes N and M of the stress plane, the vector $\dot{q}_i$ $(\dot{\varepsilon}_c\ \dot{\kappa})$ attached to the associated yield locus will be normal to the yield curve $\phi(M,N)=0$ (see Fig. 6—6).

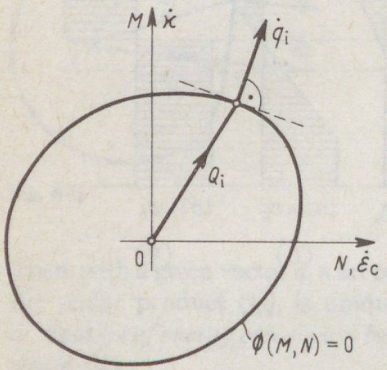


Fig. 6–6

(2) In the case of members with *rectangular cross-sections*, the fully plastic stress diagram can be divided into symmetrical and skew-symmetrical parts (Fig. 6—7) and the corresponding axial force and bending moment can be expressed as

$$N=2y_0a\sigma_0,\quad M=\left(\frac{b}{2}-y_0\right)a\sigma_0\frac{1}{2}\left(\frac{b}{2}+y_0\right).$$

Eliminating y_0 from these equations leads to

$$\phi=\left|\frac{M}{M_p}\right|+\left(\frac{N}{N_p}\right)^2-1=0. \tag{6—13}$$

Here

$$M_p=\frac{ab^2}{4}\rho_0\quad\text{and}\quad N_p=ab\sigma_0$$

are the load-carrying capacity of the member in pure bending and in pure tension, respectively, and the absolute sign expresses the fact that the same yield condition can be obtained if the bending moment has the opposite sense. Correspondingly, the yield condition is illustrated by two parabolas, as shown in Fig. 6—8. For comparison, the domain of the purely elastic state of the member is also indicated in the Figure. This *elastic domain* is bounded by four lines defined by the equation

$$\left|\frac{M}{M_e}\right|+\left|\frac{N}{N_e}\right|-1=0,$$

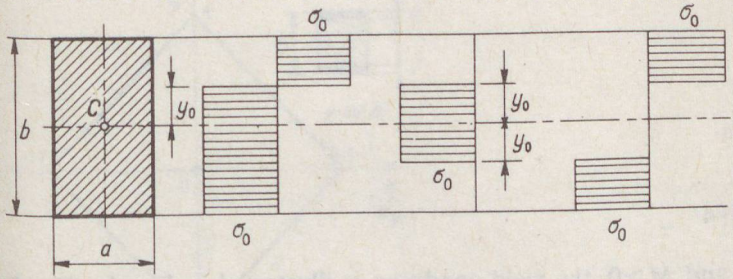


Fig. 6–7

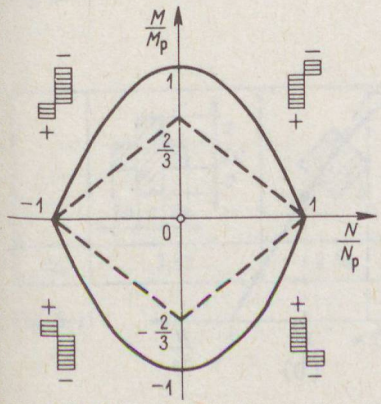


Fig. 6–8

where

$$M_e=\frac{2}{3}M_p=\frac{ab^2}{6}\sigma_0 \quad \text{and} \quad N_e=N_p=ab\sigma_0.$$

(3) In the case of *idealized I- cross-sections* we assume that the flange thickness v_1 is small compared with the height h of the cross-section, and therefore the ratio v_1/h can be neglected in the derivations (Fig. 6—9(a)). Omitting the details (see e.g. Neal 1977), the yield condition becomes

if the neutral axis intersects the web $\left(\frac{N}{N_p} \leq \kappa\right)$:

$$\phi_1 = \frac{|M|}{M_p} + \frac{1}{\kappa(2-\kappa)}\left(\frac{N}{N_p}\right)^2 - 1 = 0, \tag{6—14}$$

if the neutral axis intersects the flange $\left(\frac{N}{N_p} \geq \kappa\right)$:

$$\phi_2 = \frac{2-\kappa}{2}\frac{|M|}{M_p} + \frac{|N|}{N_p} - 1 = 0. \tag{6—15}$$

Here

$$N_p = (hv + 2av_1)\sigma_0,$$

$$M_p = \left(av_1 h + \frac{vh^2}{4}\right)\sigma_0,$$

$$\kappa = \frac{N_{wp}}{N_p}, \quad N_{wp} = hv\sigma_0.$$

For the case $N \geq 0$ and $M \geq 0$, the yield condition is illustrated in Fig. 6—9(b). It consists of a straight line and a parabola. For typical steel I-sections, κ varies between 0.3 and 0.5.

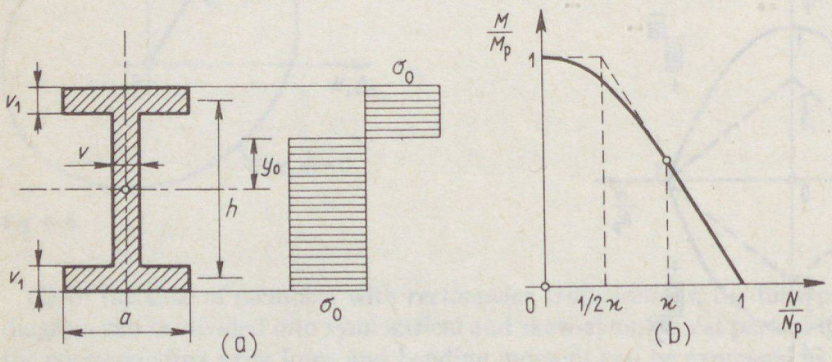


Fig. 6–9

(4) If in eq. (6—15) κ tends to zero, the yield condition for a member of a *sandwich bar* is obtained

$$\phi = \frac{|M|}{M_p} + \frac{|N|}{N_p} - 1 = 0. \tag{6—16}$$

Here $M_p = vha\sigma_0$ and $N_p = 2va\sigma_0$. This yield condition is represented by the four straight lines shown in Fig. 6—10.

(5) The yield condition for bar members with *various cross-sections* shown in Fig. 6—11 can be approximated by the following expression (Garai, Kaliszky 1957)

$$\phi = \frac{|M|}{M_p} + \left|\frac{N}{N_p}\right|^{\alpha} - 1 = 0. \tag{6—17}$$

Here M_p and N_p denote the load-carrying capacity of the members in pure bending and pure tension, respectively, and values of the exponent α are given in Fig. 6—11.

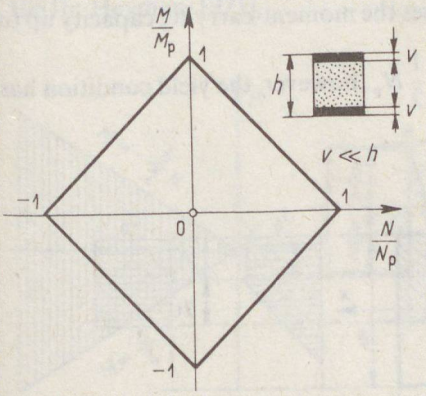


Fig. 6–10

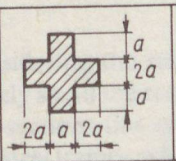
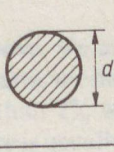
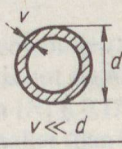
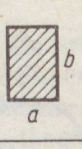
					
α	3,12	2,56	2,00	1,68	2,00

Fig. 6–11

(6) The yield condition for a bar member with a *rectangular cross-section* whose material has *no tensile strength* can be determined from the stress diagram shown in Fig. 6—12. The compression force and the bending moment, which simultaneously cause a fully plastic state in the member, are

$$N = -2y_1 a\sigma_0, \quad M = 2y_1 a\sigma_0\left(\frac{b}{2} - y_1\right).$$

Eliminating the distance y_1, the yield condition is found to be

$$\phi = 2\frac{N}{N_p} + 2\left(\frac{N}{N_p}\right)^2 + \frac{|M|}{M_p} = 0, \quad N \le 0, \tag{6—18}$$

where

$$N_p = ab\sigma_0 \quad \text{and} \quad M_p = \frac{ab^2}{4}\sigma_0.$$

This yield condition is illustrated in Fig. 6—13. We notice that in all the former cases, when the material had the same properties in tension and in compression, the increase in the axial force decreased the moment-carrying capacity of the member. In the present problem, when the material has no tensile strength, the increase in the compressive force up to $N = -\frac{1}{2}N_p$ also increases the moment-carrying capacity up to $M = \frac{1}{2}M_p = \frac{1}{8}ab^2\sigma_0$. In the region $-N_p \leq N \leq \frac{1}{2}N_p$, however, the yield condition has a decreasing character.

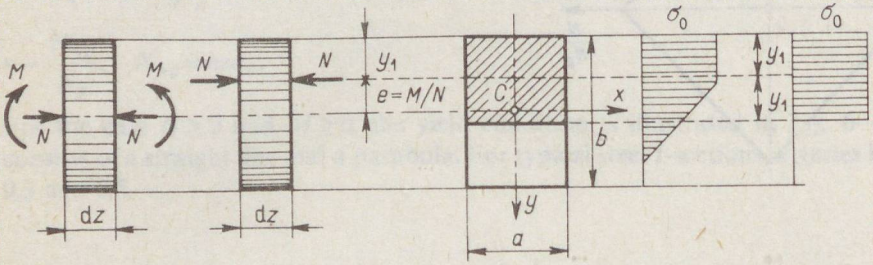


Fig. 6–12

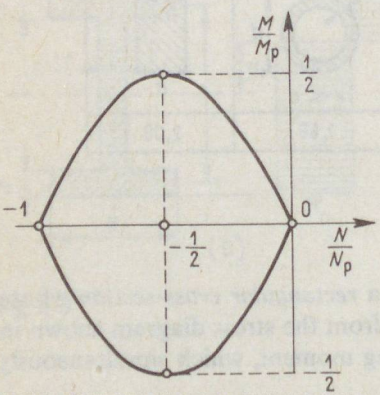


Fig. 6–13

(7) Finally, let us consider an ideal case when the material of the bar member has no *tensile strength* and its *compressional strength* is *infinite*. Then the axial compressive force N can be increased infinitely and the bending moment reaches its maximum possible value if the neutral axis is shifted to the top or to the bottom of the cross-

section, i.e. if $y_1 \to 0$ (see Fig. 6—12). Then, the corresponding moment is equal to $M = \pm N \frac{b}{2}$ and the yield condition has the form

$$\phi = \frac{b}{2} N + |M| = 0, \quad N \leq 0. \tag{6—19}$$

This yield condition, illustrated by two straight lines in Fig. 6—14, can be used for the approximate plastic analysis of structures made of concrete, stone or brick (Kaliszky 1961b; Heyman 1971).

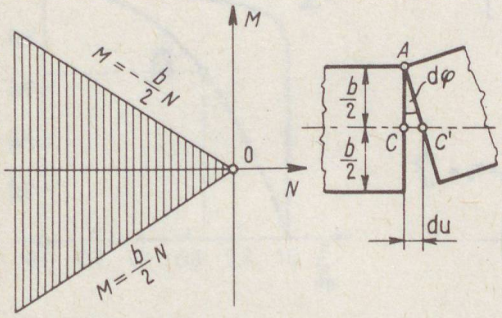


Fig. 6–14

Considering the results derived above, we can conclude that if the axial force is relatively small the reduction in the plastic moment is not significant. For example, for steel *I*-sections this reduction is less than 2% when $|N| \leq 0.1 N_p$. Therefore in single-storey steel frames, where the axial force is usually smaller than $0.1\, N_p$, the effect of axial forces can be neglected. In the columns of multi-storey frames and shallow arches, however, the interaction between the bending moment and the axial force can be of greater importance and has to be taken into account.

6.2.2.2. BENDING AND SHEAR

Under the action of bending moment and shear force the material points in a bar member are in a biaxial state of stress, and therefore the derivation of the yield condition is a more difficult problem (see e.g. Neal 1977). In the following, only the approximate solutions to this problem will be discussed.

(1) Let us consider a bar member with a *rectangular cross-section* subjected to a bending moment M and a shear force S, as shown in Fig. 6—15. An approximate stress distribution can be assumed, such that at the upper and lower parts of the member the normal stresses reach the yield stress σ_0, while in the middle portion the variations in the normal stresses and shear stresses is linear and parabolic, respectively. This stress

distribution satisfies the equilibrium equation (5—4) and, if $\tau_{max} \leq \frac{\sigma_0}{\alpha}$, then it also satisfies the yield condition

$$\sigma^2 + \alpha^2 \tau^2 \leq \sigma_0^2 \qquad (6—20)$$

at every point in the member. Here, in the case of Tresca and Huber–v. Mises–Hencky yield conditions, $\alpha = 2$ and $\alpha = \sqrt{3}$, respectively. Hence, the stress distribution shown in Fig. 6—15 is statically admissible and provides a lower bound solution for the yield condition for the member. The corresponding bending moment and shear force are

$$M = M_p \left[1 - \frac{1}{3}\left(\frac{2y_0}{b}\right)^2\right], \quad S = S_p \left[\frac{2y_0}{b}\right], \quad \text{respectively,}$$

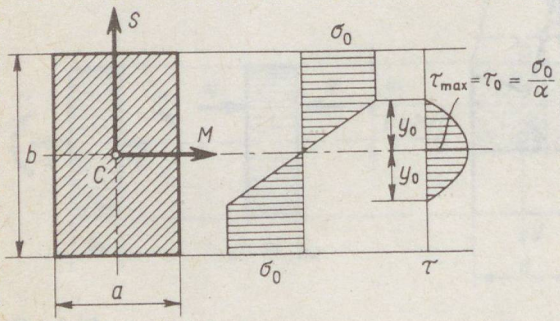


Fig. 6–15

where

$$M_p = \frac{ab^2}{4}\sigma_0 \text{ and } S_p = ab\frac{\sigma_0}{\alpha}.$$

Eliminating y_0 from these expressions, the yield condition becomes

$$\phi = \frac{|M|}{M_p} + \frac{3}{4}\left(\frac{S}{S_p}\right)^2 - 1 = 0. \qquad (6—21)$$

Since the shear force determined from the stress diagram shown in Fig. 6—15 cannot exceed $\frac{2}{3}S_p$ this yield condition is valid only when $|S| \leq \frac{2}{3}S_p$. In the range $\frac{2}{3}S_p \leq |S| \leq S_p$, the yield condition has to be derived on the basis of other assumptions which lead to fairly complicated calculations (Neal 1977). The description of this solution is omitted because the range $\frac{2}{3}S_p \leq |S| \leq S_p$ has no practical importance. The yield condition (6—21) is illustrated in Fig. 6—16.

(2) For the yield condition for members with an *idealized I-cross-section* subjected to bending and shear, various approximate solutions have been found (see e.g. Neal 1977). Heyman and Dutton (1954) suggested an empirical relationship which is in good agreement with the more accurate solutions, and has the relatively simple form

$$\frac{|M|}{M_p}+\frac{\kappa}{2-\kappa}\left[1-\sqrt{1-\left(\frac{S}{S_p}\right)^2}\right]-1=0. \tag{6—22}$$

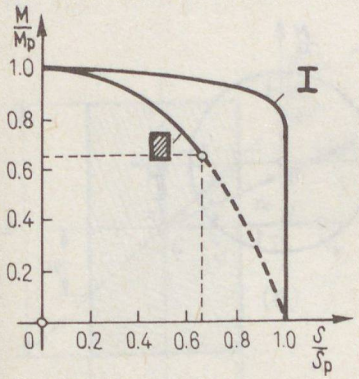


Fig. 6–16

Here $S_p=hv\frac{\sigma_0}{\alpha}$, $\kappa=\frac{hv}{hv+2av_1}$ and the notations are given in Fig. 6—9(a). The yield condition is illustrated in Fig. 6—16. It can be seen that the effect of the shear force on the moment-carrying capacity is very small, and therefore except in some special cases (e.g. short beams) can be neglected.

6.2.2.3. BENDING AND TORSION

Consider a bar member subjected to the combined action of a bending moment M and a torque T (Fig. 6—17(a)). First, let us assume the special cases when $T=0$ and $M=0$, respectively. When $T=0$, the bending moment can reach the fully plastic moment M_p and the normal stress is equal to the yield stress at every point: $|\sigma|=\sigma_0$. When, on the other hand, $M=0$, the torque can reach its plastic limit value T_p (see Section 4.2.5.) and the shear stress is equal to the yield stress in shear at every point*: $|\tau|=\tau_0=\frac{\sigma_0}{\alpha}$.

Let us now consider the general case when $M\neq 0$ and $T\neq 0$. We assume that in the plastic limit state of the member the normal and shear stress distributions are the same

* Here again, in the cases of the Tresca and the Huber–v. Mises–Hencky yield conditions, α is equal to 2 and $\sqrt{3}$, respectively.

as in pure bending and pure torsion, respectively, but that the magnitudes of the stresses are reduced to

$$|\sigma| = \frac{M}{M_p}\sigma_0 \quad \text{and} \quad |\tau| = \frac{T}{T_p}\frac{\sigma_0}{\alpha}.$$

If the yield condition

$$\sigma^2 + \alpha^2\tau = \sigma_0^2 \tag{6—23}$$

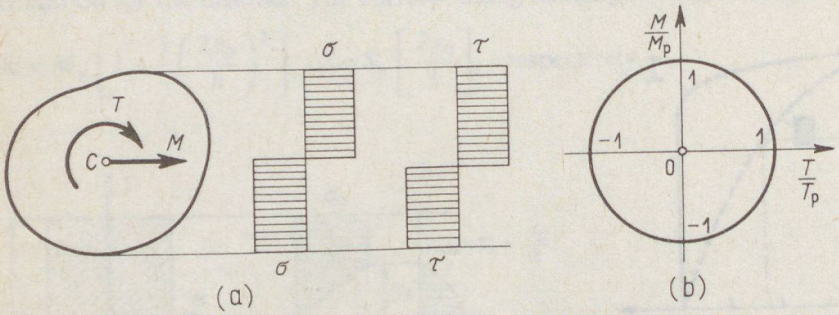


Fig. 6–17

is satisfied at every point in the member then, substituting the expressions for stresses in eq. (6—23), we obtain an approximate expression for the yield condition for members subjected to bending and torsion

$$\phi = \left(\frac{M}{M_p}\right)^2 + \left(\frac{T}{T_p}\right)^2 - 1 = 0. \tag{6—24}$$

This yield condition is illustrated by a circle shown in Fig. 6—17(b).

6.2.2.4. ASYMMETRICAL BENDING

Let us discuss the general case of bending, when the moment vector **M** is not directed along a principal centroidal axis of the cross-section. Then, the vector **M** can be resolved into two components M_x and M_y in the directions of the principal centroidal axes x and y, and the yield condition can be expressed in the general form

$$\phi(M_x, M_y) = 0.$$

(1) Let us consider the asymmetrical bending of a member with a *rectangular cross-section* (Fig. 6—18). In the fully plastic state, the normal stresses are equal to the yield stress at every point in the member and their resultant is identical to the bending moment **M**. Hence, the neutral axis divides the cross-section into two parts of equal area. Its direction, defined by the angle φ or by the distance y_0, does not generally coincide with the vector **M**. Writing the moment equations of stresses about the x and y

axes, one can determine the components M_x and M_y which together result in a fully plastic state of the member

$$\left.\begin{aligned} M_x &= |\mathbf{M}| \cos\alpha = M_{px}\left[1-\frac{4}{3}\left(\frac{y_0}{b}\right)^2\right], \\ M_y &= |\mathbf{M}| \sin\alpha = M_{py}\left(\frac{4}{3}\frac{y_0}{b}\right). \end{aligned}\right\} \tag{6—25}$$

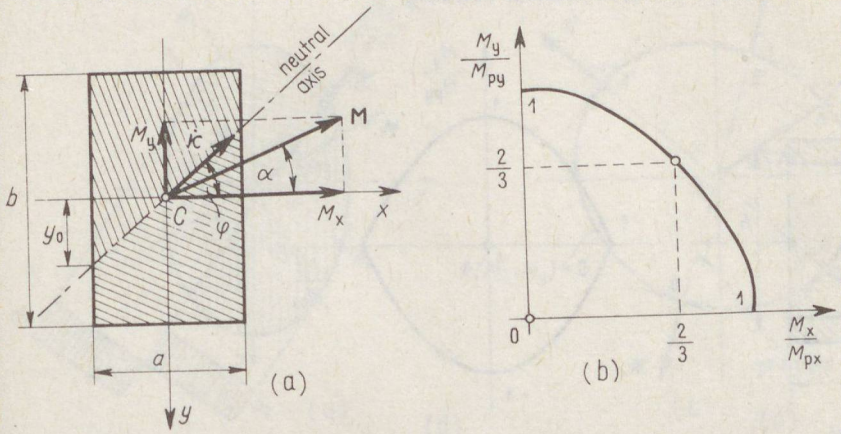


Fig. 6–18

Here $M_{px}=\dfrac{ab^2}{4}\sigma_0$ and $M_{py}=\dfrac{ba^2}{4}\sigma_0$ denote the fully plastic moments when the member is subjected to symmetrical bending about the x and y axes, respectively. Eliminating y_0 from the above expressions, the yield condition for asymmetric bending is obtained

$$\phi=\frac{|M_x|}{M_{px}}+\frac{3}{4}\left(\frac{M_y}{M_{py}}\right)^2-1=0. \tag{6—26}$$

Equations (6—25) are only valid in the range $|y_0|\leq\dfrac{b}{2}$. If $|y_0|>\dfrac{b}{2}$, the neutral axis intersects with side a rather than with side b, and therefore the derivation has to be repeated. The same expressions as eqs (6—25) can be obtained, but the roles of the components M_x and M_y have to be interchanged. Hence, the yield condition for this case has the following form

$$\phi=\frac{|M_y|}{M_{py}}+\frac{3}{4}\left(\frac{M_x}{M_{px}}\right)^2-1=0. \tag{6—27}$$

The yield conditions (6—26) and (6—27) and their ranges of validity are illustrated in Fig. 6—18(b).

(2) The yield condition for a *sandwich member* subjected to asymmetrical bending has the form (Fig. 6—19(a))

$$\phi=\frac{|M_y|}{M_{py}}+\left(\frac{M_x}{M_{px}}\right)^2-1=0, \tag{6—28}$$

where $M_{px}=avh\sigma_0$ and $M_{py}=\frac{va^2}{2}\sigma_0$.

This yield condition, illustrated in Fig. 6—19(b), can provide a good approximation for *I*-sections subjected to asymmetrical bending.

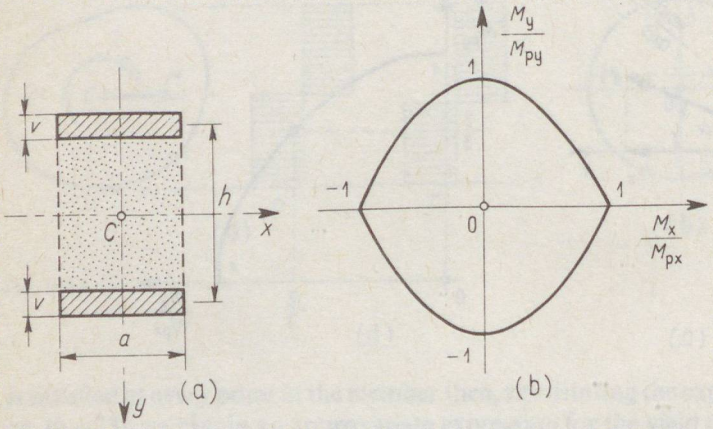


Fig. 6–19

(3) Consider the bending of a bar member with an *arbitrary cross-section* (Fig. 6—20(a)). In the fully plastic state, the normal stresses are equal to the yield stress at every point in the member and their resultant is the bending moment **M**. Hence, the neutral axis divides the cross-section into two portions of equal areas $A_1=A_2=\frac{A}{2}$ such that the resultants of the tensile and compressive stresses acting at the centroids C_1 and C_2 of these areas coincide with the plane of the bending moment. These two requirements uniquely define the position of the neutral axis. Then, the distances v_1 and v_2 of the centroids C_1 and C_2 can be determined, and the fully plastic moment is equal to

$$M_p=(A_1v_1+A_2v_2)\,\sigma_0=\frac{A}{2}(v_1+v_2)\,\sigma_0.$$

Since the first (static) moment of the entire area of a cross-section about a centroidal axis vanishes, i.e. $\frac{A}{2}v_1-\frac{A}{2}v_2=0$, $v_1=v_2=v_0$ and the fully plastic moment of the member becomes

$$M_p=Av_0\sigma_0. \tag{6—29}$$

Here v_0 is a function of the direction of the moment vector. Since both M and v_0 can be expressed in terms of the components M_x and M_y of the bending moment, the yield condition can be expressed in the general form

$$\phi(M_x, M_y)=0.$$

This is illustrated by a *closed, convex curve* in Fig. 6—20(b). Since the magnitude of the fully plastic moment is independent of the sense of the bending moment the curve is symmetrical about the origin of the coordinate system.

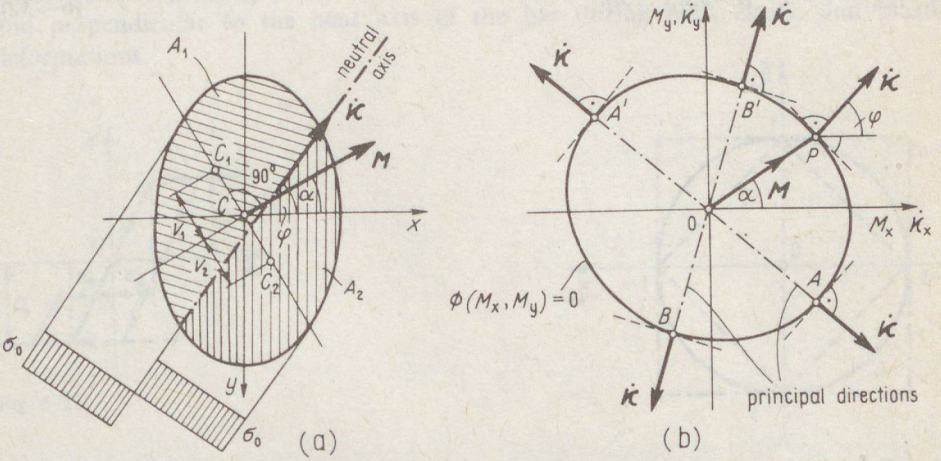


Fig. 6–20

The state of strain in the member under consideration is defined by the *curvature rate vector* $\dot{\boldsymbol{\kappa}}$, which always coincides with the neutral axis. Assuming a coordinate system $\dot{\kappa}_x$, $\dot{\kappa}_y$, coaxial with the axes M_x, M_y, according to the normality rule the vector $\dot{\boldsymbol{\kappa}}$ has to coincide with the outer normal of the yield curve at the associated yield locus. Because of the convexity and point symmetry of the yield curve, one can always find two pairs of points (A, A' and B, B') on the curve where the associated vectors of the bending moment and the curvature rate have the same direction. Since in these cases the neutral axis coincides with the vector of the bending couple, the directions AA' and BB' are called the *principal axes of plastic bending*. Unlike the case of elastic bending, these axes are generally not perpendicular to each other. In the special case, however, when the cross-section has at least one axis of symmetry, the principal axes of plastic bending will also be orthogonal and at least one of them (in the case of double symmetry, both of them) coincides with the axis of symmetry (Rzanicun 1958; Heyman 1971).

6.2.2.5. APPROXIMATE YIELD CONDITIONS

In most cases a good approximation to the yield condition of a bar member can be obtained by using the quadratic expression

$$\phi=\bar{Q}_i\bar{Q}_i-1=\bar{Q}_1^2+\bar{Q}_2^2+\ \ldots\ +\bar{Q}_n^2-1=0. \qquad (6—30)$$

Here $\bar{Q}_i$ denotes the non-dimensional generalized stresses $\bar{Q}_i = \dfrac{Q_i}{Q_{ip}}$. In the general case, the corresponding yield condition is illustrated by a hyper-sphere and in the special case of two variables by a circle, as shown in Fig. 6—21.

Using the linear expressions given below, lower and upper bounds can be obtained for the yield condition for a bar member

$$\phi = |\bar{Q}_1| + |\bar{Q}_2| + \ldots + |\bar{Q}_n| - 1 = 0, \tag{6—31}$$

$$\phi_i = |\bar{Q}_i| - 1 = 0, \quad (i = 1,2,\ldots,n). \tag{6—32}$$

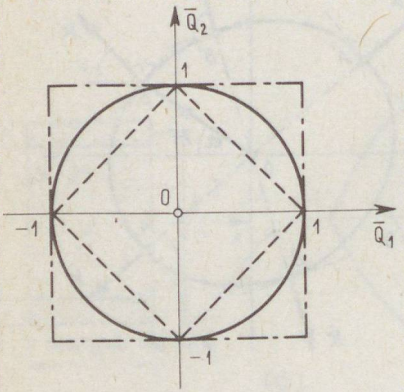


Fig. 6–21

These linear yield conditions are illustrated by hyper-planes or, in the case of two variables, by four straight lines, as shown in Fig. 6—21. The yield condition (6—32) is expressed by n independent equations, which corresponds to the assumption that there is no interaction between the generalized stresses.

Details of several yield conditions for different cross-sections and loading conditions have been published in the literature (e.g. Klöppel, Yamada 1958).

6.2.3. MEMBERS UNDER PURE BENDING

As was mentioned in Section 6.2.2., if the magnitudes of the normal and shear forces and the torque are relatively small, their effect on the plastic moment-carrying capacity of bar members can be neglected. Then, except for the bending moment, all other internal forces are *reactions* and the member can be assumed to be in a state of pure bending. Consequently, the yield condition has the simple form

$$\phi = \left(\frac{M}{M_p}\right)^2 - 1 = 0,$$

or

$$|M| = M_p \tag{6—33}$$

and the *specific dissipation of energy rate* is expressed as

$$d = M\dot{\kappa} = M_p\dot{\kappa}. \tag{6—34}$$

In these expressions, M_p and $\dot{\kappa}$ denote the fully plastic moment and the rate of curvature of the member, respectively.

Since the above approximation is widely used in the plastic analysis of bar structures, we will now study the elasto-plastic and fully plastic state of bar members subjected to symmetrical bending in more detail. We will assume that the material of the members is linearly elastic–perfectly plastic (Fig. 6—22) and that the plane sections remain plane and perpendicular to the bent axis of the bar during both elastic and plastic deformations.

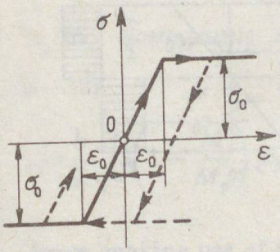


Fig. 6–22

6.2.3.1. LOADING

(1) Consider a bar member with a *rectangular cross-section* subjected to symmetrical bending, as shown in Fig. 6—23. At lower magnitudes of the bending moment M the entire member is in an elastic state and the stresses are obtained from the formula

$$\sigma = \frac{M}{I_x} y, \tag{6—35}$$

where $I_x = \dfrac{ab^2}{12}$ is the moment of inertia of the cross-sectional area with respect to the x axis. The maximum normal stresses arise in the fibres at greatest distance from the x axis and are equal to

$$\sigma_{max} = \frac{M}{Z_e}, \tag{6—36}$$

where $Z_e = \dfrac{I_x}{b/2} = \dfrac{ab^2}{6}$ is the *elastic section modulus*. As the bending moment increases, σ_{max} reaches the yield stress σ_0. The corresponding bending moment

$$M_e = Z_e\sigma_0 = \frac{ab^2}{6}\sigma_0 \tag{6—37}$$

is referred to as the *elastic limit moment* of the member.

As the bending moment increases further, plastic deformations develop in the zones where $|\varepsilon| > \varepsilon_0$, while the stresses remain unchanged*, i.e. $|\sigma| = \sigma_0$. Between the plastic zones, an elastic core exists in which the stress varies linearly. Because of the double symmetry of the cross-section, during this stress redistribution the position of the neutral axis remains unchanged. The bending moment corresponding to this elasto-plastic state of the member can be found as

$$M = \int_{(A)} y\sigma dA = 2\sigma_0 \int_{y_e}^{b/2} y a dy + \frac{\sigma_0}{y_e} \int_{y_e}^{y_e} y^2 a dy = \sigma_0 \left(\frac{ab^2}{4} - \frac{1}{3} a y_e^2 \right). \tag{6—38}$$

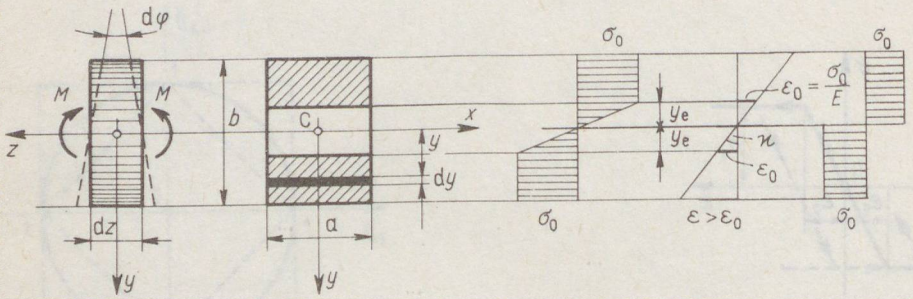


Fig. 6–23

On further increases in the bending moment, the thickness of the elastic core approaches zero ($y_e \to 0$) while M approaches the limit value M_p, called the *plastic limit moment* or *fully plastic moment* of the member. From eq. (6—38) we have

$$M_p = \frac{ab^2}{4} \sigma_0 = Z_p \sigma_0, \tag{6—39}$$

where $Z_p = \frac{ab^2}{4}$ is the *plastic section modulus*. The ratio of the plastic and elastic limit moments, or of the plastic and elastic section moduli, is called the *shape factor* of the cross-section

$$k = \frac{M_p}{M_e} = \frac{Z_p}{Z_e}. \tag{6—40}$$

Considering eqs (6—37) and (6—39) the shape factor for rectangular cross-sections is equal to 3/2, i.e. the plastic limit moment is 50% higher than the elastic limit moment.

The state of strain in the member is characterized by the relative rotation $d\varphi$ between the boundary sections of an infinitesimal element, or by its magnitude per unit length which gives the *curvature* of the member,

$$\kappa = \frac{d\varphi}{dz}. \tag{6—41}$$

* ε_0 is the strain at which the material starts to yield (see Fig. 6—22).

In the *elastic state*, i.e when $M \leq M_e$, the curvature is proportional to the bending moment

$$\kappa = \frac{M}{EI_x},$$

where EI_x is the *flexural stiffness* of the member. Introducing the curvature $\kappa_e = \frac{2\varepsilon_0}{b}$ corresponding to the elastic limit moment M_e (see Fig. 6—23), in the elastic state we can write that

$$\frac{\kappa}{\kappa_e} = \frac{M}{M_e}. \tag{6—42}$$

In the *elasto-plastic state* the curvature is equal to $\kappa = \frac{\varepsilon_0}{y_e}$, where from eq. (6—38)

$$y_e = \frac{b}{2}\sqrt{3\left(1-\frac{M}{M_p}\right)} = \frac{b}{2}\sqrt{\left(3-2\frac{M}{M_e}\right)}. \tag{6—43}$$

Hence, making use of the relationship $\kappa_e = \frac{2\varepsilon_0}{b}$

$$\frac{\kappa}{\kappa_e} = \frac{1}{\sqrt{3\left(1-\frac{M}{M_p}\right)}} = \frac{1}{\sqrt{\left(3-2\frac{M}{M_e}\right)}} \tag{6—44}$$

or

$$\frac{M}{M_e} = 1.5 - 0.5\left(\frac{\kappa_e}{\kappa}\right)^2. \tag{6—45}$$

Eq. (6—45) shows that M approaches $M_p = 1.5M_e$ only if κ tends to infinity. Consequently, the fully plastic state of a member can be reached only at infinitely large deformations. It can be shown, however, that expression (6—45) very rapidly approaches the fully plastic moment and, for example, if the strain in the outer fibres reaches $10\,\varepsilon_0$ the corresponding bending moment is equal to $M = 0.997\,M_p$. Hence, in practice, the fully plastic moment can be regarded as a good approximation to the plastic moment-carrying capacity of bar members.

(2) Consider the general case of *symmetrical bending* when the bar member's cross-section has only one axis of symmetry and the plane of the bending moment contains this axis (Fig. 6—24).

Following the analysis of members with rectangular cross-section in the elastic state the stresses and the curvature of the member are given by the expressions

$$\sigma = \frac{M}{I_x}y \quad \text{and} \quad \kappa = \frac{d\varphi}{dz} = \frac{M}{EI_x}. \tag{6—46}$$

The *elastic limit moment* M_e of the member is reached when the most remote fibre starts to yield. Hence

$$M_e = \frac{I_x}{y_{max}} \sigma_0 = Z_e \sigma_0 \tag{6—47}$$

and the corresponding *elastic limit curvature* is equal to

$$\kappa_e = \frac{M_e}{EI_x}. \tag{6—48}$$

As the bending moment increases, plastic deformations develop in the zones where $|\varepsilon| > \varepsilon_0$, while the stress remains unchanged i.e. $|\sigma| = \sigma_0$. Between the plastic zones an elastic core exists in which the stress varies linearly. Because of the symmetry of the cross-section, the neutral axis remains perpendicular to the axis of symmetry but its position is changed during the stress redistribution. Consequently, in the elasto-plastic state the neutral axis is generally not a centroidal axis of the cross-section.

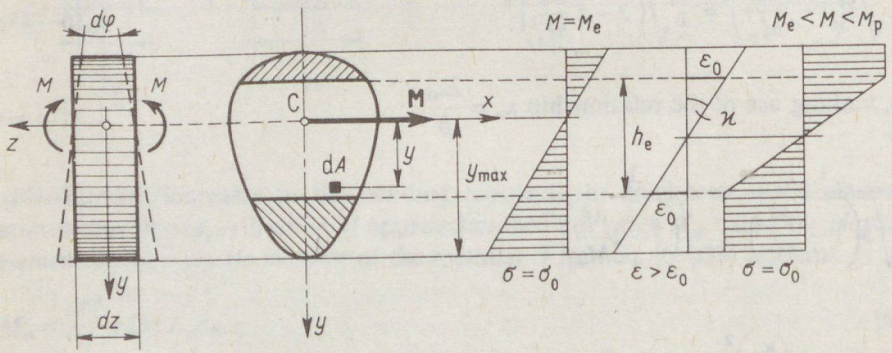


Fig. 6–24

On further increases in the bending moment, the *plastic limit moment* will be reached when the entire member becomes plastic, as shown in Fig. 6—25. Then, the force equation

$$\int_{(A)} \sigma \, dA = -\sigma_0 \int_{(A_1)} dA + \sigma_0 \int_{(A_2)} dA = \sigma_0 (A_2 - A_1) = 0$$

results in $A_1 = A_2 = \frac{A}{2}$. Hence, in the fully plastic state of members under pure bending, the neutral axis divides the cross-section into portions of equal areas.

The moment equation about the centroidal x axis provides the fully plastic moment of the member

$$M_p = \int_{(A)} \sigma y \, dA = -\sigma_0 \int_{(A_1)} y \, dA + \sigma_0 \int_{(A_2)} y \, dA = \sigma_0 (S_{2x} - S_{1x}).$$

Here $S_{1x}=-\frac{1}{2}A\bar{y}_1$ and $S_{2x}=\frac{1}{2}A\bar{y}_2$ denote the first moments of the half areas of the cross section with respect to the x axis. Since x is a centroidal axis, $S_{1x}+S_{2x}=\frac{1}{2}A(\bar{y}_1+\bar{y}_2)=0$, consequently, $|S_{1x}|=|S_{2x}|=S_{0x}$ and $|\bar{y}_1|=|\bar{y}_2|=\bar{y}_0$. Hence, the expression of the fully plastic moment reduces in this case to the general form

$$M_p=Z_p\sigma_0, \tag{6—49}$$

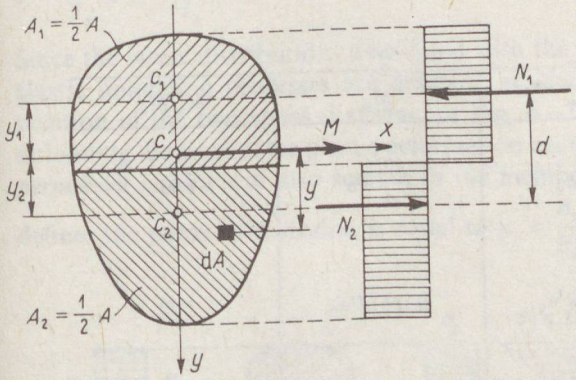


Fig. 6–25

where Z_p denotes the *plastic section modulus* defined by the expressions

$$Z_p=2S_{0x}=A\bar{y}_0=\frac{1}{2}Ad. \tag{6—50}$$

Here $d=|\bar{y}_1|+|\bar{y}_2|=2\bar{y}_0$ is the lever arm of the resultants of the tensile and compressive stresses (see Fig. 6—25).

The elastic and plastic limit moments of several members with different cross-sections are presented in Table 6—1. It can be seen that the shape factor varies within a wide range but, except for sandwich members, is always greater than 1.0. This demonstrates the *plastic reserve* of bar members made of elasto-plastic materials.

The moment-curvature diagrams of bar members with different cross-sections are presented in Fig. 6—26. As in the case of rectangular cross-sections, the diagrams show that the fully plastic state can be achieved only at infinitely large curvature; however, at relatively small curvatures the bending moment already very closely approaches the fully plastic moment. Hence, in practice, the fully plastic moment can be regarded as a good and simple approximation to the plastic moment-carrying capacity of bar members.

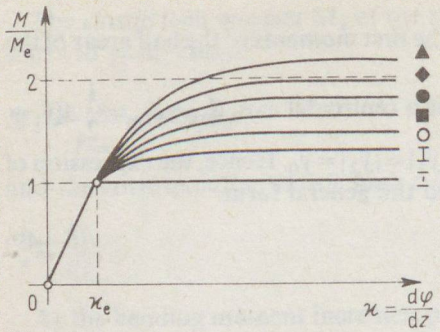
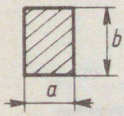
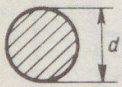
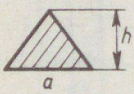
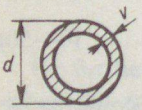
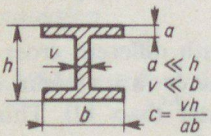
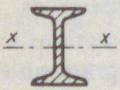
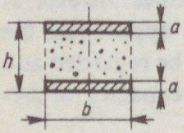


Fig. 6–26

Table 6—1

Cross-section	M_e	M_p	M_p/M_e
	$\frac{ab^2}{6}\sigma_0$	$\frac{ab^2}{4}\sigma_0$	1.50
	$0.0982d^3\sigma_0$	$0.1667d^3\sigma_0$	1.70
	$0.0417ah^2\sigma_0$	$0.0978ah^2\sigma_0$	2.34
	$0.1180a^3\sigma_0$	$0.236a^3\sigma_0$	2.00
 $v \ll d$	$0.800vd^2\sigma_0$	$1.02vd^2\sigma_0$	1.27
 $a \ll h$ $v \ll b$ $c = \frac{vh}{ab}$	$\left(1+\frac{c}{6}\right)_{bha\sigma_0}$	$\left(1+\frac{c}{4}\right)_{bh\sigma_0}$	$\frac{\left(1+\frac{c}{4}\right)}{\left(1+\frac{c}{6}\right)}$
	$Z_e\,\sigma_0$	$2S_{0x}\sigma_0$	1.14—1.16
 $a \ll h$	$abh\sigma_0$	$abh\sigma_0$	1.00

6.2.3.2. UNLOADING, RELOADING, REVERSE LOADING, CYCLIC LOADING

(a) Consider the unloading of a bar member with a doubly symmetrical cross-section, which has previously been loaded by a bending moment $M > M_e$ beyond the elastic limit* (Fig. 6—27). The unloading is achieved by keeping the moment M unchanged while another moment M', that has the same magnitude but opposite sense, is applied to the member. Then, the unloading phase can be handled by assuming the member to behave fully elastically, and the stresses corresponding to the moment M' are obtained by the formula

$$\sigma' = \frac{M'}{I_x} y = -\frac{M}{I_x} y.$$

Since the stress distributions associated with the elasto-plastic loading and the fully elastic unloading processes are different, *residual stresses*, obtained by the superposition of the two stress diagrams in Fig. 6—27 will remain in the member after unloading. Because of the plastic deformation occurring during the loading procedure, *permanent strains* will also remain in the member. The *permanent curvature*, which defines the permanent strains, is equal to $\kappa_p = \frac{\sigma_{r1}}{E y_e}$ (see the notations of Fig. 6—27).

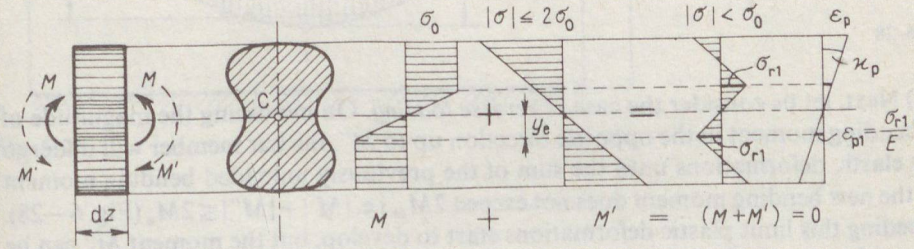


Fig. 6–27

(b) The residual stresses form a self-equilibrating system and "prestress" the bar member, so that during *reloading* the member will undergo only elastic deformations as long as the bending moment does not exceed the original bending moment. This is obvious, considering the fact that, as a consequence of the calculation of the residual stresses, the sum of the *elastic* stresses calculated from a bending moment less than M and of the residual stresses does not reach the yield stress at any point of the member. That is to say, if a member has been loaded once to the fully plastic moment M_p then, thereafter, a newly-applied bending moment $M < M_p$ will not cause any plastic deformations. Hence, the member will *shake down*.

There are a few special cases where the members subjected to repeated bending will not shake down. If the plastic limit moment M_p is higher than twice the elastic limit

* Because of the change in the position of the neutral axis during the loading and unloading process, the unloading of a member with a singly symmetrical cross-section is more complicated. Still, the statements that follow are also valid for this more general case.

moment $M_e (M_p \geqq 2M_e)$ then, during the unloading of a bending moment $M \geqq 2M_e$ the member can not behave fully elastically because in certain points the reverse stresses reach the yield stress and the material starts to yield in opposite direction. This prevents the development of residual stresses which could ensure the fully elastic behaviour of the member during the next reloading process. Hence, each time when the bending moment exceeds $2M_e$ plastic deformations take place i.e. the member will not shake down. This problem, however, does not have great practical importance, since in the case of most cross-sections M_p is less than $2M_e$ (see Table 6—1).

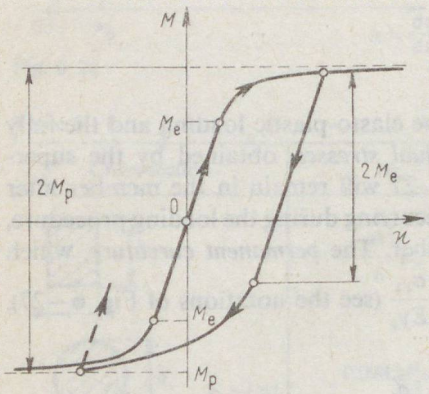


Fig. 6–28

(c) Next, let us consider the case of *reverse loading*. On increasing the magnitude of the bending moment in the opposite direction up to M'', the bar member will undergo only elastic deformations until the sum of the previously unloaded bending moment and the new bending moment does not exceed $2M_e$, i.e. $|M'|+|M''| \leq 2M_e$ (Fig. 6—28). Exceeding this limit plastic deformations start to develop, but the moment M'' can be increased up to the fully plastic moment $-M_p$ and then the member becomes fully plastic.

(d) Finally, consider the case when the member is subjected to *cyclic loading* and the bending moment varies between the limits M^+ and M^-. If the condition $|M^+|+|M^-| \leq 2M_e$ is fulfilled, the member will shake down and thereafter will undergo only elastic deformations. If, however, $|M^+|+|M^-| > 2M_e$, alternating plastic deformations will occur and the shakedown of the member will not take place.

6. 3. ELASTO-PLASTIC ANALYSIS

6.3.1. BEAMS

In the elasto-plastic analysis of beams the following assumptions will be used:

— the material of the beam is linearly elastic–perfectly plastic;

— the effect of shear stresses on the yield condition can be neglected so that the yield condition has the simple form

$$f = |\sigma| - \sigma_0 \leq 0; \qquad (6—51)$$

— the plane sections perpendicular to the axis of the beam remain plane and perpendicular to the bent axis;
— the deformations are small, and therefore the small deflection theory can be used.

Next, the elasto-plastic analysis of simply supported beams and continuous beams will be briefly discussed. More detailed treatment of these problems can be found in the literature (e.g. Prager, Hodge 1951; Neal 1977).

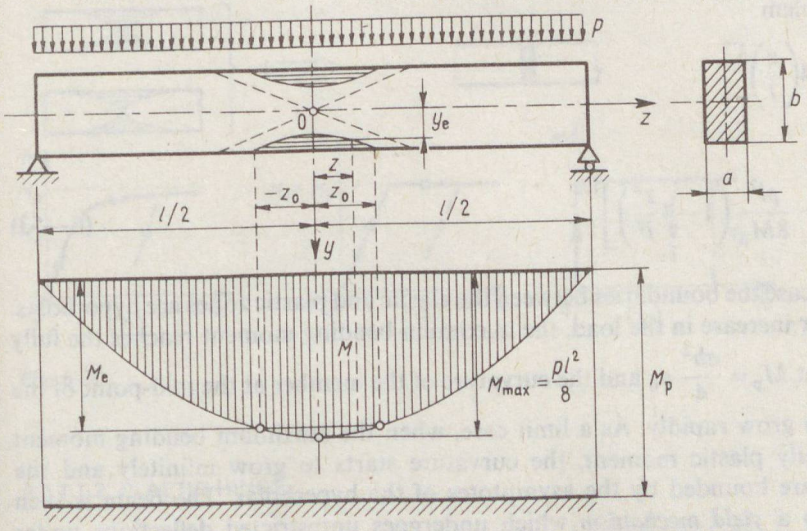


Fig. 6–29

6.3.1.1. SIMPLY SUPPORTED BEAMS

Consider a simply supported beam with a rectangular cross-section subjected to a uniformly distributed load, as shown in Fig. 6—29. Our problem is to determine the stresses and deflections in the elasto-plastic state, and to calculate the plastic limit load.

6.3.1.1.1. STRESS DISTRIBUTION

Increasing the intensity of the uniformly distributed load, the beam will be in a fully elastic state as long as the maximum normal stress does not reach the yield stress, i.e. as long as the maximum bending moment $M_{max} = \frac{pl^2}{8}$ does not reach the elastic limit moment $M_e = \frac{ab^2}{6}\sigma_0$. Hence, the *elastic limit load* of the beam is found to be

$$p_e = \frac{8M_e}{l^2}. \qquad (6—52)$$

As the load increases above the elastic limit load, yield zones develop in the upper and lower portions of the beam. The shape of the boundary surface between the elastic and plastic zones is described by a function $y_e = y_e(z)$ which according to eq. (6—43) is expressed in the form

$$y_e = \frac{b}{2}\sqrt{3\left(1-\frac{M}{M_p}\right)}.$$

In our problem

$$M = \frac{pl^2}{8}\left[1-4\left(\frac{z}{l}\right)^2\right]$$

and therefore

$$y_e = \frac{\sqrt{3}}{2} b\left[1-\frac{pl^2}{8M_p}\left(1-4\frac{z^2}{l^2}\right)\right]^{1/2}. \tag{6—53}$$

Hence, in this case the boundaries between the elastic and plastic zones are hyperbolas.

On a further increase in the load, the maximum bending moment reaches the fully plastic moment $M_p = \frac{ab^2}{4}\sigma_0$ and the curvature of the member at the mid-point of the beam starts to grow rapidly. As a limit case, when the maximum bending moment reaches the fully plastic moment, the curvature starts to grow infinitely and the plastic zones are bounded by the asymptotes of the hyperbolas. The beam is then converted into a *yield mechanism* which undergoes unrestricted deflections under constant load, indicating the exhaustion of the load-carrying capacity of the beam. Hence, we can state that if the maximum bending moment reaches the fully plastic moment, the load-carrying capacity of a simply supported beam is exhausted. From this condition, the *plastic limit load* or *collapse load* of the beam is found to be

$$p_p = \frac{8M_p}{l^2}. \tag{6—54}$$

We can conclude that in accordance with the lower and upper bound theorems of limit analysis, the plastic limit load can be defined in two different ways: the plastic limit load is the *greatest load* which can be balanced by bending moments not greater than the fully plastic moment, and is also the *smallest load* which can convert the beam into a yield mechanism.

Considering eqs (6—52) and (6—54), the ratio of the plastic and elastic limit loads of the beam is equal to

$$\frac{p_p}{p_e} = \frac{M_p}{M_e}. \tag{6—55}$$

This is a measure of the *plastic reserve* of the beam.

The results obtained above can be generalized to any type of *statically determinate structure*. The force distribution in a statically determinate structure is uniquely determined by the equilibrium equations, therefore redistribution of the internal

equilibrating forces can not be achieved. When only one cross-section of the structure becomes fully plastic, the load-carrying capacity of the entire structure is exhausted. Hence, the plastic reserve in the load-carrying capacity of a statically determinate structure is merely due to the plastic reserve of its most critical member, as it is expressed by eq. (6—55).

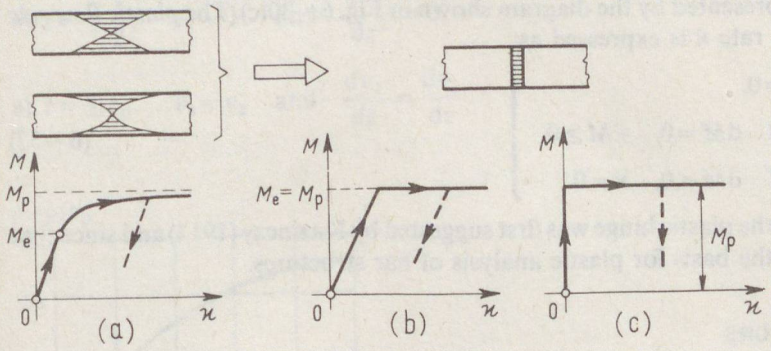


Fig. 6–30

6.3.1.1.2. PLASTIC HINGE

For the case of a uniformly distributed load, we have derived that in the plastic limit state the plastic zones of a beam with a rectangular cross-section are bounded by two straight lines (Fig. 6—30(a)). In the case of a concentrated force, these boundary lines are parabolas and for other loads and cross-sections different boundary curves can be derived (see e.g. Reckling 1967; Neal 1977).

Taking the elasto–plastic zones with various boundaries into consideration makes the plastic analysis of a structure very complicated. To avoid this difficulty, we replace the elasto-plastic regions by idealized critical segments and assume that the behaviour of these segments is also idealized so, that they are *fully elastic* as long as the bending moment is less than the fully plastic moment and become *fully plastic* when the bending moment reaches the fully plastic moment. During unloading, only elastic deformations take place. Hence, the actual moment curvature relationship shown in Fig. 6—30(a) is replaced by the bilinear diagram of Fig. 6—30(b), and the yield condition for these idealized segments has the form

$$\phi = |M| - M_p \leq 0. \tag{6—56}$$

The idealized segments are called *plastic hinges*, which can be viewed as a new type of structural member with very specific behaviour. Whenever the bending moment reaches the fully plastic moment, a plastic hinge forms at the corresponding cross-section and unrestricted rotation in the sense of the bending moment may develop while the bending moment remains constant. On decreasing the bending moment, the plastic hinge becomes *inactive and performs only elastic deformations*. Hence, the plastic

hinge can be considered a special unilateral hinge which starts to operate only if tne bending moment reaches the fully plastic moment and allows rotation only in the sense of the bending moment.

According to the theorem of constant stress (see Section 3.4.3.2.) in the plastic limit state of elastic-perfectly plastic structures no elastic deformations occur, and therefore in plastic limit analysis the concept of *rigid-perfectly plastic material* can be used. In this case a plastic hinge exhibits only plastic deformations and the moment–curvature relationship is represented by the diagram shown in Fig. 6—30(c). The *plastic flow rule* for the curvature rate $\dot{\kappa}$ is expressed as:

$$\left.\begin{aligned} &\text{if } |M|<M_p, \quad \dot{\kappa}=0, \\ &\text{if } |M|=M_p \quad \text{and} \quad dM=0, \quad \dot{\kappa}M\geq 0, \\ &\text{if } |M|=M_p \quad \text{and} \quad dM<0, \quad \dot{\kappa}=0. \end{aligned}\right\} \tag{6—57}$$

The concept of the plastic hinge was first suggested by Kazinczy (1914) and since that time has formed the basis for plastic analysis of bar structures.

6.3.1.1.3. DEFLECTIONS

(1) Consider the elasto-plastic state of the simply supported beam shown in Fig. 6—29. Assuming small deformations, the relationship between the deflections v and the curvature for both the fully elastic and the elasto-plastic parts of the beam can be expressed in the general form

$$\frac{d^2v}{dz^2}=-\kappa. \tag{6—58}$$

According to eqs (6—42) and (6—44) in the fully elastic state

$$\kappa=\frac{\kappa_e}{M_e}M,$$

while in the elasto-plastic state

$$\kappa=\frac{\kappa_e}{\sqrt{\left(3-2\frac{M}{M_e}\right)}}. \tag{6—59}$$

In both expressions, the bending moment is equal to

$$M=\frac{pl^2}{8}\left[1-4\left(\frac{z}{l}\right)^2\right].$$

Making use of the above relationships, the differential equations for the deflections have the following forms:
in the fully *elastic part*, where $|z|>z_0$,

$$\frac{d^2v_1}{dz^2}=-\frac{\kappa_e}{M_e}\frac{pl^2}{8}\left[1-4\left(\frac{z}{l}\right)^2\right],$$

in the *elasto-plastic part*, where $|z| \leq z_0$,

$$\frac{d^2 v_2}{dz^2} = -\frac{\kappa_e}{\left[3 - \frac{pl^2}{4M_e}\left(1 - 4\frac{z^2}{l^2}\right)\right]^{1/2}}.$$

In addition, the following boundary and continuity conditions have to be also satisfied:

at $z = \pm\frac{l}{2}$, $v_1 = 0$ and $\frac{d^2 v_1}{dz^2} = 0$,

at $z = \pm z_0$, $v_1 = v_2$ and $\frac{dv_1}{dz} = \frac{dv_2}{dz}$.

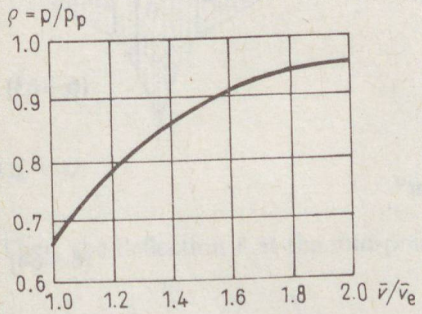


Fig. 6–31

Omitting the details of the solution to the above differential equations (see Prager, Hodge 1951), the deflection $\bar{v}$ of the middle section of the beam is found to be

$$\frac{\bar{v}}{\bar{v}_e} = 9.6\left[\frac{1}{4\sqrt{3\rho}}\sinh^{-1}\sqrt{\frac{3\rho-2}{3(1-\rho)}} + \frac{\sqrt{1-\rho}}{4\sqrt{3\rho}} + \frac{2\rho^2-1}{8\rho} - \frac{3\rho+1}{12\rho}\sqrt{\frac{\rho(3\rho-2)}{3}}\right]. \quad (6\text{—}60)$$

Here $\rho = \frac{p}{p_p}$, and $\bar{v}_e = \frac{5}{384}\frac{p_e l^4}{EI_x}$ is the deflection caused by the elastic limit load $p_e = \frac{8M_e}{l^2}$ at the middle section of the beam. From the diagram of Fig. 6—31 one can see that at the beginning of the elasto-plastic state the increase in deflections is not very rapid. For example, when the load reaches 95% of the collapse load the maximum deflection is still less than twice the elastic limit deflection. On approaching the collapse load more closely, however, the deflections start to increase very rapidly. Similar results can be obtained for other loads and cross-sections (see e.g. Neal 1977). Hence, we can state that practically the entire plastic reserve of a beam can be utilized at the cost of relatively small deflections therefore, in practice, the theoretical collapse load can be considered to be the load-carrying capacity of a beam.

(2) A more general method was suggested for the calculation of the elasto-plastic deflections of beams by Filonenko-Boroditsch (1952). The differential equation for elastic and elasto-plastic beams has the general form

$$\frac{d^2v}{dz^2} = -\kappa. \tag{6—61}$$

In the fully plastic zone, where $|M| \leq M_e$ we have $\kappa = \frac{M}{EI_x}$ and therefore

$$\frac{d^2v}{dz^2} = -\frac{M}{EI_x}. \tag{6—62}$$

In the elasto-plastic zone, where $|M| > M_e$, using eq. (6—59) and the relationship $\kappa_e = \frac{M_e}{EI_x}$, eq. (6—61) leads to

$$\frac{d^2v}{dz^2} = -\frac{\kappa_e}{\sqrt{\left(3-2\frac{M}{M_e}\right)}} = -\frac{1}{EI_x}\frac{M_e}{\sqrt{\left(3-2\frac{M}{M_e}\right)}}. \tag{6—63}$$

Then, introducing the *reduced bending moment**

$$\bar{M} = \frac{M_e}{\sqrt{\left(3-2\frac{M}{M_e}\right)}} \tag{6—64}$$

the differential equation governing the deflections can be expressed for the entire beam in the same general form

$$\frac{d^2v}{dz^2} = -\frac{\bar{M}}{EI_x}. \tag{6—65}$$

In this equation, when $|M| \leq M_e$ we have $\bar{M} = M$, and when $|M| > M_e$ eq. (6—64) determines $\bar{M}$.

To illustrate the application of the above method, consider a simply supported beam with a rectangular cross-section loaded by a *concentrated load*, and determine the deflections in the elasto-plastic state (Fig. 6—32(a)). In the fully elastic zone where $z < a$, $\bar{M} = M = \frac{F}{2}z$ while in the elasto-plastic zone where $a \leq z \leq \frac{l}{2}$,

$$\bar{M} = \frac{M_e}{\sqrt{\left(3-\frac{Fz}{M_e}\right)}}.$$

* For beams with non-rectangular cross sections this relationship has to be replaced by other appropriate expressions.

The slope of the deflected beam at the support can be obtained as the half area of the reduced bending moment diagram

$$\varphi=\frac{1}{EI_x}\int_0^{l/2}\bar{M}dz=\frac{1}{2EI_x}\int_0^{a}Fzdz+\frac{1}{EI_x}\int_a^{l/2}\frac{M_e}{\sqrt{3-\frac{Fz}{M_e}}}dz==\frac{Fa^2}{4EI_x}\left(3-2\sqrt{3-\frac{l}{a}}\right).$$

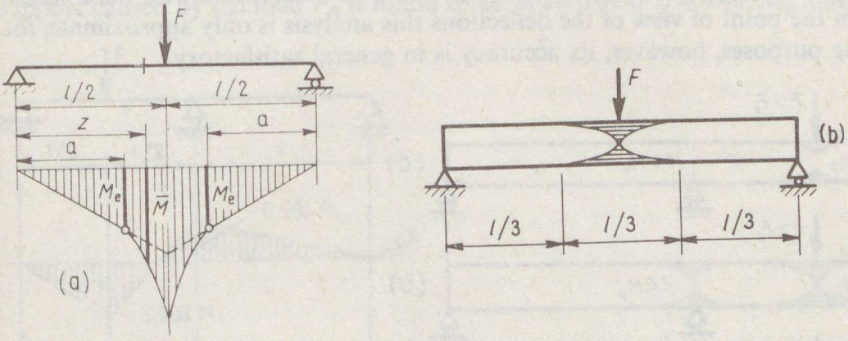


Fig. 6–32

Then, the deflection $\bar{v}$ at the mid-point of the beam is found to be

$$\bar{v}=\varphi\frac{l}{2}-\frac{1}{EI_x}\int_0^{l/2}\bar{M}\left(\frac{l}{2}-z\right)dz=$$

$$=\varphi\frac{l}{2}-\frac{1}{2EI_x}\int_0^{a}Fz\left(\frac{l}{2}-z\right)dz-\frac{1}{EI_x}\int_a^{l/2}\frac{M_e}{\sqrt{3-\frac{Fz}{M_e}}}\left(\frac{l}{2}-z\right)dz=$$

$$=\left(\frac{F_e}{F}\right)\left[5-\left(3+\frac{F}{F_e}\right)\sqrt{3-2\frac{F}{F_e}}\right]\bar{v}_e.$$

Here, $\bar{v}_e=\dfrac{F_e l^3}{48EI_x}$ is the deflection caused by the elastic limit load $F_e=\dfrac{4M_e}{l}$. It is interesting to note that in this case the collapse load $F_p=1.5F_e$ can be reached at a finite deflection $\bar{v}=3.33\,\bar{v}_e$. At this load, the plastic zone of the beam is bounded by two parabolas, shown in Fig. 6—32(b), and the deflections start to grow indefinitely.

6.3.1.2. CONTINUOUS BEAMS

Consider a uniform beam resting on three supports and loaded by a concentrated force F, as shown in Fig. 6—33. On increasing the load, first the portions below the force start to yield, and the member at the point of application of the load becomes fully plastic. A

plastic hinge develops here, but the beam still remains stable and can support additional loads. On further increases in the force, the section at the middle support also starts to yield and a second plastic hinge develops there. This converts the beam into a yield mechanism, which indicates the exhaustion of the load-carrying capacity of the beam on three supports.

In order to determine the stresses and deflections occurring in the elasto-plastic state of the beam, a step–by–step analysis is required. Making use of the concept of the plastic hinge, this analysis is very simple and provides an exact solution for the collapse load. From the point of view of the deflections this analysis is only approximate; for engineering purposes, however, its accuracy is in general satisfactory.

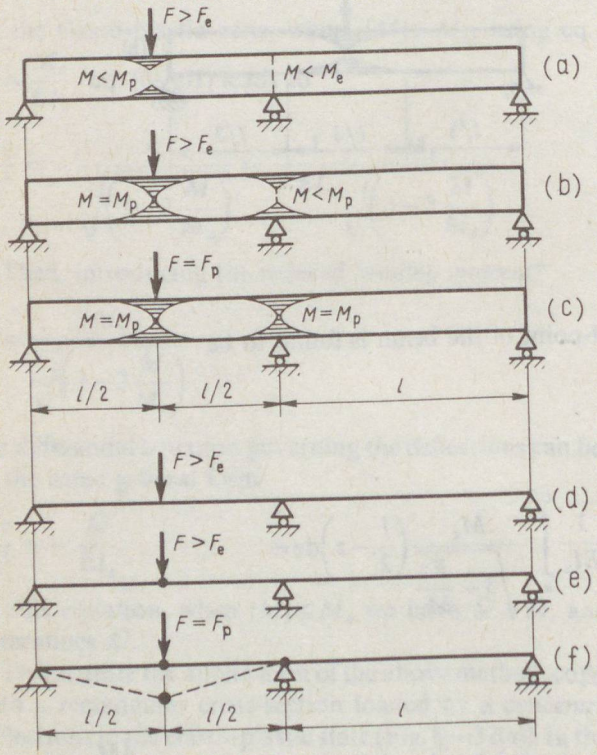


Fig. 6–33

The step–by–step solution of the problem under consideration is illustrated in Fig. 6—34. The elastic bending moment distribution in the beam is shown in Fig. 6—34(a). When the maximum bending moment $M_{max} = 0.203Fl$ reaches the elastic limit moment M_e, the beam starts to yield; thus, the *elastic limit load* is equal to

$$F_e = 4.93 \frac{M_e}{l}. \qquad (6—66)$$

On increasing the load, the cross-section at the point of application of the load becomes fully plastic and a plastic hinge develops. According to the assumptions associated with

the plastic hinge, the corresponding external force F_0 can be obtained by replacing M_e by M_p in eq. (6—66). Hence,

$$F_0 = 4.93 \frac{M_p}{l}.$$

On reaching this load, the continuous beam is transformed into a *hinged beam* which is still able to carry additional loads (Fig. 6—34(b)). The bending moment at the middle support caused by the load F_0 is found to be $M_0 = 0.094 F_0 l = 0.465 M_p$ and therefore

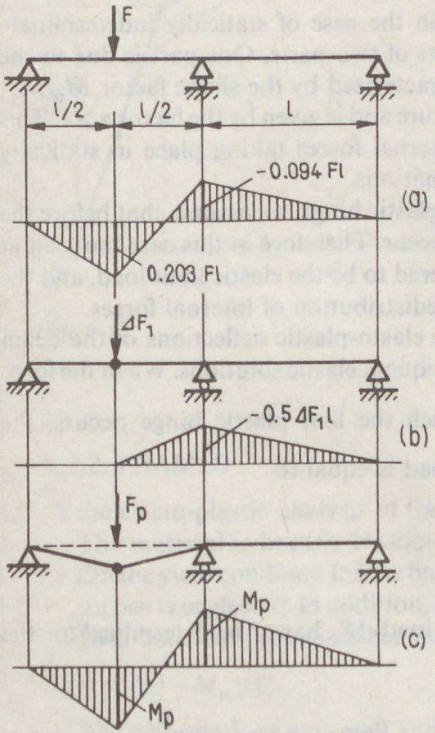


Fig. 6–34

the remaining moment capacity of the corresponding member is equal to $\Delta M_1 = = M_p - M_0 = 0.535\, M_p$. Hence, the magnitude of the additional force ΔF_1 which causes the plastic hinge to develop in this section can be obtained from the equation $0.50\, \Delta F_1 l = = 0.535 M_p$, and becomes

$$\Delta F_1 = 1.07 \frac{M_p}{l}.$$

The total load $F_0 + \Delta F_1$ converts the beam into a yield mechanism, and therefore the *plastic limit load* is given by the following expression

$$F_p = F_0 + \Delta F_1 = 6 \frac{M_p}{l}.$$

The ratio of the plastic and elastic limit loads becomes

$$\frac{F_p}{F_e} = 1.22 \frac{M_p}{M_e},$$

or in a general form

$$\frac{F_p}{F_e} = \alpha \frac{M_p}{M_e}, \quad \alpha \geq 1.$$

Considering this result, we can state that in the case of statically indeterminate structures, the plastic reserve generally consists of two parts. One part is due to the plastic reserve of the bar members and is characterized by the shape factor M_p/M_e, while the other part is associated with the structure and is given by the factor $\alpha \geq 1$. This latter is the result of the redistribution of internal forces taking place in statically indeterminate structures during plastic deformations.

We note that when using the concept of the plastic hinge, we assume that before the fully plastic moment no plastic deformations occur. Therefore in this case the load at which the first plastic hinge develops is considered to be the elastic limit load, and the plastic reserve is merely associated with the redistribution of internal forces.

As in the case of the stress distribution, the elasto-plastic deflections of the beam under consideration can be determined by subsequent elastic solutions. When the force reaches the magnitude $F_0 = 4.93 \frac{M_p}{l}$, at which the first plastic hinge occurs, the deflection at the point of application of the load is equal to

$$\bar{v}_0 = 0.01496 \frac{F_0 l^3}{EI_x} = 0.07375 \frac{M_p l^2}{EI_x}.$$

The deflection $\Delta\bar{v}_1$ caused by the additional load ΔF_1 has to be determined for the hinged beam (see Fig. 6—34(b)) and becomes

$$\Delta\bar{v}_1 = 0.125 \frac{\Delta F_1 l^3}{EI_x} = 0.13375 \frac{M_p l^2}{EI_x}.$$

Finally, at the plastic limit load $F_p = 6 \frac{M_p}{l}$, the deflection reaches the magnitude

$$\bar{v}_p = \bar{v}_0 + \Delta\bar{v}_1 = = 0.2075 \frac{M_p l^2}{EI_x}.$$

Then, under constant load unrestricted deflections start to develop. The ratio $\bar{v}_p/\bar{v}_0 = = 2.81$ shows that the plastic limit load can be reached at relatively low deflections. The force–deflection relationship is shown in Fig. 6—35.

Using the concept of plastic hinges in the computation of the deflections, the plastic deformations at the elasto-plastic zones of the beam are neglected. Since this effect is generally not significant (see e.g. Neal 1977) this approximation provides reliable

results and can be applied to the elasto-plastic analysis of beam structures. In Fig. 6—35 the dashed curve shows schematically the force–displacement relationship which can be obtained if the plastic hinge approach is not applied.

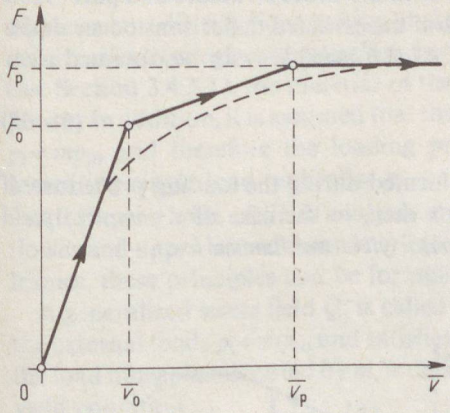


Fig. 6–35

6.3.2. FRAMES

In the elasto-plastic analysis of frames, the following assumptions are used:

— The material is linearly elastic–perfectly plastic;

— On the yield condition for the bar members the effect of normal and shear forces and torque is neglected. In addition, the plastic hinge approach is used and therefore the yield condition of a member has the form

$$\phi = |M| - M_p \leq 0; \tag{6—67}$$

— The deformations are small and therefore the small deflection theory can be used.

In a more advanced analysis, the effect of normal and shear forces and torque on the yield condition and the influence of large deflections can also be taken into consideration. These problems will be discussed in Section 6.7.

To illustrate the elasto-plastic analysis of frames, consider a frame subjected to *proportional loading* $p_i = mp_{io}$ (Fig. 6—36(a)). Here p_{io} defines the positions and directions of the forces and m is a monotonically increasing parameter, called the *load multiplier* or *load intensity*.

At lower intensities of the load, the frame is in a fully elastic state and the relationship between the load intensity m and the deflection e of a characteristic point of the frame is linear (Fig. 6—36(b)). Elastic behaviour ceases when a plastic hinge develops and the corresponding multiplier m_e is called the *elastic limit load multiplier*. On further increase the *load increment* $\Delta m F_{io}$ will be carried by a modified structure which has a hinge at the cross-section where the plastic moment has been reached and, in this manner, the redundancy of the structure is decreased by one. At a certain magnitude of the load

increment denoted by $\Delta m_1 p_{io}$, a further plastic hinge forms which will again decrease the redundancy of the structure by one. Hence, the next load increment will be carried by the structure which has two hinges and the load increment can be increased until the next plastic hinge.

This step–by–step process can be continued until the entire structure or a part of it is converted into an unstable yield mechanism and unrestricted deflections occur under constant load. Then, the corresponding *plastic load multiplier* can be obtained as

$$m_p = m_0 + \sum_{i=1}^{k-1} \Delta m_i, \tag{6—68}$$

where k denotes the number of plastic hinges formed during the loading procedure. If the degree of redundancy of the structure is r then, in the case of a *complete yield mechanism* $k = r+1$, while in the case of a *partial yield mechanism* $k < r+1$.

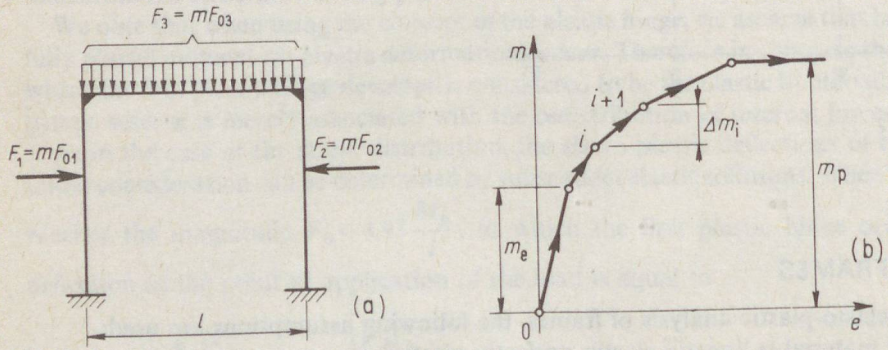


Fig. 6–36

The incremental elasto-plastic analysis described above requires the repeated *elastic* solution for the structure. This computation can easily be computerized. A difficulty arises, however, from the fact that after each step a hinge has to be inserted and the stiffness matrix of the structure modified. Hence, the step–by–step analysis requires the repeated inversion of the *modified* stiffness matrix, which may represent a significant problem. This difficulty can be overcome by applying "kinematic loads", as proposed by Kurutz (1974).

Another computational difficulty arises from the fact that during the loading process some plastic hinges may become *inactive*. Hence, at each loading step the senses of the plastic hinge rotations have to be determined and where they are opposite, as the senses of the plastic moments, the hinges have to be cancelled and the step under consideration repeated. In the case of proportional loading the occurrence of inactive hinges is rare, but in structures subjected to multi-parameter and cyclic loading this phenomenon is of great importance.

Details of the incremental elasto-plastic analysis of frame structures based on mathematical programming will be presented in Section 6.8. The approximate calculation of the deflections will be discussed in Section 6.4.

6.4. LIMIT ANALYSIS

6.4.1. THEOREMS OF LIMIT ANALYSIS

The aim of limit analysis is to determine the *plastic limit load*, also called the *collapse load*, of a structure and to provide information about the internal force and displacement distributions arising at the plastic limit state. In the analysis the effect of deformations is neglected; therefore, in accordance with the theorem of constant stress (see Section 3.4.3.2.), the material of the structure can be considered as *rigid-perfectly plastic*. In addition, it is assumed that the structure is subjected to a *proportional loading* $p_i = mp_{i0}$ and therefore the loading process is characterized by the monotonically increasing single load multiplier m.

All the methods of limit analysis are based on the *static and kinematic principles* (lower and upper bound theorems) derived and discussed in detail in Section 3.4.3. For frames, these principles can be formulated in a special form to be described below.

A generalized stress field Q_j^s is called *statically admissible* if it is in equilibrium with the external loads $p_i = mp_{i0}$ and satisfies the static boundary conditions. If, in addition, the load multiplier denoted by m_s is chosen so that in every member of the structure the yield condition

$$\phi(Q_j^s, Q_0) \leq 0 \tag{6—69}$$

is also satisfied, then m_s is called a *statically admissible stable load multiplier*.

The *static principle* (lower bound theorem) of limit analysis states that
any statically admissible stable load multiplier is less than or equal to the collapse load multiplier, i.e.

$$m_s \leq m_p.$$

A generalized strain rate and velocity field $\dot{q}_j^k, v_j^k$ is called *kinematically admissible* if it satisfies the kinematic equations and kinematic boundary conditions. If, in addition, the load multiplier denoted by m_k is defined by the equations

$$\left.\begin{aligned} m_k &= \frac{\int Q_j^k \dot{q}_j^k \, ds}{\int p_{i0} v_i^k \, ds} = \frac{D(\dot{q}_j^k)}{\int p_{i0} v_i^k \, ds}, \\ \int p_{i0} v_i^k \, ds &\geq 0, \end{aligned}\right\} \tag{6—70}$$

then m_k is called a *kinematically admissible unstable multiplier*. Here $D(\dot{q}_j^k)$ designates the total energy rate dissipated by the structure.

The *kinematic principle* (upper bound theorem) of limit analysis states that
any kinematically admissible unstable load multiplier is greater than or equal to the collapse load multiplier, i.e.

$$m_k \geq m_p.$$

In the following, we will assume that the effect of the normal and shear forces and the torque on the yield condition can be neglected, and that the concept of the plastic hinge can be used in the analysis. For the sake of simplicity, we will also assume that all the members of the frame have the same plastic moment M_p and the load contains only

concentrated forces $F_i = mF_{i0}$. These assumptions make possible the simplified formulation of the above principles, to be described below.

Applying the static principle only, the *statically admissible bending moment fields* M_j should be considered. These can easily be obtained on the *statically determinate released* structure if we choose the magnitudes of the redundant forces arbitrarily and determine the bending moment distribution of the structure by the use of equilibrium equations. Then, a statically admissible stable load multiplier can be obtained from the condition that even the maximum bending moment does not exceed the fully plastic moment, i.e.

$$\max |M_j| \leq M_p. \tag{6—71}$$

Introducing the plastic hinge approach, the kinematically admissible strain rate and velocity fields can be constructed by assuming plastic hinges at an adequate number of cross-sections of the structure so that the entire structure or a part of it is transformed into an unstable mechanism, called a *yield mechanism.* At the plastic hinges, the moments are equal to the fully plastic moment M_p and the senses of the fully plastic moments are identical to those of the corresponding rotations. Hence, the power absorbed in the plastic hinges is always positive, regardless of the sense of rotation. Then, denoting the rates of rotation in the plastic hinges by ω_j^k and the velocities at the points of application of the forces by v_i^k, a kinematically admissible unstable load multiplier can be determined from the equation

$$\left.\begin{aligned} m_k \sum_{i=1}^{n} F_{i0} v_i^k &= M_p \sum_{j=1}^{l} \omega_j^k, \\ \sum_{i=1}^{n} F_{i0} v_i^k &> 0. \end{aligned}\right\} \tag{6—72}$$

In the next section, the application of the static and kinematic principles of limit analysis will be illustrated by the solution to several problems. A more detailed systematic description of the methods applied to the limit analysis of frames can be found in the literature (see e.g. Baker, Horn, Heyman 1956; Phillips 1956; Hodge 1959; Beedle 1958; Neal 1956, 1977; Heyman 1957, 1971; Baker, Heyman 1969; Moy 1981). As indicated earlier, the mathematical programming formulation of the limit analysis of frames will be discussed in Section 6.8.

6.4.2. APPLICATIONS

(1) Determine the lower and upper bounds and the exact magnitude of the plastic limit load of the frame shown in Fig. 6—37(a).

In order to construct a statically admissible bending moment distribution, we "remove" the horizontal constraint at the support A and replace it by a redundant horizontal force of arbitrary magnitude, say $H = m_s$ (Fig. 6—37(b)). Then the bending moment diagram can be plotted, with the maximum bending moment occurring at point D and equal to $M_{max} = lm_s$. To obtain a statically admissible stable load multiplier, the yield condition $M_{max} \leq M_p$ has to be satisfied. This leads to

$$m_s = \frac{M_p}{l} \leq m_p.$$

A yield mechanism of the frame can be obtained by assuming plastic hinges at the points C and D (Fig. 6—37(c)). Then, the rates of rotation in the plastic hinges and the velocities at the points of application of the forces during a small motion in the yield mechanisms can be determined. Finally, the equation for external and internal powers (see eq. (6—72)) is found to be*

$$m_k[2 \times 0.8\,\omega l] = M_p[\omega + \omega].$$

Hence

$$m_k = 1.25\frac{M_p}{l} \geq m_p.$$

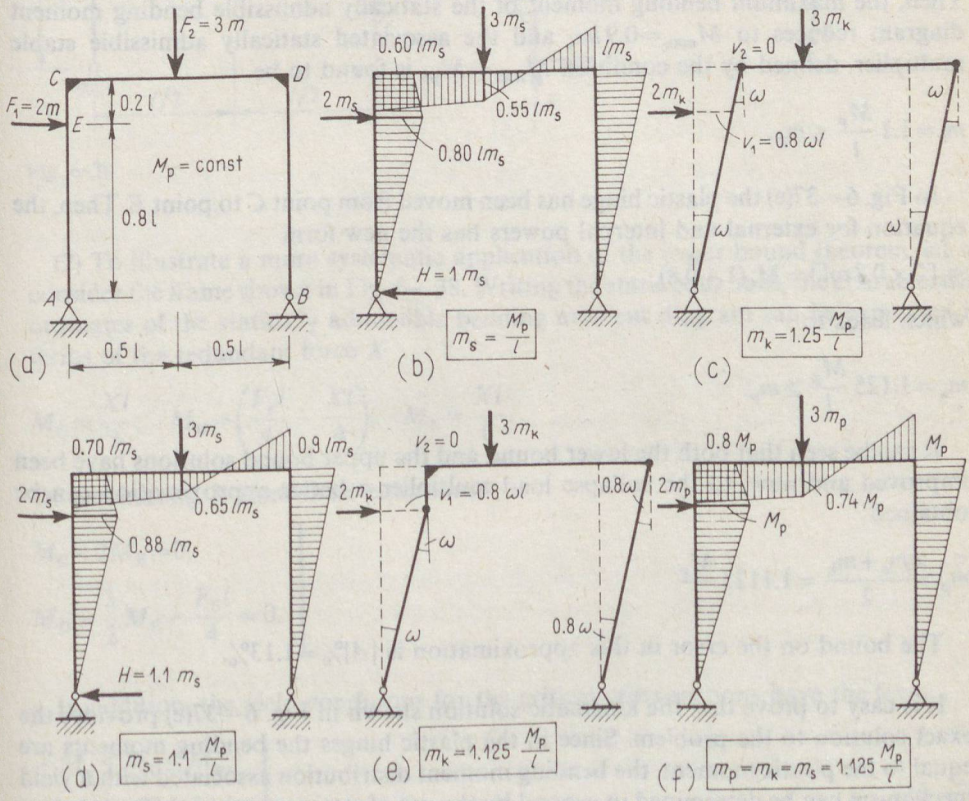


Fig. 6–37

* In the following the kinematically admissible rotation rates and velocities will simply be denoted by ω and v. Since the plastic moments and the plastic hinge rotations have the same sense by definition, all terms of the internal power are always *positive*.

The average of the lower and upper bound solutions provides a reasonable approximation for the collapse load multiplier

$$m_p \approx \frac{m_s + m_k}{2} = 1.125 \frac{M_p}{l}.$$

The bound on the error in this approximation is

$$|\Delta|\% \leq \frac{m_k - m_s}{2 m_s} 100\% = 12.5\%.$$

In order to improve the accuracy of the above solution we have to change the statically admissible moment distribution and/or the yield mechanism.

In Fig. 6—37(d) the magnitude of the redundant force is assumed to be $H = 1.1\, m_s$. Then, the maximum bending moment of the statically admissible bending moment diagram reduces to $M_{max} = 0.9\, l m_s$ and the associated statically admissible stable multiplier, defined by the condition $M_{max} \leq M_p$, is found to be

$$m_s = 1.1 \frac{M_p}{l} \leq m_p.$$

In Fig. 6—37(e) the plastic hinge has been moved from point C to point E. Then, the equation for external and internal powers has the new form

$$m_k[2 \times 0.8\, \omega l] = M_p(1 + 0.8),$$

which leads to

$$m_k = 1.125 \frac{M_p}{l} \geq m_p.$$

It can be seen that both the lower bound and the upper bound solutions have been improved and now, to the collapse load multiplier a better approximation can be obtained

$$m_p \approx \frac{m_s + m_k}{2} = 1.1125 \frac{M_p}{l}.$$

The bound on the error in this approximation is $|\Delta|\% = 1.13\%$.

It is easy to prove that the kinematic solution shown in Fig. 6—37(e) provides the exact solution to the problem. Since in the plastic hinges the bending moments are equal to the plastic moment, the bending moment distribution associated with a yield mechanism can be determined in general by the use of static equations.* The bending moment diagram associated with the yield mechanism of Fig. 6—37(e) is shown in Fig. 6—37(f). This is a statically admissible moment distribution since it nowhere exceeds

* In the case of partial yield mechanisms, the bending moments of those parts of the structure which do not undergo motion cannot be determined from equilibrium equations.

the plastic moment. Hence, the corresponding kinematically admissible multiplier $m_k = 1.125 \frac{M_p}{l}$ is, at the same time, also statically admissible, and is therefore identical to the collapse load multiplier

$$m_p = m_k = m_s = 1.125 \frac{m_p}{l}.$$

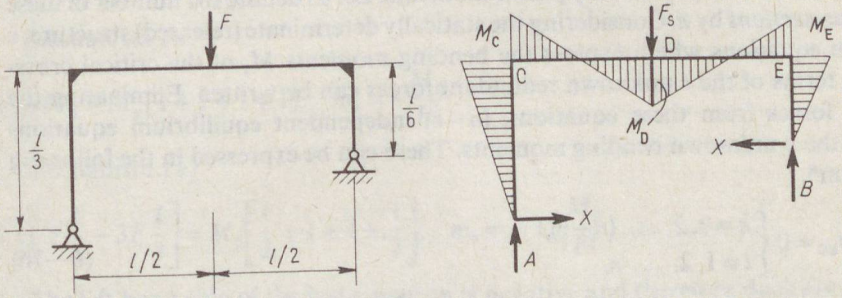


Fig. 6–38

(2) To illustrate a more systematic application of the lower bound theorem, let us consider the frame shown in Fig. 6—38. Writing the static equations, the characteristic ordinates of the statically admissible bending moment diagram can be expressed in terms of the redundant force X

$$M_C = \frac{Xl}{3}; \quad M_D = \left(\frac{F_s l}{4} - \frac{Xl}{4}\right); \quad M_E = \frac{Xl}{6}.$$

Or eliminating X from these equations,

$$\left.\begin{aligned} &M_C - 2M_E = 0, \\ &M_D - \frac{3}{2} M_E - \frac{F_S l}{4} = 0. \end{aligned}\right\} \qquad (6—73)$$

In addition, the yield conditions for the critical cross-sections have the form

$$\left.\begin{aligned} &-M_p \le M_C \le M_p, \\ &-M_p \le M_D \le M_p, \\ &-M_p \le M_E \le M_p. \end{aligned}\right\} \qquad (6—74)$$

Equations (6—73) and (6—74) define all the statically admissible stable loads F_s of the frame. To obtain the collapse load, one has to determine the greatest value of F_s, i.e. the above equations have to be supplemented by the condition

$$F_s = \max! \qquad (6—75)$$

This extreme condition, together with the linear equations and inequalities (6—73) and (6—74) is a problem of *linear programming* which leads to the solution $F_p = 7\frac{M_p}{l}$.

(3) Consider a general case when the degree of statical indeterminacy of the structure is r. Assume that the structure is made of bars with uniform or linearly varying plastic moments, and that the external load consists only of concentrated forces. Then, plastic hinges can occur only at the points of application of the concentrated forces and at the joints of the bars with different fully plastic moments. Let us denote the number of these *critical cross-sections* by n. Considering the statically determinate (released) structure, n equilibrium equations which express the bending moments M_i of the critical cross-sections in terms of the r unknown redundant forces can be written. Eliminating the redundant forces from these equations, $(n-r)$ independent equilibrium equations remain for the n unknown bending moments. These can be expressed in the following general form*

$$a_{ki}M_i + m_s a_{k0} = 0 \begin{cases} k = 1, 2, \ldots (n-r), \\ i = 1, 2, \ldots n. \end{cases} \qquad (6—76)$$

These equations define all the possible statically admissible bending moment distributions of the structure. The parameter m_s appearing in these equations is considered a statically admissible stable multiplier if in all the critical cross-sections the yield conditions are satisfied, i.e.

$$-M_{ip} \leq M_i \leq M_{ip}; \quad i = 1, 2, \ldots n. \qquad (6—77)$$

Here M_{ip} denotes the fully plastic moments of the critical cross-sections.

Finally, the collapse load multiplier is equal to the greatest statically admissible stable load multiplier, i.e. it can be obtained by the condition

$$m_s = \max! \qquad (6—78)$$

Considering the linear equations and inequalities (6—76) and (6—77) and the extreme condition (6—78) we can state, in general, that the limit analysis of bar structures based on the lower bound theorem is a *linear programming problem.*

(4) Let us determine the collapse load of the frame with uniform plastic moment M_p shown in Fig. 6—39(a), by the use of the kinematic principle. Plastic hinges can develop at the supports and the joints of the bars and at the point of application of the vertical force; hence, the frame has 5 critical cross-sections. By a suitable combination of plastic hinges four yield mechanisms can be constructed, as they are shown in Figs 6—39(b—e). The yield mechanisms of Figs 6—39(c—e) are complete mechanisms, while in Fig. 6—39(b) a partial yield mechanism is shown. The relationships between the velocities and rates of rotations can easily be determined by writing geometrical equations. The corresponding magnitudes are indicated in the Figures. Then, applying the principle of virtual velocities the following equations can be obtained:

* In this equation the summation convention is applied.

mechanism *(b)*

$$m_k\left[3F\frac{l}{4}\right]=M_p\left[\frac{1}{2}+1+\frac{1}{2}\right];\quad m_k=\frac{8}{3}\frac{M_p}{Fl},$$

mechanism *(c)*

$$m_k\left[F\frac{l}{2}+3F\frac{l}{4}\right]=M_p\left[\frac{1}{2}+1+1+\frac{1}{2}\right];\quad m_k=\frac{12}{5}\frac{M_p}{Fl},$$

mechanism *(d)*

$$m_k[Fl]=M_p[1+1+1+1];\quad m_k=4\frac{M_p}{Fl},$$

mechanism *(e)*

$$m_k\left[F\frac{l}{2}-3F\frac{l}{4}\right]=M_p\left[\frac{1}{2}+1+1+\frac{1}{2}\right];\quad m_k=-12\frac{M_p}{Fl}.$$

The left hand side of the last equation is negative and therefore does not satisfy the condition $\sum_{i=1}^{n} F_{i0}v_i>0$ given by eq. (6—72). Hence the associated load multiplier is not a kinematically admissible unstable multiplier and is therefore not considered further.

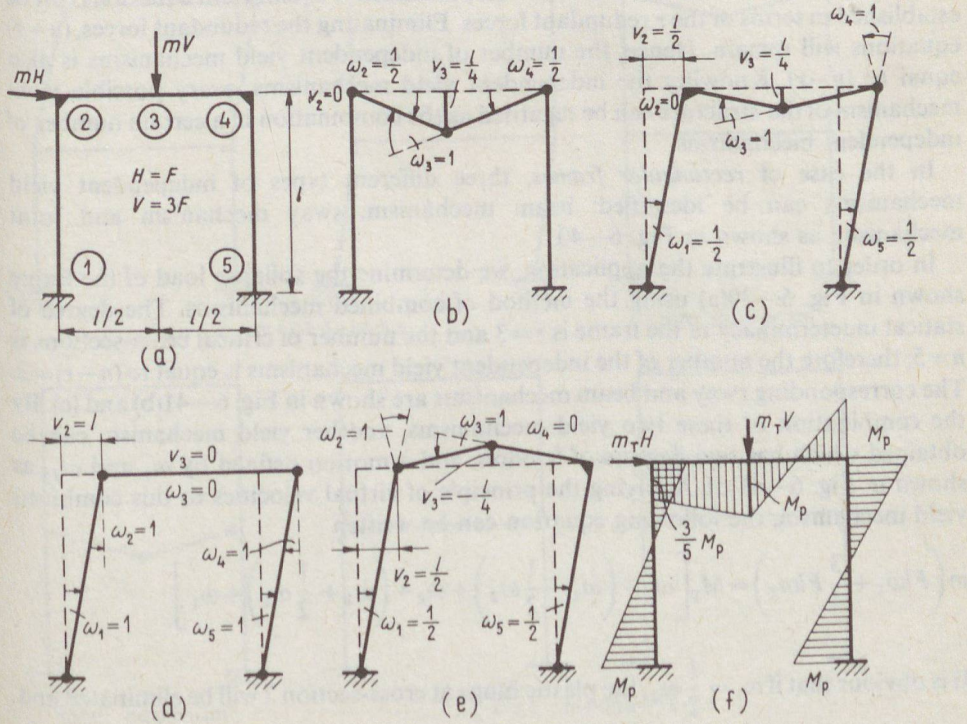


Fig. 6–39

Among the remaining three kinematically admissible unstable multipliers, the smallest one provides the collapse load multiplier, i.e.

$$m_p = \min m_k = \frac{12}{5}\frac{M_p}{Fl}.$$

The yield mechanism shown in Fig. 6—39(c) gives the collapse mechanism of the frame.

(5) In more complex structures the number of possible yield mechanisms can be very high, and therefore it is desirable to develop a systematic procedure for the determination of the yield mechanisms. Such a procedure was developed by Symonds and Neal (1952) and is called the *method of combined mechanisms*. To see the basic idea of this method, consider a frame with r degrees of statical indeterminacy subjected to concentrated forces, and assume that the number of critical cross-sections is n. Since in a complex structure n is large, the number of possible yield mechanisms is generally significant. A set of these yield mechanisms is *independent* and the remaining sets can be obtained by a suitable combination of the independent yield mechanisms.

A yield mechanism is considered to be independent if the associated power equation cannot be derived by the superposition of the power equations of other yield mechanisms. Every power equation expresses an equilibrium relationship between the moments acting at the critical cross-sections. Hence, the number of independent yield mechanisms is equal to the number of independent equations relating the moments acting in the critical cross sections. For these moments n equilibrium equations can be established in terms of the r redundant forces. Eliminating the redundant forces, $(n-r)$ equations will remain. Hence, the number of independent yield mechanisms is also equal to $(n-r)$. Knowing the independent yield mechanisms, every possible yield mechanism of the structure can be regarded as the combination of a certain number of independent mechanisms.

In the case of *rectangular frames*, three different types of independent yield mechanisms can be identified: beam mechanism, sway mechanism and joint mechanism, as shown in Fig. 6—40.

In order to illustrate the application, we determine the collapse load of the frame shown in Fig. 6—39(a) using the method of combined mechanisms. The degree of statical indeterminacy of the frame is $r=3$ and the number of critical cross-sections is $n=5$; therefore the number of the independent yield mechanisms is equal to $(n-r)=2$. The corresponding sway and beam mechanisms are shown in Fig. 6—41(b) and (c). By the combination of these two yield mechanisms, another yield mechanism can be obtained which has two degrees of freedom and a motion defined by ω_1 and ω_2, as shown in Fig. 6—41(d). Applying the principle of virtual velocities to this combined yield mechanism, the following equation can be written

$$m\left(Fl\omega_1 + \frac{3}{4}Fl\omega_2\right) = M_p\left[\omega_1 + \left(\omega_1 - \frac{1}{2}\omega_2\right) + \omega_2 + \left(\omega_1 + \frac{1}{2}\omega_2\right) + \omega_1\right].$$

It is obvious that if $\omega_1 = \frac{1}{2}\omega_2$, the plastic hinge at cross-section 2 will be eliminated and

we will obtain a yield mechanism with one degree of freedom which is identical with the yield mechanism of Fig. 6—39(c). Then the above equation yields

$$m = \frac{12}{5}\frac{M_p}{Fl}$$

which is, of course, the same as was obtained by the direct analysis of the yield mechanism of Fig. 6—39(c).

Let us now consider the sway and beam mechanisms independently, and write the power equations

$$m_1 Fl\omega_1 = 4M_p\omega_1,$$

$$m_2 \frac{3}{4} Fl\omega_2 = 2M_p\omega_2.$$

In order to eliminate the plastic hinge at cross-section 2 we assume that $\omega_1 = \frac{1}{2}\omega_2$ and add the two equations. Then, however, the work done by the plastic moment in cross-section 2 will not disappear since the terms in the right hand side of the equation, independently of the sense of rotations, are always positive. Hence, to obtain

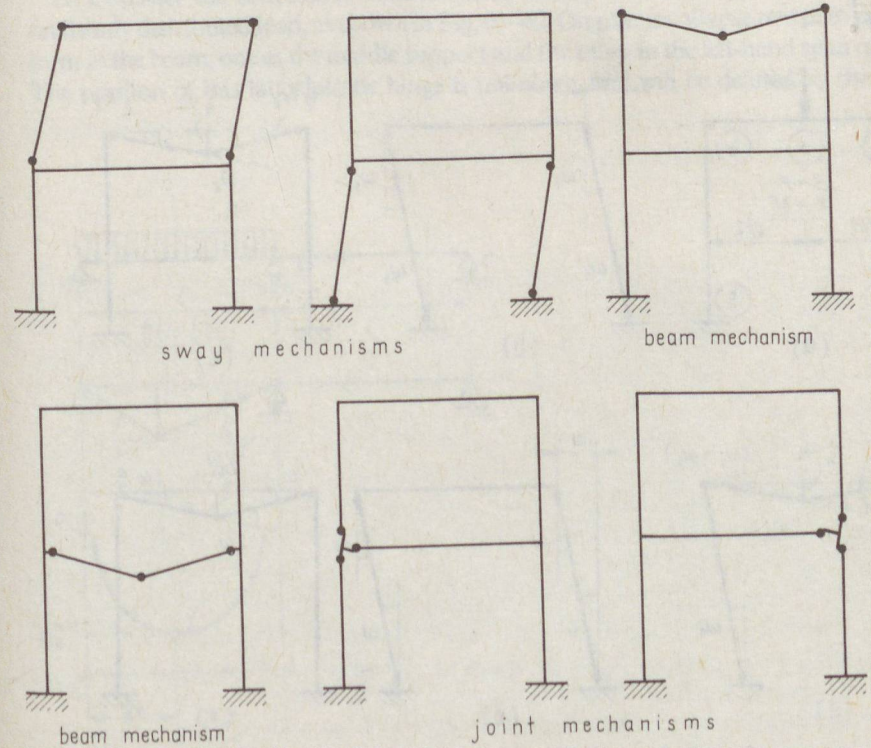


Fig. 6–40

the correct power equation, the internal power should be decreased by the power exerted in the eliminated plastic hinge. In our example this power is $M_p \frac{1}{2}\omega_2 + M_p \frac{1}{2}\omega_2 = M_p\omega_2$. Thus, the steps of computation are as follows:

$$\left.\begin{aligned} m\frac{1}{2}Fl\omega_2 &= 2M_p\omega_2 \\ m\frac{3}{4}Fl\omega_2 &= 2M_p\omega_2 \end{aligned}\right\} +$$

$$\left.\begin{aligned} m\frac{5}{4}Fl\omega_2 &= 4M_p\omega_2 \\ -M_p\omega_2 & \end{aligned}\right\} +$$

$$m\frac{5}{4}Fl\omega_2 = 3M_p\omega_2,$$

from which

$$m = \frac{12}{5}\frac{M_p}{Fl}.$$

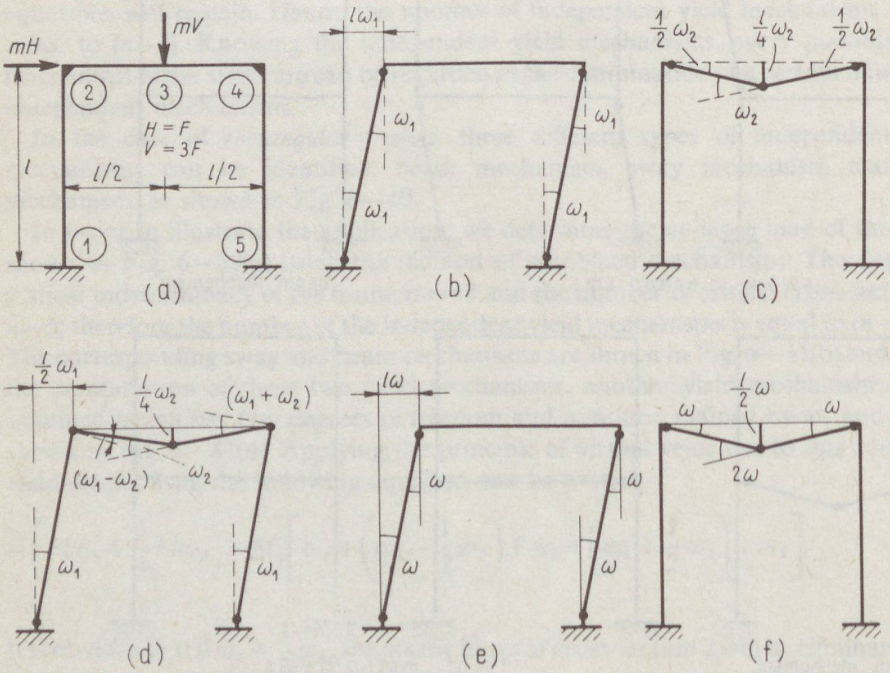


Fig. 6–41

In this manner, by the suitable combination of the power equations of the independent yield mechanisms we can obtain the kinematically admissible load multiplier associated with a combined mechanism.

The systematic application of the above method makes possible the improvement of the upper bound solutions and the determination of the collapse load multipliers of more complex structures. Combining this method with the *plastic moment distribution method* developed by Horne (1954), statically admissible moment distributions and lower bound solutions can also be obtained. More details and the applications of these methods can be found in the literature (see e.g. Hodge 1959; Neal 1977).

6.4.3. DISTRIBUTED LOADING

In all the methods and problems discussed so far, we have assumed that the structure is loaded by concentrated forces and that the positions of the critical sections, where plastic hinges may form, are therefore known "a priori". In the case of distributed loads, however, maximum bending moments may occur at any position and therefore in an exact analysis the locations of these hinges have to be determined. This, in general, leads to lengthy and complicated computations and therefore in practice different approximations are used. Before discussing these methods, the exact solution will be illustrated with a simple problem.

(1) Consider the continuous uniform beam resting on three supports and loaded by a uniformly distributed load, as shown in Fig. 6—42. On plastic collapse two plastic hinges will form in the beam, one at the middle support and the other in the left-hand span of the beam. The position of this latter plastic hinge is unknown, and will be defined by the distance ξ

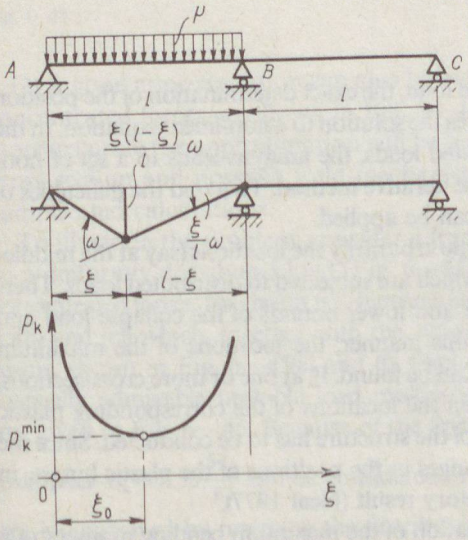


Fig. 6–42

measured from support A. Then, considering the notations of Fig. 6—42, the external power is found to be

$$\int_0^l pv\,dx = p\frac{\xi(l-\xi)}{2}\omega.$$

Hence, the principle of virtual velocity leads to the equation

$$p_k\frac{\xi(l-\xi)}{2}\omega = M_p\left(\omega+\frac{\xi}{l}\omega\right),$$

from which the kinematically admissible unstable load intensity can be expressed in terms of the parameter ξ as

$$p_k = \frac{2M_p}{l}\frac{l+\xi}{\xi(l-\xi)}. \qquad (6—79)$$

From this equation, for every value of ξ $(0<\xi<l)$ a kinematically admissible unstable load intensity can be obtained, as illustrated symbolically in Fig. 6—42. To determine the best upper bound, one has to minimize the function in (6—79). This leads to the equation

$$\frac{dp_k}{d\xi} = \frac{2M_p}{l}\frac{\xi(l-\xi)-(l-2\xi)(l+\xi)}{\xi^2(l-\xi)^2} = 0$$

from which

$$\xi_0 = \left(\sqrt{2}-1\right)l.$$

Substituting this result in eq. (6—79) we get the best upper bound which, for this simple problem, also gives the collapse load of the beam as

$$p_p = \min p_k = 11.64\frac{M_p}{l^2}.$$

It can be seen that, because of the distributed load, the exact determination of the position of the plastic hinge and the collapse load requires the solution to a non-linear equation. In the case of more complex structures with distributed loads, the analysis leads to a set of non-linear equations to be solved by an appropriate iterative method. To avoid the difficulties of iterative solutions, different approximations can be applied.

(2) The simplest approximation is if we assume arbitrarily the locations (say at the middle-cross-section of the bars) of the plastic hinges which are subjected to distributed loads. Then, with this assumption, we determine the upper and lower bounds of the collapse load and construct the bending moment diagram. In this manner, the locations of the maximum bending moments under the distributed loads can be found. If, at one or more cross-sections, these moments exceed the plastic moment then the locations of the corresponding plastic hinges have to be changed and a new analysis of the structure has to be conducted. Since the collapse load is not very sensitive to small changes in the positions of the plastic hinges, in most cases the second trial leads to a satisfactory result (Neal 1977).

Formulae are available to determine the location of the maximum bending moment of a bar. When a bar is loaded by a uniformly distributed load and the moments M_A and M_B

acting at the ends of the bar are known, the location and the magnitude of the maximum bending moment are found to be

$$x_0 = \frac{M_A + M_B}{pl},$$

$$M_{max} = M_K + \frac{px_0^2}{2}.$$

Here

$$M_K = \frac{pl^2}{8} + \frac{M_B - M_A}{2}$$

is the bending moment at the middle-section of the bar. The notations, the positive senses of the moments M_A and M_B and the distance x_0 are shown in Fig. 6—43.

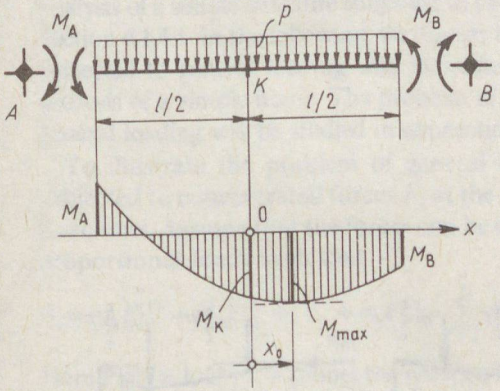


Fig. 6–43

(3) A good approximation can also be obtained by replacing the distributed load by concentrated forces, as shown in Fig. 6—44. The more concentrated forces used, the more accurate the approximation will be but, on the other hand, the number of critical cross-section and possible yield mechanisms will also be increased, leading to more complicated calculations.

To illustrate the problem, consider a frame with uniform plastic moments subjected to a uniformly distributed load (Fig. 6—45). On replacing the distributed load by two concentrated forces, two beam mechanisms should be taken into consideration (Figures 6—45(b) and (c)) which, together with the sway mechanism, result in two combined mechanisms, shown in Fig. 6—45(e) and (f). Omitting the details of the calculations, the kinematically admissible unstable load multipliers associated with the five yield mechanisms are given in Fig. 6—45. Because of the approximation applied here, even the smallest multiplier $m_k = 2.55\frac{M_p}{Fl}$ can be considered only as an approximate solution. The accuracy can be improved by replacing the distributed load by more concentrated forces. Still, the result obtained above is very likely to be sufficiently accurate for most practical purposes.

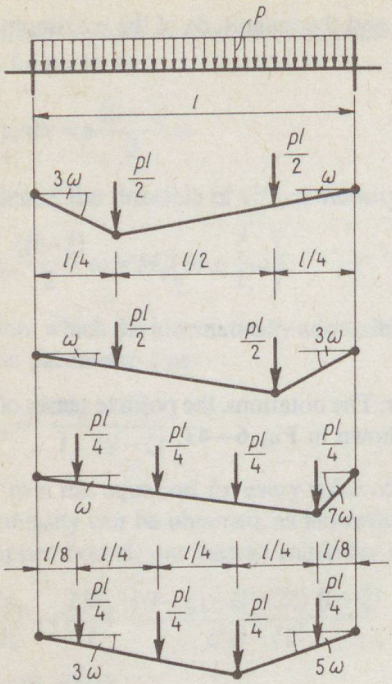


Fig. 6–44

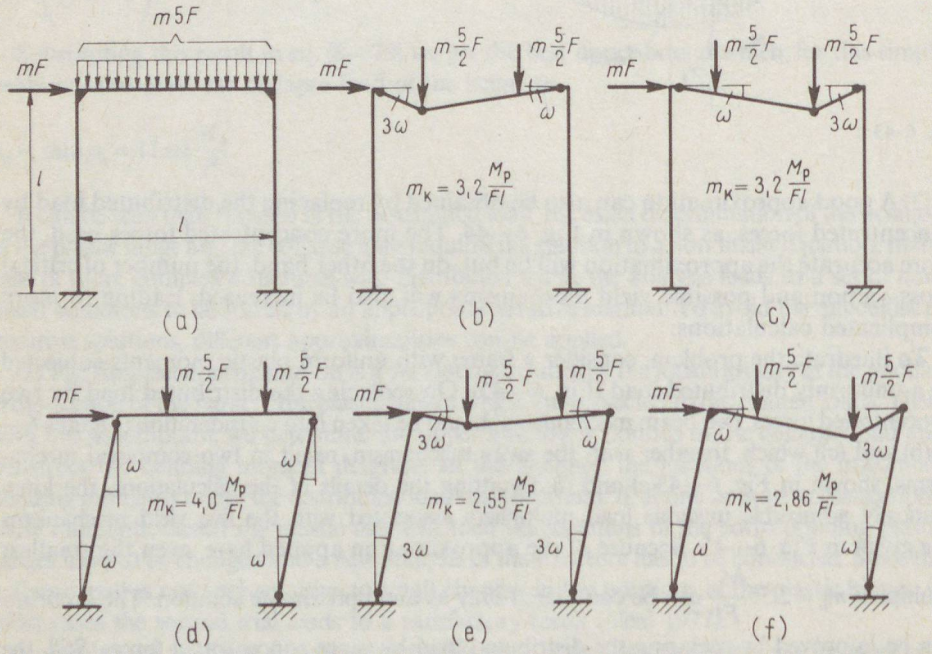


Fig. 6–45

6.4.4. GENERAL LOADING

6.4.4.1. BASIC RELATIONSHIPS

So far we have considered only the problem of *proportional loading* when the locations, directions and ratios of forces are fixed and the loading process is characterized by a monotonically increasing single parameter, called the load multiplier. In this simple case the purpose of limit analysis is to determine that specific value of the load multiplier at which plastic collapse will occur.

In most practical cases, however, structures are subjected to *general loading* which consists of a set of proportional loads which can vary independently of each other. In this general case, the load-carrying capacity of a structure cannot be characterized by a single collapse load multiplier but all the combinations of the independent loads under which the structure will collapse have to be defined.

The concept of general loading has already been presented in Section 3.4.4., and the limit analysis of a simple structure subjected to two independent forces has also been described in Section 4.1.4.1. In the following, we discuss the basic problem of limit analysis of structures subjected to general loading, and illustrate the exact and approximate solutions by the analysis of a simple frame. The problem of alternating and progressive plastic flow under general loading will be studied in connection with the shakedown analysis in Section 6.5.

To illustrate the problem of general loading, consider a bar structure which is subjected to concentrated forces F_i at the points $i=1,2,\ldots,s$ with given locations and directions. Assume that the forces can be divided into groups which form independent proportional loads such that

$$F_i = m_1 F_{i0}^{(1)} + m_2 F_{i0}^{(2)} + \ldots + m_r F_{i0}^{(r)} = \sum_{l=1}^{r} m_l F_{i0}^{l}. \tag{6—80}$$

Here $F_{i0}^{(1)}$ $l=1, 2, \ldots r$ denote the independent groups of forces, and m_l are the associated load multipliers. These multipliers can vary independently but are limited by the relationship

$$L(m_l) \leq 0, \tag{6—81}$$

which defines all the possible combinations of the external loads which can occur during the loading process. As already stated in Section 3.4.4., in an r-dimensional *load space* with the coordinate axes $m_1, m_2, \ldots, m_r$ the function $L(m_l)=0$ is illustrated by a closed hyper-surface bounding the *domain of possible loads*, and the curves inside this domain represent the *load paths*, as shown for the case $r=2$ in Fig. 6—46(a). In the case of proportional loading the ratios of m_l are kept unchanged during the loading process and the load path is illustrated by a straight line (see line OQ in Fig. 6—46(a)).

The combinations of the forces at which plastic deformation starts to develop and plastic collapse occurs are defined by two other functions

$$E(m_l, M_e)=0, \tag{6—82}$$

$$P(m_l, M_p)=0, \tag{6—83}$$

respectively, where M_e and M_p designate the elastic limit moment and the fully plastic moment of the structure, respectively. In the load space, these two functions are represented

by two closed hyper-surfaces and the two bounded domains correspond to loads which do not cause any plastic deformations and do not result in the plastic collapse of the structure, respectively (Fig. 6—46(b)). As described in Section 3.4.4., as a consequence of the residual stresses the *elastic limit surface* $E(m_1, M_e)=0$ is path-dependent; it will move and form subsequent surfaces during a general loading process. In accordance with the theory of limit analysis, on the other hand, the *plastic limit surface* $P(m_1, M_p)=0$ is path-independent. It is obvious that the elastic domain is the subset of the plastic domain, i.e.

$E(m_1, M_e) \subseteq P(M_1, M_p)$.

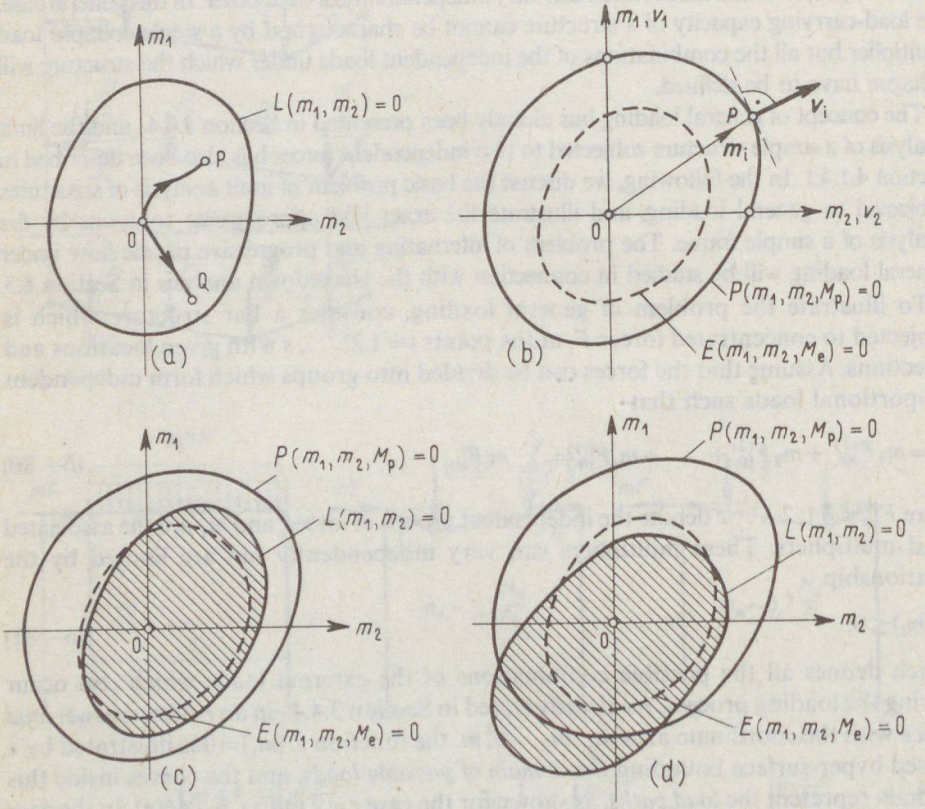


Fig. 6–46

If the domain of possible loads is included in the domain P, i.e. if

$$L(m_1) \subseteq P(m_1, M_p), \tag{6—84}$$

then the structure can carry all the loads without collapse (Fig. 6—46(c)). If, in addition, the condition

$$L(m_1) \subseteq E(m_1, M_e) \tag{6—85}$$

is satisfied then the structure will undergo only elastic deformations during the entire loading process. Finally, if the domain L is only partially included in the domain P, the structure will not be able to carry all the combinations of the loads which occur during the loading process, and will collapse (Fig. 6—46(d)).

In the case of general loading, the aim of limit analysis is to determine the plastic limit surface $P(m_1, M_p)=0$ which can be considered the yield condition for the entire structure. It can be proved that, like the yield surface $f(\sigma_{ij}, k)=0$, the plastic limit surface $P(m_1, M_p)=0$ is also convex and the normality rule is also valid (Hodge 1963). To prove the latter statement, consider an arbitrary yield mechanism of the structure designated by j, and denote the velocities of this mechanism at the points of application $i=1, 2, \ldots, s$ of the concentrated forces F_i by $v_1^{(j)}, v_2^{(j)}, \ldots, v_i^{(j)}, \ldots, v_s^{(j)}$ or by the super vector $v_i^{(j)}$. Then, making use of eq. (6—80) and applying the principle of virtual velocities the following equation can be obtained*

$$P^{(j)}=m_1 F_{i0}^{(1)} v_i^{(j)}+m_2 F_{i0}^{(2)} v_i^{(j)}+\ldots m_l F_{i0}^{(l)} v_i^{(j)}+\ldots+m_r F_{i0}^{(r)} v_i^{(j)}-P_M^{(j)}=0. \tag{6—86}$$

Here $P_M^{(j)}$ denotes the power exerted by the plastic moments M_p at the plastic hinges, and $F_{i0}^{(l)} v_i^{(j)}$ can be considered as *generalized velocity vectors* $V_l^{(j)}$ associated with the plastic multipliers m_l, i.e.

$$V_l^{(j)}=F_{i0}^{(l)} v_i^{(j)}. \tag{6—87}$$

Then, eq. (6—86) can be rewritten in the form

$$\left.\begin{aligned} &P^{(j)}=m_1 V_1^{(j)}+m_2 V_2^{(j)}+\ldots m_l V_l^{(j)}+\ldots m_r V_r^{(j)}-P_M^{(j)}=0 \\ &\text{or shortly} \\ &P^{(j)}=m_l V_l^{(j)}-P_M^{(j)}=0. \end{aligned}\right\} \tag{6—88}$$

For each yield mechanism, a similar equation can be obtained and the entire set of these equations defines the plastic limit surface $P(m_1, M_p)=0$ of the structure

$$P^{(j)}(m_l, M_p)=m_l V_l^{(j)}-P_M^{(j)}=0; \quad j=1,2,\ldots n. \tag{6—89}$$

It can be seen that *in the case of concentrated forces, the plastic limit surface consists of n hyper-planes*, where n is the number of possible yield mechanisms of the structure.

Considering eq. (6—88), one can write

$$\frac{\partial P^{(j)}}{\partial m_l}=V_l^{(j)}.$$

Since the magnitude of the generalized velocity vector defined by eq. (6—87) is not specified, the above relationship can be expressed in a more general form

$$V_l^{(j)}=\psi^{(j)}\frac{\partial P^{(j)}}{\partial m_l}, \quad j=1,2,\ldots n \tag{6—90}$$

or shortly

$$V_l=\psi\frac{\partial P}{\partial m_l}, \tag{6—91}$$

* In the following expressions the summation convention has to be applied.

where $\psi^{(j)} > 0$ denotes scalar multipliers. From these relationships it is evident that in the *velocity space* $V_1, V_2, \ldots, V_r$ coaxial with the load space $m_1, m_2, \ldots, m_r$, *the generalized velocity vector* V_1 associated with a point on the plastic limit surface $P(m_1, M_p) = 0$ will coincide with the outer normal of the surface at that point. Thus, with respect to the plastic limit surface $P(m_1, M_p) = 0$ the generalized velocities V_1 obey the normality rule.

Several methods have been suggested for the determination of the plastic limit surface (e.g. Prager 1953; Hodge 1957). One possible method of solution will now be illustrated by a simple example.

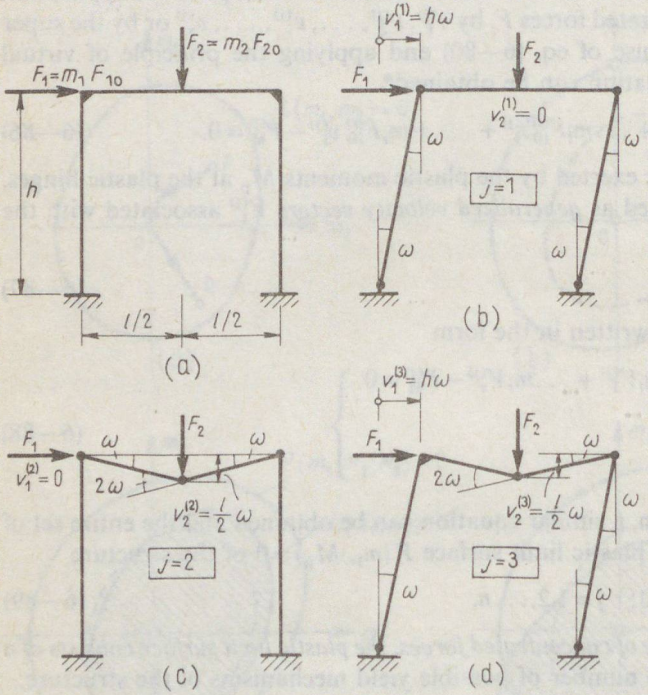


Fig. 6–47

6.4.4.2. ILLUSTRATIVE EXAMPLE

To illustrate the determination of the plastic limit surface $P(m_1, M_p) = 0$, consider the frame with constant plastic moment M_p shown in Fig. 6—47(a). The frame is subjected to two forces F_1 and F_2 which can vary independently, i.e. they are expressed in the forms* $F_1 = m_1 F_{10}^{(1)}$ and $F_2 = mF_{20}^{(2)}$. Considering the possible locations of plastic hinges, three yield mechanisms ($j = 1,2,3$) can develop, as shown in Fig. 6—47(b—c).

* In this simple problem, where the independent groups of loads consists of only one force, the use of the multipliers m_1 and m_2 is not necessary. Still, in accordance with the former section, we express the forces in a general form where $F_{10}^{(1)}$ and $F_{20}^{(2)}$ denote arbitrarily specified constants.

Then, on applying the principle of virtual velocities to these mechanisms, the following equations are obtained

$$P^{(1)} = m_1 F_{10}^{(1)} v_1^{(1)} - 4\omega M_p = 0,$$

$$P^{(2)} = m_2 F_{20}^{(2)} v_2^{(2)} - 4\omega M_p = 0,$$

$$P^{(3)} = m_1 F_{10}^{(1)} v_1^{(3)} + m_2 F_{20}^{(2)} v_2^{(3)} - 6\omega M_p = 0.$$

Using the relationships between the velocities and the rates of rotation illustrated in Fig. 6—47(b—c) leads to

$$\left.\begin{aligned} P^{(1)} &= m_1 (F_{10}^{(1)} h) - 4M_p = 0, \\ P^{(2)} &= m_2 (F_{20}^{(2)} l) - 8M_p = 0, \\ P^{(3)} &= m_1 (F_{10}^{(1)} h) + m_2 \left(F_{20}^{(2)} \frac{l}{2} \right) - 6M_p = 0. \end{aligned}\right\} \qquad (6—92)$$

Assuming that $m_1 \geq 0$ and $m_2 \geq 0$, in the load plane m_1, m_2 the above equations are represented by three straight lines illustrated in Fig. 6—48. These lines bound the domains of loads which can be carried by the frame without collapse. If the domain of possible loads is specified the comparison of these two domains makes possible the prediction of the behaviour of the frame during its loading history.

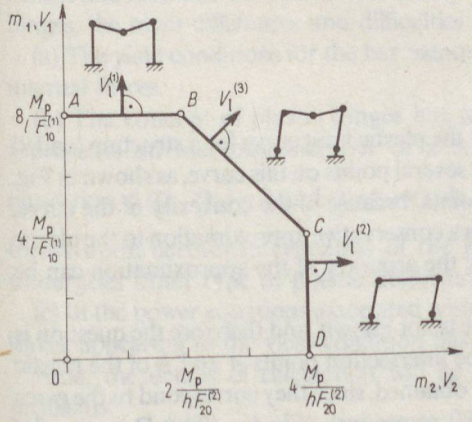


Fig. 6–48

In eq. (6—92), the terms in brackets give the components of the generalized velocity vectors associated with the three yield mechanisms

$$V_1^{(1)} (F_{10}^{(1)} h, 0); \quad V_1^{(2)} (0, F_{20}^{(2)} l); \quad V_1^{(3)} \left(F_{10}^{(1)} h, F_{20}^{(2)} \frac{l}{2} \right).$$

In the coordinate system V_1, V_2 coaxial with the axes m_1 and m_2 of the load plane, these vectors are perpendicular to the lines associated with the corresponding yield mechanisms (Fig. 6—48).

6.4.4.3. APPROXIMATE SOLUTIONS

In more complex problems, the exact determination of the plastic limit surface is complicated and needs a great deal of computation, mostly because of the great number of possible yield mechanisms. The convex property of the plastic limit surface allows the use of a simple and reliable approximation, which provides sufficiently accurate results for most practical purposes.

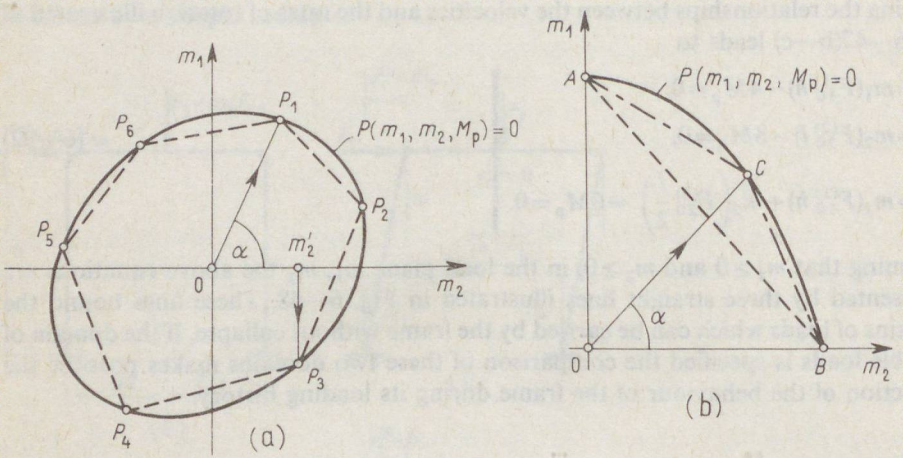


Fig. 6–49

To illustrate this approach, let us assume that the plastic limit curve for a structure loaded by a two-parameter loading is known, and select several points on this curve, as shown in Fig. 6—49(a). Then, the polygon defined by these points, because of the convexity of the curve, stays everywhere inside the domain and provides a conservative approximation to the plastic limit curve. By increasing the number of points, the accuracy of the approximation can be improved.

In an actual problem, of course, the limit curve is not known, and therefore the question is how one can determine its individual points. The intersection points A and B of the plastic limit curve with the axes m_1 and m_2 can easily be obtained, since they correspond to the cases of one-parameter loading, when $m_2 = 0$ and $m_1 = 0$, respectively (Fig. 6—49(b)). Denoting the associated collapse load multipliers by m_{10} and m_{20}, the straight line

$$\frac{m_1}{m_{10}} + \frac{m_2}{m_{20}} - 1 = 0$$

passing through the points A and B can already be considered a rough but conservative approximation to the plastic limit curve in the range $m_1 \geq 0$ and $m_2 \geq 0$. A further point (say C) on the curve can be obtained if we keep one of the multipliers or the ratio

$$\frac{m_1}{m_2} = \tan \alpha$$

fixed, and solve this one-parameter loading problem. Then, the lines defined by the points AC and BC will provide a more accurate approximation to the plastic limit curve. By determining further points, the accuracy can be improved to any desired degree.

The approach described can of course, be generalized to the case of multi-parameter loading.

6.4.5. EFFECT OF COMBINED INTERNAL FORCES

6.4.5.1. GENERAL REMARKS

Up to now we have assumed that the effect of the normal and shear forces and torque on the yield condition for the bar members can be neglected. This assumption leads to the concept of plastic hinges and significantly simplifies the elasto-plastic and limit analysis of bar structures. In most cases, the results obtained by this approximation are sufficiently accurate for practical purposes. There are, however, problems (e.g. multi-storey frames, arches) where the magnitudes of the internal forces, other than the bending moment, are large and their effect on the yield condition cannot be neglected. Next, we will briefly show how this effect can be taken into account in the limit analysis of bar structures.

In Section 6.2. we described the plastic behaviour of bar members under combined internal forces and in Section 6.4.1. we discussed the theorems of limit analysis in the general case, where all the internal forces are taken into account in the yield condition. Comparing these results and methods with the simple theory of limit analysis based on the concept of plastic hinges, the main differences and difficulties arising in the exact analysis are as follows:

(a) The yield conditions for the bar members are generally non-linear and contain all the internal forces.

(b) The concept of plastic hinges has to be generalized. A *generalized plastic hinge* represents an idealized member of a bar structure which obeys the general yield condition $\phi(Q_i, Q_0) = 0$ and the flow rule $\dot{q}_i = \dot{\lambda} \dfrac{\partial \phi}{\partial Q_i}$. Thus, a generalized plastic hinge forms upon certain interactions of the generalized stresses Q_i and besides rotation undergoes other type of plastic deformation.

(c) In the power equations associated with the yield mechanisms, the power of all internal forces appearing in the yield condition has to be taken into consideration.

Next, the details of calculation will be illustrated by the solutions to several simple problems.

6.4.5.2. ILLUSTRATIVE EXAMPLES

(1) Consider a *circular ring* with a uniform sandwich cross-section loaded by two concentrated forces, and determine the collapse load by taking the effects of normal forces in the yield condition into account (Fig. 6—50 (a)). Since in the cross-sections 1 and 1′ both the bending moments and the normal forces have extremal values, generalized plastic hinges will form here. Two more generalized plastic hinges are expected to develop at the points of application of the forces; hence, the yield mechanism of the ring will be the one shown in Fig. 6—50 (b). Considering the

equilibrium of the individual parts between the plastic hinges, it can be shown that the normal forces N_2 at the points 2 and 2′ are equal to zero, and therefore the corresponding bar members work as simple plastic hinges where only rotations ω_2 can occur and the strain rates v_2 vanish. In the generalized plastic hinges at points 1 and 1′, both rotations ω_1 and strain rates v_1 will develop. Then, considering the geometry of the yield mechanism, the relationships

$$\omega_1 = \omega_2 = \omega,$$

$$\dot{w}_F = \frac{1}{2} v_1 + \frac{1}{4} D\omega_1$$

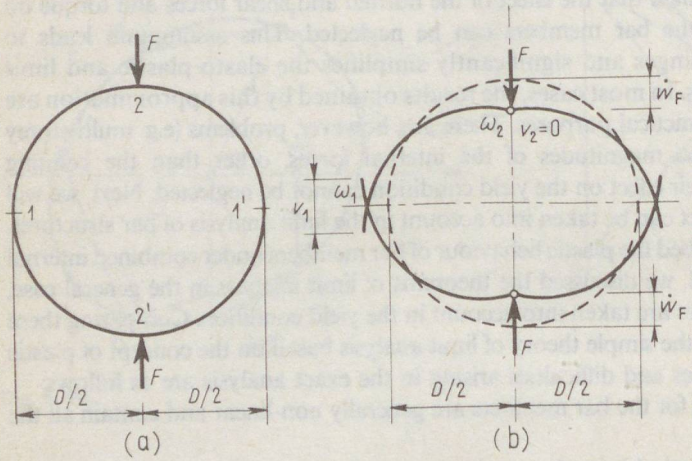


Fig. 5–50

are obtained and using eq. (6—16) the yield conditions of the plastic hinges have the form

$$\phi_1 = \frac{|M_1|}{M_p} + \frac{|N_1|}{N_p} - 1 = 0,$$

$$\phi_2 = \frac{|M_2|}{M_p} - 1 = 0.$$

In addition, according to the plastic flow rule given by eq. (6—13), the generalized strains ω_1 and v_1 satisfy the relationship

$$\frac{v_1}{\omega_1} = \frac{\partial\phi_1/\partial N_1}{\partial\phi_1/\partial M_1} = \frac{M_p}{N_p}.$$

Here for sandwich cross-sections $M_p/N_p = h/2$, where h denotes the height of the cross-section.

Finally, the power equation for the yield mechanism is found to be

$$2F_k\dot{w}_F = 2M_1\omega_1 + N_1 v_1 + M_2\omega_2.$$

Solving the above equations, the kinematically admissible load is obtained as

$$F_k = \left[\frac{1}{1+h/D}\right]\frac{8M_p}{D}.$$

It can be proved that the above solution is also statically admissible, therefore it gives the collapse load of the ring. The term in the bracket expresses the effect of the normal forces. Since this is always less than 1, the effect of normal forces is to decrease the collapse load. If, for example, $h/D=0.10$, the reduction is 9.9%.

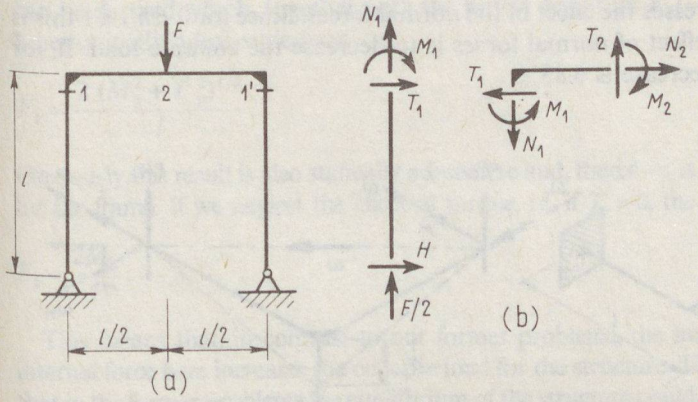


Fig. 6–51

(2) Let us calculate the collapse load of the *frame* with uniform sandwich cross-section shown in Fig. 6—51(a) by taking the interaction between the bending moments and the normal forces into consideration. Assuming generalized plastic hinges at the corners and under the concentrated force, the following equilibrium equations are obtained for the individual members of the frame shown in Fig. 6—51(b)

$$N_1 + \frac{F}{2} = 0, \quad N_2 - T_1 = 0,$$

$$T_1 + H = 0, \quad T_2 - N_1 = 0,$$

$$M_1 - Hl = 0, \quad M_2 - M_1 - N_1\frac{l}{2} = 0.$$

In addition, the yield conditions for the cross-sections 1 and 2 can be expressed in the form

$$\phi_1 = \frac{|M_1|}{M_p} + \frac{|N_1|}{N_p} - 1 = 0,$$

$$\phi_2 = \frac{|M_2|}{M_p} + \frac{|N_2|}{N_p} - 1 = 0.$$

From these equations the kinematically admissible load can be calculated from the expression

$$F_k = \left[\frac{1+\frac{1}{4}\left(\frac{h}{l}\right)}{1+\left(\frac{h}{l}\right)-\frac{1}{2}\left(\frac{h}{l}\right)^2} \right] \frac{8M_p}{l},$$

where h is the height of the sandwich cross-section. It can easily be proved that this result is also statically admissible therefore, it gives the collapse load of the frame. The term in the bracket expresses the effect of the normal forces. Since for $0<h/l<1$ this is always less than 1 the effect of normal forces is to decrease the collapse load. If, for example, $h/l=0.1$ the decrease is 6.85%.

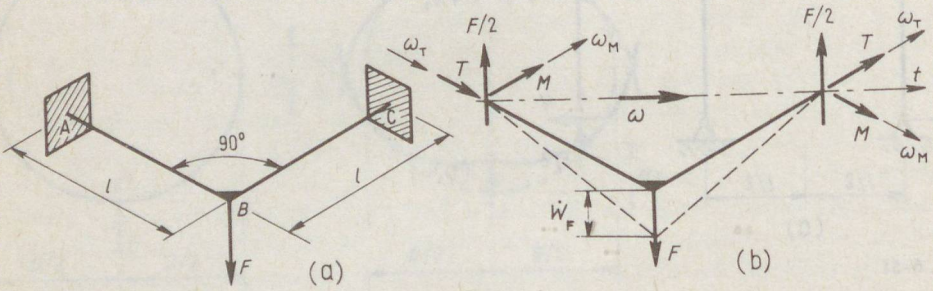


Fig. 6–52

(3) Determine the collapse load of the *frame* with uniform cross-section loaded by a concentrated force perpendicularly to its plane (Fig. 6—52(a)). In the analysis, the interaction between the bending moment and torque T will be taken into consideration, and the following approximate yield condition (see eq. (6—24)) will be used

$$\phi=\left(\frac{M}{M_p}\right)^2+\left(\frac{T}{T_p}\right)^2-1=0.$$

Assume that at collapse two generalized plastic hinges develop at the fixed ends, which allow the rotation ω of the frame about the axis t, as shown in Fig. 6—52(b). Then, the power equation for the yield mechanism becomes

$$F_k\dot{w}_F=2\,(M\omega_M+T\omega_T),$$

where $\omega_M=\omega_T=\frac{1}{\sqrt{2}}\omega$ denote the components of ω and $\dot{w}_F=\frac{l}{\sqrt{2}}\omega$ is the velocity at the point of application of the force. Substituting these relationships into the above equation yields

$$F_k l=2(M+T).$$

In addition, the plastic flow rule together with the result $\omega_M = \omega_T$ leads to the relationship

$$\frac{\omega_M}{\omega_T} = \frac{\partial\phi/\partial M}{\partial\phi/\partial T} = \frac{T_p^2}{M_p^2}\frac{M}{T} = 1.$$

Substituting this relationship into the yield condition, the expressions

$$M = \frac{M_p^2}{(M_p^2 + T_p^2)^{1/2}}, \quad T = \frac{T_p^2}{(M_p^2 + T_p^2)^{1/2}}$$

can be derived which, together with the power equation $F_k l = 2(M + T)$, provide the kinematically admissible load

$$F_k = \frac{2(M_p^2 + T_p^2)^{1/2}}{l}.$$

Obviously this result is also statically admissible and, therefore, is equal to the collapse load for the frame. If we neglect the effect of torque, i.e. if $T_p = 0$, the collapse load becomes

$$F_p = \frac{2M_p}{l}.$$

This means that, in contrast to our former problems, the interaction of an additional internal force here increases the collapse load for the structure. This is explained by the fact that in the former problems the equilibrium of the structure could not have been maintained without normal forces, while in the last problem the torque is a redundant internal force which can be omitted without violating the equilibrium of the frame. Hence, by taking the torque into consideration, we introduce an additional constraint which, according to the theorem presented in Section 3.4.3.5., cannot cause a decrease in the collapse load.

(4) In more complex structures the methods of solution described above lead to fairly complicated calculations, and therefore it is often preferable to apply approximate methods. One of these is a successive approximation, based on the repeated solution of the structure taking only the bending moments into consideration for the yield condition. The steps of this approximate solution are as follows.

(a) Determine the collapse load of the structure by taking only the bending moments into account for the yield condition.

(b) Calculate the internal forces (normal and shear forces and torques) arising in the plastic limit state of the structure, and modify the fully plastic moments in the plastic hinges by making use of the yield condition.

(c) Repeat the first step using the modified plastic moments.

The above procedure should be repeated until the difference between the collapse loads obtained by two successive steps is sufficiently small. The convergence of this approximate method is very good therefore, for practical purposes, sufficiently accurate results can be obtained after one or two repetitions.

Several other methods which take the interaction of the internal forces into consideration in the calculation of the collapse load have been published in the literature (see e.g. Hodge 1959; Heyman 1971; Horne 1971; Nonaka 1972).

6.5. DEFLECTIONS

6.5.1. INTRODUCTORY REMARKS

Applying the lower and upper bound theorems to the limit analysis of a structure subjected to proportional loading, one can determine the collapse load, the collapse mechanism and the corresponding internal force distribution but no information can be obtained about the deflections and deformations which may be expected on collapse. It is possible, however, that excessive deflections and deformations could occur before reaching the plastic limit, violating the serviceability criteria and causing other modes of failure. Besides, the bounding theorems are based on the assumption that the deflections are small and, therefore, their effects on the change in geometry of the structure are negligible. To check this assumption, it may be advisable in some cases to estimate the magnitudes of deflections at collapse.

The changes in geometry caused by large deflections may significantly influence the response of a structure. In the case of slender structures this effect must be taken into consideration. This can be achieved by exact or approximate methods dealing with the *large deflection theory* of elasto-plastic structures.

In the case of *general loading*, the deflections can play an even more important role. In structures under cyclic loading *alternating plastic flow* may occur, while under variable repeated loading conditions the accumulation of plastic deformations can lead to *progressive plastic flow*. In order to prevent these dangerous phenomena, the magnitudes of cyclic and variable loads should be kept below certain limits determined by *shakedown analysis*.

Next, the problems described above will be discussed in more detail.

6.5.2. DEFLECTIONS IN THE CASE OF PROPORTIONAL LOADING

6.5.2.1. ESTIMATE OF DEFLECTIONS AT COLLAPSE

6.5.2.1.1. ASSUMPTIONS AND BASIC RELATIONSHIPS

Applying the elasto-plastic incremental analysis described in Section 6.3.2., one can always determine the deflections which occur in a structure just before collapse. This analysis, however, needs lengthy calculations and therefore, as in the case of limit analysis, there is a need for methods which allow the direct calculation of the deflections at the point of collapse, without following the behaviour of the structure in the elastic and elasto-plastic state. Such a method was suggested by Symonds and Neal (1952) and is based on the following assumptions:

— the structure is subjected to proportional loading;
— the plastic deformations are concentrated into plastic hinges;
— the rotation of a plastic hinge never ceases, i.e. the plastic hinges do not become inactive during the loading process.

The first two assumptions are commonly used in limit analysis. In the case of proportional loading, the occurrence of inactive hinges is very rare, and therefore the method based on the above assumptions generally yields good approximate solutions.

To illustrate the idea of the method, consider a bar structure with r degrees of statical indeterminacy, and assume that the collapse mechanism is a complete yield mechanism with $r+1$ plastic hinges. Then, on increasing the proportional load more and more

plastic hinges develop in the bar structure and, in accordance with the above assumptions, continue to undergo rotation. Thus, just before the collapse load is reached, all except one of the hinges of the collapse mechanism will have formed and undergone rotation. At the point of collapse the bending moment at the location of the *last hinge* also reaches the fully plastic moment, but the rotation at this hinge will still be zero. At this instant, the structure has $r+1$ hinges where the moments $M_1, M_2, \ldots M_{r+1}$ are equal to the fully plastic moment and the rotations $\theta_1, \theta_2, \ldots \theta_{r+1}$ are unknown except for the rotation at the "last hinge", which is zero. Since the segments between the hinges are assumed to be perfectly elastic, the deflections of this special statically determinate structure can be calculated by the use of any method of elastic structural analysis.

The method described is based on the assumption that it is "a priori" known which is the last hinge to form in the collapse mechanism. The sequence of formation of plastic hinges, however, cannot be determined by the use of the bounding theorems of limit analysis, and therefore a general technique has to be developed where the last plastic hinge to form need not be specified in advance. Then, each plastic hinge can be assumed to be the last to form and for each case the corresponding displacements can be determined. It has been shown (Hodge 1959) that these displacements are *lower bounds* for the actual displacements in the idealized structure at collapse, and that location of the last plastic hinge which leads to the largest displacements provides the correct solution.*

The calculation of the deflections in the special structure described above is a simple problem which can be solved by many techniques of elastic structural analysis. Next, a method suggested by Heyman (1971) and Neal (1977) and based on the application of the principle of virtual forces will be briefly presented.

Consider a frame with r statical redundancies subjected to concentrated forces. Assume that the collapse mechanism is known, and that the deflection δ at a particular point in the frame at the instant when the collapse load is reached has to be calculated. In order to obtain δ, a virtual unit force corresponding to δ has to be applied to the collapse mechanism of the frame in which, for the time being, the last plastic hinge is not yet specified. Applying the principle of virtual forces (see Section 3.2.) the following equation can be obtained

$$\delta = \int \frac{M M^s}{EI} \, dx + \Sigma M_i^s \theta_i. \qquad (6—93)$$

Here M denotes the actual bending moments of the elastic segments between the plastic hinges of the collapse mechanism, M^s and M_i^s represent a statically admissible bending moment distribution and bending moments in the plastic hinges i, respectively, which satisfy the requirements of equilibrium with the virtual unit force, and θ_i designates the actual plastic hinge rotations. The integration of expression (6—93) is extended to all

* It has also been proved that, if inactive plastic hinges develop during the proportional loading process, the largest predicted displacement will be greater than the correct displacement (Hodge 1959).

segments in the frame, and the summation covers all positions where plastic hinge rotation occurs in the collapse mechanism. In the case of a complete collapse mechanism, the associated actual moment distribution in the frame is known and a statically admissible moment distribution can also be easily constructed. The plastic hinge rotations, however, are unknown and therefore, in order to be able to solve the problem, the equations of compatibility of the collapse mechanism also have to be taken into consideration. For a frame with r degrees of statical indeterminacy, r independent compatibility equations can be constructed. Making use again of the principle of virtual forces, one of these equations can be expressed in the following general form

$$\int \frac{\bar{M}^s M}{EI}\,dx + \Sigma \bar{M}_i^s \theta_i = 0. \tag{6—94}$$

Here $\bar{M}_s$ and $\bar{M}_i^s$ designate an *arbitrary* statically admissible *self-equilibrating* bending moment distribution maintaining equilibrium with zero external loads, and M and θ_i have the same meanings as defined in connection with eq. (6—93). In the case of a frame with r degrees of statical redundancy, r *independent* self-equilibrating moment distributions can be constructed, and by the repeated use of eq. (6—94), the r independent compatibility equations can be produced.

The compatibility equations together with eq. (6—93) uniquely define the geometry of motion of the collapse mechanism. If one of the hinge rotations is cancelled they give the displacement δ and hinge rotations θ_i which correspond to the case when the last plastic hinge is assumed to occur at the location of the cancelled rotation. Repeating this calculation for all the plastic hinges, $(r+1)$ values can be calculated for δ and the largest of them gives the correct displacement in the frame at the instant of collapse.

In the typical case where the frame has uniform straight segments, and within the segments M, M^s and $\bar{M}^s$ vary linearly, the integrals of eqs (6—93) and (6—94) for a segment AB of length L can be expressed in the following forms

$$\int_A^B \frac{M^s M}{EI}\,dx = \frac{L}{6EI}[M_A^s(2M_A + M_B) + M_B^s(2M_B + M_A)], \tag{6—95}$$

$$\int_A^B \frac{\bar{M}^s M}{EI}\,dx = \frac{L}{6EI}[\bar{M}_A^s(2M_A + M_B) + \bar{M}_B^s(2M_B + M_A)]. \tag{6—96}$$

Here the subscripts A and B refer to the moments at the points A and B of the segment. If plastic hinges develop at these points of the collapse mechanism, M_A and M_B are equal to either $+M_p$ or $-M_p$.

Finally, we note that in the case of a partial collapse mechanism, the corresponding moment distribution cannot be uniquely determined by equilibrium equations alone. However, this does not represent any additional difficulties in determining the deflections at collapse (see e.g. Hodge 1959; Neal 1977).

6.5.2.1.2. ILLUSTRATIVE EXAMPLE

In order to illustrate the application of the method described above, consider the rectangular frame with uniform flexural rigidity EI and fully plastic moment M_p shown in Fig. 6—53(a), and determine the horizontal deflection at point 2 which will occur at the instant of collapse.

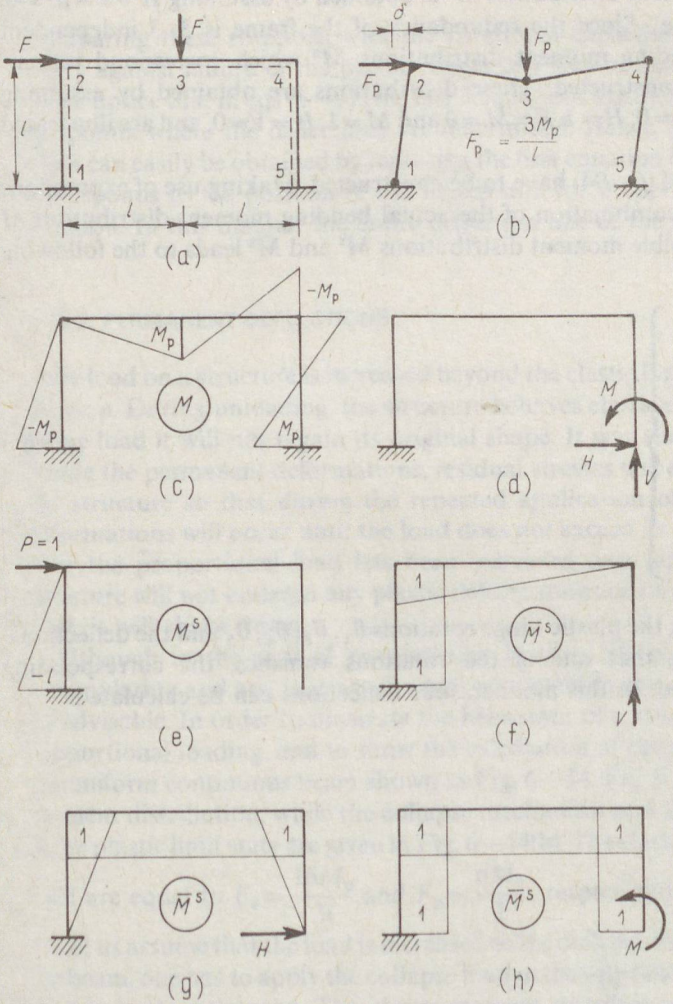


Fig. 6–53

In the following, a bending moment will be considered positive if it causes tension in the fibres adjacent to the broken line in Fig. 6—53(a). Positive hinge rotations correspond to positive bending moments.

The collapse mechanism of the frame is illustrated in Fig. 6—53(b). The associated collapse load is equal to $F_p = \frac{3M_p}{l}$, and the corresponding bending moment

distribution obtained by simple equilibrium considerations is given in Fig. 6—53(c). The statically admissible bending moment distributions M^s and $\bar{M}^s$ can be constructed on one of the statically determinate released systems of the frame which is shown in Fig. 6—53(d). In order to determine the horizontal deflection δ at point 2, a horizontal unit force has to be applied at the same point. The corresponding statically admissible moment distribution M^s is obtained by assuming $H = V = M = 0$, as shown in Fig. 6—53(e). Since the redundancy of the frame is 3, 3 independent statically admissible bending moment distributions $\bar{M}^s$ which correspond to zero external forces can be constructed. These distributions are obtained by assuming successively $V = 1, H = M = 0$; $H = 1, V = M = 0$ and $M = 1, H = V = 0$, and are illustrated in Fig. 6—53(f – h).

Finally, eqs (6—93) and (6—94) have to be constructed. Making use of expressions (6—95) and (6—96) the combination of the actual bending moment distribution M with the statically admissible moment distributions M^s and $\bar{M}^s$ leads to the following equations

$$\left.\begin{aligned} &\delta = \frac{M_p l^2}{3EI} - l\,\theta_1, \\ &-\frac{M_p l}{12EI} + \theta_1 + 0.5\theta_3 = 0, \\ &\frac{M_p l}{6EI} + \theta_3 + \theta_4 = 0, \\ &\theta_1 + \theta_3 + \theta_4 + \theta_5 = 0. \end{aligned}\right\} \qquad (6—97)$$

In these four equations, the plastic hinge rotations $\theta_1, \theta_3, \theta_4, \theta_5$ and the deflection δ are unknown. Assuming that one of the rotations vanishes, the corresponding deflection can be obtained. In this manner, four deflections can be calculated:

$$\text{if } \theta_1 = 0, \quad \delta_1 = \frac{M_p l^2}{3EI},$$

$$\text{if } \theta_3 = 0, \quad \delta_3 = \frac{M_p l^2}{4EI},$$

$$\text{if } \theta_4 = 0, \quad \delta_4 = \frac{M_p l^2}{6EI},$$

$$\text{if } \theta_5 = 0, \quad \delta_5 = \frac{M_p l^2}{6EI}.$$

The largest of these deflections is the correct solution which is associated here with the case $\theta_1 = 0$. Hence, the last plastic hinge will develop in section 1 and the horizontal deflection in the frame at the instant of collapse is equal to

$$\delta_{coll} = \frac{M_p l^2}{3EI}.$$

The corresponding plastic hinge rotations are as follows:

$$\theta_1 = 0, \quad \theta_3 = \frac{M_p l}{6EI}, \quad \theta_4 = -\frac{M_p l}{3EI}, \quad \theta_5 = \frac{M_p l}{6EI}.$$

Comparing these rotations with the rotational capacities of the plastic hinges, the safety against failure of the plastic hinges can also be estimated.

We notice that in eqs (6—97) the last 3 equations are independent of the locations of the points where the deflections are determined. Hence, the deflection at any other point can easily be obtained by replacing the first equation by a new relationship which corresponds to the position of the virtual unit force appropriate to the deflection in question. In this manner the entire deflection line of the frame can be constructed.

6.5.2.2. PERMANENT DEFLECTIONS

If the load on a structure is increased beyond the elastic limit, plastic deformations will develop. During unloading, the structure behaves elastically and after removal of the entire load it will not regain its original shape. It was shown in section 4.1.2.2. that, beside the permanent deformations, residual stresses will also remain which prestress the structure so that during the repeated application of the same load no plastic deformations will occur until the load does not exceed its original magnitude. Hence, after the proportional load has been increased once up to the collapse load, the structure will not undergo any plastic deformations during further applications of the load; it will shake down.

Although in the case of proportional loading the plastic deformations are not accumulating and are, in general, small; in certain problems their determination may be advisable. In order to illustrate the behaviour of a structure subjected to repeated proportional loading, and to show the calculation of permanent deflections, consider the uniform continuous beam shown in Fig. 6—54. Fig. 6—54(a) illustrates the elastic moment distribution, while the collapse mechanism and the moment distribution M^p in the plastic limit state are given in Fig. 6—54(b). The elastic limit load and the collapse load are equal to $F_e = \frac{16M_p}{3l}$ and $F_p = \frac{6M_p}{l}$, respectively.

Let us assume that the load is increased to the collapse load. Then, in order to unload the beam, one has to apply the collapse load in the opposite direction while the original load is kept unchanged. The *elastic* moment distribution M^e corresponding to the opposite load is shown in Fig. 6—54(c). The residual moments M^r are then equal to the sum of the two moment distributions, $M^r = M^p + M^e$. In a similar manner, denoting by u^p and u^e the deflections corresponding to the plastic limit state and to the *elastic* unloading, respectively, the permanent (residual) deflections are $u^r = u^p + u^e$. Here u^p can be determined by a step-by-step analysis, or by the method described in the previous section, while for the computation of u^e any method of elastic structural analysis can be used.

In our example, the residual moment at the middle support is found to be

$$M_B^r = -M_p + \frac{9}{8}M = \frac{1}{8}M_p$$

and the residual moment distribution is illustrated in Fig. 6—54(d).

The deflection under the force at the instant of collapse is $u_F^p = \frac{15}{128}\frac{M_p l^2}{EI}$, while the deflection corresponding to the elastic unloading is found to be $u_F^e = -\frac{7}{128}\frac{M_p l^2}{EI}$.

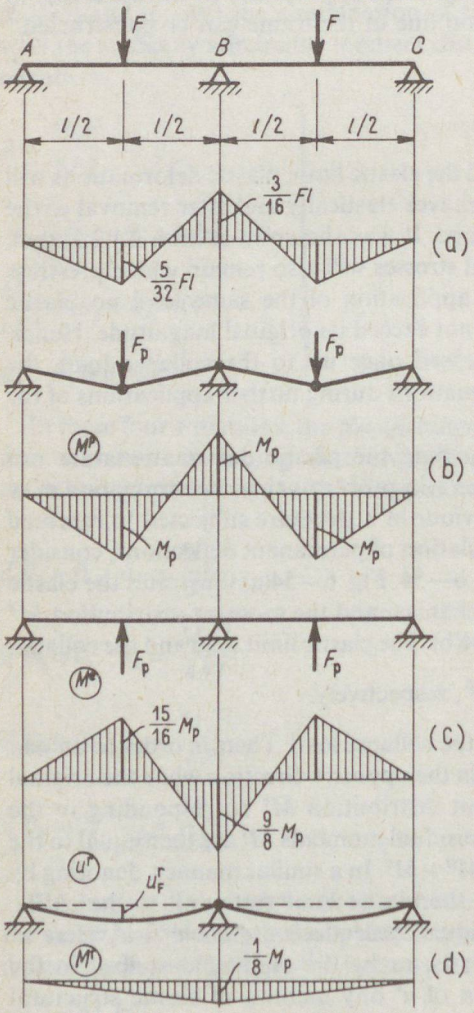


Fig. 6–54

Hence, the permanent deflection is obtained as

$$u_F^r = \frac{15}{128}\frac{M_p l^2}{EI} - \frac{7}{128}\frac{M_p l^2}{EI} = \frac{8}{128}\frac{M_p l^2}{EI} = \frac{M_p l^2}{16EI}.$$

The permanent deflections in the beam are illustrated in Fig. 6—54(d).

The residual moments prestress the beam so that on applying the same load repeatedly no further plastic deformations and permanent deflections will occur, provided that the load is less than the collapse load. Considering the definition of the residual moments, this statement is obvious.

The above statements are not valid in those cases where the collapse load is larger than twice the elastic limit load, i.e. if $F_p > 2F_e$. By definition, the maximum elastic bending moment associated with the elastic limit load is equal to M_p, and therefore the fictitious elastic bending moments which correspond to a load larger than $2F_e$ will exceed $2M_p$ in certain sections. Consequently, during unloading with a load $F > 2F_e$, the structure cannot behave wholly elastically and plastic deformations will occur in the opposite direction. Therefore a residual moment distribution which could permit the wholly elastic behaviour of the structure during the next loading process cannot develop. This means that the structure will not shake down. Because, except in a few special cases, the condition $F_p < 2F_e$ is satisfied for most structures, the phenomenon described above has no practical importance.

6.5.3. DEFLECTIONS IN THE CASE OF GENERAL LOADING

The problems of the elasto-plastic behaviour of bodies and structures subjected to general loading have already been discussed in detail in Section 3.4.4. There are three ways in which failure can occur due to general loading conditions.

(a) Under certain combinations of loads, *unrestricted plastic deformations* can occur which lead to the *plastic collapse* of the structure. This problem has already been discussed in Section 6.4.4.

(b) Under the repeated application of a certain load, even though no single combination is sufficiently large to cause plastic collapse, the structure may undergo plastic deformations each time which may *accumulate* without limit and lead to *incremental (progressive) collapse.*

(c) If the general loading is cyclic in character, then even though the loads are less than the plastic collapse load, at each cycle *alternating plastic deformations* may arise which can eventually lead to failure by low cycle fatigue.

The accumulating and alternating plastic deformations of bar structures will be studied next. First, the phenomenon will be illustrated by a simple problem and then the general theory of shakedown analysis presented in Section 3.4.4. will be applied to bar structures.

6.5.3.1. ACCUMULATING AND ALTERNATING PLASTIC DEFORMATIONS

In order to illustrate the problem of accumulating plastic deformations, consider a continuous uniform beam which is subjected to two independent loads F_1 and F_2 (Fig. 6—55). Assume that during the repeated application of these loads, both of them

are increased up to their collapse magnitudes, which are the same and equal to $F_{1p}=F_{2p}=\dfrac{6M_p}{l}$.

Figure 6—55(a) shows the permanent deflections and residual moments which correspond to the case when F_{1p} is applied to the beam and then removed. In this case, the first plastic moment develops at the middle-support and here the residual moment is equal to $+\dfrac{1}{8}M_p$.

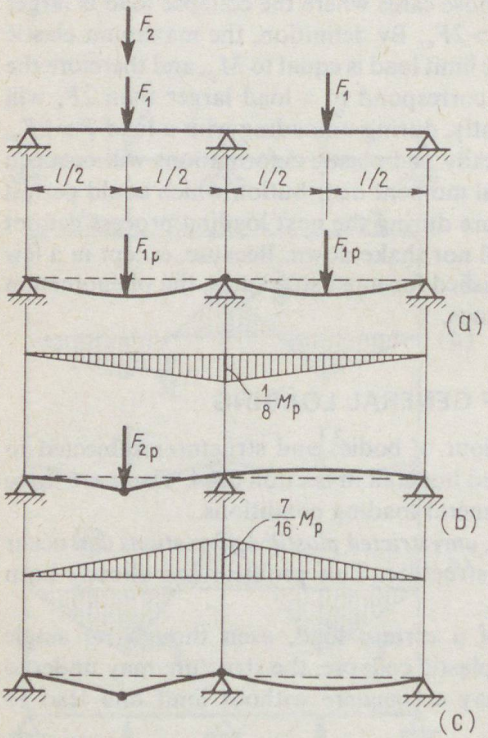


Fig. 6–55

Applying the load F_{2p} the first plastic hinge will form under the force, and after unloading the residual moment at the middle-support will be $-\dfrac{7}{16}M_p$ (Fig. 6—55(b)).

Now let us assume that the loads F_{1p} and F_{2p} are applied repeatedly one after the other. Then, after each repetition, the residual moments associated with the loads F_{1p} and F_{2p} will cancel each other out, and during reloading further plastic deformations will occur. These plastic deformations will accumulate and will lead to incremental (progressive) collapse of the beam (Fig. 6—55(c)).

In order to avoid incremental collapse, the forces F_1 and F_2 have to be kept below certain limits, lower than F_{1p} and F_{2p}, which allows the development of sufficient

residual moments for the plastic deformations not to accumulate and for the beam to shake down. The determination of these limits is the subject of shakedown analysis.

Next, consider a *cyclic loading* when a single load varies in magnitude between the limits $F^+ > 0$ and $F^- < 0$. This cyclic loading can be considered a special two-parameter loading in which the repeatedly applied independent loads are $0 \leq F_1 \leq F^+$ and $0 \geq F_2 \geq F^-$. Hence, in this case the cyclic loading is merely a special case of the problem of variable repeated loading. One can determine those upper and lower limits of the load which allow the development of residual moments, at which the structure ceases to undergo alternating plastic deformations and will shake down. As will be proved in the next section, in the case of cyclic loading the condition for shakedown is expressed in the simple form

$$(F^+ - F^-) \leq 2F_e, \tag{6—98}$$

where F_e designates the elastic limit load of the structure.

6.5.3.2. SHAKEDOWN ANALYSIS

The goal of shakedown analysis is to determine those conditions and bounds for a general loading process at which plastic deformations will eventually cease and the structure will shake down. The static theorem of shakedown analysis has already been discussed and proved for linearly elastic-perfectly plastic bodies in Section 3.4.4.2. Next, we will apply this general theorem to bar structures. In this analysis we will use the plastic hinge approach, i.e. we will assume that all the plastic deformations are concentrated in plastic hinges and that in the yield conditions for the bar members only the bending moments have to be taken into account. In addition, the small deformation theory will be applied.

(1) Consider a bar structure with the fully plastic moments M_{pi} in the critical cross-sections $i = 1, 2, \ldots, n$. The structure is subjected to a general loading which consists of the concentrated forces F_j. Assume that these forces can be divided into independent groups $F_j^{(l)} = m_l F_{j0}^{(l)}$ where $F_{j0}^{(l)}$ denotes time-independent force vectors and the multipliers m_l can vary independently of each other during the loading process.

First, the elastic moment distributions in the structure have to be considered. Denote the *elastic moments* calculated from the independent loads $F_{j0}^{(l)}$ by $\mathcal{M}_{i0}^{(l)}$. Then, using the principle of superposition the minimum and maximum possible values of the elastic moments at the critical cross-sections can be determined when all the possible combinations of the loads between their prescribed limits are taken into account. In elastic structural analysis, these are called the maximum and minimum bending moment distributions and will be denoted by $(\mathcal{M}_i)_{max}$ and $(\mathcal{M}_i)_{min}$, respectively.

To establish the shakedown theorem the *residual moment distributions*, which maintain equilibrium with zero external loads, have also to be considered. Let us denote the values of an arbitrary residual moment distribution at the critical cross-sections by M_i^r. It is evident, that if in the structure such residual moment distribution M_i^r develops which, together with the maximum and minimum elastic bending moments, respectively, nowhere exceeds the fully plastic moments, then the structure will have no further plastic deformations. According to the static theorem of

shakedown analysis presented in Section 3.4.4., if there exists such a residual moment distribution then this distribution or an other one, which also satisfies the above conditions, will actually develop and the structure will shake down. Hence, the static theorem of shakedown analysis for bar structures is formulated as below.

If at least one residual moment distribution M_i^r exists such that the conditions

$$\left.\begin{aligned} (\mathcal{M}_i)_{max} + M_i^r \leq M_{pi}, \\ (\mathcal{M}_i)_{min} + M_i^r \geq -M_{pi}, \end{aligned}\right\} \quad (i = 1, 2, \ldots n) \tag{6—99}$$

are satisfied, then this residual moment distribution, or another one which also fulfils the above conditions, will develop and the structure will shake down.

It is evident that if no such residual moment distribution exists which satisfies the conditions (6—99) then shakedown cannot occur. Next, the general formulation of shakedown given above will be applied to special loading processes.

(2) Let us consider the problem when a *common maximum value* m_{sh} of the load multipliers $m_l \leq 0$ has to be determined, such that if $m_l \leq m_{sh}$ then the structure will shake down. This common maximum value is called the *shakedown load multiplier*. In this special case, the maximum and minimum elastic bending moments of the critical cross-sections can be expressed as

$$(\mathcal{M}_i)_{max} = m_{sh}(\mathcal{M}_i^0)_{max},$$

$$(\mathcal{M}_i)_{min} = m_{sh}(\mathcal{M}_i^0)_{min},$$

where $(\mathcal{M}_i^0)_{max}$ and $(\mathcal{M}_i^0)_{min}$ denote the maximum and minimum elastic bending moments calculated from all the possible combinations of the loads $F_{j0}^{(1)}$ (i.e. when $m_1 = 1$ for each load group). Then, making use of the general shakedown condition (6—99) the problem of determination of the shakedown load multiplier m_{sh} is formulated as follows

$$\left.\begin{aligned} & m_{sh}(\mathcal{M}_i^0)_{max} + M_i^r \leq M_{pi}, \\ & m_{sh}(\mathcal{M}_i^0)_{min} + M_i^r \geq -M_{pi}, \\ & m_{sh} = \max! \end{aligned}\right\} \quad i = 1, 2, \ldots n. \tag{6—100}$$

Here the unknown residual moments M_i^r have to satisfy the equilibrium equations expressed in the general linear form*

$$a_{ki} M_i^r = 0 \begin{cases} k = 1, 2, \ldots (n-r), \\ i = 1, 2, \ldots n, \end{cases} \tag{6—101}$$

where n and r are the number of critical cross-sections and the degree of statical redundancy of the structure, respectively. As can be seen, the determination of the shakedown load multiplier is a *linear programming* problem, which will be discussed in that context in more detail in Section 6.7.

* For the subscript i, the summation convention applies.

In most practical problems certain groups among the loads (e.g. the dead load) remain unchanged during the loading process, and for them the common multiplier m_{sh} should not be applied. Then, eqs (6—100) have to be modified as

$$\left.\begin{aligned} m_{sh}(\mathcal{M}_i^0)_{max}+\mathcal{M}_i^s+M_i^r \le M_{pi},\\ m_{sh}(\mathcal{M}_i^0)_{min}+\mathcal{M}_i^s+M_i^r \ge -M_{pi}, \end{aligned}\right\} \quad i=1,\,2,\,\ldots,\,n \tag{6—102}$$

where $\mathcal{M}_i^s$ denotes the bending moments associated with the loads remaining constant during the loading process.

(3) Considering the static theorem of shakedown analysis defined by eqs (6—102) it is obvious that if we assume an arbitrary residual moment distribution $\bar{M}_i^r$, the load multiplier m_{sh}^s which satisfies the conditions

$$\left.\begin{aligned} m_{sh}^s(\mathcal{M}_i^0)_{max}+\bar{M}_i^r \le M_{pi},\\ m_{sh}^s(\mathcal{M}_i^0)_{min}+\bar{M}_i^r \ge -M_{pi}, \end{aligned}\right\} \quad i=1,\,2,\,\ldots,\,n \tag{6—103}$$

is a lower bound of the shakedown load multiplier, i.e.

$$m_{sh}^s \le m_{sh}. \tag{6—104}$$

In this case the multiplier m_{sh}^s can be determined from the bending moments of the mostly exhausted cross-section, i.e.

$$m_{sh}^s = \min\left[\left|\frac{M_{pi}-\bar{M}_i^r}{(\mathcal{M}_i^0)_{max}}\right|, \left|\frac{-M_{pi}-\bar{M}_i^r}{(\mathcal{M}_i^0)_{min}}\right|\right]. \tag{6—105}$$

Equations (6—103)—(6—105) are valid also in the special case when the residual moments are choosen to be zero along the entire structure. Then, eqs (6—103) can be expressed in the simple form

$$m_{sh}^s\,|\mathcal{M}_i^0|_{max} \le M_{pi} \tag{6—106}$$

and eq. (6—105) leads to

$$m_{sh}^s = \min \frac{M_{pi}}{|\mathcal{M}_i^0|_{max}}. \tag{6—107}$$

Here $|\mathcal{M}_i^0|_{max}$ denotes the larger of the values $|(\mathcal{M}_i^0)_{max}|$ and $|(\mathcal{M}_i^0)_{min}|$. It is obvious that if the load multipliers m_1 of the multi-parameter loading do not exceed the common multiplier m_{sh}^E defined by eq. (6—107), then during the entire loading procedure the structure will not undergo plastic deformations at all. Thus, choosing the lower bound given by eq. (6—107) as an allowable limit for the multipliers m_1 corresponds to the elastic design of the structure.

(4) Finally, consider the problem of *alternating cyclic loading*, when the structure is subjected to a proportional load the magnitude of which might vary between the limits m^+ and m^-. In this special case, the maximum and minimum elastic moments of the critical cross-sections are expressed in the form

$$\left.\begin{aligned} (\mathcal{M}_i)_{max}=m^+\mathcal{M}_i^0,\\ (\mathcal{M}_i)_{min}=m^-\mathcal{M}_i^0, \end{aligned}\right\} \quad i=1,2,\ldots\,n \tag{6—108}$$

where $\mathcal{M}_i^0$ denotes the elastic moment distribution in the case when $m=1$. The elastic limit load multiplier m_e satisfies, by definition, the condition

$$m_e \mathcal{M}_i^0 \leq M_{pi}, \quad i=1,2,\ldots n. \tag{6—109}$$

Substracting the inequalities (6—99) from each other and making use of relationships (6—108) and (6—109), the following relationship can be obtained

$$(m^+ - m^-) \leq 2m_e. \tag{6—110}$$

Hence, one can state that if the magnitude of an alternating cyclic load varies only within a range equal to twice the elastic limit load multiplier, then alternating plastic deformations will not repeat infinitely, i.e. the structure will shake down.

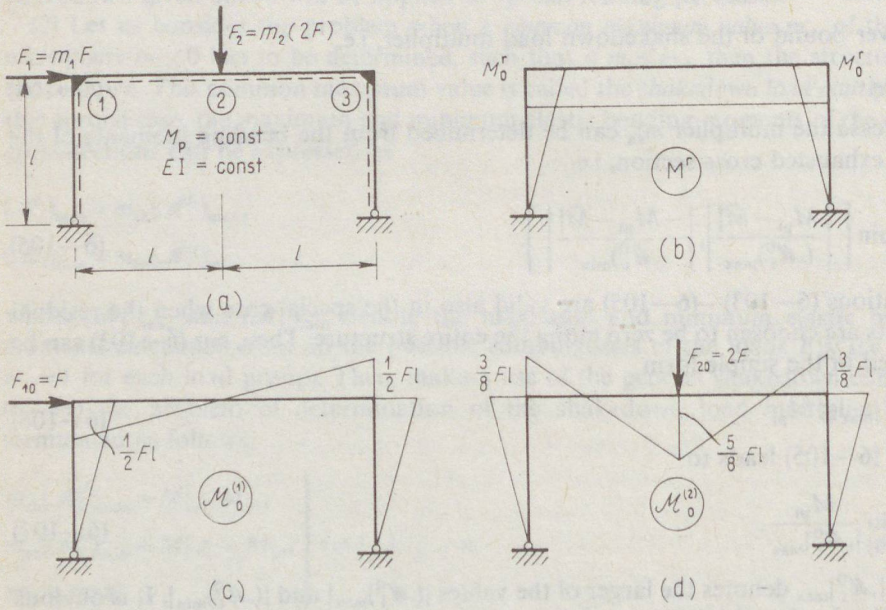


Fig. 6–56

(5) In order to illustrate the application of shakedown analysis defined by eqs (6—102) consider the frame with uniform flexural stiffness EI and fully plastic moment M_p shown in Fig. 6—56 (a). The frame is subjected to a two-parameter loading where the forces $F_1=m_1F$ and $F_2=m_2(2F)$ can vary independently. The problem is to determine the common maximum value m_{sh} of the parameters m_1 and m_2 such that if $0 \leq m_1 \leq m_{sh}$ and $0 \leq m_2 \leq m_{sh}$ then the frame will shake down. Since the degree of statical redundancy of the frame is 1, only one residual moment distribution can be constructed, as shown in Fig. 6—56(b). The elastic bending moments corresponding to the forces $F_{10}=F$ and $F_{20}=2F$ are illustrated in Fig. 6—56 (c—d) and are given in the first four columns

Table 6—2

Cross-section	$F_{10}=F$		$F_{20}=2F$		F_{10} and F_{20}		M^r
	$\mathcal{M}_{0i}^{max}$	$\mathcal{M}_{0i}^{min}$	$\mathcal{M}_{0i}^{max}$	$\mathcal{M}_{0i}^{min}$	$(\mathcal{M}_i^0)_{max}$	$(\mathcal{M}_i^0)_{min}$	
1	$\frac{1}{2}Fl$	0	0	$-\frac{3}{8}Fl$	$\frac{1}{2}Fl$	$-\frac{3}{8}Fl$	M_0^r
2	0	0	$\frac{5}{8}Fl$	0	$\frac{5}{8}Fl$	0	M_0^r
3	0	$-\frac{1}{2}Fl$	0	$-\frac{3}{8}Fl$	0	$-\frac{7}{8}Fl$	M_0^r

of Table 6—2. The next two columns of the Table show the maximum and minimum elastic bending moments obtained by the critical combinations of the forces F_{10} and F_{20}. Making use of these results, eqs. (6—102) are expressed in the following form:

$$\frac{1}{2}Flm_{sh}+M_0^r\leq M_p,$$

$$-\frac{3}{8}Flm_{sh}+M_0^r\geq -M_p,$$

$$\frac{5}{8}Flm_{sh}+M_0^r\leq M_p,$$

$$-M_0^r\geq -M_p,$$

$$+M_0^r\leq M_p,$$

$$-\frac{7}{8}Flm_{sh}+M_0^r\geq -M_p,$$

$m_{sh}=\max!$

The solution to this linear programming problem leads to

$$m_{sh}=\frac{4}{3}\frac{M_p}{Fl} \quad \text{and} \quad M_0^r=\frac{1}{8}M_p.$$

In connection with eqs (6—103)—(6—107) it has been shown that a lower bound solution can be obtained by the use of an arbitrary residual moment distribution. Assuming e.g. that $M_0^r=0$, the above equations will provide the lower bound

$$m_{sh}^s=\frac{8}{7}\frac{M_p}{Fl}\leq m_{sh}.$$

(6) Finally, it is important to note that shakedown analysis does not provide any information about the permanent deflections which will accumulate in the structure

before shakedown occurs. There are, however, a number of other methods and theorems which allow the estimation of the approximate values and bounds of the permanent deflections in the case of general loading conditions (see. e.g. Koiter 1960; König 1972; Vitiello 1972; Capurso 1974; Neal 1977; Dorosz 1978).

6.5.4. EFFECT OF DEFLECTIONS ON THE COLLAPSE LOAD

6.5.4.1. INTRODUCTION

As it is known from the elastic analysis of structures, the changes in geometry caused by large deflections can influence the behaviour of structures significantly. Because the elasto-plastic deflections are larger than the elastic ones, the second order effect plays an even more important role in the case of elasto-plastic and limit analysis. Large elasto-plastic deflections can considerably decrease the plastic collapse load of slender frames. In these cases, the lower and upper bound theorems of limit analysis are not valid and the load-carrying capacity must be determined by the use of the *large deflection theory*. Because of geometrical non-linearities, this theory leads to very complicated calculations and therefore in most cases approximate and numerical methods have to be applied.

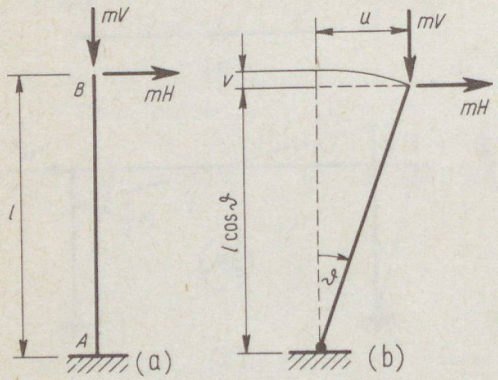


Fig. 6–57

To illustrate the effect of large deflections consider a rigid-perfectly plastic column with a constant plastic moment M_p loaded by a vertical and a horizontal force, as shown in Fig. 6—57(a). At lower values of the common multiplier m of the forces no deformations will take place. When, however, the multiplier reaches the value $m_p = \frac{M_p}{Hl}$ a plastic hinge will form at the point A and the column will undergo the lateral deflections shown in Fig. 6—57(b). In order to maintain equilibrium in the new position of the column, the equilibrium equation

$$mHl\cos\theta + mVu - M_p = 0$$

has to be satisfied. From this

$$m = \frac{M_p}{Hl\cos\theta + Vu} = \frac{M_p}{Hl\left(1 - \frac{u^2}{l^2}\right)^{1/2} + Vu}. \qquad (6—111)$$

If we assume that the deflections are relatively small, the approximation $\cos\theta \approx 1$ can be applied and the following approximate relationship between the horizontal deflection u and the load multiplier m can be obtained

$$m = \frac{M_p}{Hl + Vu}. \qquad (6—112)$$

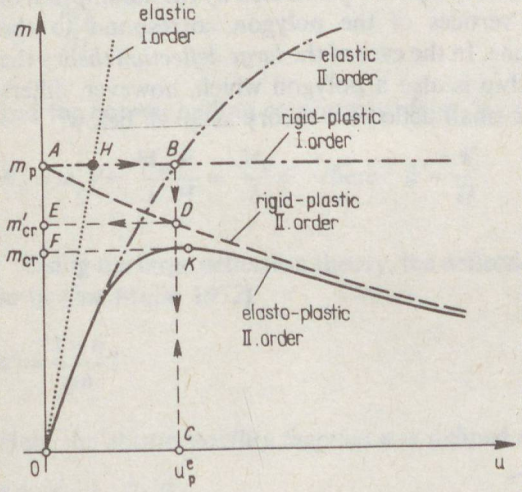


Fig. 6–58

The load–deflection diagrams of the column obtained by the use of different assumptions are shown in Fig. 6—58. First, let us suppose that the *small deflection theory* is applied. Then, assuming *perfectly elastic* material, the load–deflection relationship is represented by a straight line, while in the case of *rigid–perfectly plastic* material the deflections start to occur only if m reaches m_p and then grown indefinitely under a constant load. When the material is *elasto-plastic* the combination of these two relationships gives the appropriate load–deflection diagram (see line *O-H-B*).

Applying the *large deflection theory*, the *perfectly elastic* relationship is non-linear, and when the column is *rigid–perfectly plastic* to maintain equilibrium at increasing deflections the loads must be decreased, as defined by eqs (6—111) and (6—112). The *elasto-plastic* response of the column is represented by a curve which is below the perfectly elastic and rigid–perfectly plastic curves, and has a maximum value m_{cr}. Reaching this intensity, the equilibrium of the column becomes critical and m_{cr} gives

the load-carrying capacity of the column. The exact determination of this critical load is fairly complicated even in this simple case, and therefore approximate methods (to be discussed below) have to be applied.

6.5.4.2. NON-LINEAR ELASTO-PLASTIC ANALYSIS OF FRAMES

(1) In order to illustrate the non-linear elasto-plastic behaviour of frames, let us again consider the frame subjected to proportional loading, shown in Fig. 6—39. The relationships between the load intensity m and the horizontal deflection u at the point 2 corresponding to different assumptions and theories are illustrated by the curves of Fig. 6—59. Applying the *small deflection theory* to the analysis of the elasto-plastic frame, the load–deflection relationship is characterized by a polygon which finally reaches the horizontal line of the plastic collapse load multiplier m_p obtained by the assumption of rigid–perfectly plastic material. The vertices of the polygon correspond to the development of plastic hinges in the frame. In the case of the *large deflection theory* the elasto-plastic load–deflection relationship is also a polygon which, however, differs significantly from that obtained by the small deflection theory as given below:

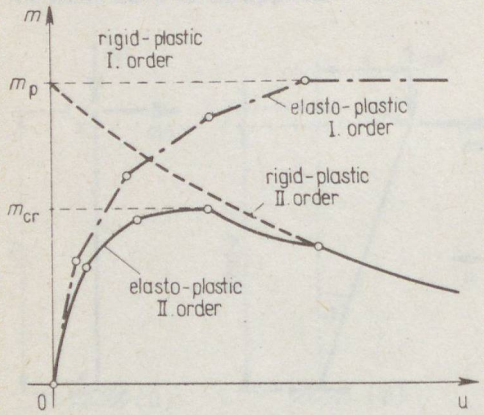


Fig. 6–59

— the lines between the vertices are curves rather than straight lines;
— the polygon is below the curve obtained by the rigid-plastic large deflection theory;
— the sequence of occurrence of plastic hinges may be different from that obtained by the small deflection theory;
— in the case of slender frames, because of the loss of stability, collapse can occur before a yield mechanism of the frame is reached.

From the above statements it is obvious that the change in geometry may significantly influence the elasto-plastic behaviour of frames; in particular, the load-carrying capacity of slender frames may be much smaller than that obtained by the small deflection theory. Because of its theoretical interest and practical importance,

several exact and approximate methods have been suggested for the solution to this problem (see. e.g. Horn 1961; Livesley 1964; Horne, Merchant 1965; Vogel 1965; Maier, 1968; Majid 1972; Moy 1981). Next, two simple approximate methods will be presented, by the use of which the elasto-plastic analysis based on the large deflection theory can be avoided.

(2) To illustrate the approximate method suggested by Majid (1972) consider again the column shown in Fig. 6—57. The idea of this method is that one first determines the deflection u_p^e caused by the plastic collapse load m_p, using the large deflection *elastic theory*. Then the load m'_{cr}, which leads to the same deflection by the use of the large deflection *rigid-plastic theory*, can be used as an approximation for the critical load of the column, i.e. $m_{cr} \approx m'_{cr}$. In Fig. 6—58, the line *A-B-C-D-E* illustrates the method of solution.

The *plastic collapse load* intensity of the column is obtained by

$$m_p = \frac{M_p}{lH}$$

and the corresponding compressive force is equal to

$$N_p = m_p V = \frac{M_p}{l}\frac{V}{H} = \frac{M_p}{l}\psi, \text{ where } \psi = \frac{V}{H}. \tag{6—113}$$

Using the large deflection theory, the deflection of the *linear elastic* column is found to be (see Majid 1972)

$$u^e = \frac{1-n}{\psi n} l. \tag{6—114}$$

Here the *elastic stability function* n is defined as

$$n = 4\phi_3 - 3\phi_2/\phi_1, \tag{6—115}$$

where

$$\left.\begin{aligned} &\phi_1 = \alpha \cot \alpha, \quad \phi_2 = \frac{\alpha^2}{3(1-\phi_1)}, \quad \phi_3 = \frac{3\phi_2 + \phi_1}{4}, \\ &\alpha = \frac{\pi}{2}\sqrt{\rho}, \quad \rho = \frac{Nl^2}{\pi^2 EI}, \end{aligned}\right\} \tag{6—116}$$

N is the compressive force and EI is the flexural stiffness of the column.

Substituting the compressive force N_p given by eq. (6—113) into eqs (6—115) and (6—116) one can calculate the value n_p of the stability function associated with the plastic limit load m_p. Then, from eq. (6—114) the corresponding elastic deflection can also be obtained

$$u_p^e = \frac{1-n_p}{\psi n_p} l. \tag{6—117}$$

Finally, the load intensity, which by the use of the large deflection rigid-plastic theory leads to the same deflection, is obtained from eq. (6—112)

$$m'_{cr} = \frac{M_p}{Hl + Vu_p^e} = \frac{M_p}{Hl\left(1 + \psi \frac{u_p^e}{l}\right)}$$

or making use of eq. (6—117)

$$m'_{cr} = n_p \frac{M_p}{Hl} = n_p m_p. \tag{6—118}$$

As can be seen, the plastic collapse load m_p multiplied by the value n_p of the elastic stability function associated with the plastic collapse load m_p gives the approximate value m'_{cr} of the critical load on the column. In this manner, the solution is reduced to the determination of the simple plastic collapse load and to the analysis based on the large deflection elastic theory.

The method described above can be generalized and provides a relatively simple tool for the approximate calculation of the critical load for elasto-plastic frames (see e.g. Majid 1972).

(3) Another approximate solution can be obtained by using the *Rankine–Merchant method*. This approximation is based on the simple observation that very stiff frames collapse at the simple plastic collapse load, while very flexible ones buckle at the elastic critical load, and therefore the behaviour of a common frame must be inbetween these two cases. Hence, the critical load multiplier m_{cr} can be approximated by the load multiplier m_R defined by the relation

$$\frac{1}{m_R} = \frac{1}{m_p} + \frac{1}{m_e}, \tag{6—119}$$

or

$$1 = \frac{m_R}{m_p} + \frac{m_R}{m_e}, \tag{6—120}$$

from which

$$m_R = \frac{m_p}{1 + m_p/m_e}. \tag{6—121}$$

Here m_p denotes the simple plastic collapse load multiplier, m_e is the elastic critical load multiplier at which the frame buckles and m_R is called the *Rankine–Merchant load multiplier*.

In the coordinate system m/m_p, m/m_e the state of equilibrium of a frame subjected to a load with intensity m is represented by a point, while eq. (6—120), which defines the approximate values m_R of the critical load multipliers m_{cr}, is illustrated by a straight line (Fig. 6–60). As long as the point is inside the region bounded by the line, buckling of the frame will not occur.

The theoretical and experimental results prove that the Rankine–Merchant formula provides reliable and conservative approximations for the critical loads of frames. On

the other hand, this method is very simple because it needs only the calculation of the simple plastic collapse load and the elastic critical load for the structure.

A number of other methods which deal with the large deflection analysis of elasto-plastic frames can be found in the literature (e.g. Freitas, Smith 1985). Among others Halász (1972, 1976) derived several theorems for the calculation of the critical load for elasto-plastic frames, and suggested design methods based on the large deflection theory for the determination of the fully plastic moments and flexural stiffnesses of "relatively stiff" frames at which a collapse mechanism develops before the critical load is reached.

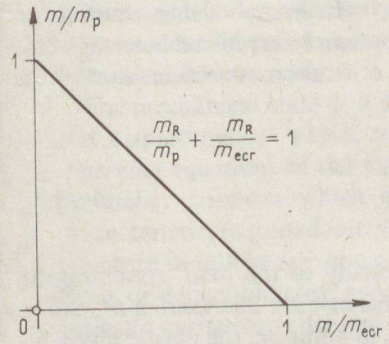


Fig. 5–60

One should note that the elasto-plastic behaviour and load-carrying capacity of steel frames can be significantly influenced by *local instability effects*, such as buckling of flanges, and torisonal and lateral buckling of individual bars. The theoretical and experimental investigation of these problems is presented in the literature (e.g. Beedle 1958; Reckling 1967; Halász 1967; Galambos 1968; Iványi 1969, 1984).

6.6. PLASTIC DESIGN

6.6.1. BASIC PRINCIPLES

In previous sections of this chapter, problems of *limit analyis*, where the basic geometry of the structure and the plastic moments of the members are fully specified and *the plastic collapse load has to be determined*, were discussed. Next, we will deal with the problem of *plastic design*, where the basic geometry of the structure and the loads are specified and *we have to find the plastic moments of the members* such that plastic collapse will occur only at the most critical magnitudes and combinations of the loads.

The concepts and methods of plastic design are widely used in engineering practice, because they provide considerable flexibility and fully utilize the plastic reserve of structures which leads to the design of highly economical structures. In addition, the calculations required by plastic theory are, in general, easier than those required by elastic theory. In certain cases, however, accumulating and alternating plastic deformations are more critical than resistance to plastic collapse or the large

deflections and stability effects significantly influence the load carrying capacity of the structure. In these cases, the applicability of plastic design is restricted; it needs to be modified or applied in combination with other methods.

In the following discussions only the bending moments will be taken into consideration in the yield condition for the members, i.e. the *plastic hinge approximation* will be used and the effects of deflections will be neglected. In addition, we assume that the structure is subjected to *proportional loading* given by the forces $F_j = mF_{j0}$.

To illustrate the concept of design based on the static theorem of limit analysis, consider a bar structure with r degree of static indeterminacy and denote the critical cross-sections, where plastic hinges can form, by $i = 1, 2, \ldots n$. Using equilibrium equations the moments M_i of the critical cross-sections can be expressed in terms of the moments M_{oi} calculated from the forces F_{jo} at the critical cross-sections and of the redundant forces X_l in the following general form*

$$M_i = mM_{oi} + b_{il}X_l \quad \begin{cases} i = 1,2,\ldots n, \\ l = 1,2,\ldots r, \end{cases} \tag{6—122}$$

Here b_{il} denotes constants and m is the given intensity of the load. Assuming an *arbitrary* set of redundant forces, a *statically admissible moment distribution* M_i can be obtained from the equilibrium equations (6—122). If, in addition, the plastic moments M_{ip} of the critical cross sections are chosen such that

$$-M_{pi} \leq M_i \leq M_{pi}; \quad i = 1,2,\ldots n, \tag{6—123}$$

then the given load multiplier is a *statically admissible safe multiplier* and, according to the static theorem of limit analysis, one can write

$$m = m_s \leq m_p. \tag{6—124}$$

We can conclude that *the plastic design for a structure can be based on any arbitrary statically admissible moment distribution.* Assuming different sets for the redundant forces, different statically admissible moment distributions can be obtained which lead to different solutions. Thus, the problem of limit design is not uniquely defined; therefore, by the suitable choice of the redundant forces, additional requirements can also be satisfied.

An important requirement is that the structure should not undergo excessive plastic deformations. This is obviously satisfied if the assumed redundant forces do not significantly deviate from those obtained by elastic theory. Hence, in plastic design, one always has to keep in mind the elastic solution to the problem.

By suitable choice of redundant forces, certain structural and economic requirements can also be satisfied, and solutions can be obtained which lead, for example, to the minimum cost or minimum weight of the structure. This is the problem of *optimal plastic design*, to be discussed next.

* In these equations the summation convention is applied.

6.6.2. OPTIMAL PLASTIC DESIGN

6.6.2.1. INTRODUCTION

The layout and mechanical state of a structure are characterized by different types of parameters and variables.

The layout of a structure denotes the arrangement of the centerlines of its members, the types and locations of its supports, the shapes and dimensions of its cross-sections and the material properties. The complete specification of a structure involves parameters with values fixed in advance or chosen by the designer. The latter are called *design variables*. The layout of a structure is, however, restricted by certain *technological* and *geometrical* constraints and the design standards also prescribe some *behaviour* constraints for the strength, stiffness and stability of structures. These are called *design constraints*.

The mechanical state of a structure is described by *state variables* (stresses, strains and displacements) which, together with the design variables, have to satisfy the *governing equations* of the structure. The idea of optimal design is to introduce an optimality criterion which expresses the requirement that certain advantageous characteristics (e.g. load-carrying capacity, energy absorption capacity, stiffness) of the structure should be maxima or certain disadvantageous characteristics (e.g. maximum stress or deflection, cost, volume or weight of the structure) should be minima. This *optimality criterion* is defined by one or more functions, called *objective functions*. The problem of optimal design is to select the design variables so that the governing equations, the design constraints and the optimality criterion are simultaneously satisfied.

In the past three decades, a great variery of optimal design methods have been developed and, especially in the field of *optimal plastic design*, very successful results have been achieved (see e.g. Johnson 1961; Wasiutynski, Brandt 1963; Gallagher, Zienkiewicz 1973; Prager 1974; Rozvany 1976; Save, Prager 1985). The main reason for this success is that, in contrast to the elastic design of statically indeterminate structures, in the case of plastic design only the equilibrium equations have to be satisfied as the governing equations which allows much more freedom for the optimal selection of the design variables. It also involves simpler calculations, which is particularly advantageous when a large number of re-analyses are needed in an iterative procedure, such as optimization.

6.6.2.2. MINIMUM WEIGHT DESIGN

A great number of optimal plastic design methods deal with the minimization of the cost of the material required for the construction of the structure. Then, the objective function expresses the cost of the material and may be called the *cost function*. Considering only homogeneous structures, the cost of the material is proportional to the weight; therefore in these cases the optimal design reduces to the minimization of the weight of the structure and is called *minimum weight design*.

In homogeneous structures, the weight is proportional to the volume and therefore the problem of minimum weight design reduces to the minimization of the volume of the structure, and should be called *minimum volume design*. This terminology, however,

is not used in the literature. It is generally assumed that the density of the material is equal to unity, and then the magnitudes of the weight and volume are identical.

In order to construct the *weight function* W for a structure, we have to specify a relationship between the *weight per unit length* w and the fully plastic moment M_p of the bar members. This specific weight function depends on the shape and dimensions of the cross-section and on the material properties, and has the general form

$$w = w(M_p). \tag{6—125}$$

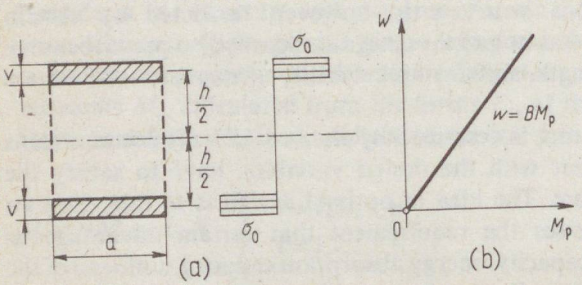


Fig. 6–61

Knowing this function, the weight of the entire structure can also be expressed in terms of the unknown plastic moments

$$W = \int_L w(M_p)\, ds. \tag{6—126}$$

Here the integral is extended over the total lengths L of the bars. In most cases, the structure consists of prismatic members with lengths l_i and constant plastic moments M_{pi}. Then, the weight function becomes

$$W = \sum l_i w_i(M_{pi}). \tag{6—127}$$

To derive the specific weight functions, first consider an idealized *sandwich bar* shown in Fig. 6—61. Denoting by γ the specific weight of the material, the weight per unit length of the bar is equal to

$$w = 2\gamma\, av$$

and the fully plastic moment is given by

$$M_p = av\, h\sigma_0.$$

Combining these two relationships, we get

$$w = KM_p \tag{6—128}$$

where $K = \dfrac{2\gamma}{\sigma_0 h}$ is a constant.

For cross-sections with other shapes, one can derive other relationships which can be described by the general formula

$$w = CM_p^{\alpha} \tag{6—129}$$

where C and α denote properly chosen constants*. For example, in the case of rectangular cross-sections with constant height or constant width we have $\alpha = 1$ and $\alpha = 1/2$, respectively.

In the case of steel I-sections, continuous functions for the specific weight function cannot be derived, but eq. (6—129) may still provide a good approximation and, depending on the type of section, α should be chosen between 1/2 and 2/3.

The use of non-linear specific weight functions generally leads to serious mathematical difficulties and therefore it appears reasonable to approximate them by a linear relationship

$$w = A + BM_p, \tag{6—130}$$

where A and B are constants. Then, using eq. (6—127) the total weight of the structure becomes

$$W = A\Sigma l_i + B\Sigma l_i M_{pi}. \tag{6—131}$$

Since here A, B and Σl_i are constants, the problem of minimizing W is equivalent to minimizing the expression

$$\Sigma l_i M_{pi}. \tag{6—132}$$

Hence, we come to the conclusion that *using linear specific weight functions, the optimal solution does not depend on the particular linear approximation used and, consequently, on the shape of the cross-sections.*

Next, we will discuss the problem of minimum weight design of bar structures with piece-wise variable and continuously variable plastic moments, respectively.

6.6.2.3. STRUCTURES WITH PIECE-WISE VARIABLE PLASTIC MOMENTS

In this section, the minimum weight design of bar structures composed of prismatic members with given lengths l_i and constant plastic moments M_{pi} will be discussed. The shape of the cross-sections of the members will not be specified, because the weight function will be approximated by the linear formula given by eq. (6—132).

(1) First consider a trivial example, when a continuous beam has a *uniform plastic moment* M_p along its entire length (Fig. 6—62). The statically admissible moments of the critical cross-sections can be expressed in terms of the redundant moment X

$$M_1 = \frac{Fl}{4} + \frac{1}{2}X, \quad M_2 = X.$$

* In finding the minimum of the weight function (6—127) the constant C does not play any role, and therefore its magnitude is irrelevant.

They have to satisfy the yield conditions

$$-M_p \leq \frac{Fl}{4} + \frac{1}{2}X \leq M_p,$$

$$-M_p \leq X \leq M_p,$$

and the optimality criterion, which in this case is minimum weight and becomes

$$\Sigma M_{pi} l_i = 2lM_p = \min!$$

This criterion expresses the trivial fact that, if the structure has a constant plastic moment, the optimal solution is obtained by minimizing the magnitude of this plastic moment.

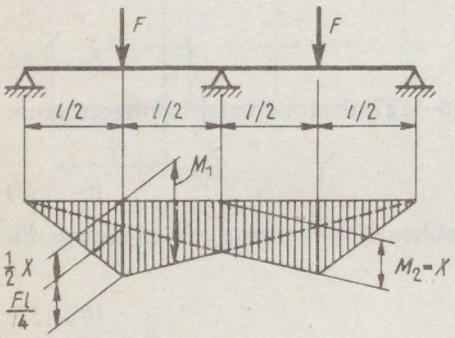


Fig. 6–62

From the first yield condition, it is evident that M_p will be a minimum if X assumes its least possible value, which according to the second yield condition is $-M_p$. Then the optimal solution becomes

$$M_p = \frac{Fl}{6}.$$

We note that in this solution, the magnitudes of the maximum positive and maximum negative moments are equal, i.e. $|M_1| = |M_2|$, which evidently provides the optimal solution to the problem.

(2) As an illustrative example consider a continuous beam constructed of two prismatic members with constant plastic moments M_{p1} and M_{p2}, as shown in Fig. 6—63 (Heyman 1971). Applying the *static theorem* of limit analysis in order to determine the optimal solution, we have to find that statically admissible moment distribution which satisfies the yield conditions and minimizes the weight of the beam. The statically admissible moments of the critical sections can be expressed in terms of the redundant moment X

$$M_1 = 60 + \frac{1}{2}X, \quad M_2 = M_3 = X,$$

$$M_4 = 30 + \frac{1}{2}X$$

and have to satisfy the yield conditions

$$\left.\begin{aligned} -M_{p1} \le 60 + \frac{1}{2} X \le M_{p1}, \\ -M_{p1} \le X \le M_{p1}, \\ -M_{p2} \le X \le M_{p2}, \\ -M_{p2} \le 30 + \frac{1}{2} X \le M_{p2}, \end{aligned}\right\} \qquad (6—133)$$

and the optimality criterion

$$W = M_{p1} + M_{p2} = \min! \qquad (6—134)$$

The solution of this *linear programming problem* is $X = -20$, $M_{p1} = 50$, $M_{p2} = 20$.

The minimum weight design can be based on the *kinematic theorem* of limit analysis, as well. It is evident that *if the plastic moments of a structure are chosen such that, for all possible yield mechanisms, the power of the external forces does not exceed the power of the plastic moments then the structure is strong enough to support the loads.* If, in addition, the function of optimality criterion is at its minimum value, this particular set of plastic moments will provide the optimal solution for the structure.

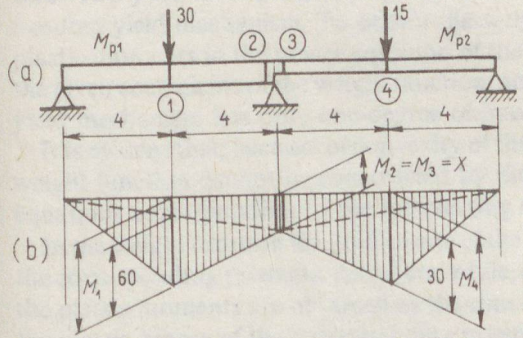


Fig. 6–63

All the possible yield mechanisms for the continuous beam under consideration are shown in (Fig. 6—64).* The corresponding power equations which express the above statement are as follows

$$\left.\begin{aligned} 3M_{p1} &\ge 120, \\ 2M_{p1} + M_{p2} &\ge 120, \\ M_{p1} + 2M_{p2} &\ge 60, \\ 3M_{p2} &\ge 60. \end{aligned}\right\} \qquad (6—135)$$

* Because of the sudden change of the plastic moment, on both sides of the middle support the possibility of forming plastic hinges has to be taken into consideration.

These equations together with the requirement of minimum weight (6—134) lead to a *linear programming problem*, and, of course, provide the same solution as was obtained by the use of the static theorem.

The concept and mechanical content of minimum weight design may be illustrated by means of a geometric interpretation. Consider the two-dimensional *design space* of the plastic moments M_{p1} and M_{p2} (Fig. 6—65). In this space eqs (6—135) are represented by four straight lines denoted by *a*, *b*, *c* and *d* in Fig. 6—65, and a particular

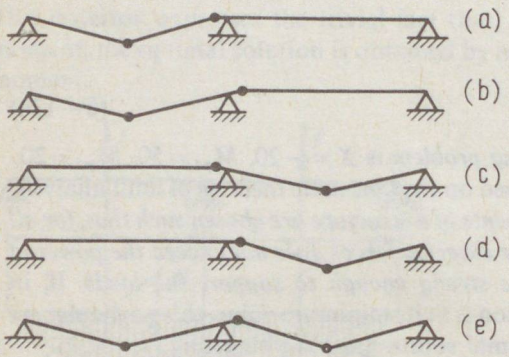


Fig. 6–64

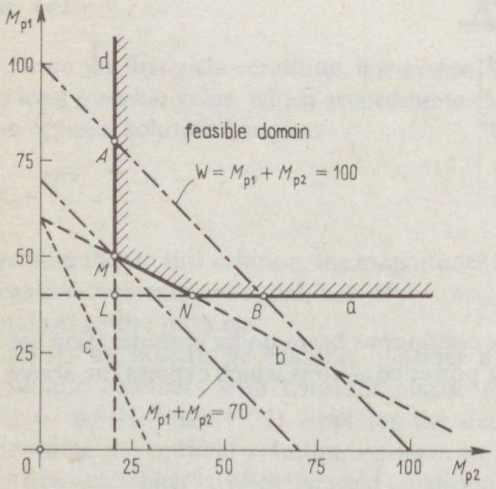


Fig. 6–65

solution is defined by a point with the coordinates M_{p1} and M_{p2}. As a consequence of the definition of plastic hinges, the coefficients of eqs (6—135) are always positive; therefore, the domain bounded by these lines is *convex* towards the origin. Any point in this domain represents a *feasible design*, since the corresponding plastic moments satisfy the inequalities of eqs (6—135) and the points on the boundary line correspond

to such solutions which provide structures that will just fail at the given load. Hence the domain is referred to as the *feasible domain.*

For a given value of W the linear weight function

$$W = M_{p1} + M_{p2}$$

can also be represented by a straight line in the design space. Let us assume that the weight of the beam is prescribed to be a given constant, say 100. Then, the corresponding line can be plotted, as shown in Fig. 6—65, and any point on the segment AB of this line, which is in the feasible domain, represents a feasible design with weight 100.

Since the magnitude of W decreases as the position of the line moves toward the origin, the minimum weight design will correspond to the weight represented by the line which is just tangential to the feasible domain. In our problem, the minimum weight corresponds to the line passing through the corner M and the coordinates $M_{p1} = 50$ and $M_{p2} = 20$ of this point give the optimal solution.*

The equation of the constant weight line passing through the corner M may be obtained by the linear combination with *positive multipliers* of the equations corresponding to the two sides of the feasible domain intersecting at point M. Since these two sides are associated with two yield mechanisms, the constant weight line may also be considered to represent a yield mechanism obtained by the combination of these two yield mechanisms. In general, this combination leads to a two-degree-of-freedom yield mechanism. To obtain the weight line, however, the coefficients of the plastic moments in the power equation of the combined mechanism must be equal to the given coefficients of the weight function, and therefore the corresponding combined yield mechanism has only one-degree-of-freedom.

It is evident that, because of convexity of the feasible domain, in its other corners the weight function cannot be constructed by the use of solely *positive* multipliers of the equations corresponding to the intersecting sides.

In the weight function the coefficients of the plastic moments designate the lengths of the corresponding prismatic members, while, in the power equations the coefficients of the plastic moments are obtained as the sum of the absolute values of the rotations in the plastic hinges of the corresponding prismatic members. Hence, if we are going to combine two yield mechanisms so that the function of the power equation of the combined mechanism will be identical to the weight function, then *for every prismatic member the sum of the absolute magnitude of the rotations in the plastic hinges must be equal to the length of the member. In this case the magnitude of the power of the external loads gives the magnitude of the weight of the structure.* Restricting the combination of the yield mechanisms to the cases where solely *positive* multipliers are used, these special one-degree-of-freedom combined yield mechanisms are called *Foulkes-mechanisms* (Foulkes 1954; Heyman 1971).

Considering the convexity of the feasible domain there is only one such Foulkes-mechanism which leads to a feasible design, i.e. which is represented by a constant

* In special cases, the constant weight line may coincide with a side of the feasible domain. Then, any point on this side provides the same (minimum) weight of the structure and therefore a *unique* optimal solution cannot be established.

weight line passing through a corner of the feasible domain, and this provides the optimal solution (see point M in Fig. 6—65). There are, however, other intersection points *outside* the feasible domain (see e.g. point L) for which Foulkes-mechanisms can also be constructed. These lead to less weight than the optimal solution, but do not provide a feasible design. Hence, we can state, that *among all possible Foulkes-mechanisms, the one that gives the optimal solution is the one for which the weight of the structure, i.e. the power of the external loads, is a maximum.*

(3) To generalize the above results, let us consider a bar structure loaded by concentrated forces F_j and composed of n prismatic members with given lengths l_i and unknown constant plastic moments M_{pi}. The problem of minimum weight design is to determine the plastic moments such that

$$W = \Sigma l_i M_{pi} = \min! \tag{6—136}$$

subject to

$$\Sigma M_{pi} \dot{\kappa}_i \geq \Sigma F_j v_j. \tag{6—137}$$

The latter restriction has to be satisfied for *all the possible yield mechanisms* of the structure. In eq. (6—137) $\dot{\kappa}_i$ designates the sum of the absolute values of the rotation rates in the plastic hinges forming in the member i, and v_j is the velocity component at the point of application of the force F_j. In an n-dimensional design space of the plastic moments M_{pi}, eqs (6—137) are represented by hyperplanes which divide the space into a feasible and an unfeasible domain. Because the coefficients $\dot{\kappa}_i$ are always positive, the *feasible domain* defined by eqs (6—137) is *convex* towards the origin.

For a fixed value of the weight of the structure the weight function W given by eq. (6—136) is also represented by a hyperplane called *constant weight plane*. The closer this plane is to the origin, the smaller the weight of the structure is. Therefore, the minimum weight design corresponds to the constant weight plane which is just tangential to the feasible domain, passing through a vertex of the domain.*

By the combination of the simple yield mechanisms defined by eqs (6—137) n degree-of-freedom combined yield mechanisms can be obtained. A combined yield mechanism is represented in the design space by hyperplanes passing through a vertex formed by the intersection of the hyperplanes of the corresponding simple yield mechanisms, and its power equation can be obtained by the linear combination of eqs (6—137). If we restrict our investigations to combinations obtained by the use of *positive* multipliers for eqs (6—137) and assume that for each member $\dot{\kappa}_i = l_i$, then these special one-degree-of-freedom yield mechanisms are called *Foulkes-mechanisms*. The power equation for a Foulkes-mechanism is represented by a hyperplane passing through the corresponding vertex and the power of the external forces is identical in magnitude to the weight of the structure.

Considering the above definition, *outside* the feasible domain a number of vertices, formed by the intersection of the hyperplanes of the simple yield mechanisms, can be found for which Foulkes-mechanisms can be constructed. *Inside* the feasible domain,

* In special cases, the plane may contain an edge or a plane of the boundary of the feasible domain. Then, any point on this edge or plane provides the same (minimum) weight of the structure and thus a *unique* optimal solution cannot be established. Still, the statements made above are also valid for these special cases.

however, such vertices cannot be found, and there is only one Foulkes-mechanism which corresponds to a vertex *on the boundary* of the feasible domain. This gives the optimum solution to the problem. Hence, considering the convexity of the feasible domain, we can state that *among all possible Foulkes-mechanisms, the one that gives the optimal solution is the one which leads to the maximum power of external forces.* Since in eqs (6—137) the external power is equal to the internal power, we can also conclude that *that particular set of plastic moments which leads to the minimum weight of a structure is the one which exerts the maximum resistance against the external forces.*

From the above theorem, it is evident that any arbitrary Foulkes-mechanism yields a *lower bound solution* for the weight and provides an *unsafe design.* On the other hand, any arbitrary statically admissible moment distribution is an *upper bound* solution for the weight and results in a *safe design.*

The optimal design based on the Foulkes-theorem is a *linear programming* problem which will be discussed in more detail in Section 6.7.

(4) To illustrate the application of the Foulkes-theorem, consider a continuous beam constructed of two prismatic members with unknown plastic moments M_{p1} and M_{p2}, as shown in Fig. 6—66 (Heyman 1971). The possible simple yield mechanisms are shown in Fig. 6—66 (a—d). By the use of these mechanisms and positive multipliers combined yield mechanisms can be constructed which have two degrees of freedom and are illustrated in Fig. 6—66 (e—g). To obtain Foulkes-mechanisms in each prismatic member the sum of the absolute magnitudes of the rotation rates must be equal to the magnitude of the length of the member. This condition makes it possible to construct the power equation for each combined mechanism and then the Foulkes-mechanism, which leads to the maximum external power, gives the optimal solution for the beam.

Starting with the combined yield mechanism of Fig. 6—66(e), the definition of the Foulkes-mechanism leads to the relationships

$$\dot{\kappa}_1 = 3\omega_1 + \omega_2 = 8 \quad \text{and} \quad \dot{\kappa}_2 = 2\omega_2 = 10,$$

from which $\omega_1 = 1$ and $\omega_2 = 5$ and the power equation becomes

$$8M_{p1} + 10M_{p2} = 4 \times 15 + 25 \times 10 = 310. \tag{6—138}$$

In the case of the combined yield mechanism shown in Fig. 6—66(f) the rotation rates have to satisfy the relationships

$$\dot{\kappa}_1 = 2\omega_1 = 8 \quad \text{and} \quad \dot{\kappa}_2 = \omega_1 + 3\omega_2 = 10.$$

Hence, $\omega_1 = 4$ and $\omega_2 = 2$ and the power equation results in

$$8M_{p1} + 10M_{p2} = 15 \times 16 + 10 \times 10 = 340. \tag{6—139}$$

Finally, considering the combined mechanisms of Fig. 6—66(g) the definition of Foulkes-mechanism leads to the relationships

$$\dot{\kappa}_1 = 3\omega_1 = 8 \quad \text{and} \quad \dot{\kappa}_2 = 3\omega_2 = 10.$$

Hence, $\omega_1 = \frac{8}{3}$ and $\omega_2 = \frac{10}{3}$ and the power equation becomes

$$8M_{p1} + 10M_{p2} = 336.66. \tag{6—140}$$

Comparing the three power equations derived above one can see that eq. (6—139) leads to the maximum external power (340) and therefore the associated Foulkes-mechanism shown in Fig. 6—66(f) provides the optimal solution for the beam. To obtain the corresponding plastic moments, one has to consider the two simple yield mechanisms used to construct the Foulkes-mechanism. According to Fig. 6—66(b) and Fig. 6—66(d), the power equations of these two simple yield mechanisms are

$$2M_{p1} + M_{p2} = 60,$$

$$3M_{p2} = 50.$$

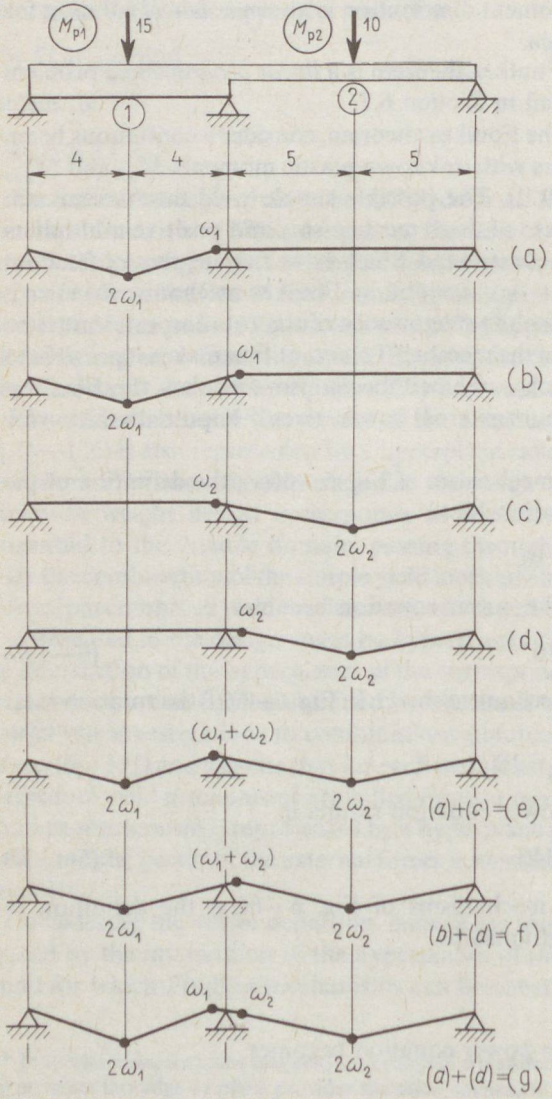


Fig. 6–66

The simultaneous solution of these equations provides the optimal solution of the beam: $M_{p1}=\frac{65}{3}$, $M_{p2}=\frac{50}{3}$.

6.6.2.4. STRUCTURES WITH CONTINUOUSLY VARIABLE PLASTIC MOMENTS

In the following, we will assume that the plastic moments of the bar structure can vary continuously. If no constraints are prescibed for the magnitudes of the plastic moments they can exactly follow the moment distribution and the optimum design based on this condition yields the *absolute minimum weight* of the structure. In practice, however, because of constructional and safety reasons, the cross-sectional dimensions cannot be reduced below certain limits, and this determines the minimum applicable magnitude of plastic moments. The introduction of side constraints for the plastic moments makes the optimal design solution more difficult but, in general, leads to more realistic results.

First, we will discuss the problem where the minimum magnitude of the plastic moments is prescribed, and present an approximate optimal design method based on a quadratic weight function. Then, we will deal with the unconstrained minimum weight design problem, based on both linear and arbitrary convex weight functions.

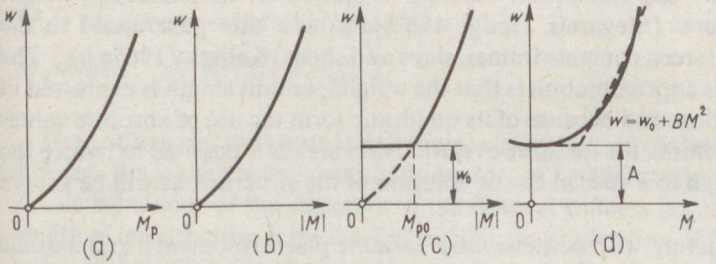


Fig. 6–67

6.6.2.4.1. CONSTRAINED MINIMUM WEIGHT DESIGN

Let us assume that the specific weight of a structure is defined by the function $w=w(M_p)$, as illustrated in Fig. 6—67(a). It is evident that, if the plastic moments can vary continuously, then a necessary but not sufficient condition of minimum weight design is that the plastic moments $M_p(s)$ should exactly follow the moment distribution $M(s)$, i.e. at every point in the structure the relationship $M_p(s)=|M(s)|$ must be satisfied. Here s denotes the coordinate measured along the axis of the bars. Substituting this relationship into the weight function, the weight per unit length can be expressed in terms of the magnitude of the *actual bending moments* (see Fig. 6—67(b)):

$$w=w(|M|). \qquad (6—141)$$

For practical reasons, the cross-sectional dimensions cannot generally be reduced below certain limits. Let us denote the weight per unit length of the members with the

minimum applicable dimensions by w_0, and the corresponding plastic moment by M_{p0}. Then, in the regions of the structure where $|M| \leq M_{p0}$, the weight per unit length is equal to w_0 and eq. (6—141) applies only to the regions where $|M| \geq M_{p0}$. Hence, in the case of *constrained minimum weight design*, the specific weight function is expressed in the form

$$\left.\begin{aligned} &\text{if} \quad |M| \leq M_{p0}, \quad w = w_0, \\ &\text{if} \quad |M| \geq M_{p0}, \quad w = w(|M|). \end{aligned}\right\} \tag{6—142}$$

This general relationship is illustrated by the full line in Fig. 6—67(c). On the basis of these weight functions analytical solutions cannot be achieved and even the numerical solutions lead to complicated calculations. In order to avoid these difficulties, the relationships (6—142) may be approximated by a single *quadratic function*

$$w = w_0 + BM^2, \tag{6—143}$$

which is represented by a second order parabola shown in Fig. 6—67(d). Here the constants w_0 and B are chosen so that the deviation between the exact curve and the parabola is minimum.

The use of the above approximation was first suggested for the minimum weight design of steel structures (Megarefs, Hodge 1963) and was later generalized to the optimal design of reinforced concrete frames, slabs and shells (Kaliszky 1965a,b,c). The main advantage of this approximation is that the weight per unit length is expressed in terms of a single function, and because of its quadratic form the use of absolute values can be omitted. In addition, the quadratic relationship makes it possible to reduce the minimum weight design to a special elastic solution of the structure, as will be shown next.

Consider a bar structure with continuously variable plastic moments, and assume that the weight per unit length of the members is described by the same weight function, i.e. w_0 and B in eq. (6—143) are constant along the entire length L of the structure. Then, the total weight of the structure is expressed in the form

$$W = \int_L (w_0 + BM^2)\, \mathrm{d}s = w_0 + B \int_L M^2 \mathrm{d}s, \tag{6—144}$$

where W_0 is a constant. According to the static theorem of limit analysis, any arbitrary *statically admissible moment distribution* leads to a safe design. To find the optimal solution, one has to determine that particular statically admissible moment distribution which minimizes the above weight function, i.e. for which*

$$\int_L M^2 \mathrm{d}s = \min! \tag{6—145}$$

* In the minimization process, the constants w_0 and B do not play any role and can therefore be omitted.

The *elastic strain energy* of a bar structure with *constant* flexural stiffness EI is defined by the expression

$$U = \frac{1}{EJ} \int_L M^2 \mathrm{d}s. \tag{6—146}$$

According to *Castigliano's theorem* (see Section 3.3.2.) among all statically admissible moment distributions the one that minimizes the elastic strain energy, i.e. for which

$$\int_L M^2 \mathrm{d}s = \min! \tag{6—147}$$

provides the elastic solution for a bar structure.

Since the minimum weight solution and the elastic solution are defined by the same conditions, we can conclude that *the optimal plastic solution for a bar structure based on a quadratic weight function is identical to the linear elastic solution for the same structure with constant flexural stiffness.* Hence, the plastic moment distribution which satisfies the condition $M_p \geq M_{p0}$ and leads to minimum weight becomes

$$\left.\begin{aligned} M_p &= M_{p0}, \quad \text{where } |M| \leq M_{p0}, \\ M_p &= |M|, \quad \text{where } |M| > M_{p0}. \end{aligned}\right\} \tag{6—148}$$

Here M denotes the linear elastic moment distribution in the structure with constant stiffness. Since the linear elastic solution does not significantly deviate from the actual elastic behaviour of the structure (if the flexural stiffness is constant along the entire length of the structure, it is identical with it), the application of the above method leads to a well-balanced design where the structure satisfies the equilibrium and optimality conditions and, in addition, does not undergo excessive plastic deformations.

The application of the quadratic weight function to the optimal design of reinforced slabs and shells will be discussed in Chapter 7.

6.6.2.4.2. UNCONSTRAINED MINIMUM WEIGHT DESIGN

(1) Consider the problem of minimum weight design where the weight per unit length of members is defined by a *convex* function

$$w = BM_p^{\alpha}, \quad \alpha \geqq 1 \tag{6—149}$$

and assume that for the continuously variable plastic moments no constraints are prescribed, i.e. they exactly follow the actual moment distribution M such that everywhere $M_p = |M|$ (Marcal, Prager 1964; Prager, Shield 1967). Then, eq. (6—149) becomes

$$w = B|M|^{\alpha} \quad \alpha \geq 1 \tag{6—150}$$

and assuming that B is constant along the entire length L of the structure the total weight is found to be

$$W = B \int_L |M|^{\alpha} ds. \tag{6—151}$$

The problem of optimal design is reduced again to finding that statically admissible moment distribution which minimizes the weight of the structure, i.e. for which

$$\int_L |M|^{\alpha} ds = \min! \tag{6—152}$$

In order to find an analogy between the optimal plastic solution and the elastic solution for structures, consider a fictitious *non-linearly elastic* structure with uniform cross-sections and with the same layout as those of the original structure and the same arrangement of loads and assume that its specific *complementary strain energy* is expressed by the same functional as the specific weight in eq. (6—151). Then, according to the *principle of minimum complementary energy* (see Section 3.3.2.), the solution for this non-linearly elastic structure is obtained by a statically admissible moment distribution which minimizes the complementary strain energy defined by the same expression as eq. (6—152). Hence, *the optimal plastic solution for a bar structure is identical to the non-linearly elastic solution for the same structure with uniform cross-sections, provided that the specific complementary strain energy of the non-linear structure is defined by the same function as the specific weight.**

As is well known, the curvature–moment relationship for a bar member can be derived from the specific complementary strain energy function U_0 by the relationship $\kappa = \dfrac{dU_0}{dM}$. In our case, U_0 is identical to the specific weight function w given by eq. (6—149), and therefore the curvature–moment relationship for the non-linearly elastic members becomes

$$|\kappa| = \frac{dw}{d|M|} = \alpha B |M|^{\alpha - 1} \tag{6—153}$$

and, in addition, κ and M must everywhere have the same sign. Since the multipliers α and B denote constants they can be omitted from further discussions. Then eq. (6—153) leads to

$$|\kappa| = |M|^{\alpha - 1}, \quad \text{sign } \kappa = \text{sign } M. \tag{6—154}$$

This curvature–moment relationship shown in Fig. 6—68 together with the equilibrium and compatibility equations makes possible the determination of the moment distribution which provides the minimum weight solution for a structure.

(2) Let us apply the above theorem to structures with the *linear specific weight function*

$$w = B|M| \tag{6—155}$$

* From this theorem, it is evident that in the special case when a *quadratic* weight function is applied, the optimal plastic solution is reduced to the *linear elastic* solution of the structure.

shown in Fig. 6—69(a). Then, the optimality condition becomes

$$\int_L |M| \mathrm{d}s = \min! \tag{6—156}$$

Consequently, *to obtain the minimum weight solution, the sum of the absolute values of the areas of the bending moment diagram has to be minimized.* The fulfilment of this condition leads to complicated calculation; therefore it is more convenient to determine the optimal solution by the use of the curvature–moment relationship given by eq. (6—154). In this special case the relationship becomes

$$\kappa = \kappa_0, \quad \operatorname{sign} \kappa_0 = \operatorname{sign} M. \tag{6—157}$$

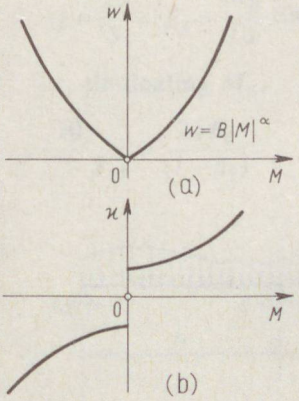


Fig. 6–68

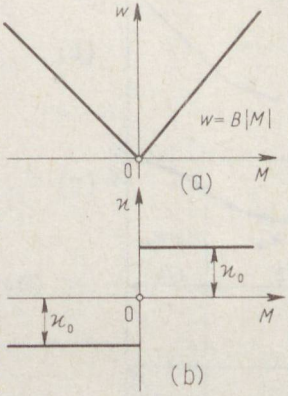


Fig. 6–69

Hence, along the entire structure, the curvature is equal to an arbitrary constant κ_0 and its sign is identical everywhere to the sign of the bending moment, as shown in Fig. 6—69(b). This special curvature–moment relationship, together with the equilibrium and compatibility equations, defines the solution for the fictitious non-linearly elastic structure which provides the optimal plastic solution.

(3) The application of the above method will be illustrated by the solution to simple problems.

Figure 6—70(a) shows a beam with fixed ends subjected to an arbitrary external load defined by the moment diagram of the released simply supported beam illustrated in Fig. 6—70(b). To determine the non-linearly elastic solution, let us start with the analysis of deflections. At the ends of the beam the deflections and rotations must vanish, and along the length of the beam the curvatures must be equal to κ_0 or $-\kappa_0$. These conditions can be satisfied by the curvature distribution shown in Fig. 6—70(c). Then, in order to satisfy eq. (6—157), the zero points of the moment diagram have to coincide with the points where the curvatures change their sign. Thus, the moment diagram for the non-linearly elastic beam which at the same time provides the optimal solution can be constructed Fig. 6—70(d).

A continuous beam subjected to arbitrary external loads and its statically admissible bending moment diagram are shown in Fig. 6—71(a) and (b). In the diagram, M_B denotes the redundant bending moment which will be determined from the condition that the beam has continuous deformations at the middle support. The curvature must be constant along the beam and its sign must be equal to the sign of the bending moments, as shown in Fig. 6—71(c).

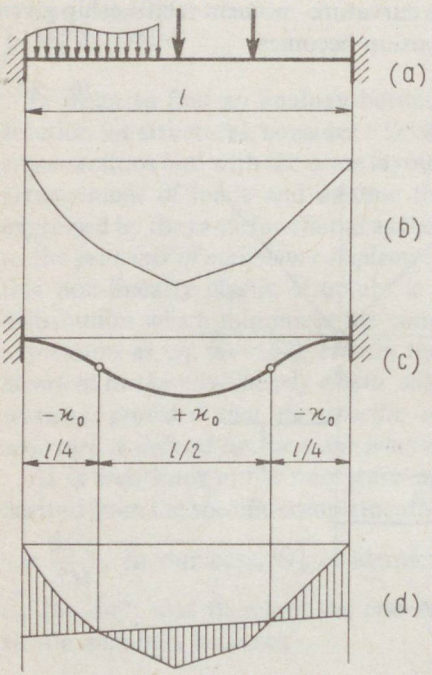


Fig. 6–70

To solve the problem, the distances $x_1=\beta_1 l_1$ and $x_2=\beta_2 l_2$ have to be expressed in terms of the redundant moment M_B and the given external loads. Then, considering the released system shown in Fig. 6—71(d), the rotations of the simply supported beams at point B can be expressed as

$$\varphi_{1B}= \quad l_1\left[\frac{1}{2}-(1-\beta_1)^2\right]\kappa_0,$$

$$\varphi_{2B}=-l_2\left[\frac{1}{2}-(1-\beta_2)^2\right]\kappa_0.$$

Because of the continuity of deflections, these two rotations must be equal, i.e. $\varphi_{1B}=\varphi_{2B}$, which leads to the relationship

$$l_1(1-\beta_1)^2+l_2(1-\beta_2)^2=\frac{1}{2}(l_1+l_2). \qquad (6—158)$$

This compatibility equation, together with the relationships between M_B, β_1 and β_2, provides the optimal solution for the beam.

To illustrate the details of calculation, determine the minimum weight solution of the continuous beam shown in Fig. 6—72. This problem has already been solved for the condition that the continuous beam is constructed of bars with *uniform* plastic moments M_{p1} and M_{p2} (see Fig. 6—66), and we have found that the optimal solution is $M_{p1}=21.66$ and $M_{p2}=16.66$. Now we assume that the plastic moments can vary continuously. Considering the statically admissible moment diagram of Fig. 6—72(b), the following relationship can be obtained

$$y_1=\frac{30}{4}8\beta_1=\frac{M_B}{8}8(1-\beta_1),$$

$$y_2=\frac{25}{5}10\beta_2=\frac{M_B}{10}10(1-\beta_2),$$

or, eliminating M_B,

$$\frac{30\beta_1}{(1-\beta_1)}=\frac{25\beta_2}{(1-\beta_2)}.$$

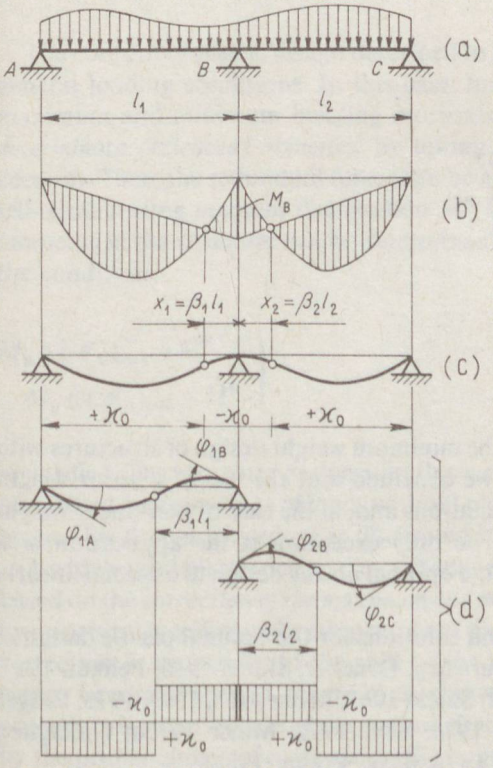


Fig. 6–71

This relationship, together with the compatibility equation

$$8(1-\beta_1)^2+10(1-\beta_2)^2=9$$

obtained from eq. (6—158) leads to $\beta_1=0.273$ and $\beta_2=0.310$, and the redundant moment which gives the optimal solution becomes $M_B=11.20$. The corresponding plastic moment distribution required for the absolute minimum weight design of the beam is shown in Fig. 6—72(b). The minimum weight solution for the same beam constructed of bars with uniform plastic moments is also illustrated in the Figure.

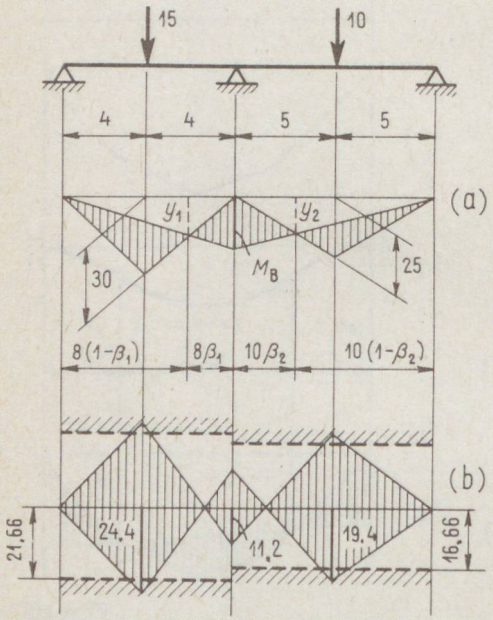


Fig. 6–72

Considering our earlier discussions of the minimum weight design of structures with continuously variable plastic moments, we conclude that the use of a linear weight function results in fairly complicated calculations and, in the case of non-linear weight functions, even more difficulties arise. The only exception is the application of a quadratic weight function, which reduces the optimal plastic design to a special linearly elastic solution.

A great number of different methods and solutions for the optimal plastic design of bar structures can be found in the literature (e.g. Drucker, Shield 1956; Pelikán 1957; Peredy 1959; Marcal, Prager 1964; Prager, Shield 1967; Mróz 1958, 1963, 1973; Prager 1970; Heyman 1971; Rozvany, Adidam 1971; Save 1972; Maier 1972a; Gallagher, Zienkiewicz 1973; Majid 1974; Rozvany 1976; Save, Prager 1985).

6.6.3. PLASTIC DESIGN OF STRUCTURES UNDER GENERAL LOADING

Having discussed the problem of plastic design and optimal plastic design of structures subjected to proportional loading, we will next briefly show the concept of plastic design of bar structures under general loading. The optimal plastic design of structures loaded by multiparameter and moving loads is described elswhere (see e.g. Save, Prager 1963; Rozvany 1976).

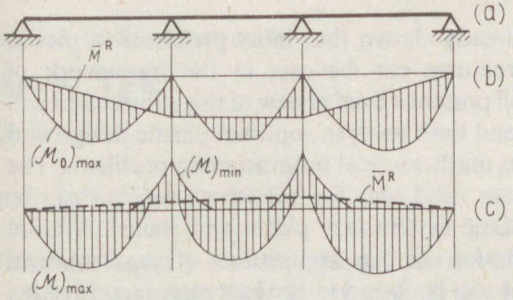


Fig. 6–73

The concept of plastic design described in Section 6.6.1. can easily be generalized for general loading conditions. In this case, first one has to determine the diagrams of maximum and minimum bending moments, $(\mathcal{M}_0)_{max}$ and $(\mathcal{M}_0)_{min}$, for the *statically determinate (released) structure* by taking all the possible load combinations into account. Then, the redundant forces can be assumed arbitrarily and the corresponding self-equilibrating moment distribution $\bar{M}^R$ has to be constructed. Finally, the plastic moments in the structure can be determined such that at every section of the structure the condition

$$\left.\begin{aligned} M_p &\geq (\mathcal{M}_0)_{max} + \bar{M}^R, \\ -M_p &\leq (\mathcal{M}_0)_{min} + \bar{M}^R \end{aligned}\right\} \qquad (6—159)$$

is satisfied. The structure designed in this way will be strong enough to support all the prescribed combinations of loads without plastic collapse. For the case of a continuous beam, this design procedure is illustrated in Fig. 6—73(a) and (b).

A widely used plastic design concept suggested first by Kazinczy (1914, 1931, 1933) is based on the *correction of the maximum and minimum elastic moments* $(\mathcal{M})_{max}$ and $(\mathcal{M})_{min}$ by an arbitrary self-equilibrating moment distribution $\bar{M}^R$. For continuous beams, this correction is equivalent to the shift of the zero-line of the maximum and minimum elastic bending moment diagram, as shown in Fig. 6—73(c). It is evident that this procedure is a special case of the method described above but, it has the advantage that, by the proper choice of corrections, the large elastic moments can be directly reduced and the expected permanent deformations can be better controlled. In addition, the

structures designed in this manner will shake down. This latter statement can easily be "confirmed" by replacing $(\mathcal{M}_0)_{max}$ and $(\mathcal{M}_0)_{min}$ in eq. (6—159) by the elastic moments $(\mathcal{M})_{max}$ and $(\mathcal{M})_{min}$ and then comparing the relationships obtained with eq. (6—99).

6.7. APPLICATION OF MATHEMATICAL PROGRAMMING

6.7.1. INTRODUCTION

In our previous discussions, we have already shown that most problems in plastic analysis and plastic design of bar structures can be cast in the framework of mathematical programming. Next, we will present a brief review of this subject and will show how the problems of incremental and limit analysis, optimal plastic design and shakedown analysis can be formulated as mathematical programming problems. The formulae and methods to be discussed are valid only for bar structures, but can be generalized to any discretized elasto-plastic system (e.g. plates and shells). A more comprehensive and systematic presentation of the application of mathematical programming to elasto-plastic structures can be found in the literature (e.g. Livesley 1964, 1966; Cyras 1969, 1974; Maier 1968, 1972a, 1972b; Grierson, Gladwell 1971; Save 1972; Maier, Srinivasan, Save 1976; Nédli 1976a, 1976b; Kaliszky, Nédli 1976; Maier, Giacomini, Paterlini 1976; Maier, Grierson, Best 1977; Cohn, Maier 1977).

6.7.2. FORMULATION OF LINEAR AND QUADRATIC PROGRAMMING

Mathematical programming is concerned with the optimization of discrete systems, and seeks the extreme values of some *objective function* when the system variables are subject to sets of inequality and equality constraints. In the case of *linear programming*, both the objective function and the inequalities and equalities are linear functions of the variables. In *quadratic programming*, the inequalities and equalities are linear but the objective function is quadratic in terms of the variables.

In linear as well as in quadratic programming, a minimization problem can be related to each maximization problem based on the same data. These problems are called *dual pairs*. Duality is an important property of mathematical programming. Generally speaking, dual formulations describe the same phenomenon but reflect a different aspect of it.

(1) In *linear programming* we present only the so-called asymmetrical dual formulation which is used in plastic analysis and design problems.

(a) The *primal or maximum problem* in this case is to maximize the objective function*

$$\mathbf{b}^*\mathbf{x} \tag{6—160}$$

subject to the constraints

$$\mathbf{A}^*\mathbf{x} \leq \mathbf{c}, \tag{6—161}$$

* The asterisk * denotes the transpose of the vector or matrix.

or briefly*

$$\max \left\{ \mathbf{b}^* \mathbf{x} \,||\, \mathbf{A}^* \mathbf{x} \leq \mathbf{c} \right\}. \tag{6—162}$$

Here the vector $\mathbf{x}$ contains the unknown variables and $\mathbf{A}$, $\mathbf{b}$ and $\mathbf{c}$ designate a constant matrix and two constant vectors. respectivelv.

(b) The corresponding *dual or minimum problem* is to minimize the objective function

$$\mathbf{c}^* \mathbf{y} \tag{6—163}$$

subject to the constraints

$$\mathbf{A}\mathbf{y} = \mathbf{b}, \quad \mathbf{y} \geqq \mathbf{0}, \tag{6—164}$$

or briefly

$$\min \left\{ \mathbf{c}^* \mathbf{y} \,||\, \mathbf{A}\mathbf{y} = \mathbf{b}, \quad \mathbf{y} \geqq \mathbf{0} \right\}. \tag{6—165}$$

Here the vector $\mathbf{y}$ contains the unknown variables.

Any $\mathbf{x}$ and $\mathbf{y}$ satisfying the constraints (6—161) and (6—164), respectively, is said to be a *feasible solution*, and the particular feasible solution $\hat{\mathbf{x}}$ and $\hat{\mathbf{y}}$ satisfying the optimality conditions (6—162) and (6—165), respectively, is called the *optimal solution*. The solutions to the primal and dual problems are connected by the following relationships:

weak duality

$$\mathbf{b}^* \mathbf{x} \leqq \mathbf{c}^* \mathbf{y}, \tag{6—166}$$

strong duality

$$\mathbf{b}^* \hat{\mathbf{x}} = \mathbf{c}^* \hat{\mathbf{y}}.$$

The minimum problem of linear programming can be solved by the *simplex method*, which approaches the optimal solution by successive iterations (Hadley 1964; Gass 1969; Cohn, Maier 1977). Using eq. (6—166) the solution of the maximum problem can easily be obtained from the solution of the minimum problem.

(2) In *quadratic programming*, the dual formulation which is used in incremental elastic–plastic analysis is the following:

primal problem

$$\min \left\{ \frac{1}{2} \mathbf{x}^* \mathbf{D} \mathbf{x} + \mathbf{p}^* \mathbf{x} \,||\, \mathbf{A}\mathbf{x} \leq \mathbf{b} \right\} \tag{6—167a}$$

dual problem

$$\min \left\{ -\frac{1}{2} \mathbf{x}^* \mathbf{D} \mathbf{x} - \mathbf{b}^* \mathbf{y} \,||\, \mathbf{A}^* \mathbf{y} + \mathbf{D}\mathbf{x} + \mathbf{p} = \mathbf{0}, \ \mathbf{y} \geqq \mathbf{0} \right\}. \tag{6—167b}$$

Here $\mathbf{p}$, $\mathbf{b}$ and $\mathbf{D}$, $\mathbf{A}$ denote constant vectors and matrices, respectively.

* In the following, the expressions behind the sign || designate the constraints associated with the expression standing before this sign.

If $\mathbf{x}^*\mathbf{D}\mathbf{x} \geq \mathbf{0}$ for all $\mathbf{x}$, i.e. $\mathbf{D}$ is positive semidefinite, then the above problem is called *convex quadratic programming* and can be solved by *Wolfe's simplex method* (Wolfe 1959).

The solution to the previous dual quadratic programming problem is equivalent to the solution to the following set of relationships, which is called the *linear complementary problem*, and can also be used in incremental elastic–plastic analysis

$$\mathbf{A}\mathbf{x} \leqq \mathbf{b}, \quad \mathbf{A}^*\mathbf{y} + \mathbf{D}\mathbf{x} + \mathbf{p} = \mathbf{0},$$
$$\mathbf{y}^*(\mathbf{A}\mathbf{x} - \mathbf{b}) = \mathbf{0}. \tag{6—168}$$

6.7.3. GOVERNING EQUATIONS OF ELASTO-PLASTIC DISCRETIZED BAR STRUCTURES

(1) In order to apply mathematical programming to the solution of elasto-plastic problems, discrete structural models must be used. The bar structures must be divided into straight members with uniform cross-sections, and the loads should be concentrated at the nodes of the members. Then, the state of the entire *elastic–perfectly plastic* bar structure undergoing small deflections is described by the following *generalized vectors*:

- $\mathbf{p}$ nodal forces;
- $\mathbf{u}$ nodal displacements;
- $\mathbf{Q}$ generalized stresses associated with one of the end-sections of the individual members,*
- $\mathbf{q} = \mathbf{q}^e + \mathbf{q}^p$ generalized strains associated with one of the end-sections of the individual members;* these express the elastic and plastic relative deformations of the members.

Here the vectors $\mathbf{Q}$ and $\mathbf{q}$ are defined such that their dot product provides the strain energy of the entire structure.

(2) By the use of the above state variables, the *equilibrium* and *compatibility equations* of the discretized structure are expressed as follows

$$\mathbf{G}^*\mathbf{Q} + \mathbf{p} = \mathbf{0},$$
$$\mathbf{G}\mathbf{u} + \mathbf{q} = \mathbf{0}. \tag{6—169}$$

Here $\mathbf{G}^*$ and $\mathbf{G}$ designate the equilibrium and compatibility matrices of the structure.

(3) The *yield conditions* for the cross-sections will be *linearized*. For example, the yield condition for the end-section of the i-th member, where the generalized stresses $\mathbf{Q}_i$ are specified, is expressed in the form

$$\boldsymbol{\phi}_i^0 = \mathbf{N}_i^{0*}\mathbf{Q}_i - \mathbf{k}_i^0 \leq \mathbf{0}. \tag{6—170}$$

Here the rows of matrix $\mathbf{N}_i^{0*}$ contain the exterior unit normals $\mathbf{n}_{ij}^0$ of the hyperplanes of the yield surface associated with the section under consideration, and the elements k_{ij}^0

* This specified end can be e.g. the end having the smaller node number.

of the vector $\mathbf{k}_i^0$ denote the distances of these hyperplanes from the origin, as shown in Fig. 6—74. The generalized stresses acting on the other end-section of the i-th member can be expressed by equilibrium equations in terms of $\mathbf{Q}_i$, and then for these generalized stresses another yield condition, similar to eq. (6—170), is obtained. These two yield conditions provide the yield condition of the i-th member

$$\boldsymbol{\phi}_i = \mathbf{N}_i^* \mathbf{Q}_i - \mathbf{k}_i \leqq \mathbf{0}.$$

Finally, the set of yield conditions of all members comprises the yield condition of the entire structure

$$\boldsymbol{\phi} = \mathbf{N}^* \mathbf{Q} - \mathbf{k} \leq \mathbf{0}. \tag{6—171}$$

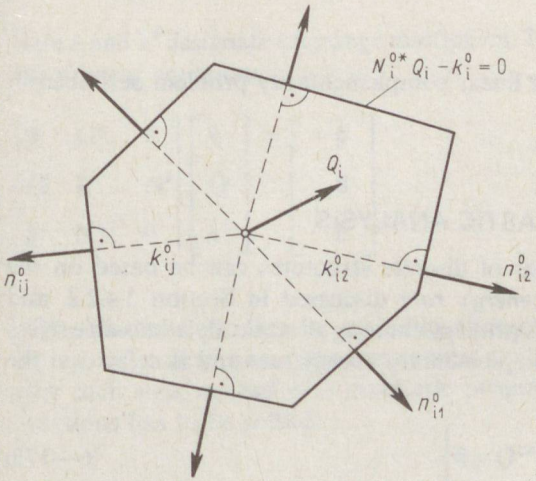


Fig. 6–74

(4) The *constitutive equations* of the discretized structure are expressed in two parts. For the generalized elastic strains, the relationship

$$\mathbf{q}^e = \mathbf{F}\mathbf{Q} \tag{6—172}$$

holds, where $\mathbf{F}$ is the elastic flexibility matrix of the structure. Using the associated flow rule (2—92) and eq. (6—171) the generalized plastic strain rates are defined by the relationship

$$\dot{\mathbf{q}}^p = \dot{\boldsymbol{\lambda}} \frac{\partial \boldsymbol{\phi}}{\partial \mathbf{Q}} = \mathbf{N}^J \dot{\boldsymbol{\lambda}}^J, \quad \dot{\boldsymbol{\lambda}}^J \geqq \mathbf{0}, \quad \dot{\boldsymbol{\lambda}}^{\bar{J}} = \mathbf{0}. \tag{6—173}$$

Here J designates the set of subscripts associated with the zero elements of the vector $\boldsymbol{\phi}$ i.e. J: $\{j \,|\, \phi_j = 0\}$ and $\bar{J}$ is the complementary set of J.

(5) Finally, using the equilibrium, compatibility and constitutive equations and yield conditions described above, the *governing equations* for discretized elastic–perfectly plastic bar structures have the following form.

$$\begin{bmatrix} \mathbf{0} & \mathbf{G}^* & \mathbf{0} \\ \mathbf{G} & \mathbf{F} & \mathbf{N}^J \\ \mathbf{0} & \mathbf{N}^{*J} & \mathbf{0} \end{bmatrix} = \begin{bmatrix} \dot{\mathbf{u}} \\ \dot{\mathbf{Q}} \\ \dot{\lambda}^J \end{bmatrix} + \begin{bmatrix} \dot{\mathbf{p}} \\ \mathbf{0} \\ -\dot{\boldsymbol{\phi}}^J \end{bmatrix} = \mathbf{0},$$

$$J: \{j \mid\mid \phi_j = 0\},$$
$$\dot{\lambda}^J \geqq 0, \quad \dot{\lambda}^{\bar{J}} = 0, \quad \dot{\boldsymbol{\phi}}^{*J} \dot{\lambda}^J = 0, \tag{6—174}$$
$$\boldsymbol{\phi} = \mathbf{N}^* \mathbf{Q} - \mathbf{k}.$$

This corresponds mathematically to a linear complementarity problem described in (6—168).

6.7.4. INCREMENTAL ELASTO-PLASTIC ANALYSIS

The incremental elasto-plastic analysis of discrete structures can be based on the *principle of minimum complementary energy rate* discussed in Section 3.4.2.2. and defined by eq. (3—43). According to this principle, among all statically admissible stress rates the actual one minimizes the complementary energy rate and is defined in the following form*

$$\min \left\{ \frac{1}{2} \dot{\mathbf{Q}}^* \mathbf{F} \dot{\mathbf{Q}} \mid\mid \mathbf{G}^* \dot{\mathbf{Q}} + \dot{\mathbf{p}} = \mathbf{0}, \quad \boldsymbol{\phi}^J = \mathbf{N}^{*J} \dot{\mathbf{Q}} \leq \mathbf{0} \right\} \tag{6—175}$$

where $J: \{j \mid\mid \phi_j = 0\}$.

This formulation corresponds to the convex quadratic programming problem defined by relationship (6—167a) and can be solved by Wolfe's simplex method (see e.g. Cohn, Maier 1977).

The incremental analysis of a structure based on the above principle is an initial value problem. Let us assume that the state of the structure corresponding to the load $\mathbf{p}_0$ is known and characterized by the state variables $\mathbf{u}_0, \mathbf{Q}_0, \mathbf{q}_0, \boldsymbol{\phi}_0$. Then, solving the quadratic programming problem defined by eq. (6—175) the rates $\dot{\mathbf{u}}_0, \dot{\mathbf{Q}}_0, \dot{\mathbf{q}}_0, \dot{\boldsymbol{\phi}}_0$ corresponding to the load rate $\dot{\mathbf{p}}$ can be determined. These rates are constant during the "time increment" $\Delta\tau$ as long as $\dot{\mathbf{p}}$ is a constant and no elastic members start to yield, i.e. the matrix $\mathbf{N}^{*J}$ remains unchanged. Then, the state variables $\mathbf{u}_1 = \mathbf{u}_0 + \dot{\mathbf{u}}_0 \Delta\tau, \mathbf{Q}_1 = \mathbf{Q}_0 + \dot{\mathbf{Q}}_0 \Delta\tau$, etc., corresponding to the load $\mathbf{p}_1 = \mathbf{p}_0 + \dot{\mathbf{p}} \Delta\tau \mid\mid \Delta\tau \leq \Delta\tau_1$ can be calculated. Here $\Delta\tau_1$ denotes the "time increment" during which $\dot{\mathbf{p}}$ and $\mathbf{N}^{*J}$ are unchanged.

* For the sake of simplicity, we assume that the surface displacements are kept constant and therefore the second term in eq. (3—43) vanishes.

The above procedure can be repeated until the requested load or the plastic limit load of the structure is reached. Since at every step a quadratic programming problem must be solved, the incremental analysis based on the above concepts leads to fairly time consuming calculations.

The solution can be simplified if we assume that the plastified cross-sections of the structure remain plastic during the entire loading process, i.e. no local unloading takes place in the member. This condition is generally satisfied in case of monotonically increasing proportional loading. Applying this assumption the inequality in eq. (6—175) becomes the equality $\dot{\boldsymbol{\phi}}^J = \mathbf{N}^{*J}\dot{\mathbf{Q}}^J = \mathbf{0}$ and the quadratic programming problem is reduced to a minimum value problem with constraints expressed by a set of linear equations

$$\frac{1}{2}\dot{\mathbf{Q}}^*\mathbf{F}\dot{\mathbf{Q}} + \dot{\mathbf{u}}^*(\mathbf{G}^*\dot{\mathbf{Q}} + \dot{\mathbf{p}}) + \dot{\boldsymbol{\lambda}}^{*J}(\mathbf{N}^{*J}\dot{\mathbf{Q}}^J) = \min! \qquad (6—176)$$

Here $\dot{\mathbf{u}}$ and $\dot{\boldsymbol{\lambda}}^J$ designate Lagrange multipliers. This minimum value problem leads to a set of linear equations

$$\begin{bmatrix} \mathbf{0} & \mathbf{G}^* & \mathbf{0} \\ \mathbf{G} & \mathbf{F} & \mathbf{N}^J \\ \mathbf{0} & \mathbf{N}^{*J} & \mathbf{0} \end{bmatrix} \begin{bmatrix} \dot{\mathbf{u}} \\ \dot{\mathbf{Q}} \\ \dot{\boldsymbol{\lambda}}^J \end{bmatrix} = \begin{bmatrix} -\dot{\mathbf{p}} \\ \mathbf{0} \\ \mathbf{0} \end{bmatrix}$$

We can conclude that by excluding the possibility of unloading of the members during the loading process the incremental analysis can be significantly simplified since after each step, instead of a quadratic programming problem, only a set of linear equations has to be solved.

6.7.5. LIMIT ANALYSIS

As stated earlier, the plastic limit state of a perfectly plastic structure subjected to the proportional loading

$$\mathbf{p}(\mathbf{x}, t) = m(t)\,\mathbf{p}_0(\mathbf{x})$$

is characterized by the condition that, under a constant load $\mathbf{p}_p = m_p\mathbf{p}_0$, the entire structure or one or several parts of it undergoes unrestricted plastic deformations. The goal of limit analysis is to determine the plastic limit load multiplier m_p.

(a) Any stress distribution $\mathbf{Q}^s$ and the associated load multiplier m_s are called *statically admissible* if they satisfy the equilibrium equations and the yield conditions

$$\mathbf{G}^*\mathbf{Q}^s + m_s\mathbf{p}_0 = \mathbf{0}, \quad \mathbf{N}^*\mathbf{Q}^s - \mathbf{k} \le \mathbf{0}.$$

According to the *static theorem* of limit analysis the plastic limit load multiplier m_p is defined as

$$m_p = \max\{m_s \,|\, \mathbf{G}^*\mathbf{Q}^s + m_s\mathbf{p}_0 = \mathbf{0},\ \mathbf{N}^*\mathbf{Q}^s - \mathbf{k} \le \mathbf{0}\}. \qquad (6—177)$$

(b) Any kinematically admissible plastic strain rate and velocity distribution $\dot{\mathbf{q}}_p^k$, $\dot{\mathbf{u}}^k$ and the associated multiplier m_k are called *kinematically admissible* if they satisfy the compatibility equation, the plastic flow rule and the power equation

$$\mathbf{G}\dot{\mathbf{u}}^k + \dot{\mathbf{q}}^k = \mathbf{0}, \quad \dot{\mathbf{q}}_p^k = \mathbf{N}\dot{\boldsymbol{\lambda}}^k, \quad m_k = \frac{\mathbf{Q}^*\dot{\mathbf{q}}_p^k}{\mathbf{p}_0^*\dot{\mathbf{u}}^k}, \quad \mathbf{p}_0^*\dot{\mathbf{u}}^k \geq \mathbf{0}. \tag{6—178}$$

Since the magnitude of the kinematically admissible strain rates and velocities are not specified, the external power in eq. (6—178) can be normalized such that $\mathbf{p}_0^*\dot{\mathbf{u}}^k = 1$. Then, making use of the yield condition $\boldsymbol{\phi} = \mathbf{N}^*\mathbf{Q} - \mathbf{k} = \mathbf{0}$, eqs (6—178) are expressed in the form

$$\mathbf{G}\dot{\mathbf{u}}^k + \mathbf{N}\dot{\boldsymbol{\lambda}}^k = \mathbf{0}, \quad m_k = \mathbf{k}^*\dot{\boldsymbol{\lambda}}^k, \quad \mathbf{p}_0^*\dot{\mathbf{u}}^k = 1.$$

According to the *kinematic theorem* of limit analysis, the plastic limit load multiplier m_p is defined as

$$m_p = \min\left\{\mathbf{k}^*\dot{\boldsymbol{\lambda}}^k \,\|\, \mathbf{G}\dot{\mathbf{u}}^k + \mathbf{N}\dot{\boldsymbol{\lambda}}^k = \mathbf{0}, \quad \mathbf{p}_0^*\dot{\mathbf{u}}^k = 1, \quad \dot{\boldsymbol{\lambda}} \geq \mathbf{0}\right\}. \tag{6—179}$$

The linear programming problems defined by eqs (6—177) and (6—179) can easily be reduced to the primal and dual problems given by eqs (6—162) and (6—165), and then their solution can be obtained by the simplex method.

6.7.6. SHAKEDOWN ANALYSIS

Next, we will discuss the special problem of shakedown analysis where the *common* maximum intensity m_{sh} of the multi-parameter loads has to be determined such that, if the loads do not exceed this intensity, the structure will shake down.

First, assume that in the yield conditions for the members, only the bending moments are taken into consideration. Then, according to the static theorem of shakedown analysis expressed by eqs (6—100) and (6—101) the common *shakedown parameter* m_{sh} is defined as

$$m_{sh} = \max\left\{m \,\|\, m\mathbf{M}_{max}^0 + \mathbf{M}^R \leq \mathbf{M}_p, \quad m\mathbf{M}_{min}^0 + \mathbf{M}^R \geqq -\mathbf{M}_p, \; \mathbf{C}^*\mathbf{M}^R = \mathbf{0}\right\}. \tag{6—180}$$

Here $\mathbf{M}_{max}^0$ and $\mathbf{M}_{min}^0$, respectively, denote the maximum and minimum *elastic* bending moments calculated from all the possible combinations of the external loads with unit intensity, $\mathbf{M}^R$ is the unknown residual moment distribution, $\mathbf{C}^*$ is the equilibrium matrix and $\mathbf{M}_p$ denotes the plastic moments of the members.

If in the yield conditions for the members, other internal forces beside the bending moments are also taken into consideration the shakedown parameter is defined in the more general form

$$m_{sh} = \max\left\{m \,\|\, m\mathbf{N}^*\mathbf{Q}_{max}^0 + \mathbf{N}^*\mathbf{Q}^R \leq \mathbf{k}, \; \mathbf{G}^*\mathbf{Q}^R = \mathbf{0}\right\}. \tag{6—181}$$

Here $\mathbf{Q}^R$ denotes the unknown residual stress distribution and $\mathbf{Q}_{max}^0$ contains the maximum values of the components of the *elastic* generalized stresses in the directions

of the external normals of the hyperplanes of the yield surfaces, calculated from all the possible combinations of the external loads with unit intensity. Thus, a particular element Q^0_{ioj} of vector $\mathbf{Q}^0_{max}$ is obtained as follows. First, on the basis of all the possible load combinations, the set $\mathbf{Q}^0_{ios}$ of the *elastic* stress vectors which belong to the end section o of the member i has to be determined*. Then, $\mathbf{Q}^{0\,*}_{ios}\,\mathbf{n}^0_{ij}$ gives the components of these vectors in the direction of the external normal of the hyperplane j of the yield surface associated with the end section o of member i (see Fig. 6—74). Finally, Q^0_{ioj} is equal to the maximum value of these components, i.e. $Q^0_{ioj} = \max\{\mathbf{Q}^{0\,*}_{ios}\mathbf{n}^0_{ij}\}$. Determining these components for all external normals of the yield surface and conducting this calculation for both ends of every member of the structure the vector $\mathbf{Q}^0_{max}$ can be constructed.

It can be seen that both eq. (6—180) and eq. (6—181) represent a linear programming problem which, after some modification, can be solved by the simplex method.

6.7.7. MINIMUM WEIGHT DESIGN

Consider a bar structure constructed of uniform members with length $\mathbf{l}$ and subjected to given external loads $\mathbf{p}$, and assume that in the yield conditions for the members only the bending moments $\mathbf{M}$ are taken into consideration. Then, according to the *static theorem* of limit analysis, the plastic moments $\mathbf{M}_p$ which lead to the minimum weight of the structure are defined as

$$\min\left\{\mathbf{l}^*\mathbf{M}_p \,\middle|\, \mathbf{C}^*\mathbf{M}+\mathbf{p}=\mathbf{0},\quad |\mathbf{M}|\leq\mathbf{M}_p,\quad \mathbf{M}_p\geq\mathbf{0}\right\}. \tag{6—182}$$

Here the vector $|\mathbf{M}|$ contains the absolute values of the bending moments.

Using the *kinematic theorem* of limit analysis, the minimum weight solution can be obtained as follows.

Let us denote the rotation rates of the plastic hinges of the yield mechanism by $\dot{\boldsymbol{\lambda}}$. The criterion that the mechanism should be a *Foulkes-mechanism* can be formulated as follows:

$$\left.\begin{aligned} &\mathbf{C}\dot{\mathbf{u}}+\mathbf{N}\dot{\boldsymbol{\lambda}}=\mathbf{0},\\ &\dot{\boldsymbol{\lambda}}\geqq\mathbf{l},\\ &\mathbf{p}^*\dot{\mathbf{u}}=\mathbf{M}_p^*\dot{\boldsymbol{\lambda}}=\mathbf{M}_p^*\mathbf{l}. \end{aligned}\right\} \tag{6—183}$$

The fact that we are looking for the best Foulkes-mechanism is expressed by the following relationship

$$\max\left\{\mathbf{p}^*\dot{\mathbf{u}} \,\middle|\, \mathbf{C}\dot{\mathbf{u}}+\mathbf{N}\dot{\boldsymbol{\lambda}}=\mathbf{0},\quad \dot{\boldsymbol{\lambda}}\geqq\mathbf{l}\right\}. \tag{6—184}$$

Relationships (6—182) and (6—184) represent a pair of dual linear programming problems which can be solved by the simplex method.

* The subscript s refers to the various load combinations.

7. PLASTIC ANALYSIS AND DESIGN OF PLATES AND SHELLS

The first part of this chapter deals with the limit analysis of rigid-perfectly plastic plates. After presentation of the equilibrium and kinematic equations, the different yield conditions and the flow rule, the application is illustrated by the solution to several axially symmetrical problems. In connection with the analysis of a rectangular plate, the concept of the yield-line theory of reinforced concrete plates is also briefly described.

In the second part of the chapter, the limit analysis of rigid-perfectly plastic cylindrical and conical shells is presented. The governing equations based on different yield conditions are described and applied to the solution to several problems, including the limit analysis of shallow reinforced concrete shells.

The last part of the chapter deals with the minimum weight design of plastic plates and shells. The applications of the different theorems and methods presented are illustrated by the solution to simple problems. The minimum weight design of reinforced concrete plates and shells is also discussed.

7.1. ASSUMPTIONS

The small displacement theory of thin plates and shells is based on the following assumptions:

(a) The thickness of the plate or shell is small compared with the other dimensions.

(b) The displacements are small compared with the thickness.

(c) The straight lines normal to the middle surface of the plate or shell remain straight and normal to the middle surface during deformation (Kirchhoff—Love hypothesis).

(d) The stresses normal to the middle surface are neglected.

(e) The shear strains caused by the shear stresses normal to the middle surface are neglected.

In addition we will assume that the plate or shell

(f) is homogeneous and made of an isotropic, rigid-perfectly plastic material and

(g) is subjected to proportional loading.

The above assumptions to be applied in our further studies lead to a number of simplifications and permit the development of relatively simple theories and methods for the analysis of elastic and plastic thin plates and shells.

As in the case of beams, as a result of assumption (c), the state of stress and strain of plates and shells can be characterized by the generalized stresses and generalized strains of the infinitesimal plate and shell elements and these variables can be entirely defined by the displacements of the points of the middle surface. Considering assumptions (a) and (b), the second order effects can be neglected and the small deformation theory can be used. Assumptions (d) and (e) significantly simplify the yield conditions for plates and shells. Finally, assumption (f) excludes elasto-plastic analysis but together with assumption (g) allows the application of the theorems of limit analysis.

7.2. LIMIT ANALYSIS OF PLATES

7.2.1. GOVERNING EQUATIONS

In the derivation of the governing equations for rigid-perfectly plastic plates, we will use tensor notation and a rectangular system of coordinates in which the x_α axes ($\alpha = 1, 2$) lie in the middle plane of the plate and the z axis is perpendicular to this plane. The thickness of the plate is constant and denoted by $2h$.

7.2.1.1. KINEMATIC EQUATIONS

A rigid-perfectly plastic plate undergoes only plastic deformations. They are assumed to be small, and therefore only those displacements of the middle plane which are perpendicular to it are significant. They are called *deflections* and denoted by $w\,(x_\alpha)$. As will be shown, as a consequence of the Kirchhoff–Love hypothesis, the displacements and strains at any other point in the plate are entirely defined by the mid-surface deflections (Fig. 7—1).

Considering an arbitrary point D in the plate at a distance z from the middle plane, its vertical velocity $\dot{u}_z$ is identical to the deflection rate $\dot{w}$ of the corresponding point A in the middle plane, and its horizontal velocities, denoted by $\dot{u}_\alpha$ are obtained by making use of the Kirchhoff–Love hypothesis

$$\dot{u}_\alpha = -z\dot{w}_{,\alpha}; \quad (\alpha = 1, 2). \tag{7—1}$$

The *strain rates* of the point under consideration are related to the velocities by the strain–displacement equations (see eq. (2—67))

$$\dot{\varepsilon}_{\alpha\beta} = \frac{1}{2}(\dot{u}_{\alpha,\beta} + \dot{u}_{\beta,\alpha}), \quad (\alpha, \beta = 1, 2). \tag{7—2}$$

Hence, by substituting eq. (7—1) the strain rates can be expressed in terms of the deflection rates

$$\dot{\varepsilon}_{\alpha\beta} = -z\dot{w}_{,\alpha\beta}, \quad (\alpha, \beta = 1, 2). \tag{7—3}$$

In the case of small deflections, the *curvature rates* of the deformed middle plane are defined by the relationships

$$\left.\begin{aligned} &\dot{\kappa}_{11} = -\frac{\partial^2 \dot{w}}{\partial x_1^2}, \quad \dot{\kappa}_{22} = -\frac{\partial^2 \dot{w}}{\partial x_2^2}, \quad \dot{\kappa}_{12} = \dot{\kappa}_{21} = -\frac{\partial^2 \dot{w}}{\partial x_1 \partial x_2} \\ &\text{or} \\ &\dot{\kappa}_{\alpha\beta} = -\dot{w}_{,\alpha\beta}, \quad (\alpha, \beta = 1,2). \end{aligned}\right\} \tag{7—4}$$

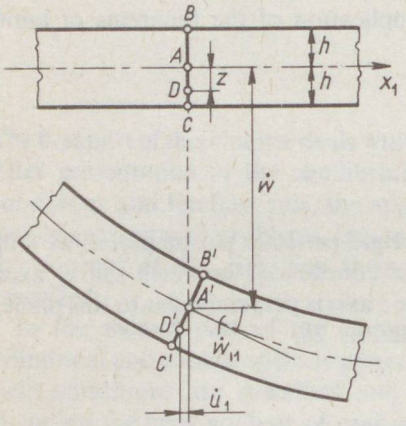


Fig. 7–1

7.2.1.2. EQUILIBRIUM EQUATIONS

Considering the assumptions described in Section 7.1. the state of stress at a point in the plate is defined by the normal and shear stresses σ_{11}, σ_{22} and $\sigma_{12} = \sigma_{21}$ acting parallel to the middle plane, and by the shear stresses σ_{1z}, σ_{2z} acting normal to the middle plane (Fig. 7—2(a)). For convenience, the stress components σ_{11}, σ_{22}, σ_{12} which correspond to the state of plane stress, will be considered to be the elements of a *stress tensor* $\sigma_{\alpha\beta}$ ($\alpha, \beta = 1,2$), while the shear stresses σ_{1z} and σ_{2z} are assumed to form the elements of a *stress vector* $\sigma_{\alpha z}$($\alpha = 1, 2$). The resultants of the stresses acting on the vertical sides of an infinitesimal element of the plate are the *moments* M_{11}, M_{22}, $M_{12} = M_{21}$ and the *shear forces* Q_1, Q_2 per unit length (Fig. 7—2(b)) and are obtained from the relationships

$$\left.\begin{aligned} M_{11} &= \int_{-h}^{h} \sigma_{11} z \mathrm{d}z, \\ M_{22} &= \int_{-h}^{h} \sigma_{22} z \mathrm{d}z, \\ M_{12} = M_{21} &= \int_{-h}^{h} \sigma_{12} z \mathrm{d}z, \end{aligned}\right\} \tag{7—5}$$

$$\left.\begin{aligned} Q_1 &= \int_{-h}^{h} \sigma_{1z}\,dz, \\ Q_2 &= \int_{-h}^{h} \sigma_{2z}\,dz. \end{aligned}\right\} \tag{7—6}$$

If the generalized stresses are assumed to form the elements of a tensor $M_{\alpha\beta}$ $(\alpha,\beta = 1,2)$ and a vector Q_α $(\alpha = 1,2)$, respectively, then relationships (7—5) and (7—6) may be written in the concise form

$$M_{\alpha\beta} = \int_{-h}^{h} \sigma_{\alpha\beta} z\,dz, \tag{7—5a}$$

$$Q_\alpha = \int_{-h}^{h} \sigma_{\alpha z}\,dz. \tag{7—6a}$$

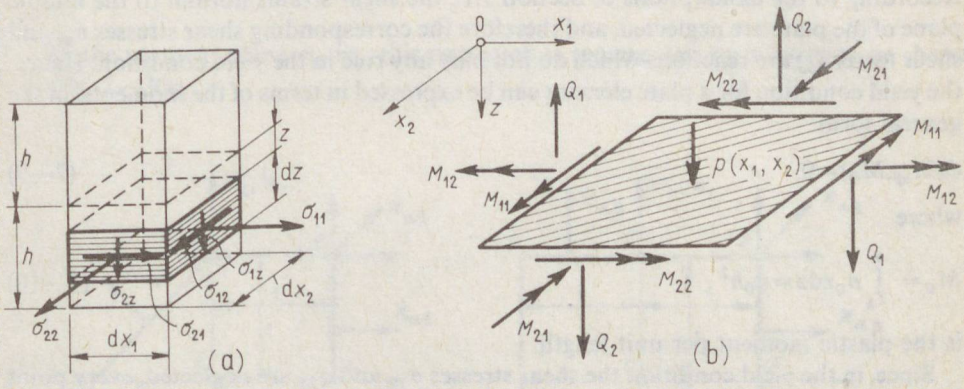


Fig. 7-2

Assuming that the load $p(x_\alpha)$ acting on the plate is normal to the middle plane, the equilibrium of an infinitesimal element is expressed as follows (see e.g. Timoshenko, Woinowsky-Krieger 1940)

$$\left.\begin{aligned} &\frac{\partial Q_1}{\partial x_1} + \frac{\partial Q_2}{\partial x_2} + p = 0, \\ &\frac{\partial M_{11}}{\partial x_1} + \frac{\partial M_{12}}{\partial x_2} - Q_1 = 0, \\ &\frac{\partial M_{21}}{\partial x_1} + \frac{\partial M_{22}}{\partial x_2} - Q_2 = 0, \end{aligned}\right\} \tag{7—7}$$

or

$$\left.\begin{aligned} &Q_{\alpha,\alpha} + p = 0, \\ &M_{\alpha\beta,\beta} - Q_\alpha = 0. \end{aligned}\right\} \quad (\alpha,\ \beta = 1.2) \tag{7—7a}$$

Substituting the last two equations into the first one, the shear forces can be eliminated and the *equilibrium* of the plate can be expressed in terms of the three unknown moments by a single equation

$$\frac{\partial^2 M_{11}}{\partial x_1^2} + \frac{\partial^2 M_{12}}{\partial x_1 x_2} + \frac{\partial^2 M_{22}}{\partial x_2^2} + p = 0, \tag{7—8}$$

or

$$M_{\alpha\beta,\beta\alpha} + p = 0, \quad (\alpha, \beta = 1, 2). \tag{7—8a}$$

7.2.1.3. YIELD CONDITIONS

According to the assumptions of Section 7.1., the shear strains normal to the middle plane of the plate are neglected, and therefore the corresponding shear stresses $\sigma_{\alpha z}$ and shear forces Q_α are reactions which do not play any role in the yield condition. Hence, the yield condition for a plate element can be expressed in terms of the moments, in the general form

$$\phi(M_{\alpha\beta}, M_0) = 0, \tag{7—9}$$

where

$$M_0 = \int_{-h}^{h} \sigma_0 z \mathrm{d}z = \sigma_0 h^2 \tag{7—10}$$

is the plastic moment per unit length.

Since, in the yield condition the shear stresses σ_{1z} and σ_{2z} are neglected, every point in the plate can be assumed to be in a state of *plane stress* defined by the stresses σ_{11}, σ_{22} and $\sigma_{12} = \sigma_{21}$, or by the principal stresses σ_{I} and σ_{II}. Let the yield condition for plane stress be written in the general form

$$f(\sigma_{11}, \sigma_{22}, \sigma_{12}) = \sigma_0. \tag{7—11}$$

If a plate element becomes perfectly plastic, the above condition has to be satisfied in every layer of the element. Therefore, integrating the stresses according to eq (7—5), *the yield condition for a plate element assumes exactly the same form for the moments as it does for the stresses*:

$$f(M_{\alpha\beta}) = f(M_{11}, M_{11}, M_{12}) = M_0. \tag{7—12}$$

For convenience, one can introduce dimensionless moments

$$\left.\begin{aligned} m_{11} &= \frac{M_{11}}{M_0}, \quad m_{22} = \frac{M_{22}}{M_0}, \quad m_{12} = \frac{M_{12}}{M_0}, \\ m_{\mathrm{I}} &= \frac{M_{\mathrm{I}}}{M_0}, \quad m_{\mathrm{II}} = \frac{M_{\mathrm{II}}}{M_0} \end{aligned}\right\} \tag{7—13}$$

and then the yield condition (7—12) becomes

$$f(m_{11}, m_{22}, m_{12}) = 1, \tag{7—14}$$

or, in terms of the *principal moments* M_I and M_{II}, as

$$f(m_I, m_{II}) = 1. \tag{7—14a}$$

Using the above results and various yield theories the yield conditions for the plate elements have the following forms.

(a) In a state of plane stress the *Tresca yield condition* becomes (see eq. (2—86))

$$f = \frac{1}{2}(|\sigma_I| + |\sigma_{II}| + |\sigma_I - \sigma_{II}|) = \sigma_0$$

and therefore the corresponding yield condition for moments is

$$f = \frac{1}{2}(|m_I| + |m_{II}| + |m_I - m_{II}|) = 1. \tag{7—15}$$

In the moment plane m_I, m_{II}, this condition is represented by a hexagon as shown in Fig. 7—3(a).

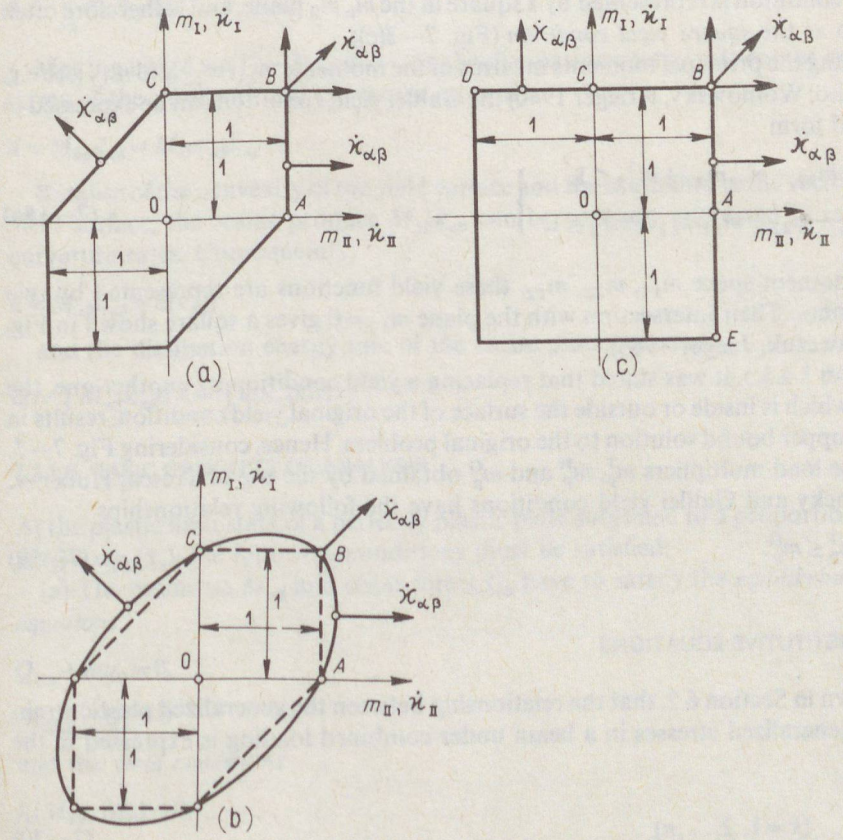


Fig. 7–3

(b) In a state of plane stress the *Huber–v. Mises–Hencky yield condition* is given by (see eq. (2—79a))

$$f=\sigma_{11}^2-\sigma_{11}\sigma_{22}+\sigma_{22}^2+3\sigma_{12}^2=\sigma_0^2,$$

and the corresponding condition for plates becomes

$$f=m_{11}^2-m_{11}m_{22}+m_{22}^2+3m_{12}^2=1. \tag{7—16}$$

In terms of the principal moments, this condition has the simpler form

$$f=m_{\mathrm{I}}^2-m_{\mathrm{I}}m_{\mathrm{II}}+m_{\mathrm{II}}^2=1 \tag{7—17}$$

and is represented by an ellipse, shown in Fig. 7—3(b).

(c) In a state of plane stress the *Galilei yield condition* has the form (Sawczuk, Jaeger 1963)

$$f=\max(|\sigma_{\mathrm{I}}|,|\sigma_{\mathrm{II}}|)=\sigma_0$$

and the corresponding condition for plates becomes

$$f=\max(|m_{\mathrm{I}}|,|m_{\mathrm{II}}|)=1. \tag{7—18}$$

This yield condition is represented by a square in the $m_{\mathrm{I}}, m_{\mathrm{II}}$ plane, and is therefore often referred to as the *square yield condition* (Fig. 7—3(c)).

Expressing the principal moments in terms of the moments m_{11}, m_{22} and m_{12} (see e.g. Timoshenko; Woinowsky, Krieger 1940) the Galilei yield condition can be expressed in the general form

$$\left.\begin{aligned} f_1&=m_{11}+m_{22}-m_{11}m_{22}+m_{12}^2\le 1,\\ f_2&=-m_{11}-m_{22}-m_{11}m_{22}+m_{12}^2\le 1. \end{aligned}\right\} \tag{7—18a}$$

In the moment space m_{11}, m_{22}, m_{12}, these yield functions are represented by two elliptical cones. Their intersection with the plane $m_{12}=0$ gives a square shown in Fig. 7—3(c) (Sawczuk, Jaeger 1963).

In Section 3.4.3.5. it was stated that replacing a yield condition by another one, the surface of which is inside or outside the surface of the original yield condition, results in a lower or upper bound solution to the original problem. Hence, considering Fig. 7—3. the collapse load multipliers $m_{\mathrm{p}}^{\mathrm{T}}$, $m_{\mathrm{p}}^{\mathrm{H}}$ and $m_{\mathrm{p}}^{\mathrm{G}}$ obtained by the use of Tresca, Huber–v. Mises–Hencky and Galilei yield conditions have the following relationships

$$m_{\mathrm{p}}^{\mathrm{T}}\le m_{\mathrm{p}}^{\mathrm{H}};\ m_{\mathrm{p}}^{\mathrm{T}}\le m_{\mathrm{p}}^{\mathrm{G}}. \tag{7—19}$$

7.2.1.4. CONSTITUTIVE EQUATIONS

It was shown in Section 6.2. that the relationship between the generalized plastic strain rates and generalized stresses in a beam under combined loading is expressed in the form

$$\dot{q}_{\mathrm{i}}^{\mathrm{P}}=\dot{\lambda}_{\mathrm{k}}\frac{\partial f}{\partial Q_{\mathrm{i}}},\quad (k=1,2,\ldots n). \tag{7—20}$$

This general form of the *plastic flow rule* can also be applied to plates and becomes

$$\dot{\kappa}_{\alpha\beta}=\dot{\kappa}^{p}_{\alpha\beta}=\dot{\lambda}_k\frac{\partial f_k}{\partial M_{\alpha\beta}},\quad (k=1, 2, \ldots, n). \tag{7—21}$$

Here

if $f_k=0$ and $\dot{f}_k=0$, then $\dot{\lambda}_k\geq 0$;
if $f_k<0$ or $f_k=0$ and $\dot{f}_k<0$, then $\dot{\lambda}_k=0$.

Illustrating the principal curvature rates $\dot{\kappa}_I$ and $\dot{\kappa}_{II}$ in a coordinate system coaxial with the coordinate system m_I, m_{II} the vectors $\dot{\kappa}_{\alpha\beta}(\dot{\kappa}_I\dot{\kappa}_{II})$ will coincide with the external normals of the corresponding points in the yield surface (see. Figs 7—3).

7.2.1.5. DISSIPATION FUNCTION

Neglecting the shear deformations caused by the vertical shear stresses $\sigma_{\alpha z}$, the *dissipation energy rate per unit area* of the plate becomes

$$d=\int_{-h}^{h}\sigma_{\alpha\beta}\dot{\varepsilon}_{\alpha\beta}\mathrm{d}z. \tag{7—22}$$

Making use of eqs (7—3) and (7—5), the dissipation energy rate can be expressed in terms of the moments and curvature rates as

$$d=M_{\alpha\beta}\dot{\kappa}_{\alpha\beta}=M_0 m_{\alpha\beta}\dot{\kappa}_{\alpha\beta}. \tag{7—23}$$

Because of the convexity of the yield surface and the normality of the vector $\dot{\kappa}_{\alpha\beta}$ to the yield surface, the scalar product $M_{\alpha\beta}\dot{\kappa}_{\alpha\beta}$ can be uniquely expressed in terms of the curvature rates. Consequently,

$$d=M_{\alpha\beta}\dot{\kappa}_{\alpha\beta}=d(\dot{\kappa}_{\alpha\beta}) \tag{7—24}$$

and the dissipation energy rate of the entire plate becomes

$$D=\int M_{\alpha\beta}\dot{\kappa}_{\alpha\beta}\mathrm{d}A=\int d(\dot{\kappa}_{\alpha\beta})\mathrm{d}A. \tag{7—25}$$

7.2.1.6. BASIC CONCEPTS OF ANALYSIS

At the plastic limit state of a perfectly plastic plate subjected to a proportional loading $p(x_\alpha)=mp_0(x_\alpha)$, the following conditions must be satisfied:

(a) The moments $M_{\alpha\beta}$ and shear forces Q_α have to satisfy the *equilibrium equations equations*

$$Q_{\alpha,\alpha}+mp_0=0,$$

$$M_{\alpha\beta,\beta}-Q_\alpha=0$$

and the *yield conditions*

$$f_k(M_{\alpha\beta}, M_0)\leq 0,$$

inside the plate and the *static boundary conditions* along the edges of the plate.

(b) The velocities $\dot{w}$ have to satisfy inside the plate the *kinematic equations*

$$\dot{\kappa}_{\alpha\beta} = -\dot{w}_{,\alpha\beta}$$

and the *constitutive equations*

$$\dot{\kappa}_{\alpha\beta} = \dot{\lambda}_k \frac{\partial f_k}{\partial M_{\alpha\beta}},$$

where

$$\dot{\lambda}_k \geq 0, \quad \text{if} \quad f_k = 0 \quad \text{and} \quad \dot{f}_k = 0;$$

$$\dot{\lambda}_k = 0, \quad \text{if} \quad f_k < 0 \quad \text{or} \quad f_k = 0 \quad \text{and} \quad \dot{f}_k < 0,$$

and the *kinematic boundary conditions* along the edges of the plate.

The solution which fulfils all the above conditions will give the collapse load multiplier m_p and the exact moment and velocity distribution in the plate at the plastic limit state. If, however, only the conditions (a) or (b) are satisfied then, according to the theorems of limit analysis, the corresponding load intensities provide only a lower bound or an upper bound for the collapse load multiplier m_p.

As with other problems of plasticity, certain *discontinuities* may occur in the moment and curvature distributions in a plastic plate which cause difficulties in the solution (Sawczuk, Jaeger 1963; Hodge 1959, 1963). In addition, using a linear (Tresca or Galilei) yield condition, in different domains with unknown boundaries the yield condition is expressed by different linear equations, and therefore the governing equations also have different forms. In the case of non-linear yield conditions, on the other hand, the governing equations are also non-linear. Both problems lead to serious mathematical difficulties; therefore, except in the case of some simple (mostly axisymmetrical) problems, no closed form solutions have been reported in the literature.

Next, the limit analysis of perfectly plastic plates will be illustrated by the solutions to several simple problems.

7.2.2. AXIALLY SYMMETRICALLY LOADED CIRCULAR PLATES

7.2.2.1. GOVERNING EQUATIONS

In polar coordinates r, φ, the state of an axially symmetrically loaded circular plate is described by the moments M_r, M_φ, the shear force Q, the curvature rates $\dot{\kappa}_r$, $\dot{\kappa}_\varphi$ and the velocity $\dot{w}$, as shown in Fig. 7—4. As a consequence of axial symmetry, these variables depend only on the coordinate r, and the radial and circumferential directions are principal directions for the moments at any point in the plate.

In polar coordinates the kinematic and equilibrium equations become (Timoshenko, Woinowsky-Krieger 1940)

$$\dot{\kappa}_r = -\dot{w}'', \quad \dot{\kappa}_\varphi = -\frac{\dot{w}'}{r}, \tag{7—26}$$

$$\left.\begin{aligned} (rQ)' + pr &= 0, \\ (rM_r)' - M_\varphi - rQ &= 0, \end{aligned}\right\} \tag{7—27}$$

where the primes denote differentiation with respect to r. Eliminating the shear force from the equilibrium equations, the equilibrium of a circular plate can be expressed in terms of the dimensionless variables $m_r = \frac{M_r}{M_0}$ and $m_\varphi = \frac{M_\varphi}{M_0}$ as

$$(rm_r)' = m_\varphi - \frac{1}{M_0}\int_0^r pr\,\mathrm{d}r. \tag{7—28}$$

In the following analysis the Tresca yield condition will be used. Since m_r and m_φ are principal moments, the Tresca yield condition is represented by the hexagon shown in (Fig. 7—5). The associated curvature rates defined by the flow rule (7—20) are also illustrated in the figure.

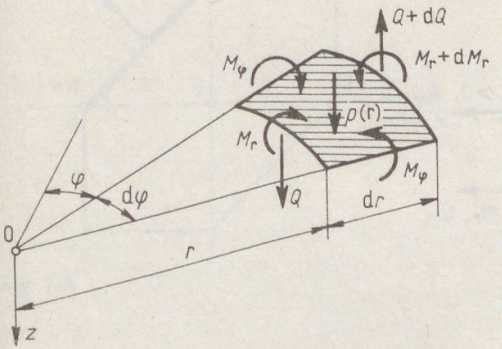


Fig. 7–4

7.2.2.2. SIMPLY SUPPORTED CIRCULAR PLATE UNDER UNIFORM LOAD

At the simply supported edge of a circular plate with radius R we must have $m_r = 0$ and at the centre $m_r = m_\varphi$. In addition, m_r and m_φ are likely to be positive throughout the entire plate, and therefore it appears reasonable to expect the moments m_r and m_φ to be entirely in the stress profile BC of the yield hexagon. Then, at every point in the plate, $m_\varphi = 1$ and eq. (7–28) leads to the expression

$$m_r = \frac{1}{r}\left\{\int_0^r\left[1 - \frac{1}{M_0}\int_0^r pr\,\mathrm{d}r\right]\mathrm{d}r + C_1\right\} = 1 - \frac{pr^2}{rM_0} + \frac{C_1}{r}. \tag{7—29}$$

Here the constant C_1 must vanish, since m_r must have a finite value at the centre of the plate. On the other hand, at $r = R$, m_r must vanish which leads to the *statically admissible multiplier* of the load

$$p_s = 6\frac{M_0}{R^2}. \tag{7—30}$$

In order to prove that this multiplier is identical to the collapse load multiplier, we have to show that the corresponding velocity field obtained by the flow rule and by the kinematic equations, satisfies the geometrical boundary conditions for the plate.

Since the curvature rate $\dot{\kappa}_r$ associated with the stress profile BC of the yield surface shown in Fig. 7—5 vanishes, the first relationship of the kinematic equations (7—26) leads to the velocity field

$$\dot{w} = C_2 r + C_3,$$

where C_2 and C_3 are constants. Considering the boundary condition $\dot{w}(R) = 0$ and denoting by $\dot{w}_0$ the unspecified velocity of the center, the velocity field of the plate is found to be

$$\dot{w} = \dot{w}_0 \left(1 - \frac{r}{R}\right).$$

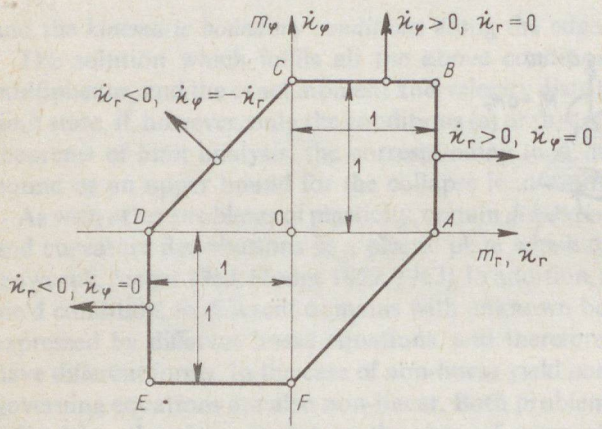


Fig. 7–5

Hence, a complete solution to the problem has been found, and therefore eq. (7—30) provides the collapse load of the plate

$$p_p = 6 \frac{M_0}{R^2}. \qquad (7—31)$$

Since the stress profile BC of the hexagon and the square shown in Fig. 7—3 coincide, it is obvious that in this particular problem the Tresca and Galilei yield conditions result in the same solution. Using the Huber–v. Mises–Hencky yield condition, the collapse load of the same problem is found to be (Sawczuk, Jaeger 1963)

$$p_p = 6.516 \frac{M_0}{R^2}. \qquad (7—31a)$$

7.2.2.3. CLAMPED CIRCULAR PLATE UNDER UNIFORM LOAD

In this case, at the centre of the plate m_r and m_φ must be equal and positive, which corresponds to the point B on the yield hexagon in Fig. 7—6. At the clamped edge, however, m_r is likely to be negative, and therefore it appears reasonable to expect the

moments to be entirely in the stress profile BCD of the hexagon. Hence, denoting by $r=\rho$ the circle where $m_r=0$, the plate has to be divided into two domains.

In the domain $0\leq r\leq\rho$, the stress profile is BC. Therefore* $m_{\varphi 1}=0$ and according to eq. (7—29)

$$m_{r1}=1-\frac{pr^2}{6M_0}. \tag{7—32}$$

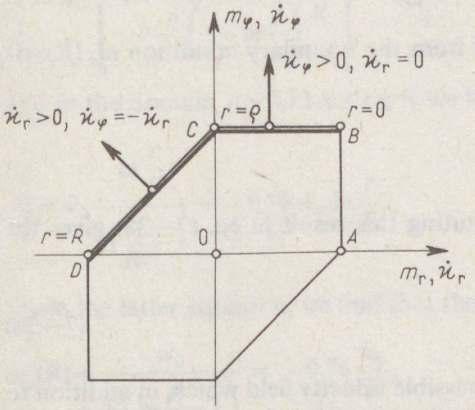


Fig. 7–6

At $r=\rho$, $m_r=0$, which gives the statically admissible multiplier in terms of ρ as

$$p_s=\frac{6M_0}{\rho^2}. \tag{7—33}$$

In the domain $\rho\leq r\leq R$, the stress profile is CD and therefore the equation

$$m_{\varphi 2}-m_{r2}=1 \tag{7—34}$$

has to be satisfied. Substituting this relasionship into eq. (7—28) leads to the differential equation

$$m'_{r2}=\frac{1}{r}-\frac{1}{rM_0}\int_0^r pr\,dr$$

the solution to which is

$$m_{r2}=\ln r-\frac{pr^2}{4M_0}+C_1. \tag{7—35}$$

* In the following, the subscripts 1 and 2 of the functions refer to the domains $0\leq r\leq\rho$ and $\rho\leq r\leq R$, respectively.

At $r=\rho$, m_{r2} must vanish, which makes it possible to express the constant C_1 in terms of ρ. Then eqs (7—34) and (7—35) lead to

$$m_{r2}=\ln\frac{r}{\rho}+\frac{3}{2}-\frac{3}{2}\frac{r^2}{\rho^2}, \tag{7—36}$$

$$m_{\varphi 2}=\ln\frac{r}{\rho}+\frac{5}{2}-\frac{3}{2}\frac{r^2}{\rho^2}. \tag{7—37}$$

Finally, the radius ρ can be determined from the boundary condition $m_\varphi(R)=0$, which results in the equation

$$2\ln\frac{\rho}{R}+3\left(\frac{R}{\rho}\right)^2-5=0,$$

the solution to which is $\rho=0.73\,R$. Substituting this result in eq. (7—33) gives the statically admissible load multiplier

$$p_s=11.26\frac{M_0}{R^2}. \tag{7—38}$$

Next, we have to find a kinematically admissible velocity field which, in addition to the kinematic equations and boundary conditions, satisfies the associated flow rule.

In the domain $0\le r\le\rho$, corresponding to the stress profile BC, $\dot\kappa_{r1}=-\dot w_1''=0$ from which

$$\dot w_1=-C_2r+\dot w_0.$$

Here C_2 is a constant and $\dot w_0$ denotes the unspecified velocity at the centre of the plate.

In the domain $\rho\le r\le R$, the associated flow rule is defined by the stress profile CD, which leads to the relationship $\dot\kappa_{\varphi 2}=-\dot\kappa_{r2}$. Thus, eqs (7—26) lead to the differential equation

$$\dot w_2''+\frac{1}{r}\dot w_2'=0$$

with the solution

$$\dot w_2=C_3\ln r+C_4.$$

At $r=R$ $\dot w_2$ must vanish. This leads to the relation $C_4=-C_3\ln R$, and then the above equation becomes

$$\dot w_2=C_3\ln\frac{r}{R}.$$

Finally, we have to satisfy the continuity of the two velocity fields at $r=\rho$. This is expressed in the form

$$\dot w_1(\rho)=\dot w_2(\rho),$$

$$\dot w_1'(\rho)=\dot w_2'(\rho),$$

and provides the following relationships for the unknown constants C_2 and C_3

$$C_2\rho + \dot{w}_0 = C_3 \ln\frac{\rho}{R}, \quad C_2 = \frac{C_3}{\rho}.$$

From the results derived above, the velocity field in the plate in the domain $0 \le r \le \rho = 0.73\,R$ is found to be

$$\dot{w}_1 = \dot{w}_0\left[1 - \frac{1}{\frac{\rho}{r}\left(1 - \ln\frac{\rho}{r}\right)}\frac{r}{R}\right] = \dot{w}_0\left(1 - 1.042\frac{r}{R}\right),$$

and in the domain $\rho = 0.73\,R \le r \le R$ we have

$$\dot{w}_2 = \dot{w}_0\frac{\ln\frac{r}{R}}{\ln\frac{\rho}{R} - 1} = -0.76\,\dot{w}_0 \ln\frac{r}{R}.$$

From the latter equation, we find that the slope of the velocity field at $r = R$ becomes

$$\dot{w}_2'(R) = \frac{w_0}{R\left(\ln\frac{\rho}{R} - 1\right)} = -0.76\frac{\dot{w}_0}{R},$$

i.e. the boundary condition $\dot{w}_2'(R) = 0$ is not satisfied at the clamped edge. The plate has a discontinuity line, called a *yield line*, along the clamped edge, which allows finite rotations. In the plastic theory of plates, this kind of discontinuity occurs very often (Sawczuk, Jaeger 1963).

The moment and velocity fields derived above represent a complete solution, and therefore the statically admissible multiplier (7—38) also gives the collapse load of the plate

$$p_p = 11.26\frac{M_0}{R^2}.$$

Using the Galilei and the Huber–v. Mises–Hencky yield conditions, the collapse load for the same problem becomes

$$p_p = 12\frac{M_0}{R^2} \quad \text{and} \quad p_p = 12.5\frac{M_0}{R^2},$$

respectively (Sawczuk, Jaeger 1963).

7.2.2.4. CIRCULAR PLATES ON PLASTIC SUBGRADE

Next we will discuss the limit analysis of rigid–perfectly plastic plates resting on a rigid–perfectly plastic subgrade. Generalizing the *Winkler model* it will be assumed that the subgrade is composed of independent elastic–perfectly plastic or, in the case of limit

analysis, rigid–perfectly plastic springs, which have unilateral contact with the plate. Figure 7—7 shows the relationship between the contact pressure σ_s and the deflection w of the plate. If $w>0$ the pressure is equal to the yield stress σ_{so} of the subgrade and if $w<0$ no contact stress occurs between the plate and the subgrade, i.e. the plate can rise freely. Hence, the plate or a part of it can deflect in three different ways:

(a) Where $\sigma_s=\sigma_{so}$ and $f(M_{\alpha\beta},M_0)=0$, both the subgrade and the plate might undergo plastic deformations resulting in deflections.

(b) Where $\sigma_s=\sigma_{so}$ and $f(M_{\alpha\beta},M_0)<0$, only the subgrade experiences plastic deformations and the plate might indentate into the subgrade as a rigid body.

(c) Where $\sigma_s=0$ and $f(M_{\alpha\beta},M_0)\leq 0$, the plate can rise up from the subgrade with or without plastic deformations.

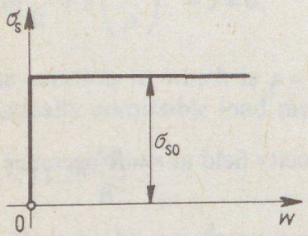


Fig. 7–7

On the basis of the above assumptions and the Galilei yield condition given by eq. (7—18) a number of different problems have been solved by the kinematic theorem of limit analysis (Kaliszky 1959b, 1962a, 1962b). Later, the method was extended to the Tresca yield condition and to the general case when the subgrade is inhomogeneous, i.e. when the yield stress of the subgrade is not constant (Sawczuk, Kaliszky 1964). Next, the solution to a simple problem will be presented.

Consider a circular plate with radius R resting on a plastic subgrade and loaded at its centre by a concentrated force F (Fig. 7—8). We will determine the load-carrying capacity of the plate, using the Galilei yield condition and the kinematic theorem of limit analysis.

The simplest yield mechanism is obtained if we assume that the plate identates into the subgrade as a rigid body. Then, the contact pressure is σ_{s0} at every point under the plate and the corresponding kinematically admissible load becomes

$$F_k=\pi R^2\sigma_{s0}. \tag{7—39}$$

Next, we assume that the yield mechanism of the plate is a cone, and that only the inner part of the cone indentates into the subgrade. The outer part rises above the subgrade and is free of contact stresses (see Fig. 7—8). Denoting the radius of the circle which separates these two parts by R_0 and using eq. (7—26), the velocities and curvature rates are found to be

$$\dot{w}=\dot{w}_0\left(1-\frac{r}{R_0}\right),\quad \dot{\kappa}_r=0,\quad \dot{\kappa}_\varphi=\frac{\dot{w}_0}{rR_0},$$

where $\dot{w}_0$ denotes the unspecified velocity of the centre of the plate. In order to determine the associated kinematically admissible load, we have to write the power equations for the external loads and internal moments. Using eq. (7—25) we obtain

$$F_k \dot{w}_0 - 2\pi \int_0^{R_0} \sigma_{s0} \dot{w} r \, dr = 2\pi \int_0^{R} \frac{\dot{w}_0}{r R_0} M_0 r \, dr, \tag{7—40}$$

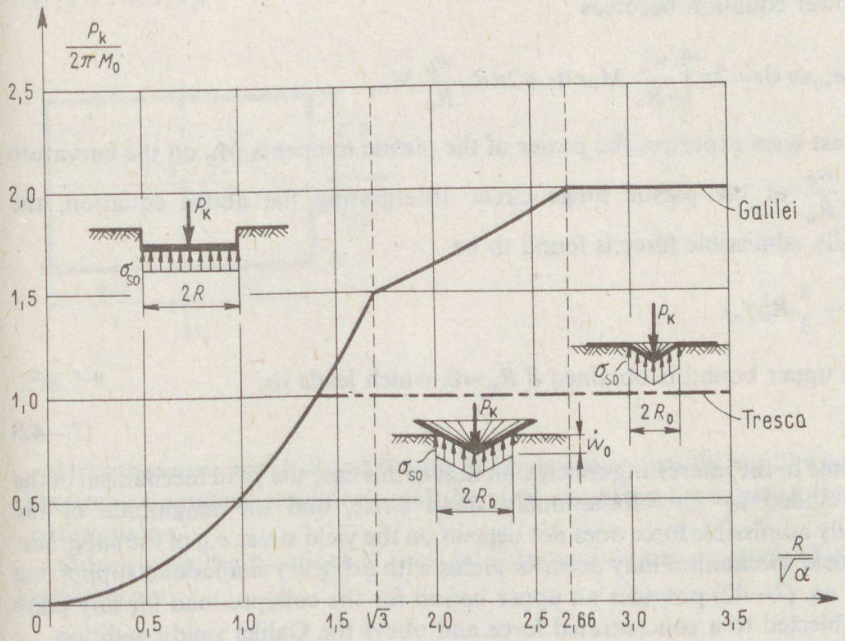


Fig. 7–8

from which the external force can be expressed in terms of the radius R_0 as

$$F_k = 2\pi \frac{R}{R_0} M_0 + \frac{\pi}{3} R_0^2 \sigma_{s0}.$$

The best upper bound is obtained by minimizing F_k. Then, equation $\frac{\partial F_k}{\partial R_0} = 0$ leads to the solution

$$R_0 = \sqrt[3]{3R\alpha}, \quad \alpha = \frac{M_0}{\sigma_{s0}},$$
$$F_k = 6.54\, \sigma_{s0} \sqrt[3]{R^2 \alpha^2}. \tag{7—41}$$

Finally, consider the yield mechanism where only the inner part of the plate, bounded by a *plastic hinge circle* with radius R_0, undergoes plastic deformations and the outer part remains rigid. The velocity field is then given by

$$\dot{w}=\dot{w}_0\left(1-\frac{r}{R_0}\right), \quad 0\le r\le R_0,$$

$$\dot{w}\equiv 0, \qquad R_0\le r\le R$$

and the power equation becomes

$$F_k\dot{w}_0-\int_0^{R_0}\sigma_{s0}\dot{w}r\,dr=2\pi\int_0^R\frac{\dot{w}_0}{rR_0}M_0 r\,dr+2\pi R_0\frac{\dot{w}_0}{R_0}M_0.$$

Here, the last term expresses the power of the plastic moments M_0 on the curvature rates $\dot{\kappa}_0=\dfrac{\dot{w}_0}{R_0}$ at the plastic hinge circle. Intergrating the above equation, the kinematically admissible force is found to be

$$F_k=4\pi M_0+\frac{\pi}{3}R_0^2\sigma_{s0}.$$

The best upper bound is obtained if $R_0\to 0$, which leads to

$$F_k=4\pi M_0. \tag{7—42}$$

We have come to the interesting conclusion that in this case the yield mechanism of the plate is bounded by an infinitesimally small circle, and the magnitude of the kinematically admissible force does not depend on the yield stress σ_{s0} of the subgrade. Since this yield mechanism may occur in plates with arbitrary shapes and supporting conditions, eq. (7—42) provides an upper bound for the collapse load for any plate which is subjected to a concentrated force and obeys the Galilei yield condition.

Considering eqs (7—39), (7—41) and (7—42), one can see that the magnitude of the kinematically admissible force depends on the radius R and the ratio $\alpha=\dfrac{M_0}{\sigma_{s0}}$. In a particular problem, the lowest value of the forces obtained by these equations provides the best upper bound solution which is, at the same time, the collapse load for the plate. These results are illustrated in Fig. 7—8.

Finally, it should be mentioned that, using the Tresca yield condition, eqs (7—39) and (7—41) are unchanged but eq. (7—42) has to be replaced by the relationship

$$F_k=2\pi M_0. \tag{7—43}$$

This is illustrated by a dashed line in Fig. 7—8.

7.2.3. RECTANGULAR PLATES

As our next example, we will determine the lower and upper bounds of the collapse load for a simply supported rectangular plate subjected to a uniformly distributed load p (Fig. 7—9). We assume that the plate obeys the Galilei yield condition and $a\ge b$.

7.2.3.1. LOWER BOUND SOLUTION

Considering the double symmetry, let us try to find the statically admissible moment distribution in the plate in the following form

$$M_{11}=M_0-Ax_1^2,$$
$$M_{22}=M_0-Bx_2^2, \qquad (7—44)$$
$$M_{12}=-Cx_1x_2.$$

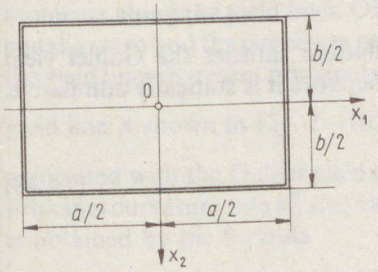


Fig. 7–9

Here the constants A, B and C have to be chosen so that the equilibrium equations, the static boundary conditions and the yield condition are satisfied throughout the entire plate.

Substituting the functions (7—44) into the equilibrium equation (7—8) yields the relationship

$$-2A-2C-2B+p=0. \qquad (7—45)$$

The static boundary conditions are expressed in the form

$$M_{11}\left(\pm\frac{a}{2}, x_2\right)=0,$$
$$M_{22}\left(x_1, \pm\frac{b}{2}\right)=0,$$

and provide the results

$$A=\frac{4M_0}{a^2}, \quad B=\frac{4M_0}{b^2}.$$

In order to satisfy the yield condition, consider first only the corners of the plate. Here, according to eqs (7—44) $M_{11}=M_{22}=0$ and $M_{12}=\pm C\frac{ab}{4}$. Substituting these moments into the Galilei yield condition given by eq. (7—18a) gives $C\frac{ab}{4}\leqq M_0$.

Considering eq. (7—45), the best lower bound is obtained if C takes its maximum value, i.e. if $C=\dfrac{4M_0}{ab}$. Then, using eqs (7—44), the moment distibution in the plate becomes

$$\left.\begin{aligned} M_{11}&=M_0\left(1-4\frac{x_1^2}{a^2}\right),\\ M_{22}&=M_0\left(1-4\frac{x_2^2}{b^2}\right),\\ M_{12}&=-4M_0\frac{x_1x_2}{ab}. \end{aligned}\right\} \qquad (7—46)$$

It can be proved that the above moment distribution satisfies the Galilei yield condition (7—18a) at every point in the plate, and therefore it is statically admissible. Consequently, eq. (7—45) gives

$$p_s=\left[1+\frac{b}{a}+\left(\frac{b}{a}\right)^2\right]\frac{8M_0}{b^2} \qquad (7—47)$$

as a lower bound solution to the problem.

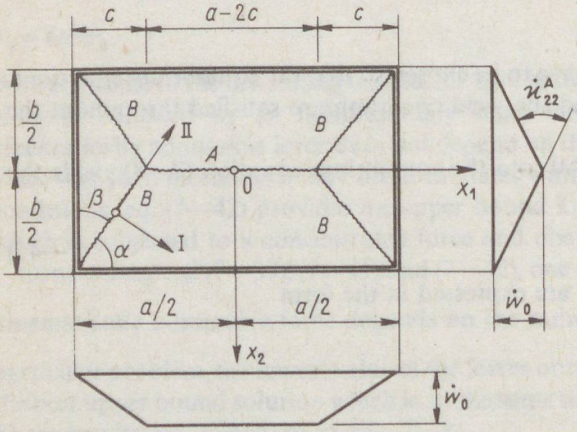


Fig. 7-10

7.2.3.2. UPPER BOUND SOLUTION

To obtain an upper bound solution, let us assume a yield mechanism in which plastic deformations occur only along several straight discontinuity lines, called *yield lines* (Fig. 7—10). Here, finite rotations which allow the rigid body motion of regions bounded by the yield lines can develop. In the yield mechanism shown in Fig. 7—10 the distance c of the joints of the yield lines from the supports is unknown and the velocity $\dot{w}_0$ of these joints is unspecified.

The power equation for the yield mechanism is expressed in the general form

$$p_k \int \dot{w} \mathrm{d}A = \int M_{\alpha\beta} \dot{\kappa}_{\alpha\beta} \mathrm{d}A. \tag{7—48}$$

The integral on the left hand side is equal to the volume of the polyhedron formed by the yield mechanism and is found to be

$$p_k \int \dot{w} \mathrm{d}A = p_k \left(\frac{ab}{2} \dot{w}_0 - 2 \frac{bc}{2} \frac{1}{3} \dot{w}_0 \right) = p_k b \left(\frac{a}{2} - \frac{c}{3} \right) \dot{w}_0. \tag{7—49}$$

To determine the internal power, we have to calculate the curvature rates and moments along the yield lines. Obviously, along a straight yield line the twist must be equal to zero and the curvature parallel to the yield line also vanishes. This implies that the yield lines represent principal directions for the curvatures. Consequently, along the yield line A shown in Fig. 7—10, $\dot{\kappa}^A_{11} = \dot{\kappa}^A_{12} = 0$ and $\dot{\kappa}^A_{22} = \dot{\kappa}^A_{\mathrm{I}} = 4 \frac{\dot{w}_0}{b}$, and the moment associated with the Galilei yield condition is equal to M_0. Along the yield lines B the principal curvature rate $\dot{\kappa}^B_{\mathrm{II}}$ also vanishes and the curvature rate normal to the yield line is obtained by the formula

$$\dot{\kappa}^B_{\mathrm{I}} = \frac{\dot{w}_0}{s} \left(\cot \alpha + \cot \beta \right) = \frac{\dot{w}_0}{s} \left(\frac{2c}{b} + \frac{b}{2c} \right),$$

where s is the length of the yield line (see e.g. Wood 1961). According to the Galilei yield condition the associated moment is equal to M_0.

Now the power of the moments on the curvature rates is expressed as

$$\int M_{\alpha\beta} \dot{\kappa}_{\alpha\beta} \mathrm{d}A = (a - 2c) 4 \frac{\dot{w}_0}{b} M_0 + 4s \frac{\dot{w}_0}{s} \left(\frac{2c}{b} + \frac{b}{2c} \right) M_0 =$$

$$= 4 \left(\frac{a}{b} + \frac{b}{2c} \right) M_0 \dot{w}_0.$$

This result together with eq. (7—49) provides the kinematically admissible load in terms of the parameter c

$$p_k = \frac{\frac{a}{b} + \frac{b}{2c}}{\frac{3a}{b} - \frac{2c}{b}} \frac{24 M_0}{b^2}. \tag{7—50}$$

To obtain the best upper bound, we have to minimize this expression. Equation $\frac{\partial p_k}{\partial c} = 0$ leads to the solution

$$p_k = \frac{3}{\left[\sqrt{3 + \left(\frac{b}{a} \right)^2} - \frac{b}{a} \right]^2} \frac{8 M_0}{b^2}. \tag{7—51}$$

Considering also the lower bound solution given by eq. (7—47), the collapse load for the plate is bounded by the expressions

$$\left[1+\frac{b}{a}+\left(\frac{b}{a}\right)^2\right]\frac{8M_0}{b^2}\leq p_p\leq \frac{3}{\left[\sqrt{3+\left(\frac{b}{a}\right)^2}-\frac{b}{a}\right]^2}\frac{8M_0}{b^2}. \tag{7—52}$$

The lower and upper bounds are shown in Table 7—1. As can be seen, the bounds are quite close to each other, and in the special cases when $\frac{a}{b}=1$ and $\frac{a}{b}\to\infty$, give the exact solution to the problem.

Table 7—1

a/b	1.0	1.5	2.0	3.0	∞
$\frac{p_s b^2}{M_0}$	24	16.89	14	11.55	8
$\frac{p_k b^2}{M_0}$	24	16.97	14.14	11.73	8

7.2.4. YIELD-LINE THEORY OF REINFORCED CONCRETE PLATES

The yield-line theory of reinforced concrete plates was first suggested by Ingerslev (1921) and Johansen (1932), and later developed and experimentally proved by others (see e.g. Gvozdev 1936; Wood 1961; Johansen 1962; Sawczuk, Jaeger 1963; Kaliszky 1967; Wood, Jones 1967; Kwiecinski 1986).

The theory is based on the kinematic theorem of limit analysis, and therefore provides upper bound solutions for the collapse load. Since the reinforcement may be different in different directions and at different points in the plate, the plastic moment is in general a function of the directions and the coordinates. The analysis is based on the generalized Galilei yield condition, which takes the orthotropy of the plate into consideration.

The theory assumes that all the plastic deformations of the plate are concentrated in discontinuity lines, called *yield lines*, about which the rigid parts of the plate can undergo rotations. Consequently, the yield mechanism consists of rigid regions of the plate bounded by yield lines. The arrangement of the yield lines is assumed on the basis of experimental results and/or geometrical and mechanical considerations, and the unknown parameters of the yield mechanism can be determined by minimizing the kinematically admissible load multiplier.

The solution presented in Section 7.2.3.2. was based on the principles of yield-line theory, therefore, further illustrations are not necessary to show its application. On the basis of this theory, several methods have been obtained and widely used in engineering practice.

7.3. LIMIT ANALYSIS OF SHELLS

Because of the great variety of possible shapes and loading conditions, the general governing equations for shells are very complicated. Much simpler equations can be obtained if they are derived for various particular shapes separately, which also makes the solutions easier to obtain. Our next discussion will be restricted to the limit analysis of cylindrical and conical shells. In addition, the solution for a shallow reinforced shell will also be presented. A broader treatment of the plastic analysis of shells can be found in the literature (Hodge 1959, 1963; Mikeladze 1963; Olszak, Sawczuk 1964, 1967; Save, Massonnet 1972; Save 1985).

It should be noted that the application of the theory of limit analysis to thin shells is limited, because failure may occur due to loss of stability either in the entire shell or in a significant part of it before the plastic collapse load reached. Hence, to determine the load-carrying capacity in many practical cases an elasto-plastic analysis based on the large deflection theory of shells has to be applied using numerical methods, generally the finite element method. The discussion of such problems is beyond the scope of this brief survey.

7.3.1. CIRCULAR CYLINDRICAL SHELLS

7.3.1.1. GOVERNING EQUATIONS

(1) Consider a circular cylindrical shell with radius R, length $2L$ and thickness $2h$, subjected to a uniformly distributed radial pressure P (Fig. 7—11) (Hodge 1954, 1959, 1963; Drucker 1954; Prager 1955; Onat 1955). In a cylindrical coordinate system r, ϕ, X the radial and axial displacements of the points on the middle surface will be denoted by W and U and the radial and axial displacements of an arbitrary point of the shell will be designated by and U_r, U_x, respectively. Because of axial symmetry, W and U are independent of ϕ and the circumferential displacements U_ϕ vanish at every point of the shell. Remembering the assumption that elements normal to the middle surface remain straight and normal after deformation, the following relationships are obtained:

$$U_x = U + \frac{dW}{dX} Z, \quad U_r = -W, \quad U_\phi = 0. \tag{7—53}$$

Here Z is the distance of a point of the shell through the shell thickness measured from the middle surface. U_r and Z are positive in the outward direction, while W is assumed to be positive in the inward direction.

As a consequence of axial symmetry, the shear strains $\varepsilon_{x\phi}$ and $\varepsilon_{r\phi}$ are zero. Besides this, ε_{xr} can be neglected because of the assumptions of Section 7.1, and the radial strain ε_{rr} does not appear in the derivation of the equations. Therefore, using eqs (6—67b) and (7—53) the only strains of relevance are found to be

$$\varepsilon_{\phi\phi} = \frac{U_r}{R} = \frac{-W}{R},$$

$$\varepsilon_{xx} = \frac{dU_x}{dX} = \frac{dU}{dX} + \frac{d^2W}{dX^2} Z. \tag{7—54}$$

(2) The *dissipation energy* per unit area of the plate becomes

$$\mathrm{d}=\int_{-h}^{h}(\sigma_{xx}\varepsilon_{xx}+\sigma_{\phi\phi}\varepsilon_{\phi\phi})\mathrm{d}Z$$

or, by substituting eqs (7—54),

$$d=\frac{\mathrm{d}U}{\mathrm{d}X}\int_{-h}^{h}\sigma_{xx}\mathrm{d}Z-\frac{\mathrm{d}^2W}{\mathrm{d}X^2}\int_{-h}^{h}(-Z\sigma_{xx})\mathrm{d}Z-\frac{W}{R}\int_{-h}^{h}\sigma_{\phi\phi}\mathrm{d}Z. \tag{7—55}$$

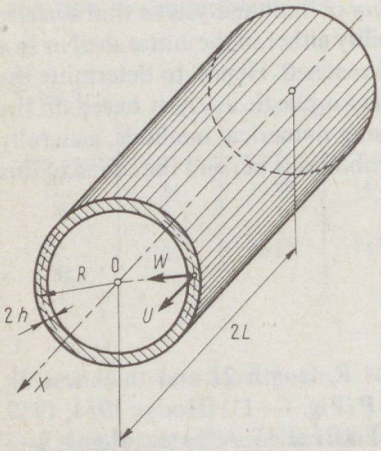


Fig. 7–11

Here the integrals

$$\left.\begin{aligned}N_x&=\int_{-h}^{h}\sigma_{xx}\mathrm{d}Z,\\ N_\phi&=\int_{-h}^{h}\sigma_{\phi\phi}\mathrm{d}Z,\\ M_x&=-\int_{-h}^{h}\sigma_{xx}Z\mathrm{d}Z\end{aligned}\right\} \tag{7—56}$$

denote the generalized stresses per unit length, as shown in Fig. 7—12, and the corresponding generalized strains are

$$V_x=\frac{\mathrm{d}U}{\mathrm{d}X},\quad V_\phi=-\frac{W}{R},\quad K_x=-\frac{\mathrm{d}^2W}{\mathrm{d}X^2}. \tag{7—57}$$

Using these notations, the dissipation energy of the entire shell can be written in the form

$$D=2\pi R\int_{-L}^{L}(N_xV_x+N_\phi N_\phi+M_xK_x)\mathrm{d}X. \tag{7—58}$$

As can be seen, the shear force Q_x and moment M_ϕ do not occur in the expression for the dissipation energy. They are "reactions", and consequently will also be missing from the yield condition.

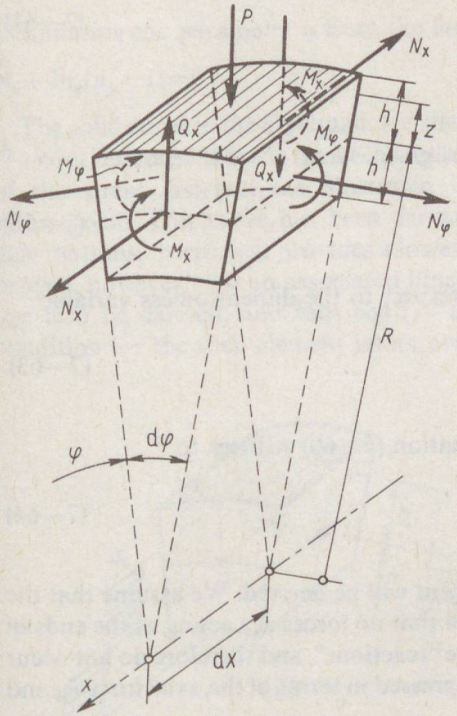


Fig. 7–12

(3) The *equilibrium* of a shell element shown in Fig. 7—12 is expressed by the differential equations

$$\left.\begin{aligned} \frac{dQ_x}{dX} + \frac{N_\phi}{R} + P = 0, \\ \frac{dM_x}{dX} - Q_x = 0, \\ \frac{dN_x}{dX} = 0. \end{aligned}\right\} \qquad (7—59)$$

The last equations results in $N_x = \text{constant}$. Consequently, if no axial forces are acting on the ends of the shell, $N_x = 0$. In this special case, eliminating Q_x from the above equations, the equilibrium of the shell is expressed by a single differential equation:

$$\frac{d^2M_x}{dX^2} + \frac{N_\phi}{R} + P = 0. \qquad (7—60)$$

In order to simplify the equations, let us introduce the following dimensionless variables

$$\left.\begin{aligned} &n_x=\frac{N_x}{N_0}, n_\phi=\frac{N_\phi}{N_0}, m_x=\frac{M_x}{M_0}, p=\frac{PR}{N_0},\\ &u=\frac{U}{L}, w=\frac{W}{L}, N_0=2h\sigma_0, M_0=h^2\sigma_0. \end{aligned}\right\} \tag{7—61}$$

Then, the dimensionless generalized strains given by eq. (7—57) become

$$v_x=u', \quad v_\phi=-w, \quad \kappa_x=-\frac{w''}{2\psi^2}. \tag{7—62}$$

Here the primes denote differentiation with respect to the dimensionless variable

$$x=\frac{X}{L} \quad \text{and} \quad \psi=\frac{L}{\sqrt{Rh}}. \tag{7—63}$$

Using the new variables the equilibrium equation (7—60) reduces to

$$\frac{1}{2\psi^2}m_x''+n_\phi+p=0. \tag{7—64}$$

(4) Next, the *yield condition* for a shell element will be derived. We assume that the material follows the *Tresca yield condition* and that no forces are acting at the ends of the shell, i.e. $N_x\equiv 0$. In addition, Q_x and M_ϕ are "reactions", and therefore do not occur in the yield condition, therefore this can be expressed in terms of the axial force n_ϕ and the moment m_x as

$$f(n_\phi,m_x)=0. \tag{7—65}$$

Approaching the problem from the stress viewpoint, we can state that in the yield condition for a point only the stresses σ_{xx} and $\sigma_{\phi\phi}$ will occur. Since the principal directions are axial and circumferential, the Tresca yield condition may be written in the form

$$\max(|\sigma_{xx}|, |\sigma_{\phi\phi}|, |\sigma_{xx}-\sigma_{\phi\phi}|)\leq\sigma_0. \tag{7—66}$$

A shell element becomes perfectly plastic if, at every point, the above relationship becomes an equality. However, the same relationship is not necessarily valid throughout the entire element, and therefore the form of the yield condition for an entire shell element is generally different from that given by eq. (7—66) for a point.

The possible stress distributions of an element in the fully plastic state are shown in Fig. 7—13. From Fig. 7—13(a) one obtains

$$m_x=1, \quad 0\leq n_\phi\leq\frac{1}{2}, \tag{7—67a}$$

while the stress distribution of Fig. 7—13(b) gives

$$m_x = 1-\eta^2,$$
$$n_\phi = \frac{1}{2}(1+\eta). \qquad (7—67b)$$

Eliminating the parameter η from the last two equations leads to

$$m_x + 2n_\phi(n_\phi - 1) = 0. \qquad (7—67c)$$

The solid curve in the first quadrant shown in Fig. 7—14 represents eqs (7—67a) and (7—67c). The curves in the remaining quadrants can be obtained by suitable reflection of the stress distributions illustrated in Fig. 7—13. Hence, the yield curve is symmetrical. This curve has been derived by the use of statically admissible stress distributions; therefore it provides a lower bound for the true yield condition. It can be proved, however, that an associated kinematically admissible strain rate distribution can also be derived, and thus eqs (7—67a) and (7—67c) represent the exact yield condition for the shell element under consideration (Hodge 1959).

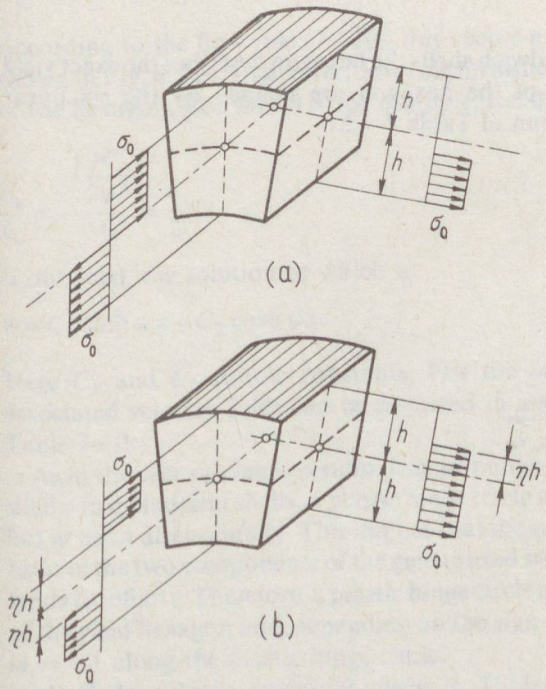


Fig. 7–13

In order to simplify our analysis, it seems desirable to linearize the above yield condition. This is indicated by the dashed line in Fig. 7—14. The corresponding hexagon is inside the exact yield curve and therefore provides a lower bound solution.

Table 7–2

Side	f	n_ϕ	m_x	$\dot{w}$
AB	$n_\phi + \frac{1}{2} m_x - 1 = 0$	$K_1 \sinh\psi x + K_2 \cosh\psi x - p$	$2(1-n_\phi)$	$C_1 \sinh\psi x + C_2 \cosh\psi x$
BC	$m_x - 1 = 0$	$-p$	1	0
CD	$-n_\phi + \frac{1}{2} m_x - 1 = 0$	$K_1 \sin\psi x + K_2 \cos\psi x - p$	$2(1+n_\phi)$	$C_1 \sin\psi x + C_2 \cos\psi x$
DE	$-n_\phi - \frac{1}{2} m_x - 1 = 0$	$K_1 \sinh\psi x + K_2 \cosh\psi x - p$	$-2(1+n_\phi)$	$C_1 \sinh\psi x + C_2 \cosh\psi x$
EF	$-m_x - 1 = 0$	$-p$	-1	0
FA	$n_\phi - \frac{1}{2} m_x - 1 = 0$	$K_1 \sin\psi x + K_2 \cos\psi x - p$	$2(n_\phi - 1)$	$C_1 \sin\psi x + C_2 \cos\psi x$

It can be proved that in the case of sandwich shells the hexagon describes the exact yield condition (Hodge 1959). The sides of the hexagon are defined by the six linear relationships shown in the first column of Table 7—2.

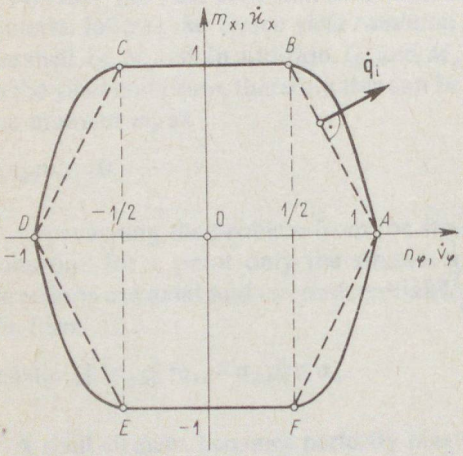


Fig. 7–14

The equilibrium equation (7—64) and the yield condition contain two unknown functions m_x and n_ϕ and therefore if only static boundary conditions are prescribed the solution can be obtained without considering the velocities and strains. The problem is, however, that the yield condition is defined by six different equations and each equation results in a different solution. For example the stress profile CD in Fig. 7—14

defined by the equation

$$-n_\phi + \frac{1}{2} m_x - 1 = 0$$

together with the equilibrium equation (7—61a) leads to the solution

$$n_\phi = K_1 \sin \psi x + K_2 \cos \psi x - p,$$

$$m_x = 2(1 + n_\phi).$$

Here K_1 and K_2 are constants to be determined from the boundary conditions. The solutions corresponding to the other sides of the yield hexagon are given in Table 7—2.

When geometrical boundary conditions are prescribed, the velocities and strains in the shell must also be taken into consideration. This problem will be discussed next.

(5) Making use of the kinematic equation (7—63), the *generalized strain rate vector* $\dot{q}_i[\dot{v}_\phi \; \dot{\kappa}_x]$ can be expressed in terms of the velocity $\dot{w}$ as

$$\dot{q}_i \left[-\dot{w} \quad -\frac{\dot{w}''}{2\psi^2} \right]. \tag{7—68}$$

According to the flow rule (7—20), this vector must be normal to the yield hexagon shown in Fig. 6—14. Hence, the flow rule furnishes a differential equation for each side of the hexagon. For side AB, for example, the differential equation

$$\frac{\dot{\kappa}_x}{\dot{v}_x} = \frac{-\frac{\dot{w}''}{2\psi^2}}{-\dot{w}} = \frac{1}{2} \tag{7—69}$$

is obtained, the solution to which is

$$\dot{w} = C_1 \sinh \psi x + C_2 \cosh \psi x.$$

Here C_1 and C_2 denote constants. For the other sides of the yield hexagon the associated velocity fields can be obtained in a similar manner, and are tabulated in Table 7—2.

As in the case of plates, certain discontinuities can also occur in the velocity field of shells. In cylindrical shells, a *plastic hinge circle* can form along which $\dot{w}$ is continuous but $\dot{w}'$ has a discontinuity. This implies that the curvature rate $\dot{\kappa}_x$, and consequently the ratio of the two components of the generalized strain rate vector $\dot{q}_i$ given by eq. (7—69), tends to infinity. Therefore, a plastic hinge circle must correspond to the sides BC or EF of the yield hexagon and, depending on the sign of the discontinuity in slope, $m_x = 1$ or $m_x = -1$ along the plastic hinge circle.

(6) If the velocity functions given in Table 7—2 are known, the solution to a particular problem reduces to the determination of the constants in Table 7—2. First, using mechanical and geometrical considerations, we assume the stress profiles in different domains of the shell. Then, we determine the constants from the boundary conditions and the continuity conditions along the boundaries of the different plastic domains. Finally, to find the exact solution to a problem, we have to check that

(a) the stress profile lies everywhere on or inside the yield hexagon and,

(b) the associated strain-rate vectors are directed everywhere *outward* and lie between the normal vectors of the neighbouring sides at a corner of the yield hexagon.

Solutions which satisfy only the first condition are *statically admissible* and provide lower bounds for the collapse load. On the other hand, solutions which satisfy only the second condition are *kinematically admissible* and provide upper bounds for the collapse load.

The main difficulty in finding the exact solution is assuming the correct hypothesis for the different plastic domains of the shell. If the first attempt fails, one may obtain the correct hypothesis by a suitable change in the first assumption.

The application of the theory will next be illustrated by the solution to an example.

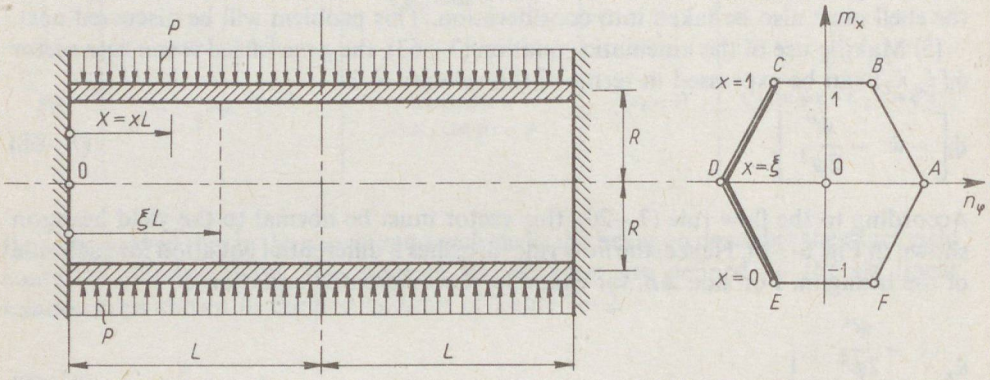


Fig. 7–15

7.3.1.2. CLAMPED CYLINDRICAL SHELL UNDER UNIFORM RADIAL PRESSURE

The problem to be solved is shown in Fig. 7—15 (Hodge 1963). In the analysis, the linearized yield condition given in Fig. 7—14 will be used, and because of symmetry only the left hand side of the shell will be taken into consideration.

Using the dimensionless coordinates defined by eqs (7—61) and (7—62) the boundary conditions are as follows:

(a) at the clamped end

$$\left.\begin{aligned} &\dot{w}(0)=0 \\ &\text{and} \\ &\dot{w}'(0)=0 \text{ or } m_x(0)=-1; \end{aligned}\right\} \qquad (7—70)$$

(b) in the plane of symmetry

$$\left.\begin{aligned} &m_x'(1)=0 \\ &\text{and} \\ &\dot{w}'(1)=0 \text{ or } m_x(1)=1. \end{aligned}\right\} \qquad (7—71)$$

Here the conditions $m_x(0) = -1$ and $m_x(1) = 1$ correspond to the cases when *plastic hinge circles* develop at the clamped end and at the middle section of the shell, respectively. This can occur when the shell is relatively short and the behaviour of the axial strips is similar to that of a clamped beam. First, we will assume that the shell is "short" and that the stress profile is *EDC* in Fig. 7—15. The points *E* and *C* correspond to the plastic hinge circles at $x = 0$ and $x = 1$, respectively, while the point *D* corresponds to the section $x = \xi$, where $m_x = 0$. This section divides the shell into two domains where the stress distributions are defined by the lines *ED* and *DC*. Denoting the moments in the domains $0 \le x \le \xi$ and $\xi \le x \le 1$ by m_x^- and m_x^+, respectively, the following conditions should be satisfied at $x = \xi$

$$\left.\begin{aligned} &m_x^-(\xi) = 0, \quad m_x^+(\xi) = 0, \\ &[m_x^-(\xi)]' = [m_x^+(\xi)]'. \end{aligned}\right\} \tag{7—72}$$

The stress distribution in the shell can be determined by considering the boundary conditions (7—70) and (7—71), the first condition of eq. (7—72) and the equations given in Table 7—2.

In the domain $0 \le x \le \xi$

$$\left.\begin{aligned} &n_\phi = \left(p - \frac{1}{2}\right)\frac{\sinh\psi(\xi - x)}{\sinh\psi\xi} + (p-1)\frac{\sinh\psi x}{\sinh\psi\xi} - p, \\ &m_x = -2n_\phi - 2, \end{aligned}\right\} \tag{7—73a}$$

in the domain $\xi \le x \le 1$,

$$\left.\begin{aligned} &n_\phi = \left(p - \frac{1}{2}\right)\cos\psi(1-x) - p, \\ &m_x = 2n_\phi + 2. \end{aligned}\right\} \tag{7—73b}$$

Finally, the last two conditions of eq. (7—72) provide two equations, which make the determination of the distance ξ and the load intensity p possible. They have the forms

$$\left.\begin{aligned} &\frac{2p-1}{2p-2} = \frac{1}{\cos\psi(1-\xi)}, \\ &\sinh\psi\xi = \frac{\sin\psi(1-\xi)}{\sqrt{2}\cos\psi(1-\xi)+1}. \end{aligned}\right\} \tag{7—74}$$

Since the above results are based on certain assumptions about the stress profile in the shell, we now have to determine the conditions under which the solution is statically and kinematically admissible.

The solution will be statically admissible as long as the stress profile associated with eq. (7—73) is nowhere outside the corners *E*, *D* and *C* of the sides *ED* and *DC* of the yield hexagon. Since $m_x(x)$ is a monotonic function for all values of ψ, this condition is satisfied, and therefore eq. (7—74) provides a statically admissible solution.

The velocity distribution corresponding to the stress distribution (7—73) can be determined from Table 7—2 and from the boundary conditions (7—70) and (7—71). It becomes

$$\left.\begin{aligned} &\dot{w}=\dot{w}_0\frac{\sinh\psi x}{\cosh\psi\xi} \quad \text{for } 0\le x\le\xi \\ &\text{and} \\ &\dot{w}=\frac{\dot{w}_0}{\sinh\psi\xi}\left[\sinh\psi\xi\cos\psi(x-\xi)+\cos h\psi\xi\sin\psi(x-\xi)\right] \\ &\text{for} \quad \xi\le x\le 1, \end{aligned}\right\} \tag{7—75}$$

where $\dot{w}_0$ designates the unspecified velocity at $x=\xi$.

The vectors $\dot{q}_i$ corresponding to the above velocity distribution are normal to the appropriate sides of the yield hexagon by virtue of the method of their derivation. The velocities, however, will not be positive everywhere for larger values of ψ. That would imply an inward-directed normal, which would not be kinematically admissible. To avoid this contradiction, the slope at $x=1$ given by eq. (7—75) must be positive, which leads to the condition

$$-\sinh\psi\xi\sin\psi(1-\xi)+\cosh\psi\xi\cos\psi(1-\xi)\ge 0.$$

This expression together with the second equation of (7—74) provides the bounds $0\le\psi\le 1.649$ for which eqs (7—73) – (7—75) give the complete solution to the problem. If $\psi>1.649$ only a lower bound solution can be obtained by the use of eqs (7—73) and (7—74).

To determine a complete solution for the case $\psi>1.649$, one has to modify the above solution by omitting the plastic hinge circle at $x=1$. The stress profile will then terminate at some interior point G of the line CD, as shown in Fig. 7—16. The solution under this assumption is easily obtained form Table 7—2 and the boundary conditions (7—70) and (7—71), and is found to be as follows:

in the domain $0\le x\le\xi$

$$\left.\begin{aligned} n_\phi&=\left(p-\frac{1}{2}\right)\frac{\sinh\psi(\xi-x)}{\sinh\psi\xi}+(p-1)\frac{\sinh\psi x}{\sinh\psi\xi}-p, \\ m_x&=2n_\phi-2, \\ \dot{w}&=\dot{w}_0\frac{\sinh\psi x}{\cosh\psi\xi}, \end{aligned}\right\} \tag{7—76a}$$

in the domain $\xi\le x\le 1$

$$\left.\begin{aligned} n_\phi&=(p-1)\frac{\cos\psi(1-x)}{\cos\psi(1-\xi)}-p, \\ m_x&=2n_\phi+2, \\ \dot{w}&=\dot{w}_0\frac{\cos\psi(1-x)}{\sin\psi(1-\xi)}. \end{aligned}\right\} \tag{7—76b}$$

Here $\dot{w}_0$ denotes the unspecified velocity at $x=\xi$. The distance ξ and the load intensity p are defined by the equations

$$\left.\begin{aligned} &\tan\psi(1-\xi)=\coth\psi\xi,\\ &p=1+\frac{1}{2\,(2\cosh\psi\xi-1)}. \end{aligned}\right\} \qquad (7—77)$$

It has been proved (Hodge 1954) that the above equations provide a complete solution for $\psi>1.649$.

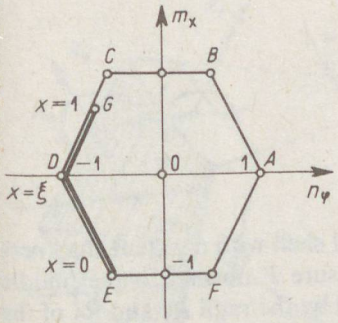


Fig. 7–16

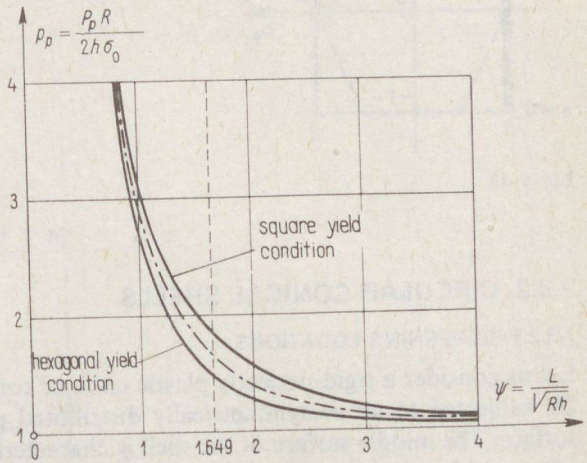


Fig. 7–17

The collapse load for the shell defined by eqs (7—74) and (7—77) is plotted in Fig. 7—17. At larger values of ψ, $p_p=\dfrac{P_pR}{2h\sigma_0}$ tends to 1 which corresponds to the collapse load for a cylindrical *membrane shell*. This result is in agreement with the obvious fact that for long shells the effect of clamped edges is negligible.

The solution to the previous problem is much easier if the *square yield condition* shown in Fig. 7—18 is used. It leads to the following results

$$\left.\begin{aligned} &n_\varphi=-1,\ m_x=-1+4x-2x^2,\\ &\dot{w}=\dot{w}_0x,\ p_p=1+\frac{2}{\psi^2}. \end{aligned}\right\} \qquad (7—78)$$

This collapse load is also plotted in Fig. 7—17 and, as can be seen, the difference between the two solutions is not significant. Since the curve for the exact yield condition for a shell element (see Fig. 7—14) lies between the square and the hexagon shown in Fig. 7—18, the solid lines of Fig. 7—17 give lower and upper bounds for the collapse load for the shell. Thus, the average values of these bounds, indicated by the dashed line in Fig. 7—17, provide good approximations for practical purposes.

The elasto-plastic and limit analysis of cylindrical shells with different loading and boundary conditions is widely discussed in the literature (see e.g. Drucker 1953; Hodge 1959, 1963; Kozák 1966).

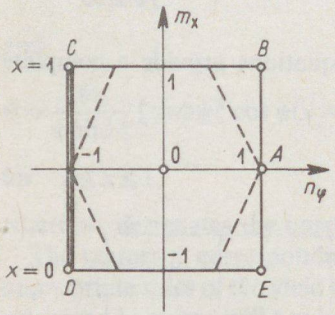


Fig. 7–18

7.3.2. CIRCULAR CONICAL SHELLS

7.3.2.1. GOVERNING EQUATIONS

Let us consider a rigid-perfectly plastic circular conical shell with constant thickness $2h$, subjected to an axisymmetrically distributed pressure P normal to the middle surface. The middle surface of the shell is characterized by the radii R_1 and R_2 of the edges and by the angle α between the generators and the axis of symmetry, while the position of an arbitrary point on the median surface is defined by the radius R (Fig. 7—19). The boundary conditions will be specified later.

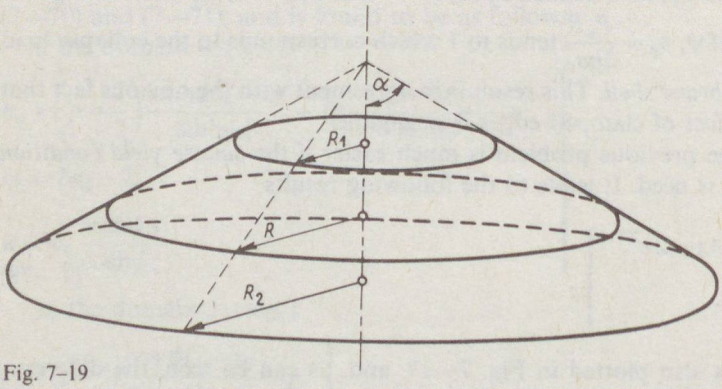


Fig. 7–19

The displacement of the middle surface of the shell in the direction of the generators and in the inward normal direction will be denoted by U and W, respectively. The state of strain of a shell element is characterized by the generalized strains V_r and V_ϕ and the

curvatures K_r and K_ϕ. They have the following *kinematic relationships* with the displacements (see e.g. Timoshenko, Woinowsky–Krieger 1940)

$$\left.\begin{aligned} V_r &= \frac{dU}{dR}\sin\alpha, \\ V_\phi &= \frac{U\sin\alpha - W\cos\alpha}{R}, \\ K_r &= -\frac{d^2W}{dR^2}\sin^2\alpha, \\ K_\phi &= -\frac{1}{R}\frac{dW}{dR}\sin^2\alpha. \end{aligned}\right\} \tag{7—79}$$

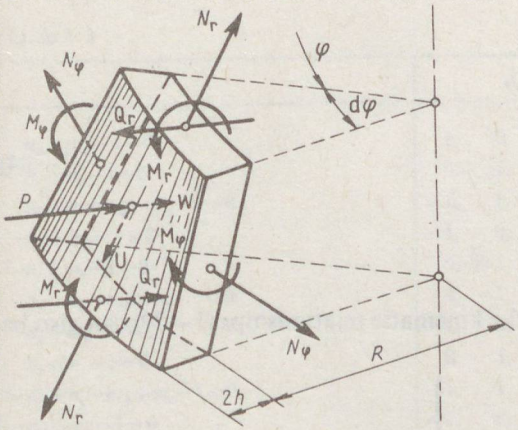


Fig. 7–20

The state of stress of a shell element is characterized by the generalized stresses N_r, N_ϕ, Q_r, M_r and M_ϕ shown in Fig. 7—20. They have to satisfy the *equilibrium equations*

$$\left.\begin{aligned} &\frac{d}{dR}(RN_r) - N_\phi = 0, \\ &\frac{d}{dR}(RQ_r) + N_\phi\cot\alpha + \frac{RP}{\sin\alpha} = 0, \\ &\frac{d}{dR}(RM_r) - M_\phi - \frac{R}{\sin\alpha}Q_r = 0. \end{aligned}\right\} \tag{7—80}$$

The elimination of the shear force Q_r yields the expressions

$$\left.\begin{aligned} &\frac{d}{dR}(RN_r) - N_\phi = 0, \\ &\frac{d^2}{dR^2}(RM_r) - \frac{dM_\phi}{dR} + \frac{\cos\alpha}{\sin^2\alpha}N_\phi + \frac{R}{\sin^2\alpha}P = 0. \end{aligned}\right\} \tag{7—81}$$

Finally, the *dissipation energy* of the entire shell is expressed in the form*

$$D=\frac{2\pi}{\sin\alpha}\int_{R_1}^{R_2}(N_r V_r+N_\phi V_\phi+M_r K_r+M_\phi K_\phi)R\,dR. \tag{7—82}$$

Introducing the dimensionless variables

$$\left.\begin{aligned} &r=\frac{R}{R_2},\ p=\frac{PL}{N_0},\\ &n_r=\frac{N_r}{N_0},\ n_\phi=\frac{N_\phi}{N_0},\\ &m_r=\frac{M_r}{M_0},\ m_\phi=\frac{M_\phi}{M_0}, \end{aligned}\right\} \tag{7—83}$$

$$\left.\begin{aligned} &u=\frac{U}{R_2},\ w=\frac{W}{R_2},\\ &v_r=V_r,\ v_\phi=V_\phi,\\ &\kappa_r=\frac{M_0}{N_0}K_r,\ \kappa_\phi=\frac{M_0}{N_0}K_\phi \end{aligned}\right\} \tag{7—84}$$

the equilibrium equations (7—81) and the kinematic relationships (7—79) can also be expressed in dimensionless form

$$\left.\begin{aligned} &\frac{d}{dr}(rn_r)-n_\phi=0,\\ &k\frac{d^2}{dr^2}(rm_r)-k\frac{dm_\phi}{dr}+\frac{\cos\alpha}{\sin^2\alpha}n_\phi+\frac{rp}{\sin^2\alpha}=0, \end{aligned}\right\} \tag{7—85}$$

$$\left.\begin{aligned} &v_r=\frac{du}{dr}\sin\alpha,\ v_\phi=\frac{u\sin\alpha-w\cos\alpha}{r},\\ &\kappa_r=-k\frac{d^2w}{dr^2}\sin^2\alpha,\ \kappa_\phi=-k\frac{dw}{rdr}\sin^2\alpha. \end{aligned}\right\} \tag{7—86}$$

Here

$$\left.\begin{aligned} &k=\frac{M_0}{N_0R_2},\\ &M_0=h^2\sigma_0,\ N_0=2h\sigma_0. \end{aligned}\right\} \tag{7—87}$$

* Since the shear deformations are neglected, the shear force Q_r does not contribute to the dissipation energy.

The *yield condition* for an element of the conical shell has the general form

$$f(n_\phi, n_r, m_\phi, m_r)=0. \tag{7—88}$$

This yield function is, in general, non-linear but it can be linearized by using the Tresca yield condition and by considering an ideal sandwich shell. The yield condition is then defined by the twelve linear functions given in Table 7—3 (see Hodge 1959).

The generalized strain rate vector

$$\dot{q}_i[\dot{v}_\phi \ \dot{v}_r \ \dot{\kappa}_\phi \ \dot{\kappa}_r]$$

is normal to the yield hypersurface. Its direction cosines associated with the different hyperplanes can easily be obtained, and are also given in Table 7—3.

Table 7–3

f	$\dot{q}_{0i}$
$n_\phi-m_\phi-1=0$	1, 0, −1, 0
$n_r-m_r-1=0$	0, 1, 0, −1
$-n_\phi+n_r+m_\phi-m_r-1=0$	−1, 1, 1, −1
$-n_\phi+m_\phi-1=0$	−1, 0, 1, 0
$-n_r+m_r-1=0$	0, −1, 0, 1
$n_\phi-n_r-m_\phi+m_r-1=0$	1, −1, −1, 1
$n_\phi+m_\phi-1=0$	1, 0, 1, 0
$n_r+m_r-1=0$	0, 1, 0, 1
$-n_\phi+n_r-m_\phi+m_r-1=0$	−1, 1, −1, 1
$-n_\phi-m_\phi-1=0$	−1, 0, −1, 0
$-n_r-m_r-1=0$	0, −1, 0, −1
$n_\phi-n_r+m_\phi-m_r-1=0$	1, −1, 1, −1

The equilibrium and kinematic equations (7—85) and (7—86) together with the yield condition and the flow rule given in Table 7—3, provide the governing equations for plastic conical shells. In spite of the fact that all the equations are linear, the solution to a particular problem is fairly complicated, since the analysis involves several domains with different yield conditions and flow rules the boundaries of which are, in general, unknown. In addition, the singular points (edges, vertices) of the yield hyper-surface and the possible discontinuities (plastic hinge circles) in the velocity field result in further difficulties.

To simplify the solution, one may assume that, similarly to the shear force Q_r, the moment M_ϕ is also a reaction and it can then be omitted from the yield condition. In cylindrical shells κ_ϕ is equal to zero, and therefore M_ϕ is a reaction. In conical shells K_ϕ does not vanish, but if the angle α of the cone is small neglecting M_ϕ in the yield condition leads to a reasonably good approximation.

A further simplification can be obtained by the use of a yield condition described by the expressions

$$\left.\begin{aligned} &|n_r|-1\leq 0,\\ &|n_\phi|-1\leq 0,\\ &|m_r|-1\leq 0, \end{aligned}\right\} \tag{7—89}$$

and illustrated by a cube in Fig. 7—21. Our further investigations will be based on this yield condition which obviously leads to upper bound solutions.

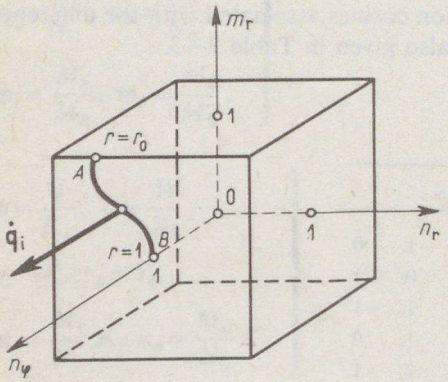


Fig. 7–21

7.3.2.2. CLAMPED CONICAL SHELL UNDER UNIFORM PRESSURE

Let us consider a conical shell, with a clamped edge at $R=R_1$ and a free edge at $R=R_2$, subjected to a uniform internal pressure P_0 normal to the middle surface (Kaliszky 1961a, 1963a).

(1) First, let us solve the problem by using the *kinematic principle*. The yield mechanism for the shell, which forms the basis of solution, is shown in Fig. 7—22. A plastic hinge circle at $R=R_0$ divides the shell into two domains; in the domain $R\leq R_0$ the shell remains motionless, while in the domain $R>R_0$ cracks develop in the direction of the generators and the displacements of the shell are normal to the middle surface. Hence, the yield mechanism is defined by the following velocity distribution:

$$\dot{u}(r)\equiv 0,$$

and in the domain $r_1\leq r\leq r_0$

$$\dot{w}(r)\equiv 0, \tag{7—90}$$

while in the domain $r_0\leq r\leq 1$

$$\dot{w}(r)=-\frac{r-r_0}{1-r_0}\dot{w}_0. \tag{7—91}$$

Here $\dot{w}_0$ is the unspecified velocity of the lower edge of the shell and $r_0 = \dfrac{R_0}{R_2}$ denotes the unknown position of the plastic hinge circle. Using eqs (7—86) and (7—91), the generalized strain rates for a shell element become

$$\left.\begin{aligned} &\dot{v}_r = 0, \\ &\dot{v}_\phi = \frac{\cos\alpha}{r}\frac{r-r_0}{1-r_0}\dot{w}_0, \\ &\dot{\kappa}_r = 0, \quad \dot{\kappa}_\phi = 0. \end{aligned}\right\} \tag{7—92}$$

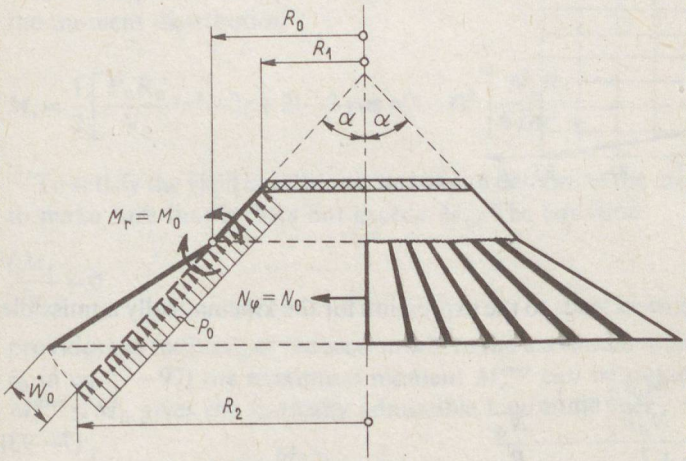


Fig. 7–22

The rotation in the plastic hinge circle can be obtained from Fig. 7—22 and is equal to

$$\dot{\phi}_0 = \frac{\sin\alpha}{1-r_0}\dot{w}_0.$$

From eq. (7—92) it is obvious that the strain-rate vector $\dot{q}_i\,(1, 0, 0)$ is parallel to the n_ϕ axis of the stress space shown in Fig. 7—21, consequently, the stress profile of the domain $r_0 \le r \le 1$ lies on the side $n_\phi = 1$ of the yield cube, and everywhere in this domain $N = N_0$. In addition, at $r = r_0$, $M_r = M_0$, while at $r = 1$, $M_r = 0$ and $N_r = 0$.

Using eq. (7—82), the dissipation energy of the shell has the form

$$D = \frac{2\pi R_2^2}{\sin\alpha}\int_{r_0}^{1} N_\phi \dot{v}_\phi dr + 2\pi R_0 M_0 \dot{\phi}_0 =$$

$$= \frac{2\pi R_2^2}{1-r_0} N_0 \left[\frac{1}{2}(1-r_0)^2 \cot\alpha + \frac{M_0 \sin\alpha}{N_0 R_2} r_0\right]\dot{w}_0,$$

while the power of the external load becomes

$$\frac{2\pi R_2^3}{\sin\alpha}\int_{r_0}^{1} P\dot{w}r\,dr = \frac{2\pi P_0 R_2^3}{6\sin\alpha(1-r_0)}(r_0^3-3r_0+2)\dot{w}_0.$$

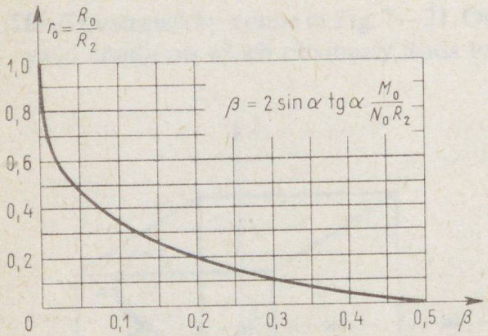


Fig. 7–23

The equality of these powers leads to the expression for the kinematically admissible load multiplier

$$P_{0k} = 6\frac{\frac{1}{2}\cos\alpha(1-r_0)^2+\frac{M_0 r_0}{N_0R_2}\sin^2\alpha}{r_0^3-3r_0+2}\frac{N_0}{R_2}. \qquad (7—93)$$

Any arbitrary value of r_0 satisfying the condition $r_1 \le r_0 \le 1$ provides an upper bound for the collapse load. The best approximation can be obtained by applying the minimum condition

$$\frac{\partial P_{0k}}{\partial r_0} = 0. \qquad (7—94)$$

The result of this calculation in terms of the parameter

$$\beta = 2\sin\alpha\,\mathrm{tg}\,\alpha\frac{M_0}{N_0R_2}$$

is plotted in Fig. 7—23. Knowing r_0, the best upper bound solution is obtained from eq. (7—93). If in a particular problem r_0, determined by the diagram of Fig. 7—23, is smaller than r_1 then the plastic hinge circle will form at the clamped edge $r=r_1$; and therefore, $r_0=r_1$ has to be substituted in eq. (7—93)

(2) Next, let us solve the problem by the use of the *static principle*. The equilibrium conditions for the shell are defined by the three equilibrium equations (7—80) and the boundary conditions

$$N_r(1)=M_r(1)=Q_r(1)=0. \qquad (7—95)$$

In the three equilibrium equations there are five unknown internal forces. To obtain a statically admissible stress field, two of these internal forces may be arbitrarily assumed and then the three remaining functions can be obtained from the equilibrium equations and boundary conditions. If, in addition, the yield condition (7—89) is also satisfied at every point in the shell, then the corresponding load multiplier will be statically admissible.

Let us make the following assumption

$$\left.\begin{aligned} M_\phi &\equiv 0, \\ N_\phi &\equiv N_0. \end{aligned}\right\} \tag{7—96}$$

Then the equilibrium equations (7—80) and the boundary conditions (7—95) lead to the moment distribution

$$M_r = \frac{1}{2}\left[\frac{P_0 R_2}{N_0}(r^3 - 3r + 2) - 3\cos\alpha(1-r)^2\right]\frac{N_0 R_2}{6\sin^2\alpha}. \tag{7—97}$$

To satisfy the yield conditions, we have to determine the maximum moment, in order to make sure that is does not exceed M_0. The equation

$$\frac{\partial M_r}{\partial r} = 0 \tag{7—98}$$

provides the radius $\bar{r}_0$ of the section where the maximum moment occurs. Substituting $\bar{r}_0$ in eq. (7—97) the maximum moment M_r^{max} can be obtained. Then the condition $M_r^{max} \leq M_0$ gives the statically admissible load multiplier

$$P_{os} = 6\frac{\frac{1}{2}\cos\alpha(1-\bar{r}_0)^2 + \frac{M_0\bar{r}_0}{N_0 R_2}\sin^2\alpha}{\bar{r}_0^3 - 3\bar{r}_0 + 2}\frac{N_0}{R_2}. \tag{7—99}$$

As can be seen, the expressions for the kinematically and statically admissible load multipliers given by eqs (7—93) and (7—99) have the same form. The only difference is that the parameters r_0 and $\bar{r}_0$ are defined by eq. (7—94) and eq. (7—98), respectively. It is easy to prove, however, that these two equations lead to the same solution, i.e. $r_0 = \bar{r}_0$, and therefore the kinematically and statically admissible multipliers are identical (Kaliszky 1961a, 1963a).

Finally, we have to prove that the normal forces N_r also do not violate the yield condition, i.e. that at every point of the shell the condition $|N_r| \leq N_0$ is fulfilled. From eqs (7—70), (7—95) and (7—96) we have

$$N_r = \frac{1-r}{r}N_0 \tag{7—100}$$

from which one can see that in the domain $\frac{1}{2} \leq r \leq 1$, N_r does not exceed N_0. Hence, in those cases where $r_1 = \frac{R_1}{R_2} \geq \frac{1}{2}$ both the moments and the normal forces satisfy the yield

condition; therefore, eq. (7—93) provides the collapse load of the shell. If, however, $r_1 = \frac{R_1}{R_2} < \frac{1}{2}$ the load multiplier (7—99) cannot be considered statically admissible; therefore eq. (7—93) gives only an upper bound solution.

Several publications on the plastic analysis of conical shells can be found in the literature (e.g. Hodge 1960; Onat 1960; Hodge, 1963; Olszak, Sawczuk 1967; Save, Massonnet 1972).

7.3.3. SHALLOW REINFORCED CONCRETE SHELL

The concept of the yield line theory of reinforced concrete plates discussed briefly in Section 7.2.4 can be generalized to the limit analysis of reinforced concrete shells. In this case, a generalized yield line has to be used in which in addition to rotation relative displacements can also occur therefore the power of the axial forces also has to be taken into consideration in the dissipation energy. The kinematic solution for the conical shell presented in Section 7.3.2 was based on this approach.

To illustrate the application, let us consider a shallow reinforced concrete shell simply supported along its straight polygonal edges and subjected to a concentrated force, as shown in Fig. 7—24 (Rzanicin 1956). We assume that the reinforcement is placed in the middle surface of the shell, and therefore the moment-carrying capacity of the shell elements is negligibly small. Thus, only *membrane forces* will arise in the shell.

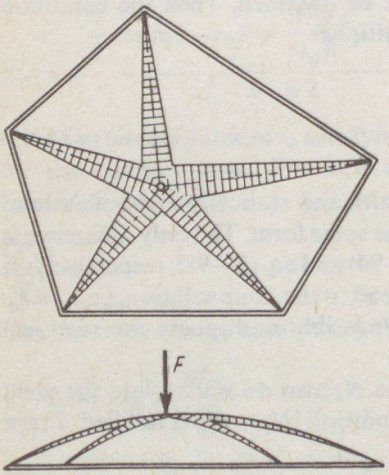


Fig. 7–24

The yield mechanism consists of yield lines, directed from the point of application of the force to the corners of the polygon, which divide the shell into rigid sections. Along the yield lines relative rotations and displacements can occur; the bending moment is zero and the normal force is equal to the load-carrying capacity in tension of the cross-

section, denoted by N_0 per unit length. Then, the equation for the power of the external and internal forces becomes

$$F\dot{w}_0 = \sum_{i=1}^{n} \left[\int_0^{s_i} N_0 \dot{v}_i \mathrm{d}S \right]. \tag{7—101}$$

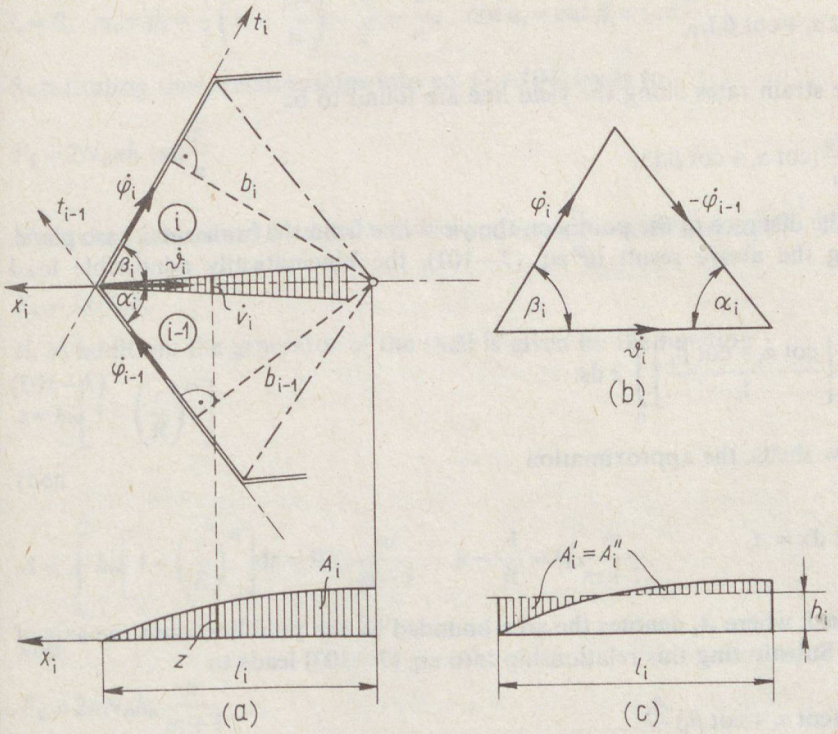


Fig. 7–25

Here $\dot{w}_0$ and $\dot{v}_i$ denote the velocity under the force and the strain rates along the yield lines, respectively as it is shown in Fig. 7—25(a). The summation is extended to all the yield lines $i = 1,2 \ldots n$. To determine $\dot{v}_i$, first we have to calculate the rotation rates of the sectors i and $i-1$ about the edges t_i and t_{i-1}. They become

$$\dot{\varphi}_i = \frac{\dot{w}_0}{b_i} \quad \text{and} \quad \dot{\varphi}_{i-1} = \frac{\dot{w}_0}{b_{i-1}}$$

or using the relationships $b_i = l_i \sin \alpha_i$ and $b_{i-1} = l_i \sin \beta_i$, we obtain

$$\dot{\varphi}_i = \frac{\dot{w}_0}{l_i \sin \alpha_i}, \quad \dot{\varphi}_{i-1} = \frac{\dot{w}_0}{l_i \sin \beta_i}. \tag{7—102}$$

The axis x_i of the *relative* rotation rate ϑ_i between the two sectors passes through the point of intersection of the axes t_i and t_{i-1}, and is equal to the difference between $\dot{\varphi}_i$ and $\dot{\varphi}_{i-1}$. Thus, from Fig. 7—25(b), one can obtain the relationship

$$\vartheta_i = \dot{\varphi}_i \cos \beta_i + \dot{\varphi}_{i-1} \cos \alpha_i$$

or, substituting eq. (7—102), it becomes

$$\vartheta_i = \frac{\dot{w}_0}{l_i} (\cot \alpha_i + \cot \beta_i).$$

Finally, the strain rates along the yield line are found to be

$$\vartheta_i = \vartheta_i z = \frac{\dot{w}_0}{l_i} (\cot \alpha_i + \cot \beta_i) z,$$

where z is the distance of the points on the yield line from the horizontal base plane. Substituting the above result in eq. (7—101), the kinematically admissible load becomes

$$F_k = N_0 \sum_{i=1}^{n} \left[\frac{\cot \alpha_i + \cot \beta_i}{l_i} \right] \int_0^{s_i} z \, ds. \qquad (7—103)$$

In shallow shells, the approximation

$$\int_0^{s_i} z \, ds \approx \int_0^{l_i} z \, dx = A_i$$

can be applied, where A_i denotes the area bounded by the yield line i and the axis of rotation x_i. Substituting this relationship into eq. (7—103) leads to

$$F_k = N_0 \sum_{i=1}^{n} (\cot \alpha_i + \cot \beta_i) \frac{A_i}{l_i}.$$

Considering Fig. 7—25(c), $\frac{A_i}{l_i}$ is equal to the average height h_i of the yield line above the axis x_i. Hence, the kinematically admissible load multiplier is finally expressed in the following simple form

$$F_k = N_0 \sum_{i=1}^{n} (\cot \alpha_i + \cot \beta_i) h_i. \qquad (7—104)$$

It is interesting to note that the kinematically admissible load multiplier for a plate with the same geometrical arrangement and loading is equal to (Wood 1961)

$$F_k = \sum_{i=1}^{n} (\cot \alpha_i + \cot \beta_i) M_{0i},$$

where M_{0i} denotes the plastic moment of the plate along the yield line i. Comparing these two results, we can state that the kinematically admissible load multiplier for a

membrane shell is identical to that of a plate with the same arrangement, provided that the relationship $M_{0i}=N_0 h_i$ is satisfied for all the yield lines.

Let us apply eq. (7—104) to the special case where the edges of the shell form a *regular polygon* with n sides and the corners of the polygon lie on a circle with radius R. Assuming that the force is acting on the centre of the circle, the following relationships can be obtained

$$l_i=R, \quad \alpha_i=\beta_i=\frac{1}{2}\left(\pi-\frac{2\pi}{n}\right)=\frac{\pi}{2}-\frac{\pi}{n}, \quad \cot\alpha_i=\cot\beta_i=\tan\frac{\pi}{n}.$$

Substituting these relationships into eq. (7—104) leads to

$$F_k=2N_0 nh\tan\frac{\pi}{n}. \tag{7—105}$$

If the shell is bounded by a *circle* $n\to\infty$ and $n\tan\frac{\pi}{n}\to\pi$. Hence, eq. (7—105) becomes

$$F_k=2\pi N_0 h. \tag{7—106}$$

If, in addition, the generator of the shell is given by the function

$$z=h_0\left[1-\left(\frac{r}{R}\right)^m\right]$$

then

$$A=\int_0^R h_0\left[1-\left(\frac{r}{R}\right)^m\right]dr=Rh_0\frac{m}{m+1}, \quad h=\frac{A}{R}=h_0\frac{m}{m+1}$$

and

$$F_k=2\pi N_0 h_0\frac{m}{m+1}. \tag{7—107}$$

Here h_0 denotes the height of the mid-point of the shell above the horizontal base plane.

More details of the plastic analysis of reinforced concrete shells can be found in the literature (e.g. Menyhárd 1956; Szmodits 1959; Ovetskin 1960; Kaliszky 1963a; König 1962; Olszak, Sawczuk 1964, 1967; Save, Massonnet 1972).

7.4. OPTIMAL DESIGN OF PLATES AND SHELLS

7.4.1. FUNDAMENTALS

(1) In Section 6.6.2.4 it was shown that the optimal plastic design of bar structures with continuously variable cross-sections can be reduced to the solution for fictitious elastic structures for which the expression for the complementary energy is identical to that of the weight (volume) function. It has been proved that this theorem can be generalized to plates and shells as well (Marcal, Prager 1964; Prager, Shield 1967; Rozvany 1976, Zyczkowski 1985).

Let us consider a homogeneous, perfectly plastic plate or shell with known shape and supports and with continuously variable thickness $2h$ subjected to proportional loading. The problem is to determine the function $h=h(x_i)$ such that the plate or shell can carry the given load, and the weight (volume)

$$W=2\int_S h(x_i)\,dS$$

of the structure is a minimum. The state of an element of a plate or shell is characterized by the generalized stresses Q_i, generalized strain-rates $\dot{q}_i$ and a scalar quantity, say the plastic moment M_0, which is a function of the thickness and defines the strength of the element. The specific weight per unit area and the yield condition for an element can be expressed in terms of the plastic moment in the forms

$$w=w(M_0),\quad f(Q_i)\leq M_0. \tag{7—108}$$

Let us assume that no constraints are prescribed for the thickness of the plate or shell. Then, at the plastic limit state of an optimally designed structure, all the elements are fully utilized; consequently, for each element, the condition $f(Q_i)=M_0$ is fulfilled. Substituting this relationship in the specific weight function we obtain

$$w=w(M_0)=w[f(Q_i)]=\bar{w}(Q_i). \tag{7—108a}$$

The problem of minimum weight design is to determine the thickness $h(x_i)$ of the plate or shell, on the following conditions:

(a) The *generalized stresses* Q_i must satisfy the equilibrium equations, the static boundary conditions and the yield condition and, at the same time, the weight of the structure must be a minimum. Making use of eq. (7—108a), this latter condition together with the satisfaction of the yield condition can be expressed in the concise form

$$W=\int_S \bar{w}(Q_i)dS=\min! \tag{7—109}$$

(b) The *generalized plastic strain-rates* $\dot{q}_i$ obtained from the generalized stresses by the plastic flow rule

$$\dot{q}_i=\dot{\lambda}\frac{\partial f}{\partial Q_i};\quad \dot{\lambda}\geq 0 \tag{7—110}$$

must satisfy the kinematic equations and the kinematic boundary conditions.

In order to reduce the above problem to a fictitious elastic solution, let us consider a non-linearly elastic plate or shell with the same shape, supports and loading and assume that its specific complementary energy (energy per unit area) is specified by the function $\phi(Q_i)$. Then, from the definition of the complementary energy, the generalized elastic strains are obtained as

$$q_i=\frac{\partial \phi}{\partial Q_i}. \tag{7—111}$$

If the specific complementary energy function is identical to the specific weight function, i.e.

$$\phi(Q_i) \equiv \bar{w}(Q_i) = w[f(Q_i)] \tag{7—112}$$

expression (7—111) becomes

$$q_i = \frac{\partial \phi}{\partial Q_i} = \frac{\partial w}{\partial f}\frac{\partial f}{\partial Q_i} = \frac{\partial w}{\partial M_0}\frac{\partial f}{\partial Q_i}. \tag{7—113}$$

Assuming that the specific weight function $w(M_0)$ is *convex*, the differential quotient

$$k = \frac{\partial w}{\partial M_0} \tag{7—114}$$

cannot be negative. Hence eq. (7—113) can be expressed in the form

$$q_i = k\frac{\partial f}{\partial Q_i}, \quad k > 0. \tag{7—115}$$

Then, the solution for the fictitious elastic structure under consideration is defined as follows:

(a) The *generalized stresses* Q_i must satisfy the equilibrium equations and static boundary conditions.

(b) The *generalized elastic strains* q_i obtained from the elastic stress-strain relationship

$$q_i = k\frac{\partial f}{\partial Q_i}; \quad k \geq 0 \tag{7—116}$$

must satisfy the compatibility equations and the kinematic boundary conditions.

According to the *principle of minimum complementary energy*, the condition for compatibility is expressed in the form

$$\int_S \phi(Q_i)\,dS = \int_S \bar{w}(Q_i)\,dS = \min! \tag{7—117}$$

Considering eqs (7—109), (7—110), (7—116) and (7—117), we can state that *the minimum weight design of plastic plates or shells is reduced to the solution for fictitious nonlinearly elastic plates or shells with the same shape, supports and loading provided that their specific complementary energy function is identical to the specific weight function of the original structure.*

(2) As a special application, consider the minimum weight design of *sandwich plates and shells* which obey the *Tresca yield condition*. In this case, both the specific weight function and the yield condition are linear functions of the generalized stresses.

The sandwich plate or shell has a soft core with constant thickness $2H$ and no axial strength, and two thin layers with *variable thickness* v, as shown in Fig. 7—26. In the

case of minimum weight design, the function $v(x_i)$ has to be determined such that the weight (volume)

$$W = 2\int_S v(x_i)\,dS$$

of the layers is a minimum*.

For the sake of simplicity our further discussion will be restricted to sandwich plates, the results obtained, however, can easily be generalized to sandwich shells.

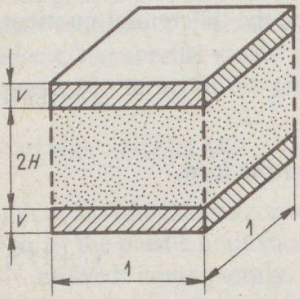


Fig. 7–26

When no restrictions are prescribed for the thickness v then each element of the plate is fully utilized and according to the Tresca yield condition (7—15) the equation

$$f(M_i) = \frac{1}{2}(|M_I| + |M_{II}| + |M_I - M_{II}|) = M_0 \tag{7—118}$$

is satisfied. Here $M_0 = 2Hv\sigma_0$ designates the plastic moment per unit length. Making use of eq. (7—118) the specific weight function can be expressed in terms of the moments as follows

$$w = 2v = \frac{M_0}{H\sigma_0} = kf(M_i) = \frac{k}{2}(|M_I| + |M_{II}| + |M_I - M_{II}|) \tag{7—119}$$

where

$$k = \frac{\partial w}{\partial M_0} = \frac{1}{H\sigma_0}. \tag{7—120}$$

In the coordinate system M_I, M_{II}, for a particular value of w (say $w = 1$) the specific weight function is represented by a hexagon, as shown in Fig. 7—27(a).

In order to obtain the minimum weight solution we consider a non-linearly elastic plate, the complementary energy per unit area of which is identical to the specific weight function (7—119). Then, according to eqs (7—111) and (7—117) the curvature vector $\kappa_i[\kappa_I\ \kappa_{II}]$ is obtained as the gradient of the specific weight function. Hence, the

* In the optimization procedure the constant weight of the core can be disregarded.

vector is normal to the hexagon shown in Fig. 7—27(a) and its length is defined by the constant k.

The locus of all weight gradient vectors κ_i defines a weight gradient surface which is also a hexagon, as is shown in Fig. 7—27(b). The edges of this hexagon correspond to the corners of the hexagon of the specific weight function and vice versa, and the exterior normals define the moment vector $M_i[M_I\ M_{II}]$.

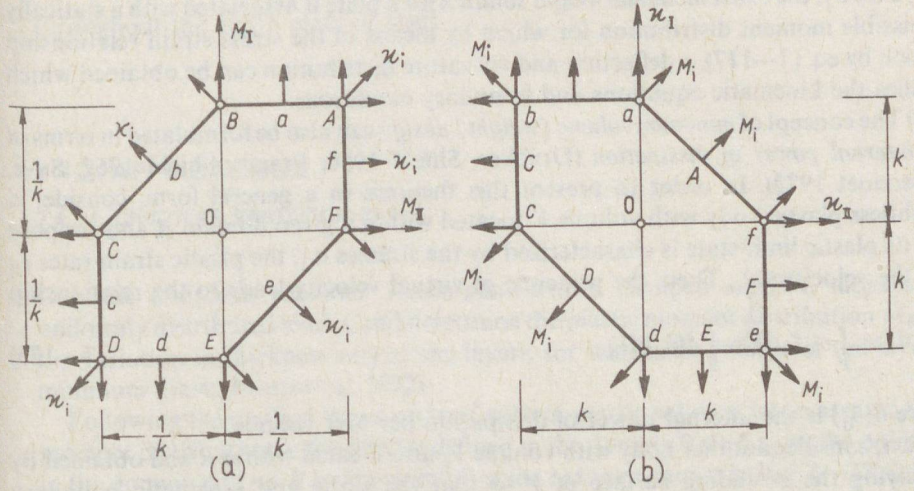


Fig. 7–27

On the basis of the above results the following theorems can be established (Melchers, Rozvany 1970; Rozvany, Adidam 1971, 1972; Prager 1974; Rozvany 1976).

(a) The weight W^s of a plate obtained by the use of any arbitrary *statically admissible moment distribution* M_i^s is an *upper bound* for the minimum weight of the plate

$$W^s = \int_S \bar{w}(M_i^s)\mathrm{d}S \geq W^{\min}. \tag{7—121}$$

(b) The weight W^k of a plate obtained by any arbitrary *kinematically admissible deflection and curvature distribution* u_i^k, κ_i^k is a *lower bound* for the minimum weight of the plate

$$W^k \leq W^{\min}. \tag{7—122}$$

A deflection and curvature distribution is considered kinematically admissible if the curvatures κ_i^k represent points on or inside the hexagon of the weight gradient illustrated in Fig. 7—27(b), and the deflections u_i^k satisfy the kinematic equations and boundary conditions. To obtain the corresponding weight W^k, one can make use of eqs (7—117) and (7—119) and the fact that the yield condition is linear. Then we obtain

$$W^k = \int_S \bar{w}(M_i^k)\mathrm{d}S = \int_S k f(M_i^k)\mathrm{d}S = \int_S k \frac{\partial f}{\partial M_i^k} M_i^k \mathrm{d}S = \int_S M_i^k \kappa_i^k \mathrm{d}S. \tag{7—123}$$

Here the last integral denotes the internal work which according to the principle of virtual displacements is equal to the work done by the external loads. Hence, relationship (7—122) becomes

$$W^{k} = \int_{S} p_i u_i^{k} \mathrm{d}S \leq W^{\min}. \tag{7—124}$$

(c) Finally, the *exact minimum weight solution* for a plate is associated with a statically admissible moment distribution for which by means of the stress-strain relationship defined by eq. (7—117), a deflection and curvature distribution can be obtained which satisfies the kinematic equations and boundary conditions.

(3) The concept of *minimum volume (weight) design* can also be formulated in terms of the *internal power of dissipation* (Drucker, Shield 1956; Prager, Shield 1967; Save, Massonnet 1972). In order to present this theorem in a general form, consider a weightless plastic body with volume V located within a given domain R and suppose that its plastic limit state is characterized by the stresses σ_{ij}, the plastic strain rates $\dot{\varepsilon}_{ij}$ and the velocities $\dot{u}_i$. Then, the principle of virtual velocity leads to the relationship

$$\int_{S} p_i \dot{u}_i \mathrm{d}S = \int_{V} \sigma_{ij} \dot{\varepsilon}_{ij} \mathrm{d}V = \int_{V} d(\dot{\varepsilon}_{ij}) \mathrm{d}V, \tag{7—125}$$

where $d(\dot{\varepsilon}_{ij})$ is the internal power of dissipation per unit volume.

Next, consider another body with volume V_1 also located within R and obtained by modifying the bounding surface of V so that the static and kinematic boundary conditions remain unchanged. Imagine, moreover, that the field $\dot{\varepsilon}_{ij}$ can be extended in a kinematically admissible manner throughout the entire domain R. If the second body does not collapse under a load smaller than p_i, then one can write the relationship

$$\int_{S} p_i \dot{u}_i \mathrm{d}S \leq \int_{V_1} \mathrm{d}(\dot{\varepsilon}_{ij}) \mathrm{d}V. \tag{7—126}$$

Comparison of relationships (7—125) and (7—126) furnishes

$$\int_{V} \mathrm{d}(\dot{\varepsilon}_{ij}) \mathrm{d}V \leq \int_{V_1} \mathrm{d}(\dot{\varepsilon}_{ij}) \mathrm{d}V. \tag{7—127}$$

To obtain an inequality relating the volumes instead of the dissipation, it is sufficient that the rate of dissipation per unit volume should be a constant throughout R, i.e.

$$\mathrm{d}(\dot{\varepsilon}_{ij}) = \alpha = \text{constant in } R. \tag{7—128}$$

If this condition is satisfied, eq. (7—127) gives

$$\alpha \int_{V} \mathrm{d}V \leq \alpha \int_{V_1} \mathrm{d}V, \tag{7—129}$$

indicating that V is an absolute minimum.

Hence, we can state that *the minimum volume solution for a plastic body is defined by a kinematically admissible strain rate and velocity field at which the rate of dissipation per unit volume is a constant throughout the entire body.*

In the case of *sandwich plates or shells* with variable thickness $v(x_i)$ of the layers, the rate of dissipation per unit volume is equal to $\frac{d(\dot{q}_i)}{v}$. Thus, in the case of the minimum volume solution

$$\frac{d(\dot{q}_i)}{v} = \alpha = \text{constant} \tag{7—130}$$

throughout the entire plate or shell.

7.4.2. APPLICATIONS

7.4.2.1. CIRCULAR SANDWICH PLATE

Consider a circular *sandwich Tresca-plate* with a clamped support, subjected to a uniformly distributed load p, and determine the plastic moment distribution $M_0(r)$ and the variation in thickness $v(r)$ of the layers, for which the volume of the layers is a minimum (Save, Massonnet 1972).

Following the method based on the fictitious elastic solution let us assume that the moment distribution in the plate is defined in the domain $0 \le r \le r_0$ by the point A and in the domain $r_0 \le r \le R$ by the point C of the hexagon shown in Fig. 7—27(a). Here R denotes the radius of the plate and r_0 is an unknown radius, to be determined later. The moment distribution in this plate becomes

$$\left.\begin{aligned} &\text{if} \quad 0 \le r \le r_0: \\ &M_r = M_\phi = M_0 \\ &\text{if} \quad r_0 \le r \le R: \\ &M_r = -M_0, \quad M_\phi = 0. \end{aligned}\right\} \tag{7—131}$$

Considering Fig. 7—27(b), the corresponding curvatures of the fictitious elastic plate are as follows

$$\left.\begin{aligned} &\text{if} \quad 0 \le r \le r_0: \\ &\kappa_r + \kappa_\phi = k, \\ &\text{if} \quad r_0 \le r \le R: \\ &\kappa_r = -k, \quad \kappa_\phi < k. \end{aligned}\right\} \tag{7—132}$$

Then, the kinematic equations

$$\kappa_r = -\frac{d^2w}{dr^2}, \quad \kappa_\phi = -\frac{1}{r}\frac{dw}{dr}$$

of axisymmetric plates (see eq. (7—26)) together with the above relationship lead to the following differential equations and solutions for the deflection of the elastic plate:
if $0 \leq r \leq r_0$:

$$\frac{d^2 w_1}{dr^2} + \frac{1}{r}\frac{dw_1}{dr} = -k$$

$$w_1 = a - \frac{1}{4} kr^2 + \frac{1}{2} kb^2 \ln \frac{b}{r},$$

if $r_0 \leq r \leq R$:

$$\frac{d^2 w_2}{dr^2} = k,$$

$$w_2 = \frac{1}{2} kr(r - 2c) + d.$$

Since at $r = 0$ the deflection cannot be infinite, the constant b must be zero in the expression for w_1.

In addition, at the clamped support $r = R$ the boundary conditions $w_2 = \frac{dw_2}{dr} = 0$ have to be satisfied, and at $r = r_0$ the continuity condition leads to the relationships $w_1 = w_2$ and $\frac{dw_1}{dr} = \frac{dw_2}{dr}$. These conditions allow the determination of the constants a, c, d and r_0. This latter is equal to $\frac{2}{3} R$. Then, the deflection of the fictitious elastic plate can be determined

$$\left.\begin{aligned} &\text{if } 0 \leq r \leq \frac{2}{3} R: \\ &w_1 = \frac{k}{12}(2R^2 - 3r^2), \\ &\text{if } \frac{2}{3} R \leq r \leq R: \\ &w_2 = \frac{k}{2}(r - R)^2. \end{aligned}\right\} \qquad (7—133)$$

Finally, substituting eq. (7—131) into the equilibrium equation

$$\frac{d^2}{dr^2}(r M_r) - \frac{M_\phi}{dr} + pr = 0$$

we obtain the differential equations

if $0 \leq r \leq \frac{2}{3}R$:

$$r\frac{d^2M_0}{dr^2} + \frac{dM_0}{dr} + pr = 0,$$

if $\frac{2}{3}R \leq r \leq R$:

$$\frac{d}{dr^2}(r\,M_0) - pr = 0.$$

In solving these equations one has to take into account that at $r=0$ the shear force must be equal to zero and at $r=\frac{2}{3}R$ both the shear force and the bending moment must be continuous. The latter condition can only be satisfied if at $r=\frac{2}{3}R$, $M_0=0$. Then, the moment distribution becomes

$$\left.\begin{aligned} &\text{if } 0 \leq r \leq \frac{2}{3}R: \\ &M_0 = \frac{p}{4}\left(\frac{4}{9}R^2 - r^2\right), \\ &\text{if } \frac{2}{3}R \leq r \leq R: \\ &M_0 = \frac{p}{6r}\left(r^3 - \frac{8}{27}R^3\right). \end{aligned}\right\} \qquad (7—134)$$

As can be seen, the deflection and moment distributions given by eqs (7—133) and (7—134) satisfy the equilibrium and kinematic conditions and the moment-curvature relationships, and therefore they provide the complete solution of the fictitious elastic plate and, at the same time, the minimum volume solution for the real sandwich plate.

From the optimal plastic moment distribution the variation in the thickness of the layers can easily be obtained

$$v = \frac{M_0}{2H\sigma_0}.$$

This function is represented in Fig. 7—28(a). The total volume of the layers is equal to

$$V^{\min} = 0.117\frac{\pi p R^4}{\sigma_0 H}.$$

The solution of the same sandwich plate with *constant thickness* of layers needs a volume

$$V=0.178\frac{\pi pR^4}{\sigma_0 H}.$$

Hence the saving is 34%, which can be obtained by allowing the thickness to vary and applying the optimal design method.

Finally, Fig. 7—28(b) illustrates the variation in the thickness of a *solid plate* determined by minimum weight design.

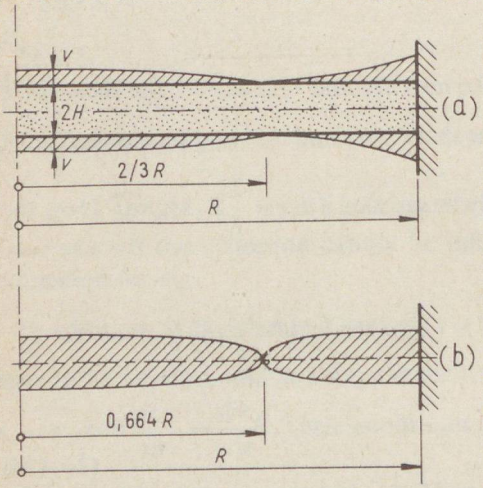


Fig. 7–28

7.4.2.2. REINFORCED CONCRETE PLATES

In Section 6.6.2.4 it was shown that the minimum weight design of reinforced concrete beams and frames can be reduced to a special elastic solution by the use of a quadratic weight function. Generalizing this idea, let us assume that the weight of reinforcement per unit area of reinforced concrete plates is expressed in the form

$$w=w_0+B(M_{\mathrm{I}}^2+M_{\mathrm{II}}^2). \tag{7—135}$$

Here M_{I} and M_{II} denote the principal moments, w_0 is the minimum amount of reinforcement to be applied per unit area and B is a constant. Using this weight function for plates with constant thickness, the condition for minimum weight of the total reinforcement becomes

$$W=W_0+B\int(M_{\mathrm{I}}^2=M_{\mathrm{II}}^2)\mathrm{d}S=\min! \tag{7—136}$$

where W_0 denotes a constant.

In addition to this minimum condition, the moments M_{I} and M_{II} have to satisfy the equilibrium equations and static boundary conditions, and hence the solution leads to a problem in the calculus of variations, with side constraints.

To reduce this problem to a special elastic solution, let us consider a homogeneous, isotropic, *linearly elastic plate* with zero Poisson's ratio and constant thickness, subjected to the same loading and boundary conditions as the actual plate. According to the principle of minimum elastic strain energy, the solution to this problem is defined by the condition

$$\frac{1}{EI}\int (M_{\mathrm{I}}^2 + M_{\mathrm{II}}^2)\mathrm{d}S = \min! \tag{7—137}$$

where the moments M_{I} and M_{II} must also be statically admissible. Comparing eqs (7—136) and (7—137) and the corresponding side constraints, it is obvious that the minimum weight solution and the special elastic solution are identical. Hence, *the optimal solution of a reinforced concrete plate with constant thickness, which leads to the minimum weight of reinforcement, is identical to the solution for a homogeneous, isotropic linearly elastic plate with zero Poisson's ratio and constant thickness, provided that this elastic plate has the same loading and boundary conditions as the actual one* (Kaliszky 1965a, 1968a).

7.4.2.3. AXISYMMETRIC REINFORCED CONCRETE SHELLS

The concept of optimum design of reinforced concrete plates can be generalized for axisymmetric reinforced concrete shells with constant thickness (Kaliszky 1965a, 1965c, 1968a). Our further discussions will be restricted to problems where the loading and boundary conditions are also axisymmetrical and no compressive forces arise in the sections of the shell. Then, the weight of reinforcement per unit area can be approximated by the quadratic formula

$$w = w_0 + B(M_r^2 + M_\varphi^2) + C(N_r^2 + N_\varphi^2), \quad N_r \geq 0, \quad N_\varphi \geq 0, \tag{7—138}$$

and the minimum of the weight of the total reinforcement is expressed as

$$W = W_0 + \int [B(M_r^2 + M_\varphi^2) + C(N_r^2 + N_\varphi^2)]\mathrm{d}S = \min! \tag{7—139}$$

In addition, the moments M_r, M_φ and the axial forces N_r, N_φ must be statically admissible. This requirement together with the above minimum condition, uniquely defines the optimal solution to the problem under consideration.

It can be seen that the function in eq. (7—139) is identical to the expression for the strain energy of a homogeneous, linearly elastic axisymmetric shell with constant flexural and tensile stiffness $EI = \frac{1}{B}$ and $EA = \frac{1}{C}$, respectively and with zero Poisson's ratio. Hence, considering the principle of minimum strain energy, the solutions for these special elastic structures provide the minimum weight solutions for reinforced concrete shells.

To illustrate the application of the above theorem let us consider a cylindrical shell with constant thickness $2H$, a free edge at the top and clamped edge at the bottom, which is subjected to a linearly variable internal pressure (Fig. 7—29).

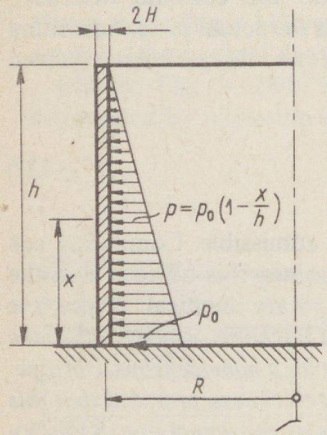


Fig. 7–29

First, we determine the solution for *the linear elastic shell* with constant flexural and axial stiffness EI and EA respectively and zero Poisson's ratio. The internal stresses of this shell have to satisfy

(a) the *equilibrium equations*

$$\left.\begin{aligned}\frac{dQ_x}{dx}+\frac{N_\varphi}{R}&=p_0\left(1-\frac{x}{h}\right),\\ \frac{dM_x}{dx}-Q_x&=0,\end{aligned}\right\} \tag{7—140}$$

which can be expressed on eliminating the shear force Q_x, by a single equation

$$\frac{d^2M_x}{dx^2}+\frac{N_\varphi}{R}=p_0\left(1-\frac{x}{h}\right); \tag{7—141}$$

(b) the *static boundary conditions*

$$Q_x(h)=M_x(h)=0; \tag{7—142}$$

(c) and the condition of *minimum strain energy*

$$2\pi R\int_0^h\left(\frac{M_x^2}{EI}+\frac{N_\varphi^2}{EA}\right)dx=\min! \tag{7—143}$$

This variational problem leads to the differential equation (Timoshenko, Woinowsky-Krieger 1940)

$$\frac{d^4 M_x}{dx^4} + 4\lambda_e^4 M_x = 0, \tag{7—144}$$

where

$$\lambda_e = \sqrt[4]{\frac{EA}{4R^2 EI}} = \frac{1.31}{\sqrt{2RH}} \tag{7—145}$$

is the *elastic damping factor.*

The solution to this differential equation results in

$$\left.\begin{aligned} M_x &= M_{x0}\eta + \frac{Q_{x0}}{\lambda_e}\xi, \\ Q_x &= Q_{x0}\psi - 2\lambda_e M_{x0}\xi, \\ N_\phi &= Rp_0\left(1 - \frac{x}{h}\right) + 2R\lambda_e^2\left(M_{x0} + \frac{Q_{x0}}{\lambda_e}\theta\right), \\ M_\phi &= 0. \end{aligned}\right\} \tag{7—146}$$

Here

$$Q_{x0} = \frac{p_0}{\lambda_e}\left(1 - \frac{1}{2\lambda_e h}\right) \quad \text{and} \quad M_{x0} = \frac{p_0}{2\lambda_e^2}\left(1 - \frac{1}{\lambda_e h}\right), \tag{7—147}$$

respectively, denote the shear force and moment along the bottom edge of the shell, and the functions η, ψ, θ and ξ are as follows

$$\left.\begin{aligned} \eta &= e^{-\lambda_e x}(\cos\lambda_e x + \sin\lambda_e x), \\ \psi &= e^{-\lambda_e x}(\cos\lambda_e x - \sin\lambda_e x), \\ \theta &= e^{-\lambda_e x}\cos\lambda_e x, \\ \xi &= e^{-\lambda_e x}\sin\lambda_e x. \end{aligned}\right\} \tag{7—148}$$

In order to obtain the *minimum weight solution*, the flexural stiffness EI and tensile stiffness EA of the elastic shell have to be replaced by the constants $\frac{1}{B}$ and $\frac{1}{C}$, respectively. That means that instead of the elastic damping factor (7—145) the *"optimal" damping factor*

$$\lambda_0 = \sqrt[4]{\frac{B}{4R^2 C}} = \frac{\alpha}{\sqrt{2RH}} \tag{7—149}$$

has to be used, but otherwise all the results presented above remain unchanged and provide the optimal internal stress distribution in the reinforced concrete shell. The constant α in eq. (7—149) depends on the constants B and C, and in practical cases its value varies between 0.60 and 0.9. It means that $\lambda_0 < \lambda_e$ and, therefore in the optimal

solution there is less damping of the moments in the vicinity of the bottom edge of the shell than in the elastic solution. Hence, in the optimal solution a larger portion of the load is carried by the moments and shear forces than by the circumferential axial forces.

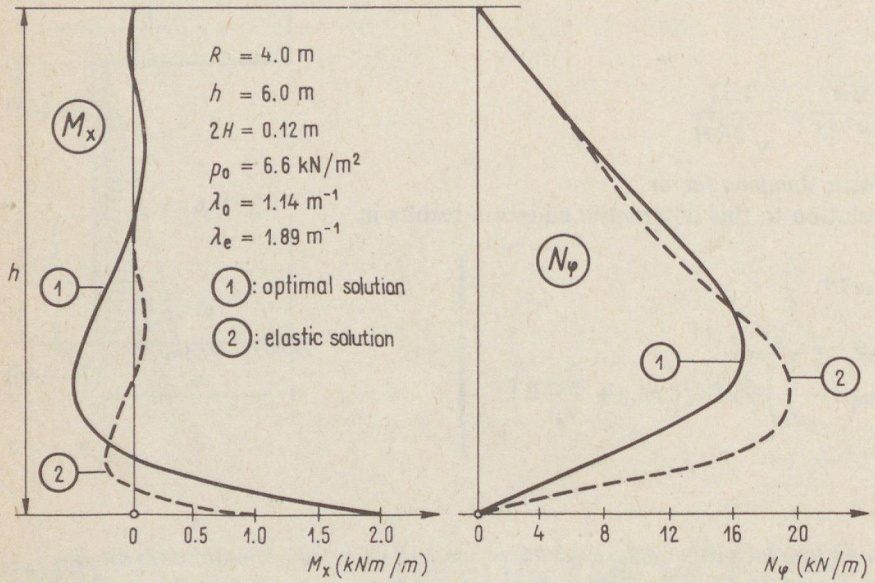


Fig. 7–30

Figure 7—30 shows the numerical data and the moment and axial force distributions for a reinforced concrete cylindrical shell. As can be seen, the difference between the elastic and optimal solutions is significant. The savings in reinforcement which can be obtained by the application of the optimal design method is about 17%.

8. VARIOUS INELASTIC MATERIAL PROPERTIES

In the first part of this chapter the general phenomena of plastic hardening are discussed, and the subsequent yield conditions and the flow rule of isotropic and kinematic hardening materials are presented. Next, the mechanical behaviour of granular materials with and without cohesion are described and the Coulomb, the generalized Huber–v. Mises–Hencky, the generalized Tresca and the Stassi D'Alia yield contitions are presented.

In the last part of the chapter the viscous properties of materials are treated, and various material models and constitutive equations of visco-elastic and visco-plastic materials are briefly described.

8.1. INTRODUCTORY REMARKS

The linearly elastic–perfectly plastic model used in the previous chapters is based on the assumption that the material behaviour is path-, time- and temperature-independent and that the strength is the same in tension and in compression. In many cases these simplifications lead to acceptable results, actual material properties are, however, much more complex and there are several other inelastic phenomena which can play an important role for certain kinds of materials and in the solutions to certain mechanical problems.

During plastic deformation the structure of the material changes, which may increase its plastic resistance. The behaviour of these *plastic hardening materials* depends not only on the instantaneous state of stress but also on the previous plastic deformation process; thus, the plastic hardening materials are *path-dependent*.

There are several materials in which deformations take place under constant state of stress (creep) and the stresses change under a constant state of deformation (relaxation). In addition, the behaviour of these materials depends on the rate of deformations. This *time-dependent* phenomenon is called *viscosity*.

Most materials are *temperature-dependent*, i.e. their behaviour and strength are influenced by the change of temperature. For some materials (e.q. plastics) already a smaller change in temperature can have a significant effect on the material behaviour, in general, however, only large temperature variations result in any considerable change in the material properties.

The strength of *granular materials* (e.g. stone, concrete, soil) is much less in tension than in compression. This phenomenon significantly changes the yield conditions used in the previous chapters, and has an important influence on the solution to problems.

Next, the various inelastic material properties described above will be briefly presented. Our discussion will be restricted only to the yield conditions and constitutive equations and only a few applications will be presented.

8.2. PLASTIC HARDENING MATERIALS

8.2.1. FUNDAMENTAL RELATIONSHIPS

The main feature of *perfectly plastic materials* is that in a uniaxial state of stress they undergo plastic deformations under *constant* stress and their yield does not depend on the previous states of stress and strain, i.e. they are *path-independent.*

The *plastic hardening materials* in a uniaxial state of stress perform plastic deformations only upon *increasing* the stress level and the yield condition for plastic deformations changes during the loading process. It depends on the previous states of stress and strain, i.e. the plastic hardening materials are *path-dependent.*

The elastic behaviour of plastic hardening material does not differ from that of perfectly plastic materials. It is also assumed that the yield condition which defines the *first plastic deformations* has the same form $f(\sigma_{ij}, k)=0$, as was discussed in connection with perfectly plastic bodies. In the case of perfectly plastic materials, the yield function $f(\sigma_{ij}, k)$ entirely defines the further plastic deformations at a point. The *subsequent* plastic behaviour of a plastic hardening material is, however, characterized by another function, called the *hardening function*, expressed in a general form

$$g(\sigma_{ij}, \varepsilon_{ij}^{p}, W^{p}, k).$$

Here ε_{ij}^{p} and W^{p} denote the previous plastic deformations and plastic work, respectively at the point under consideration. At a point where no plastic deformations have previously occurred the relationship

$$g(\sigma_{ij}, 0, 0, k)=f(\sigma_{ij}, k)$$

has to be satisfied. The condition

$$g(\sigma_{ij}, \varepsilon_{ij}^{p}, W^{p}, k)=0 \qquad (8—1)$$

defines the *subsequent yield conditions* for plastic hardening materials and, at the same time, forms the basis for the construction of the constitutive equations. In the stress space σ_{ij}, the relationships given by eq. (8—1) are illustrated by *hypersurfaces*, as shown symbolically in Fig. 8—1. According to Drucker's postulate, the plastic hardening materials are *stable* materials, consequently eq. (8—1) is represented by *convex* hypersurfaces (Drucker 1952a).

Let us assume that in the stress space σ_{ij} the loading path of a point in a body is illustrated by the line *O-A-B*. Reaching the yield surface $f=0$ the material point under consideration starts to yield but, in contrast to perfectly plastic materials, the stress intensity can be further increased. The point *B* on the hypersurface $g(\sigma_{ij}, \varepsilon_{ij}^{p}, W^{p}, k)=0$

represents a subsequent plastic state. Now, let us assume that the state of stress is changed by $d\sigma_{ij}$, resulting in a change in the hardening function

$$dg = \frac{\partial g}{\partial \sigma_{ij}} d\sigma_{ij} + \frac{\partial g}{\partial \varepsilon_{ij}^{p}} d\varepsilon_{ij}^{p} + \frac{\partial g}{\partial W^{p}} dW^{p}. \tag{8—2}$$

Depending on the value of this total differential three different cases can be distinguished.

(a) *Active loading* ($dg > 0$). If the increment vector $d\sigma_{ij}$ points outward the domain bounded by the surface $g = 0$, plastic deformations can occur i.e. $d\varepsilon_{ij}^{p} \geq 0$ and $dW^{p} \geq 0$.

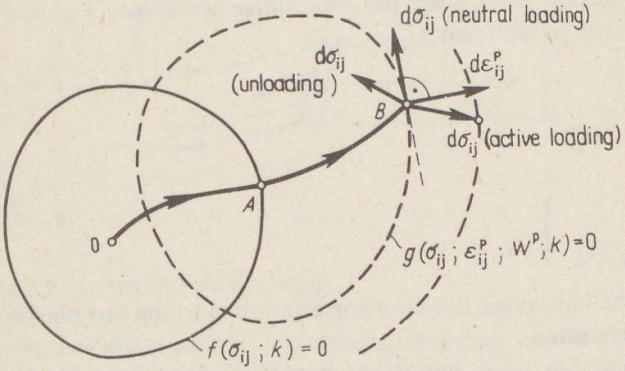


Fig. 8–1

Since $\frac{\partial g}{\partial \sigma_{ij}}$ represents the outer normal to the surface $g = 0$, in this case

$$\frac{\partial \sigma}{\partial \sigma_{ij}} d\sigma_{ij} > 0$$

and consequently, $dg > 0$.

It follows from Drucker's postulate that the plastic strain increment vector $d\varepsilon_{ij}^{p}$ is normal to the surface $g = 0$, i.e. the *hardening function is a potential function of the plastic strain increments*. Hence, the *flow rule* of plastic hardening materials has the form

$$d\varepsilon_{ij}^{p} = d\lambda \frac{\partial g}{\partial \sigma_{ij}}. \tag{8—3}$$

(b) *Neutral loading*. If the increment vector $d\sigma_{ij}$ lies on the surface $g = 0$ then

$$\frac{\partial g}{\partial \sigma_{ij}} d\sigma_{ij} = 0.$$

In this case, no plastic deformations occur, hence $d\varepsilon_{ij}^{p} = dW^{p} = 0$ and consequently, $dg = 0$.

(c) *Unloading.* If the increment vector $d\sigma_{ij}$ points inward the domain bounded by the surface $g=0$, then

$$\frac{\partial g}{\partial \sigma_{ij}} d\sigma_{ij} < 0.$$

In this case no plastic deformations occur, hence $d\varepsilon_{ij}^{p} = dW^{p} = 0$ and consequently, $dg < 0$.

In all the cases described above, the *elastic* strain increments are defined by Hooke's law

$$d\varepsilon_{ij}^{e} = H_{ijkl} d\sigma_{kl}.$$

Making use of the relationship $d\varepsilon_{ij} = d\varepsilon_{ij}^{e} + d\varepsilon_{ij}^{p}$ the *constitutive equations for plastic hardening materials* are expressed in the form

$$d\varepsilon_{kl} = H_{ijkl} d\sigma_{kl} + d\lambda \frac{\partial g}{\partial \sigma_{ij}},$$

where

$$\left.\begin{aligned} &d\lambda \geq 0, \text{ if } g=0 \text{ and } dg>0; \\ &d\lambda = 0, \text{ if } g<0 \text{ or } g=0 \text{ and } dg \leq 0; \end{aligned}\right\} \qquad (8—4)$$

and $g(\sigma_{ij}, \varepsilon_{ij}^{p}, W^{p}, k)$ denotes the hardening function corresponding to the *last* plastic state at the point under consideration.

Next, we will briefly discuss the most important hardening theories and the corresponding hardening functions.

8.2.2. PLASTIC HARDENING THEORIES

8.2.2.1. UNIAXIAL STATE OF STRESS

Before a general discussion of the theories of plastic hardening, it is useful to consider the case of uniaxial state of stress. Fig. 8—2 shows the idealized stress-strain diagrams for different plastic hardening materials. The only difference between the diagrams is due to the stress at which, in the case of reverse loading, the material starts to yield. Three cases can be distinguished.

(a) In the case of *isotropic hardening* (line *OABEH*) if the tensile stress reaches the value σ_1 during plastic deformations, then on reverse loading the material starts to yield at the same magnitude of the compressive stress, i.e. at $\sigma = -\sigma_1$. Hence, as a consequence of plastic deformations, the elastic range of the material increases by the same amount in tension and in compression.

(b) In case of *kinematic hardening* (line *OABCF*) if the tensile stress reaches the value σ_1 during plastic deformations, then on reverse loading the material starts to yield at a compressive stress $\sigma_1' = \sigma_1 - 2\sigma_0$. This means that the plastic deformations do not change the elastic range of the material (equal to $2\sigma_0$) but cause a change in the magnitude of the yield stresses in tension and compression.

(c) A general case can be obtained by the combination of isotropic and kinematic hardening. This is represented by the line *OABIK*.

Next, we will discuss the above cases for three-dimensional state of stress.

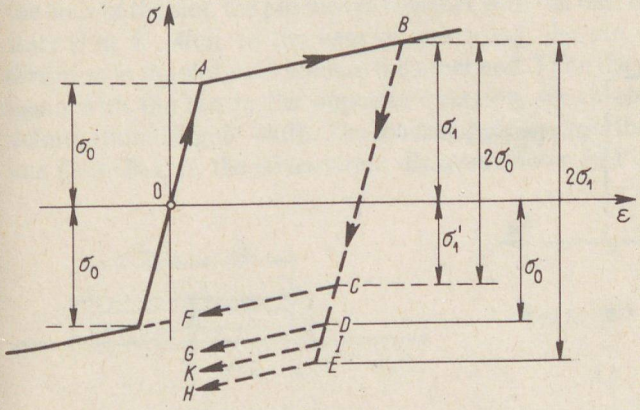


Fig. 8–2

8.2.2.2. ISOTROPIC HARDENING

In the case of isotropic hardening, two cases can be distinguished depending on the form of the hardening function.

(a) In the case of *isotropic work hardening* the hardening function has the form

$$g(\sigma_{ij}, W^p, k)=f(\sigma_{ij}, k)-W^p, \tag{8—5}$$

where

$$W^p=\int \sigma_{ij}d\varepsilon^p_{ij}$$

is the *plastic work* done during the previous plastic deformations. For each value of W^p, we have a geometrically similar, centrally located surface defined by the equation

$$f(\sigma_{ij}, k)-W^p=0.$$

The sizes of these surfaces increase monotonically with W^p, as it is illustrated for the Tresca yield condition and for plane stress in Fig. 8—3.

(b) In the case of *isotropic strain hardening*, the hardening function has the form

$$g(\sigma_{ij}, \varepsilon^p_{ij}, k)=f(\sigma_{ij}, k)-\varepsilon_p, \tag{8—6}$$

where

$$\varepsilon_p=f(I_p)$$

is a monotonically increasing function and

$$I_p=\int \sqrt{d\varepsilon^p_{ij}d\varepsilon^p_{ij}}\,dt$$

denotes the length of the trajectory of plastic deformations.

Since in the hardening functions (8—5) and (8—6) only the monotonically increasing scalar functions W^p and ε_p are different the geometrical representation of strain hardening materials is the same as it has been described for work hardening materials.

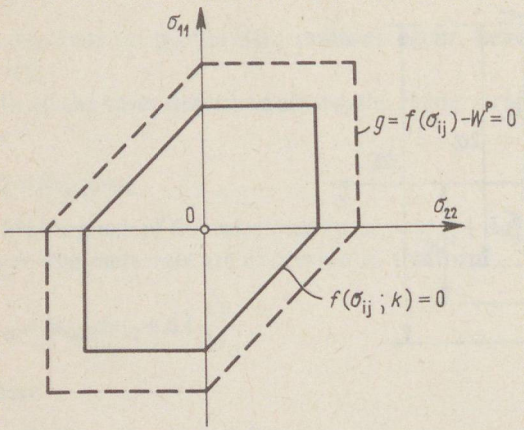


Fig. 8–3

8.2.2.3. KINEMATIC HARDENING

In the case of kinematic hardening the hardening function has the form

$$g=f[(\sigma_{ij}-\alpha_{ij}), k] \tag{8—7}$$

where

$$\alpha_{ij}=c\int d\varepsilon_{ij}^p$$

and c is a constant.

For each α_{ij} vector the equation

$$f[(\sigma_{ij}-\alpha_{ij}), k]=0$$

represents geometrically identical surfaces the centres of which are, however, different and defined by the vector α_{ij}. Hence, the subsequent surfaces are obtained by the simple translation of the initial yield surface $f(\sigma_{ij}, k)=0$.

Kinematic hardening can be represented by simple *kinematic models*, to be described below.

Fig. 8—4(a) illustrates a model of rigid–kinematic hardening plastic materials under uniaxial stress (Prager 1959; Onat 1966). The slotted bar slides freely on a frictionless surface and the pin P slides without friction in the slot. The bar, the surface and the pin each carry a vertical mark. The displacement of the pin's mark P with respect to the surface's mark O represents the stress σ, and the displacement of the bar's mark I with

respect to the surface's mark 0 represents the strain ε. The length of the slot is equal to twice the yield stress σ_0.

Until the pin does not reach either end of the slot the bar does not move on the surface, and consequently the strain is equal to zero (Fig. 8—4(b)). On reaching one of the ends of the slot, the pin moves together with the bar; this corresponds to the plastic state (Fig. 8—4(c)). In the case of unloading, the pin slides freely in the opposite direction in the slot until reaches the other end. Then the pin and the bar start to move again with the pin in the opposite direction, which corresponds to reverse plastic deformations (Fig. 8—4(d)). The loading process described above is illustrated by the line *O–A–B–C* in the stress-strain diagram shown in Fig. 8—4(e).

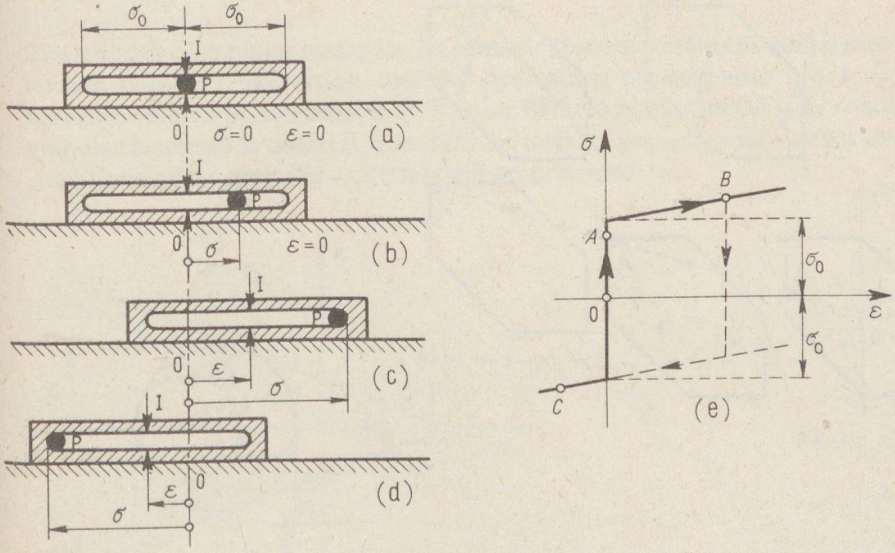


Fig. 8–4

For a *biaxial state of stress*, the kinematic model may be generalized as follows. A rigid frame is mounted so that it can perform any translation in its plane without rotation. The shape of the frame is identical to the shape of the curve of the yield condition for a biaxial state of stress. For example, in the case of the Tresca yield condition the frame is a hexagon, as illustrated in Fig. 8—5. The perfectly smooth pin *P*, free to move inside the frame, imparts a motion to the frame only when it pushes against a side or engages with a corner.

Initially, the centre *P* of the pin and the centre *I* of the frame coincide with the origin *O* of the coordinate system σ_{I}, σ_{II}. Then the pin is moved according to a given loading process, and at any instant the vector defined by the origin *O* and the centre of the pin represents the stresses.

When the pin pushes against a side of the frame, the frame will move in the direction of the external normal of the frame at the point of contact. When the pin engages with a

corner the frame will move in a direction which lies between the external normals to the sides at the vertex under consideration. Considering the normality rule, it is evident that the increment vector defined by the incremental movement of the centre of the frame represents the plastic strain increments.

In Fig. 8—5 a loading process is illustrated by the line $P_1 \ldots P_8$ and the corresponding motion of the frame is also shown.

It is obvious that by replacing the frame by a "box" with the shape of the yield surface, and the pin by a sphere, the kinematic model can be generalized to a triaxial state of stress, as well.

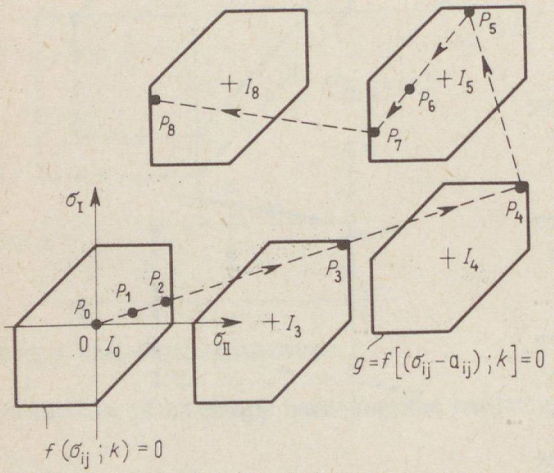


Fig. 8–5

8.2.2.4. GENERALIZED HARDENING RULES

By the combination of isotropic and kinematic hardenings a generalized hardening function

$$g=f[(\sigma_{ij}-\alpha_{ij}),\ k]-W^p \qquad (8—8)$$

can be introduced, where W^p and α_{ij} have already been defined in connection with eqs (8—5) and (8—7). In this case during plastic deformations the surface $g=0$ undergoes a uniform expansion and translation.

In the literature, several other hardening rules have been published the description of which is beyond the scope of this book (e.g. Hill 1950; Hoffman, Sachs 1953; Johnson, Mellor 1962; Mendelson 1968; Kachanov 1971; Zyczkowski 1981).

8.3. GRANULAR MATERIALS

In this section the most important properties and some problems of granular materials will be briefly presented. First, several yield conditions and the problems of the constitutive equations will be discussed and then the plane strain problem will be briefly described. More details of theory and solutions for granular materials can be found in the literature (e.g. Terzaghi 1943; Sokolowski 1950; Kézdi 1962, 1964; Nádai 1963; Chen, Drucker 1969; Gudehus 1972; Chen, 1975; Salenčon 1977; Z. P. Bažant 1985, Cristescu 1985).

8.3.1. YIELD CONDITIONS

The strength of granular materials (for example stone, concrete and soil) is much less in tension than in compression, and the hydrostatic pressure also has a significant influence on their plastic behaviour. Because of these properties the yield condition for granular materials is different from that for metals. Next, the most widely used yield conditions of the granular materials will be presented.

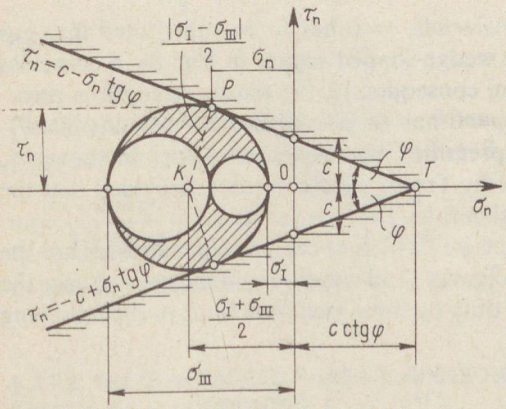


Fig. 8–6

8.3.1.1. COULOMB YIELD CONDITION

Coulomb (1773) assumed that at a point of a granular solid plastic flow occurs when on any section the shear stress τ_n and the normal stress σ_n satisfy the relationship

$$|\tau_n| = c - \mu\sigma_n. \tag{8—9}$$

Here $\mu = \tan\varphi$ is the *coefficient of internal friction*, φ and c denote the *angle of internal friction* and *cohesion*, respectively, and the tensile normal stress is supposed to be positive.

This *Columb yield condition* is represented in Fig. 8—6 by two straight lines which start from the point ($c \cot\varphi$, 0) and are inclined at angles φ to the σ_n axis. The state of

stress at the point is characterized by the principal stresses σ_I, σ_{II}, σ_{III}, and can be illustrated in the same coordinate system by three Mohr's circles. When the circles lie within the wedge-shaped region, the point is in the elastic range. Plastic flow can occur when the largest of the Mohr's circles touches the two straight lines. In order to express the yield condition (8—9) in terms of the principal stresses, we have to consider the relationship obtained from the triangle KPT of Fig. 8—6

$$\frac{1}{2}(\sigma_I - \sigma_{III}) = \left[-\frac{1}{2}(\sigma_I + \sigma_{III}) + c \cot \varphi \right] \sin \varphi$$

or

$$\frac{1}{2}(\sigma_I - \sigma_{III}) = c \cos \varphi - \frac{1}{2}(\sigma_I + \sigma_{III}) \sin \varphi. \tag{8—10}$$

Hence, the Coulomb yield condition for *granular materials with cohesion* has the form

$$f = \frac{1}{2}(\sigma_I - \sigma_{III}) - c \cos \varphi + \frac{1}{2}(\sigma_I + \sigma_{III}) \sin \varphi = 0. \tag{8—11}$$

In the case of *cohesionless granular materials*, $c = 0$ has to be substituted into eqs (8—9)—(8—11). Then the corner of the wedge-shaped region in Fig. 8—6 coincides with the origin of the coordinate system; consequently, the tensile strength is zero.

In the case of *frictionless materials*, $\varphi = 0$ has to be substituted into eqs (8—9)–(8—11). Then, the yield condition is represented by two parallel lines in the σ_n, τ_n coordinate system, which correspond to the Tresca yield condition provided that the cohesion is equal to the yield stress in shear, i.e. $c = \tau_0$.

In most problems it is not known "a priori" which of the principal stresses are the largest and the smallest; hence, as for the Tresca yield condition, in the general case the Coulomb yield condition can be defined only by three yield functions in the following form

$$\left.\begin{aligned} f_1 &= \frac{1}{2}(\sigma_I - \sigma_{II})^2 - \left[c \cos \varphi - \frac{1}{2}(\sigma_I + \sigma_{II}) \sin \varphi \right]^2 \leq 0, \\ f_2 &= \frac{1}{2}(\sigma_{II} - \sigma_{III})^2 - \left[c \cos \varphi - \frac{1}{2}(\sigma_{II} + \sigma_{III}) \sin \varphi \right]^2 \leq 0, \\ f_3 &= \frac{1}{2}(\sigma_I - \sigma_{III})^2 - \left[c \cos \varphi - \frac{1}{2}(\sigma_I + \sigma_{III}) \sin \varphi \right]^2 \leq 0. \end{aligned}\right\} \tag{8—12}$$

When at least one of the above relationships becomes an equality, plastic flow can occur. In the stress space σ_I, σ_{II}, σ_{III} the yield condition (8—12) is represented by an irregular *hexagonal pyramid* with sides equally inclined to the axes σ_I, σ_{II} and σ_{III}. The distance of its vertex from the origin is $\sqrt{3}\, c \cot \varphi$. Its intersection with the plane $\sigma_I + \sigma_{II} + \sigma_{III} = 0$, together with the corresponding curves of the Huber–v. Mises–

Hencky and Tresca yield conditions, is shown in Fig. 8—7. The distances indicated in this Figure are as follows

$$\overline{OA}=\frac{2\sqrt{6}\cos\varphi}{3+\sin\varphi}c, \quad \overline{OB}=\frac{2\sqrt{6}\cos\varphi}{3-\sin\varphi}c.$$

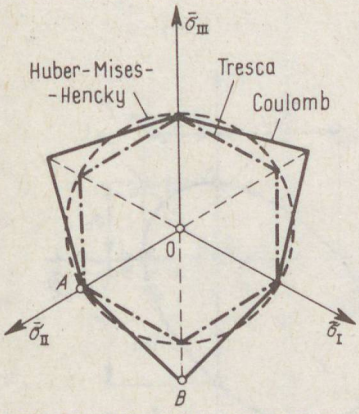


Fig. 8–7

Finally, in the case of *plane stress*, when $\sigma_{III}=0$, the Coulomb yield condition is represented by a hexagon, shown in Fig. 8—8. Here

$$\sigma_0=\frac{2\cos\varphi}{1+\sin\varphi}c \quad \text{and} \quad \sigma_0'=\frac{2\cos\varphi}{1-\sin\varphi}c \tag{8—13}$$

denote the yield stress in pure tension and compression, respectively.

8.3.1.2. THE GENERALIZED HUBER–V. MISES–HENCKY AND TRESCA YIELD CONDITIONS

(a) Drucker and Prager (1952c) proposed the generalization of the Huber–v. Mises–Hencky yield condition for granular materials in the following form

$$f=\alpha\sigma_{oct}+K_2^{1/2}-k=0, \tag{8—14}$$

where K_2 is the second invariant of the stress deviator tensor and α and k denote material constants. If

$$\alpha=\frac{3\tan\varphi}{\sqrt{9+12\tan^2\varphi}} \quad \text{and} \quad k=\frac{3c}{\sqrt{9+12\tan^2\varphi}} \tag{8—15}$$

the yield condition (8—14) reduces to the Coulomb yield condition in the case of *plane strain*. If $\alpha=0$ and $k=\tau_0$, we obtain the Huber–v. Mises–Hencky yield condition for metals.

In the stress space σ_I, σ_{II}, σ_{III}, the generalized Huber–v. Mises–Hencky yield condition is represented by a right *circular cone* with its axis equally inclined to the axes σ_I, σ_{II} and σ_{III}. The distance of its vertex from the origin is $\sqrt{3}\frac{k}{\alpha}$ and its intersection with the plane $\sigma_{III}=0$, which corresponds to the case of *plane stress*, is an ellipse shown in Fig. 8—9.

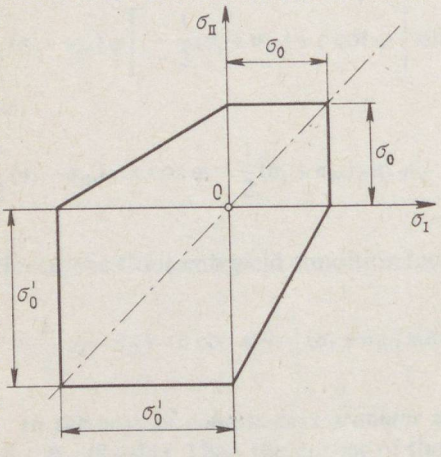


Fig. 8–8

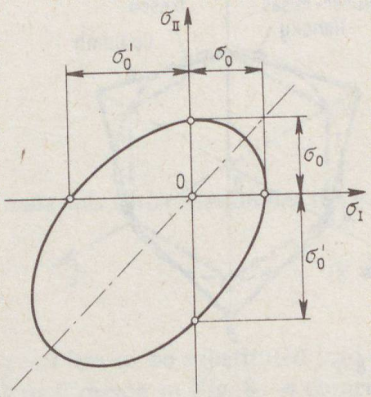


Fig. 8–9

(b) Similarly, Drucker (1953) proposed the generalization of the Tresca yield condition for granular materials. In the stress space σ_I, σ_{II}, σ_{III}, the proposed yield surface is a *right hexagonal pyramid*. In the case of *plane strain*, if its dimensions are properly chosen, this generalized yield condition can also be reduced to the Coulomb yield condition.

8.3.1.3. STASSI D'ALIA YIELD CONDITION

For granular materials Stassi D'Alia (1951, 1957, 1967) proposed the following yield condition

$$f=(\sigma_I^2+\sigma_{II}^2+\sigma_{III}^2)+A(\sigma_I\sigma_{II}+\sigma_{II}\sigma_{III}+\sigma_I\sigma_{III})+ \\ +B(\sigma_I+\sigma_{II}+\sigma_{III})+C=0 \qquad (8—16)$$

or, in terms of the invariants I_1, I_2, I_3 of the stress tensor,

$$(2-A)I_2+BI_1+I_1^2+C=0. \qquad (8—17)$$

Here the constants A, B and C can be expressed in terms of the yield stress σ_0 in pure tension, of the yield stress $\sigma_0'=\rho\sigma_0$ $(\rho\geqq 0)$ in pure compression and of the stress σ_h,

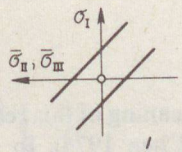
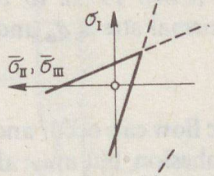
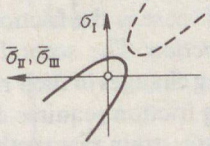
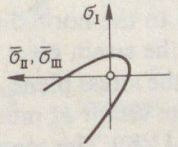
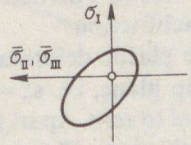
Parameter	Yield surface	Intersection through the axis of the surface
$\frac{\sigma_h}{\sigma_0}=\infty$ $\rho=1$	circular cylinder	
$\frac{\sigma_h}{\sigma_0}=\frac{2}{3}\frac{\rho}{\rho-1}$ $\rho>1$	circular cone	
$\frac{1}{3}\frac{\rho}{\rho-1}<\frac{\sigma_h}{\sigma_0}<\frac{2}{3}\frac{\rho}{\rho-1}$ $\rho>1$	rotational hyperboloid	
$\frac{\sigma_h}{\sigma_0}=\frac{1}{3}\frac{\rho}{\rho-1}$ $\rho>1$	rotational paraboloid	
$\frac{\sigma_h}{\sigma_0}<\frac{1}{3}\frac{\rho}{\rho-1}$ $\rho>1$	rotational ellipsoid	

Fig. 8–10

which causes plastic flow in a hydrostatic state of stress, as follows

$$\left.\begin{aligned} A&=-1-(\rho-1)\frac{\sigma_0}{\sigma_h}+\frac{\rho}{3}\left(\frac{\sigma_0}{\sigma_h}\right)^2,\\ B&=(\rho-1)\sigma_0, \quad C=-\rho\sigma_0^2. \end{aligned}\right\} \tag{8—18}$$

In the stress space the yield condition (8—16) is represented by a *second order surface* which, depending on the values of the material constants, may be a circular cylinder, a cone, a rotational hyperboloid or paraboloid or an ellipsoid, as shown in Fig. 8—10. The ratio $\rho=\frac{\sigma_0'}{\sigma_0}$ has the following values: for metals 1.0, for cast iron 2.5—4.0, for concrete 10—12, for stones 20—30 and in case of loose granular materials infinity.

8.3.2. FLOW RULE

(1) If we assume that the theory of perfectly plastic solids can be applied to granular materials then the plastic strain rates are defined by the *associated flow rule*

$$\dot{\varepsilon}_{ij}^{p} = \dot{\lambda} \frac{\partial f}{\partial \sigma_{ij}}. \tag{8—19}$$

To illustrate the meaning of this relationship let us consider the physical model shown in Fig. 8—11(a) (Chen 1975). In the model, a layer of dense granular material is subjected to a normal stress σ_n and a shear stress τ_n. When the relationship

$$|\tau_n| = c - \mu\sigma_n \tag{8—20}$$

is satisfied, plastic flow can occur and during the deformation the shear stress must not only overcome cohesion, but must also exceed two types of resistance displayed by the particles. One of these is the friction on the contact surfaces between particles and is called *surface friction*. The second is due to the interference between the particles themselves during changes in their relative positions, and is termed *interlocking friction*. This interlocking friction requires displacement normal to the vertical slip plane, and therefore the plastic strain rate vector $\dot{\boldsymbol{e}}_n^p$ has two components; $\dot{\gamma}_n^p$ corresponds to sliding and $\dot{\varepsilon}_n^p$ corresponds to the normal displacement.

Let us illustrate the strain rates $\dot{\varepsilon}_n^p$ and $\dot{\gamma}_n^p$ in a coordinate system coaxial with the coordinate axes of the stress plane σ_n, τ_n. Then, according to the associated flow rule, the plastic strain rate vector $\dot{\boldsymbol{e}}_n^p$ must be normal to one of the limit lines defined by eq. (8—20) (see Fig. 8—11(b)). This means that the angle θ in Fig. 8—11(a) must be equal to the angle of internal friction.

Since during the plastic deformation described above no strain takes place in the direction of the slip plane, i.e. $\varepsilon_n^p = 0$, it is evident that the change in volume of the material is not equal to zero. Apart from this difference, however, all the principles and methods of elasto-plastic and limit analysis can be used for the model shown in Fig. 8—11(a) and 8—11(b).

(2) In contrast to the approach described above, one may idealize the granular materials as *frictional materials* for which the interlocking friction is ignored and deformation occurs only by the smooth sliding of adjacent surfaces of material points. The physical model of a frictional material is a block which can slide on a rough surface when the condition (8—20) is satisfied (see Fig. 8—11(c)). This corresponds to the well known *Coulomb friction law*. Since in this case the block does not move in the normal direction, $\dot{\varepsilon}_n^p = 0$, and, consequently, the plastic strain rate vector $\dot{\boldsymbol{e}}_n^p$ is *not normal* to the corresponding limit line illustrated in the stress and strain rate plane (see Fig. 8—11(d)). Hence, a frictional material belongs to the class of materials which have *non-associated flow rules*. For these materials the limit theorems of plasticity, which are based on the normality rule, are inapplicable. However, there are special conditions for frictional materials to which the limit theorems of plastic bodies fully apply (Mróz 1963; Dais 1970; Chen 1975; Livesley 1978).

(3) The behaviour of real granular materials (stones, concrete, soil, etc.) is partly perfectly plastic and partly frictional in character, and therefore they do not exactly follow either of the two material models described above. Since the theory based on the

associated flow rule is relatively simple and well established, most of the solutions published in the literature in connection with granular materials have been obtained by the assumption of a perfectly plastic material. Still, several other theories have been developed for granular materials which are based on other different assumptions (e.g. Drucker 1951; Weidler, Paslay 1969).

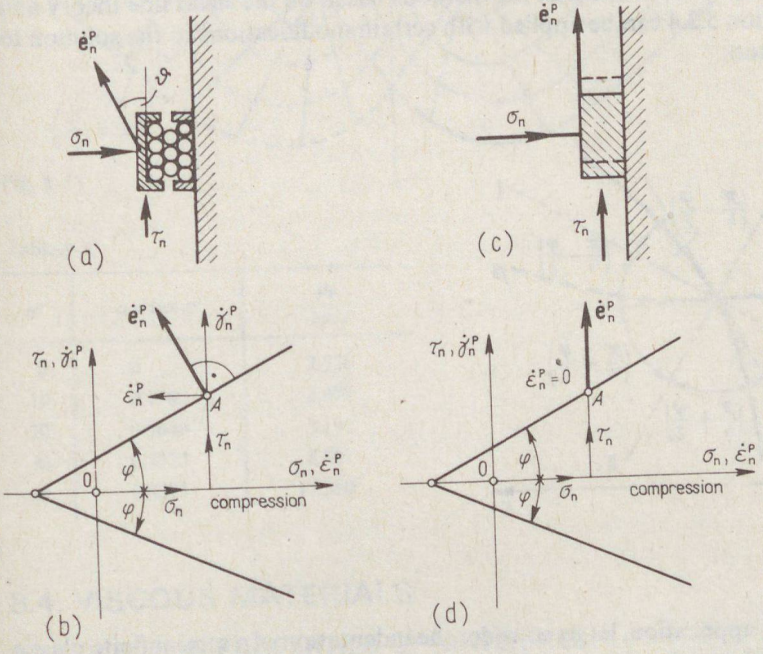


Fig. 8–11

8.3.3. PLANE STRAIN PROBLEM

In the case of plane strain, the Coulomb yield condition (8—11) for granular materials becomes

$$f = \frac{\sigma_{xx}+\sigma_{yy}}{2}\sin\varphi + \frac{1}{2}\sqrt{\left(\frac{\sigma_{xx}-\sigma_{yy}}{2}\right)^2+\sigma_{xy}^2} - \cos\varphi = 0 \tag{8—21}$$

which, together with the equilibrium equations

$$\left.\begin{aligned}\frac{\partial\sigma_{xx}}{\partial x}+\frac{\partial\sigma_{xy}}{\partial y}=0,\\ \frac{\partial\sigma_{yx}}{\partial x}+\frac{\partial\sigma_{yy}}{\partial y}=0,\end{aligned}\right\} \tag{8—22}$$

uniquely defines the plastic stress distribution in a continuum, provided that only static boundary conditions are prescribed. The above system of differential equations is *hyperbolic*, giving two sets of characteristic lines. They are symmetrically arranged with respect to the principal directions of stresses and at each point intersect each other at the angles $\frac{\pi}{2}+\varphi$ and $\frac{\pi}{2}-\varphi$, respectively, as shown in Fig. 8—12. Omitting the detailed discussion, we can state that the methods based on the shear line theory and presented in Section 5.2.4 can be applied with certain modifications to the solution to these problems, too.

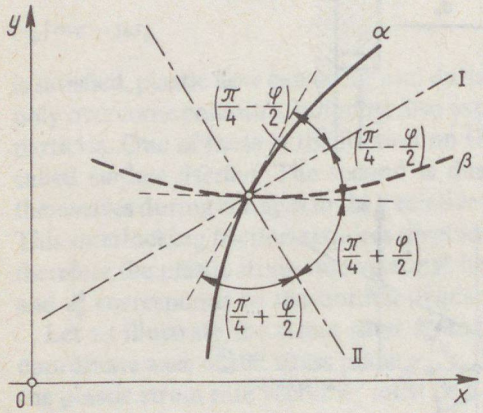


Fig. 8–12

To illustrate the application, let us consider the indentation of a semi-infinite plastic sheet by a flat rigid punch, under conditions of plane strain.

The solution to this problem, based on the Huber–v. Mises–Hencky or Tresca yield condition, has been presented in Section 5.2.5. The shear line field is illustrated by Fig. 5—14 and the pressure for plastic flow is

$$p_p = 4s\left(1+\frac{\pi}{2}\right)\tau_0 = 2s\left(1+\frac{\pi}{2}\right)\sigma_0. \tag{8—23}$$

The shear line field for the same problem based on the Coulomb yield condition is shown in Fig. 8—13, and the corresponding limit pressure is equal to (Prandtl 1920; Nádai 1963; Chen 1975)

$$p_p = \frac{s}{\sin\varphi}\left[(1+\sin\varphi)e^{\pi\tan\varphi}-1+\sin\varphi\right]\sigma_0'. \tag{8—24}$$

Here σ_0' designates the yield stress for the granular material in pure compression. The magnitudes of the limit pressure for different values of the coefficient of internal friction are given in Table 8—1. As can be seen, when μ tends to zero and $\sigma_0' = \sigma_0$, (8—24) is identical to the same solution obtained on the basis of the Huber–v. Mises–Hencky or Tresca yield condition.

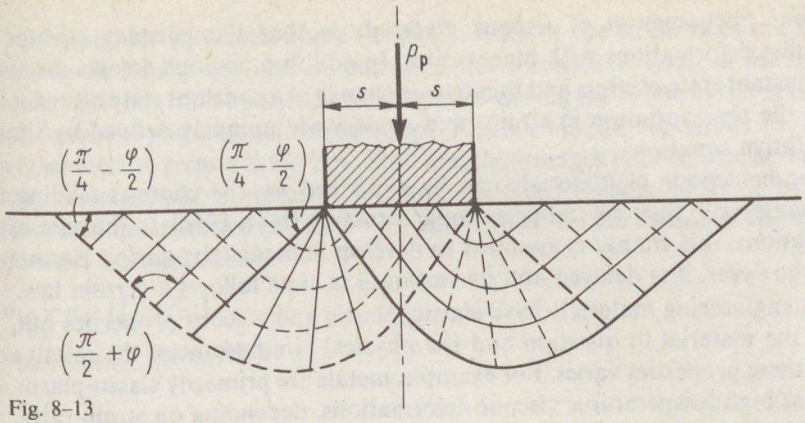


Fig. 8–13

Table 8–1

φ°	$\mu=\tan\varphi$	$\frac{p_F}{2s\sigma'_F}$
0	0	2.571
10	0.1763	3.499
20	0.3640	5.194
30	0.5773	8.701
40	0.8391	17.560

8.4. VISCOUS MATERIALS

8.4.1. VISCOUS PROPERTIES OF MATERIALS

(1) The principal phenomenological models introduced in order to describe material inelasticity can be classified into two groups: *plastic and viscous materials*. The main differences between these two material behaviours can be summarized as below.

Plastic deformations can occur only when certain combinations of stresses defined by the yield condition are reached. The coefficients appearing with the stress and strain components in the constitutive equations for plastic materials are not material constants; they depend upon the instantaneous state of stress or strain. The plastic deformations accumulate during the loading process. They are *path-dependent*, but do not depend on time.

Viscous deformations can occur at any level of stress. The coefficients appearing with the stress and strain components in the constitutive equations of viscous materials are material constants; they do not depend upon the instantaneous state of stress or strain. The development of viscous deformations is a function of time; hence, viscous materials are *time-dependent*.*

* In certain special cases, by the application of Laplace transformation the time dependence of the constitutive equations can be formally removed and solutions can be obtained in terms of the associated elastic problem (Olszak, Sawczuk 1967).

An important phenomenon of viscous materials is that they display greater resistance against deformations with higher rates. In addition, viscous deformations develop at a constant state of stress and the stresses change at a constant state of strain. In both cases, the time variation in strains and stresses are uniquely defined by the viscous constitutive equations.

The inelastic behaviour of materials can be explained by the changes (sliding, dislocation) occurring in their crystal or granular structure (Hult 1966). In the case of plastic deformations, this change is assumed to develop immediately; during viscous deformations, however, it is delayed and its variation in time follows a certain law.

In principle, engineering materials have elastic, plastic and viscous properties but, depending on the material in question and the physical circumstances, the relative significance of these properties varies. For example, metals are primarily elasto-plastic materials but, at high temperatures viscous deformations, depending on strain rates, may play an important role and therefore can not be neglected. Concrete and especially plastics are primarily visco-elastic materials, but at higher stresses they can also display significant plastic deformations.

(2) It follows from the above that the basic variables in a phenomenological theory of viscosity are stress σ, strain ε, stress rate $\dot{\sigma}$, strain rate $\dot{\varepsilon}$ and time t. In addition, the material parameters are temperature dependent. In the following, assuming isothermal conditions, this latter effect will be ignored. Hence, in a uniaxial state of stress, the constitutive equation for viscous materials has the general form

$$F(\sigma, \varepsilon, \dot{\sigma}, \dot{\varepsilon}, t) = 0.$$

In order to find out the specific forms of this equation, and to illustrate the most important viscous properties of materials, the results of a few basic experiments will now be discussed.

(a) First consider the case where a tensile test specimen made of viscous material is subjected to a *constant stress*, i.e. $\dot{\sigma} = 0$, and the strain is recorded at subsequent times. Then, essentially immediately upon the application of the load an instantaneous strain occurs, which is considered to be the elastic or elasto-plastic deformation, and is denoted by ε^{ep}. In the case of a viscous material, however, the strain, does not remain unchanged under a constant load but increases monotonically. This is the viscous part of the strain, denoted by ε^{v}, and the phenomenon is called *creep*. Typical creep curves obtained for different constant stress levels are shown in Fig. 8—14(a). These curves can all be divided into two parts: in the first part the creep rate $\frac{d\varepsilon}{dt}$ is decreasing and showing *primary creep*, while in the second part the creep rate remains essentially constant, and this showing *secondary creep*.*

(b) Next, consider the case where a tensile specimen made of viscous material is subjected to a *constant strain*, i.e. $\dot{\varepsilon} = 0$. Then, it will be observed that under constant strain the stress does not remain unchanged but decreases monotonically. This phenomenon is called *relaxation*. Typical relaxation curves obtained for different constant strain levels are shown in Fig. 8—14(b).

* Following secondary creep, a *tertiary creep* can also be observed, when the creep rate is increasing. This part of the curve, however, does not have practical importance.

(c) Consider the cases where the strain rates or the stress rates are kept constant during the tensile tests, i.e. $\dot{\varepsilon} =$ constant or $\dot{\sigma} =$ constant. Then, in the case of viscous materials, the strain and stress rates applied during the experiments may significantly influence the stress-strain relationships (Fig. 8—14(c,d)); the higher the strain rate or stress rate, the greater is the yield limit and the strength of the material. The yield stress may be expressed in terms of the strain rate either by a linear or by a non-linear relationship, as shown in Fig. 8—15 and defined by the formulae (Wierzbicki 1967a, Bodner, Symonds 1962)

$$\sigma_{0d} = \sigma_{0s}\,(1 + \dot{\varepsilon}/\dot{\gamma}_0), \tag{8—25}$$

$$\sigma_{0d} = \sigma_{0s}\,[1 + (\varepsilon/\dot{\eta}_0)^{1/n}]. \tag{8—26}$$

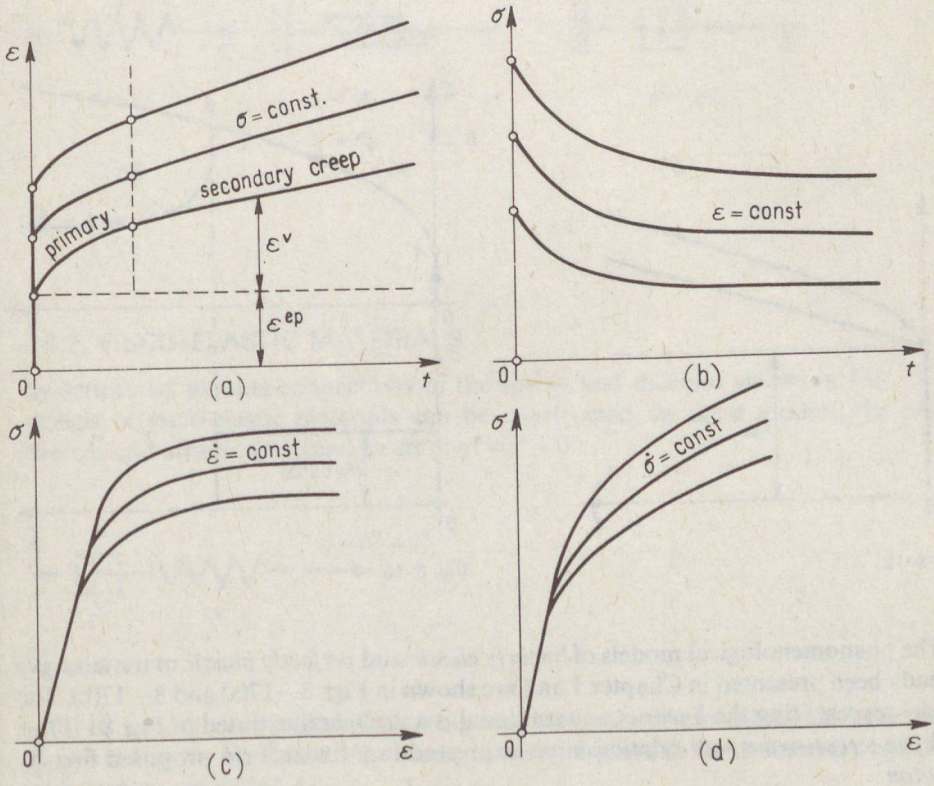


Fig. 8–14

Here σ_{0s} denotes the *static yield stress* which corresponds to quasi-static loading ($\dot{\varepsilon} \to 0$), σ_{0d} is called the *dynamic yield stress* and $\dot{\eta}_0$, $\dot{\gamma}_0$ and n are material constants which can be determined by experiment. For example, for steel the values $\dot{\gamma}_0 = 100 - 300\ \mathrm{s}^{-1}$, $\dot{\eta}_0 = 40\ \mathrm{s}^{-1}$ and $n = 5$ could be used.

(d) Finally, consider the case where the constant stress on a specimen is suddenly decreased to zero. Then, time-dependent diminishing of the previous viscous strain can be observed. This phenomenon is called *creep recovery* (Fig. 8—16).

(3) From the experimental results briefly described above, it can be seen that the behaviour of viscous materials even in a uniaxial state of stress is very complex, and therefore in order to develop a relatively simple phenomenological theory a number of simplifications have to be made. The most important assumption is that *the elastic, plastic and viscous properties of the material are independent and can therefore be superimposed.* Hence, the strains and stresses can be subdivided into elastic, plastic and viscous parts

$$\varepsilon = \varepsilon^{e} + \varepsilon^{p} + \varepsilon^{v},$$

$$\sigma = \sigma^{e} + \sigma^{p} + \sigma^{v}.$$

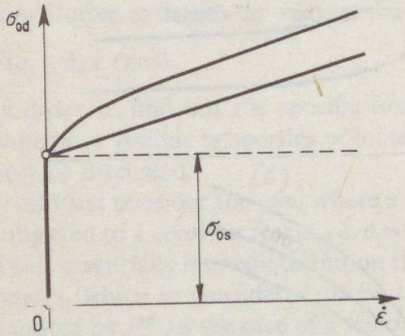


Fig. 8–15

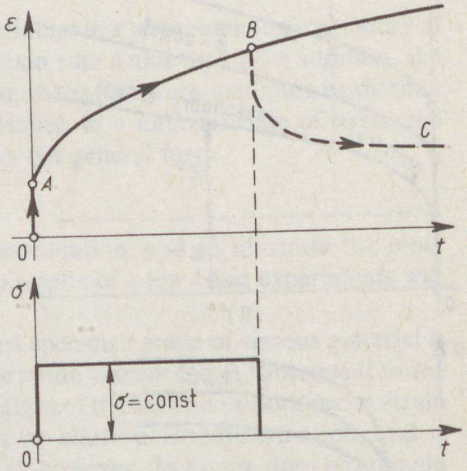


Fig. 8–16

The phenomenological models of *linearly elastic* and *perfectly plastic* materials have already been presented in Chapter 1 and are shown in Figs 8—17(a) and 8—17(b). The model representing the *linear viscous* material is a *dashpot* illustrated in Fig. 8—17(c), and the *stress-strain rate relationship* is expressed in a linear form proposed first by *Newton*

$$\sigma = \mu\dot{\varepsilon}. \tag{8—27}$$

Here μ denotes a *viscous coefficient*, its unit being $\frac{\text{Ns}}{\text{m}^2}$ and its magnitude can be obtained by experiments (Hult 1966). The linear equation (8—27) corresponds to the secondary creep shown in Fig. 8—14(a). For the description of primary creep, different nonlinear stress-strain rate relationships are proposed in the literature (Hult 1966).

By *parallel and series connections* of the simple models shown in Fig. 8—17 different complex models which describe the elastic, plastic and viscous properties of the material can be constructed. Next, these complex models will be presented, first for uniaxial states of stress and then for multi-axial states.

Other phenomenological and mathematical models and theories for viscous materials can be found in the literature (e.g. Olszak, Sawczuk 1964; Hult 1962, 1966; Flügge 1975; Malmeisters, Tamuzs, Teters 1977; Valanis, 1971, 1980; Valanis, Lee 1982).

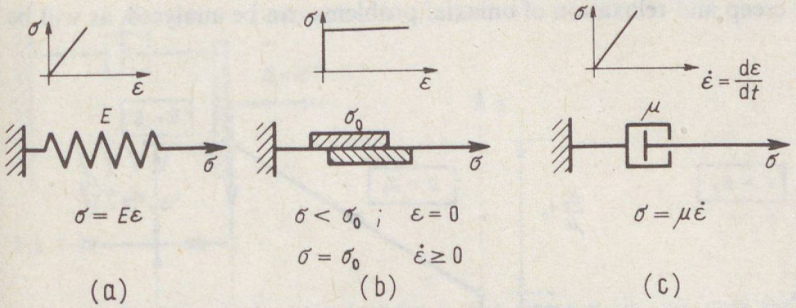


Fig. 8–17

8.4.2. VISCO-ELASTIC MATERIALS

By series and parallel connections of the spring and dashpot shown in Fig. 8—17, models of visco-elastic materials can be constructed. In these models, the plastic stresses and strains are equal to zero: $\sigma^p = \varepsilon^p = 0$.

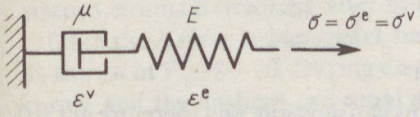


Fig. 8–18

(1) In the *Maxwell model*, the spring and the dashpot are connected in *series*, as shown in Fig. 8—18. Hence, the stresses in the spring and in the dashpot are equal and their strains are added, i.e.

$$\sigma^e = \sigma^v = \sigma,$$

$$\varepsilon = \varepsilon^e + \varepsilon^v, \quad \dot{\varepsilon} = \dot{\varepsilon}^e + \dot{\varepsilon}^v.$$

Here

$$\varepsilon^e = \frac{\sigma}{E}, \quad \dot{\varepsilon}^e = \frac{\dot{\sigma}}{E} \quad \text{and} \quad \dot{\varepsilon}^v = \frac{\sigma}{\mu},$$

which leads to the constitutive equation for the Maxwell model

$$\dot{\varepsilon}=\dot{\varepsilon}^{e}+\dot{\varepsilon}^{v}=\frac{\dot{\sigma}}{E}+\frac{\sigma}{\mu}, \tag{8—28}$$

or in a more detailed form

$$\frac{d\varepsilon}{dt}=\frac{1}{E}\frac{d\sigma}{dt}+\frac{1}{\mu}\sigma. \tag{8—29}$$

By the solution of this differential equation and by the suitable choice of the initial conditions, the creep and relaxation of uniaxial problems can be analysed, as will be shown below.

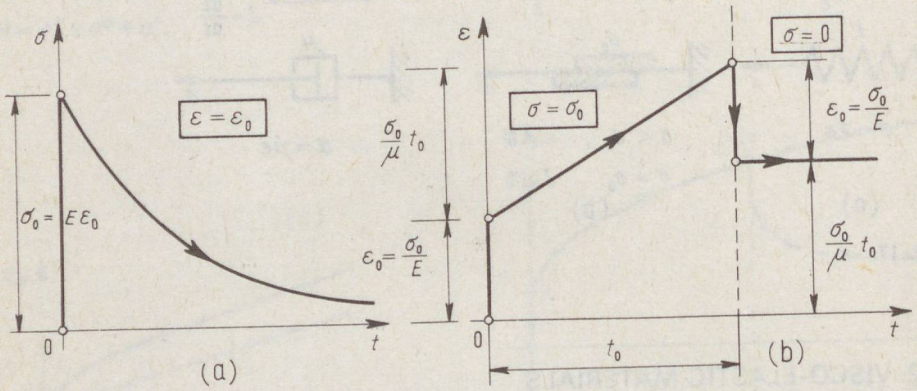


Fig. 8–19

(a) First, let us consider the case of *relaxation* when at the instant $t=0$ the strain is suddenly increased from zero to ε_0 and remains unchanged, i.e. $\dot{\varepsilon}=0$. Then eq. (8—29) becomes

$$\frac{d\sigma}{dt}+\frac{E}{\mu}\sigma=0.$$

During a sudden change in strain, no viscous strains can develop, and therefore at $t=0$, $\varepsilon^{v}=0$ and $\sigma=\sigma_0=E\varepsilon_0$. Using this initial condition, the solution to the above differential equation yields

$$\sigma=E\varepsilon_0\exp\left(-\frac{E}{\mu}t\right). \tag{8—30}$$

This relationship is illustrated in Fig. 8—19(a).

(b) Considering the case of *creep*, we assume that at the instant $t=0$ the stress is suddenly increased from zero to σ_0 and remains unchanged, i.e. $\dot{\sigma}=0$. Then eq. (8—29) becomes

$$\frac{d\varepsilon}{dt}=\frac{\sigma_0}{\mu}.$$

During a sudden change in stress, no viscous strains can develop, and therefore at $t=0$, $\varepsilon^v=0$ and $\varepsilon=\varepsilon_0=\dfrac{\sigma_0}{E}$. Using this initial condition, the solution to the above differential equation becomes

$$\varepsilon=\varepsilon_0+\frac{\sigma_0}{\mu}t=\varepsilon_0\left(1+\frac{E}{\mu}t\right). \tag{8—31}$$

This relationship is illustrated in Fig. 8—19(b).

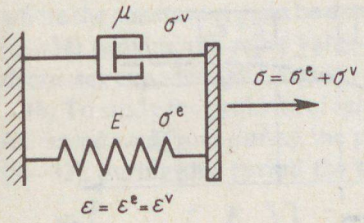


Fig. 8–20

Let us assume that at the instant t_0 the stress σ_0 is suddenly decreased to zero. Then, the corresponding elastic strain $\varepsilon_0=\dfrac{\sigma_0}{E}$ will also disappear and since for $t>t_0$ $\sigma=\dfrac{d\sigma}{dt}=0$, according to eq. (8—31) $\dfrac{d\varepsilon}{dt}=0$. Hence, after unloading, a permanent strain remains, the magnitude of which is equal to $\dfrac{\sigma_0}{\mu}t_0$.

Comparison of the diagrams of Fig. 8—14(a,b) and Fig. 8—19 shows that the Maxwell model describes relaxation reasonably well. In the case of creep, however, the model is only accurate for the stage of secondary creep and is unable to account for the viscous strains developing after unloading.

(2) In the *Kelvin—Voigt model*, the spring and the dashpot are connected in *parallel*, as shown in Fig. 8—20. During displacement of the rigid plate, the elongations in the spring and the dashpot are equal and the stresses are added, i.e.

$$\varepsilon^e=\varepsilon^v=\varepsilon,$$

$$\sigma=\sigma^e+\sigma^v.$$

Here

$$\sigma^e=E\varepsilon \quad \text{and} \quad \sigma^v=\mu\dot{\varepsilon},$$

which leads to the constitutive equation for the Kelvin—Voight model*

$$\sigma=E\varepsilon+\mu\dot{\varepsilon} \tag{8—32}$$

* For the sake of simplicity, in this equation the viscous coefficient is also denoted by μ. In this case, however, μ has a different physical content and value and is often called the *internal viscous coefficient* (Nádai 1963).

or, in a more detailed form,

$$\sigma = E\varepsilon + \mu \frac{d\varepsilon}{dt}. \tag{8—32a}$$

By the solution to this differential equation and by the suitable choice of the initial conditions, the uniaxial creep and relaxation can be analysed, as will be described below.

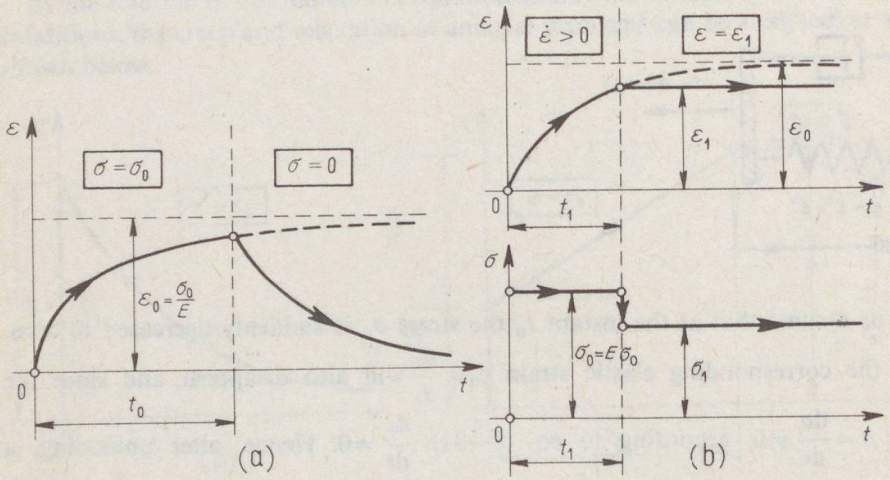


Fig. 8–21

(a) In the case of *creep* we assume that at the instant $t=0$ the stress is suddenly increased from zero to σ_0 and remains unchanged, i.e. $\dot{\sigma}=0$. Then eq. (8—32) becomes

$$\frac{d\varepsilon}{dt} + \frac{E}{\mu}\varepsilon = \frac{\sigma_0}{\mu}.$$

Since during the sudden change in stress no viscous strain can develop, the initial condition has the form: at $t=0$ $\varepsilon=\varepsilon^v=0$. This leads to the following solution to the above differential equation

$$\varepsilon = \frac{\sigma_0}{E}\left[1-\exp\left(-\frac{E}{\mu}t\right)\right]. \tag{8—33}$$

This relationship is illustrated in Fig. 8—21(a). It can be seen that if $t\to\infty$, $\varepsilon\to\varepsilon_0=\dfrac{\sigma_0}{E}$.

Now let us assume that at the instant t_0 the stress σ_0 is suddenly decreased to zero. Since the viscous strains cannot change suddenly, and the parallel connection also prevents a sudden change in the elastic strains, at $t=t_0$ the strain diagram does not

show discontinuity. In the unloaded state (when $t>t_0$) the behaviour of the model is described by eq. (8—32a) if there $\sigma=0$ is substituted

$$\frac{d\varepsilon}{dt}+\frac{E}{\mu}\varepsilon=0.$$

The solution to this differential equation yields

$$\varepsilon=K_0\exp\left(-\frac{E}{\mu}t\right), \tag{8—34}$$

where the constant K_0 can be determined on the condition that at $t=t_0$ eqs. (8—33) and (8—34) provide the same value for ε. It can be seen that after unloading the strain decreases exponentially and if $t\to\infty$, $\varepsilon\to 0$.

(b) To study the problem of *relaxation*, first assume that at $t=0$ the stress is suddenly increased to σ_0 and during the period $0\le t\le t_1$ remains unchanged. According to eq. (8—33), during this period the strain reaches the value

$$\varepsilon_1=\frac{\sigma_0}{E}\left[1-\exp\left(-\frac{E}{\mu}t_1\right)\right].$$

Next, we assume that the strain is kept unchanged during the period $t>t_1$ and consider the subsequent variation in the stress. Since at $t=t_0$ $\dfrac{d\varepsilon}{dt}$ suddenly becomes zero, according to eq. (8—32) a sudden change will take place in the stress as well and its value

$$\sigma=E\varepsilon_1=\sigma_0\left[1-\exp\left(-\frac{E}{\mu}t_1\right)\right] \tag{8—35}$$

remains unchanged for $t>t_1$, as shown in Fig. 8—21(b). Hence, in this model the relaxation occurs suddenly, and the longer is the period t_1 during which the stress has been kept constant, the smaller is its value.

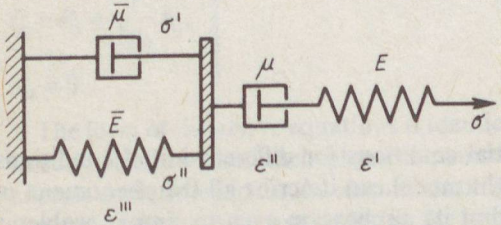


Fig. 8–22

Comparison of the diagrams of Figs 8—14 and (8—21) shows that the Kelvin—Voigt model describes the phenomenon of primary creep and the following unloading behaviour reasonably well, but is not suitable for the characterization of relaxation.

(3) According to the above results, the Maxwell and Kelvin—Voigt models separately are not able to describe all the properties of visco-elastic materials. It can be seen, however, that they complement each other, and therefore it can be expected that

more refined models can be obtained by their combination. Figure 8—22 shows the series connection of these two models. Using the notations of Fig. 8—22, the following relationships can be obtained:

$$\varepsilon = \varepsilon' + \varepsilon'' + \varepsilon''',$$

$$\sigma = \sigma' + \sigma'',$$

$$\varepsilon' = \frac{\sigma}{E}, \quad \dot{\varepsilon}'' = \frac{\dot{\sigma}}{\mu},$$

$$\varepsilon''' = \frac{\sigma''}{\bar{E}}, \quad \dot{\varepsilon}''' = \frac{\dot{\sigma}'}{\bar{\mu}},$$

where E, μ, $\bar{E}$ and $\bar{\mu}$ denote suitably chosen material constants. Using these relationships, the constitutive equations for the combined model become

$$\dot{\varepsilon} = \frac{\dot{\sigma}}{E} + \frac{\sigma}{\mu} + \dot{\varepsilon}''',$$
$$\sigma = \bar{\mu}\dot{\varepsilon}''' + \bar{E}\varepsilon'''. \qquad (8—36)$$

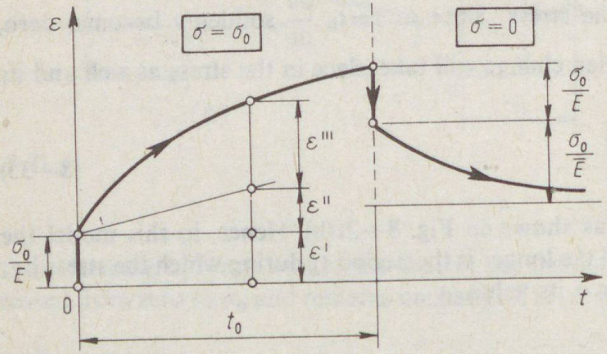


Fig. 8–23

The solution to this system of differential equations for different initial conditions shows that the Maxwell—Kelvin—Voight model can describe all the phenomena of visco-elastic materials reasonably well, but its application even to simple problems results in complicated calculations. As an example, the diagram of Fig. 8—23 illustrates the problem of creep when for $0 \leq t \leq t_0$, $\sigma = \sigma_0$ and for $t > t_0$, $\sigma = 0$. Other applications can be found elsewhere (Odqvist, Hult 1962; Nádai 1963; Hult 1966; Lin 1968).

(4) The uniaxial Newton model of ideal viscous materials given by eq. (8—27) can be generalized to three-dimensional problems by assuming that the *viscous dilatation* is zero

$$\varepsilon^{\nu}_{kk} = 0, \qquad (8—37)$$

and in pure shear a relationship similar to that for pure tension or compression can be used, namely

$$\tau = \mu_0 \dot{\gamma}^v. \tag{8—38}$$

Here τ and $\dot{\gamma}^v$ denote the shear stress and the viscous shear strain, respectively, and μ_0 is a viscous coefficient for pure shear. This is not an independent material constant, since by the use of the incompressibility condition (8—37) it can be expressed in terms of μ

$$\mu_0 = \frac{1}{3}\mu. \tag{8—39}$$

Similarly, because of incompressibility, Poisson's ratio is equal to 1/2 and the viscous strain tensor is equal to the viscous strain deviator

$$\varepsilon_{ij}^v = e_{ij}^v. \tag{8—40}$$

Then, the generalized *constitutive equations for ideal viscous bodies* are expressed as below

$$\left.\begin{aligned}
\dot{\varepsilon}_{xx}^v &= \frac{1}{\mu}\left[\sigma_{xx} - \frac{1}{2}(\sigma_{yy}+\sigma_{zz})\right],\\
\dot{\varepsilon}_{yy}^v &= \frac{1}{\mu}\left[\sigma_{yy} - \frac{1}{2}(\sigma_{xx}+\sigma_{zz})\right],\\
\dot{\varepsilon}_{zz}^v &= \frac{1}{\mu}\left[\sigma_{zz} - \frac{1}{2}(\sigma_{xx}+\sigma_{yy})\right],\\
\dot{\varepsilon}_{xy}^v &= \frac{1}{2\mu_0}\sigma_{xy}, \quad \dot{\varepsilon}_{xz}^v = \frac{1}{2\mu_0}\sigma_{xz}, \quad \dot{\varepsilon}_{yz}^v = \frac{1}{2\mu_0}\sigma_{yz}.
\end{aligned}\right\} \tag{8—41}$$

Making use of eqs (8—39) and (8—40) these equations can be written in terms of the stress and strain deviators

$$\left.\begin{aligned}
\dot{\varepsilon}_{ij}^v &= \dot{e}_{ij}^v = \frac{1}{2\mu_0} s_{ij},\\
\dot{\varepsilon}_{kk}^v &= 0.
\end{aligned}\right\} \tag{8—42}$$

The form of the above equations is identical to that of the constitutive equations for linearly elastic bodies; their physical meaning however is entirely different, since they express a relationship for the viscous strain rates rather than for the elastic strains, and the material constants appearing in the two constitutive equations are also different. There is also formal similarity between the constitutive equations of the ideal viscous and rigid-perfectly plastic bodies (see eq. 2—99(b)). In eq. (8—42), however, $\frac{1}{2\mu_0}$ denotes a *material constant*, while in eq. (2—99b) the plastic multiplier $d\lambda$ is a function of the coordinates and instantaneous stresses. In addition, viscous strains develop at any magnitude of stress, but plastic strains occur only at certain level of stresses when the yield function f satisfies the conditions $f = 0$ and $df = 0$.

The formal similarity of the different constitutive equations makes it possible to describe them in the following unified form

$$\left.\begin{aligned} \dot{e}_{ij} &= \psi s_{ij}, \\ \dot{\varepsilon}_{kk} &= \phi \sigma_{kk}. \end{aligned}\right\} \tag{8—43}$$

Here

(a) for *linearly elastic bodies*

$$\psi = \frac{1}{2G}\frac{\partial}{\partial t}, \quad \phi = \frac{1-2\nu}{E}\frac{\partial}{\partial t} = \frac{1}{3K}\frac{\partial}{\partial t}. \tag{8—44a}$$

(b) *for rigid–perfectly plastic bodies*

$$\left.\begin{aligned} &\text{if } f=0 \text{ and } \dot{f}=0, \text{ then } \psi = \dot{\lambda} \geq 0 \\ &\text{if } f<0 \text{ or } f=0 \text{ and } \dot{f}<0, \text{ then } \psi = \dot{\lambda} = 0 \text{ and } \phi = 0. \end{aligned}\right\} \tag{8—44b}$$

(c) *for ideal viscous bodies*

$$\psi = \frac{1}{2\mu_0}, \quad \phi = 0. \tag{8—44c}$$

(5) Next, we will construct the constitutive equations for *visco-elastic bodies*. As in the case of a uniaxial state of stress, we will assume that the stress and strain deviator tensors can again be separated into elastic and viscous parts

$$s_{ij} = s^{e}_{ij} + s^{v}_{ij}, \quad e_{ij} = e^{e}_{ij} + e^{v}_{ij}. \tag{8—45}$$

(a) In the case of the *Maxwell model* (see Fig. 8—18) we have the relationships

$$e_{ij} = e^{e}_{ij} + e^{v}_{ij},$$

$$e^{e}_{ij} = \frac{1}{2G} s_{ij}, \quad \dot{e}^{v}_{ij} = \frac{1}{2\mu_0} s_{ij},$$

which lead to the following constitutive equation

$$\left.\begin{aligned} \dot{e}_{ij} &= \frac{1}{2G}\dot{s}_{ij} + \frac{1}{2\mu_0} s_{ij}, \\ \dot{\varepsilon}_{kk} &= \frac{1}{3K}\dot{\sigma}_{kk}. \end{aligned}\right\} \tag{8—46}$$

(b) In the case of the *Kelvin–Voight model* (see Fig. 8—20), the relationships

$$s_{ij} = s^{e}_{ij} + s^{v}_{ij},$$

$$s^{e}_{ij} = 2Ge_{ij}, \quad s^{v}_{ij} = 2\mu_0 \dot{e}_{ij}$$

can be obtained and the constitutive equation then has the form

$$\left.\begin{aligned} s_{ij} &= 2Ge_{ij} + 2\mu_0 \dot{e}_{ij}, \\ \dot{\varepsilon}_{kk} &= \frac{1}{3K}\dot{\sigma}_{kk}. \end{aligned}\right\} \tag{8—47}$$

8.4.3. VISCO-PLASTIC MATERIALS

(1) By the combination of the perfectly plastic and ideally viscous material models different models of visco-plastic materials can be obtained. This will now be briefly discussed.

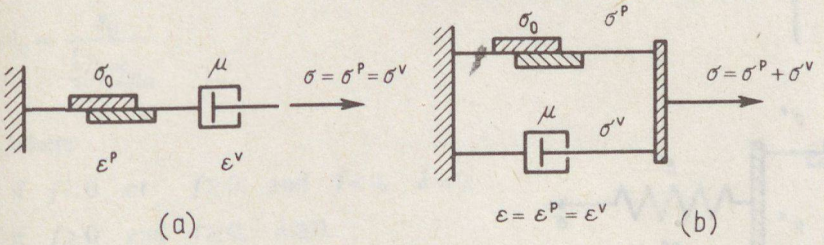


Fig. 8–24

(a) When the models of viscous and plastic materials are connected in *series*, at stresses lower than the yield stress only viscous strains occur; upon reaching the yield stress, however, plastic strains will also develop. Considering Fig. 8—24(a), the following relationships can be written

$$\left.\begin{aligned} &\text{if} \quad \sigma < \sigma_0, \quad \dot{\varepsilon} = \frac{\dot{\sigma}}{\mu}, \\ &\text{if} \quad \sigma = \sigma_0, \quad \dot{\varepsilon} = \frac{\dot{\sigma}}{\mu} + \dot{\varepsilon}^P. \end{aligned}\right\} \tag{8—48}$$

Here the plastic strain rate $\dot{\varepsilon}^P$ depends on the load path of the material.

(b) The model obtained by *connection in parallel* of the models of viscous and plastic materials is called the *Bingham model*. Considering Fig. 8—24(b), the following relationships can be written in this case

$$\left.\begin{aligned} &\text{if} \quad \sigma < \sigma_0, \quad \varepsilon = 0, \\ &\text{if} \quad \sigma \geq \sigma_0, \quad \sigma = \sigma_0 + \mu\dot{\varepsilon}. \end{aligned}\right\} \tag{8—49}$$

Accordingly, at stresses lower than the yield stress no strains occur, and in the plastic range the yield stress increases in proportion to the strain rate. This phenomenon shows a formal similarity to the behaviour of strain hardening materials. There is a fundamental difference, however, between these two materials because for strain hardening materials the increase in yield stress depends on the strains rather than on the strain rates.

The Bingham model describes the visco-plastic behaviour of metals reasonably well and, therefore it is widely used in the analysis of different dynamic problems.

(c) By the combination of the Bingham model and the linearly elastic model, one can construct the model of *elasto-visco-plastic materials*. Considering Fig. 8—25,

$$\left.\begin{aligned} &\varepsilon=\varepsilon^{e}+\varepsilon^{vp},\\ &\varepsilon^{vp}=\varepsilon^{v}=\varepsilon^{p},\\ &\sigma=\sigma^{p}+\sigma^{v},\\ &\sigma^{e}=\sigma. \end{aligned}\right\} \tag{8—50}$$

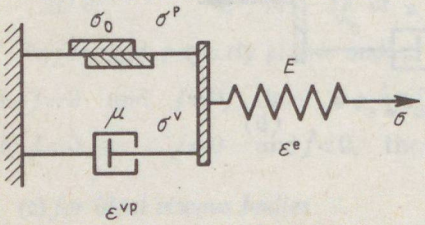


Fig. 8–25

Using these relationships the constitutive equations for elasto-visco-plastic materials become

$$\left.\begin{aligned} &\text{if } \sigma<\sigma_0\\ &\varepsilon^{v}=\varepsilon^{p}=0,\ \varepsilon=\frac{\sigma}{E}; \end{aligned}\right\} \tag{8—51}$$

$$\left.\begin{aligned} &\text{if } \sigma\geq\sigma_0\\ &\varepsilon^{e}=\frac{\sigma}{E},\quad \dot{\varepsilon}^{p}=\dot{\varepsilon}^{v}=\frac{\sigma^{v}}{\mu},\\ &\sigma^{p}=\sigma_0,\quad \sigma^{v}=\sigma-\sigma_0,\\ &\dot{\varepsilon}=\frac{\dot{\sigma}}{E}+\frac{1}{\mu}(\sigma-\sigma_0). \end{aligned}\right\} \tag{8—52}$$

(2) The visco-plastic models described above can be generalized to multi-axial states of stress and strain. As an example, we will next discuss the generalized constitutive equations for *Bingham bodies* (see Fig. 8—24(b)). We assume that the material is imcompressible, i.e.

$$\dot{\varepsilon}_{kk}=\dot{\varepsilon}^{p}_{kk}=\dot{\varepsilon}^{v}_{kk}=0. \tag{8—53}$$

As a consequence of parallel connection, we can write

$$s_{ij}=s^{p}_{ij}+s^{v}_{ij}, \tag{8—54}$$

where according to eqs (2—99b) and (8—43)

$$s_{ij}^{p}=\frac{1}{\dot{\lambda}}\dot{\varepsilon}_{ij},\quad s_{ij}^{v}=2\mu_0\dot{\varepsilon}_{ij}. \tag{8—55}$$

Substituting these relationships into eq. (8—54), and using the yield function f, we obtain the *constitutive equations for Bingham bodies*

$$\dot{\varepsilon}_{ij}=\frac{s_{ij}}{\frac{1}{\dot{\lambda}}+2\mu_0}, \tag{8—56}$$

where

if $f<0$ or $f\geq 0$ and $\dot{f}<0$, $\dot{\lambda}=0$;

if $f\geq 0$ and $\dot{f}\geq 0$, $\dot{\lambda}\geq 0$.

(3) There are several constitutive equations for visco-plastic bodies which are not constructed by the combination of the simple models of viscous and plastic materials. One of these constitutive equations, proposed by *Perzyna* (1966, 1968), has the following form

$$\dot{\varepsilon}_{ij}=\dot{\eta}\phi(F)\frac{\partial F}{\partial\sigma_{ij}},\quad \dot{\varepsilon}_{kk}=0. \tag{8—57}$$

Here $\dot{\eta}$ is a viscous coefficient and F denotes the yield function for the material. For example, in the case of the Huber–v. Mises–Hencky yield condition $F=\left(\frac{s_{ij}s_{ij}}{2}\right)^{1/2}$. $\phi(F)$ is a scalar function controlled by the following conditions

$$\left.\begin{aligned}&\phi=0 \quad \text{if} \quad F<k,\\ &\phi>0 \quad \text{if} \quad F\geq k,\end{aligned}\right\} \tag{8—58}$$

where k is a plastic material constant.

(a) According to the results of experiments (Aspden, Campbell 1966) a suitable form for the function ϕ is

$$\phi=\left(\frac{F}{k}-1\right)^{n}. \tag{8—59}$$

Then, the constitutive equation (8—57) becomes

$$\dot{\varepsilon}_{ij}=\dot{\eta}\left(\frac{F}{k}-1\right)^{n}\frac{\partial F}{\partial\sigma_{ij}},\quad \dot{\varepsilon}_{kk}=0. \tag{8—60}$$

Using the Huber–v. Mises–Hencky yield condition and applying the above constitutive equation for a uniaxial state of stress, we get $k=\frac{\sigma_0}{\sqrt{3}}$, $F=\frac{\sigma}{\sqrt{3}}$ and

$$\sigma=\left[1-\left(\frac{\dot{\varepsilon}}{\dot{\eta}_0}\right)^{1/n}\right]\sigma_0, \tag{8—61}$$

where $\dot{\eta}_0 = = \frac{\dot{\eta}}{\sqrt{3}}$. This special form agrees with the constitutive equation for visco-plastic materials given by eq. (8—26). For example, for steel the values $\dot{\eta} = 40\, s^{-1}$ and $n = 5$ can be assumed.

(b) The constitutive equation described above is nonlinear, and therefore its application causes mathematical difficulties. In order to linearize eq. (8—60), first we assume that $n = 1$ and replace $\dot{\eta}$ by an other properly chosen constant $\dot{\gamma}$. Then we get

$$\dot{\varepsilon}_{ij} = \dot{\gamma}\left(\frac{F}{k} - 1\right)\frac{\partial F}{\partial \sigma_{ij}}, \quad \dot{\varepsilon}_{kk} = 0, \tag{8—62}$$

where, using the Huber–v. Mises–Hencky yield condition,

$$F = \left(\frac{s_{ij}s_{ij}}{2}\right)^{1/2}. \tag{8—63}$$

In addition, we assume that in the plastic stage at each point of the body the stresses are increasing *proportionally*. Consequently, if at a certain point in the body the stresses $\bar{s}_{ij}$ cause the first yield in the material, i.e. $F(\bar{s}_{ij}) = k$, then for the subsequent stresses s_{ij} the following relationship can be written

$$s_{ij} = \frac{F(s_{ij})}{F(\bar{s}_{ij})}\bar{s}_{ij} = \frac{F(s_{ij})}{k}\bar{s}_{ij}. \tag{8—64}$$

Furthermore, because of the proportionality of stresses we obtain

$$\frac{\partial F(s_{ij})}{\partial s_{ij}} = \frac{\partial F(\bar{s}_{ij})}{\partial \bar{s}_{ij}} = \frac{\bar{s}_{ij}}{\left(\frac{\bar{s}_{ij}\bar{s}_{ij}}{2}\right)^{1/2}} = \frac{\bar{s}_{ij}}{F(\bar{s}_{ij})} = \frac{\bar{s}_{ij}}{k}. \tag{8—65}$$

Substituting eqs (8—64) and (8—65) into eq. (8—62) we get *the linear constitutive equations for visco-plastic bodies* (Wierzbicki, Florence 1970)

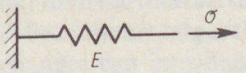
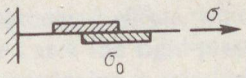
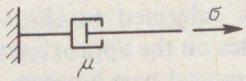
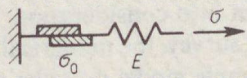
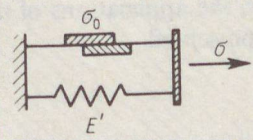
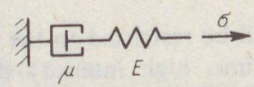
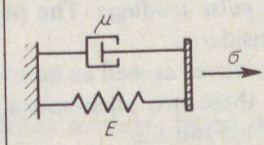
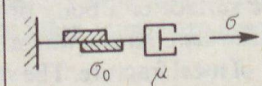
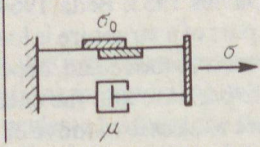
$$\left.\begin{aligned} &\text{if} \quad s_{ij} < \bar{s}_{ij}, \quad \dot{\varepsilon}_{ij} = 0; \\ &\text{if} \quad s_{ij} \geq \bar{s}_{ij}, \quad \dot{\varepsilon}_{ij} = \frac{\dot{\gamma}}{k}(s_{ij} - \bar{s}_{ij}), \\ &\left(\frac{\bar{s}_{ij}s_{ij}}{2}\right)^{1/2} = k \text{ and } \dot{\varepsilon}_{kk} = 0. \end{aligned}\right\} \tag{8—66}$$

In the case of a uniaxial state of stress, eq. (8—66) becomes

$$\sigma = \left(1 + \frac{\dot{\varepsilon}}{\dot{\gamma}_0}\right)\sigma_0, \tag{8—67}$$

where $\dot{\gamma}_0 = \frac{2}{\sqrt{3}}\dot{\gamma}$. This is in agreement with the linear constitutive equation for visco-plastic materials given by eq. (8—25).

Finally, the material models discussed in this chapter are illustrated for uniaxial states of stress in Fig. 8—26.

Material	Model	Constitutive equation*
ideally elastic (Hooke)		$\varepsilon = \frac{\sigma}{E}$
ideally plastic (Saint-Venant)		$\varepsilon = 0$, if $\sigma < \sigma_0$ $\varepsilon \geq 0$, if $\sigma = \sigma_0$
ideally viscous (Newton)		$\dot{\varepsilon} = \frac{\sigma}{\mu}$
elasto-plastic		$\varepsilon = \frac{\sigma}{E}$, if $\sigma < \sigma_0$ $\varepsilon = \geq 0$, if $\sigma = \sigma_0$
rigid-hardening		$\varepsilon = 0$, if $\sigma < \sigma_0$ $\varepsilon = \frac{\sigma - \sigma_0}{E'}$, if $\sigma \geq \sigma_0$
visco-elastic (Maxwell)		$\dot{\varepsilon} = \frac{\dot{\sigma}}{E} + \frac{\sigma}{\mu}$
visco-elastic (Kelvin–Voigt)		$\sigma = E\varepsilon + \mu\dot{\varepsilon}$
visco-plastic		$\dot{\varepsilon} = \frac{\sigma}{\mu}$, if $\sigma < \sigma_0$ $\varepsilon \geq 0$, if $\sigma = \sigma_0$
visco-plastic (Bingham)		$\varepsilon = 0$, if $\sigma < \sigma_0$ $\sigma = \sigma_0 + \mu\dot{\varepsilon}$, if $\sigma \geq \sigma_0$

* The equations are only valid if $\sigma \geq 0$.

Fig. 8–26

9. DYNAMIC RESPONSE OF PLASTIC STRUCTURES

This chapter contains a review of the basic principles and methods of the overall inelastic response of structures subjected to short-time, high intensity dynamic pressures. The review concentrates on the approximate methods based on the simple rigid-plastic idealization; in the second part however the problems, including elastic and viscous effects and large deformations, are also discussed. In the solutions pulse and impulsive loadings are taken into consideration.

In the course of the theoretical survey, the numerical analysis of a two-mass discrete beam model is discussed. This simple model provides a clear insight into the physical background of the theorems and approximations.

In the last part of the chapter, the applications of the methods described to a few structural problems are briefly presented.

9.1. INTRODUCTION

The contents of this chapter will be restricted to the analysis of plastic bodies and structures subjected to short-time, high intensity dynamic pressures caused by explosion or impact and called *pulse loadings*. The problem of repeated and cyclic dynamic loading will not be considered.

Pulse loading can cause stress waves as well as an overall structural response. It is customary practice to uncouple these two phenomena, because their time durations usually differ by a few orders of magnitude.

When only a small part of the surface of a body or structure is subjected to high intensity pressure or impact, transient stress waves will develop which may be important from the point of view of local fracture. The study of this problem is beyond the scope of this book (see e.g. Davies 1953; Béda 1964; Cristescu 1967; Ionescu 1979). When, on the other hand, a large part of a structure is loaded by a pulse load, the entire structure or a large part of it may start to move and, depending on the magnitude of the energy transferred by the dynamic pressure and the energy absorption capacity of the structure, after a while the structure will cease to move or will collapse. The study of this overall response will form the subject of our further investigations.

In the *overall inelastic dynamic response*, the following phenomena can play an important role: elastic and plastic deformations, strain rate sensitivity, strain hardening

and large deflections. In a great number of studies, rigid-perfectly plastic material is assumed and the effect of large deflections is neglected. This idealization leads to considerable simplifications and yet generally provides reliable information. The assumptions in this simple rigid-plastic theory are, however, to some extent contradictory, since the elastic deformations can only be neglected when the external energy input is several times greater than the total elastic strain energy capacity. On the other hand, when the transverse deflections are larger than the corresponding thickness of the structure, the geometry changes can introduce in-plane or membrane forces which may exert a significant effect. Similarly, the dynamic buckling or unstable behaviour of structures can also have an important influence. Finally, the strain–rate–sensitive behaviour exerts strengthening effects, which at higher strain rates can be significant. Therefore in certain cases the rigid-plastic approximation may require further refinements. The strain hardening is relatively unimportant compared with other effects, and so it can usually be neglected.

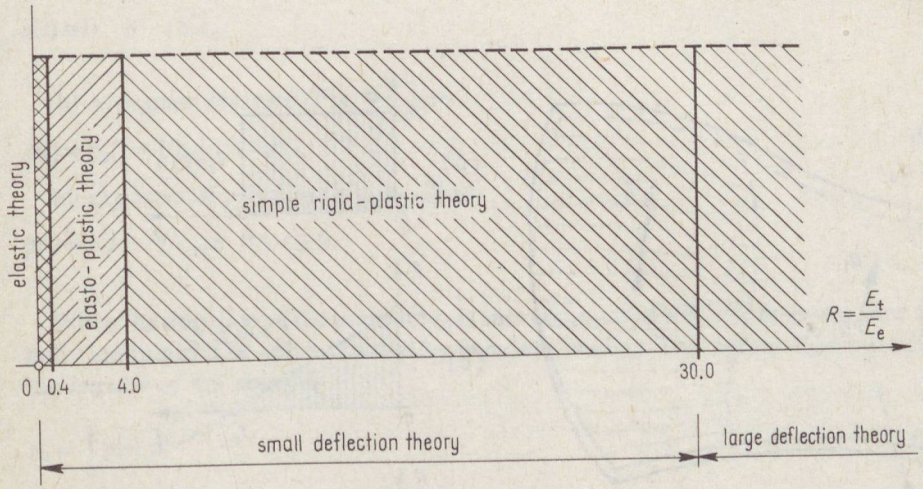


Fig. 9–1

The range of applicability of the methods based on different assumptions can be illustrated by the problem of a simply supported beam subjected to dynamic pressure (Wierzbicki 1976). The limits of these ranges are described in terms of the ratio

$$R=\frac{\text{total energy input}}{\text{elastic energy capacity}}.$$

In Fig. 9—1 it can be seen from this symbolical representation that at low values of R the influence of elastic deformations is important, while at higher values the effect of large deformations cannot be neglected. Hence, in this simple problem, the range of applicability of the simple rigid-plastic theory can be approximately given by $4<R<$ <30. Even in this case, however, the effect of strain rate sensitivity may play an important role.

9.2. FUNDAMENTAL RELATIONSHIPS

In the following, one- and two-dimensional structures will be considered and the following notation will be used (Fig. 9—2(a).

x_i, t: space and time variable ($i = 1,2,3$),
$m(x_i)$: mass per unit length or per unit surface area,
$u_i(x_i,t)$: displacement field,
$q_j(x_i,t)$; $Q_j(x_i,t)$: generalized strain and stress field ($j = 1,2,\ldots n$),
$T_i(x_j,t)$: dynamic surface pressure,
$p(t)$; $T_i^0(x_j)$: pressure parameter and pressure distribution function,
$v_i^0(x_j)$: initial velocity field,
$f(Q_j, x_i)$: yield function,
p_k; p_c: kinematically admissible and collapse load multiplier,
p_0; t_0: peak value and duration of the pulse load,
t_f: response time.

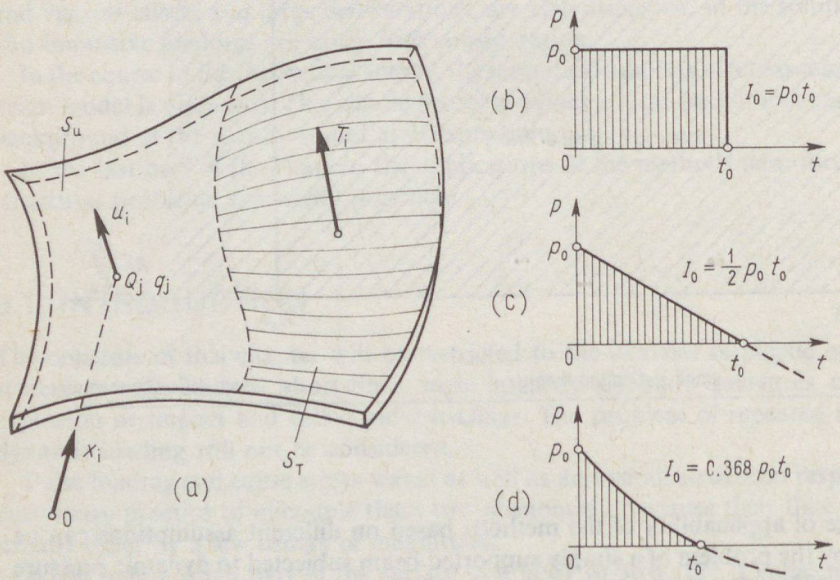


Fig. 9–2

A dot denotes differentiation with respect to time. In a part of the total domain S of the structure, denoted by S_T, dynamic surface pressures $T_i(X_j,t)$ are given and initial velocities $v_i^0(x_j)$ can also be prescribed. On the remainder of S, denoted by S_u, the velocities $\dot{u}_i(x_j,t)$ are set equal to zero. The initial displacements $u_i(x_j, o)$ are assumed to be zero on the total surface S. The weight of the structure is disregarded, but the inertia forces will be taken into consideration.

The primary goal of investigation is to calculate the *response time* t_f at which the structure ceases to move and to determine the *final* (permanent) *displacements* $u_i^f(x_j) = u_i(x_j,t_f)$. In some cases the complete determination of the state variables u_i, $\dot{u}_i$, q_j, $\dot{q}_j$ and Q_j is also required.

In the following it will be assumed that the structure is subjected to a *proportional dynamic pressure*, i.e. the dynamic surface tractions will be specified in a separated-variable form

$$T_i(x_j,t) = p(t)T_i^0(x_j). \tag{9—1}$$

Here the vector-valued function $T_i^0(x_j)$ defines the distribution of the surface pressure, and the pressure parameter function $p(t)$ describes the time variation of the pressure. The most widely used pressure parameter functions are as follows:

(a) *rectangular pressure* (Fig. 9—2(b))

$$\begin{aligned} &p(t) = p_0 \quad \text{if} \quad 0 \le t \le t_0, \\ &p(t) \equiv 0 \quad \text{if} \quad t > t_0; \end{aligned} \tag{9—2}$$

(b) *triangular pressure* (Fig. 9—2(c))

$$p(t) = p_0(1 - t/t_0), \quad t \ge 0; \tag{9—3}$$

(c) *exponential pressure* (Fig. 9—2(d))

$$p(t) = p_0(1 - t/t_0)\,e^{-t/t_0}, \; t \ge 0. \tag{9—4}$$

When the duration of the pressure t_0 is short compared with the response time t_f, the pulse loading can be approximated by *impulsive loading*. This means that, introducing the *impulse of the pressure*

$$I_0 = \int_0^{t_0} p(t)\,dt \tag{9—5}$$

eq. (9—1) is expressed in the form

$$T_i(x_j,t) = T_i^0(x_j)\, I_0\, \delta(t)$$

where $\delta(t)$ is the unit Dirac delta function. In this case, the solution to the problem is reduced to the dynamic analysis of an unloaded structure with prescribed *initial velocity* field:

$$\left.\begin{aligned} &T_i(x_j,t) = 0 && \text{on } S_T, \\ &u_i(x_j,0) = 0 && \text{on } S, \\ &\dot{u}_i(x_j,0) = v_i^0(x_j) = \frac{T_i^0(x_j)}{m(x_j)}\, I_0 && \text{on } S_T. \end{aligned}\right\} \tag{9—6}$$

9.3. SIMPLE RIGID-PLASTIC THEORY

9.3.1. GENERAL RELATIONSHIPS

In the simple rigid-plastic theory we assume that the structure is composed of a path-, time- and temperature-independent, rigid-perfectly plastic material, and neglect the effect of changes in geometry. Then, introducing a convex yield function $f(Q_j, x_i)$, the constitutive equation has the form

$$\dot{q}_j = \dot{\lambda} \frac{\partial f}{\partial Q_j}, \tag{9—7}$$

where $\lambda(x_i, t) \geq 0$ is the scalar multiplier of plastic strain-rates.

Because of the convexity of the yield surface $f(Q_j, x_i) = 0$, the *specific rate of dissipation energy function* d is uniquely determined if $\dot{q}_j$ is given

$$d = Q_j \dot{q}_j = d(\dot{q}_j) \tag{9—8}$$

and from this

$$Q_j = \frac{\partial d}{\partial \dot{q}_j}. \tag{9—9}$$

Considering a quasi-static one parameter loading, defined by the surface tractions $T_i^0(x_j)$ and a kinematically admissible strain-rate and velocity field $\dot{q}_i^k, \dot{u}_i^k$, the corresponding kinematically admissible load multiplier is given by

$$p_k = \frac{\int_S Q_j^k \dot{q}_j^k \mathrm{d}S}{\int_S T_i^0 \dot{u}_i^k \mathrm{d}S} = \frac{\int d(\dot{q}_j^k) \mathrm{d}S}{\int_S T_i^0 \dot{u}_i^k \mathrm{d}S}. \tag{9—10}$$

Next, the application of the simple rigid-plastic theory to the exact and approximate analysis and optimal design of structures subjected to pulse or impulsive loading will be presented.

9.3.2. SOLUTIONS TO SIMPLE PROBLEMS

In order to illustrate the application of the simple rigid–plastic theory to the analysis of dynamically loaded structures, solutions for simple models will first be presented.

9.3.2.1. ONE-DEGREE-OF-FREEDOM MODEL

Let us consider a one-degree-of-freedom model which consists of a block with mass M, resting on a frictionless surface and subjected to a pulse load $P(t)$, and supported by an ideal rigid-plastic connection with yield force R_0, as shown in Fig. 9—3. As long as the force R acting in the connection is smaller than R_0 the displacement W of the block will be zero, while on reaching the yield force R_0 unrestricted displacements can take place. In the following, it will be assumed that the function $P(t)$ has a decreasing character

and its peak value P_0 at $t=0$ is higher than R_0. Then, at the instant $t=0$ the block will start to move, but after a period of time denoted by t_f will stop moving and come to a standstill. The problem is to determine the response time t_f and the permanent displacement W_f which are defined by the conditions

$$\dot{W}(t_f)=0, \tag{9—11}$$

$$W_f=W(t_f). \tag{9—12}$$

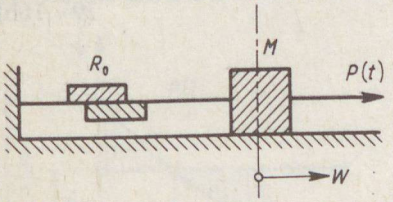


Fig. 9–3

The differential equation of motion of the block has the form

$$M\ddot{W}=P(t)-R_0, \quad 0\leq t\leq t_f. \tag{9—13}$$

By the use of the initial condition $\dot{W}(0)=0$ we obtain

$$\dot{W}=\frac{1}{M}\left[\int_0^t P(t)\mathrm{d}t-R_0t\right], \quad 0<t<t_f. \tag{9—14}$$

Substituting eq. (9—11) into this equation, the response time can be expressed in the form

$$t_f=\frac{\int_0^{t_f} P(t)\mathrm{d}t}{R_0}=\frac{I_{t_f}}{R_0}. \tag{9—15}$$

In the case of *rectangular pressure* given by eq. (9—2) we get

$$t_f=t_0\frac{P_0}{R_0}, \tag{9—15a}$$

while in the case of *exponential pressure* defined by eq. (9—4) the response time becomes

$$t_f=t_0\ln\left(\frac{P_0}{R_0}\right). \tag{9—15b}$$

Using the initial condition $W(0)=0$, eq. (9—14) can be written in the form

$$W=\frac{1}{M}\int_0^t\left[\int_0^t P(t)\mathrm{d}t-R_0t\right]\mathrm{d}t, \quad 0<t<t_f. \tag{9—16}$$

Making use of this relationship and of eqs (9—12) and (9—15), the permanent displacement W_f of the block can be obtained. For example, in the case of *quadratic pressure* we get

$$W_f = \frac{1}{2}\frac{P_0 t_0^2}{M}\left(\frac{P_0}{R_0} - 1\right) \tag{9—16a}$$

and in the case of *exponential pressure* eq. (9—16) results in

$$W_f = \frac{P_0 t_0^2}{M}\left[1 - \frac{R_0}{P_0}\left(1 + \ln\frac{P_0}{R_0} + \frac{1}{2}\ln^2\frac{P_0}{R_0}\right)\right]. \tag{9—16b}$$

Table 9—1

$\frac{P_0}{R_0}$	$\frac{t_f}{t_0}$	$\frac{MW_f}{P_0 t_0^2}$
1.00	0.000 00	0.000 000 00
1.02	0.019 80	0.000 001 28
1.04	0.039 22	0.000 009 76
1.06	0.058 27	0.000 031 57
1.08	0.076 96	0,000 071 72
1.10	0.095 31	0.000 134 37
1.12	0.113 33	0.000 222 87
1.14	0.131 03	0.000 339 94
1.16	0.148 42	0.000 487 71
1.18	0.165 51	0.000 667 84
1.20	0.182 32	0.000 881 56
1.22	0.198 85	0.001 129 76
1.24	0.215 11	0.001 413 04
1.26	0.231 11	0.001 731 72
1.28	0.246 86	0.002 085 92
1.30	0.262 36	0.002 475 56
1.32	0.277 63	0.002 900 43
1.34	0.292 67	0.003 360 18
1.36	0.307 48	0.003 854 32
1.38	0.322 08	0.004 382 33
1.40	0.336 47	0.004 943 56
1.42	0.350 66	0.005 537 33
1.44	0.364 64	0.006 162 91
1.46	0.378 44	0.006 819 52
1.48	0.392 04	0.007 506 36
1.50	0.405 47	0.008 222 61

The values of the functions in eqs (9—15b) and (9—16b) are given in Table 9—1. The acceleration, velocity and displacement functions are illustrated in Fig. 9—4.

Considering *pressure functions with arbitrary shapes* a general closed-form solution can also be derived for the permanent displacement, provided that the pressure function satisfies the following restrictions (Krajcinovic 1972).

The initial velocity is assumed to be zero and the time is measured from the moment when the motion commences, i.e. when $P(t)$ first exceeds R_0 (Fig. 9—5). In addition, it is also assumed that

$$\text{if} \quad t > t_0, \; P(t) \equiv 0 \text{ and } I_0 = \int_0^{t_0} P(t)\mathrm{d}t \geq R_0 t_0. \tag{9—17}$$

Otherwise, the function $P(t)$ can be of arbitrary form. Considering eq. (9—15), the physical meaning of the second restriction of eqs (9—17) is that the response time must exceed the duration of the pressure i.e. $t_f \geq t_0$.

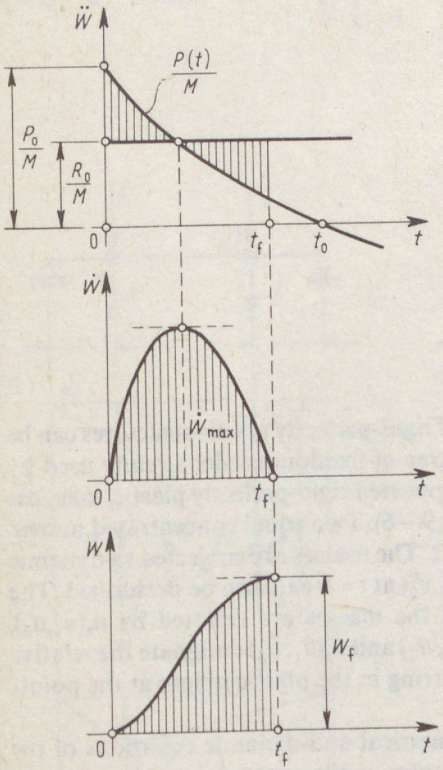


Fig. 9–4

Using the above assumptions and eq. (9—16), the following result can be derived for the permanent displacement

$$W_f = \frac{I_0}{M}\left(\frac{I_0}{2R_0} - t_c\right) = \frac{S_0}{M}\left(\frac{R_e}{R_0} - 1\right), \tag{9—18}$$

where

$$I_0 = \int_0^{t_0} P(t)\mathrm{d}t, \quad S_0 = \int_0^{t_0} tP(t)\mathrm{d}t, \quad t_c = \frac{S_0}{I_0}, \quad P_e = \frac{I_0^2}{2S_0}. \tag{9—19}$$

In this general case the formula (9—15) derived for the response time is also valid.

The significance of the expression (9—18) is in eliminating the influence of the pulse shape on the final results. In this way, if the solution for one pulse shape is known it is immediately possible to compute results for another pulse, through simple conversion.

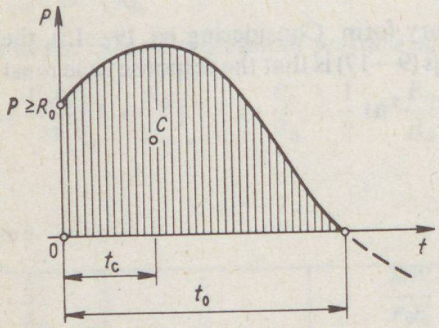


Fig. 9–5

9.3.2.2. TWO-DEGREE-OF-FREEDOM MODEL

The problems arising in the dynamic analysis of rigid-perfectly plastic structures can be very clearly illustrated by means of a two-degree-of-freedom model already used by several other authors. The model is a simply supported rigid-perfectly plastic, massless beam with a constant plastic moment M_0 (Fig. 9—6). Two equal concentrated masses M are attached to the beam at the points $\alpha = 1,2$. The masses are subjected to dynamic forces $F_\alpha(F_1,F_2)$ and their initial velocities $v_\alpha^0(v_1^0,v_2^0)$ at $t=0$ can also be prescribed. The displacements, velocities and accelerations of the masses are denoted by $u_\alpha(u_1,u_2)$, $\dot{u}_\alpha(\dot{u}_1,\dot{u}_2)$ and $\ddot{u}_\alpha(\ddot{u}_1,\ddot{u}_2)$, respectively, while $\theta_\alpha(\theta_1,\theta_2)$ and $\dot{\theta}_\alpha(\dot{\theta}_1,\dot{\theta}_2)$ designate the relative rotations and rotation rates, respectively, occurring in the plastic hinges at the points $\alpha = 1,2$.

(1) First, let us derive the fundamental geometrical and dynamic equations of the model. Considering Fig. 9—6(a), the rotation rates at the supports are expressed as

$$\dot{\varphi}_A = \frac{3}{4}\dot{\theta}_1 + \frac{1}{2}\dot{\theta}_2 \quad \text{and} \quad \dot{\varphi}_B = \frac{1}{4}\dot{\theta}_1 + \frac{3}{4}\dot{\theta}_2,$$

and then then following *geometrical relationships* between the relative rates and the velocities can be obtained

$$\left.\begin{aligned} \dot{u}_1 &= \dot{\varphi}_A l = \left(\frac{3}{4}\dot{\theta}_1 + \frac{1}{4}\dot{\theta}_2\right) l, \\ \dot{u}_2 &= \dot{\varphi}_B l = \left(\frac{1}{4}\dot{\theta}_1 + \frac{3}{4}\dot{\theta}_2\right) l, \end{aligned}\right\} \qquad (9—20)$$

or briefly

$$\dot{u}_\alpha = G\dot{\theta}_\alpha, \quad \text{where} \quad G = \frac{l}{4}\begin{bmatrix} 3 & 1 \\ 1 & 3 \end{bmatrix} \tag{9—20a}$$

From this equation

$$\dot{\theta}_\alpha = G^{-1}\dot{u}_\alpha, \quad \text{where} \quad G^{-1} = \frac{1}{2l}\begin{bmatrix} 3 & -1 \\ -1 & 3 \end{bmatrix} \tag{9—21}$$

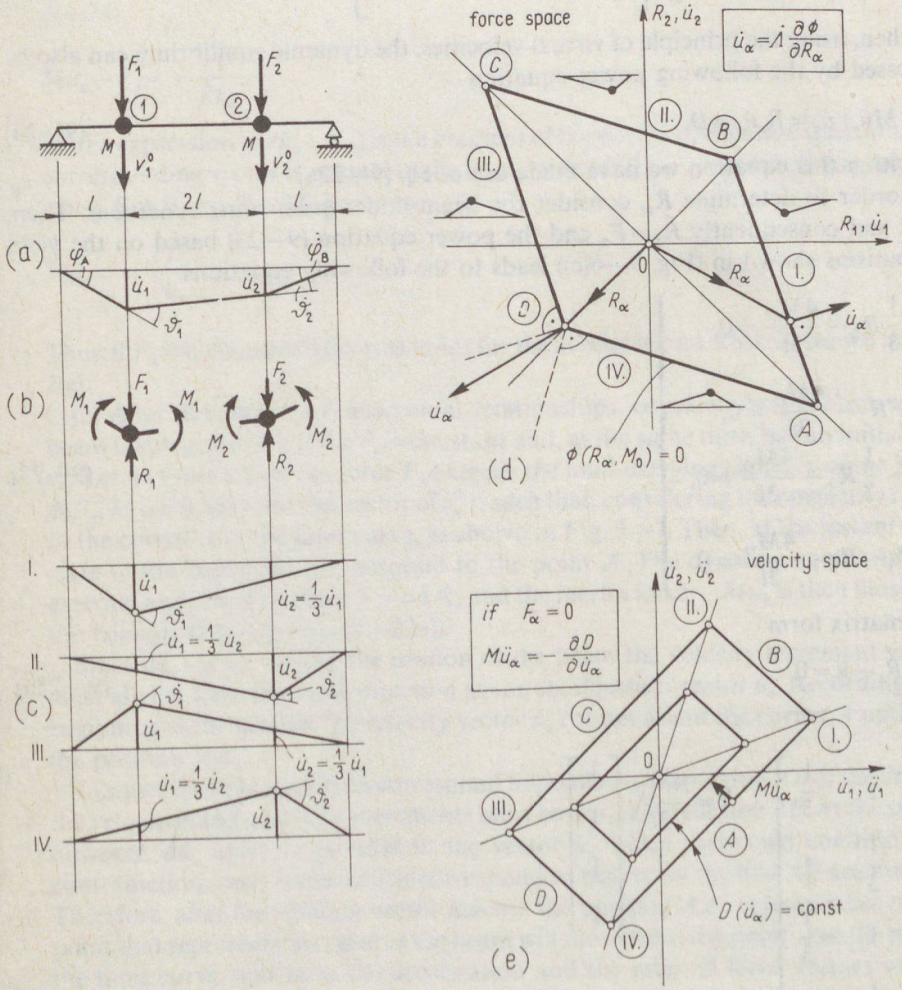


Fig. 9–6

Next, considering Fig. 9—6(b), the *dynamic equations* for the masses can be expressed in the following form

$$\left.\begin{aligned} F_1 - R_1 &= M\ddot{u}_1, \\ F_2 - R_2 &= M\ddot{u}_2, \end{aligned}\right\} \tag{9—22}$$

or in vector form

$$F_\alpha - R_\alpha = M\ddot{u}_\alpha. \tag{9—22a}$$

Here $R_\alpha(R_1, R_2)$ denotes the internal forces in the beam at the points $\alpha = 1,2$. Their magnitudes will be determined later.

Using eq. (9—21), the *energy dissipation function* for the beam becomes

$$D = M_0|\dot{\vartheta}_1| + M_0|\dot{\vartheta}_2| = \frac{M_0}{2}\left[|3\dot{u}_1 - \dot{u}_2| + |-\dot{u}_1 + 3\dot{u}_2|\right] \tag{9—23}$$

and then, using the principle of virtual velocities, the dynamic equilibrium can also be expressed by the following power equation

$$(F_\alpha - M\ddot{u}_\alpha)\,\dot{u}_\alpha = R_\alpha \dot{u}_\alpha = D. \tag{9—24}$$

In writing this equation we have made use of eq. (9—22a).

In order to determine R_α, consider the beam under *quasi-static conditions*. Then, $\ddot{u}_\alpha = 0$ and consequently $R_\alpha = F_\alpha$ and the power equation (9—23) based on the yield mechanisms shown in (Fig. 9—6(c)) leads to the following equations

$$\left.\begin{aligned} R_1 + \frac{1}{3}R_2 - \frac{4M_0}{3l} &= 0, \\ \frac{1}{3}R_1 + R_2 - \frac{4M_0}{3l} &= 0, \\ -R_1 - \frac{1}{3}R_2 - \frac{4M_0}{3l} &= 0, \\ -\frac{1}{3}R_1 - R_2 - \frac{4M_0}{3l} &= 0, \end{aligned}\right\} \tag{9—25}$$

or in matrix form

$$\phi = \mathbf{N}R_\alpha - \mathbf{k} = 0, \tag{9—25a}$$

where

$$\mathbf{N} = \begin{bmatrix} 1 & \frac{1}{3} \\ \frac{1}{3} & 1 \\ -1 & -\frac{1}{3} \\ -\frac{1}{3} & -1 \end{bmatrix}, \quad \mathbf{k} = \frac{4M_0}{3l}\begin{bmatrix} 1 \\ 1 \\ 1 \\ 1 \end{bmatrix}.$$

In the *force space* shown in (Fig. 9—6(d) eqs (9—25) are illustrated by four straight lines which bound the *feasible domain* of the internal forces R_α. This domain, defined in the general form $\phi(R_\alpha, M_0) \leq 0$, represents the load-carrying capacity of the beam subjected to the two-parameter quasi-static loading $F_\alpha(F_1, F_2)$. Considering eq. (9—24) for the *limit curve* $\phi(R_\alpha, M_0) = 0$ the *normality rule* holds, i.e. using eq. (9—25a) we have the relationship

$$\dot{u}_\alpha = \dot{\Lambda} \frac{\partial \phi}{\partial R_\alpha} = \dot{\Lambda} N. \tag{9—26}$$

Here $\dot{\Lambda} \geqq 0$ is a scalar multiplier.

In the *velocity space* shown in Fig. 9—6(e), the levels $D(\dot{u}_\alpha) =$ constant of the energy dissipation function given by eq. (9—23) are illustrated by rectangles. The lines of these *level curves* correspond to the corners of the limit curve and vice versa. According to eq. (9—24)

$$M\ddot{u}_\alpha - F_\alpha = -\frac{\partial D}{\partial \dot{u}_\alpha}, \tag{9—27}$$

i.e. the expression $[M\ddot{u}_\alpha - F_\alpha]$ is the gradient of the energy dissipation function, and the corresponding vector is normal to the level curves $D(\dot{u}_\alpha) =$ constant. In the special case when $F_\alpha = 0$, eq. (9—27) becomes

$$M\ddot{u}_\alpha = -\frac{\partial D}{\partial \dot{u}_\alpha}. \tag{9—28}$$

Thus, if $F_\alpha = 0$, the normality rule holds for the acceleration vector, as shown in Fig. 9—6(e).

(2) After deriving the fundamental relationships, consider the problem where the beam is subjected to a force $F_\alpha =$ constant and, at the same time, has an initial velocity v_α^0. Let us assume that the force F_α exceeds the load-carrying capacity of the beam, i.e. $\phi(F_\alpha, M_0) > 0$, and that the vector of v_α^0 is such that, considering the normality rule, it fits to the corner A of the limit curve, as shown in Fig. 9—7. Then, at the instant $t = 0$, the state of the beam must correspond to the point A. The dynamic equilibrium of the external and internal forces F_α and R_α and the inertia force $-M\ddot{u}_\alpha$ is then illustrated by the triangle OAG (see eq. (9—22a)).

Since $d\dot{u}_\alpha = \ddot{u}_\alpha dt$, during the motion of the beam the velocity increment vector $d\dot{u}_\alpha$ must always have the same direction as the acceleration vector $\ddot{u}_\alpha$. Accordingly, at the beginning of the motion the velocity vector $\dot{u}_\alpha$ rotates about the corner A until reaches the position AA_2.

In states of the beam which correspond to points on the portion AB of the limit curve, the velocities and also their increments must be normal to the line AB. At the same time, however, $d\dot{u}_\alpha$ must be parallel to the vector $\ddot{u}_\alpha$. Since these two conditions are in contradiction, such states which correspond to points on the line AB are not feasible. Therefore, after the velocity vector reaches the position AA_2, a *jump* takes place. The point that represents the state of the beam will move from the point A to the point B on the limit curve, and both the acceleration and the internal force vectors will have a *discontinuous change* in time.

In the state corresponding to the corner B on the limit curve, the phenomenon described above will be repeated. When $\dot{u}_\alpha$ reaches the direction BB_2, a jump takes place and the point that represents the state of the beam moves to the point E on the limit curve. In the state corresponding to this point, the velocity vector coincides with the acceleration vector, i.e. $\dot{u}_\alpha = \psi(t)\ddot{u}_\alpha$, where $\psi(t)$ is a scalar function of time. Therefore, during further response, only the magnitude of the velocity vector will increase by the increments $d\dot{u}_\alpha = \ddot{u}_\alpha dt$ while its direction remains unchanged. This means that the beam will undergo a *stationary motion* during which the shape of the velocity field and the internal force distribution remains unchanged.

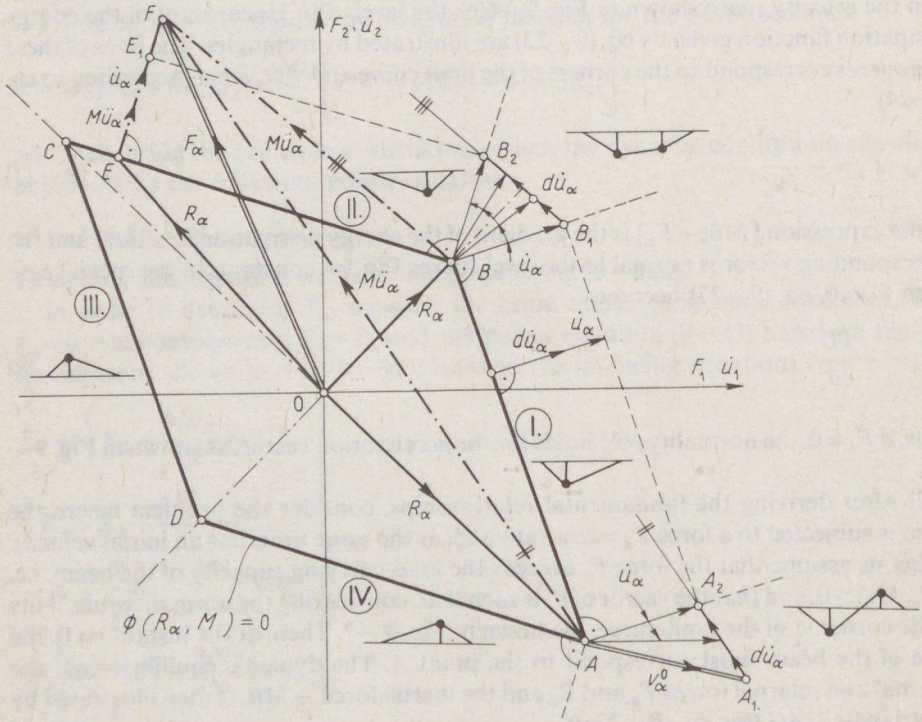


Fig. 9–7

From the above investigations, we conclude that during the dynamic response of a rigid-perfectly plastic structure

— the acceleration and internal force distribution fields may be *discontinuous* in time and

— under the action of constant external loads, the response tends towards a *stationary mode form motion* which is a *mode shape* of the structure.

(3) Next, consider the case of *impulsive loading*, i.e. where the one-parameter dynamic load $F_\alpha = F_\alpha^0 p(t)$ is replaced by an initial velocity field $v_\alpha^0 = \dfrac{I_o}{M} F_\alpha^0$ (Fig. 9—8a). Here the constant F_α^0 defines the ratio of the external forces and I_0 is the impulse of the external

load defined by eq. (9—5). Assuming the numerical values $F_\alpha^0(1, 2/3)$, the initial velocity vector $v_\alpha^0\left(\frac{I_0}{M}, \frac{2}{3}\frac{I_0}{M}\right)$ which corresponds to the normality rule fits in to the corner B on the limit curve shown in Fig. 9—8(b).

Consequently, at the instant $t=0$ the state of the beam must correspond to the point B. Then during the response the velocity vector changes, with the increments $d\dot{u}_\alpha$ being parallel to the acceleration vector $\ddot{u}_\alpha$ until $\dot{u}_\alpha$ reaches the direction BB_2. Then, for the reason described above, the point representing the state of the beam jumps from the point B to the point E, while $\ddot{u}_\alpha$ and R_α are changing discontinuously. At the point E the velocity vector coincides with the acceleration vector and therefore during further response only its magnitude will decrease while its direction remains unchanged. In this phase the beam undergoes a stationary mode form motion until the velocity diminishes to zero.

Figure 9—8(c) shows the level lines of the energy dissipation function given by eq. (9—23). Corresponding to relationship (9—28), during the motion the velocity increment vectors $d\dot{u}_\alpha = \ddot{u}_\alpha\, dt$ are normal to the level lines. Reaching the position OE_2, the velocity vector coincides with the acceleration vector and therefore during further response its direction remains unchanged. Thus, a stationary motion takes place until the beam comes to a standstill.

In the numerical solution to the problem, we have to investigate the two phases of the motion separately.

In the *first phase* $(0 \le t \le t_1)$, the state of the beam is defined by the point B in Fig. 9—8(b). Hence, according to the first relationship of eqs (9—25), $R_1 = R_2 = \frac{M_0}{l}$ and the equation of motion of the masses becomes

$$M\ddot{u}_1 = -\frac{M_0}{l}, \quad M\ddot{u}_2 = -\frac{M_0}{l}.$$

Considering the initial conditions $\dot{u}_1(0) = v_1^0 = \frac{I_0}{M}$ and $\dot{u}_2(0) = \frac{2}{3}\frac{I_0}{M}$, we obtain

$$M\dot{u}_1 = -\frac{M_0}{l}t + I_0, \quad M\dot{u}_2 = -\frac{M_0}{l}t + \frac{2}{3}I_0.$$

At the end of this phase

$$\dot{u}_2(t_1) = \frac{1}{3}\dot{u}_1(t_1)$$

and consequently

$$M\dot{u}_1(t_1) = -\frac{M_0}{l}t_1 + I_0, \quad \frac{1}{3}M\dot{u}_1(t_1) = M\dot{u}_2(t_1) = -\frac{M_0}{l}t_1 + \frac{2}{3}I_0,$$

from which

$$t_1 = \frac{I_0 l}{2M_0}, \quad \dot{u}_1(t_1) = \frac{I_0}{2M} \quad \text{and} \quad \dot{u}_2(t_1) = \frac{I_0}{6M}.$$

Finally, considering the initial conditions $u_1(0)=0$ and $u_2(0)=0$, we can calculate the displacements at the end of the first phase

$$u_1(t_1)=\frac{1}{M}\left[-\frac{M_0}{2l}t_1^2+I_0t_1\right]=\frac{3}{8}\frac{I_0^2l}{M_0M},$$

$$u_2(t_1)=\frac{1}{M}\left[-\frac{M_0}{2l}t_1^2+\frac{2}{3}I_0t_1\right]=\frac{5}{24}\frac{I_0^2l}{M_0M}.$$

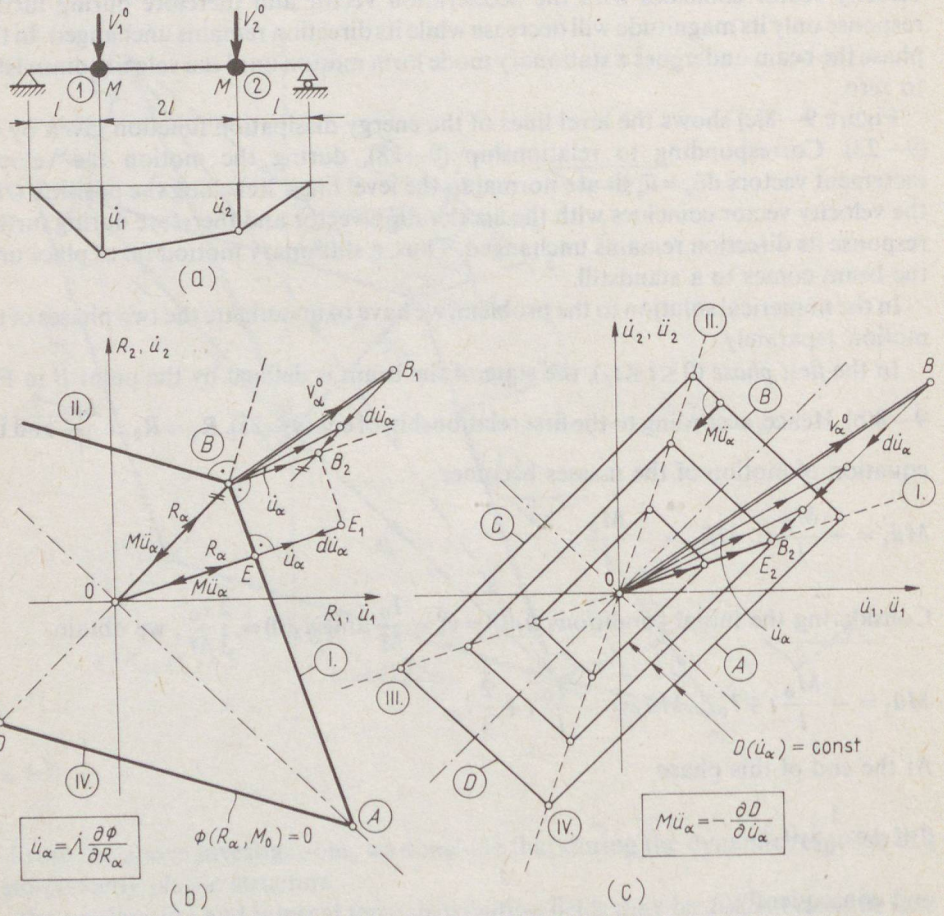


Fig. 9–8

In the *second phase* $[t_1 \le t \le t_2]$ the state of the beam is defined by the point E in Fig. 9—8(b). Hence, according to the first relationship of eqs (9—25), $R_1=3R_2=\frac{6}{5}\frac{M_0}{l}$ and $\dot{u}_1=3\dot{u}_2$. Then, the equation of motion of the mass 1 becomes

$$M\ddot{u}_1 = -\frac{6M_0}{5l}.$$

At $t=t_1$, $\dot{u}_1(t_1)=\frac{I_0}{2M}$ and consequently

$$M\dot{u}_1 = -\frac{6}{5}\frac{M_0}{l}t+\frac{I_0}{2}.$$

At $t=t_2$ the beam ceases to move, therefore $\dot{u}_1(t_2)=0.$. This leads to $t_2=\frac{5}{12}\frac{I_0 l}{M_0}$. Then, the displacements at $t=t_2$ become

$$u_1(t_2)=\frac{1}{M}\left[-\frac{6}{10}\frac{M_0}{l}t_2^2+\frac{I_0}{2}t_2\right]=\frac{5}{48}\frac{I_0^2 l}{M_0 M}.$$

$$u_2(t_2)=\frac{1}{3}u_1(t_1)=\frac{5}{144}\frac{I_0^2 l}{M_0 M}.$$

Finally, the solutions for the two phases provide the response time and the permanent displacements of the beam

$$\left.\begin{aligned} t_f &= t_1+t_2=\frac{I_0 l}{2M_0}+\frac{5}{12}\frac{I_0 l}{M_0}=0.91667\frac{I_0 l}{M_0},\\ u_{1f} &= u_1(t_1)+u_1(t_2)=\frac{3}{8}\frac{I_0^2 l}{M_0 M}+\frac{5}{48}\frac{I_0^2 l}{M_0 M}=0.47917\frac{I_0^2 l}{M_0 M},\\ u_{2f} &= u_2(t_1)+u_2(t_2)=\frac{5}{24}\frac{I_0^2 l}{M_0 M}+\frac{5}{144}\frac{I_0^2 l}{M_0 M}=0.2426\frac{I_0^2 l}{M_0 M}. \end{aligned}\right\} \quad (9—29)$$

9.3.3. TIME HISTORY ANALYSIS

9.3.3.1. GENERAL REMARKS

From the investigation of the two-degree-of-freedom model presented above, it is evident that analytical solutions for multi-degree-of-freedom structures subjected to general dynamic loading cannot be achieved. Instead, a step-by-step numerical procedure, called *time history analysis* has to be carried out, in which the response time is devided into sufficiently small time intervals, and for each time increment the corresponding increments in the state variables of the structure have to be determined. Hence, the basic problem in time history analysis is determining the acceleration field $\ddot{u}_i(x_j, t)$ at an instant t, when the velocity field $\dot{u}_i(x_j, t)$ is known. After solving this problem, the entire dynamic solution can be obtained by considering successive

instants, in which the velocity fields are determined from the velocities and accelerations at preceding instants by the use of the relationship $\dot{u}_i^{(n+1)} = \dot{u}_i^{(n)} + \ddot{u}_i^{(n)} \Delta t$.

In the case of rigid–perfectly plastic structures, difficulties arise from the possibility of time discontinuities in the acceleration field. Besides, where at the instant under consideration plastic flow starts to occur in the rigid regions, the stresses cannot be determined from eq. (9—9).

The time history analysis of rigid-perfectly plastic structures can be conducted by the use of extremum principles. Two of these extremum principles will be briefly presented next.

9.3.3.2. KINEMATIC PRINCIPLE

Suppose that at an instant t the state variables u_i, $\dot{u}_i$ and $\dot{q}_j$ of a rigid-perfectly plastic structure are known and consider kinematically admissible velocity fields $\dot{u}_i^k(x_j, t)$ defined for $t_1 \geq t$, wich fulfil the condition $\dot{u}_i^k = \dot{u}_i$ at time t. From the function $\dot{u}_i^k$ the velocity and acceleration fields $\dot{q}_j^k$, $\ddot{q}_j^k$ and $\ddot{u}_i^k$ can be derived and then *Tamuzh's principle*, which is the generalization of *Gauss' principle of least constraint* to rigid–plastic problems, states that the function

$$J(\ddot{u}_i^k) = \frac{1}{2}\int_S m\,\ddot{u}_i^k \ddot{u}_i^k \mathrm{d}S - \int_{S_T} T_i \ddot{u}_i^k \mathrm{d}S + \int_{S_1} Q_j^k \ddot{q}_j^k \mathrm{d}S + \int_{S_2} Q_j{}^* \ddot{q}_j^k \mathrm{d}S \qquad (9—30)$$

takes on its least value when $\ddot{u}_i^k = \ddot{u}_i$ (Tamuzh 1962). Here $\ddot{u}_i$ denotes the actual acceleration field in the structure at the instant t. In the function in eq. (9—30), S_1 denotes the domain where at the moment t, $\dot{q}_j = \dot{q}_j^k \neq 0$ and $d(\dot{q}_j^k)$ has continuous derivatives, while S_2 is the domain where at the moment t, $\dot{q}_j = \dot{q}_j^k = 0$ or $\dot{q}_j^k = 0$, but $d(\dot{q}_j^k)$ has discontinuous derivatives. In S_1 Q_j^k is defined by eq. (9—9) and in S_2 Q_j^* is associated with $\ddot{q}_j^k$ through eq. (9—7) if $\ddot{q}_j^k$ were a strain rate.

Using piecewise linear yield functions, Capurso modified Tamuzh's principle. Then the determination of the acceleration field became a quadratic programming problem (Capurso 1975).

9.3.3.3. DYNAMIC PRINCIPLE

Consider again the problem, described in Section 9.3.3.2 and let $\ddot{u}_i^d(x_j, t)$ and $Q_j^d(x_i, t)$ denote dynamically admissible acceleration and stress fields for $t_1 \geq t$ which satisfy the yield conditions at each point in the rigid-perfectly plastic structure.* Then, the principle derived by Martin states that the function

* The acceleration and stress fields are called dynamically admissible if they satisfy the dynamic equilibrium equations.

$$J(\ddot{u}_i^d) = \int_S m\ddot{u}_i^d u_i \mathrm{d}S \tag{9—31}$$

takes on its least value when $\ddot{u}_i^d = \ddot{u}_i$ (Martin 1972). Here again $\ddot{u}_i$ denotes the actual acceleration field in the structure at the instant t.

9.3.4. MODE APPROXIMATION

9.3.4.1. BASIC CONCEPTS

It was shown in Section 9.3.2.2 that the dynamic response or rigid-perfectly plastic structures subjected to a constant external pressure or to an initial velocity tends toward a stationary mode form motion. This mode form motion is defined by

$$\dot{u}_i^*(x_j, t) = \psi(t)\ddot{u}_i^*(x_j) = \dot{W}(t)u_i^m(x_j) \tag{9—32a}$$

where $\psi(t)$ and $\dot{W}(t)$ are functions of time and $u_i^m(x_j)$ is the *mode shape* of the structure.

The concept of the mode solution proposed by Martin and Symonds (1966) is based on two approximations:

— the pulse loading is replaced by impulsive loading with the initial velocity field $v_i^0(x_j)$ defined by eq. (9—6);

— the initial velocity field $v_i^0(x_j)$ is replaced by an other equivalent initial velocity field, which corresponds to a mode shape. This initial velocity field is expressed in the form

$$\dot{u}_i^*(x_j, 0) = \dot{W}(0)u_i^m(x_j) = V_0 u_i^m(x_j), \tag{9—32b}$$

where V_0 is a properly chosen initial velocity amplitude. Consequently, the mode approximation solves a different initial value problem and therefore does not satisfy the original initial conditions. The advantage of this approximation is that, after introduction of the modified initial condition, the structure undergoes solely mode form motion which can be solved in a simple closed form. The only problem is to select the mode shape $u_i^m(x_j)$ and to determine the initial velocity amplitude V_0.

9.3.4.2. SOLUTION TECHNIQUE

Let us suppose that the mode shape $u_i^m(x_j)$ used for the mode solution has already been selected. Then the problem is to find the velocity amplitude V_0. This amplitude can be chosen so as to provide a "best fit" to the given initial velocity field in a mean square sense, i.e. so as to minimize the expression

$$\Delta_0(V_0) = \frac{1}{2}\int_S m(v_i^0 - V_0 u_i^m)(v_i^0 - V_0 u_i^m)\mathrm{d}S. \tag{9—33}$$

This leads to the solution

$$V_0 = \frac{\int_S m v_i^0 u_i^m \mathrm{d}S}{\int_S m u_i^m u_i^m \mathrm{d}S}. \tag{9—34}$$

Using this parameter, the response time t_f and the parameter $W_f = W(t_f)$ can easily be obtained. Omitting the details, we obtain

$$t_f = \frac{\int_S m v_i^0 u_i^m \mathrm{d}S}{\int_S Q_j^m q_j^m \mathrm{d}S} = \frac{I_0}{p_k}, \tag{9—35}$$

$$W_f = W(t_f) = \frac{\left[\int_S m v_i^0 u_i^m \mathrm{d}S\right]^2}{2\int_S m u_i^m u_i^m \mathrm{d}S \int_S Q_j^m q_j^m \mathrm{d}S} = \frac{1}{2} K \frac{I_0^2}{p_k}, \tag{9—36}$$

where p_k is the kinematically admissible load multiplier associated with the displacement filed $u_i^m(x_j)$ and defined by eq. (9—10) and the constant K is expressed in the form

$$K = \frac{\int_S T_i^0 u_i^m \mathrm{d}S}{\int_S m u_i^m u_i^m \mathrm{d}S}. \tag{9—37}$$

Whenever W_f is known, the permanent displacements of the structure can be approximated as

$u_{if}(x_j) \approx W_f u_i^m(x_j)$.

The mode shapes form a class of kinematically admissible displacement fields. At constant external loads, the structure will reach one or other of these modes. For the selection of the mode shape which leads to the best approximation, different rules and methods have been suggested (Symonds 1978).

9.3.4.3. EXAMPLE

Let us consider again the impulsively loaded two–degree–of–freedom model shown in Fig. 9—8(a). As was shown in Section 9.3.2.2. the actual response of the structure corresponding to the initial velocity v_α^0 is characterized by the line B_1—B_2—O in the velocity space illustrated in Fig. 9—9. Applying the mode approximation, let us choose the first yield mechanism shown in Fig. 9—6(c) as a mode shape to be used in the solution. In the velocity space, the direction of the velocity vector corresponding to this mode shape is defined by the line OG. Choosing an arbitrary value for the initial velocity amplitude V_0, the corresponding initial velocity is represented by the vector

OF and the value of the Δ_0 function defined by eq. (9—33) is proportional to the distance B_1F. Thus, the least value of Δ_0 is obtained by the distance B_1H and the best value of V_0 is equal to the length OH.

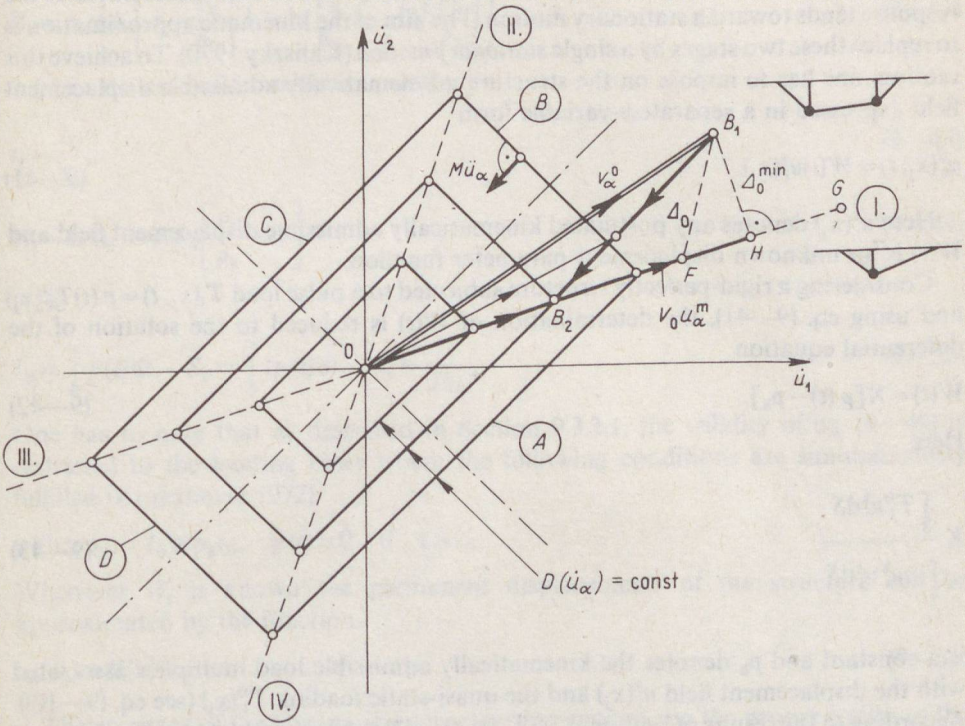


Fig. 9–9

Using the numerical data $v_\alpha^0 = \frac{I_0}{M}\left(1, \frac{2}{3}\right)$ and $u_\alpha^m\left(1, \frac{1}{3}\right)$, eqs (9—34)—(9—37) lead to the solution

$$V_0 = \frac{Mv_\alpha^0 u_\alpha^m}{Mu_\alpha^m u_\alpha^m} = 0.91667 \frac{I_0}{M},$$

$$t_f = \frac{Mv_\alpha^0 u_\alpha^m}{Q_\alpha^m q_\alpha^m} = 0.91667 \frac{I_0 l}{M_0}, \tag{9—38}$$

$$u_{1f} = W_f = \frac{[Mv_\alpha^0 u_\alpha^m]^2}{2[Mu_\alpha^m u_\alpha^m]\,[Q_\alpha^m q_\alpha^m]} = 0.50417 \frac{I_0^2 l}{M_0 M}, \tag{9—39}$$

$$u_{2f} = \frac{1}{3} W_f = 0.1680 \frac{I_0^2 l}{M_0 M}. \tag{9—40}$$

9.3.5. KINEMATIC APPROXIMATION

9.3.5.1. BASIC CONCEPTS

The response of rigid-perfectly plastic structures subjected to pulse or impulsive loading generally has two phases: first a non-stationary motion takes place but later the response tends toward a stationary motion. The aim of the kinematic approximation is to replace these two stages by a single *stationary motion* (Kaliszky 1970). To achieve this motion, one has to impose on the structure a kinematically admissible displacement field expressed in a separated–variable form

$$u_i^0(x_j, t) = W(t) u_i^k(x_j). \tag{9—41}$$

Here $u_i^k(x_j)$ denotes any postulated kinematically admissible displacement field and $W(t)$ is an unknown displacement parameter function.

Considering a rigid-perfectly structure subjected to a pulse load $T_i(x_j, t) = p(t) T_i^0(x_j)$ and using eq. (9—41), the determination of $W(t)$ is reduced to the solution of the differential equation

$$\ddot{W}(t) = K[p(t) - p_k]. \tag{9—42}$$

Here

$$K \frac{\int_S T_i^0 u_i^k \mathrm{d}S}{\int_S m u_i^k u_i^k \mathrm{d}S} \tag{9—43}$$

is a constant and p_k denotes the kinematically admissible load multiplier associated with the displacement field $u_i^k(x_j)$ and the quasi-static loading $T_i^0(x_j)$ (see eq. (9—10)). According to the results of Section 9.3.2.1. eq. (9—42) can be considered as the dynamic equation for a single mass point. Thus, the kinematic approximation reduces the problem to the solution of the equivalent quasi-static problem and to the analysis of the one-degree-of-freedom model described in Section 9.3.2.1.

9.3.5.2. RESPONSE TIME AND FINAL DISPLACEMENTS

As a consequence of the above statements, by means of a suitable change in the notations, the results presented in Section 9.3.2.1. for a one-degree-of-freedom model can be used in the application of the kinematic approximation as well. Hence,

(a) in the case of *rectangular pressure*

$$t_f = \frac{p_0}{p_k} t_0, \tag{9—44}$$

$$W_f = \frac{1}{2} p_0 t_0^2 K \left(\frac{p_0}{p_k} - 1 \right); \tag{9—45}$$

(b) in the case of *exponential pressure*

$$t_f = t_0 \ln\left(\frac{p_0}{p_k}\right), \tag{9—46}$$

$$W_f = p_0 t_0^2 K\left[1 - \frac{p_k}{p_0}\left(1 + \ln\frac{p_0}{p_k} + \frac{1}{2}\ln^2\frac{p_0}{p_k}\right)\right]; \tag{9—47}$$

(c) in the case of an *arbitrary pressure*

$$t_f = \frac{I_0}{p_k}, \tag{9—48}$$

$$W_f = W(t_f) = KS_0\left[\frac{p_e}{p_k} - 1\right]. \tag{9—49}$$

Here

$$I_0 = \int_0^{t_0} p(t)\mathrm{d}t, \quad S_0 = \int_0^{t_0} tp(t)\mathrm{d}t, \quad p_e = \frac{I_0^2}{2S_0}. \tag{9—50}$$

One has to note that as described in Section 9.3.2.1, the validity of eq. (9—49) is restricted to the loading cases where the following conditions are simultaneously fulfilled (Krajcinovic 1972)

$$p(0) \geq p_k, \quad I_0 \geq p_k t_0, \quad p(t) \equiv 0 \quad \text{if} \quad t > t_0.$$

Whenever W_f is known the permanent displacements of the structure can be approximated by the function

$$u_{if}(x_j) \approx W_f u_i^k(x_j). \tag{9—51}$$

The accuracy of the kinematic approximation depends on the proper choice of the kinematically admissible displacement field. It has been proved that eq. (9—48) gives a lower bound for the response time. Since $p_k \geq p_c$, from eq. (9—48) it is evident that the best lower bound can be obtained if p_k is equal to the collapse load multiplier p_c. For the final displacements a similar statement cannot be made. Still, even in this case, the use of the collapse mechanism obtained under quasi-static condition is recommended as giving the best approximation.

It can be proved that in the case of impulsive pressure, when in the mode approximation and in the kinematic approximation the same kinematically admissible displacement fields are used, both methods yield the same results. Hence, we can conclude that the kinematic solution is equally suitable for the analysis of pulse and impulsive loading and, as a special case, can provide the mode solution.

9.3.5.3. EXAMPLE

Consider again the two-degree-of-freedom model shown in Fig. 9—10(a). Assuming a pulse loading $F_\alpha = p(t)F_\alpha^0$, the exact solution to the problem is illustrated in Fig. 9—10(a). Here the triangle OAA_1 represents the dynamic equilibrium at the instant $t = 0$

and, while the forces are proportionally decreasing, the acceleration and velocity vectors rotate from the direction AA_1 to AA_3 and the model performs an unstationary motion. After this phase, however, the model undergoes stationary motion which corresponds to the yield mechanism I of Fig. 9—6(c).

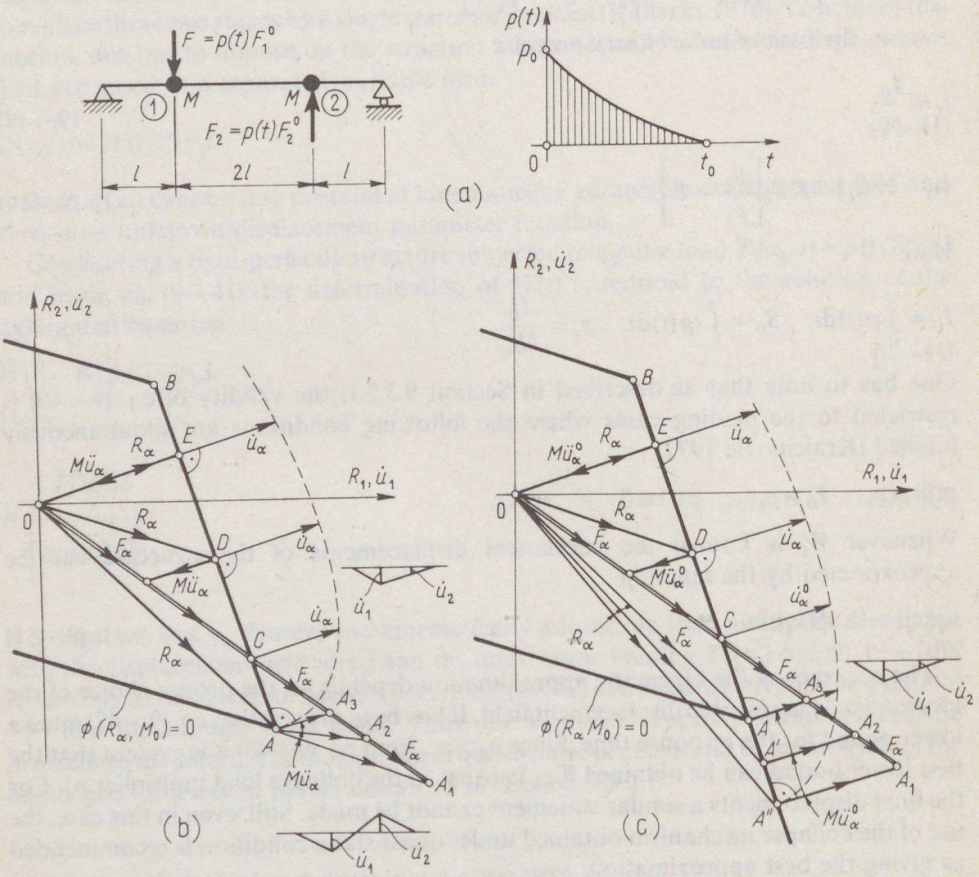


Fig. 9–10

Applying the kinematic approximation, first the quasi-static solution to the problem has to be determined. This is defined by the intersection of the vector F_α with the limit surface $\phi(R_\alpha, M_0)=0$, as shown in Fig. 9—10(c). The length OC gives the magnitude of the collapse load multiplier p_c, and the vector normal to the line AB corresponds to the collapse mechanism $\dot{u}_\alpha^0$ which may form the basis of the solution. Since the direction of $\dot{u}_\alpha^0$ does not change during the entire response, $\ddot{u}_\alpha^0$ must also be normal to the line AB. Hence, at the instant $t=0$, dynamic equilibrium can be achieved only if the vector R_α passes through the limit curve. This stage is valid only until the load intensity decreases

to the value OA_3. Thereafter R_α remains inside the limit curve and the motion of the model will be identical to that described in the exact solution.

We can conclude that in the kinematic approximation the yield condition may be violated in the first phase of the motion. This occurs in those cases where the peak value of the pulse load is large and therefore the end point of F_α does not remain inside the shaded regions I, II, III and IV shown in Fig. 9—11. Otherwise, exact solutions can be obtained by the use of the kinematic approach.

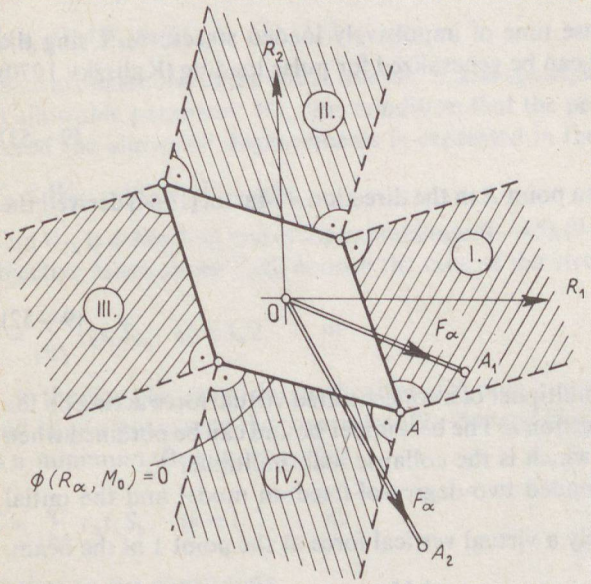


Fig. 9–11

Finally, let us consider the numerical values $P_\alpha^0\left(1, \frac{2}{3}\right)$ and the collapse mechanism I shown in Fig. 9—6(c). Then the corresponding kinematically admissible multiplier is $p_k = 1.0909 \frac{M_0}{l}$ and using the "square" load parameter function defined by eq. (9—2), (9—44) and (9—45) provide the following results

$$t_f = 0.916\,67 \frac{I_0 l}{M_0}, \tag{9—48}$$

$$W_f = 0.504\,17 \frac{I_0^2 l}{M_0 M} - 0.550\, I_0 t_0. \tag{9—49}$$

In the case of impulsive loading, i.e. when $t_0 \to 0$, these results are identical to those obtained by the mode approximation and given by eqs (9—38) and (9—39).

9.3.6. BOUNDING THEOREMS

A number of theorems to obtain bounds for the response time and on the final displacements of impulsively loaded structures has been published in the literature (e.g. Martin 1968, 1972; Symonds, Wierzbicki 1975). Here only the theorem based on the simple rigid-plastic theory will be briefly described.

The expression obtained by the mode approximation and given in the form

$$t_f = \frac{I_0}{p_k} \tag{9—50}$$

is a lower bound for the response time of impulsively loaded structures. Using the kinematic solution, this theorem can be generalized for pulse loading (Kaliszky 1970)

$$t_f \geq \frac{I(t_f)}{p_k}. \tag{9—51}$$

For a single final displacement at a point A in the direction n Martin (1964) derived the following upper bound

$$u^f_{An} \leq \frac{1}{2F_s} \int_S m v_i^0 v_i^0 \, dS. \tag{9—52}$$

Here F_s is a statically admissible multiplier of a concentrated virtual force acting on the structure at the point A in the direction n. The best upper bound can be obtained when F_s assumes its maximum value, which is the collapse load multiplier F_c.

Considering the impulsively loaded two-degree-of-freedom model and the initial velocity $v_\alpha^0 = \frac{I_0}{M}\left(1, \frac{2}{3}\right)$, let us apply a virtual vertical force at the point 1 of the beam. The collapse load intensity of this force is $F_c = \frac{4}{3}\frac{M_0}{l}$, so that using expression (9—52) the following upper bound can be calculated for the final vertical displacement at the point 1

$$u_{1f} - \frac{1}{F_c}\left[\frac{1}{2} M v_\alpha^0 v_\alpha^0\right] = 0.54167 \frac{I_0^2}{M M_0}. \tag{9—53}$$

9.3.7. OPTIMAL DESIGN

9.3.7.1. BASIC CONCEPTS

Only a few papers which deal with the optimal design of plastic structures exposed to dynamic pressure have been published (e.g. Reitman, Shapiro 1974; Lepik, Mróz 1977). In the following, an approximate method for the optimal design of perfectly plastic inhomogeneous structures subjected to pulse or impulsive loading will be presented. The solution is based on the kinematic approach (Heinloo, Kaliszky 1981).

It is assumed that the surface S of the rigid-perfectly plastic inhomogeneous structure under consideration is divided into regions S_k, $(k=1, 2, \ldots n)$ in which the density ρ_k, the specific cost c_k and the yield stress σ_0^k of the material are given constants. The size of S_k and the thickness of the structure (t_k), which is also constant in each region, are design variables restricted by the design constraints

$$S'_k \subset S_k \subset S''_k, \quad t'_k \leq t_k \leq t''_k. \tag{9—54}$$

Here S'_k, S''_k, t'_k, t''_k are prescribed bounds for S_k and t_k, respectively. Assuming different kinematically admissible displacement fields

$$u^0_{ih}(x_j, t) = W_h(t) u^k_{ih}(x_j), \quad (h=1, 2, \ldots m) \tag{9—55}$$

which are extended to the entire domain S, and specifying for each displacement mode an allowable parameter W_{0h}, the condition that the permanent displacements do not exceed the allowable displacements is expressed in the form

$$W_{fh} \leq W_{0h}, \quad (h=1, 2, \ldots m). \tag{9—56}$$

Here W_{fh} is defined by one of the expressions (9—45), (9—47) or (9—49). Finally, for the objective function we shall choose the cost of the structure which has the form

$$C = \sum_{k=1}^{n} c_k t_k S_k, \quad (k=1, 2, \ldots n). \tag{9—57}$$

In the case of optimal design the sizes of S_k and t_k are to be determined such that S_k, t_k and W_{fh} do not exceed the constraints (9—54) and (9—56) and the cost of the structure is a minimum. Briefly, minimize

$$C = \sum_{k=1}^{n} c_k t_k S_k, \quad (k=1, 2, \ldots n) \tag{9—58}$$

subject to the constraints

$$S'_k \subset S_k \subset S''_k, \quad t'_k \leq t_k \leq t''_k, \tag{9—59}$$

$$W_{fh} = K_h S_0 \left[\frac{p_e}{p_{kh}} - 1 \right] \leq W_{0h}, \quad (h=1, 2, \ldots m). \tag{9—60}$$

In eqs (9—58)–(9—60) p_{kh}, K_h, p_e and S_0 are defined by eqs. (9—10), (9—43) and (9—50). It can be seen that the optimal design is a mathematical programming problem.

9.3.7.2. EXAMPLE

Consider again the two-degree-of-freedom model shown in Fig. 9—12. Now we assume that the massless beam has clamped ends and is subjected to a square-type pulse loading defined by eq. (9—2) and by the vector $F^0_\alpha\left(1, \frac{2}{3}\right)$. The allowable final displacements for both mass points are identical and denoted by W_0.

The beam is divided by the masses into three regions S_1, S_2 and S_3. We assume that these regions are fixed and that their plastic moments M_{01}. M_{02} and M_{03} are unknown

constants. If the cost per unit length of the beam is proportional to the plastic moment, then the cost of the entire beam can be expressed in the form

$$C = M_{01} + 2M_{02} + M_{03}, \tag{9—61}$$

where the following restrictions are prescribed on the plastic moments

$$M_{01} \geq 0, \quad M_{02} \geq 0, \quad M_{03} \geq 0. \tag{9—62}$$

The problem is to determine the plastic moments such that the permanent displacements do not exceed the allowable value and the cost of the beam is a minimum.

In order to express the final displacements, four kinematically admissible displacement fields will be considered (see Fig. 9—12). The corresponding kinematically admissible load multipliers are

$$p_{k1} = \frac{3}{11l}(7M_{01} + M_{03}), \qquad p_{k3} = \frac{3}{11l}(M_{01} + 4M_{02} + 3M_{03}),$$

$$p_{k2} = \frac{3}{11l}(3M_{01} + 4M_{02} + M_{03}), \qquad p_{k4} = \frac{3}{11l}(M_{01} + 7M_{03}).$$

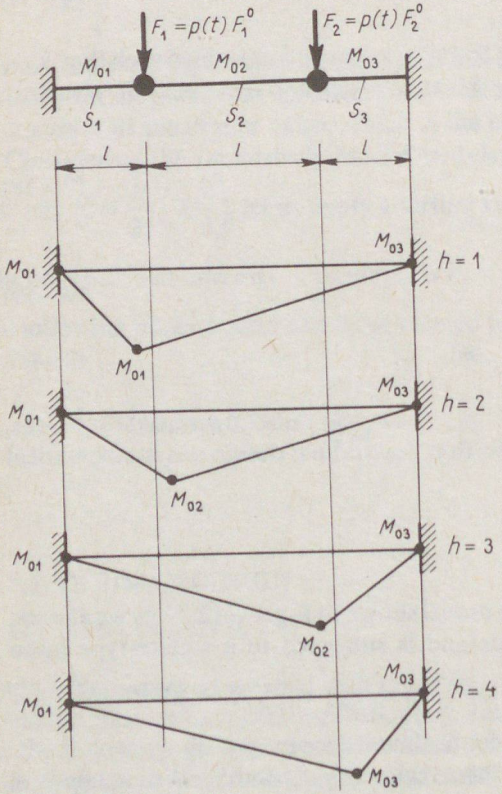


Fig. 9–12

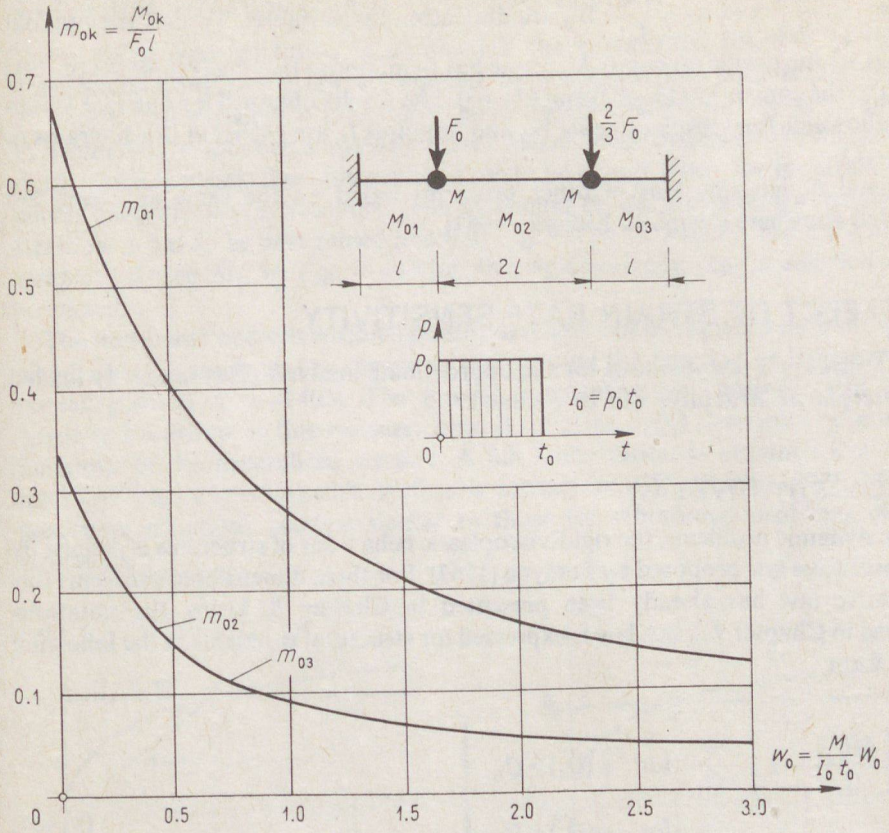


Fig. 9–13

From eq. (9—43) $K_1 = K_2 = \dfrac{11}{10M}$ and $K_3 = K_4 = \dfrac{9}{10M}$ and applying formula (9—60), for each yield mechanism the following inequalities can be obtained

$$\left.\begin{aligned}
7m_{01} + \quad\quad m_{03} &\geq \frac{2.016}{w_0 + 0.550}, \\
3m_{01} + 4m_{02} + m_{03} &\geq \frac{2.016}{w_0 + 0.550}, \\
m_{01} + 4m_{02} + 3m_{03} &\geq \frac{1.35}{w_0 + 0.450}, \\
m_{01} + \quad\quad 7m_{03} &\geq \frac{1.35}{w_0 + 0.450}.
\end{aligned}\right\} \qquad (9—63)$$

Here $m_{0k}=\dfrac{M_{0k}}{p_0 l}$ and $w_0=\dfrac{M}{I_0 t_0}W_0$ are dimensionless variables. To find the optimal solution for the plastic moments M_{0k}, one has to minimize the object function (9—61) subject to the constraints (9—62) and (9—63). The results obtained for different values of the allowable final displacements W_0 and impulses I_0 are ploted in the diagrams of Fig. 9—13.

Optimal design solutions of other problems based on the same approach are presented elsewhere (Heinloo, Kaliszky 1981).

9.4. EFFECT OF STRAIN RATE SENSITIVITY

In the following a few methods for the approximate analysis of dynamically loaded *rigid-viscoplastic* structures will be outlined.

9.4.1. CONSTITUTIVE LAW

In most dynamic problems, the rigid-viscoplastic behaviour of structures is defined by the constitutive law proposed by Perzyna (1963). For three dimensional problems this constitutive law has already been presented in Chapter 8. Using the notations described in Chapter 9.2, this law is expressed for structural problems in the following special form

$$\left.\begin{aligned} \dot{q}_j &= \dot{q}_0\left[\frac{\psi(Q_j)}{Q_0}-1\right]^n\frac{\partial\psi}{\partial Q_j} \quad \text{for} \quad \psi(Q_j)\geq Q_0,\\ \dot{q}_j &= 0 \qquad\qquad\qquad\qquad\quad \text{for} \quad \psi(Q_j)<Q_0. \end{aligned}\right\} \tag{9—64}$$

In the case of *simple bending*, $Q_j=M$, $Q_0=M_0$, $\dot{q}_j=\dot{\kappa}$, $\dot{q}_0=\dot{\kappa}_0=\dfrac{2\dot{\varepsilon}_0}{H}\left(1+\dfrac{1}{2n}\right)^n$, hence

$$\left.\begin{aligned} \dot{\kappa} &= (\operatorname{sign} M)\,\dot{\kappa}_0\left[\frac{|M|}{M_0}-1\right]^n\\ M &= (\operatorname{sign}\dot{\kappa})M_0\left[1+\left(\frac{|\dot{\kappa}|}{\dot{\kappa}_0}\right)\right]^{1/n} \quad \text{for } |M|\geq M_0,\\ \dot{\kappa} &= 0 \qquad\qquad\qquad\qquad\qquad\quad \text{for } |M|<M_0. \end{aligned}\right\} \tag{9—65}$$

Here $\dot{\kappa}$ is the curvature rate, H and M_0 are the thickness and plastic moment, respectively of the beam and n and $\dot{\varepsilon}_0$ denote viscous constants (e.g. for mild steel $\dot{\varepsilon}_0=40\ \mathrm{s}^{-1}$ and $n=5$). When $n=1$ we obtain the case of linear viscosity, and when $n\to\infty$ the behaviour approaches that of a rigid–plastic material with doubled yield stress (Fig. 9—14(a)).

9.4.2. LINEARIZATION OF THE CONSTITUTIVE LAW

The simplest approximation is obtained if the exponential function of the one-dimensional constitutive law is replaced by a straight line with zero slope (Fig. 9—14(b)). This provides a reasonably good approximation for higher strain rates. Perrone (1965) elaborated a quasi-iterative method, based on this idea in which first the rigid–perfectly plastic dynamic problem has to be solved. Then, for the strain rate, at which the correction is computed, the maximum or the time-average magnitude of strain rates has to be determined (see $\dot{\bar{\kappa}}$ in Fig. 9—14(b)). Finally, using the modified yield stress (see $\bar{M}_0$ in Fig. 9—14(b)), the rigid-perfectly plastic solution can be corrected.

The non-linear one-dimensional constitutive law can be replaced by a straight line which either is tangential to the curve representing the function or intersects it at a chosen point (Fig. 9—14(c)). The general constitutive law, however, can only be partially linearized in this manner, since it involves $\psi(Q_j)$ described by non-linear functions of the generalized stresses. A full linearization is obtained if a suitably modified statically admissible system is introduced (Wierzbicki 1977). Then, the governing equations become similar to those for vibrational problems of elastic structures.

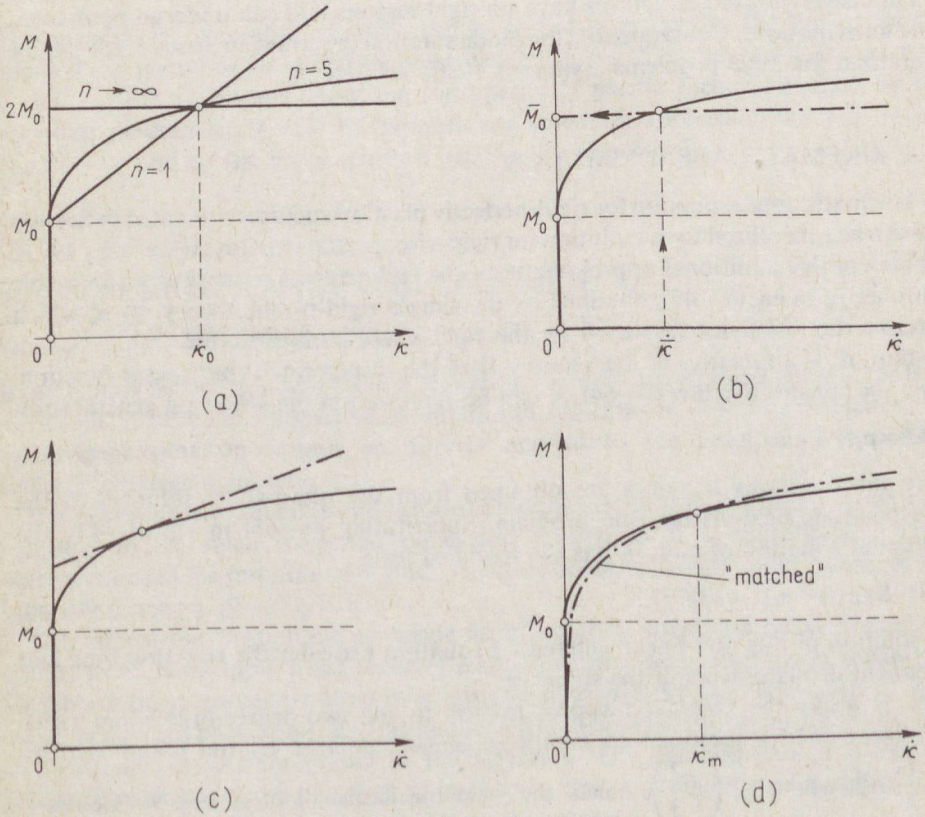


Fig. 9–14

9.4.3. MODE APPROXIMATION

Inhomogeneous stress-strain rate relationships do not allow mode form solutions in the sense of separated variable forms, that hold for the entire motion. Physically, this is due to the fact that the interfaces between the rigid and deformable regions of the structure are not fixed during the response. This difficulty may be overcome by the use of a *homogeneous viscous* rather than a rigid-viscoplastic constitutive law, replacing eqs. (9—64) and (9—65) by a "matched" viscous representation as below (Symonds, Cohn 1973)

$$\dot{\kappa}=(\text{sign } M)\dot{\kappa}'_0\left[\frac{|M|}{M'_0}\right]^{n'} \quad \text{or} \quad M=(\text{sign } \dot{\kappa})M'_0\left[\frac{|\dot{\kappa}|}{\dot{\kappa}'_0}\right]^{1/n'}. \tag{9—66}$$

Here $M'_0=\mu M_0$, $\dot{\kappa}'_0=\dfrac{4\dot{\varepsilon}_0}{H}$ and $n'=\nu n$. Choosing $\dot{\kappa}_m=\beta\dot{\kappa}'_0$ as a "matching" point (see Fig. 9—14(a)), μ and ν are determined by the relationships

$$\mu=\frac{1+\beta^{1/n}}{\beta^{1/n'}}, \quad \nu=\frac{1+\beta^{1/n}}{\beta^{1/n}}. \tag{9—67}$$

After the introduction of the homogeneous "matched" viscous constitutive law (9—66), the impulsively loaded structures have no rigid regions and can undergo permanent mode form motions. Consequently, the mode solution described in Section 9.34 can be generalized for these problems (Symonds 1980).

9.4.4. KINEMATIC APPROXIMATION

The kinematic approximation for rigid-perfectly plastic structures presented in Section 9.3.5 can be generalized to the solution for rigid-viscoplastic structures (Kaliszky 1973). The idea of this additional approximation is to replace the kinematically admissible multiplier p_k in eq. (9—42), obtained by the simple rigid-plastic theory, by p_k^v which expresses the resistance displayed by the rigid-viscoplastic structure. While p_k is a constant, p_k^v is a function of the velocity $\dot{W}$ of the displacement parameter function. Using the constitutive law (9—64), p_k^v can be expressed in the following general form

$$p_k^v(\dot{W})=p_k(1+a\dot{W}^\alpha), \tag{9—68}$$

where the constants a and α are obtained from the quasi-static solution to the corresponding rigid-viscoplastic problem. Substituting (9—68) in eq. (9—42), the differential equation of motion has the modified form

$$\ddot{W}(t)=K[p(t)-p_k(1+a\dot{W}^\alpha)]. \tag{9—69}$$

The solution of this non-linear differential equation provides the response time and permanent displacements of the structure.

Let us apply the kinematic approximation to the two-degree-of-freedom rigid-viscoplastic model subjected to *impulsive loading*, defined by the initial velocity $v_\alpha^0=\dfrac{I_0}{M}F_\alpha^0$, where $F_\alpha^0\left(1\,\dfrac{2}{3}\right)$. Select the yield mechanism I of of Fig. 9—6(c) as a

kinematically admissible displacement field. Then, the kinematically admissible load multiplier of the rigid–viscoplastic model associated with the assumed yield mechanism can be calculated by making use of eq. (9—65)

$$p_k^v = \frac{12}{11}\frac{M_0}{l}\left[1+\left(\frac{4}{3}\frac{H}{l}\right)^{1/n}\left(\frac{\dot{w}}{\dot{\kappa}_0}\right)^{1/n}\right]. \tag{9—70}$$

Here H is the thickness of the beam, $\dot{w}=\dot{W}/H$ and $\dot{\kappa}_0=\frac{2\dot{\varepsilon}_0}{H}\left(1+\frac{1}{2n}\right)^n$. Let us assume the numerical values $n=5$, $\dot{\varepsilon}_0=40\,\mathrm{s}^{-1}$ and $H/l=0.25$ and modify the differential equation (9—69) so that $p(t)=0$ but an equivalent initial velocity $V_0=KI_0$ is taken into account. Then, the following equation can be derived for the problem under consideration

$$\frac{\mathrm{d}^2w}{\mathrm{d}t^2}+0.9917\frac{v_0^2}{\lambda}\left[1+0.3036\left(\frac{\mathrm{d}w}{\mathrm{d}t}\right)^{1/5}\right]=0, \tag{9—71}$$

where

$$w=\frac{W}{H},\quad v_0=\frac{W_0}{H}\quad\text{and}\quad \lambda=\frac{I_0^2 l}{MM_0H}. \tag{9—72}$$

This non-linear differential equation can be solved numerically. The final displacements of the point 1 of the model are presented in Fig. 9—15 by diagram 4. Diagrams 1, 2 and 3 show the results using the rigid-perfectly plastic theory obtained by the bounding theorem (eq. 9—53), by the mode and kinematic approximations (eqs 9—39) and (9—49) and by the exact solution (eq. 9—29), respectively.

9.5. EFFECT OF LARGE DISPLACEMENTS

9.5.1. MODE APPROXIMATION

It can readily be seen that when non-linear terms for finite deflections appear in the field equations, it becomes impossible to obtain full solutions in mode form. Hence, the mode approximation cannot be directly applied to the analysis of structures undergoing large deformations.

It is possible to obtain quasi-mode form solutions that start out as simple mode form solutions in the small deflection range and take account of the effects of large deformations as the response continues. In these solutions the minimum Δ_0 choice can be applied (see eq. (9—33)).

The aim of the "instantaneous mode form" solution suggested by Symonds and Chon (1978) is to apply a sequence of instantaneous mode solutions in separated-variable form to successive time intervals. These satisfy the field equations at each stage, but do not provide a smoothly connected system of solutions, since continuity is imposed only at certain points in the structure. This method should provide a satisfactory simple approximation, at least for a structure whose configuration does not change in considerable manner during the response.

9.5.2. KINEMATIC APPROXIMATION

The kinematic approximation can be generalized to structures undergoing moderately large displacements (Kaliszky 1973). The idea of this further approximation is to replace in eq. (9—42) the kinematically admissible multiplier p_k, obtained by the simple rigid-plastic theory, by another one denoted by p_k^1, which expresses the resistance displayed by the structure undergoing large deflections. While p_k is a constant, p_k^1 can be expressed in terms of the displacement parameter function $p_k^1 = p_k^1(W)$. In most cases this function can be written in the following general form

$$p_k^1(W) = p_k(1 + bW^\beta). \tag{9—73}$$

Here the constants b and β are obtained from the quasi-static solution to the problem, taking into consideration the effects of deflections. Substituting (9—73) in eq. (9—42), the differential equation of motion has a modified form

$$\ddot{W}(t) = K[p(t) - p_k(1 + bW^\beta)]. \tag{9—74}$$

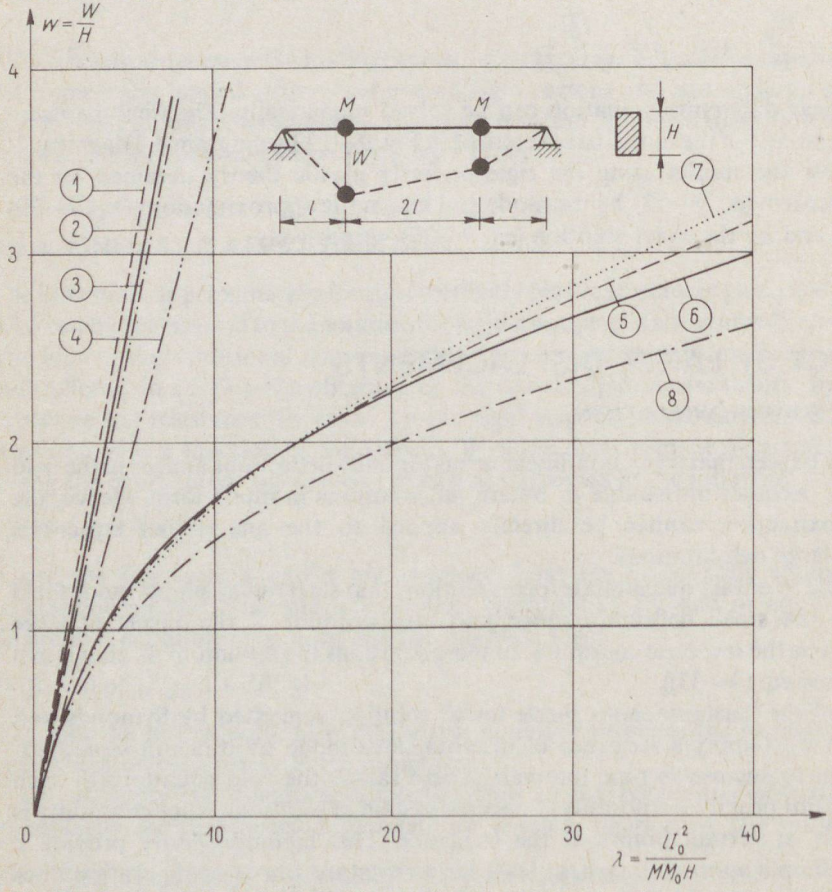


Fig. 9–15

By the combination of eqs (9—69) and (9—74), the kinematic approach can be extended to the dynamic analysis of problems in which both the effect of strain rate sensitivity and the influence of large displacements are taken into consideration. Then, the differential equation of motion has the following general form

$$\ddot{W}(t)=K[p(t)-p_k(1+a\dot{W}^{\alpha})(1+bW^{\beta})]. \tag{9—75}$$

9.5.3. BOUNDING THEOREM

The bounding theorem described below was proposed by Ploch and Wierzbicki (1974) for impulsively loaded rigid-perfectly plastic structures undergoing moderately large deformations.

Let us apply a quasi-static concentrated virtual force F_s to the structure at the point A in the direction n and denote the corresponding statically admissible stress and displacement fields by σ_{ij}^s and u_i^s. The system F_s, σ_{ij}^s has to satisfy the equilibrium equations and yield conditions, taking into consideration the second-order effects caused by the assumed displacements u_i^s. Then, an upper bound for a single final displacement of the point A in the direction n can be obtained as

$$u_{An}^f \leq \frac{1}{F_s}\left[\frac{1}{2}\int_S m v_i^0 v_i^0 \mathrm{d}S + \frac{1}{2}\int_V \sigma_{ij}^s u_{i,j}^s u_{j,i}^s \mathrm{d}V\right], \tag{9—76}$$

where v_i^0 is the initial velocity field corresponding to the impulsive loading. When the effect of large deformations is neglected, the second term of the right side equals zero and (9—76) gives the bound (9—52) derived by Martin for structures with small deformations.

9.5.4. EXAMPLE

Consider again the two-degree-of-freedom model subjected to impulsive loading defined by the initial velocity $v_\alpha^0 = \frac{I_0}{M} F_\alpha^p$, where $F_\alpha^p\left(1, \frac{2}{3}\right)$. Suppose that the beam is fully restrained from axial motion and for its rectangular cross-section the yield condition has the form

$$f = \frac{|M|}{M_0} + \left(\frac{N}{N_0}\right)^2 - 1 = 0. \tag{9—77}$$

Here $M_0 = \frac{H^2}{4}\sigma_0$ and $N_0 = H\sigma_0$ denote the fully plastic moment and axial force, respectively, and H is the height of the beam.*

* The width of the beam is assumed to be equal to the unit

(a) First, let us apply the kinematic approximation and assume the kinematically admissible velocity field shown in Fig. 9—16(a). Considering moderately large deflections and the notations of the Figure, the following geometrical relationships can be obtained

$$\varphi_1=\frac{3}{4}\theta,\quad \varphi_2=\frac{1}{4}\theta,\quad W=\varphi_1 l=\frac{3}{4}\theta l,$$
$$e=e_1+e_2=W\varphi_1+W\varphi_2=W\theta. \tag{9—78}$$

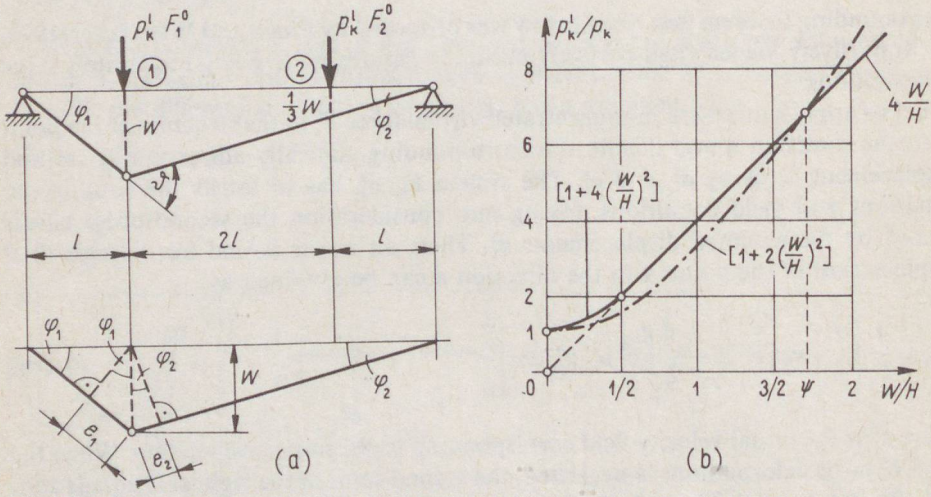


Fig. 9–16

The normality rule and the yield condition (9—77) lead to

$$\frac{e}{\theta}=\frac{\dfrac{\partial f}{\partial N}}{\dfrac{\partial f}{\partial M}}=2\frac{M_0}{N_0}\frac{N}{N_0}=\frac{H}{2}\frac{N}{N_0}, \tag{9—79}$$

or making use of the last relationship of eqs (9—78)

$$W=\frac{H}{2}\frac{N}{N_0}. \tag{9—80}$$

Finally, applying the principle of virtual displacements to the yield mechanism we get

$$p_k^1\left(W+\frac{2}{9}W\right)=M\theta+Ne. \tag{9—81}$$

Substituting eqs (9—78)—(9—80) in this relationship, the kinematically admissible load multiplier can be obtained

$$p_k^1=p_k\left[1+4\left(\frac{W}{H}\right)^2\right]. \tag{9—82}$$

Here $p_k = \frac{12}{11}\frac{M_0}{l}$ denotes the kinematically admissible multiplier calculated on the basis of the small deformation theory.

The relationship (9—80) is only valid, however, when $N \leq N_0$, i.e. $W \leq \frac{H}{2}$. If $W > \frac{H}{2}$, $N = N_0$ and $M = 0$, therefore eq. (9—82) has to be replaced by another equation also derived from eq. (9—81). This is

$$p_k = 4p_k \frac{W}{H}. \tag{9—83}$$

The relationships (9—82) and (9—83) are illustrated in Fig. 9—16(b).

In the range of larger deflections, a good approximation can be expected from the use of (9—83). Then, the differential equation (9—74) becomes

$$\frac{d^2w}{dt^2} + 3.967\frac{v_0^2}{\lambda}w = 0 \tag{9—84}$$

and after its solution the final value of the displacement parameter function is

$$w_f = \frac{W_f}{H} = 0.5021\sqrt{\lambda},$$

where

$$\lambda = \frac{I_0^2 l}{M M_0 H}. \tag{9—85}$$

This result is illustrated in Fig. 9—15 by diagram 5.

(b) Eqs (9—82) and (9—83) can be approximated by the single equation

$$p_k^1 = p_k\left[1 + 2\left(\frac{W}{H}\right)^2\right]. \tag{9—86}$$

The differential equation (9—74) then has the form

$$\frac{d^2w}{dt^2} + 0.9917\frac{v_0^2}{\lambda}[1 + 2w^2] = 0. \tag{9—87}$$

The results of the numerical solution of this non-linear differential equation are given in Fig. 9—15 by diagram 6.

(c) Solving the same problem by the use of the bounding theorem described in Section 9.5.3, the following upper bound is obtained

$$w_f = \frac{W_f}{H} = 0.5204\sqrt{\lambda}. \tag{9—88}$$

This upper bound is illustrated in Fig. 9—15 by diagram 7.

(d) Finally, consider the problem where both the effect of strain rate sensitivity and the influence of large deformations are taken into consideration. Using the kinematic

approach and eq. (9—75), by the combination of eqs (9—71) and (9—87) the following differential equation is obtained

$$\frac{d^2w}{dt^2}+0.9917\frac{v_0^2}{\lambda}\left[1+2w^2\right]\left[1+0.3036\left(\frac{dw}{dt}\right)^{1/5}\right]=0. \tag{9—89}$$

The numerical solution of this non-linear differential equation gives the final displacements illustrated in Fig. 9—15 by diagram 8.

9.6. EFFECT OF ELASTIC DEFORMATIONS

9.6.1. GENERAL REMARKS

The exact dynamic analysis involving elastic and plastic deformations is more difficult than the elastic, the rigid-plastic or the rigid-viscoplastic solutions. In the elasto-plastic structure, several plastic regions may develop which increase or decrease in size during the response. This complicated behaviour can be followed only by numerical methods. Next, two simple approximate methods will be briefly described.

9.6.2. MODE APPROXIMATION

The concept of this approach proposed by Symonds (1980) is to divide the response of the structure into two sharply-separated phases; in the first phase, the structure performs solely linear elastic deformations, while in the second phase a rigid-plastic behaviour is assumed.

The linear elastic phase is treated by the elastic dynamic equations. This phase is terminated at time t_1 when a global criterion of plastic yielding is satisfied. For this purpose a "*global average stress*" has to be calculated from the elastic stresses in the regions where plastic flow occurs.

In the rigid–plastic phase, an appropriate mode form has to be assumed, expressed in a separated–variable form $W(t)\,u_i^m(x_j)$. The initial velocity amplitude V_0 is determined from the elastic velocity field $\dot{u}_i^e(x_j,t_1)$ by minimizing the "difference" function Δ_0, as described in Section 9.3.4.2. Finally, the response time and the maximum displacements of the elasto–plastic structure are equal to the sum of the corresponding values of the elastic and plastic phases.

In the method described, the effect of strain rate sensitivity can also be taken into consideration and the solution has been extended to the analysis of large plastic deformations, as well.

9.6.3. KINEMATIC APPROXIMATION

The idea of the solution is again to impose a kinematically admissible displacement field $u_i^k(x_j)$ on the structure, but now the domains of the structure which perform deformations are elasto-plastic rather than perfectly plastic (Kaliszky, Duong 1984). Then, during the entire response the structure undergoes stationary displacements expressed in the form $u_i^0(x_j,t)=W(t)u_i^k(x_j)$. For example, in the case of frames the

kinematically admissible displacement field is obtained by introducing *elasto–plastic hinges* while the other parts of the frame are assumed to be perfectly rigid. The elastic properties of the hinges can be calculated approximately from the elastic stiffnesses of the neighbouring parts of the frame, and their plastic properties are determined from the plastic moments of the cross-sections. This frame undergoes only stationary displacements during the entire response, and forms a one-degree-of-freedom system. Still, the states of the hinges are changing; some of them are in elastic state and others in plastic state during the response, and therefore the resistance displayed by the system is not constant. Therefore a step-by-step time history analysis is needed for the solution to the problem.

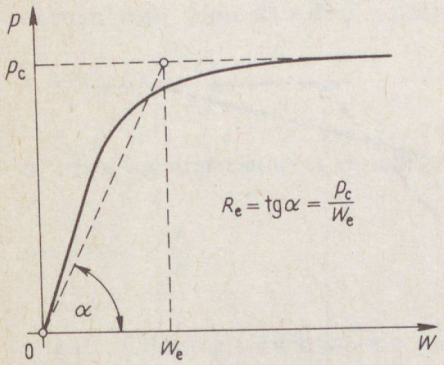


Fig. 9–17

The computational work can be further reduced by introducing the concept of the "*global average elastic stiffness*" of the structure. Let us suppose that the elasto-plastic solution of the structure subjected to the quasi-static loading $p(t)T_i^0(x_j)$ is known, and that the relationship between the load parameter p and the displacement W of a chosen point in the structure is also given (Fig. 9—17). Then the "global average elastic stiffness" of the elasto-plastic structure can be chosen: $R_e = p_c/W_e$, where p_c is the collapse load parameter and W_e is an appropriately chosen value of the displacements. Now, imposing the collapse mechanism on the structure, two phases of motion can be distinguished, described by the following two differential equations:

$$\text{if} \quad W < W_e, \quad \text{then} \quad W(t) = K\left[p(t) - \frac{p_c}{W_e} W(t)\right], \tag{9—90}$$

$$\text{if} \quad W \geq W_e, \quad \text{then} \quad W(t) = K[p(t) - p_c]. \tag{9—91}$$

The solution of these differential equations provides the maximum displacements of the elasto-plastic structure under consideration.

To illustrate the application of the kinematic method, consider the two-degree-of-freedom model. We assume that the ends of the beam are clamped and that the constant flexural stiffness is denoted by EJ (Fig. 9—18(a)). The pulse load $p(t)F_\alpha^0\left(1, \frac{2}{3}\right)$ is

replaced by impulsive loading, characterized by the impulse I_0. The relationship between the load multiplier p and the displacement W of the point 1 of the beam determined under quasi-static conditions is shown in Fig. 9—18(b). To obtain the "global average elastic stiffness" of the model we chose $W_e = 0.620 \frac{M_0 l^2}{EJ}$ and then $R_e = \frac{p_c}{W_e} = 3.519 \frac{EJ}{l^3}$. Using the collapse mechanism of Fig. 9—18(c) and eqs (9—90) and (9—91), we obtain the differential equations of motion which can be solved analytically. The maximum displacements of the point 1 of the beam are plotted in Fig. 9—18(d).

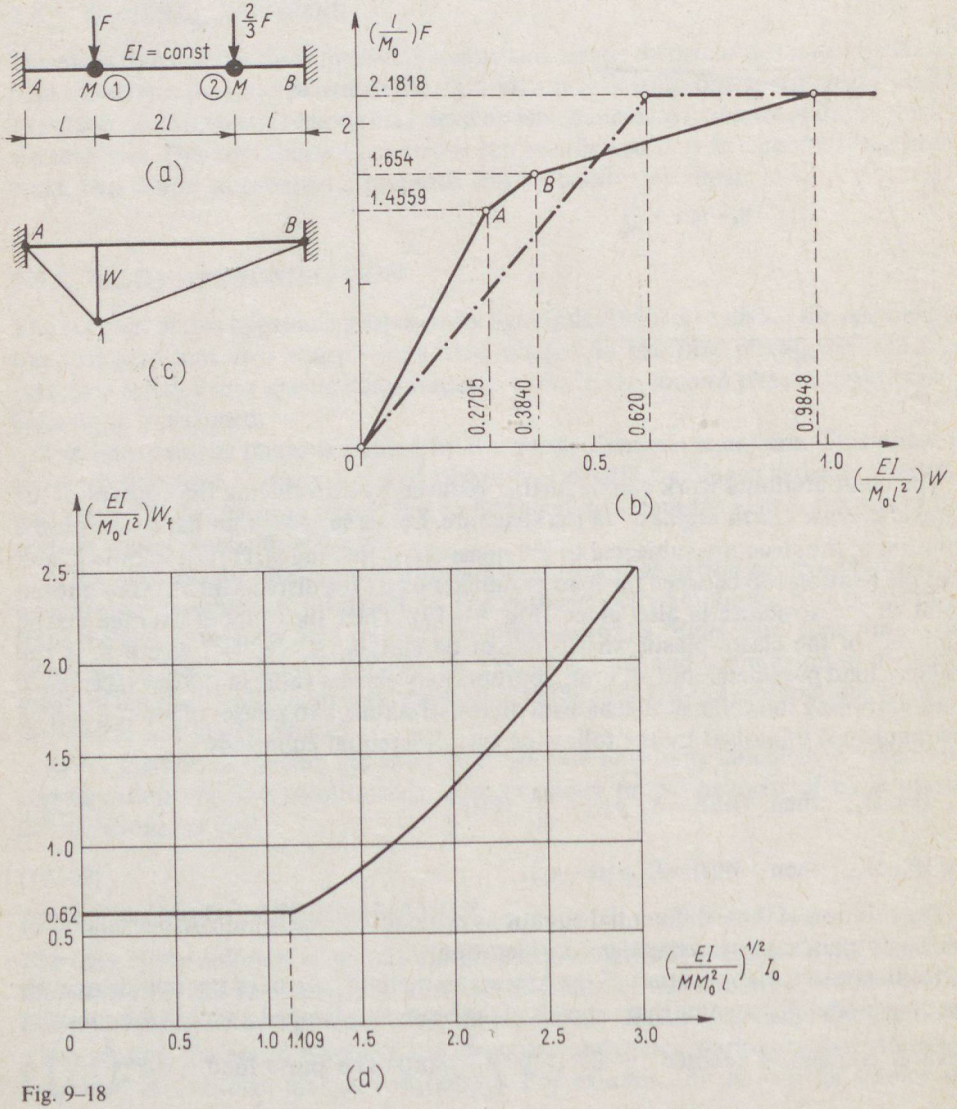


Fig. 9–18

9.7. APPLICATIONS

Next, a few applications of the kinematic approximation will be briefly presented. The details of these solutions have been published in the literature (Kaliszky 1970; 1972; 1973; Heinloo, Kaliszky 1981; Kaliszky 1981; Kaliszky 1984).

9.7.1. CIRCULAR PLATE

Consider a simply supported circular plate of radius R, thickness H, constant mass per unit surface area m and plastic moment per unit length M_0. Applying the kinematic approximation, let us assume for the transverse deflections of the middle surface the kinematically admissible displacement field

$$U = W(t)\left(1 - \frac{r}{R}\right),$$

or using the dimensionless variables $u = \frac{U}{H}$ and $w(t) = \frac{W(t)}{H}$

$$u = w(t)\left(1 - \frac{r}{R}\right). \tag{9—92}$$

In the following, we will consider pulse and impulsive loading and will take the effects of large deformations and viscosity into consideration.

(a) Considering a *uniformly distributed pulse load* and the Tresca or the square yield condition, the kinematically admissible multiplier of the rigid-perfectly plastic plate with small deflections becomes

$$p_k = \frac{6M_0}{R^2}, \tag{9—93}$$

and the constant K defined by eq. (9—43) is $K = \frac{2}{m}$.

Taking the effect of moderately large deflections into consideration, the external force-displacement relationship can be determined under quasi-static conditions (Wierzbicki, Florence 1970) and is expressed as

$$p_k^1 = p_k\left(1 + \frac{1}{3}w^2\right). \tag{9—94}$$

Then, assuming a rectangular pressure given by eq. (9—2) and using eq. (9—74), the differential equation of motion of the rigid-perfectly plastic plate with moderately large deflections has the form

$$\frac{d^2w}{d\tau^2} + \frac{\lambda}{3\eta^2}\left(1 + \frac{1}{3}w^2\right) = \delta\frac{\lambda}{3\eta}, \tag{9—95}$$

where

$$\tau=\frac{t}{t_0},\quad \eta=\frac{p_0}{p_k},\quad \lambda=\frac{I_0^2R^2}{mM_0H}$$

and

$$\delta=1,\ \text{if}\ 0\le\tau\le1;\quad \delta=0,\ \text{if}\ \tau>1.$$

Solving this non linear differential equation numerically, the maximum permanent deflections W_f of the mid-point of the plate can be expressed as functions of the parameters λ and η. The results are plotted in Fig. 9—19. The limit case $\eta\to\infty$ gives the solution for an impulsively loaded plate with a uniformly distributed initial velocity field.

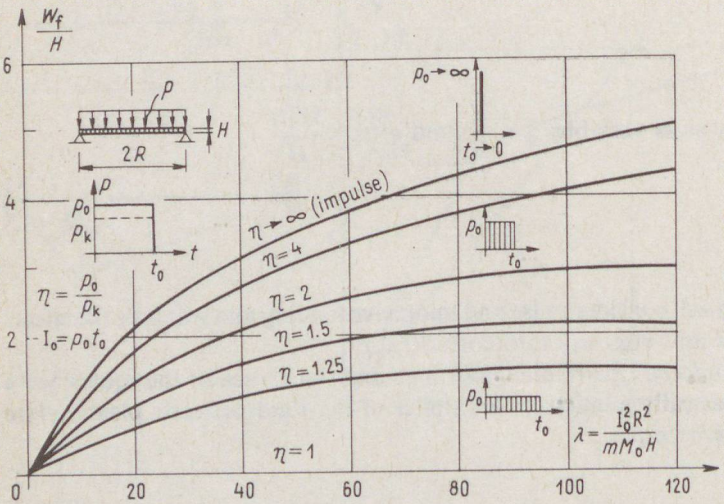


Fig. 9–19

As a special case, the permanent deflections of the rigid-perfectly plastic plate with small deformations are illustrated in Fig. 9—20. Comparison of the diagrams of Fig. 9—19 and Fig. 9—20 shows that at larger deflections the effect of deformations significantly influences the dynamic response of the plate. Similarly, assuming a constant impulse I_0, the duration t_0 of the pressure also plays an important role; the smaller t_0 is, the larger are the permanent deflections are. Thus, the maximum permanent displacements are obtained by the use of impulsive loading. This means that replacing the pulse load by an impulsive load leads to a safe approximation.

(b) Next, let us consider *impulsive loading* and assume the initial velocity field as follows

$$V=V_0\left(1-\frac{r}{R}\right),\qquad (9—96)$$

where $V_0=\dfrac{I_0}{m}$.

Using the linear constitutive equation of rigid-viscoplastic materials given by eq. (8—67), the external force-displacement relationship of the plate determined under quasi-static conditions is expressed as

$$p_k^v = p_k\left(1+\beta\frac{\dot{w}}{v_0}\right). \tag{9—97}$$

Here $\beta = 0.8\left(\frac{HV_0}{\dot{\gamma}_0 R^2}\right)$ and $v_0 = \frac{V_0}{H}$.

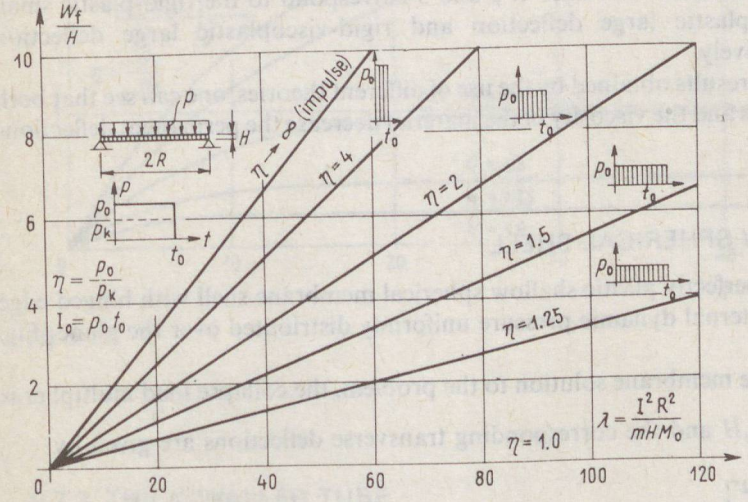


Fig. 9–20

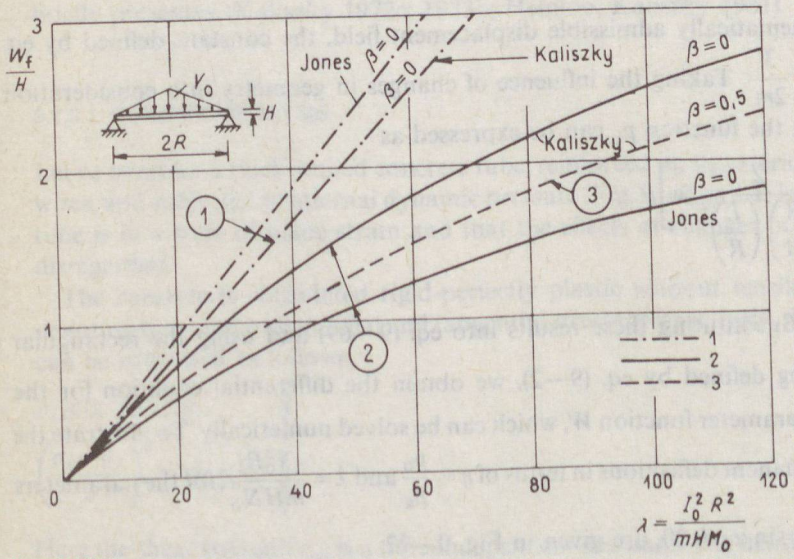


Fig. 9–21

The relationships (9—94) and (9—97) make it possible to take both the effect of large deflections and the influence of strain-rate sensitivity into consideration. Then, eq. (9—75) becomes

$$\ddot{w}+\frac{12v_0}{\lambda}\left(1+\frac{1}{3}w^2\right)\left(1+\beta\frac{\dot{w}}{v_0}\right)=0.$$

The numerical solution of this non-linear differential equation provides the results shown in Fig. 9—21. Here, for the sake of comparison, the results obtained by Jones (1968) are also illustrated. The lines 1, 2 and 3 correspond to the rigid-plastic small deflection, rigid-plastic large deflection and rigid-viscoplastic large deflection solutions, respectively.

Comparing the results obtained by the use of different theories, one can see that both large deformations and the viscosity of the material decrease the permanent deflections of the plate.

9.7.2. SHALLOW SPHERICAL SHELL

Consider a rigid-perfectly plastic shallow spherical membrane shell with hinged edge subjected to an internal dynamic pressure uniformly distributed over the plane (Fig. 9—22).

According to the membrane solution to the problem, the collapse load multiplier is $p_k=\dfrac{2N_0}{R}$, $N_0=\sigma_0 H$ and the corresponding transverse deflections are given by

$$U=W(t)\left[1-\left(\frac{r}{R}\right)^2\right].$$

Using this kinematically admissible displacement field, the constant defined by eq. (9—43) is $K=\dfrac{3}{2m}$. Taking the influence of changes in geometry into consideration (Duszek 1967), the function p_k can be expressed as

$$p_k^1=p_k\left[1+\frac{2}{\left(\frac{R}{H}\right)\left(\frac{L}{R}\right)^2}w\right],$$

where $w=\dfrac{W}{H}$. Substituting these results into eq. (9—69) and using the rectangular pressure loading defined by eq. (9—2), we obtain the differential equation for the displacement parameter function W, which can be solved numerically. To illustrate the results, the permanent deflections in terms of $\eta=\dfrac{p_0}{p_k}$ and $\lambda=\dfrac{I_0^2R}{mHN_0}$, for the parameters $\dfrac{R}{H}=25$ and $\dfrac{L}{R}=\sin\alpha=0.20$, are given in Fig. 9—22.

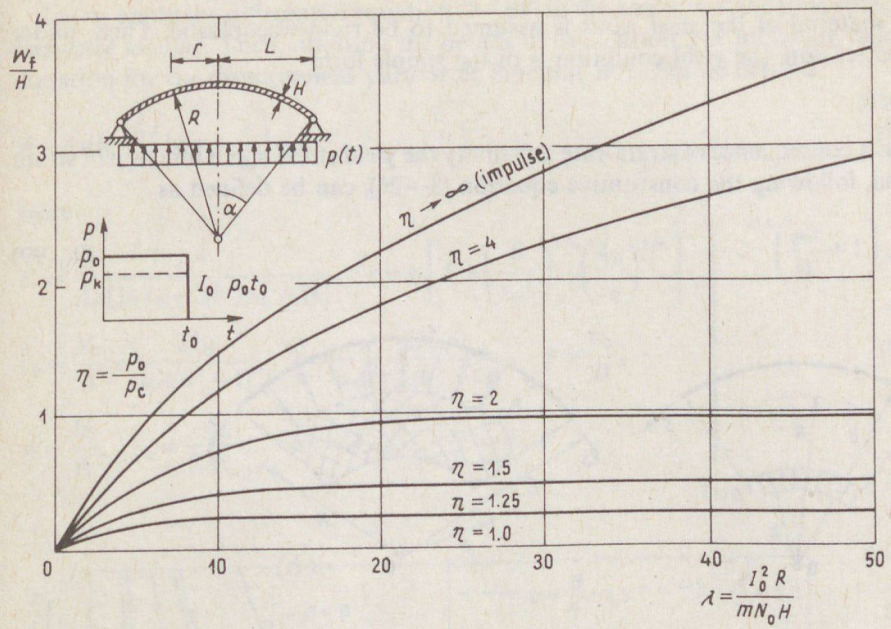


Fig. 9–22

9.7.3. THICK-WALLED TUBE

Next, the dynamic analysis and optimal design of a thick-walled concrete tube will be briefly presented (Kaliszky 1972c; 1973b; Heinloo, Kaliszky 1981).

9.7.3.1. DYNAMIC ANALYSIS

Let us consider a thick-walled concrete tube, reinforced on its exterior surface by steel wires, and subjected to internal dynamic pressure (Fig. 9—23(a)). It is assumed that the tube is in a state of plane strain and that the effects of changes in geometry can be disregarded.

The *concrete* is considered rigid-perfectly plastic without tensile strength. Then, denoting by σ_r and σ_ϑ the radial and tangential stresses respectively, the yield condition can be expressed as follows

$$\left.\begin{aligned} &\sigma_r \leq 0, \quad \sigma_\vartheta \leq 0, \\ &\left(\frac{\sigma_r - \sigma_\vartheta}{2}\right)^2 - \tau_{c0}^2 \leq 0. \end{aligned}\right\} \tag{9—98}$$

Here the shear strength τ_{c0} is a time-independent constant. The density of the concrete will be denoted by ρ.

The material of the *steel wires* is assumed to be rigid-viscoplastic. Then, under uniaxial tension, the yield condition is of the simple form

$$\sigma - \sigma_s \leq 0.$$

Here, as a consequence of strain-rate sensitivity the yield stress σ_s is a function of strain rate and, following the constitutive equation (8—26), can be defined as

$$\sigma_s = \sigma_{s0}\left(1 + \frac{\dot{\varepsilon}_{\theta S}}{D}\right)^{1/n}. \tag{9—99}$$

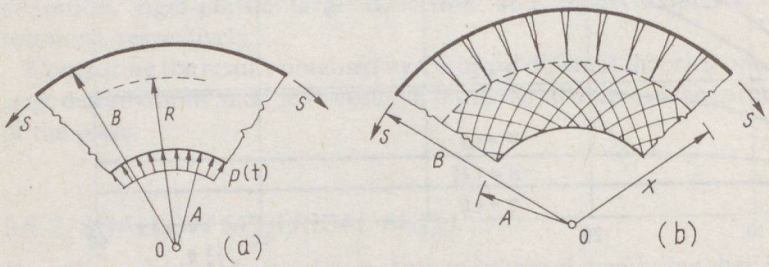


Fig. 9-23

Here $\dot{\varepsilon}_{\theta S}$ denotes the strain-rate of the steel wires, σ_{s0} is the yield stress of steel under static conditions, while D and n are viscous constants. The mass of the steel wires will be disregarded.

The yield mechanism of the tube consists of two parts (Fig. 9—23(b)). In the inner part of the concrete ($A \leq R \leq X$) shear lines develop, while in the outer part ($X \leq R \leq B$) radial cracks divide the concrete into rigid elements. The steel wires are yielding, and the force arising in them is equal to $S = A_s \sigma_s$. Here A_s denotes the area of steel wires per unit length of the tube. Using this yield mechanism, the kinematically admissible load of the rigid-viscoplastic tube under quasi-static conditions can be expressed in terms of the parameter X

$$p_k^v = 2\tau_{c0}\left(\ln x + \frac{s}{x}\right). \tag{9—100}$$

Here

$$\left.\begin{aligned} &x = 1, \quad \text{if} \quad s \leq 1; \\ &x = s, \quad \text{if} \quad 1 \leq s \leq b; \\ &x = b, \quad \text{if} \quad s > b; \end{aligned}\right\} \tag{9—101}$$

and

$$x = \frac{X}{A}, \quad s = \frac{S}{2A\tau_{c0}}, \quad b = \frac{B}{A}.$$

Let us apply the differential equation (9—69) to the analysis of the tube subjected to *impulsive loading*. Then, omitting the details of calculation, the following differential equation for the displacement parameter function $W(t)$ can be derived

$$\ddot{w}+\rho AK\frac{v_0^2}{\lambda}\left(\ln x+\frac{s}{x}\right)=0. \tag{9—102}$$

Here

$$\left.\begin{aligned} &K=\frac{1}{A\rho[\ln x_0+2(b^2/x_0^2-1)]}, \quad s=s_0\left[1+\left(\frac{\beta}{x_0 b}\right)^{1/n}\left(\frac{\dot{w}_0}{v_0}\right)^{1/n}\right] \\ &v_0=\frac{V_0}{A}=\frac{2I_0}{\rho A(b^2-1)}, \quad \lambda=\frac{2I_0^2}{\rho A^2\tau_{c0}(b^2-1)^2}, \quad \beta=\frac{v_0}{D}, \\ &w=\frac{W}{A}, \quad s_0=\frac{S_0}{2A\tau_{c0}}, \quad S_0=A_s\sigma_{s0}, \end{aligned}\right\} \tag{9—103}$$

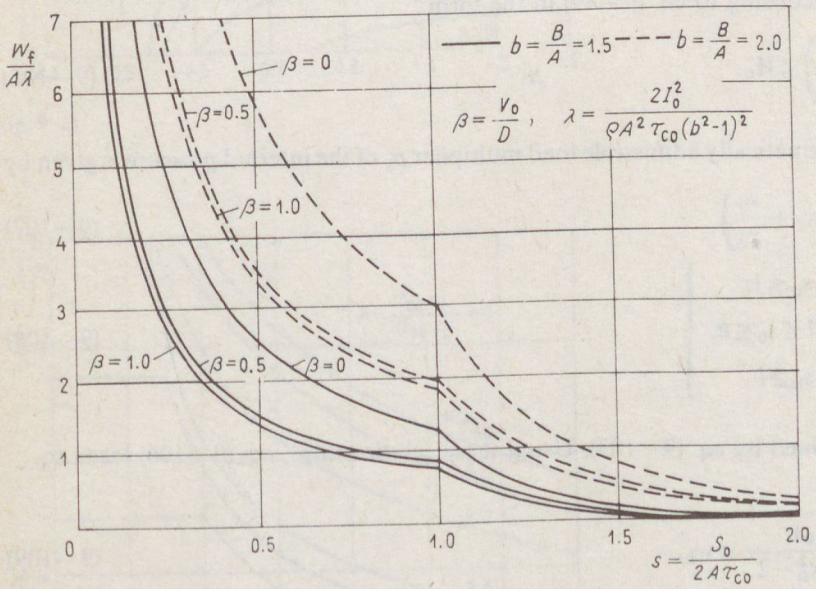


Fig. 9–24

and between $x_0=X_0/A$ and s_0 the same relationships are valid as are given by eq. (9—101) for x and s.

Using Runge–Kutta's method, the differential equation (9—102) can be solved numerically. The maximum permanent radial displacements w_f obtained in terms of s_0 for the parameters $b=1.5-2.0$, $\beta=0.0-0.5-1.0$ and $n=5$ are plotted in Fig. 9—24. The case $\beta=0$ (i.e. when $D\to\infty$) corresponds to the simple rigid-plastic theory.

9.7.3.2. OPTIMAL DESIGN

In the case of the optimal design of the thick-walled concrete tube under consideration, we assume that the external radius B and the area A_s of the steel wires per unit length of the tube are design variables. They have to be determined so that the cost of the materials used for the tube is a minimum

$$C=\pi(B^2-A^2)c_c+2\pi BA_sc_s=\min! \tag{9—104}$$

Or, using the dimansionless variables introduced above,

$$c=\frac{C}{\pi A^2c_c}=b^2+4s_0kb-1=\min! \tag{9—105}$$

Here c_c and c_s denote the specific costs of the concrete and the steel wires, respectively, and $k=\tau_{c0}c_s/\sigma_{s0}c_c$. Neglecting the effect of the viscosity of the steel wires, and taking only small deformations into consideration, the condition that the permanent radial displacements should not exceed the prescribed permissible displacement W_0 can be expressed according to eq. (9—49) in the form

$$KS_0\left(\frac{p_e}{p_k}-1\right)\leq W_0. \tag{9—106}$$

Here the kinematically admissible load multiplier p_k of the internal pressure is given by

$$p_k=2\tau_{c0}\left(\ln x_0+\frac{s_0}{x_0}\right). \tag{9—107}$$

$$\left.\begin{aligned} &x_0=1 \quad \text{if} \quad s_0\leq 1;\\ &x_0=s_0 \quad \text{if} \quad 1\leq s_0\leq b;\\ &x_0=b \quad \text{if} \quad s_0\geq b \end{aligned}\right\} \tag{9—108}$$

and K is defined by eq. (9—103). Using these relationships, eq. (9—106) leads to

$$\frac{\frac{\psi}{2(\ln x_0+s_0/x_0)}-1}{\ln x_0+2b^2/x_0^2-2}\leq w_0, \tag{9—109}$$

where $\psi=p_e/\tau_{c0}$ and $w_0=(\rho A/S_0)W_0$ are dimensionless variables. Finally, the following design constraints should be introduced

$$b>1, \quad s_0\geq 0. \tag{9—110}$$

The problem of the optimal design formulated by eqs (9—105)—(9—10) can be solved analytically (Heinloo, Kaliszky 1981). Omitting the details of the lengthy calculation, the results, in terms of w_0 and ψ for the parameter $k=\tau_{c0}c_s/\sigma_{s0}c_c=1$, are illustrated by the diagrams in Figs. 9—25 and 9—26.

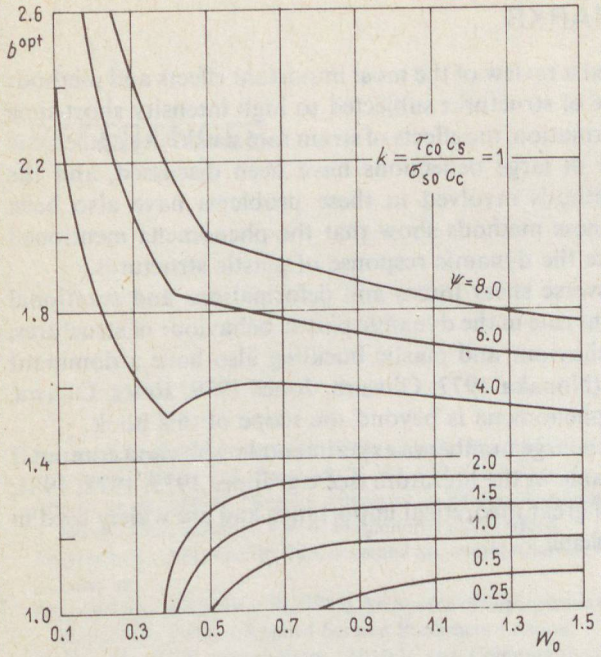


Fig. 9–25

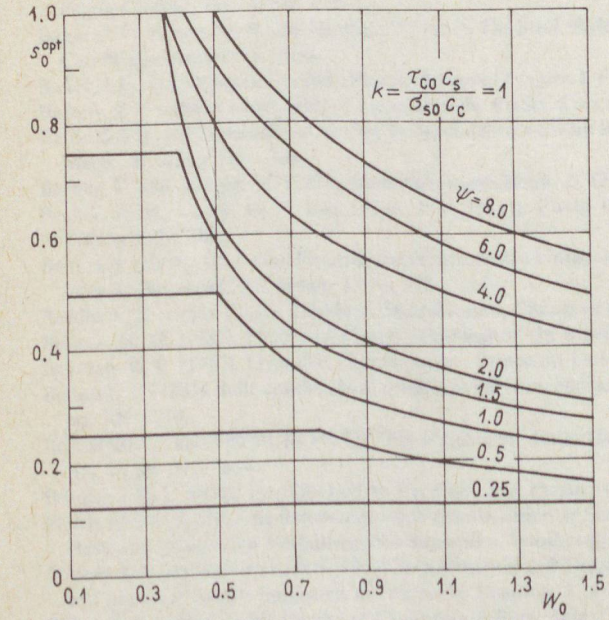


Fig. 9–26

9.8. CONCLUDING REMARKS

In this chapter, we have presented a review of the most important effects and methods for the dynamic plastic response of structures subjected to high intensity short-time pressure. Besides the plastic deformation, the effects of strain rate sensitivity and elastic deformations and the influence of large deflections have been discussed, and the principles and approximate methods involved in these problems have also been described. The applications of these methods show that the phenomena mentioned above may significantly influence the dynamic response of plastic structures.

Plastic hardening, large transverse shear forces and deformations and rotational inertia may also play an important role in the dynamic plastic behaviour of structures, and in certain cases unstable behaviour and plastic buckling also have a dominant effect on the dynamic response (Nonaka 1977; Oliveira, Jones 1979, Jones, Okawa, 1976). The description of these phenomena is beyond the scope of this book.

Finally, it should be noted that a large number of experimental results and computer methods and solutions are available in the literature (see e.g. Jones 1975, 1978, 1981; Symonds 1984). These are also of great theoretical importance and are widely used in the solution of engineering problems.

REFERENCES

Anand, C. and Weisgerber, F. E. (1977), Inelastic Finite Element Analysis Using the Tresca Yield Condition, J. Engng. Mech. Div. Proc. ASCE 103, EM 1, Febr.

Argyris, J. H. (1964), "Recent Advances in Matrix Methods of Structural Analysis", in: Progress in Aeronautical Sciences, Vol. 4. Pergamon Press, Oxford.

Argyris, J. H. (1971), Energy Theorems and Structural Analysis, 4th ed. Butterworths Sciencific Publications, London.

Argyris, J. and Doltsinis, J. St. (1985), An Apercu of Superplastic Forming. Plasticity Today, eds., Sawczuk A., Bianchi G., Elsevier Applied Science Publishers London.

Armen, H. (1979), Assumptions, Models and Computational Methods for Plasticity. Computers and Structures, Vol. 10 pp. 161—174.

Aspden, R. J. and Campbell, J. D. (1966), "The Effect of Loading Rate on the Elastic-Plastic Flexure of Steel Beams", Proc. Roy. Soc. A. 290 pp. 266—285.

Baker, J. F. and Roderick, J. W. (1938), An Experimental Investigation of the Strength of Seven Portal Frames, Trans. Inst. Weld. Vol. 1.

Baker, J. F., Horne, M. R. and Heyman, J. (1956), The Steel Skeleton. Vol. II. Plastic Behaviour and Design, Cambridge University Press.

Baker, J. F. and Heyman, J. (1969), Plastic Design of Frames. I. Fundamentals, Cambridge University Press.

Bažant, Z. P. (1985), Mechanics of Geomaterials: Rocks, Concretes, Soils, John Willey, New York.

Batdorf, S. B. and Budiansky, B. (1954), 'Polyaxial Stress-Strain Relation of Strain Hardening Metal', J. Appl. Mech., 21, 4, pp 323—326.

Becker, E. and Bürger, W. (1975), Kontinuumsmechanik, B. G. Teubner, Stuttgart.

Becker, E. B., Carey, G. F. and Oden, J. T. (1981), Finite Elements. An Introduction, Prentice Hall, Englewood Cliffs.

Béda, Gy. (1964), 'Über eine Frage der experimentellen Untersuchung des dynamischen plastischen Zuges', Acta Techn. Acad. Sci. Hung. 49 pp. 311—316.

Beedle, L. S. (1958), Plastic Design of Steel Frames, Chapman and Hall, London; John Wiley, New York.

Beljaev, N. M. (1937), Theory of Plastic Deformation (In Russian), Izvest. Akad. Nauk SSSR, pp. 49—70.

Bellman, R. E. (1957), Dynamic Programming, Princeton University Press.

Beltrami, E. (1885), Sulle conditioni di resistenza dei corpi elastici, Rend. ist. lomb. d. sci. lett. Cl. mat. not., 18 pp. 705—714.

Belytschko, T. and Velebit, M. (1972), "Finite Element Method for Elastic Plates", J. Engng. Mech. Div. Proc. ASCE, pp. 672—694.

Bezuhov, N. I. (1950): Introduction to Elasticity and Plasticity (In Russian), Moscow, Gosstroizdat

Bleich, H. (1932), Über die Bemessung statisch unbestimmter Stahltragwerke unter der Berücksichtigung des elastische-plastischen Verhaltens des Baustoffes, Bauingenieur, 13 pp. 261—267.

Bodner, S. R. and Symonds, P. S. (1962), Experimental and Theoretical Investigation of Plastic Deformations of Cantilever Beams Subjected to Impulsive Loading, J. Appl. Mech., 29 pp. 719–728.

Bölcskei, E. (1956), Limit Design of Compressed Bars, Acta Techn. Acad., Sci. Hung., 15 pp. 19—25.

Brandt, A. M. (1984), Criteria and Methods of Structural Optimization, Martinus Nijhoff Publishers, The Hague.

Brebbia, C. A. (1982), Boundary Element Methods in Engineering, Proc. 4th Int. Seminar, Springer Verlag, Southampton, Berlin.
Bridgman, P. W. (1947), The Effect of Hydrostatic Pressure on the Fracture of Brittle Substances, J. Appl. Phys., 18 p. 246.
Bruhns, O. (1978), Grundlagen der Plastizitätstheorie und ihre Anwendungen UDI-Z., No. 8. pp. 381—385.
Capurso, M. (1974), A Displacement Bounding Principle in Shakedown of Structures Subjected to Cyclic Loads, Int. J. of Solids and Structures 10 pp. 77—92.
Chen, W. F. (1975), Limit Analysis and Soil Plasticity, Elsevier, Amsterdam, Oxford, New York.
Chen, W. F.—Drucker, D. C. (1969), Bearing capacity of Concrete Blocks or Rock, J. Engng. Mech. Div. Proc. ASCE, 95 EM 4.
Christopherson, D. G. (1940), A Theoretical Investigation of Plastic Torsion in an I-Beam, J. Appl. Mech., 7 pp. 1—4.
Cohn, M. Z. and Maier, G. (1977), Engineering Plasticity by Mathematical Programming, Proc. of the NATO Advanced Study Inst., Pergamon Press, New York, Oxford, Frankfurt, Paris
Colonnetti, G. (1938), De l'équilibre des systèmes élastiques dans lesquelles se produisent des déformations plastiques, J. Math. Pur. Appel, 9, 17, pp. 233—255.
Corradi, L. and Gioda, G. (1979), A Plane Strain Formulation of Elastic-Plastic Constitutive Laws, J. Struct. Mech., 7, 3 pp. 325—264.
Cosserat, E. and Cosserat, F. (1909), Théorie des corps déformables, Paris.
Coulomb, C. A. (1773), Essai sur une application des regles de maximis et minimis a quelques problemes de statique relatifs a l'architecture, Mémoires de Math. et de Phys. L'Academie Royale des Sciences par divers savants.
Cristescu, N. (1967), Dynamic plasticity. In Applied Mathematics, and Mechanics North-Holland Publishing Co., Amsterdam.
Cristescu, N. (1985), Rock Plasticity. Plasticity Today, eds., Sawczuk, A. and Bianchi, G. Elsevier, London.
Cyras, A. (1975), Optimization Theory in the Design of Elastic-Plastic Structures. Springer Verlag, Vienna.
Dais, J. L. (1970), Nonuniqueness of Collapse Load for a Frictional Material, Int. J. of Solids and Structures, 6 pp. 1315—1319.
Davies, R. M. (1953), Stress Waves in Solids, Appl. Mech. Revs., 6 pp. 1—3.
Dewhurst, P. and Collins, I. F. (1973), A Matrix Technique for Constructing Slip-Line Field Solutions to a Class of Plane Strain Plasticity Problems, Int. J. Numer. Methods in Engng. 7 pp. 357—378.
Dines, L. L. (1918), Systems of Linear Inequalities, Ann. Math., Princeton 20 pp. 191—199.
Dorosz, S. (1978), An Improved Upper Bound to Maximum Deflections of Elastic-Plastic Structures at Shakedown, J. Struct. Mech., 6, pp. 267—287.
Dorosz, S. (1985), Note on Displacement in Shakedown of Elasto-Plastic-Creeping Structures, Archives of Mechanics, Vol. 37. 4—5. pp. 337—342.
Drucker, D. C. (1949), Some Implications of Work-Hardening and Ideal Plasticity, Quart. Appl. Math., 7, 2 pp. 411—418.
Drucker, D. C. (1951), A More Fundamental Approach to Plastic Stress–Strain relations, Proc. lst. US Nat. Congr. Appl. Mech., Chicago, Edwards Brothers Inc. pp. 484—491.
Drucker, D. C. (1952), A More Fundamental Approach to Plastic Stress-Strain Relations, Proc. lst US Nat. Congr. Appl. Mech., Chicago, Edwards Brothers Inc. pp. 487—491.
Drucker, D. C. (1953), Limit Analysis of Two- and Three-Dimensional Soil Mechanics Problems, J. Mech. Phys. Solid, 1 pp. 217—226.
Drucker, D. C. (1954), Limit Analysis of Cylindrical Shells under Axially-Symmetric Loading, Proc. lst Midwestern Conf. Solid Mech., Urbana, 1953 pp. 158—163.
Drucker, D. C. (1959), A Definition of Stable Inelastic Material, J. Appl Mech., Vol. 26. No 1. pp. 101—106.
Drucker, D. C. (1985), Appropriate Simple Idealizations for Finite Plasticity. Plasticity Today, eds., Sawczuk, A. and Bianchi, G., Elsevier, London.
Drucker, D. C. Greenberg, H. J. and Prager, W. (1951), The Safety Factor of an Elastic-Plastic Body in Plane Stress, J. Appl. Mech. 18 pp 317—378.
Drucker, D. C., Prager, W. and Greenberg, H. J. (1952b), Extended Limit Design Theorems for Continuous Media, Quart. Appl. Math., 9 pp. 381—394.
Drucker, D. C. and Prager, W. (1952c), Soil Mechanics and Plastic Analysis or Limit Design, Quart. Appl. Math., 10 pp. 157—165.

Drucker, D. C. and Shield, R. T. (1956), Design for Minimum Weight, Proc. 9th Int. Cong. Appl. Mech., Brussels, Book 5 pp. 212—222.
Dubinski, A. M. (1961), Limit Analysis of Reinforced Concrete Plates (In Russian), Gosstroizdat, Kiev.
Duszek, M. (1967), Plastic Analysis of Shallow Spherical Shells at Moderately Large Deflections, Proc. IUTAM Symposium, Coppenhagen.
Eason, G. and Shield, R. T. (1956), Dynamic Loading of Rigi-Plastic Cylindrical Shells, J. Mech. Phys. Solids, 4 pp. 53—71.
Filonenko-Boroditsch, M. M. (1952), Festigkeitslehre, Bd. 1—2 Berlin, VEB Verlag Technik.
Flügge, W. (1962), Handbook of Engineering Mechanics, McGraw-Hill, New York, Toronto, London,
Flügge, W. (1972), Tensor Analysis and Continuum Mechanics, Springer Verlag, Berlin.
Flügge, W. (1975), Viscoelasticity, Springer Verlag, Berlin.
Foulkes, J. (1954), Minium Weight Design of Structural Frames, Proc. Roy. Soc., London, A. 223 pp. 482—494.
Freitas, J. A. T. and Smith, D. L. (1985), Elasto-plastic Analysis of Planar Structures for Large Displacements, J. Struct. Mech., Vol. 12., No. 4. pp. 419—446.
Freudenthal, A. M. (1955), The Inelastic Behavior of Engineering Materials and Structures, John Wiley, New York.
Freudenthal, A. M. (1955), Inelastisches Verhalten von Werkstoffen, VEB Verlag Technik, Berlin.
Galambos, T. V. (1968), Structural Members and Frames, Prentice Hall Inc., New York.
Galilei, G. (1638), Discorsi e dimostrazioni matematiche intorno a due nuove scienze, Leyden.
Galin, L. A. (1949), Elasto-Plastic Torsion of Prismatic Bars (In Russian), Prikl. Mat. i Mekh., 13 pp. 285—296.
Galin, M. P. (1959), Propagation of Elastic-Plastic Bending Shearing Waves in Beams, (in Russian), Izv. Akad. Nauk SSSR OTN 2 pp. 88—99.
Gallagher, R. M. and Zienkiewicz, O. C. (1973), Optimal Structural Design: Theory and Applications, John Wiley, London.
Garai, T. and Kaliszky, S. (1957), Limit Analysis of Eccentrically Loaded Cross-Sections (In Hungarian), Építésügyi Szemle, 1 pp. 33—48.
Gass, S. I. (1969), Linear Programming, McGraw-Hill, New York.
Geiringer, H. (1953), 'Some Recent results in the Theory of an Ideal Plastic Body', in Advances in Applied Mechanics, Vol. III., Academic Press New York, pp. 197—294.
Geiringer, H. and Pollaczek (1930), Beitrag zum vollständigen ebenen Plastizitätsproblem, III. Int. Cong. Techn. Mech., Stockholm, 2.
Geleji, S. (1960), Bildsame Formung der Metalle in Rechnung und Versuch, Akademie-Verlag, Berlin.
Girkmann, K. (1931), Bemessungen von Rahmentragwerken unter Zugrundelegung eines ideal-plastischen Stahles. Sitzungsberichte der Akademie der Wissenschaften in Wien, Springer Verlag, Vienna.
Greenberg, H. J. (1949), Complementary Minimum Principles for an Elasto-Plastic Material, Quart. Appl. Math., 7 pp 85—95.
Grierson, D. E. and Gladwell, G. M. L. (1971), Collapse Load Analysis Using Linear Programming, J. Struct. Div. ASCE, 97 ST 5 pp. 1561—1573.
Grüning, M. (1926), Die Tragfähigkeit statisch unbestimmter Tragwerke aus Stahl bei beliebig häufig wiederholter Belastung. Springer Verlag, Berlin.
Gudehus, G. (1972), Elastic-Plastic Constitutive Equations for Dry Sand, Arch. Mech., Warszawa, 24 pp. 395—402.
Gvozdev, A. A. (1936), The Determination of the Value of the Collapse Load for Statically Indeterminate Systems Undergoing Plastic Deformation, Int. J. Mech. Sci., 1960, London pp. 322—335.
Gvozdev, A. A. (1949), Limit Analysis of Structures (In Russian), Stroizdat, Leningrad.
Hadley, G. (1964), Non-linear and Dynamic Programming, Addison-Wesley Publishing Co, London.
Halász, O. (1967), Adoption for the Theory of Plasticity to Steel Structures, Acta Techn. Acad. Sci. Hung., 59 pp. 55—74.
Halász, O. (1969), Design of Elastic-Plastic Frames Under Primary Bending Moments, Periodica Polytechnica, Budapest 13, 3—4 pp. 38—44.
Halász, O. (1972), Theorems for a Simplified Second Order Limit Analysis of Elastic-Plastic Frames, Proc. IX. Congr. Int. Ass. Bridge Struct. Engng., Preliminary Report, Amsterdam pp. 11—19.
Halász, O. (1976), Limit Analysis of Frames, II. Order Problems (In Hungarian), Dissertation, Budapest.
Hearmon, R. F. S. (1961), An Introduction to Applied Anistropic Elasticity, Oxford University Press.

Heinloo, M. and Kaliszky, S. (1981), Optimal Design of Dynamically Loaded Rigid-Plastic Structures. Application: Thick-Walled Concrete Tubes, J. Struct. Mech., 9, 3 pp. 235—251.
Hencky, H. (1923), Über einige statisch bestimmte Fälle des Gleichgewichts im plastischen Körper, Z. Ang. Math. Mech., 3 pp. 241—251.
Hencky, H. (1924), Zur Theorie plastischer Deformationen und der hierdurch im Material hervorgerufenen Nachspannungen, Z. Ang. Math. Mech., 4 pp 323—334.
Hencky, H. (1925), Zur Theorie plastischer Deformationen und der hierdurch im Material hervorgerufenen Nebenspannungen, Proc. lst Int. Congr. Appl. Mech. Delft. Technische Boekhandel en Druckerij, J. Waltman, Jr. Delft pp. 312—317.
Heyman, J. and Dutton, V. L. (1954), Plastic Design of Plate Girders with Unstiffened Webs. Welding and Metal Fabrication, 22 p. 265.
Heyman, J. (1957), Plastic Design of Portal Frames, Cambridge University Press.
Heyman, J. (1971), Plastic Design of Frames. 2. Applications, Cambridge University Press.
Hill, R. (1948), A Variational Principle of Maximum Plastic Work in Classical Plasticity, Quart. J. Mech. Appl. Math., 1, 1 pp. 18—28.
Hill, R. (1949), The Plastic Yielding of Notched Bars under Tension, Quart. J. Mech. App. Math., 2 pp 40—52.
Hill, R. (1950), The Mathematical Theory of Plasticity, Clarendon Press, Oxford.
Hinton, E. and Owen, D. R. J. (1979), An Introduction to Finite Element Computations, Pineridge Press Ltd., Swansea.
Hodge, P. G. Jr. (1954), The Rigid-Plastic Analysis of Symmetrically Loaded Cylindrical Shells, J. App. Mech., 21 pp. 336—342.
Hodge, P. G. Jr. (1956), Ultimate Dynamic Load of a Circular Cylindrical Shell, proc. 2nd Midwest. Conf. Solid Mech., Lafayette. 1955 pp. 150—177.
Hodge, P. G. Jr. (1958), "The Mathematical Theory of Plasticity", in: Surveys in Applied Mahematics I. John Wiley, New York.
Hodge, P. G. Jr. (1959), Plastic Analysis of Structures, McGraw-Hill, New York, Toronto, London.
Hodge, P. G. Jr. (1960), Plastic Analysis of Circular Conical Shells, J. Appl. Mech., 27 pp. 696—700.
Hodge, P. G. Jr. (1963), 'Limit Analysis of Rotationally Symmetric Plates and Shells', in: Prentice-Hall International Series in Theoretical and Applied Mechanics, Prentice-Hall, Englewood Cliffs, N. J.
Hoff, N. J. (1952), Complementary Energy Analysis of the Failing Load of a Clamped Beam, J. Appl. mech., 19 pp 563—564.
Hoff, N. J. (1954), Approximate Analysis of structures in the Presence of Moderately Large Creep Deformation, Quart. Appl. Math., 12 pp. 49—55.
Hoff, N. J. (1959), On a Critical Strain Approach to Creep Buckling of Plates and Shells, J. Aero/Space Sci., 26 pp. 117—118.
Hoff, N. J. (1960), Mechanics Applied to Creep Testing, Proc. Soc. Experimental Stress Analysis, 18 pp 1—32.
Hoffmann, I. and Sachs, G. (1953), Introduction to the Theory of Plasticity for Engineers, McGraw-Hill, New York, Toronto, London.
Hopkins, H. G. and Prager, W. (1954), On the Dynamics of Plastic Circular Plates, ZAMP, 6 pp. 317—330.
Horne, M. R. (1954), A Moment Distribution Method for the Analysis and Design of Structures by the Plastic Theory, Proc. Inst. Civil Engng., London, 3 pp. 51—76.
Horne, M. R. (1961), 'The Stability of Elastic–Plastic Structures', in: Progress in Solid Mechanics. Vol. II. North-Holland, Amsterdam.
Horne, M. R. (1971), Plastic Theory of Structures. Nelson, London.
Horne, M. R. (1978), Plastic Theory of Structures, 2nd ed., University of Manchester.
Horne, M. R. and Merchant, W. (1965), The Stability of Frames, Pergamon Press, London.
Huber, M. T. (1904), Wlasciva praca odksztalcenia jako miara witezenia materialu, Czas. Techn., Lwów, 22 pp. 38—81.
Huebner, K. H. (1975), The Finite Element Method for Engineers, John Wiley, New York.
Hult, J. (1966), Creep in Engineering Structures, Waltham, Mass., Blaisdele Publishing Co., Toronto, London.
Hundy, B. (1954), Plane Plasticity, Metallurgia.
Ilyushin, A. A. (1948), Plasticity (In Russian), Moscow Gosstroizdat, Leningrad.
Ilyushin, A. A. (1960), Problems of the Theory of Plasticity (In Russian), Prikl. Mat. i Mekh., XXIV pp. 339—441.

Ilyushin, A. A. and Lenski, V. S. (1959), Strength of Materials, (In Russian), Fizmatgiz, Moscow.
Ilyushin, A. A. and Lenski, V. S. (1967), Strength of Materials. Pergamon Press, Oxford.
Ismar, H. and Mahrenholtz, O. (1979), Technische Plasto-mechanik, Vieweg und Sohn, Braunschweig, Wiesbaden.
Ingerslev, A. (1921), Om en elementaer beregningsmetode of krydsarmbrede Plader, Ingenioren, 30 pp. 507—515.
Iványi, M. (1969), Effect of Strain-Hardening on the Elastic–Plastic Behaviour of Beams, Periodica Polytechnica Civil Eng., 13 pp 3—4.
Johansen, K. W. (1932), Bruchmomente der kranzweise bewehrten Platten, Abhandlungen, Int. Ver. Brücken- und Hochbau, Zürich pp. 227—296.
Johansen, K. W. (1962), Yield-Line Theory, Cement and Concrete Association, London.
Johanson, R. C. (1961), Optimum Design of Mechanical Elements, John Wiley, New York.
Johnson, W. and Mellor, P. B. (1962), Plasticity for Mechanical Engineers, D. Van Nostrand Co., London, Toronto, New York, Princeton.
Jones, N. (1968), Impulsive Loading of a Simply Supported Circular Rigid-Plastic Plate, Trans. ASME J. Appl. Mech., 35, 1 pp. 59—65.
Jones, N. (1971), A Theoretical Study of the Dynamic Plastic Behavior of Beams and Plates with Finite Deflections, Int. J. of Solids and Structures, 7 pp. 1007—1029.
Jones, N. (1975), A Literature Review of the Dynamic Plastic Response of Structures, The Shock and Vibration Digest, 7, 8 pp 89—105.
Jones, N. (1978), Recent Progress in the Dynamic Plastic Behavior of Structures, The Shock and Vibration Digest, 10, 9 pp. 21—33, 10 pp. 13—19.
Jones, N. (1979), Response of Structures to Dynamic Loading, Inst. Phys. Conf., 47, 3 pp 254—276.
Jones, N. and Okawa, D. M. (1976), Dynamic Plastic Buçkling of Rings and Cylindrical Shells, Nuclear Engineering and Design, 37 pp. 125—147 North-Holland Publishing Company, Amsterdam.
Kachanov, L. M. (1971), 'Foundations of the Theory of Plasticity', in: Applied Mathematics and Mechanics, North-Holland Publishing Co., Amsterdam.
Kaliszky, S. (1959a), Limit Analysis of Plastic Beams and Plates on Plastic Subgrade, (In Hungarian) ÉKME Tud. Közl. V. pp. 39—53.
Kaliszky, S. (1959b), Plasticity, Engineering Handbook. (In Hungarian) Budapest, Műszaki Könyvkiadó, pp. 248—278.
Kaliszky, S. (1960), Calculation of the Load Bearing Capacity of Concrete and Reinforced Concrete Walls Loaded in their own Plane, Acta Techn. Acad. Sci. Hung., 28, 3—4, pp. 441—473.
Kaliszky, S. (1961a), Untersuchung einer Kegelstumpf-Schale aus Stahlbeton auf der Grundlage des Traglastverfahrers, Acta Techn. Acad. Sci. Hung., 34 1—2, pp. 159—175.
Kaliszky, S. (1961b), Limit Analysis of Stone, Brick and Concrete Arches, (In Hungarian) Mélyépítéstudományi Szemle, 11, 10 pp 469—474.
Kaliszky, S. (1962a), Berechnung der Trägfähigkeit von plastischen Balken und Platten auf plastischer Unterlage, Bulletin de l'Académie Polonaise des Sciences, X. pp. 151—158.
Kaliszky, S. (1962b), Load Carrying Capacity of Plastic Beams and Plates on Plastic Foundation, Archivum Inzynierii Ladowej, VI pp. 19—38.
Kaliszky, S. (1963a), Limit Design of Truncated Cone-Shaped Reinforced Concrete Shells. Non-Classical Shell Problems, Proc. of IASS Symposium, Warsaw pp. 1011—1029.
Kaliszky, S. (1963b), Problems of Plastic Analysis and Design of Reinforced Concrete Slabs (In Hungarian) ÉKME. Tud. Közl. IX pp. 107—125.
Kaliszky, S. (1965a), Optimal Design of Reinforced Concrete Tanks (In Hungarian), Mélyépítéstudományi Szemle XV. pp. 449—456.
Kaliszky, S. (1965b), Optimum Limit Design for Reinforced Concrete Structures, Report. The University of Southampton, England.
Kaliszky, S. (1965c), Economic Design by the Ultimate-Load Method, Concrete and Constructional Engineering IX pp. 365—372, 424—433, 461—467.
Kaliszky, S. (1967), Plastic design of Reinforced Concrete Slabs (In Hungarian) Műszaki Könyvkiadó, Budapest.
Kaliszky, S. (1968), On the Optimum Design for Reinforced Concrete Structures, Acta Techn. Acad. Sci. Hung. 60 pp. 257—264.

Kaliszky, S. (1969), Approximate Solutions for Impulsively Loaded Rigid-Plastic Structures and Continua. Bulletin de l'Académie Polonaise des Sciences, Warsaw *XVII* pp. 164—268.
Kaliszky, S. (1970), Approximate Solutions for Impulsively Loaded Inelastic Structures and Continua, Int. J. Non-Linear Mechanics, 5 pp. 143—158.
Kaliszky, S. (1971), Optimum Design of Reinforced Concrete Tanks, J. Engng. Mech. Div. Proc. ASCE, 97, EM 4 pp. 1299—1302.
Kaliszky, S. (1972a), Large Plastic and Viscous Deformations of Dynamically Loaded Structures, IXth Congr. Int. Ass. Bridge Struct. Engng., Amsterdam.
Kaliszky, S. (1972b), Plastic Deformation of Thick-Walled Concrete Tubes under Dynamic Internal Pressure, Archives of Mechanics, Warsaw 24, pp. 5—6 pp. 1013—1021.
Kaliszky, S. (1973a), Large Deformations of Rigid-Viscoplastic Structures under Impulsive and Pressure Loading, J. Struct. Mech., I, 3 pp. 295—317.
Kaliszky, S. (1973b), Limit Analysis of Post-Stressed Thick-walled Concrete Tubes, Acta Techn. Acad. Sci. Hung., 75, 1—4 pp. 193—202.
Kaliszky, S. (1979), Statically Admissible Stress Field in Plane Plastic Problems, Bulletin de l'Academie Polonaise des Sciences, XXVII., 5—6 pp. 51—55.
Kaliszky, S. (1981), Kinematical Method for the Analysis of Inelastic Structures under Dynamic Loading, Advances in Mechanics, Vol. 4. No. 1. pp. 30—47.
Kaliszky, S. (1984), 'Dynamic Plastic Response of Structures', in Proc. Symposium on Plasticity Today. eds Sawczuk, A. and Bianchi, G., Elsevier, London.
Kaliszky, S., Halász, O. and Kollár, L. (1959), Limit Analysis and Design of Frames (In Hungarian), Mérnöki Továbbképző Intézet, Budapest.
Kaliszky, S. and Györgyi, J. (1972), Limit Analysis of Grillages, (In Hungarian) Magyar Építőipar, XXI pp. 4—5.
Kaliszky, S. and Nédli, P. (1976), Analysis of Elasto-Plastic Structures by Mathematical Programming, Acta Techn. Acad. Sci. Hung., 83, 3—4 pp. 205—212.
Kaliszky, S., Nédli, P. and Tornyos, Á. (1985), Progressive Collapse Analysis of Large Panel Buildings, Proc. 3rd Int. Symp. on Wall Structures. Warsaw pp. 161—165.
Kaliszky, S. and Dong, T. (1984), Approximate Analysis of Elasto–Plastic Frames Under Impulsive Loading, (In Hungarian) Építés- Építészettudomány XVI. 1—2, 125—38.
Kármán, T., (1925), Beitrag zur Theorie des Walzvorganges. Z. Ang. Math. Mech., 5 pp. 139.
Kauderer, H. (1958), Nichtlineare Mechanik, Springer Verlag, Berlin, Göttingen, Heidelberg.
Kazinczy, G. (1914), Experiments with Clamped Beams (In Hungarian), Betonszemle 2, No. 4, 5, 6 pp. 68—71, 83—87, 101—104.
Kazinczy, G. (1931), Statisch unbestimmte Tragwerke unter Berücksichtigung der Plastizität, Der Stahlbau 4 pp. 5—8.
Kazinczy, G. (1933), Die Bemessung unvollkommen eingespannter Stahl-I-Deckenträger unter Berücksichtigung der plastischen Formänderungen, Int. Ver. Brücken- und Hochbau, Berlin, Abhandlungen 2.
Kazinczy, G. (1936), Kritische Betrachtungen zur Plastizitätstheorie, Int. Ver. Brücken- und Hochbau, Berlin, Schlussbericht, pp. 56—69.
Kazinczy, G. (1942), The Importance of the Plastic Behaviour of Materials from the Point of View of the Load Carrying Capacity of Structures (In Hungarian), Budapest, Mérnöki Továbbképző Intézet, Bd. III. H. 13.
Kazinczy, G. (1952), Zulässigkeit der Anwendung des Traglastverfahrens bei Stahlbeton, Int. Ver. Brücken- und Hochbau, London, Schlussbericht.
Kennedy, A. J. (1962), Progress of Creep and Fatigue in Metals, Oliver and Boyd, Edinburg.
Ketter, R. L. and Prawel, S. P. (1969), Modern Methods of Engineering Computation, McGraw-Hill, New York.
Kézdi, Á. (1952), Soil Mechanics I—II (In Hungarian), Tankönyvkiadó, Budapest.
Kézdi, Á. (1962), Erddrucktheorien, Springer Verlag, Berlin, Göttingen, Heidelberg.
Kézdi, Á. (1964), Bodenmechanik, Bd. 1. VEB Verlag für Bauwesen Berlin; Akadémiai Kiadó, Budapest.
Kist, N. C. (1917), Führt eine auf das Hookesche Gesetz gegründete Spannungsberechnung zu einer befriedigenden Bemessung von Stahlbrücken and Gebäuden? (In Holland), De Ingenieur.
Kleiber, M. and Raniecki, B. (1985), Elastic-plastic materials at finite strains. Plasticity Today, eds.: Sawczuk, A., Bianchi, G. Elsevier Applied Science Publishers, London.

Klöppel, K. and Yamada, Y. (1958), Fliesspolyeder des Rechteck- und I-Querschnittes unter der Wirkung von Biegemoment. Normalkraft und Querkraft, Der Stahlbau, H. 11.
Koiter, W. T. (1953), Stress-Strain Relation, Uniqueness and Variational Theorem for Elastic-Plastic Materials with a Singular Yield Surface, Quart. Appl. Math., 11, 3 pp. 350—354.
Koiter, W. T. (1956), A New General Theorem on Shake-down of Elastic-Plastic Structures, Proc. Koninkl. Ned. Akad. Wetenshap, B. 59 pp. 24—34.
Koiter, W. T. (1960), 'General Theorems for Elastic-Plastic Solids', in: Progress in Solid Mechanics, North-Holland Publishing Co., Amsterdam.
Kolar, V. et al. (1972), Die Berechnung ebener und räumlicher Tragwerke durch die Methode der finiten Elemente (In Czech), SNTL. Naklada telsoi Technicke Literature, Prague.
König, J. A. (1972), Shakedown Deflections. A Finite Element Approach, Bulg. Acad. Sci. Theor. Appl. Mech., Sofia 3 pp 65—69.
Korn, G. A. and Korn, T. M. (1968), Mathematical Handbook for Scientists and Engineers, McGraw-Hill, New York.
Kötter, F. (1899), Der Bodendruck von Sand in verticalen, cylindrischen Gefässen. J. reine und angew. Math. 120.
Kozák, I. (1966), Small Elastic-Plastic Deformation of a Thin Walled Tube Clamped at one of its Ends to a Rigid Support, Acta Techn. Sci. Hung., 55, 1—2 pp. 7—26.
Krajcinovic, D. (1972), On Approximate Solutions for Rigid-Plastic Structures Subjected to Dynamic Loading, Int. J. Non-Linear Mechanics, 7 pp. 571—575.
Krekó, B. (1962), Linear Programming (In Hungarian), Közgazdasági Kiadó, Budapest.
Kröner, E. (1958), Kontinuumstheorie der Versetzungen und Eigenspannungen, Springer Verlag, Berlin, Göttingen, Heidelberg.
Küpfer, H., Hilsdorf, H. K. and Rüsch, H. (1969), Behavior of Concrete under Biaxial Stresses, ACI Journal, 9.
Kurutz, M. (1974), Analysis of Plastic Load Capacity of Plane Framework by Kinematic Loading, Periodica Polytechnica Civ. Engng., 18, 1—2 pp. 71—81.
La Hire, P., de (1695), Traité de Mécanique, Paris, S. A.: Sur la construction des voutes dans les édifices, Histoire de l'Académie Royal des Sciences, Année 1712.
Lamé, G., and Clapeyron, E. (1823), Sur la stabilité des voutes, Annales des Mines 8.
Lee, F. H. and Symonds, P. S. (1952), Large Plastic Deformation of Beams under Transverse Impact, J. App. Mech., 19, pp. 308—314.
Kruzelecki, J. and Zyczkowski, M. (1985), Optimal Structural Design of Shells—a Survey, SM Archives 10. pp. 101—170.
Kwiecinski, M. (1986), Plastic Design of Slab-Beam Systems, (In Polish) Warsaw. Panstwowe Wysawnictwo Naukowe.
Lehmann, Th. (1979), Elemente der Mechanik I—IV. Vieweg and Sohn, Braunschweig, Wiesbaden.
Lehmann, Th. (1985), On a Generalized Constitutive Law in Thermoplasticity. Plasticity Today, eds.: Sawczuk, A. and Bianchi, G., Elsevier London.
Lepik, Ü. and Mróz, Z. (1977), Optimal Design of Plastic Structures under Impulsive and Dynamic Pressure Loading, Int. J. of Solids and Structures, 13 pp. 657—674.
Lévy, M. (1870), Mémoire sur les équations générales des mouvements intérieurs des corps solides ductiles au dela des limites où l'élasticité pourrait les ramener à leur premier état, Compt. Rend. Acad. Sci., Paris 70 pp. 1323—1325.
Lin, T. H. (1955), A Proposed Theory of Plasticity Based on Slip, Proc. 2nd US Nat. Congr. Appl. Mech., New York pp. 461—468.
Lin, T. H. (1968), Theory of Inelastic Structures, John Wiley New York, London, Sydney, Toronto.
Lippmann, H. (1981), Mechanik des plastischen Fliessens, Grundlagen und Technische Anwendungen, Springer Verlag, Berlin, Heidelberg, New York.
Lippmann, H. and Mahrenholtz, O. (1967), Plastomechanik der Umformung metallischer Werkstoffe. Springer Verlag, Berlin.
Livesley, R. K. (1956), The Automatic Design of Structural Frames., Quart. J. Mech. Appl. Math. 9, 3 pp. 257—278.
Livesley, R. K. (1964), Matrix Methods of Structural Analysis, Pergamon Press, New York, Oxford.
Livesley, R. K. (1966), Notes on Linear Programming. Cambridge University Engineering Laboratory, Techn. Report, No. 9.

Livesley, R. K. (1967), The Flection of Redundant Forces in Structures with an Application to the Collapse Analysis of Frameworks, Proc. Roy. Soc. A., 301 pp. 493—505.
Livesley, R. K. (1978), Limit Analysis of Structures Formed from Rigid Blocks, Int. Journ. Numerical Methods in Engineering, 12 pp. 1853—1871.
Lode, W. (1926), Versuche über den Einfluss der mittleren Hauptspannung auf das Fliessen der Metalle Eisen, Kupfer und Nickel, Z. Physik 36 pp. 913—939.
Magnusson, A. W. and Baldwin, W. M. (1957), Low Temperature Brittleness. J. Mech. Phys. Solids, 5 pp. 19—57.
Maier, G. (1968), Quadratic Programming and Theory of Elastic Perfectly-Plastic Structures, Meccanica 4, Vol. III.
Maier, G. (1972a), Limit Design in the Absence of a Given Layout. A Finite Element, Zero–One Programming Approach. J. Struct. Mech. 1 pp. 213—230.
Maier, G. (1972b), A Shake-down Matrix Theory Allowing for Workhardening and Second-Order Geometric Effects. Symposium on Foundations of Plasticity, Nordhoff International Publishing Co., Warsaw, Groningen.
Maier, G. and Corradi, L. (1974), Upper Bounds on Dynamic Deformations of Elastoplastic Continua, Meccanica, 1, Vol. IX.
Maier, G., Giacomini, S. and Paterlini, F. (1976), Elastoplastic and Limit Analysis of Discretized Structures by Restricted Basis Linear Porgramming, 3rd Congress of AIMETA, Cagliari.
Maier, G., Srinivasan, R. and Save, M. A. (1976), On Limit Design of Frames Using Linear Programming, J. Struct. Mech., 4, 4 pp. 349—378.
Maier, G., Grierson, D. E. and Biest, M. J. (1977), Mathematical Programming Methods for Deformation Analysis at Plastic Collapse, Computers, Structures, 7 pp. 599—612.
Maier, G. and Munro, J. (1982), Mathematical Programming Applications to Engineering Plastic Analysis, Appl. Mech. Rev., Vol. 35. No. 12. pp. 1631—1643.
Maier-Leibnitz, H. (1928), Beitrag zur Frage der tatsächlichen Tragfähigkeit einfacher und durchlaufender Balkenträger aus St 37 und aus Holz, Bautechnik 6.
Majid, K. I. (1972), Non-Linear Structures, Matrix Methods of Analysis and Design by Computers, Butterworths, London.
Majid, K. I. (1974), Optimum Design of Structures, Newnes-Butterworths, London.
Malmeisters, A., Tamuzs, V. and Teters, G. (1977), Mechanik der Polymerwerkstoffe, Akademie-Verlag, Berlin,
Manjoine, M. J. (1944), Influence of Rate of Strain and Temperature on Yield Stresses of Mild Steel, J. Appl. Mech., 11, pp. 211.
Marcal, P. V. and Prager, W. (1964), A Method of Optimal Plastic Design, J. Mécanique 3 pp. 509—530.
Markov, A. A. (1947), On Variational Principles in the Theory of Plasticity, (In Russian) Prikladaia Matematika i Mekhanika 11. pp. 339—350.
Martin, J. B. (1972), Extremum Principles for a Class of Dynamic Rigid-Plastic Problems, Int. J. of Solids and Structures, 8 pp. 1185—1204.
Martin, J. B. (1975), Plasticity. Fundamentals and General Results, MIT Press, Cambridge, Mass.
Martin, J. B. and Symonds, P. S. (1966), Mode Approximations for Impulsively-Loaded Rigid-Plastic Structures, J. Engng. Mech. Div. Proc., ASCE 92, EM 5 p. 43.
Martin, J. B. and Ponter, A. R. S. (1972), Bounds for Impulsively-Loaded Plastic Structures, Journ. Engng. Mech. Div. Proc. ASCE 98, EM 1 pp. 107—119.
Massau, J. (1899), Mémoire sur l'intégration des équations aux dérivées partielles, Ghent.
Massonnet, Ch. and Save, M. (1961), Calcul Plastique des Constructions. Centre Belgo-Luxembourgeois d'Information de l'Acier, Vol. 1. Bruxelles, Vol. 2, 1963.
Massonnet, Ch., Olszak, W. and Phillips, A. (1979), Plasticity in Structural Engineering. Fundamentals and Applications, Springer Verlag, Vienna, New York.
Megarefs, G. J. and Hodge, P. G. (1963), Method for Plastic Design of Frames, J. Struct. Mechn. Div. Proc. ASCE 89, St. 1.
Melan, E. (1936), Theorie statisch unbestimmter Systeme, Prelim. Publ. 2nd Congr. Int. Ass. Bridge Struct. Engng., Berlin pp. 43—64.
Melan, E. (1938), Der Spannungszustand eines Mieses-Henckyschen Kontinuums bei veränderlichen Belastung, Sitz. Berg. Akad. Wis. Wien, Abt. 11/a. pp. 147—173.

Melchers, R. E. and Rozvany, G. I. N. (1970), Optimum Design of Reinforced Concrete Tanks, J. Engng. Mech. Div. Proc. ASCE, 96, EM 6, 11.
Mendelson, A. (1968), Plasticity: Theory and Application, MacMillan, New York.
Menyhárd, I. (1956), Die statische Berechnung von zylindrischen Stahlbeton-Behältern auf Grund der Bruchtheorie, Vorbericht V. Kongr. Int. Ver. Brücken- und Hochbau, Lissabon.
Mikeladze, M. S. (1963), Statics of Anisotropic Plastic Shells, (In Russian) Izd. Akad. Nauk Gruzinskoi SSSR, Tiflis.
Mises, R. (1913), Mechanik der festen Körper im plastisch-deformablen Zustand, Göttingen Nachr. Math. Phys. K., 1 pp. 582—592.
Mises, R. (1928), Mechanik der plastischen Formänderung von Kristallen, Z. Ang. Math. Mech., 8, 3 pp. 161—185.
Mises, R. (1949), Three Remarks on the Theory of the Ideal Plastic Body, Reissner Anniversary Volume, Edwards Brothers Inc. pp. 415—429.
Moseley, H. (1943), The Mechanical Principles of Engineering and Architecture, part IV., London.
Moy, S. J. (1981), Plastic Methods for Steel and Concrete Structures, John Wiley, New York.
Mróz, Z. (1952), Plastic Deformations of Annular Plates under Dynamic Loads, Arch. Mech. Stos., 10 pp. 499—516.
Mróz, Z. (1958), On the Design of Non-Homogeneous Technically Orthtropic Plates, Proc. Symposium IUTAM, Warsaw.
Mróz, Z. (1963), Non-Associated Flow Laws in Plasticity. J. Mécanique, 2 pp. 21—42.
Mróz, Z. (1973), Multiparameter Optimal Design of Plates and Shells, J. Struct. Mech., 1 pp. 371—392.
Muskelisvili, N. I. (1953), Some Basic Problems of the Mathematical Theory of Elasticity, Nordhoff International Publishing Co., Groningen.
Nádai, Á. (1927), Der bildsame Zustand der Werkstoffe, Springer Verlag, Berlin.
Nádai, Á. (1950), Theory of Flow and Fracture of Solids, McGraw-Hill, Vol. 1., New York, Toronto, London.
Nádai, Á. (1963), Theory of Flow and Fracture of Solids, Vol. 2., McGraw-Hill, New York, Toronto, London.
Neal, B. G. (1950), Plastic Collapse and Shake-down Theorems for Structures of Strain-hardening Material, J. Aeronaut. Sci. 17 pp. 297—306.
Neal, B. G. (1951), The Behaviour of Framed Structures under Repeated Loading, Quart. J. Mech. Appl. Math., 4 pp. 78—84.
Neal, B. G. (1956), The Plastic Methods of Structural Analysis, Chapman and Hall, London.; 2nd ed., 1963, Chapman and Hall, London.
Neal, B. G. (1958), Die Verfahren der plastischen Berechnung biegesteifer Stahlstabwerke, Springer Verlag, Berlin, Göttingen, Heidelberg.
Neal, B. G. (1977), The Plastic Methods of Structural Analysis, Chapman and Hall, London.
Neal, B. G. and Symonds, P. S. (1950), The Calculation of Collapse Loads for Framed Structures, J. Inst. Civil Engrs., London 35 pp. 21—40.
Neal, B. G. and Symonds, P. S. (1952), The Rapid Calculation of the Plastic Collapse Load for a Framed Structure, Proc. Inst. Civil Engrs., London 1 pp. 58—71.
Nédli, P. (1976), Elasto–Plastic Analysis of Frames by Wolfe's Short Algorithm, Periodica Polytechnica. Civ. Eng., 20, 3—4 pp. 127—134.
Ngyen, D. H. (1983), Aspect of Analysis and Optimization of Structures under Proportional and Variable Loadings, Engineering Optimization. Vol. 7. No. 1. pp. 35—77.
Nonaka, T. (1967), Some Interaction Effects in Problems of Plastic Beam Dynamics, J. App. Mech., 34 pp. 623—643.
Nonaka, T. (1972), A Kinematical Approach to the Plastic Collapse Load of a Rectangular Frame with Consideration of Axial Forces, Symposium, Iasi (Rumania).
Nonaka, T. (1977), Shear and Bending Response of a Rigid-Plastic Beam to Blast-Type Loading, Ing. Arch., 46 pp. 35—52.
Norris, C. H. et al. (1959), Structural Design for Dynamic Loads, McGraw-Hill, New York, Toronto, London.
Oden, T. J. (1972), Finite Elements of Nonlinear Continua, McGraw-Hill, New York.
Oden, T. J. and Bathe, K. J. (1978), A Commentary on Computational Mechanics, Appl. Mech. Rev. Vol. 31. No. 8. pp. 1053—1058.

Odquist, F. K. G. and Hult, J. (1962), Kriechfestigkeit metallischer Werkstoffe, Springer Verlag, Berlin.
Olszak, W. and Perzyna, P. (1957), Extremum Theorems in the Theory of Non-Homogeneous and Anisotropic Bodies, Arch. Mech. Stos., 9, 6 pp. 695—712.
Olszak, W. and Perzyna, P. (1958), Variational Theorems in the Theory of Non-Homogeneous Elastic-Plastic Bodies, Bull. Acad. Pol. Sci. Ser. Techn. Sci., No. 2.
Olszak, W., Mróz, Z. and Perzyna, P. (1963), Recent Trends in the Development of the Theory of Plasticity, Pergamon Press; Oxford, London, New York, Paris.
Olszak, W. and Sawczuk, A. (1964), Non-Classical Shell Problems, IASS Proceedings Symposium, North-Holland, Warsaw, Amsterdam.
Olszak, W. and Sawczuk, A. (1967), 'Inelastic Behaviour in Shells', in: Noordhoff Series of Monographs and Textbooks on Pure and Applied Mathematics, Noordhoff International Publishing Co., Groningen.
Onat, E. T. (1955), Plastic Collapse of Cylindrical Shells under Axially Symmetrical Loading, Quart. Appl. Math., 13, pp. 63—72.
Onat, E. T. (1960), Plastic Analysis of Shallow Conical Shells, J. Engng. Mech. Div. Proc., ASCE 86, 6 pp. 1—12.
Onat, E. T. (1966), Description of Mechanical Behavior of Inelastic Solids, Proc. 6th US National Congr. Appl. Mech. ASME, pp. 421—433.
Owen, D. R. J. and Hinton, E. (1980), Finite Elements in Plasticity: Theory and Practice, Pineridge Press Ltd., Swansea.
Ovechkin, A. M. (1960), Design of Axisymmetric Reinforced Concrete Structures (In Russian) Gosstroizdat, Moscow.
Palotás, L. (1962), Versuche mit Stahlbetonplatten und Pilzdecken und ihre Auswertung auf Grund der Bruchtheorie. Wissenschaftliche Zeitschrift der Hochschule für Bauwesen Cottbus, 5, 3—4.
Pande, G. N. and Zienkiewicz, O. C. (1980), Soils under Cyclic and Transient Loading, Proc. Int. Symp., Balkema, Swansea, Rotterdam.
Peano, A. (1977), Limit Analysis Via Stress Functions, Limit Analysis Using Finite Elements, ASME Special Publication Book, No. 109.
Pelikán, J. (1957), Theory of Highly Economical Reinforced Concrete Beams, Acta Techn. Acad. Sci. Hung., XVIII, pp. 1—2.
Peredy, J. (1959), Über eine neue Minimumaufgabe der Technischen Festigkeitslehre, Acta Techn. Acad. Sci. Hung., XXIV, pp. 3—4.
Perzyna, P. (1963), The Constitutive Equations of Rate Sensitive Plastic Materials, Quart. Appl. Mech. 20. pp. 321—332.
Perzyna, P. (1966), 'Fundamental Problems in Visco-Plasticity', in: Recent Advances in Applied Mechanics 9., Academic Press, New York.
Perzyna, P. (1968), Problems of Viscoplasticity (In Russian), Izd. Mir., Moskva.
Phillips, A. (1956), Introduction to Plasticity, The Ronald Press Co., New York.
Ploch, J. and Wierzbicki, T. (1974), Bounds in Large Melastic Deformations of Dynamically Loaded Structures, (In Polish) Proc. 3rd Symposium on Dynamic Stability of Structures, Warsaw.
Polizzotto, C. (1978), Adaptation of Rigid-Plastic Continua under Dynamic Loading, J. Struct. Mech., 6, 3 pp. 319—329.
Polizzotto, C. (1984), Dynamic Shakedown by Modal Analysis, Meccanica. 19, 2. pp. 133—144.
Polizzotto, C. (1985), New Developments in the Theory of Dynamic Shakedown, Plasticity Today, eds.: Sawczuk, A. end Biachi, G. Elsevier, London.
Poncelet, J. V. (1840), Mémoire sur la stabilité de revetements et de leurs fondations, Mémoires de l'Officier du Génie 13.
Pope, G. G. (1965), The Application of Matrix Displacement Method in Plane Elastoplastic Problems, Proc. Conf. Matrix Methods in Structural Mechanics, Wright–Patterson Air Force Base.
Prager, W. (1952), General Theory of Limit Design, Proc. 8th Int. Congr. Appl. Mech. 2., Istambul pp. 65—72.
Prager, W. (1955), Probleme der Plastizitätstheorie. Birkhäuser, Basel, Stuttgart.
Prager, W. (1959), An Introduction to Plasticity, Addison-Wesley, Reading, Mass., London.
Prager, W. (1961), Einführung in die Kontinuumsmechanik, Birkhäuser, Basel, Stuttgart.
Prager, W. (1966), Models of Plastic Behaviour, Proc. 6th US Nat. Congr. Appl. Mech., ASME pp. 435—450.
Prager, W. (1970), Optimization of Structural Design, J. Optimiz. Theory Appl., 6, 1 pp. 1—21.

Prager, W. (1974), Introduction to Structural Optimization, Int. Centre for Mech. Sci. Udine, No. 212. Springer Verlag, Vienna.
Prager, W.—Hodge, P. G. Jr. (1951), Theory of Perfectly-Plastic Solids, John Wiley, New York.
Prager, W. and Hodge, P. G. Jr. (1954), Theorie ideal-plastischer Körper, Springer-Verlag, Vienna.
Prager, W. and Hodge, P. G. Jr. (1965), Theory of Perfectly-Plastic Solids (In Hungarian), Műszaki Könyvkiadó, Budapest.
Prager, W. and Shield, R. T. (1967), A General Theory of Optimal Plastic Design, J. Appl. Mech. Trans. ASME, 34 pp. 86—97.
Prager, W. and Sheu, C. (1968), Recent Developments in Optimal Structural Design, Appl. Mech. Rev., 10.
Prandtl, L. (1903), Zur Torsion von prismatischen Stäben, Z. Physik, 4 pp. 758—759.
Prandtl, L. (1920), Über die Härte plastischer Körper, Göttingen Nachr. Math. Physik Kl., 12.
Prandtl, L. (1924), Spannungsverteilung in plastischen Körpern. Proc. lst Int. Congr. Appl. Mech. Delft. Technische Boekhandel en Druckerij, J. Waltman, Jr. pp. 43—54.
Przemieniecki, J. S. (1966), Theory of Matrix Structural Analysis, McGraw-Hill, New York.
Rabotnov (1962), Strength of Materials, (In Russian) Fizmatgiz, Moscow.
Radenkovic. D. (1961), Theorèmes limites pour un material de Coulomb à dilatation non standardisée, C. R. Acad. Sci. Paris, 252 pp. 4103—4104.
Ramberg, W. and Osgood, W. R. (1943), Description of Stress-strain Curves by three Parameters, NACA Technical Note No. 902, July.
Rankine, W. J. M. (1859), On the Stability of Loose Earth. Phil. Trans. Roy. Soc., p. 147.
Rebhann, G. (1871), Theorie des Erddrucks und der Futtermauern mit besonderer Rücksicht auf das Bauwesen, Vienna.
Reckling, K. A. (1967), Plastizitätstheorie und ihre Anwendung auf Festgkeitsprobleme, Springer Verlag, Berlin.
Reuss, E. (1930), Berücksichtigung der elastischen Formänderungen in der Plastizitätstheorie, Z. Angew, Math. Mech. 10 pp. 266—274.
Reuss, E. (1932), Fliesspotential der Gleitebenen, Z. Angew. Math. Mech., 12 p. 15.
Reuss, E. (1933), Vereinfachte Berechnung der plastischen Formänderungsgeschwindigkeiten bei Voraussetzung der Schubspannungsfliessbedingung, Z. Angew. Math. Mech. 13 p. 356.
Reuss, E. (1938), Über Lüders–Harmannsche Linien, Z. Angew. Math. Mech., 18 pp. 347—357.
Reuss, E. (1961), Mechanics of Plastic Bodies (In Hungarian), Műszaki Könyvkiadó, Budapest, pp. 983—998.
Rozvany, G. I. N. (1971), Concave Programming and Piecewise Linear Programming, Int. J. Numerical Methods in Engng., 3 pp. 131—144.
Rozvany, G. I. N. (1976), Optimal Design of Flexural Systems: Beams, Grillages, Slabs, Plates and Shells, Pergamon Press, Oxford, New York, Toronto, Sydney, Paris, Frankfurt.
Rozvany, G. I. N. and Adidam, S. R. (1971), Dual Formulation of Variational Problems in Optimal Design, Proc. Int. Conf. Design Automation., New York.
Rozvany, G. I. N. and Adidam, S. R. (1972), Recent Advances in Plastic Optimal Design, Symposium on Foundations of Plasticity, Warsaw, Noordhoff International Publishing Co., Groningen.
Rzhanitsyn, A. R. (1956), The Design of Plates and Shells by the Kinematical Method of Limit Equilibrium, Proc. IX. Int. Cong. Appl. Math. Mech., Bruxelles, pp. 331—340.
Rzhanitsyn, A. R. (1958), The Investigation of Problems of Plasticity and the Limit Analysis of Structures (In Russian), Gosstroizdat, Moscow.
Sachs, G. (1927), Zur Theorie des Ziehvorgangs, Z. Angew. Math. Mech., 7 p. 235.
Saint-Venant, B. (1856), Mémoire sur la torsion des prismes, Mem. Acad. Sci. Math. Phys., 14 pp. 233—560.
Saint-Venant, B. (1870), Mémoire sur l'établissement des équations différentielles de mouvements intérieurs opérés dans les corps solides ductiles au dela des limites où l'élasticité pourrait les ramener à leur premier état, Compt. Rend., 70 pp. 473—480.
Salençon, J. (1977), Applications of the Theory of Plasticity in Soil Mechanics, John Wiley Chichester, New York.
Save, M. A. (1972), A Unified Formulation of the Theory of Optimal Plastic Design with Convex Cost Function. J. Struct. Mech., 1 pp. 247—276.
Save, M. A. and Prager, W. (1963), Minimum Weight Design of Beams Subjected to Fixed and Moving Loads. J. Mech. Phys. Solids, 11 pp. 255—267.

Save, M. A. and Massonnet, Ch. (1972), 'Plastic Analysis and design of Plates, Shells and Disks', in: Applied Mathematics and Mechanics, North-Holland, Amsterdam.
Save, M. A. and Massonnet, Ch. (1972a), L'influence de la plasticité et de la viscosité sur la résistance et la déformation des constructions, IX. Cong. Int. Ass. Bridge Struct. Engng., Amsterdam.
Save, M. (1985a), Limit Analysis and Design: an Up-to-date Subject of Engineering Plasticity. Plasticity Today, eds.: Sawczuk, A., Bianchi, G. Elsevier Applied Science Publishers, London.
Save, M. (1985b), Limit Analysis of Plates and Shells: Research over Two Decades, J. Struct. Mech. 13 (3—4) 343—370.
Save, M. and Prager, W. (1985), Structural Optimisation, Vol. 1. Optimality Criteria, Plenum Press, New York, London.
Sayir, M. and Frommer, H. (1985), Singular Perturbations in Plasticity: Application to Plane-strain Slip-line Fields. Plasticity Today, eds.: Sawczuk, A., Bianchi, G. London, Elsevier Applied Science Publishers.
Sawczuk, A. (1978), Wprowadzenie do mechaniki konstrukcji plastycznych, Wroclaw, Wydsawnictwo Politechniki, Wroclawskiej.
Sawczuk, A. and Hodge, P. G. (1960), Comparison of Yield Conditions for Circular Cylindrical Shells, J. Franklin Inst., 269 pp. 362—374.
Sawczuk, A. and König, J. A. (1962), Limit Analysis of Reinforced Concrete Cylindrical Silos, Arch. Inz. Lad., 8 pp. 161—183.
Sawczuk, A. and Jaeger, Th. (1963), Grenztragfähigkeits-Theorie der Platten, Springer Verlag, Berlin, Göttingen, Heidelberg.
Sawczuk, A. and Kaliszky, S. (1964), On the Limit Analysis of Plates Supported by a Nonhomogeneous Plastic Subgrade under Rotational-Symmetric Conditions, Acta Techn. Acad. Sci. Hung., 48 pp. 186—201.
Sawczuk, A. and Bianchi, G. (1983), Plasticity Today, Proc. Symposium Elsevier, London.
Sayegh, A. F. and Rubinstein, M. F. (1972), Elastic-Plastic Analysis by Quadratic Programming, Journ. Engng. Mech. Div. Proc. ASCE, EM 6 pp. 1547—1572.
Shapiro, G. Sh. (1959), Impulsively Loaded Rigid-Plastic Circular Plate, (In Russian) Prikl. Mat. i Mekh., XXIII pp. 172—175.
Shapiro, G. Sh. and Reitman, M. I. (1974), Optimal Design of Structures under Dynamic Loading, Vilnius
Save, M. (1985), Limit Analysis of Plates and Shells: Research over two Decades, J. Struct. Mech. 13 (3—4) (343—370)
Shaw, F. S. (1944), The Torsion of Solid and Hollow Prisms in the Elastic and Plastic Range by Relaxation Methods, Australian Council for Aeronautics, Rep. ACA—11.
Shield, R. T. and Drucker, D. C. (1953), The Application of Limit Analysis to Punch-Indentation Problems, J. Appl. Mech., 20 pp. 453—460.
Siebel, E. and Fangmeier, E. (1931), Researches on Power Consumption in Extrusion and Punching of Metal, Mitt. K.-W.-Inst., Eisenforsch. 13 p. 29.
Slater, R. A. C. (1977), Engineering Plasticity: Theory and Application to Mechanical Processes, John Wiley, New York.
Smith, J. O. and Sidebottom, O. M. (1965), Inelastic Behaviour of Load-Carrying Members, John Wiley, New York, London, Sydney.
Sokolnikoff, I. S. (1956), Mathematical Theory of Elasticity, 2nd ed., McGraw-Hill, New York.
Sokolovski, V. V. (1942), On a Problem of Elasto-Plastic Torsion (In Russian), Prikl. Mat. i Mekh., IV pp. 241—246.
Sokolovski, V. V. (1950), Theory of Plasticity, (In Russian) Gostekhizdat, Moskva, Leningrad.
Sokolovski, V. V. (1969), Theory of Plasticity, (In Russian) Izd. Vysshaia shkola, Moskva.
Southwell, R. V. (1946), Relaxation Methods in Theoretical Physics, Oxford University Press.
Stassi D'Alia, F. (1951), Un paraboloide di rivoluzione quale condizione di plastizita, L'ingegnere.
Stassi D'Alia, F. (1957), La condizione di plastizita, Politecnico di Milano. Rendiconti, XI pp. 60—75.
Stassi D'Alia, F. (1967), Flow and Fracture of Materials According to a New Limiting Condition of Yielding, Meccanica 2. pp. 178—195.
Swida, W. (1950), Über die Restspannungen bei der elastisch-plastischen Biegung des krummen Stabes, Ing. Arch. 18 pp. 77—83.
Symonds, P. S. (1951), Shake-down in Continuous Media, J. Appl. Mech., 18 pp. 85—89.
Symonds, P. S. (1953), Dynamic Load Characteristics in Plastic Bending of Beams, J. Appl. Mech., 20 pp. 475—481.

Symonds, P. S. (1955), Large Plastic Deformation of Beams under Blast-Type Loading, Proc. 2nd US Nat. Congr. Appl. Mech. Ann. Arbor. Mich, Ed. Naghdi, P. M., ASME, New York.

Symonds, P. S. (1973), Approximation Techniques for Impulsively Loaded Structures with Rate Sensitive Plastic Behaviour, SIAM J. Appl. Math., 25, 3 pp. 41—60.

Symonds, P. S. (1984), Twenty Years of Developments in Inelastic Dynamics, Proc. 5th Eng. Mech. Div. Speciality Conference. EM Division/ASCE Laramie, Wyoming pp. 1—23.

Symonds, P. S. and Prager, W. (1950), Elastic-Plastic Analysis of Structures Subjected to Loads Varying Arbitrarily Between Limits., J. Appl. Mech., 17 pp. 315—323.

Symonds, P. S. and Neal, B. G. (1952), The Interpretation of Failure Loads in the Plastic Theory of Continuous Beams and Frames, Journ. Aero. Sci., 19. p. 15.

Symonds, P. S. and Chon, C. T. (1975), Bounds for Finite Deflections of Impulsively Loaded Structures with Time-dependent Plastic Behaviour, Int. J. of Solids and Structures, 11 pp. 403—423.

Symonds, P. S. and Wierzbicki, T. (1975), On an Extremum Principle for Mode Form Solutions in Plastic Structural Dynamics, J. Appl. Mech., 42 pp. 630—640.

Symonds, P. S. and Yu, T. X. (1985), Counterintuitive Behavior in a Problem of Elastic–Plastic Beam Dynamics, Journ. Appl. Mech. Vol. 107. pp. 517—522.

Szabó, I. (1977), Höhere technische Mechanik, 5. Aufl. Berlin, Heidelberg, Springer Verlag, New York.

Szabó, J. and Roller, B. (1978), Anwendung der Matrizenrechnung auf Stabwerke, Akadémiai Kiadó, Budapest.

Szmodits, K. (1959), Limit Analysis of Hyperbolic Paraboloid Shells (In Hungarian), ÉKME Tud. Közl., III.

Tamuzh, B. P. (1962), On a Minimum Principle of the Dynamics of Rigid–Plastic Bodies, (In Russian) Prikl. Mat. i Mekh., XXVI pp. 715—722.

Taylor, G. I. and Quinney, H. (1931), The Plastic Distorsion of Metals, Phil. Trans. Roy. Soc., London A 230 pp. 323—362.

Terzaghi, K. (1943), Theoretical Soil Mechanics, John Wiley, New York.

Timoshenko, S. (1961), Theory of Elastic Stability, 2nd ed. New York, Toronto, London, Mchraw-Hill.

Timoshenko, S. and Woinowsky-Krieger, S. (1940), Theory of Plates and Shells. New York, London, McGraw-Hill Co.

Timoshenko, S. and Goordier, J. N. (1970), Theory of Elasticity, New York, Toronto, London, McGraw-Hill.

Tottenham, H. and Brebbia, C. (1970), Finite Element Techniques in Structural Mechanics, Proc. Seminar at University of Southampton. Southampton University Press.

Tresca, H. (1964), Mémoire sur l'écoulement des corps solides soumis à les fortes pressions, Compt. Rend. Acad. Sci. Paris 59 pp. 754.

Valanis, K. C. (1971), A Theory of Viscoplasticity without a Yield Surface, Archives of Mechanics. 23 pp. 517—533, 535—551.

Valanis, K. C. (1980), Fundamental Consequences of a New Intrinsic Time Measure Plasticity as a Limit of the Endochronic Theory, Arch. Mech. 32.2 pp. 171—191.

Valanis, K. C. and Lee C. F. (1982), Some Recent Developments at the Endochronic Theory with Applications, Nuclear Eng. Design 69. pp. 327—344.

Visy, Z. (1959), Iterative Method for the Calculation of Moments in Highly Economical Reinforced Concrete Beams. Acta Techn. Acad. Sci. Hung., XXII pp. 1—2.

Vitiello, E. (1972), Upper Bounds to Plastic Strains in Shakedown of Structures Subjected to Cyclic Loads. Meccanica 7 pp. 205—213.

Vogel, U. (1965), Die Traglastberechnung stählerner Rahmentragwerke nach der Plastizitätstheorie II. Ordnung, Köln, Stahlbauverlag.

Wang, A. J. (1955), The Permanent Deflection of a Plastic Plate under Blast Loading, J. Appl. Mech. 22 pp. 375—376.

Washizu, K. (1975), Variational Methods in Elasticity and Plasticity, In: International Series of Monographs in Aeronautics and Astronautics, 1. division. Solid and Structural Mechanics, Vol. 9. Oxford, Pergamon Press. 2nd Ed.

Wasiutynski, Z. and Brandt, A. (1963), The Present State of Knowledge in the Field of Optimum Design of Structures, Appl. Mech. Rev. 16, 5 pp. 1—6.

Weidler, J. B. and Paslay, P. R. (1969), Analytical Description of Behaviour of Granular Media. J. Engng. Mech. Div. Proc. ASCE 95, EM 2, 4.

Westergaard, H. M. (1952), Theory of Elasticity and Plasticity, Cambridge, Harvard University Press.

Wierzbicki, T. (1967a), Impulsive Loading of Rigid Visco-plastic Plates, Int. J. of Solids and Structures 3 pp. 365—647.
Wierzbicki, T. (1967b), A Method of Approximate Solution of Boundary Value Problems for Rigid–Viscoplastic Structures, Acta Mech. II/I. pp. 60—72.
Wierzbicki, T. and Florence, A. L. (1970), A Theoretical and Experimental Investigation of Impulsively Loaded Clamped Circular Plastic and Viscoplastic Plates, Int. J. of Solids and Structures 6 pp. 553—568.
Wierzbicki, T. (1976), Response of Dynamically Loaded Structures. (In Polish) Arkady, Warsaw.
Wolfe, P. (1959): The Simplex Method for Quadratic Programming, Econometrica 27, 3 pp. 382—398.
Wood, R. H. (1961), Plastic and Elastic Design of Slabs and Plates, London, Thames and Hudson.
Wood, R. H. and Jones, L. L. (1967), Yield-line Analysis of Slabs, Thames and Hudson-Chatto and Vindus.
Zavelani, A. (1973), A Compact Linear Programming Procedure for Optimal Design in Plane Stress, J. Struct. Mech. 2, 4 301—324.
Zyczkowski, M. (1981), Combined Loading in the Theory of Plasticity, Warsaw. PWN-Polish Scientific Publishers.
Ziegler, H. (1972), Thermomechanics, Quart. Appl. Math. 30.
Zienkiewicz, O. C. (1971), The Finite Element Method in Engineering Science, London, McGraw-Hill. 3rd. ed. (1977).
Zienkiewicz, O. C. (1974), Methode der finiten Elemente, Leipzig, VEB Fachbuchverlag.
Zienkiewicz, O. C., Valliappan, S. and King, I. P. (1969), Elasto-Plastic Solutions of Engineering Problems. "Initial stress" Finite Element Approach, Int. J. Numer. Methods in Engng. 1 pp. 75—100.
Zurmühl, R. (1964) Matrizen, Berlin, Springer Verlag.

SUBJECT INDEX

absolute minimum weight 341
accumulating plastic deformation 309
Airy's stress function 179, 234
alternating plastic deformation 112, 238, 309

Bauschinger effect 23
beam mechanism 284
Beltrami–Michell equation 86
Bingham model 435
body force 45
bulk modulus 34, 59

Cartesian tensor notation 31
Castigliano's theorem 98, 335
Cauchy equilibrium equations 45
centred fan 191
cohesion 415
collapse load 104
compatibility equations 57
complementary virtual work 91
– – –, principle of 93
constitutive equations 58
– – of elastic bodies 58
– – of Prandtl–Reuss 73
– – of Lévy–Mises 75
– – of Hencky 77
continuity equations 57
convexity rule 70
Cosserat-continuum 38
cost function 323
creep 20, 424, 428, 430
–, primary 424
–, secondary 424
creep recovery 426
critical cross-section 282
critical load 237
cyclic loading 112, 311, 313

damping factor 405
– –, elastic 405
– –, optimal 406
deformation theory 77
design constraints 323
design variable 323
differential convention 33
dilatation 34, 52
discontinuity
– in stress field 120, 219
– in velocity field 121, 192, 219
discontinuity line 120, 121, 192
displacement method 225
dissipation energy 108, 242
distorsion energy theory 65
Drucker's stability postulate 21, 69

elastic hysteresis 23
elastic limit load 104, 237, 265, 275
– – moment 257
– – surface 392
– – torque 147
elastic material 20
elastic section modulus 257
elastic stability function 319
elasto-plastic material 21

Foulkes-mechanism 329, 349
flexibility method 225
flow rule 71, 240
– –, associated 71
– –, generalized 241
– –, nonassociated 71
flow theory 77
force method 225
fully plastic moment 258

generalized strain 239
generalized stress 239

hardening
–, isotropic 410, 411
–, kinematic 410, 412
–, plastic 408
hardening function 408
Helliger–Reisner principle 99
Hencky constitutive equations 77
– elasto-plastic body 85
homogeneous body 20
Hooke's law 25, 58
Hu-Washizu principle 96

incipient plastic deformation 104
incremental analysis 346
incremental collapse 112, 238, 309
incremental plastic deformation 112, 238, 309
incremental theory 77
internal friction 415
isotropic material 20

Kelvin–Voigt model 429, 434
kinematic boundary conditions 56
kinematic equations 56
kinematic principle
– – of limit analysis 107, 277
– – of shakedown analysis 118
kinematically admissible multiplier 35, 108, 277, 348
– – strain and displacement field 89, 100, 348
Kirchhoff–Love hypothesis 350
Kronecker delta 32

Lagrangian formulation 47
Lamé's modulus 59
Lamé–Navier equations 82
large deflection theory 237, 316
Lévy–Mises constitutive equations 75
– – rigid-plastic body 86
limit analysis 104, 133, 136, 237, 347
linearly elastic body 82
linearly elastic — perfectly plastic material 24
load intensity 104, 275
load multiplier 104, 275

mathematical programming 342
maximum shear stress theory 65
Maxwell model 428, 434
membrane analogy 148, 154
method of combined mechanisms 284
minimum volume design 323
minimum weight design 323, 349
mode form motion 452
mode shape 452, 457
Mohr's circle 43, 183
multiple loading 112

normality rule 70, 240

objective function 323, 342
one-parameter loading 104
optimal design 140
optimal plastic design 323

plastic deformation 20
– –, accumulating 309
– –, alternating 112, 238, 309
– –, incipient 104
– –, incremental 112, 238, 309
– –, progressive 112, 238
– –, unrestricted 104, 309
plastic design 237
plastic hardening 407
plastic hinge 267, 377
– –, generalized 297
plastic limit load 104, 237, 277
– – moment 258, 260
– – state 104
– – surface 297
plastic material 20
– – modulus 78
– – multiplier 35, 71, 75, 241
– – reserve 266
– – section modulus 258, 261
permanent stress 115
Poisson's ratio 58
Prandtl–Reuss constitutive equations 73
– – elasto-plastic body 83
principal direction 38
– normal strain 34, 52
– normal stress 34, 38
– shear strain 34, 53
– shear stress 34, 41
principle of complementary virtual power 94, 346
– – complementary virtual work 93
– – minimum complementary energy 97
– – minimum complementary energy rate 101
– – minimum elastic strain energy 98
– – minimum potential energy rate 103
– – stationary potential energy 94
– – virtual power 93
– – virtual work 91
proportional loading 104, 275

Rankine–Merchant method 320
relative displacement tensor 47
relaxation 20, 424, 428, 431
residual moment 311
residual stress 113, 114, 263
rigid-plastic material 24
rotation tensor 49

sand hill analogy 157
secant modulus 78
shakedown 112, 138, 238, 263, 348
– analysis 114
– load multiplier 118, 312
shape factor 258
shape function 225
shear line 181, 184, 188
–– theory 189
shear modulus 34, 58
simplex method 344
slip line 122, 189
small deflection theory 237, 317
soap film analogy 149
stability postulate 21, 69
stable material 21
state variable 323
static principle of limit analysis 106, 277
––– shakedown analysis 114
statically admissible stress and force field 89, 100, 348
–– multiplier 35, 106, 277, 348
stiffness matrix 229
stiffness method 225
stiffness
–, initial 231
–, tangential 231
strain 33
– deviator 34, 54
– energy 239
– increment tensor 54
– invariant 34, 52
– rate tensor 34, 55
– tensor 34, 50
– vector 50
–, generalized 239
–, mean normal 34, 53
–, octahedral normal 34, 53
–, octahedral shear 34, 53
–, principal normal 34, 52
–, principal shear 34, 53
–, spherical 53
stress 31
– deviator 34, 52
– function 145, 179
– increment tensor 55
– invariant 34, 39, 43
– rate tensor 34, 55
– tensor 33, 77
– vector 36
–, couple 38
–, generalized 238
–, hydrostatic 40
–, mean normal 34, 41
–, octahedral shear 34, 41
–, principal normal 34, 52
–, principal shear 34, 53
summation convention 31
surface force 46
sway mechanism 284

Thamuz's principle 466
theorem of constant stress 105

unrestricted plastic flow 104, 309
unstable material 21

virtual strain 90
virtual stress 90
virtual work 91
––, principle of 91
viscosity 20, 407
viscosity coefficient 34, 426
––, internal 429

warping 142
weight function 324

yield condition 60, 239
––, Coulomb 415
––, Galilei 356
––, Huber–v. Mises–Hencky 63, 355, 417
––, Stassi D'Alia 418
––, Tresca 65, 354, 417
yield criterion 60
yield function 35, 60
yield line 368, 370
–– theory 370
yield mechanism 266, 278
yield stress 21, 24, 34
yield surface 61, 240
––, dynamic 425
Young's modulus 34, 58

Bibliotheca Academiae Scientiarum Hungaricae
MAGYAR TUDOMÁNYOS AKADÉMIA KÖNYVTÁRA

There are many problems arising in the design of structures and machine parts, in the analysis of metal-forming processes and in the field of geotechnics and mining which cannot be solved without taking into consideration the plastic properties of materials. The theory of plasticity also provides an efficient tool for the basic understanding of several mechanical phenomena and obtaining more accurate and economical solutions. This knowledge is indispensable for researchers and engineers active in the field of mechanics.

Considering these aspects and demands the author presents a comprehensive survey of the theory and applications of plasticity in this monograph which can be equally useful as a text book for the use of university teachers and graduate students and as a handbook for the use of research workers and professional engineers.

In the first part of the book the flow theory and the extremum theorems of linearly elastic–perfectly plastic bodies are treated, while in the second part the following engineering applications are discussed: elasto-plastic analysis of thick-walled cylinders and spheres under internal pressure, elasto-plastic torsion of bars, methods and solutions of plane strain, plane stress problems of plasticity and elasto-plastic and limit analysis and optimal design of bar structures, plates and shells. Besides the analytical solutions the numerical methods based on the finite element method and mathematical programming are also presented.

In the last two chapters of the book the yield conditions and constitutive equations of strain hardening, viscous and granual materials are briefly discussed and the fundamental principles and the exact and approximate methods of the analysis of dynamically loaded plastic structures are presented.

A great number of illustrative examples, figures and nearly 400 references are given which facilitate the better understanding of the applications of the theorems and methods and provide help to deeper study and further research.

ISBN 963 05 4708 2

507680

PLASTICITY. THEORY AND ENGINEERING APPLICATIONS

SÁNDOR KALISZKY

